COMPARATIVE STUDY OF LOSS OF FLOW ACCIDENT AT PAKISTAN RESEARCH REACTOR-1 (PARR-1) WITH HIGH DENSITY LOW ENRICHED URANIUM DISPERSED FUEL (U_3SI_2-Al)

M. Iqbal, A. Muhammad, T. Mahmood

Nuclear Engineering Division, Pakistan Institute of Nuclear Science and Technology (PINSTECH)
Nilore, Islamabad, Pakistan

ABSTRACT

Analysis has been carried out for Loss of flow Accident (LOFA) for the equilibrium core of Pakistan Research Reactor-1 (PARR-1) utilizing high density (4.8 g/cc) low enriched uranium dispersed fuel (U_3Si_2-Al) at proposed power i.e 9 MW. Comparison made with reference operating core of PARR-1 at 10 and 9 MW. Computer code PARET/ANL used for evaluation of maximum fuel centre line temperature, maximum clad temperature, maximum coolant temperature and flow inversion time. Results predict that nucleate boiling starts in all three cores but the clad temperatures would remain far below the fuel clad melting point. Calculations reveal that high density fuel core maximum clad temperature is the highest i.e. 157.0°C and operating cores at 10 MW and 9 MW clad temperatures are 128.75°C and 128.25°C respectively.

1. Introduction

Pakistan Research Reactor-1 (PARR-1) is basically a swimming pool type material testing research reactor (MTR), having a parallelepiped core comprising LEU (U_3Si_2-Al) fuel, containing 19.99% ^{235}U. Demineralized light water is used as coolant and moderator. One side of the parallelepiped core is reflected by graphite, i.e. thermal column, while opposite side is reflected by a blend of graphite reflector elements and light water. The bottom side is reflected by a combination of aluminum and water. Rest of the three sides, i.e. top and two lateral sides, are reflected by light water only. At PARR-1, five (Ag-In-Cd alloy) control rods are employed for reactor operating power level control and safe shut down in normal or any anticipated accidental condition [1]. PARR-1 core provides numerous irradiation facilities, which include water boxes, graphite thermal column, pneumatic rabbit tubes, beam port tubes, dry gamma cell, and bulk irradiation areal.

Different types of transients have already been simulated for earlier PARR-1 cores. Among those transients analysis are; Sensitivity of reactivity insertion limits with respect to safety parameters in typical MTR, LEU-MTR transients under reactivity insertion [2], loss of flow conditions [3], analysis of reactivity induced accidents at Pakistan Research Reactor-1[4], simulation of burn-up effect on inherent safety parameters and reactivity insertion transient analysis of Pakistan Research Reactor-1 [5]. In the current study, Loss of flow Accident (LOFA) has been evaluated for the proposed equilibrium core of Pakistan Research Reactor-1 (PARR-1) utilizing high density (4.8 g/cc) low enriched uranium dispersed fuel (U_3Si_2-Al) at proposed power of 9 MW. The core was proposed in our previous study on improved performance base [6]. The proposed core containing 15 standard and 4 control fuel elements is shown in Fig 1. Comparison has been made with reference operating core of PARR-1 shown in Fig 2.

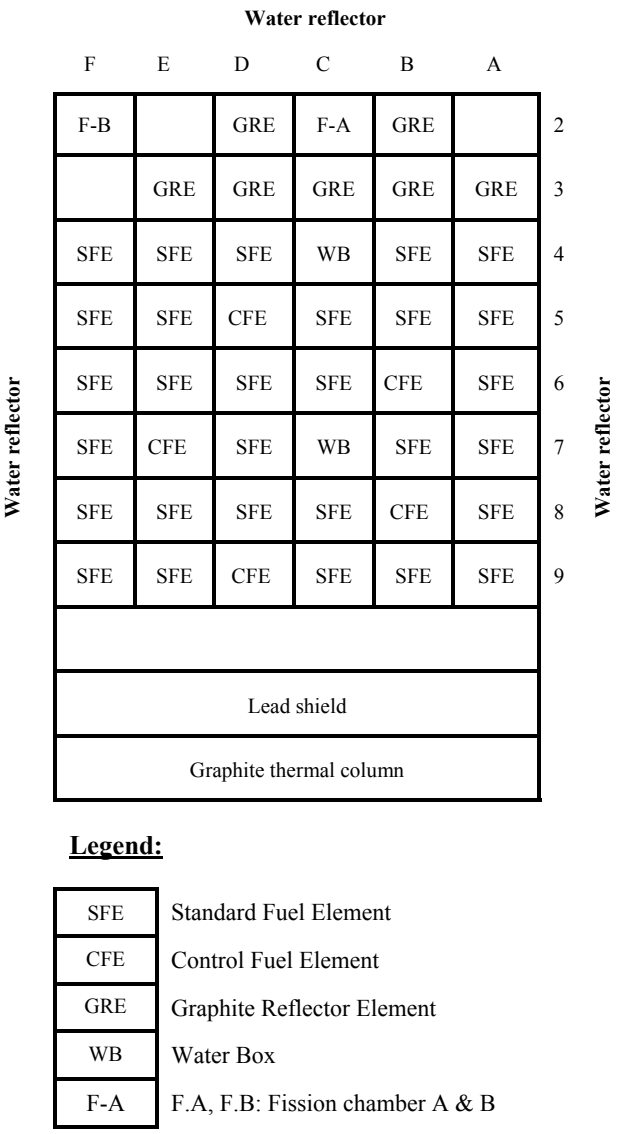

Fig 1. Reference Operational Core of PARR-1

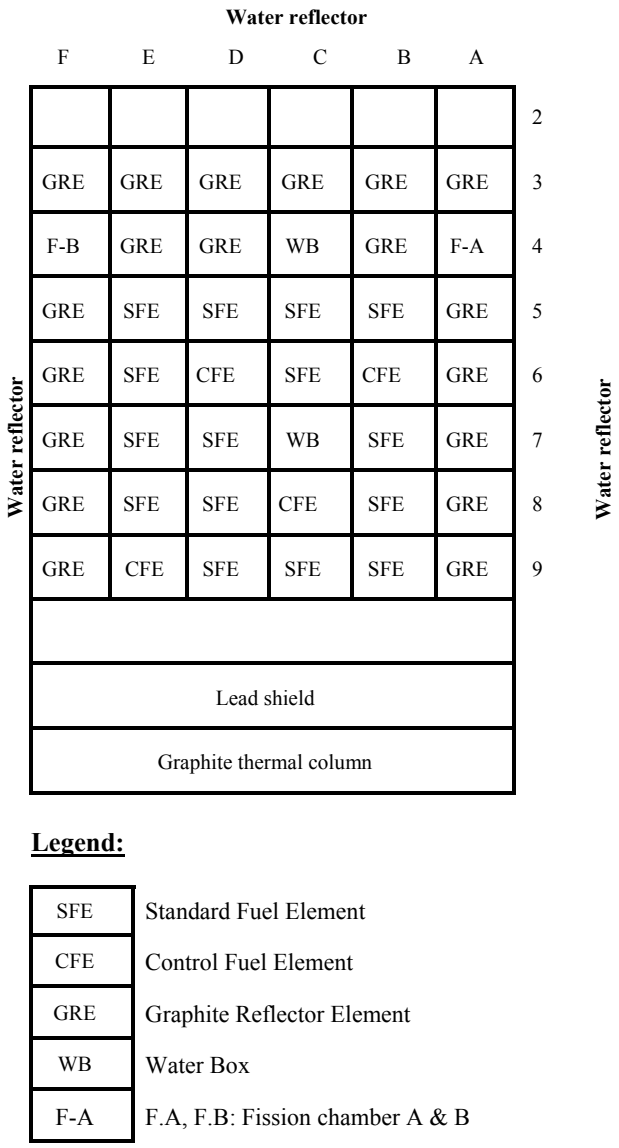

Fig 2. Proposed Equilibrium Core

At PARR-1, the primary cooling water during forced convection mode flows under gravity downward through the core. The flow rate is regulated by means of butterfly valves installed in the shielded valve pit and are operated manually.

2. Methodology

Computer code PARET [7] was employed to carry out the analysis. The code was originally developed for power reactors for the analysis of SPERT-III experiments [8], which was later modified [9] to include library of various parameters suitable to research reactors. It is basically a coupled neutronics-hydrodynamics- heat transfer code employing point kinetics, one-dimensional hydrodynamics, and one-dimensional heat transfer. Core parameters used for this study are listed in Table 1. Two channels model approach was adopted i.e hottest plate with associated flow channel and other being an average plate with associated

flow channel. Axial peaking profiles, represented by 21 equidistant mesh points calculated through deterministic neutronics calculation; were incorporated in this study. Engineering hot channel factor of 1.584 was incorporated using the conservative multiplicative method [1, 3, 4] to account for the: Uncertainties in coolant temperature rise due to manufacturing tolerances in the coolant channel spacing, uncertainties in film temperature rise due to uncertainties in the heat transfer coefficient and in-homogeneities in ^{235}U distribution and uncertainties in the calculated power distribution.

Table 1: Reactor parameters used in analyses

Parameter	Proposed High density Core	Reference operating core of PARR-1
Radial peaking Factor	1.951	1.586
Axial peaking factor	1.567	1.888
Engineering Peaking factor	1.584	1.584
Total Peaking Factor	4.843	4.74
Flow (m^3/h)	950	950
Coolant velocity (m/sec)	4.23	2.21

Study has been performed for LOFA due to closure of the outlet valve during full power operation. Reactor will scram due to low flow signal (at 90% of normal flow rate) and the safety flapper will open (at 22% of normal flow rate). It is assumed that 90% of the total fission energy is deposited in fuel section, about 4% in moderator, about 1% in other reactor materials and remaining 5% is carried away by neutrinos [10]. The reactor has low-flow trip setting at 90% of the normal flow rate (950 m^3/hr)[4]. Decay heat now will be removed by natural convection in upward direction. In transition from forced to natural convection mode, a period of very low flow and flow inversion will occur. This situation has been analyzed to estimate the peak clad temperature using the conservative approach.

3. Results and discussion

Results of the loss of flow accident analysis have been shown in Table 2. In the accident, the flow coast down was initiated after one second of reactor as shown in Table 3. The flow control valve at the core outlet was closed at its maximum speed. Low-flow trip level is always set at 90% of the full flow. Safety flapper opened at 22% of full flow. Clad temperature reached a peak value of 157 ^{0}C in the proposed core with high density fuel. For the reference operating core, maximum values of clad temperatures were 128.25°C and 128.75°C at 9 MW and 10 MW respectively.

Table 2: Transient response to loss of flow accident

Parameter	Proposed High Density Equilibrium core	Reference operating Core	
Power (MW)	9	9	10
Low-flow trip at (s)	1.56	1.46	1.43
Flow reversal at (s)	7.36	7.35	7.30
Peak Clad Temperature(^{0}C)	157	128.25	128.75

Table 3: Coolant flow during loss of flow

Time(s)	Fraction of the full flow	Time(s)	Fraction of the full flow
0	1.00	4.0	0.398
1.0	1.00	4.5	0.351
1.4	0.936	5.3	0.292
2.2	0.819	6.4	0.234
2.6	0.702	6.58	0.222
3.2	0.585	7.0	0.00
3.7	0.468		

4. Conclusion

The integrity of the core remains intact as the clad surface temperatures remains far below the melting point of the clad material. The proposed high density core is compact with small heat transfer area. Therefore peak clad temperature is higher as compared to reference operating core of PARR-1.

5. Reference

[1]. FSAR, Final Safety Analysis Report of PARR-1 (2001).

[2]. Nasir, R., Mirza, N.M., Mirza, S.M., Sensitivity of reactivity insertion limits with respect to safety parameters in a typical MTR. Annals of Nuclear Energy 26, 1517–1535 (1999).

[3]. Bokhari, I.H., Mahmood,T., Analysis of loss of flow accident at Pakistan research reactor-1. Annals of Nuclear Energy 32, 1963–1968 (2005).

[4]. Bokhari, I.H., Israr, M., Pervez, S., Analysis of reactivity induced accidents at Pakistan Research Reactor-1. Annals of Nuclear Energy 29, 2225–2234 (2002).

[5]. Muhammad, A., Iqbal, M., Mahmood, T., Burn-up effect on inherent safety parameters and reactivity insertion transient analysis of Pakistan Research Reactor-1. Progress in Nuclear Energy 58, 1-5 (2012).
[6]. Muhammad, A., Iqbal, M., Mahmood, T., A study on improving the performance of a research reactor's equilibrium core. Nuclear Technology & Radiation Protection 28, Volume 28, No. 4, pp. 362-369 (2013).
[7]. Obenchain, C.F., PARET-A Program for the Analysis of Reactor Transients. ACE Research and Development Report, IDO-17282 (1969).
[8]. Scott, R. Jr., Hale, C.L., Hagen, R.N., Transient Tests of Fully Enriched Uranium Oxide Stainless Steel Plate Type C-Core in the SPERT-III Reactor. Data Summary Report, IDO-17223 (1967).
[9]. Woodruff, W.L., Smith, R.S, 2001. A Users guide for the ANL version of the PARET code, PARET/ANL Argonne National Laboratory, Argonne, IL 60439-4841 USA (2001).
[10]. El-Wakil M.M., Nuclear Heat Transport, International Textbook Company (1971).

Thermalhydraulic analysis of control rods effect on safty parameters in Tehran Research Reactor

MINA TORABI[1] , AHMAD LASHKARI[2] , FARHAD MASOUDI[1]
1) K.N. Toosi University of Technology Faculty of science Physics department
2) Research school of reactor and nuclear safety, Nuclear Science and Technology Research Institute (NSTRI), Atomic Energy Organization of Iran (AEOI), Tehran 14399-51113, Iran

ABSTRACT

The measurement of thermalhydraulic parameters is very essensial to operate the reactor in safe situation. The position of control rods in the core effect these in safty parameters. In This paper, the control rod position in the core of Tehran Research Reactor has been investigated in Steady-State and transiate.The MTR-PC package has been used to investigate the neutronic and thermalhydraulic parameters. Termic, Caudvap and Paret codes have been used to calculate thermalhydraulic parameters. For 0% and 70% control rods position. The simulation result show that the core become more safe with injection of control rods in transiate.

Keywords: thermalhydraulic parameters, steady-state, transiate, control rods effect,safty parameters, safty of research reactors

Nomenclature	
TRR	Tehran Research Reactor
PPF	Power peaking Factor
LEU	Low Enriched Uranium
SFE	Standard Fuel Element
CFE	Control Fuel Element
LEU-CFE	Low Enriched Uranium- Control Fuel Element
BOC	Begin Of Cycle
EOC	End Of Cycle
RR	Regulating Rod
HCF	Hot Channel Factor
SAR	Safety Analysis Report
GR.B	Graphite Box
E.B	Empty Box
SR	Shim Safety Rod

1. Introduction

Research reactors have various roles in the development of nuclear science and technology. They are used in research, testing and analysis. They are also used for different applications in the fields of nuclear engineering, nuclear physics, radiochemistry, materials sciences, nuclear medicine, agriculture, etc.[1]. In all of these applications, research reactors must be operated in safe condition. Several activities related to normal operation involve safety evaluation. Generally, any activity or modification that influence Neutronic, thermal-hydraulic and mechanical properties of the reactor should be supported by safety analyses. NS-R-4 establishes safety requirements for the utilization and modification of research reactors [2]. SS 35-G21Provides guidance on the safety categorization of modification and utilization projects and the associated approval routes. Generally, any activity or modification that

influence Neutronic, thermal-hydraulic and mechanical properties of the reactor should be supported by safety analyses. In principle, Safety parameters are divided in two Neutronic and thermal-hydraulic categories. Neutronic parameters connects to Thermalhydraulic parameters from PPF. To ensure the safe operation of reactor in both steady state and transient situation, all safety parameters must be analysed in any modification.
The effect of control rods on neutronic parameters has been evaluated in my previous paper[3]. The presence of control rods result in the peak of power and the margin of safty. The main purpose of this work is evaluation of the effect of control rods movement on the thermalhydraulic parameters in steady and transiate state in TRR and their relationship to the core safety [4, 5].

1.1. Description of TRR

The TRR is pool type, heterogeneous, solid fuel, light water moderated nuclear research reactor, in which the light water is also used for cooling, shielding and reflecting. The reactor has been designed and licensed to operate at maximum thermal power level of 5 MW with forced cooling mode. The reactor core assembly has been located in two-section pool and may be operated in either of two sections of the pool. One of the sections contains experimental facilities like beam tubes, rabbit system, and thermal column. The other section is an open area for bulk irradiation studies. The major components of TRR are the pool (including embedment and accessories), bridge and support structure, core, cooling system, control and instrumentation, ventilation system, and the experimental facilities. Other details of reactor description and core parameters are given
in TRR- Safety Analysis Reports (SAR2). Elements of the reactor core are arranged in a 9 by 6 grid plate structure. The core configuration of the reference core and the burn-up of the fuel elements (in percent of the initial value of 235U) at the BOC is given in Fig. 1.

1.2. TRR Reactivity Control System

TRR is controlled by positioning of four shim safety rods made of neutron absorbing materials including Silver (Ag), Indium (In) and Cadmium (Cd) alloy (80%, 15%, 5% respectively) and one stainless steel regulating rod within the core lattice. Material selected to made control rods should have good absorption cross-section for neutrons and long lifetime as an absorber (not burn out rapidly). Silver-indium-cadmium rods are excellent neutron absorbers over a large energy range. The silver-indium-cadmium rods absorb essentially all neutrons from thermal energy to approximately 50 eV (reference). Fork type assembly is used for both of safety and regulating
rods. In any core configuration, the reactivity worth of the shim safety rods is sufficient to keep the core in a deep sub-criticality in normal operating conditions as well as abnormal occurrences such as stuck rod. The drive mechanism moves the neutron absorbing materials in specified speed as it is determined in the OLCs. The drop time of the fork type absorber rods are always less than 700 ms to compromise the fast shut down of the reactor. For each core lattice configuration, calibration of shim safety rod worth is independently performed to assure provision of safe condition.

2. Methodology

The MTR_PC package has been developed by INVAP (Argentina) in order to perform neutronic, thermal hydraulic and shielding calculations of MTR-type reactors. In this research, WIMSD-5B[4] POS_WIMS, HXS, BORGES, CITVAP v.3.1, TERMIC V 4.1, CAUDVAP V 3.60 and PARET[6,7]. WIMSD with ENDF/B-IV library was employed for macroscopic cross-section generation which provides nuclear cross-sections in the form of 69-energygroup structure. POS_WIMS is a post processor program of WIMS code used to condense and homogenizes macroscopic cross section for CITVAP from WIMS output for neutronic and reactivity feedback coefficient calculations. The HXS program (Handle Cross-Section) makes the connection between cell and core calculations. The BORGES code prepares microscopic cross section libraries for CITVAP from WIMS output for kinetic

[2] AEOI, 2001. Safety Analysis Report for the Tehran Research Reactor (LEU), Tehran-Iran.

parameters calculations. This code homogenizes and condenses microscopic cross section in any region and energy group structures. Energy group structures for calculation of neutronic and kinetic parameters are given in Table 1. Five and twelve energy croup structures were sued to calculate the cross section of SFEs and CFEs in WIMS code, respectively. Core calculations are performed with the CITVAP code using the three-group energy structure according to table1.This energy structure agrees with the 5-45-69 partition of the 69 groups WIMS library. CAUDVAP was employed in steady-state bevavior of reactor to calculate the distribution of coolant flow velocity of different parallel channels which have the same input and output polonium. the input of this code is the data of channels geometric. This code calculates the flow in channels using of iterative scheme. TREMIC code, was employed to calculate thermalhydraulic parameters in steady-state. this code calculates the temperature of fuel and coolant in channels, critical thermal flux, etc. PARET is a dynamic code to calculate the thermalhydraulic parameters. This code solves the dynamic equations of the reactor and simulates the cooling channel, clade and fule plate as a single channel axially and radially.

Table 1 - Energy group structures used in the calculations.

	Energy range	Energy group		
		12 groups	5 groups	3 groups
1	10–0.821 MeV	10–0.821 MeV	10–0.821 MeV	
2	0.821–0.00553 MeV	0.821– 0.00553 MeV	821000 – 0.625 eV	
3	5530 - 367.262 eV	5530 – 0.625 eV	0.625 – 0.00001 eV	
4	367.262 - 48.052 eV	0.625-0.08 eV		
5	48.052 - 15.968 eV	0.08 – 0.00001 eV		
6	15.968 - 4.00 eV			
7	4.00-2.10 eV			
8	210-1.123 eV			
9	1.123 - 0.625 eV			
10	0.625 - 0.280 eV			
11	0.280 - 0.080 eV			
12	0.080 - 0.00001 eV			

A	*B*	*C*	*D*	*E*	*F*	
E.B	GR	GR	GR	E.B	GR	*9*
SFE 8.15	RR CFE	SFE 28.44	SFE 28.94	SFE 18.26	SFE 11.45	*8*
SFE 24.51	SFE 36.09	SFE 46.53	SFE 52.53	SR2 CFE 1.10	SFE 28.55	*7*
SFE 21.37	SR1 CFE 36.07	SFE 50.24	E.B	SFE 44.07	SFE 28.55	*6*
SFE 31.66	SFE 31.36	SFE 42.08	SFE 55.62	SR3 CFE 58.03	SFE 15.70	*5*
SFE 4.03	SFE 22.59	SR4 CFE 48.71	SFE 54.00	SFE 39.15	SFE 3.62	*4*
E.B	SFE 13.07	SFE 23.99	SFE 37.84	SFE 3.79	E.B	*3*
GR	E.B	E.B	GR	GR	GR	*2*
GR	GR	GR	GR	GR	GR	*1*

SFE: STANDARD FUEL ELEMENT **CFE**: CONTROL FUEL ELEMENT
GR-BOX: GRAPHITE BOX **E.B:** EMPTY BOX
SR: SHIM SAFETY ROD **RR:** REGULATING ROD
Fig.1.TRR 61 core configuration

3. Result and discussion

3.1. The effect of control rods position on thermalhydraulic parameters.

The effect of control rods position on neutronic parameters in the core configuration of TRR has been calculated in my previous paper[3]. The neutronic part of result was inserted in TERMIC and PARET input for both %0 and 70% control rod positions. In this paper, the effect of power distribution has been compared with the parameters of the maximum value of fuel temperature, clade and coolant.

TERMIC code has been utilized to produce the thermalhydraulic parameters in steady-state situation.The results are compatible with safty criteria.

Parametr	Value		Safty Criteria (SAR)
	0%	70%	
Coolant flow, m3/hr	500	500	-
Coolant velocity, m/s	1.252	1.252	< 15.3
Margin to ONB SFE	2.23	1.88	>1.3
Margin to DNB SFE	12.286	10.219	>2
Peak cladding temp. (℃) SFE	79.7	84.3	<105
Peak fuel temp. (℃) SFE	87.8	94.0	<650
Margin to Twall=105 (℃) SFE	1.73	1.45	>1

The studies of transiat behaviour of TRR is consist of different scenarios. In this research, we just evaluate one of standard scenarios. This scenario is reactivity injection of 1.5$/0.5s without scram condition with primary power of 1mw in TRR. The power and temperature of fuel, clade and coolant has been shown in fig.1 for both 0% and 70% rod positions. The reactivity coefficients and kinetic parameters has been shown in table 1 . in 0% rod position. When control rods are out of the core, the maximum level of power of reactor reached to 508MW in 0.07s. further, the maximum value of fuel reched to 384°C (the melting point of Aluminium is 600°C). If the temperature of fuel reaches to the melting point of Aluminium in ceramic, begings to melt and causing turbulence in clade. Although the maximum temperature of clade reached to 260°C in this scenario and did not reach to the melting point of Aluminium, the point is the maximum value of fuel . In this scenario, the maximum value of coolant reached to 118°C which is less than the saturation point. Thus, the water in coolant channels is not boiling throughout the reactivity injection of 1.5$/0.5s. In next step, the safty parameters has been evaluated in 70% control rods position. The shape of distribution of thermal flux changes when control rods inject to the core in 70%. The results has been put in code and the scenario has been evaluated.

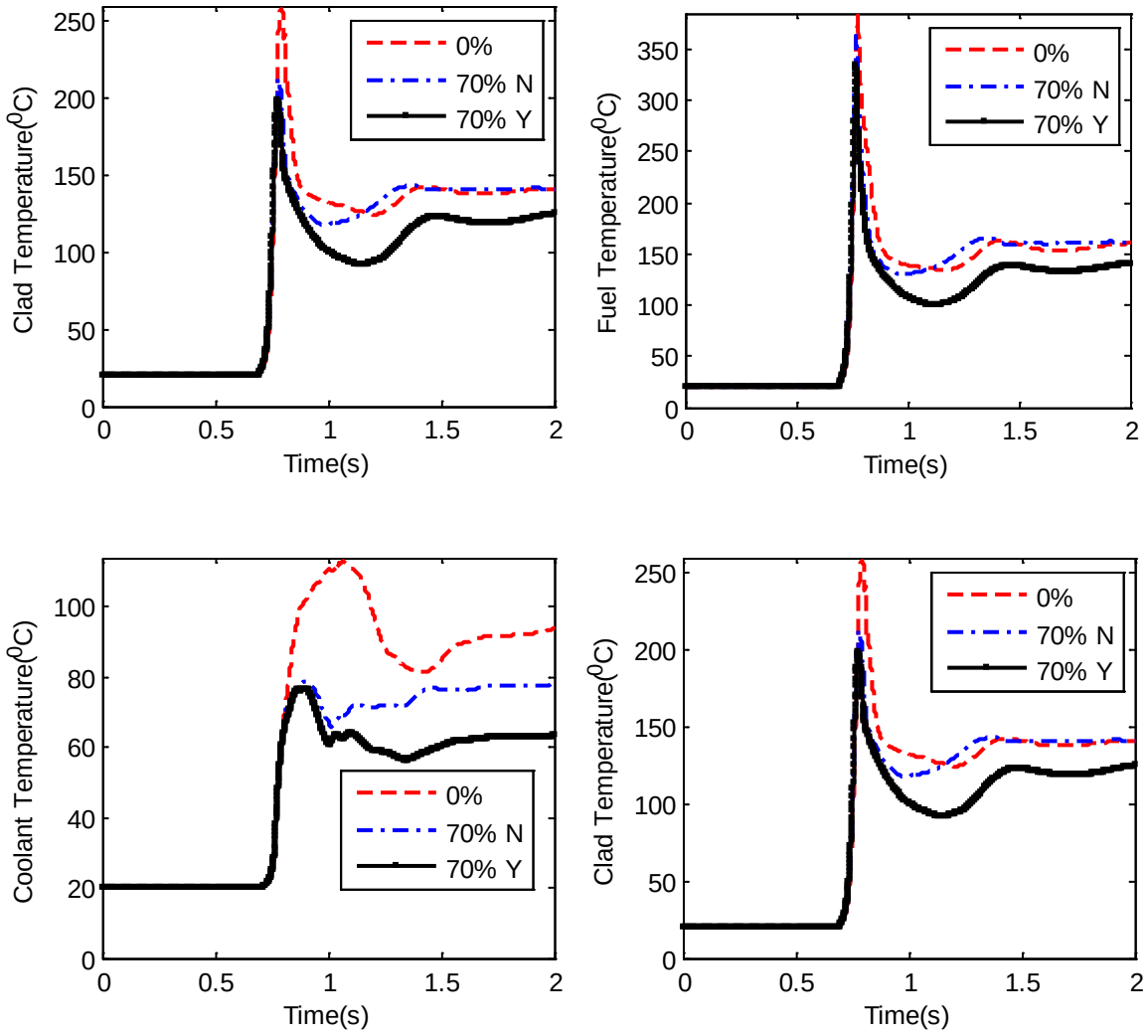

Fig 2. The time behavior of power parameters A)The maximum value of fuel temperature, B) The maximum value of clade temperature C) The maximum value of coolant temperature in positive reactivity injection scenario of 1.5$/0.5s without shutting down

As it is obvious, the power peak has been decreased and reached from 435.3MW to 508MW. The fuel temperature has not been significantly changed in 70%.however it shows a little drop. As well as this, the temperature of clade has been decreased as much as 20°C. Further more, there is 30°C temperature drop. In this study, the most important point, was more safty situation when control rods are inserted into the core as much as 70%. We should attention all of safty parameters such as reactivity coefficients and kinetic parameters in transiate state. we evaluated revolution of these parameters in presence of control rods into the core.

Table1. reactivity coefficient of void and kinetic parameters of core 61.

	fuel (pcm/oC)	moderator (pcm/oC)	Vapor 0 to 40) (percent	Delayed neutron fraction(pcm)	prompt neutron lifetime (µs)
% 0	1.4	19.92	400	769	55
%70	1.46	29.14	650	769	55

3.2. The calculation of thermal reactivity coefficient in 70%

In this section, the value of reactivity coefficients have been calculated when control rods are injected as much as 70% into the core. The reactivity coefficients have been shown in table.1 for both 0% and 70%. The results shows the ractivity coefficient with injection of control rods.we put the results into the input of PARET code and the scenario was repeated. according in fig 2.

the power peak has been decreased with input of coefficient reactivity. As well as this, the maximum value of fuel temperature has been decreased for 70%. The point is that reactivity coefficient is more effective than the injection of control rods in reactor core. According in fig.2 the temperature of clade and coolant has been decreased. This is because the reactivity coefficient increases with injection of control rod in the core. This leads to the increase of the effect of feedbacks and causes the reactor to be shut down faster during accidents.

4- Conclusion

As far as mentioned in the introduction of this paper, the main objective of this work is calculatatin of the effect of the control rods on thermalhydraulic parameters.

Thermal neutrons disrtribution revoluated with inserting gradually bank of control rods into the core. In this work, safty parameters of the reactor core was calculated by PARET code and results has been shown for three steps in table2. The presence of control rods causes increase of safty in transiate state. As well as this, reactivity coefficient corrected with regarding of presence of control rods. It leaded to the mre safty of the core. In normal operating condition, the most part of control rods are into the core. It causes untisymmetry of thermal flux distribution. If an accident occurs for any reason, the reactor will be in a more safe condition.

Table2. The maximum value of fuel, clade and coolant and release energy of injection of positive reactivity scenario

Inserted Reactivity	Peak Power [MW]	Max. Energy [MJ]	Peak Fuel Temp. [oC] (*)	Peak Clad Temp. [oC] (*)	Peak Coolant Temp. [oC] (*)
0% in	508	42.7	384	258	113
70% in without R.Cs correction	411	38.1	362	212	79
70% in with R.Cs correction	366	29.4	334	198	77

(*): Values associated with hot channel

Ramp reactivity insertion (1.5 $per 0.5s)

Initial power = 10-9 MW

Reactor without scram

Refrences:

1. IAEA-TECDOC-1234, The applications of research reactors. IAEA, Viana. 2001.
2. IAEA, SAFETY OF RESEARCH REACTORS. IAEA SAFETY STANDARDS SERIES 2005. NS-R-4.
3. M. Torabi, A.Lashkari, S.F Masoudi, Neutronic analysis of control rod effect on safty parameters in Tehran Research Reactor.Nuclear engineering and Technology 2018.50(18): 1017-1023
4. Hetrick, D.L., DYNAMICS OF NUCLEAR REACTORS. 1971.
5. Mirza, A.M., S. Khanam, and N.M. Mirza, Simulation of reactivity transients in current MTRs. Annals of Nuclear Energy, 1998. 25(18): p. 1465-1484.
6. Kulikowska, T., WIMSD-5B: A Neutronic Code for Standard Lattice Physics Analysis. Distributed by NEA Data Bank. Saclay, France, 1996.
7. Lecot, E.V.a.C., Neutronic calculation code CITVAP 3.1.

INSTITUT LAUE LANGEVIN – REACTOR HIGH FLUX – STRESS TEST RESPONSE AFTER FUKUSHIMA

J. ESTRADE, H. GUYON, B. DESBRIERE,
JL. DURIEU
Institut Laue-Langevin -38000 Grenoble - France

Contact author: estrade@ill.fr

ABSTRACT

The Institut Laue-Langevin (the ILL) is an international research centre providing world-leading facilities in neutron science and technology. The Institute operates the most intense neutron source in the world, a 58.3 MW nuclear reactor designed for high brightness.

Following the nuclear disaster at Fukushima in 2011, the French regulatory body (ASN) ordered additional safety assessments to be performed on all French nuclear facilities, including the ILL.
The ILL's Reactor Division teams carried out the assessments required, analysing the behaviour of the ILL reactor under extreme conditions - an earthquake scenario involving major damage to the town of Grenoble and the failure of all the river Drac dams upstream, leaving the city centre under 8 m of water.

This safety review has had a major impact on the ILL and its budget over the past few years. The resulting "Post-Fukushima reinforcement programme" has now ended and the safety of the reactor is guaranteed even in such extreme conditions.

This paper will give an overview of the new safety systems installed and present the "defence-in-depth" approach adopted to deal with extreme events.

1. Introduction - The Institut Laue-Langevin (ILL)

The Institut Laue Langevin (ILL) is Europe's most advanced neutron research facility. It operates a high-flux reactor (the RHF), the world's most intense neutron source, and delivers beams of neutrons to almost 40 high-technology scientific instruments.
The ILL is managed by France, Germany and the United Kingdom. It has set up scientific partnerships with 10 other countries: Austria, Belgium, Czech Republic, Denmark, Italy, Poland, Slovakia, Spain, Sweden and Switzerland.
In conjunction with the neighbouring synchrotron facility, the ESRF, the ILL is part of a unique complex for the exploration of matter, the European Photon and Neutron science campus. It provides services and expertise for scientists from the entire world. Each year, the Institute attracts around 1,200 researchers from more than 40 countries. Research is focused on fundamental science in numerous fields including biology, chemistry, soft matter, nuclear physics and the science of materials.

Fig 1. The EPN campus

Among the 1,500 experiment proposals received each year, around 800 are selected for their excellence by the international scientific committees. The number of experiments performable is determined by the operational constraints of the reactor and the number of instruments available.
The research programmes performed over recent years at the ILL have generated over 600 scientific papers per year, some 150 of which have been published in high-impact journals.

2. Reactor design and continuous refurbishment

The reactor was designed to provide maximum brightness for the experimental programme. Its fuel assembly is located in a tank of heavy water, from which a series of neutron beam tubes made of aluminium or zircaloy deliver the high flux of neutrons to the instruments. The neutron instruments are located in the reactor building or in the two adjacent guide halls.
Due to its unique, highly compact fuel element and the excellent thermo-hydraulic conditions, the reactor can deliver a thermal neutron flux of 1.5×10^{15} n.cm-2.s-1 with a thermal power of 58.3 MW.
The reactor first went critical in 1971. Since then it has been maintained through major refurbishment programmes. The reactor core was replaced in 1995, and major work was carried out ten years ago under the Refit programme to reinforce the facilities against a severe earthquake (Richer 5.7).

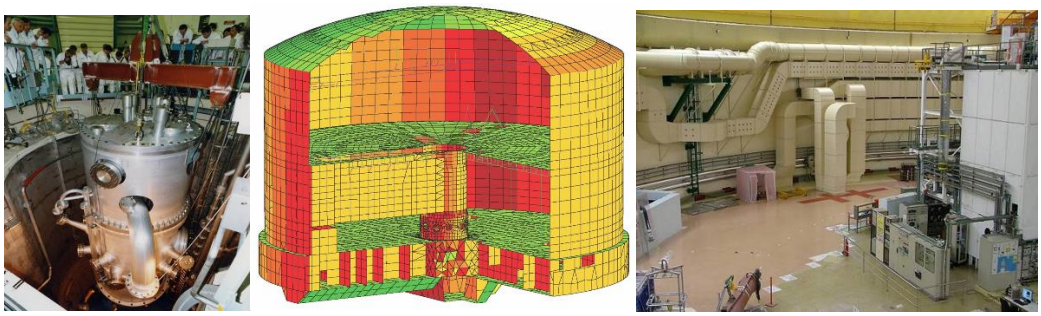

Fig 2. Replacement of the reactor core in 1995 and the 2002-2006 “Refit” reactor refurbishment programme

The reactor containment was generously dimensioned to house a significant number of instruments. It consists of a concrete housing some 40 cm thick and an 11mm external steel shell.

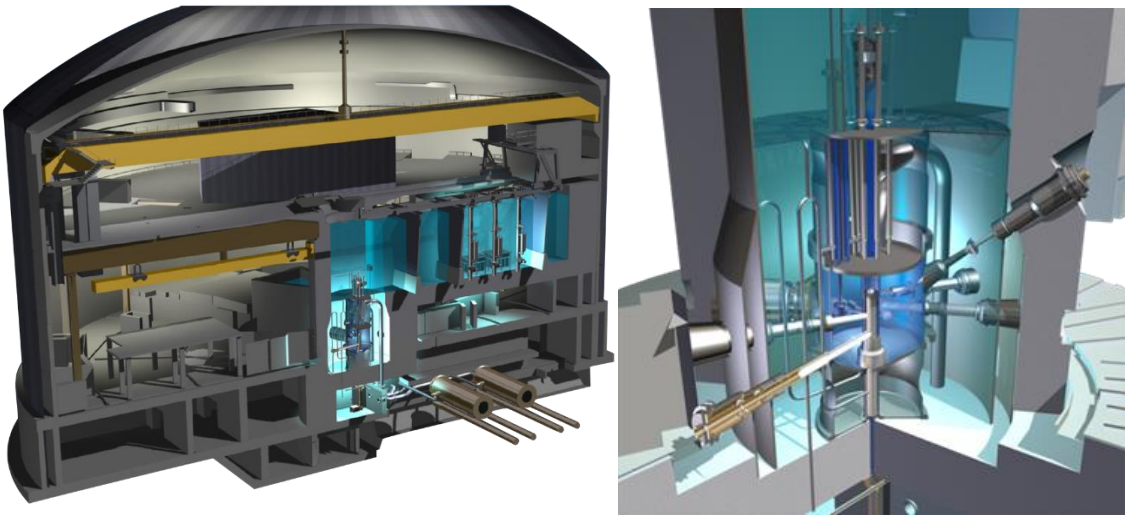

Fig 3. Reactor building and reactor core

The original design basis events underlying the reactor design were the Borax-type accident (rapid reactivity insertion) and a core meltdown in air. It is important to note that, given the type of fuel used by the reactor (high-enriched uranium), its power, and its operating mode, the ILL's inventory of radioactive material contains 100 fewer short-lived fission products and 1000 fewer long-lived fission products than that of nuclear power plants.
The ILL is located in Grenoble, close to the mountains and the Drac river. It operates within 10 kilometres of a chemical-industrial complex.

Fig 4. Panoramic view from the dome of the RHF reactor

The main characteristics of the ILL reactor

- Pool-type reactor
- Coolant: heavy water
- Reflector: heavy water
- Thermal power: 58 MW
- Max. thermal flux in the reflector: 1.5×10^{15} $n.cm^{-2}.s^{-1}$
- Fuel: UAlx with enriched uranium
- Cycle length: around 50 days
- 2 cold neutron sources and 1 hot neutron source
- 19 neutron beams
- 40 experimental areas

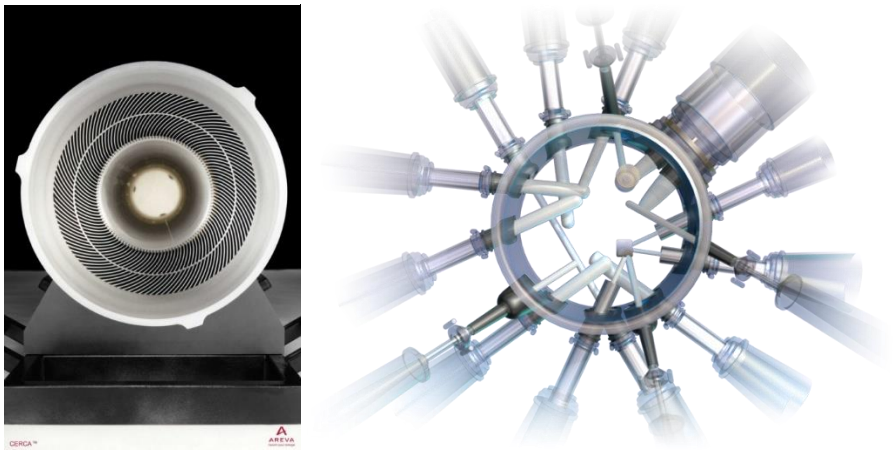

Fig 5. The fuel assembly and reactor core

3. Safety reassessment and review of extreme conditions

In 2011, after the Fukushima accident, the French authorities asked the ILL to re-assess the risk scenario used in its preparations for a natural disaster (a “stress test”). This request was made to all French nuclear operators. The ILL had to produce a report on the results of its reassessment.

The safety reassessment focused on a verification of its defence-in-depth procedures for the reactor facilities, under specific internal and external conditions: it took into account the hazards associated with the ILL’s location (earthquake, flood, and industrial environment...). In particular it examined the safety requirements addressed in the design of the facility, including its resistance to seismic events, flooding, or physical damage (from flooding and/or earthquake), the risk of loss of its electric power or heat sink, the safety of its spent fuel storage pool, as well as hydrogen control, emergency arrangements, accident management, and communications.

In the light of Fukushima, and to address the risk of “extreme external events”, the severity of the earthquake to be taken into account was raised to the Richter 7.3 level (compared to the level of 5.7 used for the relatively recent Refit reactor refurbishment programme). In addition, the authorities added the requirement that the ILL facilities be protected against the concurrence of an earthquake and extreme flooding.

The earthquake scenario the ILL had to prepare for was that of a quake such as would occur only every 20 000 years. The hypothesis is that the quake would result in the breach of the four dams upstream on the river Drac. In less than an hour the flood waters would reach the ILL and rise in a matter of minutes to the 216-metre level - with a wave 8 metres high sweeping across the town. This was the combination of catastrophes the ILL had to face. ILL is required, of course, to be able to maintain its reactor under control in these extreme conditions.

Earthquake and flooding are the main risk in the hypothesis of an extreme external event, but the ILL’s industrial environment was also reviewed, mainly in terms of the chemical risk for the reactor operator in a post-accident scenario.

The safety reassessment was based on the existing safety analysis report. Its main objective was to confirm the operability of the ILL’s basic safety functions. These involve:

- ensuring that the reactor shuts down and remains in a safe shutdown state for all design basis accidents and for all operational states;
- providing for the adequate removal of heat after shutdown, in particular from the core, including in design basis accidents;

- confining radioactive material in order to prevent or mitigate its unplanned release to the environment.

Safety reassessments are performed in phases:

- The first phase aims at ensuring that the current design requirements and the underlying data are valid and consistent with the current conditions of the reactor facility and its site.
- The second phase assesses the reactor's response to beyond-design-basis events, including this stress test. This is a highly systematic assessment focusing on defence-in-depth. It identifies specific vulnerabilities and where improvements to safety are required, including any possible mitigatory action.
- The next phase is to specify, on the basis of the results of the two points above, the preventive measures and mitigatory action to be taken. This involves redefining the "SSC" (structures, systems and components) to be targeted in reinforcing the safety of the reactor and its "hard core" safety systems, together with additional measures to reinforce the existing SSC.

Fig 6. Reinforcement of existing equipment

The reassessment therefore recalculated the ILL's safety standards to match the "new" scenario. All the studies performed and the work carried out adopted the defence-in-depth approach. This involves ensuring the resilience of the secondary lines of defence, on the hypothesis that the initial systems of protection would all fail.
The results of these new safety reassessments were submitted to the advisory group of experts, and the ILL subsequently defined its commitments to reinforce the safety of the facility. Overall, the regulatory body accepted the ILL proposals with the addition of a few more general requirements.

4. Post-Fukushima reinforcement programme

Following the conclusion of the safety reassessment and its validation by the regulatory body, in 2012 the ILL proceeded to install new safety circuits and automated systems, the so-called "hard core", in and around the reactor. There was also a focus on reducing the need for human intervention, particularly during and following an accident situation

(first 30 minutes). ILL also launched a significant programme of work to reinforce the existing “Structures, systems and components”.
This included new buildings capable of resisting “extreme external events” (earthquake conditions and flooding) and modifications to existing buildings.
All the new safety systems were installed in duplicate, to ensure that systems continue to function in the event of a failure. It is important to note that this is a unique approach, making the ILL reactor one of the safest research reactors in the world, particularly in the event of an extreme external event. Moreover, all these systems have dedicated power supplies and command and control systems. To guarantee their timely deployment instrumentation was developed to monitor and report on the state of the reactor (the level of water in the pool for example, or the pressure in the reactor building). The programme had three priorities:

- ***Ensure efficient cooling***

In the event of an emergency shutdown, the reactor core will have to be cooled by natural convection, requiring sufficient water in the reactor pool. To guarantee the water level, the existing emergency core reflood circuit (CRU) was reinforced and automated, and an additional supply of groundwater was installed (CEN). This guarantees that the supply of water to the reactor pool is sufficient to ensure that the fuel element remains under water and that the cooling process continues efficiently, even in the double occurrence of an earthquake and dam burst.

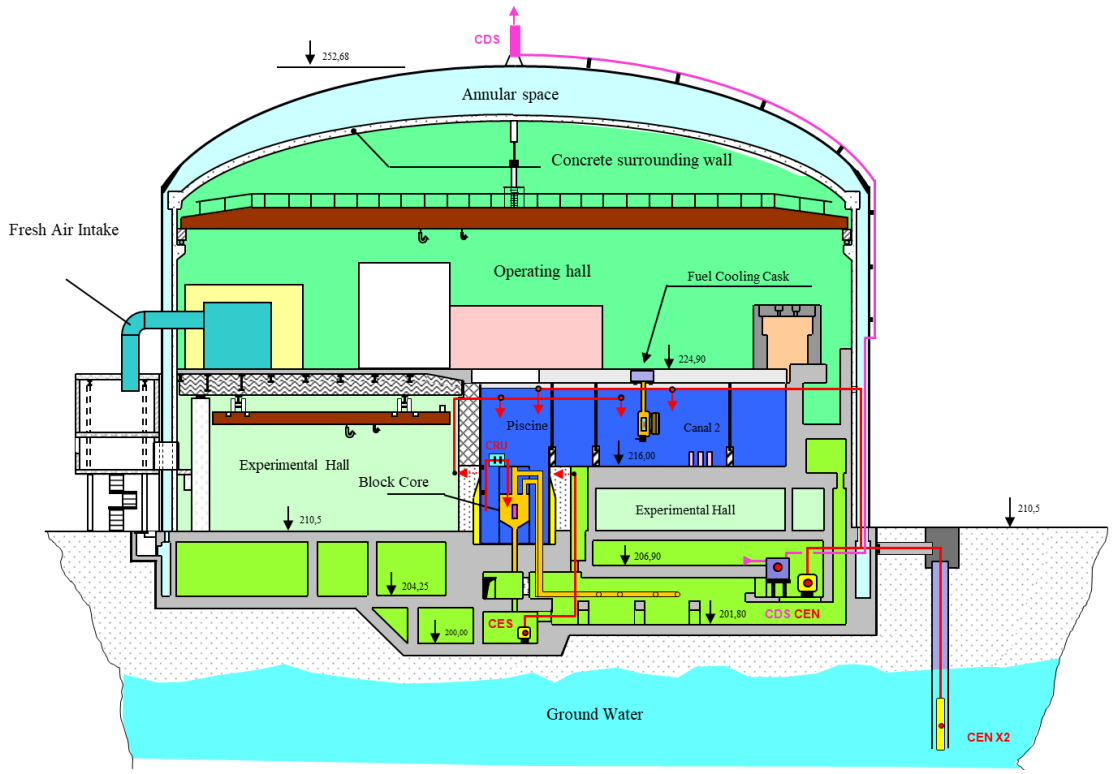

Fig 7. The CRU, CEN and CDS safety circuits

Fig 8. Groundwater well pipe and installation (CEN)

- ***Ensure confinement***

If the redundant systems and the two cooling systems (CRU & CEN) described above fail, the fuel element would overheat and melt in the reactor hall. Confinement must therefore be guaranteed for the medium- to long-term management of the emergency.
To deal with this scenario, a new seismic depressurisation circuit (CDS) was installed, to limit the effects of a meltdown to acceptable proportions.

Fig 9. Seismic depressurisation circuit (CDS)

This circuit ensures that the reactor hall (containing any radioactivity released by the melting core) remains at a slightly lower pressure than its surroundings. There should thus be no risk of uncontrolled or unfiltered releases into the environment.
In the event of an accident, the air in the basement of the reactor hall would be the least polluted. The system takes air from the basement and purifies it through two sets of very high-efficiency filters and one set of iodine traps. It then evacuates the air through the chimney on the dome of the reactor. New instrumentation was developed to control the releases.

- ***Ensure good crisis management***

To control all the safety circuits, and, more generally, to manage a major crisis on the site, the ILL has had to build a new emergency control room (PCS3), designed to house the equipment and personnel required to manage a crisis. The building is sufficiently robust to resist all the envisaged external hazards: earthquake and flood, of course, but

also clouds of toxic pollution from the chemical complex to the south and even outside explosions.

Fig 10. New emergency control room (PCS3)

The PCS3 is linked to the safety circuits (CRU, CEN and CDS) in and around the reactor building by a “motorway” of cables: 130 km in all! The cables follow two different subterranean cableways, buried at a depth of 4 metres to protect them from being swept away in the flood that would ensue if the dams were to burst upstream. Two new underground buildings protect the cableways in particular, as they cross into the reactor through 60 holes in the containment walls. The new systems are now contributing to the overall safety of the site, and will continue to be of use even during more minor incidents or safety exercises.
There are other items linked with this reinforcement programme:

- human resources and organisational factors: specific training programmes and exercises have been introduced to improve operator responses to the new scenarios,
- a review of the operating procedures (normal-, incidental-, accidental- and severe- accident instructions, maintenance, periodic testing and inspection programmes…);
- a review of certain severe-accident management procedures: measures to guarantee access to the reactor facilities to be able to replace on-duty personnel, availability of on-call personnel, availability of external response forces to reinforce and manage teams over the medium and long term. There was also the need to construct a suspended walkway from the reactor building to the new emergency centre (PCS3).

Fig 12. Access to the emergency centre (PCS3) from the reactor building

5. Conclusion

It is thanks to the quality of the initial design of the ILL reactor and its subsequent refurbishment programmes that the ILL was able to adapt, renew and reinforce its installations in response to new regulatory requirements following the accident in 2011 at the Fukushima Daiichi nuclear power plant in Japan.

The ILL reacted promptly to conduct the safety reassessment and determine the measures to be performed; the improvements were implemented from 2013 to 2018, given the commitment of the Institute's Associates and the technical and organisational capacities of the ILL staff.

No other French nuclear installation has had to reinforce its facilities against the combined risk of earthquake and dam burst flooding. Thanks to the success of this programme, there can be no doubt cast on the ILL's capacity to continue to operate safely beyond 2030.

THE EFFECT OF THE INTERACTION LAYER (IL) THERMAL CONDUCTIVITY UNCERTAINTY ON THE PERFORMANCE OF U-MO/AL DISPERSION RESEARCH REACTOR FUEL

F.B. SWEIDAN, Q. M. MISTARIHI, H.J. RYU
Department of Nuclear and Quantum Engineering, KAIST
Yuseong-gu, Daejeon 34141, Republic of Korea

ABSTRACT

U–Mo/Al dispersion fuel has been considered one of the most promising candidates for the replacement of highly enriched uranium fuel in many research reactors. One of the issues of U-Mo/Al dispersion type fuel is the formation of the interaction layer (IL) between U-Mo particles and the aluminum matrix. Several models have been developed for the estimation of the thermal conductivity of this interaction layer without providing an uncertainty analysis of the parameters involved. In this study, uncertainty ranges of the parameters used for the IL thermal conductivity are provided. These uncertainty values are used to determine the overall uncertainty effect on the IL thermal conductivity and to rank the most influential parameters.

1. Introduction

To minimize nuclear proliferation, the development of low-enriched uranium (LEU) fuels for research reactors has been pursued to replace the use of highly-enriched uranium (HEU). However, this replacement deteriorates the levels of power and neutron flux. In order to use LEU, increasing uranium loading is required. U-Mo/Al dispersion fuel has been the most potential candidate since the U-Mo alloy can increase uranium loading significantly [1-3].

Dispersion fuel offers an advantage in thermal conductivity over a monolithic fuel design [4]; that is thermal conductivity is proportional to the amount of high thermal conductivity aluminum present in the matrix. The matrix will dissipate heat faster than the lower thermal conductivity fuel phase. However, one of the main issues of U-Mo/Al dispersion type fuel is the formation of the interaction layer (IL) between U-Mo particles and the aluminum matrix.

When the dispersion fuel is irradiated, the fuel particles react with the matrix and form IL. The composition of the IL is complex. The microstructural analysis of the un-irradiated U-7Mo/Al-2Si showed that the chemical composition of the IL was dependent on the annealing temperature where a mixture of (U, Mo) Al_x-Si_y was formed [5]. After irradiation, the IL becomes amorphous and its composition is unknown [3]. Some properties including density and chemical composition that provided the best fitting for the measured fuel meat swelling were recently provided [6].

The thermal conductivity of IL is critical on the fuel performance during irradiation and has been predicted recently by Mistarihi et al. [7]. The objective of this study is to utilize the model by Mistarihi et al. in the uncertainty analysis of the interaction layer thermal conductivity to evaluate the overall effect of all the parameters' uncertainties involved and to identify the most impactful parameters on the IL thermal conductivity.

2. Parameters and Uncertainties

Two segments were selected as basic models for the simulation; one was irradiated at a low burn-up of 5.195×10^{21} f/cm^3 (referred as TL) and the other was irradiated at a high burn-up of 6.49×10^{21} f/cm^3 (referred as TK) [2], the data of these two segments are from the ATR Full-

size plate In-center flux trap Position (AFIP-1) experiment of the RERTR program [8]. The AFIP-1 experiments summarize the experiment in terms of irradiation, safety, neutronics and hydraulics analyses, and thermal analyses results. Thus far, these experiments are most representative of the operation conditions of U-Mo/Al dispersion fuel and are most reliable in terms of providing well-defined irradiated microstructures and thermal properties of irradiated U-Mo/Al dispersion fuel.
To determine dimensions of each model, the volume fraction of fuel particles, the IL, and the matrix (if applicable) were calculated using ImageJ software [9] from the images of TL and TK provided in Ref. 2. Table 1 shows the dimensions of the simulated models representing TL and TK segments with the associated uncertainties [7].

Table 1: Volume fractions of the constituent phases of the irradiated TK and TL fuel meat segments [7].

Vol%	Low burnup low heat flux (TL) fuel segment	High burnup high heat flux (TK) fuel segment
Fuel particles	59.8 ± 1.1	44.1 ± 1.3
IL	30.7 ± 1.2	52.5 ± 0.6
Matrix	7.5 ± 0.3	0.0
Porosity	2.0 ± 0.3	3.4 ± 0.1

As shown in Table 1, the study by Mistarihi et al. [7] provided the uncertainty ranges regarding the volume fractions for TK and TL. Alongside the volume fraction uncertainty, the fuel thermal conductivity uncertainty is significant to be taken into account. According to the author's previous work [10], the uncertainty ranges of the fuel thermal conductivity is approximately ±11%.

These uncertainty ranges were used to evaluate the overall effect of all the parameters' uncertainties by applying the upper and lower bounds of all the uncertainties. It is worth mentioning that in order to keep the volume fraction at 100% when applying the upper and lower bounds, the porosity was intentionally changed.

Identifying the most influential parameter is also an important part of this study, this also has been done by solely applying the upper and lower bounds of each parameter's uncertainty to evaluate the effect of the very parameter uncertainty on the interaction layer thermal conductivity.

3. Simulation and Calculations

The simulation was performed using "COMSOL Multiphysics" version 5.1 finite element analysis (FEA) software [11]. The thermal conductivity of the IL was calculated by fitting the FEA-reproduced thermal conductivity data of the U-7Mo/Al-2Si fuel meat with the experimentally measured data by assigning a random value to the IL thermal conductivity and finding the value of the IL thermal conductivity that produced U-7Mo/Al-2Si fuel meat thermal conductivities matching the average of the experimentally measured ones. More details about the modelling and simulation can be found in Ref [7]. The thermal conductivity data of irradiated U-Mo/Al dispersion fuel used in our calculation was taken from the experimentally measured data reported by Huber et al. [12].

Simulated models for TL segment consisted of three phases; fuel particles, Al matrix, and IL. The model for TK segment consisted of just two phases, fuel particles and IL. The modelling assumed that there would be no thermal expansion nor swelling due to irradiation, i.e., the IL thickness would not grow throughout the operation.

The model assumed that U-Mo particles and IL were distributed in an FCC array in the matrix. ILs were overlapped together in the model representing the TL segment. Fig. 1 showed the final dimensions for the geometry of the TL and TK model.

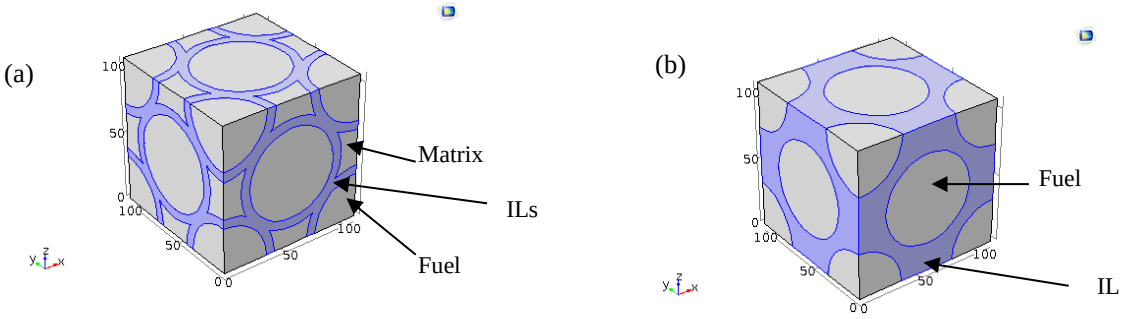

Fig 1. Simulated models generated for (a) TL with an IL thickness of 6.008 μm and (b) TK segments in COMSOL Multiphysics.

4. Results and Discussion

4.1 The Combined Uncertainty

After collecting all the parameters' uncertainties, COMSOL Multiphysics was used for the calculations of the change in the interaction layer thermal conductivity after applying the upper and lower bounds of the uncertainties. As mentioned previously, the first goal of this study is to evaluate the overall effect of all the parameters' uncertainties (the combined uncertainty) on the interaction layer thermal conductivity. Fig. 2 shows the effect of applying the uncertainties of all the parameters on the IL thermal conductivity for TL and TK.

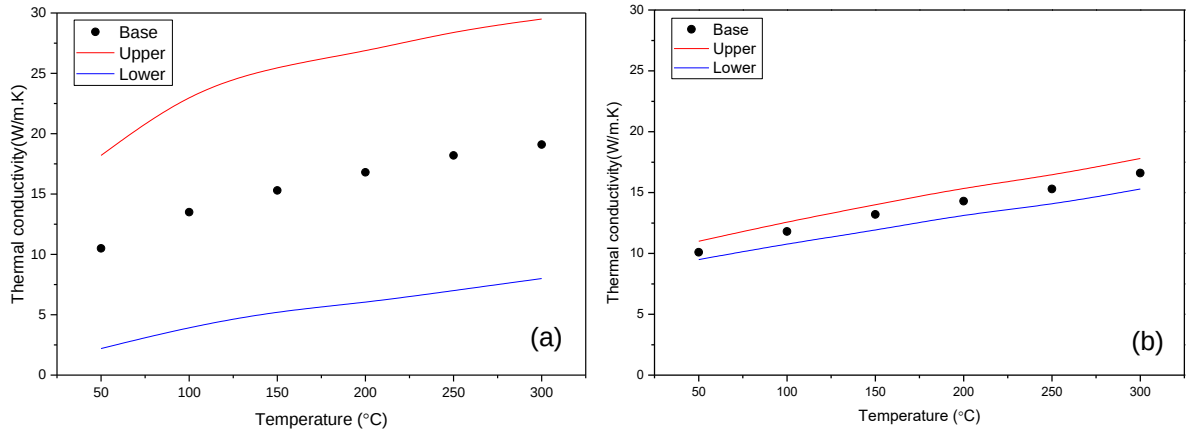

Fig 2. The overall uncertainty (the combined uncertainty) for (a) TL and (b) TK segments.

From Fig. 2, it can be noted that with applying all the uncertainties, the upper and lower bound for TK, which represents the stable case after the full consumption of the matrix by the interaction layer, are small. This result indicates the reliability of the estimated IL thermal conductivity values obtained by Mistarihi et al. model as the IL thermal conductivity TL and TK will be almost identical. Therefore, the estimated values for the IL thermal conductivity, which are 10~16 W/m-K, are reliable and meaningful. However, these values are much higher than the measured values from the results of the out-of-pile samples reported in previous studies. This difference will be one on of the issues that need further theoretical studies to be explained.

On the other hand, it is shown in Fig. 2 that the upper and lower bounds in the case of TL are higher than those of TK. This is explained as more uncertainties are involved in the TL IL thermal conductivity calculations. In the case of TL, the interaction layer is still growing as it

consumes the matrix with time while for TK, the matrix is fully consumed. Therefore, any uncertainty in the parameters can cause a large influence in the IL thermal conductivity for TL. In the case of TK, the interaction layer already consumed the Al matrix and, in turn, no major changes take place.

4.2 Identifying the Most Influential Parameters

The second goal of this study is to identify the most impactful parameter on the interaction layer thermal conductivity. This has been done by applying the upper and lower bounds of each parameter separately at a representative temperature (200 ^{o}C). Fig. 3 shows the effect of each parameter's uncertainty on the interaction layer thermal conductivity for TL and TK.

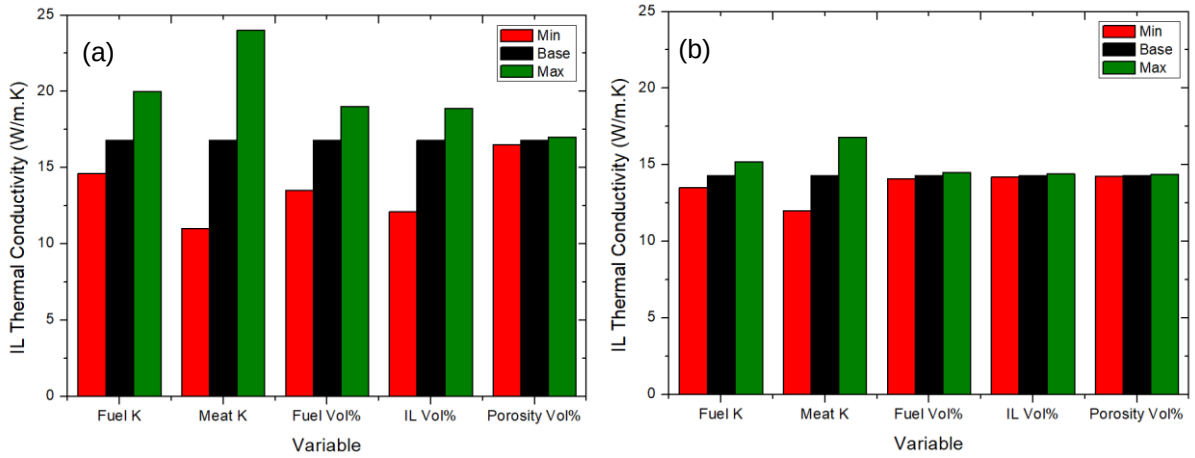

Fig 3. The effect of each parameter's uncertainty on the interaction layer thermal conductivity for (a) TL and (b) TK segments.

As explained in the previous section, the TL interaction layer thermal conductivity suffers large fluctuations if any changes happen due to uncertainties, this can be also noticed in Fig. 3 as the effect of each parameter shows a larger influence when compared to TK. However, for both cases, TL and TK, the most influential parameter is the fuel meat and the fuel particles thermal conductivity. This can be explained as the fuel thermal conductivity possesses a relatively large uncertainty compared to the other parameters and it also controls the heat dissipation from the fuel to the outer surfaces that significantly affects the IL thermal conductivity calculations. Therefore, it shows higher fluctuations when compared to other parameters.

5. Conclusion

In this study, the overall effect of five parameters' uncertainties on the interaction layer thermal conductivity has been evaluated based on the model by Mistarihi et al. for two fuel segments referred to as TL (low burnup) and TK (high burnup). The results show that TL suffers larger upper and lower bounds when compared to TK due to the continuous changes occurring as the matrix is still being consumed during operation, while in the case of TK, the matrix is fully consumed by the interaction layer. Most importantly, the results showed that the estimated values of the IL thermal conductivity are reliable and meaningful as the overall uncertainty effect on the IL thermal conductivity of TK, which represents the stable case after the full consumption of the matrix by the interaction layer, provides small upper and lower bounds when compared to the base case.

After that, the effect of each parameter's uncertainty was evaluated to identify the most impactful parameter on the IL thermal conductivity. This was done by applying the upper and lower bounds of each parameter individually in the IL thermal conductivity calculations. The

most influential parameter was the fuel meat and the fuel particles thermal conductivity as they possess a larger uncertainty and controls the heat dissipation from the fuel to the outer surface, which significantly influences the calculations of the interaction layer thermal conductivity. This study helps to identify the major parameters that can control the interaction layer thermal conductivity value that affects the overall fuel performance. This contributes to the safety analysis and the licensing process of this type of fuel to be utilized in future research reactors that will use low-enriched uranium.

6. Acknowledgments

This study is supported by the National Research Foundation, Korea (NRF-2018M2A8A1023313).

7. References

[1] M. K. Mayer, G. L. Hofman, S. L. Hayes, C. R. Clarck, T. C. Wiencek, J. L Snelgrove, R. V Strain, K. H. Kim, “Low temperature irradiation behavior of uranium-molybdenum alloy dispersion fuel”, *Journal of Nuclear Materials*, Vol. 304, 2002, P. 221.
[2] D.E. Burkes et al., "A model to predict thermal conductivity of irradiated U-Mo dispersion fuel", *Journal of Nuclear Materials* 473 (2016) 309-319
[3] Y.S. Kim, B. J. Cho, D. S. Sohn, J. M. Park, "Thermal conductivity modeling of U-Mo/Al dispersion fuel", *Journal of Nuclear Materials* 466 (2015) 576-582
[4] D.E. Burkes A. M. Casella, A. J. Casella, E. C. Buck, K. N. Pool, P. J. MacFarlan, M. K. Edwards, F. N. Smith, "Thermal properties of U–Mo alloys irradiated to moderate burnup and power", *Journal of Nuclear Materials*, 464 (2015) 331–341
[5] D. D. Keiser, J.-F. Jue, B. Yao, E. Perez, Y. Sohn, C. R. Clark, “Microstructural characterization of U-7Mo/Al-2Si dispersion fuel plates fabricated at 500^{o}C”, *Journal of Nuclear Materials*, Vol. 412, 2011, P. 90.
[6] Y. S. Kim, G. Y. Jeong, J. M. Park, A. B. Robinson, “Fission induced swelling of U-Mo/Al dispersion fuel”, *Journal of Nuclear Materials*, Vol. 465, P. 142, 2015.
[7] Q. M. Mistarihi, J. T. Hwang, H. J. Ryu, “The modelling and simulation of the thermal conductivity of irradiated U-Mo dispersion fuel: Estimation of the thermal conductivity of the interaction layer”, *Journal of Nuclear Materials*, 510 (2018) 199-209
[8] INL/EXT-11-22045, “AFIP-1 Irradiation Summary Report”, May 2011
[9] W. S. Rasband, ImageJ, U.S. national institute of health, Bethesda, Maryland, USA, (http://imagej.nih.gov/ij/).
[10] F. B. Sweidan, Y.-W. Tahk, J.-S. Yim, H. J. Ryu, “Uncertainty and sensitivity analyses for fuel temperature evaluations of U-Mo/Al plate-type dispersion fuel”, *Annals of Nuclear Energy 120* (2018) 581–592
[11] COMSOL MULTIPHYSICS, Version 5.1, COMSOL AB, Stockholm, Sweden, 2015 (http://www.comsol.com).
[12] T.K. Huber, H. Breitkreutz, D.E. Burkes, A.J. Casella, A.M. Casella, S. Elgeti, C. Reiter, A.B. Robinson, F.N. Smith, D.M. Wachs, W. Petry, “Thermal conductivity of fresh and irradiated U-Mo fuels”, *Journal of Nuclear Materials*, 503, (2018) pp.304-313.

SAFARI-1 RESEARCH REACTOR AGEING MANAGEMENT APPLICATION AND IMPLEMENTATION UPDATE

SM MALAKA, JF DU BRUYN
South African Nuclear Energy Corporation (Necsa) – SAFARI-1
P.O. Box 582, Pretoria 0001, South Africa

ABSTRACT

The objective of the paper is to provide the SAFARI-1 Research Reactor ageing management application process or methodology and implementation update. SAFARI-1 embarked on the Ageing Management, modernisation and refurbishment process around 2001 when it started the process of fuel conversion from HEU to LEU which was successfully completed in 2009. The major objective of the SAFARI-1 ageing management programme is to extend reactor life to beyond 2030.

The operation of SAFARI-1 Research Reactor covered in this paper explains the reactor operating schedule, aspects related the reactor system start up and reactor operational performance and monitoring as well as reactor in-service inspections (ISI) programme. The paper concluded by providing an update on the projects implemented for ageing management, the bulk of the projects is related to the instrumentation and control upgrades.

The paper at the end also indicated the assessment conducted to determine the remaining life of the SAFARI-1 Research Reactor, these will involve the reactor vessel and the concrete biological shield structures.

1. Introduction

SAFARI-1 is a 20 MW de-mineralised light water-cooled, beryllium reflected, tank-in-pool type research reactor situated at Pelindaba West. The reactor is owned and operated by Necsa. It is has been safely in operated since 1965.

1.1 Reactor Operations at SAFARI-1

Reactor Operating Schedule

The SAFARI-1 reactor is operated twenty-four hours a day, seven days a week. The reactor schedule or programme consist of eleven (11) cycles of 28/35 days long of operation and in each cycle there is 5 days of shutdown to cater for maintenance activities. In an annum there will always be one long shutdown programme .

Reactor System Start-up

Normal Start-up: Where the core has been critical previously, the excess reactivity of the core is known, the critical position of the control rods can be predicted from previous runs, the flux distribution in the core has been measured, and the reactor power will be raised to the desired level and maintained at that level. After mid-cycle core loading or after loading a recovery core, when poisoned out, the start-up is considered normal without flux distribution measurements.

Duty Supervisor has an overall control of the start-up procedures. He alone is responsible for the completion of the Master Start-up Checklist. Should another supervisor take the start-up over for any reason, an entry shall be made in the Reactor Log Book to this effect.

Conditions of the core at start-up, and the type of run which follows the start-up, determine the type of start-up procedure and therefore the selection of the correct check list to be used adhering to and satisfying the OTS conditions as prescribed.

Reactor Operational Performance and Monitoring

Performance Indicator FY	*1st QTR*	*2nd QTR*	*3rd QTR*	*4th QTR*	*2017/2018 FY TD*	*Estimated FY End*
Actual Operational Days	*80.4*	*66.84*	*41.14*	*46.8*	*188.38*	*305.54*
Targeted Operational Days	*75.72*	*66.32*	*72.53*	*72.43*	*287.00*	*287.00*
Days Available but not Utilised	*0*	*0*	*36.62*	*27.26*	*63.88*	*0*
Total Days Available (Excluding Gains during Shutdowns)	*80.92*	*66.84*	*77.87*	*74.05*	*299.68*	*287.00*
Reactor Availability Against Schedule%	*99.36*	*94.32*	*99.85*	*98.25*	*98.04*	*100.00*
Reactor Availability Against Target %	*106.18*	*100.79*	*107.21*	*102.24*	*104.2*	*105.00*
Reactor Utilisation Against Target %	*106.18*	*100.79*	*56.72*	*64.61*	*81.94*	*95.00*
Average Power Level (MW)	*20.07*	*19.60*	*19.36*	*19.91*	*19.78*	*19.50*

Table 1: SAFARI-1 KEY Performance Indicator for 2017/18

1.2 Reactor Maintenance at SAFARI-1

The IAEA-TECDOC-1263 explains that Maintenance is usually divided into two categories: preventive (also referred to as routine or scheduled) and corrective (or remedial). Preventive maintenance consists of regularly scheduled inspections, tests, servicing, and overhaul and replacement activities. Its purpose is to assure the continuing capability of the reactor structures, systems and components to perform their intended functions and to detect incipient failures.

It further elaborate that Corrective maintenance (or remedial maintenance) consists of repair and replacement activities not occurring on a regular schedule. The preventive maintenance programme will reduce the need for corrective maintenance and may result in extended availability and cost reductions. However, the total elimination of need for corrective actions cannot be achieved. Adequate resources, such as manpower, spares and budget should be allocated for corrective maintenance.

In SAFARI-1 the maintenance covers the planning, scheduling and execution of those inspection, tests and maintenance activities necessary to ensure that nuclear safety related and critical systems and equipment are maintained in order to operate within their design parameters. The maintenance process relates to the following activities:

- Routine maintenance.
- Periodic inspections.
- Ad-hoc maintenance.
- Functional inspection.

- Performance and functional tests.
- Training of maintenance personnel.
- Control of equipment and spares.

The maintenance shall plan all routine and special maintenance resulting from inspections of equipment and systems. In planning maintenance activities, due cognizance shall be taken of the manufacturing plants or reactor operational program as well as the nuclear safety aspects pertaining to the maintenance work. A Maintenance Shutdown Plan shall be issued detailing all maintenance schedules and ad-hoc inspections or testing to be performed during a shutdown. Maintenance work within SAFARI-1 shall, where possible, be scheduled to coincide with the SAFARI-1 shutdown program as applicable.

Maintenance work permits shall be issued by the shift supervisor and Radiological protection work permits shall be issued (as applicable) by the RPO before the related maintenance activity could commence. A post-shutdown meeting shall be held to determine the effectiveness of all maintenance and inspection activities performed.

The frequency of inspection, testing and maintenance of individual nuclear safety related equipment shall be such as to ensure reliability, taking into account the following:

- Their relative importance to safety based on design intent and experience.
- The requirements of the OTS / OLCs.
- The chance of failure to function based on experience (i.e. History of the equipment or facility).

A functional test will be done on items, equipment and systems before they are used or after they have been switched off and not been in operation. Functional tests will be used to demonstrate satisfactory performance following maintenance, modification, replacement or significant procedural changes. Functional tests should be prescribed in instructions, maintenance programmes or user manuals.

Training shall be provided or arranged for all maintenance and inspection personnel commensurate with the scope, complexity, or special nature of their activities. Normally this training shall be based on available technical documents, manuals, other training courses, on-the-job training (with emphasis on first-hand experience). Personnel who routinely conduct specific maintenance activities, inspections or tests (for example equipment adjustments, calibration checks, operation of equipment, calculations, recording and reporting of results), have to be a qualified technician or artisan.

From time to time temporary modifications may be necessary to enable particular experiments to be carried out. Any such modifications shall be approved by the Reactor Safety Committee (RSC) before implementation and shall be valid only for the duration specified by the RSC

1.3 Reactor In-service Inspections (ISI)

The SAFARI-1 in-service inspection plan (ISP) provides the necessary information with respect to inspection and tests of all relevant equipment or systems of the plant. Such equipment or systems may typically include:

- vessels (reactor vessel and components);
- containments (control areas);
- pipe systems; pumps, valves, heat exchangers, etc;

- pool liners, structures and penetrations;
- glove boxes;
- fume cupboards; vacuum induction furnaces;
- ventilation equipment, such as filter banks;
- storage tanks including their respective supports;
- specialized and critical equipment as

In SAFARI-1 an ISI Item is a component and/or an assembly of components of the highest priority that will be inspected for the safe operation of the reactor. These include items of, and items connected to, the reactor vessel and the reactor pool liners. Inspection results of these items should be reported to NNR on a yearly basis.

The ISP shall list the following information, Identification of the equipment/system, In-service inspection frequency, Maintenance Schedule (where applicable), Method of inspection or testing, Data to be recorded for evaluation purposes (eg. vibration, temperature, neutron fluency etc.); as well as Inspection and test reports to be issued

Periodic examination, such as NDE, visual inspection of components and supports, hydraulic tests, leak tests, measurements, functional tests on pumps and valves, etc., shall be performed in accordance with an approved instruction.

The regulator can request and shall have access to perform the verification that the required examinations, hydraulic tests, pressure tests, visual examinations, etc., have been conducted and the results recorded, as well as Verification that the in-service tests required on pumps, valves, components and supports have been completed and the results recorded, the NDE methods used, follow the techniques specified in the approved procedures and are carried out and interpreted by appropriately qualified and certificated personnel

2. Ageing Management Programme in SAFARI-1

In implementing Ageing Management in SAFARI-1, three documents were developed using the IAEA guideline SSG-10, Ageing Management Philosophy/ strategy, Ageing Management Plan and the list document to record annually projects progress and status on modification/upgrades and refurbishment.

The SAFARI-1 Ageing Management programme is integrated with other key facility programmes and management systems to ensure continuous safe operation of the reactor. These programmes and management system are:

- ***MAINTENACE*** *PROGRAMME &* ***ISI*** *PROGRAMME*
- *MANAGEMENT OF* ***CRITICAL SPARES***
- ***SAFETY CLASSIFICATION OF SSC'S*** *PROCESS*
- ***SAFAETY REASSESSMENTS F-D***
- ***REACTOR SAFETY COMMITTEE***
- ***INSARR*** *RECOMMENDATIONS*
- ***SSC FUNCTIONAL ASSESSMENT (PLANT*** *HEALTH STATUS)*
- ***PERIODIC SAFETY REVIEW)***

2.1. Ageing Management Plan

The currently projected end of life of the facility at the present rate of operation is provisionally set to at least the end of 2030. The design basis for the facility contains no information relating to the design life of the facility, but a preliminary assessment of, for example, the effect of neutron fluence on the fixed core structure, based on current operation, confirms that the soundness of this structure is predictable up to that date. The result of a remedial action addressing this situation may change the prediction significantly (i.e. add a decade or so to the projection), but for the purpose of this paper, the above date remains a convenient threshold separating “current lifetime” from “lifetime extension”.

SAFARI-1 diagnosis of the above state is as follows, Operation of the reactor beyond the currently projected end of life (see previous paragraph) may follow one of two paths:

- Extension of the lifetime of the facility by a few years up to a decade or so, or
- Complete rejuvenation of the facility to operate for another 40-60 years beyond 2030

As a result an Ageing Management Plan was developed, the plan included the methodology for identifying, assessing, prioritising and addressing ageing issues.

2.2. AM Methodology & Assessment

The basic causes of ageing degradation of a Systems Structures and Components (SSC) are the service conditions which support the activation of particular ageing mechanisms leading, unless properly managed, to loss (or partial loss) of the SSC functionality. These service conditions can be categorized as normal operation, anticipated operational occurrences and environmental conditions.

A further ageing “mechanism” identified in many SSCs at SAFARI-1 is technological obsolescence, where either whole technologies (e.g. vacuum tubes vs. solid state electronics) have become obsolete, or where suppliers/vendors of equipment have discontinued certain products (e.g. the primary pumps, Siemens “S5” PLCs) to the point that even their support is discontinued and spares are not available.

Ageing Management Assessment specific to the SAFARI-1 facility. This matrix is based on IAEA guidelines **Error! Reference source not found.** & 6 which were adjusted to fit the type of reactor and its components.

An ageing evaluation task group, headed by the Project Management Office Manager shall be established to identify and evaluate SSCs affected by ageing, and recommend for implementing the resulting projects related to ageing management.

All SSCs relevant to safety and sustainability were identified and divided into the following categories:

- Reactor block, fuel and internals
- Cooling systems
- Confinement / Containment
- Instrumentation and controls
- Power Supply
- Auxiliaries
- Experimental Facilities
- Documentation and Configuration Management
- Other (non-SSC)

The SSCs were evaluated against the ageing mechanisms described in Table 2.

Mechanism		Description
A	Radiation - Change of Properties	Neutron and other radiation damage. Generally well-known and predictable phenomena, for which studies and data are fairly widely available.
B	Temperature - Change of Properties	Affects many synthetic materials, electronic circuits and sensors, cables and wiring, electric motors, transformers etc., and concrete subjected to heat deposition. Also consider effects of historical fire events in the facility (also see J).
C	Creep due to Stress/Pressure	Typical examples are core components subject to the effects of A, e.g. Be reflector, Graphite components, even fuel elements that are loaded or stored for very long periods in some reactors.
D	Mech Displacement/Fatigue/Wear from Vibration, Cyclic Loads	Routine loosening and fastening of bolts, periodic repair of breakages (e.g. re-tapping of threads, re-welding etc.), changes due to operating modes, general wear and tear.
E	Material Deposition (e.g. Crud)	Particularly in inaccessible places such as regions below the reactor core, the decay tank, beam port front (core-side) chambers, experiment penetrations and cavities in the pool structure (e.g. in the space below pool gates).
F	Flow Induced Erosion	Shouldn't affect the normal flow paths of most RRs, but look e.g. for erosion of flow measuring orifices (dulling of edges) that can affect accuracy. Erosion of concrete can occur in the biological shield and other concrete structures due to pool leaks.
G	Corrosion	This is by far the biggest contributor to the record of ageing in RRs, and is not limited to old facilities. Look particularly for corrosion on the concrete side of embedded pipes, components, re-enforcing, etc. - - especially if the pool has been leaking. Note that stainless steel is not immune to corrosion! There are many instances of (e.g.) incorrect welding procedures that have promoted rapid corrosion of SS components. Look also at electronic and instrumentation components, where corrosion can lead to imperfect connections.
H	Damage due to Power Excursions, Operational Events	A single abnormal event or accident may cause permanent damage. Look also for historical handling errors and accidents causing mechanical damage. Ever dropped something heavy into the pool? Or into the reactor core? Or onto a concrete floor?
I	Flooding - Deposition; Chemical Contamination	Both internal and external flooding. The latter can cause erosion around foundations etc. (see also F). Chemical contamination can occur in demineraliser plant, pool liners (e.g. Hg/Al reactions) and may lead to corrosion (see also G)
J	Fire - effects of heat, Smoke, Reactive Gases	Both internal and external fires (induction of smoke and gases by the ventilation systems).
K	Obsolescence; Technology Change	This affects practically all aspects, especially of old facilities (design, mechanical, electrical, instrumentation, documentation, staff etc.). However, even new facilities have reported rapid obsolescence and loss of support from vendors due to discontinuation of products etc. Also look at as-built status of drawings.
L	Changes in Requirements or Acceptable Standards	This is typically applicable to regulatory requirements. Codes and standards (including IAEA Safety Series docs for RRs) also evolve with time and facilities' documentation and safety cases gradually become outdated. Furthermore, the operational focus of many RRs today is far removed from their original design intent.
M	Other (Time Dependent Phenomenon)	Typical aspects considered under this mechanism are incorrect or defective control over design or over installation - both during the original construction and during modifications or upgrades.

Table 2: Clarification of Ageing Mechanisms

Ageing Management (AM) evaluation workshops were held during which the AM assessment was developed. Remedial actions to deal with AM aspects were drawn up and these were objectively prioritised into projects. The remedial actions identified, were divided into four groups namely; Safety Critical; Mission Critical; Lifetime Extension and Organisational.

During the prioritisation workshop the classification were amended into six groups, meaning those projects addressing additional ageing-related issues as well as Refurbishment and or Maintenance.

Now all the SAFARI-1 projects are classified into 6 distinct categories namely:-

- **Compliance:** Projects / actions originating from process, regulatory; safety compliance issues identified requiring attention of the facility.
- **Infrastructure:** Safety, Health, Environment and Quality issues requiring attention to maintain and improve the safety management and culture of the facility.
- **Safety Critical:** Remedial actions without which the reactor will probably not be able to safely operate until the currently projected end of life (Not considering the purpose of operating the reactor).
- **Mission Critical:** Remedial actions without which the reactor will be safely operated until end of life but reliability and or availability may be compromised.
- **Lifetime Extension:** Remedial actions required for lifetime extension of the facility.
- **Maintenance:** Projects /actions assisting in improving the general safety and maintenance of the facility.

A quizzed mathematical model was developed to aid in the objective prioritisation of remedial actions and was applied throughout. The methodology followed is to allocate a score to each remedial action for each impact factor on a scale of 1 to 10. The impact factor is then multiplied by an urgency factor on a scale of 1 to 10. The priority is the product of these two factors with a range between 0 (lowest priority) to 100 (highest priority), see Table 3.

The identified project were documented in [7], shown in sample SAFARI-1 project list Table 3. The SAFARI-1 Project Management Office (PO) was established to facilitate the delivery of projects under the auspices of the Ageing Management Programme (AMP).

No	RA No	Remedial Action or Project Description	Priority	Status	Classification
1	1c1	Grid Plate Manufacture, including inserts	100	In Progress	Mission
2	3d	Implement Standard Charcoal Ventilation Filter Efficiency Measurement Capability	100	In Progress	Safety
3	4g2	Stack PLC	70	In Progress	Compliance
4	4l	Rehabilitate N-16 channels	70	Delayed	Maintenance
5	1e	Assess Reactor Vessel Lifetime (may lead to recommendation to replace the RV)	40	In Progress	Lifetime
6	2g2	Manufacture and Install New Heat exchanger	70	On Hold	Lifetime
6	4e	Refurbish Control Room	60	On Hold	Infrastructure
7	4b2	Replace Automatic Flux Controller	100	In Progress	Mission
8	4b4	Replace Rod Drop Monitor	100	In Progress	Mission
9	4b1	Refurbish Neutron Control Channel (WR/MRL)	100	In Progress	Mission

Table 3. A sample List of SAFARI-1 Projects

3. Regulatory review and requirements

For any plant modifications that SAFARI-1 plan to implement or commission, must meet the following Nuclear Regulatory requirements:-

- The proposed modification must comply with regulatory approved processes and procedures relating to control of such modification to the design of existing plant, facility or system design, including modifications that may be of temporary nature.
- These approved process must provide for the classifications of modifications according to their safety significance
- These modifications must be divided into stages or phases where explicit regulatory approval is pronounced to indicate where it is specified not to commence activities nor proceed from one phase to the next of the modification prior to the regulator granting the necessary approval.
- The process must include a requirement for the provision of an adequate documentation to justify the safety of the proposed modification.
- The facility is expected to implement processes for the periodic and systematic review and reassessment of safety cases.
- As far as the Nuclear Installation stipulates, the licensee must if so directed by the National Nuclear Regulator carry out a review and reassessments of safety and submit a report of the said review and reassessment to the regulator at such intervals, within such period and for such matters or operations as may be specified in the directive.

4. Ageing Management Implementation update

5.1. Instrumentation and maintenance upgrades

The SAFARI-1 Research Reactor Instrumentation and Control system as depicted in Figure 1 comprises, amongst others, the following major instrumentation subsystems**:**

- Reactor Protection System (RPS)
    - Nuclear Safety Instrumentation
        - Neutron Safety Channels for measuring neutron flux
        - Gamma Safety Channels for monitoring gamma flux
- Process Safety Instrumentation
- Rod Control System
- Reactor Automatic Flux Controller
- Process Instrumentation and Controls
- Radiation Protection Monitoring

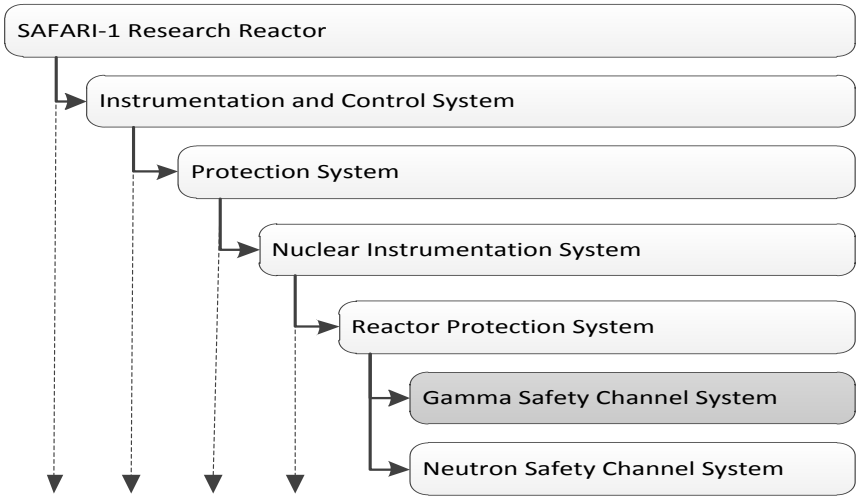

Figure 1: Relevant Section of the SAFARI-1 System Breakdown Structure

Most of the instrumentation projects undertaken to date under the auspices of the ageing management projects are in the installation and commissioning phase. The instrumentation and maintenance projects were largely mission critical i.e. the reactor will be safely operated until end of life but reliability and or availability may be compromised if not addressed.

5.2. Reactor Vessel Assessment

SAFARI-1 reactor vessel and support structures are made from aluminium alloy of 5052-O ASTM designation. This aluminium alloy is a non-heat treatable wrought Al-Mg alloy for sheets/plates with very good formability and weldability and excellent corrosion resistant properties. The "-O" indicates that after they have been manufactured aluminium plates were fully annealed. [9].

The reactor vessel was designed in accordance with the Unfired Pressure Vessel ASME VIII for an internal pressure of 248 kPa(g) and a temperature of 65,5 ºC. It is made of welded 5052 graded aluminium cylindrical shell of 1.66 m internal diameter and average 4.52 m height between flanges. The circulation of cooling water is driven by a pressure drop between the inlet and outlet reactor vessel pipes. The pipes and flanges are made of graded 6061-T6 aluminium [9] see Figure 2.

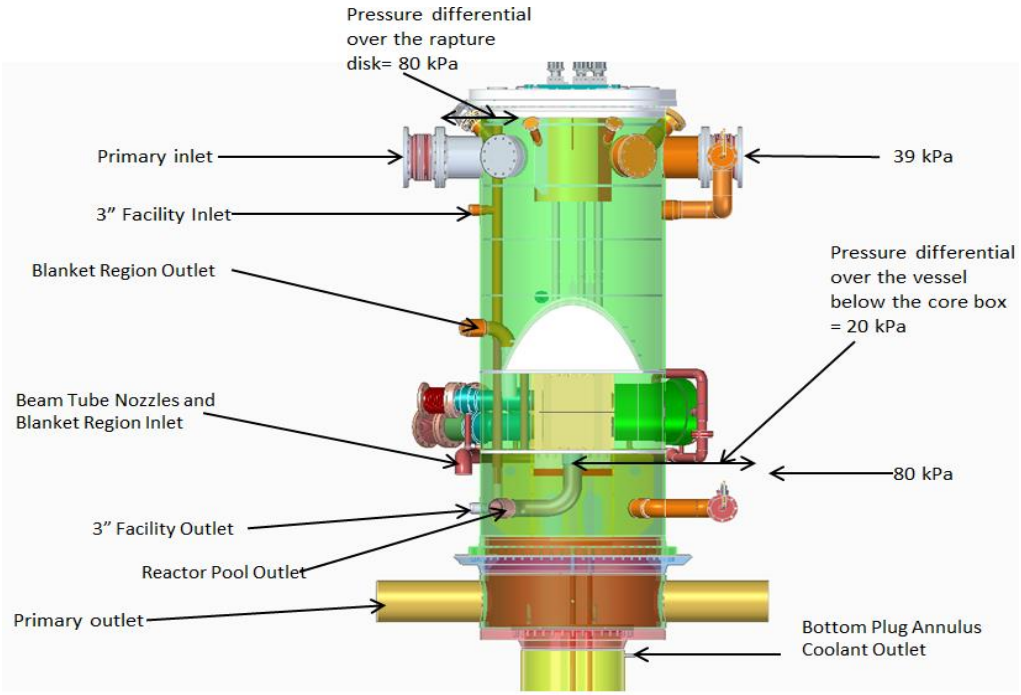

Figure 2: Reactor Vessel showing the inlet and outlet together with the pressures

SAFARI-1 reactor vessel has been bombarded with thermal neutrons for approximately more than 45 years which may negatively impact on each item's design life. In addition, during its operation over the years there were multiple minor impacts that may have impacted the reactor vessel in some ways. Changes in the material properties of the reactor vessel are expected. These changes are generally characterised by the reactor vessel material losing its plasticity and becomes brittle leading to susceptible crack propagation.

Due to the absence of surveillance program that allows monitoring ageing of components, an analytic investigation through design verifications was required to determine the mechanical integrity of SAFARI-1 reactor vessel.

The mechanical integrity of SAFARI-1 reactor vessel was investigated through structural analysis based on ASME III code requirements for the purpose of determining the fitness-for-purpose period of the reactor. A computational fluid dynamics analysis was carried out to determine the pressure and temperature distribution in the reactor structure under operating conditions. The results of this investigation showed that the highest stress area was found to be at the bottom weld. A fatigue life of approximately 300 000 cycles was calculated based on 1% probability of crack initiation, based on these calculations a conclusion was drawn that the stress intensity stays below the irradiated fracture toughness of the material and the shell will therefore not fracture (leak before break). The study recommends ultrasonic inspections of this area every ten (10) years to detect and monitor any cracks that can initiate. [9]

5.3. Biological Shield

SAFARI-1 concrete Biological Shield structure main purpose is to provide radiation shielding for the reactor vessel, for active equipment in the pools, and for active piping embedded in the concrete structure itself. As part of the Ageing Management Programme an investigation of the Biological shield was proposed, it is aimed at assessing the structural soundness of the reinforced concrete members associated with the Concrete Biological Shield, see Figure 3.

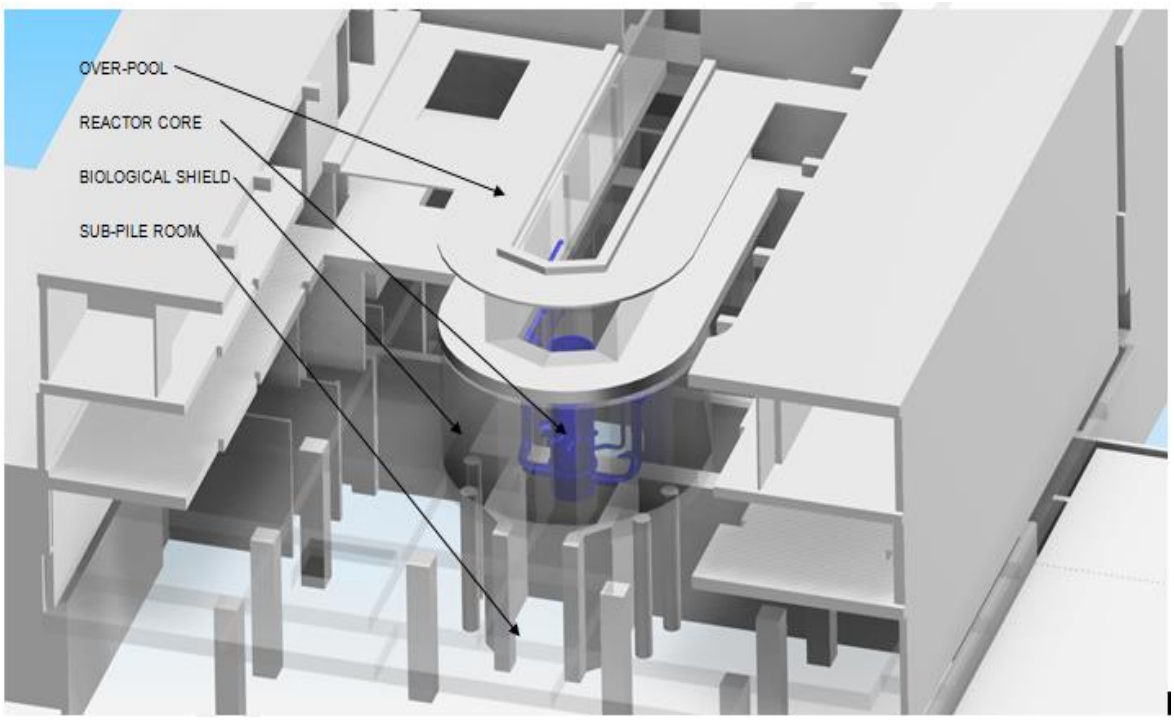

Figure 3 3D solid edge figure showing the over-pool and biological shield

A structural analysis was done to determine if there were any high stress concentrations in the structure which might cause propagation of cracks or compromise the structural integrity of the shield in any way. From the detailed stress calculations, it was found that the stresses in the biological shield and its supports were within limits. No high stress concentrations were found at the openings or cavities in the shield.

5. Conclusion

The currently projected end of life of the facility at the present rate of operation is provisionally set to at least the end of 2030. The design basis for the facility contains no information relating to the design life of the facility and as such an Ageing Management Programme (AMP) was a necessary tool to ensure safe and soundness of structures and components. The SAFARI-1 AMP is based on SSG10. The programme developed a methodology and an assessment to assist SAFARI-1 in identifying ageing mechanisms and provide remedial actions to counter the anticipated age related effects.

The major critical tasks undertaken in the SAFARI-1 AMP includes the upgrade Instrumentation and control equipment's to ensure safe and reliable operation of the reactor. The investigation of the Reactor Vessel and Biological shield was to determine the mechanical integrity of SAFARI-1 reactor vessel and structural soundness of the reinforced concrete members associated with the Concrete Biological Shield respectively.

The outcomes of the above investigations have shown that the reactor vessel stress intensity stays below the irradiated fracture toughness of the material and the shell will therefore not fracture (leak before break) and found that the stresses in the biological shield and its supports were within limits.

The ISI was performed on the SAFARI-1 reactor under the AMP, whereby the purpose was to determine wall thickness, the measurements were conducted in parts of the reactor vessel assembly and pool liners to determine material loss due to corrosion and/or other operating constrains. The conclusion from this investigation was that no reportable wall thickness have been measured during the inspection.

6. References

1. **SSG-10**: Safety Guide Ageing Management of Research Reactors", IAEA, 2010.
2. **SAR**: SAFARI-1 Safety Analysis Report
3. **RR-PLN-0052** Ageing Management plan for the SAFARI-1 Research Reactor
4. **SHEQ-INS-0890 :** Safety Classification of Structures, Systems and Components
5. **RR-PLN-0083:** Master Management Plan for Ageing Management At SAFARI-1 Research Reactor
6. **IAEA-TECDOC-1263**: Application of non-destructive testing and in-service inspection to research reactor
7. **RR-LYS-1008**: LIST OF SAFARI-1 Projects
8. **TECDOC-792:** "Management of Research Reactor Ageing", IAEA, Vienna, 1995.
9. **RR-SPE-0040** : User requirements specification for the assessment of the SAFARI-1 Reactor Vessel
10. Reference omitted

SPECIFIC SAFETY CONSIDERATIONS FOR MANAGEMENT OF RADIOACTIVE WASTE FROM DECOMMISSIONING OF RESEARCH REACTORS

M. ABDEL GELEEL

Safety of Nuclear Fuel Cycle, Nuclear and Radiological Regulatory Authority
3 Ahmed El Zomr st., Nasr city, 11762, Cairo, Egypt

ABSTRACT:

Today there aren't any decommissioning project in Egypt for research reactors in the near future, so the regulatory action is focused to the control of reports and other documents which will be necessary and applicable in due time. One of the important point that should be taken in our consideration during decommissioning of the research reactor is the radioactive waste that produced from this process.
There are different types of radioactive waste produced from decommissioning of research reactors. Owing to specific characteristics, some of these radioactive waste could be considered as being problematic, for example waste for which application of routine methods of handling, treatment and conditioning is not appropriate and therefore requires special considerations for the selection of specific radioactive waste management options. Radioactive wastes and material that produces from decommissioning process requires proper planning and selection of appropriate waste management and material management options.
In this work we will focus into six main challenges points should takes place in our considerations to implement article 26 (Decommissioning) of Joint Convention on the Safety of Spent Fuel and Radioactive Waste Management. These points are waste facilities, limited information, soil contamination, needs for trained professionals, security and cost.

1. Introduction

There are a large number and a broad range of facilities around the world, including NPPs, RRs, nuclear fuel cycle facilities, research and industrial facilities that are undergoing decommissioning or where decommissioning is planned in the near future. In particular, there will be an increasing number of NPPs and RRs closing down in the next few decades. The decommissioning of all these facilities requires adequate planning, evaluation and demonstration that decommissioning activities can be conducted safely. Radioactive waste is generated in the production of electricity in NPPs and in the use of RRs. The radioactive waste arising from NPPs and from research reactors is diverse and varied in nature and it encompasses a broad range of radionuclides, half-lives, activity concentrations, volumes, and physical and chemical properties. Typical radioactive waste from nuclear power plants and research reactors includes, but is not limited to :spent ion exchange resins, filters, activated metals, liquid and gaseous effluents, irradiated experimental components, spent nuclear fuel declared as waste and waste from decommissioning. Because of the diversity and variation in the radioactive waste streams from such facilities, particular consideration over extended periods of time has to be given to all steps of the management of the waste. Huge amount of radioactive waste are produced from decommissioning process. These types of waste should be management in a safe manner.

2. Radioactive waste produced from decommissioning and dismantling of research reactors

Although less than half of the non-operational reactors have been decommissioned so far, there is a significant experience in this field. Several of the earlier decommissioning projects in the US are summarized in reference [1] and in Russia in reference [2]. Research and development activities were performed in several projects, e.g., in the decommissioning of the CP-5 reactor [3] in the US and in the decommissioning of the BR3 [4] and JEN-1 [5] reactors in Europe. The IAEA

collected much data and operator experience, including research and development efforts, on the decommissioning of research reactors [6, 7, 8, 9, 10].
Decommissioning strategies range from immediate dismantling and removal of all radioactive materials and radioactive waste from the site, allowing unrestricted release, to an option of in situ disposal involving encapsulation of the reactor and subsequent restriction of access [11].

Immediate dismantling involves the decontamination, dismantling and removal of all equipment, structures and other parts of the facility that are contaminated, typically within three years after permanent shutdown. This option normally has the fewest uncertainties, eliminates the risk associated with the facility in a small time scale, costs less than deferred dismantling, and allows the use of operational staff who knows the history of the facility. However it may lead to higher doses to the worker, due to the relatively short decay time of the radioactive isotopes present. An obstacle to this option may be the absence of a waste disposal route, namely in the case of the spent fuel.

The deferred dismantling decommissioning strategy requires that the facility is placed and maintained in a safe, stable, and monitored condition for an extended period of time (some decades) until it is decontaminated or dismantled. A certain number of activities still need to be done immediately after shutdown the facility. This strategy minimizes the initial commitments of time, funds, radiation exposure, waste disposal capacity, and may reduce the quantities of radioactive waste produced. It is limited to facilities where the appropriate decay of the nuclides in the nuclide vector is shorter than the expected life structure. However, there are additional costs associated with providing long term surveillance and maintenance, and the operator has to ensure that sufficient expertise and knowledge will be available at the time of decommissioning. Funding and legislative uncertainties may also be higher. This option puts an undue burden on future generations, which may be socially and economically unacceptable.

The entombment is a decommissioning strategy similar to immediate dismantling, except that not all of the radioactive material is removed from the site and the radioactive contaminants are encased in a structurally long-lived material, such as concrete. The entombment structure must be appropriately maintained and surveyed until the radioactivity decays to a level permitting an unrestricted release of the facility. In principle, entombed facilities become a near surface waste repository and must comply with safety and radiological requirements for waste disposal facilities. This may be an option for countries with a very limited number of facilities, e.g., just one research reactor, and not having the resources to develop or obtain the infrastructure needed for dismantling and waste disposal [11].

The Nuclear Regulatory Commission (NRC) evaluated these strategies in the early eighties [12]. Table 1 presents the total costs of the different strategies together with the collective dose from the decommissioning operations for two reference reactors. The first reference reactor is the 1 MW Oregon State University TRIGA Reactor (OSTR), at Corvallis, while the second is the 60 MW Plum Brook Reactor Facility (PBRF), of the National Aeronautics and Space Administration (NASA) at Sandusky. The OSTR was recently converted to LEU fuel within the RERTR program [13], while the PBRF is shutdown since 1973 and its decommissioning is expected to be complete at the end of 2011 [14].

Strategy	OSTR		PBRF	
	Cost (MUSD) a)	Collective dose (man·Sv)	Cost (MUSD) a)	Collective dose (man·Sv)
Immediate	0.85	0.18	15.6	3.22
Deferred – 10 y	1.64	0.15	17.6	1.98
Deferred – 30 y	2.24	0.13	20.0	1.18
Deferred –100 y	4.50	0.13	27.2	1.12
Entombment	0.56	0.17	14.6	4.25

Table 1. NRC estimated costs and collective doses for different decommissioning strategies for two types of research reactors [12]
a) 1981 values.

NRS studied the deferred dismantling after 10, 30 and 100 years. The collective doses in the case of deferred dismantling include the operations that need to be performed immediately as well as the operations to be performed after the waiting period. The prices are given in 1983 USD, which can be converted to 2010 values multiplying by 2.40, as determined using the Consumer Price Index (CPI) inflation calculator of the US Bureau of Labor Statistics. The most cost-effective strategy is immediate dismantling. Deferred dismantling is more costly than immediate dismantling, although a 50% reduction of the collective dose is achievable after a delay of 10-15 years in the case of a large research reactor. The reduction of the collective dose is not significant for the deferred dismantling of a less complex, lower power reactor, where the amounts and activation of materials are necessarily lower.

3. Decommissioning and dismantling policies and projects

According to the law number 7 for the year 2010 (Egyptian nuclear law) a nuclear facility must be decommissioned in a manner ensuring nuclear safety and radiological protection of the staff and the whole society. The actions that could impact the future generations should be avoided during decommissioning and dismantling of the facilities. In compliance of Egyptian nuclear law decommissioning of a nuclear facility requires a license from the Egyptian Nuclear and Radiological Regulatory Authority (ENRRA). It is granted on condition that applicant shall prove fulfilment of all requirements set forth in the Egyptian nuclear law and secondary legislation related to the decommissioning (generic), as well as will be able to fulfil the conditions, related to the particular facility to be decommissioned, included in the license. The article 38 b states, that the decommissioning plan, which is obligatory to be issued along with other documentations and assessments in the licensing procedure, shall be revised and updated at least every 5 years, and in case of the early closure of the facility (which is understood as equal to reduced exploitation period), the decommissioning plan shall be revised and updated immediately and submit to the regulatory body for approval. It has to include the assessment of the costs of decommissioning According to executive legislation of the law number 7 for the year 2010, financial responsibility for decommissioning as well as radioactive waste and spent fuel management coming from the commercial facilities are to be held by the operator. The decommissioning RW-SF disposal fund(s) are to be set for any new nuclear facility. The rules and provisions for budgetary financed nuclear facilities remain the same and are guaranteed by the financing bodies/authorities. The funds for decommissioning process and RWM/SNF management are to be saved on a separate bank account every month. For NPPs, the source of funds is a designated part from the price of every 1 MWh produced by the NPP.

4. Regulatory activities

Today there aren't any decommissioning project in Egypt for research reactors in the near future, so the regulatory action is focused to the control of reports and other documents which will be necessary and applicable in due time. In addition to requirements established in the regulatory standards previously mentioned, there is a specific one included in the Operation Licences: the Preliminary Decommissioning Plan. This mandatory document, the Preliminary Decommissioning Plan, include topics related to documents management, record-keeping and special tasks oriented to decommissioning The Operating Organization must collect and archive the following documentation during the operation stage

5. Documents

o Safety analysis report
o Technical manuals
o Technical specifications (limits and conditions)
o Complete drawings, photographs and technical descriptions of building, systems, experimental facilities and components
o Design change reports and updated drawings
o Modifications to the original design
o Quality records (such as deficiencies, corrective actions, etc.)

6. Records

o Effluents management records and locations
o Waste management records and locations
o Radiation sources management records and locations
o Records of neutron flux and distribution
o Radioisotopes management and locations
o Radioprotection records (doses rates, contamination levels, radiation and contamination survey data, etc.)
o Samples of irradiated materials and probes
o Operation and maintenance reports
o Hazardous material inventories
o Abnormal events reports (fuel failures; incidents leading to spillage or inadvertent release of radioactive material)
o Staff records

On the other hand in the Operation Licence are established that at least one year before the date of the planned decommissioning, the Decommissioning Plan must be submitted to the Regulatory Body. The content of this plan must be coherent with IAEA safety standard and safety guide (IAEA SRS N° 45 Standard format and content for safety related decommissioning documents and Safety Guide WS-G-2.1 Decommissioning of nuclear power plants and research reactors).

7. Regulating decommissioning at the global level

The Joint Convention on the Safety of Spent Fuel Management and on the Safety of Radioactive Waste Management is the first legal instrument to directly address, among other issues, the management of radioactive waste from decommissioning on a global scale (IAEA 2011 a).

8. Article 26 Decommissioning

Article 26 from the joint convention specifies that "Each Contracting Party shall take the appropriate steps to ensure the safety of decommissioning of a nuclear facility. These steps shall ensure that: (i) qualified staff and adequate financial resources are available; (ii) the provisions of Article 24 with respect to operational radiation protection, discharges and unplanned and uncontrolled releases are

applied; (iii) the provisions of Article 25 “emergency preparedness “are applied; and (iv) records of information/data important to decommissioning are kept”.

8.1. Waste facilities

A large number of sites will be required to store radioactive waste from decommissioned nuclear power plants and other nuclear reactors over the long term. It is likely that additional buildings and facilities to treat, package and store resultant radioactive wastes will need to be constructed to handle output from newly decommissioned reactors.

8.2. Limited information

The Nuclear Decommissioning Authority [15] of the UK states that: "One of the biggest difficulties we face is the limited information we have for a number of legacy facilities. For instance, some do not have detailed inventories of radioactive waste. Some lack reliable design drawings. Many were one-off projects, built as experiments to test new approaches and ideas. Therefore the challenge is often not how to tackle a particular task, but rather deciding what the task is.

8.3. Soil contamination

Based on past decommissioning experiences, it has been shown that the pattern and extent of soil contamination cannot be planned until late into the decommissioning process. The boundary between the bedrock and soil deposits and the flow pathways in the soil will affect the direction and rate in which the radioactive material will be transported. Soil testing below the buildings cannot be carried out until access has been made safe. Depending on the results of these tests, varying amounts of soil might have to be removed, which cannot be determined until the decommissioning process is well underway.

8.4. Need for trained professionals

An increased number of trained professionals will be needed [16] and techniques need to be improved to ensure safer dismantling. The dismantling of the Brennilis power station was meant to be a learning experience to acquire technological knowledge to apply to other sites in France. The release of sites for other uses may help to limit the social impacts, but other constraints still need to be considered. Negative public perception remains the most serious challenge to opening radioactive waste disposal.

8.5. *Security*

Once the spent nuclear fuel is removed from the reactors prior to decommissioning, the risks to the public and environment are relatively small. But where facilities are under decommissioning, and in particular when they are placed in "safe-store" mode or entombed, site surveillance has to be maintained to protect the contents from theft, stolen and malicious use. This is a costly factor that countries will need to take into account. Concerns exist about the risks associated with the possible use of nuclear devices created from stolen nuclear material as well as sabotage of power stations [17].

8.6. Cost

Since few nuclear power plants have been fully decommissioned, the exact costs of accomplishing this phase are unknown. Estimates vary from 9% to 200% of the construction costs [18]. Information and data are often not made available to the public owing to contractual arrangements, property rights and other reasons.

9. Conclusion

Today there aren't any decommissioning project in Egypt for research reactors in the near future, so the regulatory action is focused to the control of reports and other documents which will be necessary and applicable in due time. One of the important point that should be taken in our consideration during decommissioning of the research reactor is the radioactive waste that produced from this process.

The Joint Convention on the Safety of Spent Fuel Management and on the Safety of Radioactive Waste Management is the first legal instrument to directly address, among other issues, the management of all different types of radioactive waste from decommissioning on a global scale**.** The pattern and extent of soil contamination are difficult to be planned until late into the decommissioning process.

10. References

[1] Konzek, G.J. (1983). Technology, Safety and Costs of Decommissioning eference Nuclear Research and Test Reactors. NUREG/CR-1756 Addendum, Nuclear Regulatory Commission, Washington.

[2] Morozov, S.I. (2005). Decommissioning Russian Research Facilities. Proceedings of International Conference on Research Reactor Utilization, Safety, Decommissioning, Fuel and Waste Management, Chile, 2003, IAEA, Vienna, 573-578. ISBN 92-01139047.

[3] Noakes, M.W. (1998). CP-5 Reactor Remote Dismantlement Activities: Lessons Learned in the Integration of New Technology in an Operations Environment. ORNL/CP-97762, ORNL, Oak Ridge.

[4] European Commission (1995). *Studies in the Frame of the EC Pilot Dismantling Project* BR3 Mol. EUR-16645, EC, Brussels.

[5] European Commission (1996). *Decommissioning of the JEN-1 Experimental Reactor.* EUR-16899, EC, Brussels.

[6] International Atomic Energy Agency (1999). State-of-the-art Technology for Decontamination and Dismantling of Nuclear Facilities. *Technical Reports Series No*. 395, IAEA, Vienna.

[7] International Atomic Energy Agency (2002). *Decommissioning Techniques for Research Reactors.* TECDOC-1273, IAEA, Vienna.

[8] International Atomic Energy Agency (2006). Decommissioning of Research Reactors: Evolution, State of the Art, Open Issues. *Technical Reports Series No*. 446, IAEA, Vienna.

[9] International Atomic Energy Agency (2008). Decommissioning of Research Reactors and Other Small Facilities by Making Optimal Use of Available Resources. *Technical Reports Series No*. 463, IAEA, Vienna.

[10] International Atomic Energy Agency (2008). *Innovative and Adaptive Technologies in Decommissioning of Nuclear Facilities.* TECDOC-1602, IAEA, Vienna. ISBN 978-9201100085.

[11] Sed, L.J., Reisenweaver, D. (2005). International Decommissioning Strategies. Proceedings of International Conference on Research Reactor Utilization, Safety, *Decommissioning, Fuel and Waste Management*, Chile, 2003, IAEA-CN-100/83, IAEA, Vienna, 593-602. ISBN 92-01139047.

[12] Konzek, G.J., Ludwick, J.D., Kennedy, W.E. Jr., Smith, R.I. (1982). *Technology, Safety, and Costs of Decommissioning Reference Nuclear Research and Test Reactors.* NUREG/CR-1756. NRC, Washington.

[13] Keller, S.T., Reese, S.R. (2009). Going From HEU to LEU: Conversion of the Oregon State TRIGA Reactor. *Proceedings of 31st International Meeting on Reduced Enrichment for Research and Test Reactors,* Beijing, 2009, ANL, Argonne. <http://www.rertr.anl.gov>.

[14] National Aeronautics and Space Administration (2009). *Plum Brook Reactor Facility Decommissioning Project: 10 Years of Progress.* NASA Glenn Research Center, Cleveland. <http://www.grc.nasa.gov/>.
[15] International Atomic Energy Agency, Decommissioning of Facilities Using Radioactive Material (WS-R-5), IAEA, Vienna (2006).
[16] IAEA 2005. Selection of decommissioning strategies: Issues and factors IAEA-TECDOC-1478, International Atomic Energy Agency.
[17] Bunn M and Bunn G 2008. Reducing the threat of nuclear theft and sabotage IAEA-SM-367/4/08, International Atomic Energy Agency
[18] Lenzen M 2008. Life cycle energy and greenhouse gas emissions of nuclear energy: A review. Energy Conversion and Management, vol. 49, no. 8, pp 2178-2199.

INSNU Project - FRANCE

Fuel irradiation devices

Test of sealed passages with optical fibres

in support of the development of innovative instrumentation.

AUTHORS: S.GAILLOT (1), G.CHEYMOL (2), J.BRINSTER (1), D.PICARD (1), G.CHICHEREAU (1), N.HOUSSE (1), P.DEGOUSEE (1), C.DESTOUCHES (3)

(1) CEA, French Alternative Energies and Atomic Energy Commission, Division of Nuclear Energy, DTN/STCP, CEA Cadarache.13108 Saint Paul lez Durance. France.
(2) CEA, French Alternative Energies and Atomic Energy Commission, Division of Nuclear Energy, DPC/SEARS/LISL Bât 467 CEA Saclay. 91191 Gif / Yvette Cedex. France.
(3) CEA, French Alternative Energies and Atomic. Energy Commission, Division of Nuclear Energy, DER/SPEX/LDCI Bat 238, CEA Cadarache. 13108 Saint Paul lez Durance. France

Contact Person : Stephane.Gaillot@cea.fr

ABSTRACT

Within the scope of developing the experimental reactor means for the Jules Horowitz reactor (JHR) in France, certain R&D actions are currently focusing on technological building bricks. The action covered in this paper concerns fuel irradiation devices, in particular the fabrication and testing of leak tight feedthroughs equipped with optical fibres under thermal hydraulic conditions (155 bar and 100°C) that are representative of those in certain irradiation devices heads operating under pressurised water reactor (PWR) conditions.

The test performed with these leak tight feedthroughs lasted five days and was representative of certain experimental power ramp-up scenarios on a fuel rod (conditioning, ramp-up, high power plateau for 24 hours, and cooling). The results of this test make it possible to validate the recommended technology. It therefore seems feasible to implement innovative instrumentation equipped with optical fibres in irradiation devices operating under similar experimental conditions.

Following a general description of the project and the JHR facility currently under construction at the CEA Cadarache centre in France, this paper describes the relevant fuel irradiation devices. We have focused on the leak tight feedthroughs going through the device head, in particular those containing the optical fibres.

We discuss the tests performed, their results and several future prospects with respect to the utilisation of optical fibres as a means to support the development of innovative instrumentation.

1. Introduction

In the frame of development of the experimental fleet for the RJH reactor, some measures involve the development of technological blocks. The action described in this paper concerns fuel irradiation devices and especially the realization and testing of experimental feedthroughs equipped with fibre optics to the Thermal Hydraulic conditions of the heads of certain irradiation devices (155 bar,100°C).

2. Context Reminder

The Jules Horowitz reactor currently under construction at the CEA Cadarache centre (Bouches-du-Rhone department, France) is a material testing reactor (MTR). It will be used to perform irradiation tests on Fuel and Material samples as part of support Programmes for current nuclear (Gen II and III) and future (Gen IV and fusion) reactors. This reactor will also be used to produce radioelements (mainly Mo-99) for medical purposes and will meet 50% of the European demand in this field.

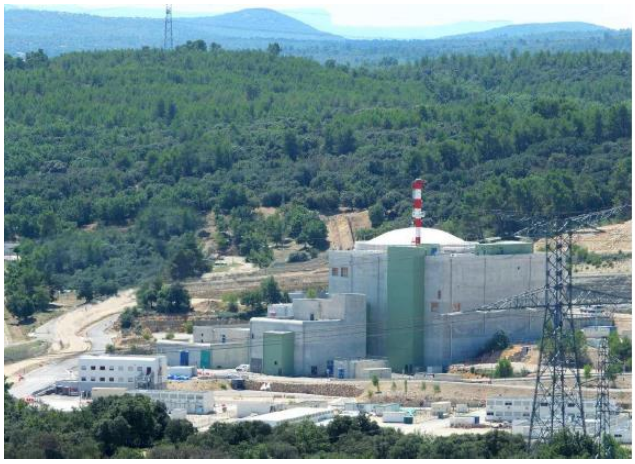

Fig.1a: JHR facility. v12-2018

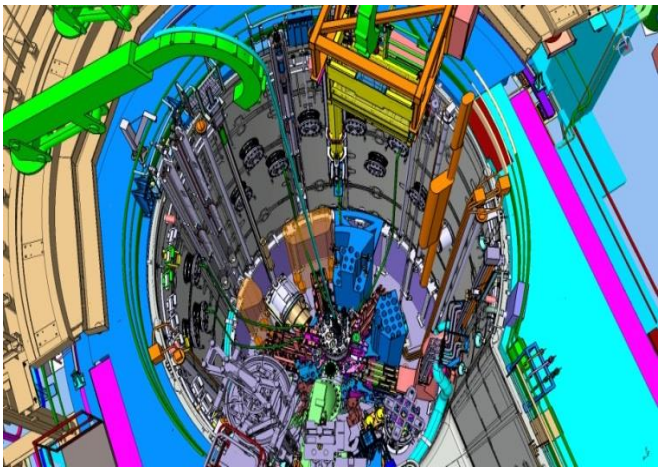

Fig.1b: JHR reactor pool overview. CAD illustration

3. Main characteristics of The Reactor

3.1 Introduction

The main characteristics of the Jules Horowitz reactor are recalled below [R1]:

- ✓ the compact core is designed to generate a nominal power up to 100 MW_{th},
- ✓ it is cylindrical in shape, with a diameter of 60 cm and a height of 60 cm,
- ✓ the reactor is immersed under 9.3 m of water (level with the mid-height plane) in a pool that is 12 m deep,
- ✓ the core is under-moderated in order to generate strong fast neutron fluxes, i.e. up to 5.10^{14} $n.cm^{2}.s^{-1}$, E > 1MeV,
- ✓ the primary system is closed and slightly pressurised (12 bar upstream of the core),
- ✓ the cooling water in the core flows upwards at a rate of about 10 m/s,
- ✓ gamma heating in the core is about 15 to 20 W/g (maximum local value),

- ✓ the beryllium reflector is 30 cm thick and surrounds the core vessel to thermalize the neutrons produced in the core.
- ✓ The thermal neutron flux in the reflector is 3.10^{14}n.cm^{-2}.s^{-1}.

Ten experimental locations will be available in the core and another ten in the reflector, including six on the displacement systems which are designed to modify the distance between the samples and the core.

After the divergence phase of the reactor, the start-up phase of the experimental equipments is planned over a one-trial period spanning 12 to 18 months. Once this stage is reached, the experimental loops will be operational and ready to meet the needs of future customers.

3.2 Experiments in the Core

In the core, various experiments are possible. The first possible configuration involves placing the irradiation device in the first crown of the core, and particularly in the center of a fuel element. This privileged position allows researchers to produce important fast neutron fluxes on the samples. These fluxes, translated into displacements per atom (dpa), are typically 15dpa/year with 100MWth reactor power. These conditions make it possible to carry out accelerated ageing campaigns on the samples. Other sites in the 2nd and 3rd crown presenting reduced fast neutron fluxes are considered. In addition, the devices can be located in the position of a fuel assembly to increase the embedded capacity of the samples.

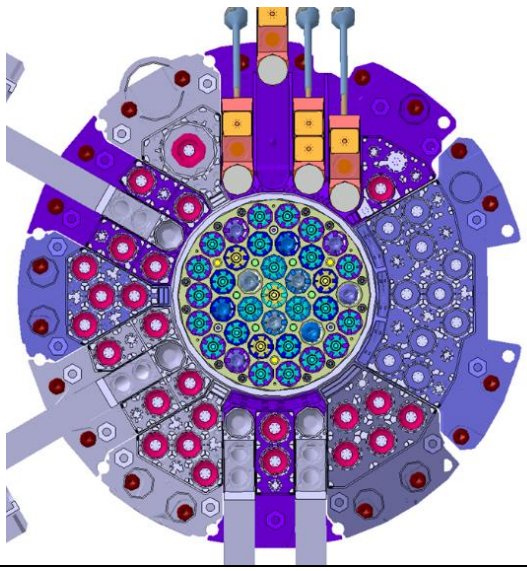

Fig.2: JHR - Cross section of the core & reflector (CEA).

3.3 Experiments in the Reflector

The Beryllium reflector has ten sites where it is possible to conduct experiments. Six sites are possible in fixed positions and four others are foreseen for mobile systems (SAD). The different positions available will enable researchers to obtain conditions of neutron fluxes compatible with the needs for fuel rod irradiation tests in LWR (PWR, BWR) or VVER conditions.

4. The JHR Irradiation Loop for Fuel Power Ramps Tests.

4.1 Main Features:

An experimental irradiation loop dedicated to rod irradiation functioning under LWR conditions in under detailed study (cf. fig.3). This loop is called ADELINE [R1,R2].

This fuel irradiation loop is composed of an in-core part located in the reactor pool and of another part located in the operation zone of the experiments (BUR, CEDE).

The in-core part includes the irradiation device equipped with a rod, the underwater lines and the fluid & electrical connections through the experimental penetrations of the pool. The other part is made up of the fluid circuit, a tight bunker and connection of the circuit with the utilities of the JHR facility. The fluid circuit is equipped with circulating pumps and pressurization systems, making it possible to obtain the circulation of water-cooling towards the device and to reach the required thermal-hydraulic conditions at the bottom of the test channel (155 bar, 270°C, 200g/s). The experimental loop under study also takes into account the feedback of this kind of loop much like the ISABELLE irradiation loop, which was used on the OSIRIS irradiation reactor located in SACLAY (France) up to 2015.

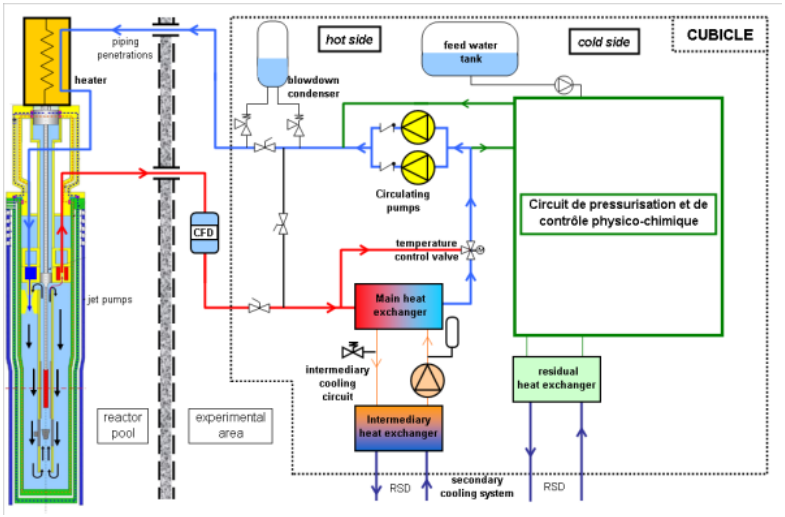

Fig.3: JHR. simplified drawing of an fuel irradiation loop (ADELINE)

4.2 Planned Performances of the Loop

The experimental rod is composed of a UO_2 type or MOx, irradiated or not.
The standard profile of power during the test is described hereafter:

- ✓ conditioning phase with low power (100W.cm^{-1}) ranging from a few hours to a few days,
- ✓ power ramp test with kinetics going up to 700W.cm^{-1}.min^{-1},
- ✓ power aimed at the high level of 620W.cm^{-1}+/-10W.cm^{-1} for one maximum duration of 24h,
- ✓ withdrawal of the device according to the power decrease scenario.

The physical parameters around the rod correspond to the following PWR conditions: 155b, 320°C with a fluid flow of 0.2kg/s and 73b, 280°C for BWR conditions.

Regarding the displacement system (SAD), it can move to or from the core tank. It allows implementing linear power variations simply and quickly on the sample and reaching representative power level and fission products inventory during conditioning phase and before a soliciting test.

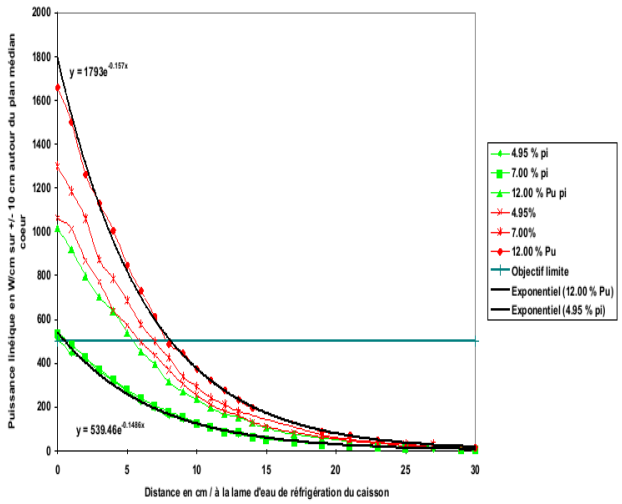

Fig.4a: Example of power evolution versus SAD displacement and fuel enrichment

(analytic calculations)

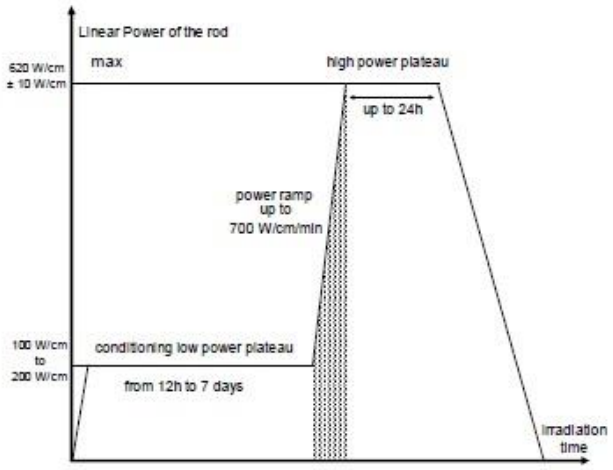

Fig.4b : Typical scenario of power ramp test

Such a concept is convenient for operation (easy to handle, even during the operating cycle of the core) and for safety, the backward position and the off normal conditions of the device are not directly coupled to the core operations.

4.3 Instrumented Experimental Rod

The experimental rod is fixed on a sample holder (PE), metallic structure, which offers an axial and radial rod position during irradiation (cf. fig.5). The head of the sample holder is used as a tight closure of the device.

For this configuration, the rod can be equipped with lengthening sensors at its ends (of LVDT type) enabling us to measure its elongation during the test. According to the objective of the test, the rod may also be more instrumented (fuel, clad temperature measurements, deformation).

This embedded instrumentation can characterize the consequences of the irradiation on the rod more precisely. Note that this instrumentation, placed on the sample holder is consumable.

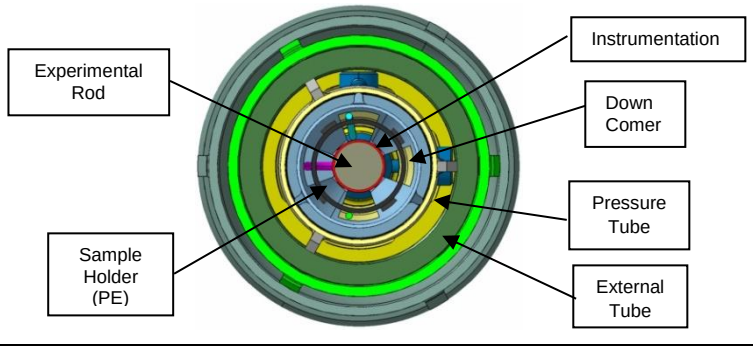

Fig.5: Cross section view of the device with the sample holder (CEA - preliminary design)

During the irradiation phase, the experimental rod can be subjected to various stresses: swelling, elongation, wear. For the purpose of following these phenomena, innovating instrumentation is now being developed. One of these R&D actions involves the use of an optical-mechanical sensor permitting the on-line deformation measurement of the rod. This low-size sensor integrates an optical module, in a pressurized and deformable tight enclosure making it possible to follow rod deformation. The range of the sensor is from 0 to 1.5 mm with a precision of 10 microns. The effective range of expected rod deformation during the test varies from about 0 to 0.5 mm [R3].

Fig.6: Optical module of the sensor inserted in a body with a piston simulating the feeler piece (CEA, R&D).

4.4 Support qualification tests

In response to the experimental requirements described above, qualification tests are required. The test described in this paper concerns the implementation of tight feedthroughs with fibre optics in a fuel irradiation device.

Optical fibres are composed of silica, diameter 125 microns and are inserted in tightness feedthroughs.

The tested FO flange is equipped with two welded tightness feedthroughs fixed on a flange and a tight passage (Pet) mounted with a screw fitting.

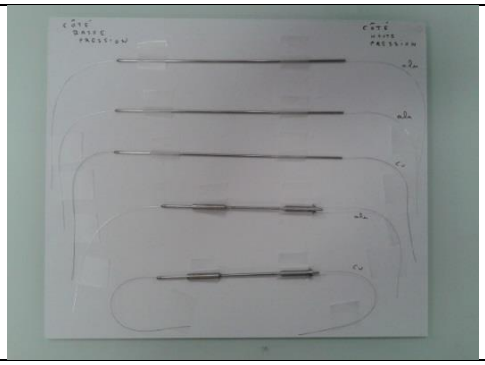

Fig.7a : Typology of tested feedthroughs.

Fig.7b : Mock-up for feedthrough welding qualification

The experimental conditions for these tests correspond to the TH conditions at the level of the heads of devices.

Numerical simulations have been carried out and led to clarify the maximum temperatures reached in this zone, which is about 100 °C.

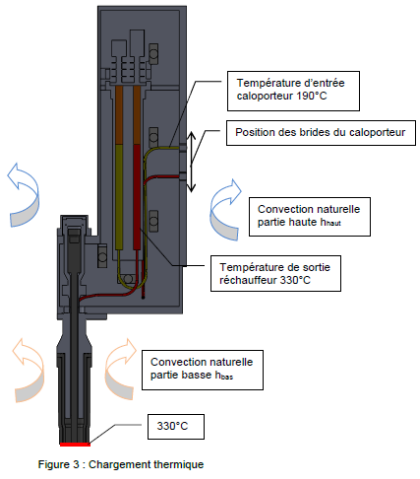

Figure 3 : Chargement thermique

Fig.8a : Head of device configuration

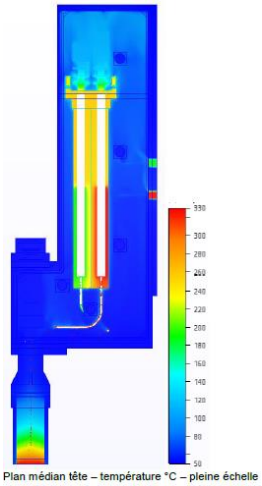

Plan médian tête – température °C – pleine échelle

Fig.8b : Thermal cartography the head zone of the device

4.5 Experimental Tests

The test facility is the experimental out of pile BIKINI loop operated by CEA-CAD-DTN. The main characteristics of this loop are recalled below:

- test section height =2,5m.
- thermal hydraulic parameters: 155 bar, 330°C, 1 to 5m^3/h.
- demineralised water : pH (25°C) = 5.45

Fig.9a: BIKINI experimental loop (HP-HT)
Operator: CEA-DTN-STCP-LETH

Fig.9b: experimental test section flanges

Hereafter are reminded the main parameters of the experimental test:

Title	Description	Note
Test startup End of Test	Me 04.07.18 14h15 Lu 09.07.18 14h30	Test duration : 5 days
Process pressure	155 bar +/2 bar	
OF Flange Temperature	100°C	Fluid TC in front of the OF Flange
Process flow rate	1000 $kg.h^{-1}$	Ascending flow
OF flange flow		No flow

During the test, control of the experimental feedthroughs called PET2 (welded), PET3 (screwed) & PET5 (welded).

Note: The rate of leakage of the sealed passages is monitored by differential pressure sensors placed below the flange (range 0-62 hPa).

The graph below shows the evolution in time of the differential pressure measurement obtained by sensors P02, P03 and P05 (these sensors permit to check the apparition of a leak at the level of the sealed passages PET2, PET3 and PET5 respectively).

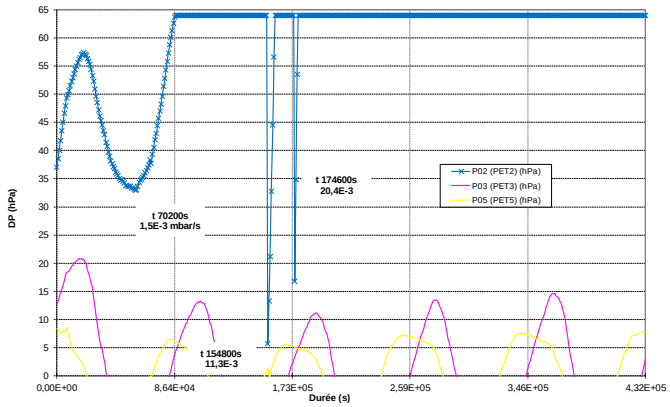

Fig.10: Control of the evolution of the pressure of individual passages tested

legend: yellow - red: (Pet welded) / blue (screwed Pet)

Note: the time t=0 s represent the beginning of the endurance phase.

After the five-day trial, the loop was operated to ambient pressure & temperature conditions.

From the completed script, it can be concluded the preliminary results below:

- ✓ The OF (Optical Fibers) flange has been tested on the test BIKINI loop to the thermal conditions of the head of the ADELINE for 5 days to 155 bar,100 °C,

- ✓ The PET3 and PET5 feedthroughs (welded passages) remain perfectly sealed throughout the test. The observed fluctuations are due to atmospheric fluctuations (pressure and temperature of the test hall).

Note: feedthrough noted PET2-sensor P02 (Pet mounted screw connection) is waterproof up to 19 h 30 min after the start of the trial. At this moment, there is the appearance of a saturation with a speed increase in the pressure of 1.5 x 10^{-3} h.Pa.s^{-1}.

After the test, the FO flange was removed for inspection.

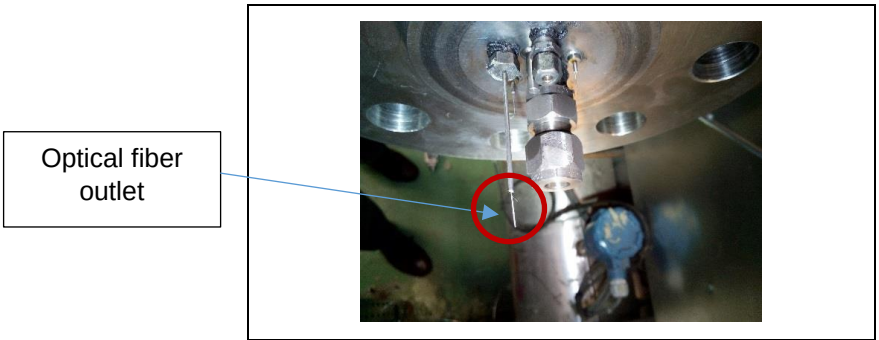

Fig.11: OF Flange.

Visual inspection of feedthroughs after the test

The visual examination of the flange shows that the ends of the tight passages (coated optical fibers) have not been altered by the endurance test.

5. Conclusion:

In the frame of JHR Program, some ongoing actions concern the development of irradiation devices. These devices will allow, among other things, the power ramps test on fuel rods. To characterize online behaviour of fuel rod during the test, innovative instrumentation is studied.

In particular, some instrumentation will integrate optical fibres in order to achieve, among others, interferometric measurements to characterize in-situ swelling of a rod (range 0-1,5 mm).

One of the point identified in the phase of development of this type of instrumentation is to check the mechanical performance of tight feedthroughs to thermal hydraulic conditions representative of ADELINE type devices (head zone, 155 bar,T=100°C). This test was performed on a duration of five days.

The first results obtained identify technology "fittings welded" potentially usable for ADELINE tight type passages.

The futures tests will be designed to validate the following points:

- Resistance of this type of feedthrough to thermal hydraulic pressurised water conditions (PWR) for 24 hours.
- Optical function verification with this type of feedthroughs test in these conditions.

6. References:

[R1] IGORR 2009
JHR. The ADELINE irradiation loop in the Jules Horowitz MTR. Testing a LWR fuel rod up to the limits with a high quality level. Experimental process.
S.GAILLOT, D.PARRAT, G.LAFFONT, C.GONNIER, C.GARNIER
CEA, DEN, CEA CADARACHE, F-13108 Saint-Paul-lez-Durance, France.

[R2] PHYSOR 2014
Jules Horowitz Reactor, France. Development of an experimental loop INTEGRATING AN optimized irradiation process.
S.GAILLOT, S.VITRY & T.DOUSSON
CEA, DEN, CEA CADARACHE, F-13108 Saint-Paul-lez-Durance, France.

[R3] IGORR 2013
JHR Project. Fuel irradiation device. Innovative instrumentation proposal for experimental real time measurement.
S.GAILLOT, G.CHEYMOL
CEA, DEN, CEA CADARACHE, F-13108 Saint-Paul-lez-Durance, FRANCE
CEA, DEN, CEA SACLAY, F-91191 Gif sur Yvette, FRANCE.

Experiencing an Extreme External Event – Bushfires near ANSTO's Lucas Heights Site, April 2018

M W Summerfield[1], D Waters[1], S Wilson[1]

1) Australian Nuclear Science and Technology Organisation (ANSTO), New Illawarra Road, Menai, NSW 2234, Australia

Corresponding author: msx@ansto.gov.au

Abstract. In April 2018, a large, fast moving bushfire originating in the outskirts of south-west Sydney led to activation of the ANSTO emergency response plans. Whilst there was no direct impact on the Lucas Heights site and no implications for nuclear or radiological safety, there was some impact on the operational activities onsite. This paper provides an overview of the bushfire and the ANSTO response in the context of the ANSTO emergency response plans. Some of the key lessons learned by ANSTO are identified as are some other lessons that may be of benefit to other research reactors and similar facilities.

1. Introduction

This paper provides an overview of the large, fast moving bushfire in south-western Sydney that resulted in the activation of the ANSTO emergency response plans in April 2018.

2. Lucas Heights Science and Technology Centre

The Lucas Heights Science and Technology Centre (LHSTC) is located approximately 30 km south-west of central Sydney. It is the principal location of the Australian Nuclear Science and Technology Organisation, the other main locations being the Camperdown campus 5 km south of central Sydney and the Clayton campus 22 km south-eats of central Melbourne. It contains a number of nuclear installations, including the OPAL Reactor, radioisotope production facilities and accelerators, as well as various other research facilities and laboratories.

The site is surrounded by a 1.6 km buffer zone centered on the now shutdown HIFAR reactor within which no permanent residential development is permitted. A main road (New Illawarra Road) runs along the north side of the site. This road intersects with another main road (Heathcote Road) that runs along the south-western side of the site. On the northern side of the New Illawarra Road is the Lucas heights Resource Recycling Centre and open bushland. To the west and south is more open bushland and to the east and north east are the suburbs of Engadine, Bardon Ridge and Menai.

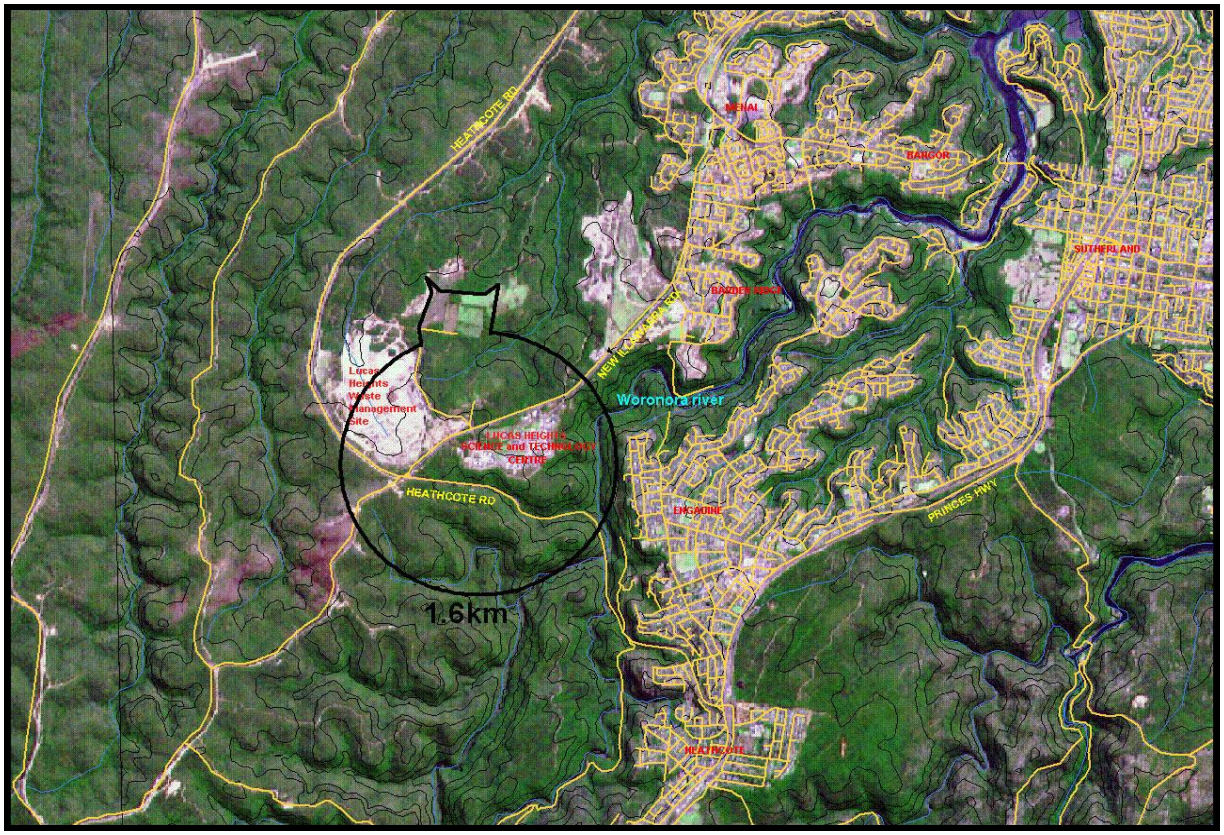

Figure 1: Map of the Lucas heights Area

The LHSTC location in bushland means that bushfires can be expected to impact the site every eight to 12 years. Previous experience has shown that such bushfires have the potential to burn to the site boundary fence although since the site itself is on generally flat ground with sparse vegetation, the intensity of most such fires is not normally high. However, due to the more dense vegetation and a drop-off to the Heathcote Road on the south-west side of the site, fires in this area can be more intense.

Hazard reduction "burning-off" is undertaken outside the site boundary to reduce the fire-load. However, the ability for this to be done to the optimal degree is dependent upon appropriate weather conditions during the non-bushfire season, the availability of external resources and the relative priority for such hazard reduction in relation to other areas in the locality. All buildings onsite are also subject to a bushfire preparedness inspection (such as verifying gutters are clear of any accumulation of flammable material) prior to the start of the bushfire danger period and resources are also made available ensure good grounds keeping across the site to minimise fuel loads.

Active protection within the LHSTC is provided by the onsite Emergency Response Team (ERT) supported by the volunteer Bushfire Response Team (BFRT) and as necessary by external emergency responders from Fire and Rescue New South Wales (FRNSW) or the NSW Rural Fire Service (RFS). They would be able to utilize over 100 fire hydrants located onsite and outside the boundary fence that may be supplied from onsite water storage facilities by dedicated fire pumps. Based on previous experience, the principal function of the onsite BFRT is to identify and extinguish spot fires started by "ember-attack", where embers from a bushfire that could be kilometers away are blown onto the site and ignite flammable material.

3. Overview of Bushfire Incident

The bushfire originated in the Sydney suburb of Casula sometime late on the Friday night or in the early hours of the Saturday morning, apparently deliberately started. This point of origin is approximately 10 km to the north west of the LHSTC.

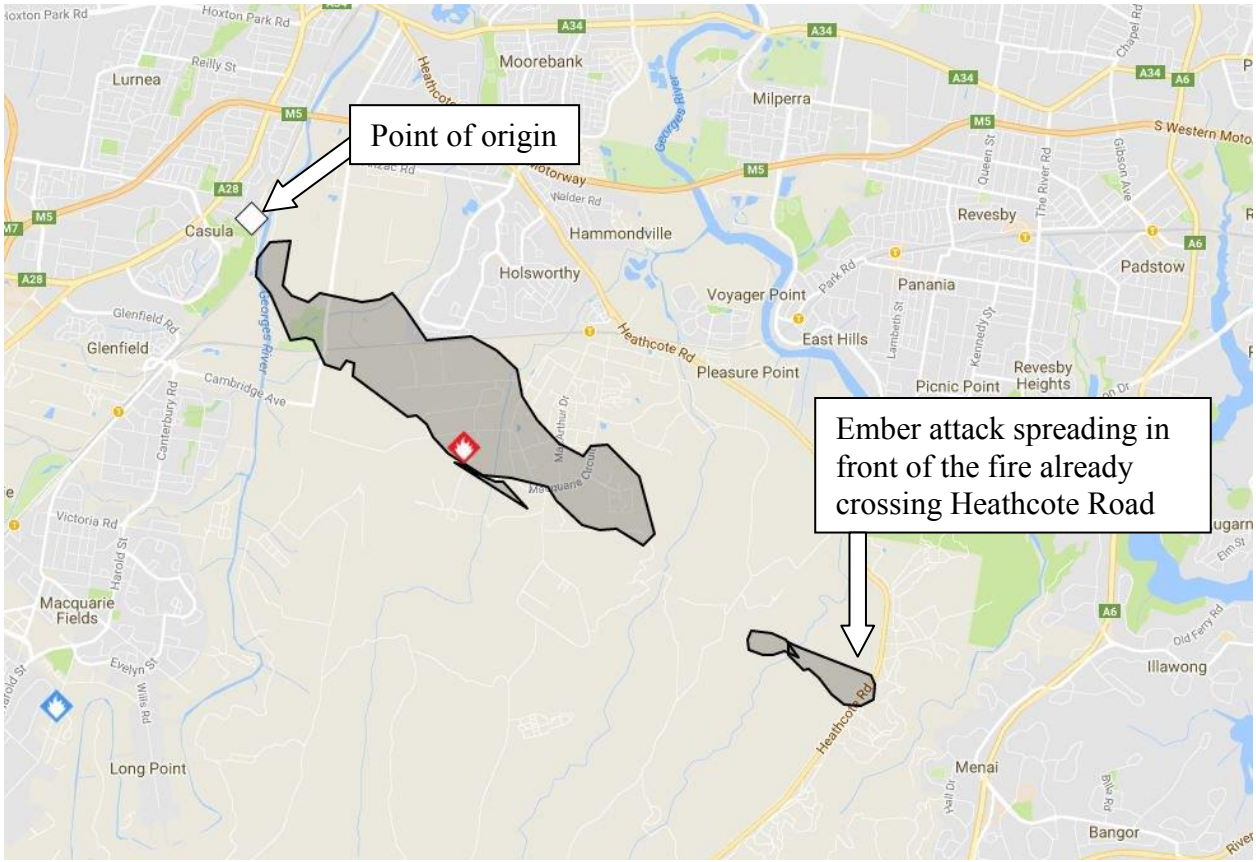

Figure 2: Status of Bushfire – Mid-afternoon, Saturday (from NSWRFS website)

By mid-morning, and fanned by a strong north-westerly wind, the fire was spreading through through open bushland as well as threatening parts of the suburb of Holsworthy. By early Saturday afternoon, whilst still threatening the suburb of Holsworthy, the fire front was spreading in an east-south-east direction towards the Heathcote Road. Embers from the fire were already igniting bushland around the Heathcote Road, forcing the closure of this road. By mid-evening on the Saturday, the fire had crossed Heathcote Road and was starting to impact the western edge of the suburb of Menai 5 km north of the LHSTC.

At this time, the LHSTC was not directly threatened by the bushfire. However, on the Saturday evening, the ANSTO Emergency Operations Centre (AEOC) was stood up, the CEO and the Consequence Assessment Team (CAT) notified and Stage 3 of the ANSTO Emergency Plan was activated due to the bushfire threat in the open bushland to the north-west of LHSTC. The ANSTO BFRT was also stood up with eight personnel responding. This team undertook roving inspections of the northern fence line of the LHSTC with the objective of identifying and extinguishing any spot fires caused by flying embers. Based on advice from the local Sutherland Shire Emergency Operations Centre (EOC) and previous

experience of bushfires in the area around the LHSTC, non-essential staff at LHSTC were requested to leave the site. This was due to the potential for road closures that could mean these staff having to stay onsite for an extended period.

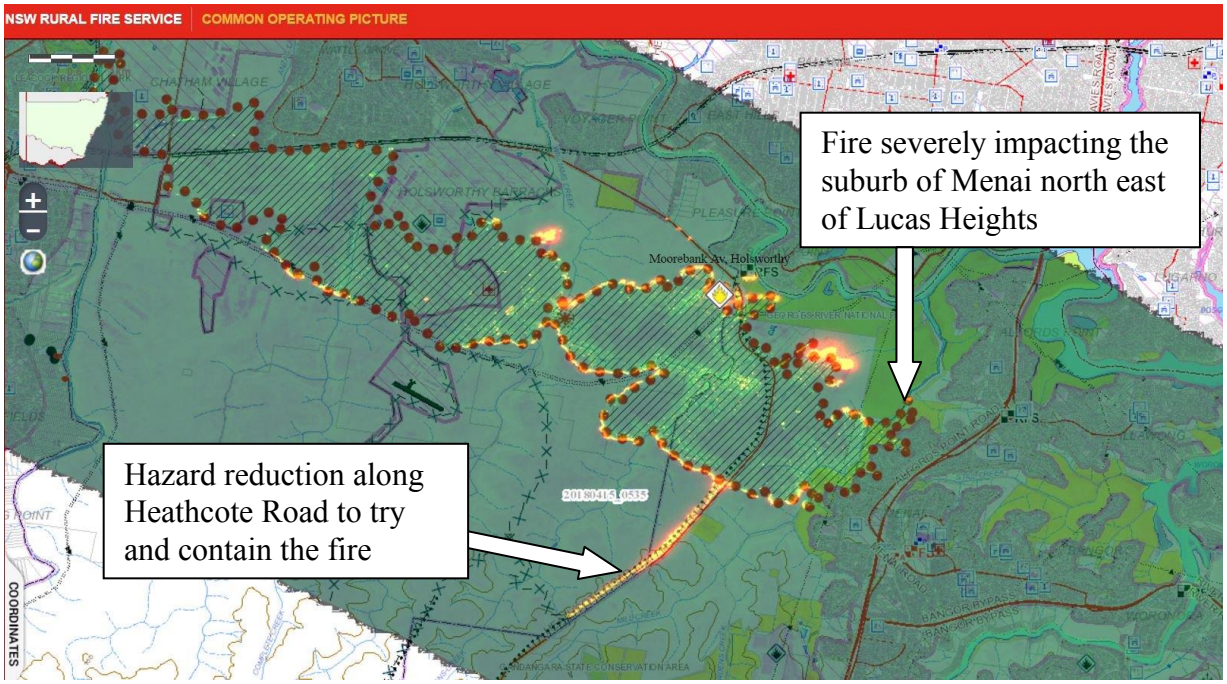

Figure 3 – Status of Bushfire, Mid-afternoon, Sunday (linescan)

The weather conditions eased over the Saturday night but the wind strengthened again on the Sunday and by the Sunday afternoon, the bushfire was severely impacting the suburbs to the north east of the LHSTC whilst also continuing to spread in the open bushland north west of LHSTC. The main firefighting activities were focused on protecting properties in the suburb of Menai but to try and contain the bushfire within this open bushland, back-burning operations were also undertaken along the Heathcote Road.

At ANSTO, the BFRT had been stood down but remained on call to respond to any change in conditions, particularly any change in wind direction or a new bushfire south of the main fire. The ANSTO canteen located outside the site fence was also opened and made available to the emergency services as a rest area whilst NSWRFS and FRNSW appliances were able to refill from ANSTO hydrants and swimming pool. The ANSTO Crisis Management Team (CMT), made of members of the Executive and other senior managers, was also activated at ANSTO's Camperdown campus. The CMT determined that the LHSTC would be closed to non-essential staff on the Monday due to both the potential for road closures isolating the site and to reduce traffic volumes on the Heathcote and New Illawarra Roads.

On the Monday, the bushfire was partially contained but a forecast change in wind direction to a northerly wind meant that further back-burning was required to create appropriate fire breaks against the southwards spread of the fire. This included hazard reduction along the new Illawarra Road opposite the LHSTC starting at 8 pm on the Monday night.

Figure 4 – Hazard reduction on the Monday night opposite Lucas Heights as seen from main entrance

The ANSTO BFRT was stood up to cover the hazard reduction operations, particularly in relation to any potential for spot fires to break out on the ANSTO site due to flying embers. The AEOC continued to provide support to the local area Fire Control Centre (FCC), including placing a liaison officer at the FCC to facilitate communications and coordinate such support. In addition, due to further hazard reduction operations being planned for the Tuesday, the CMT again determined that the LHSTC would remain closed to non-essential staff on the Tuesday.

By 6 pm on the Tuesday, the fire was still active but classed as "contained" and under control with back burning operations complete and mop up and patrol activities being undertaken. At this time, both the local area FCC and the AEOC were stood down and the ANSTO BFRT put on standby. NSWRFS and FRNSW appliances continued to refill from ANSTO hydrants and swimming pool during this time whilst the ANSTO canteen remained open to support both external emergency services and ANSTO personnel. The ANSTO CMT determined that is was appropriate to re-open the LHSTC to non-essential staff although those considered "high-risk" (e.g. asthmatics) would be assessed on a case-by-case basis. As a result, normal operations were resumed at the LHSTC on the Wednesday.

At this time the fire was classed as under control, the NSWRFS impact assessment estimated that the fire had burnt out more than 3800 hectares but that only five properties were damaged and one outbuilding lost out of nearly 900 properties that were directly impacted.

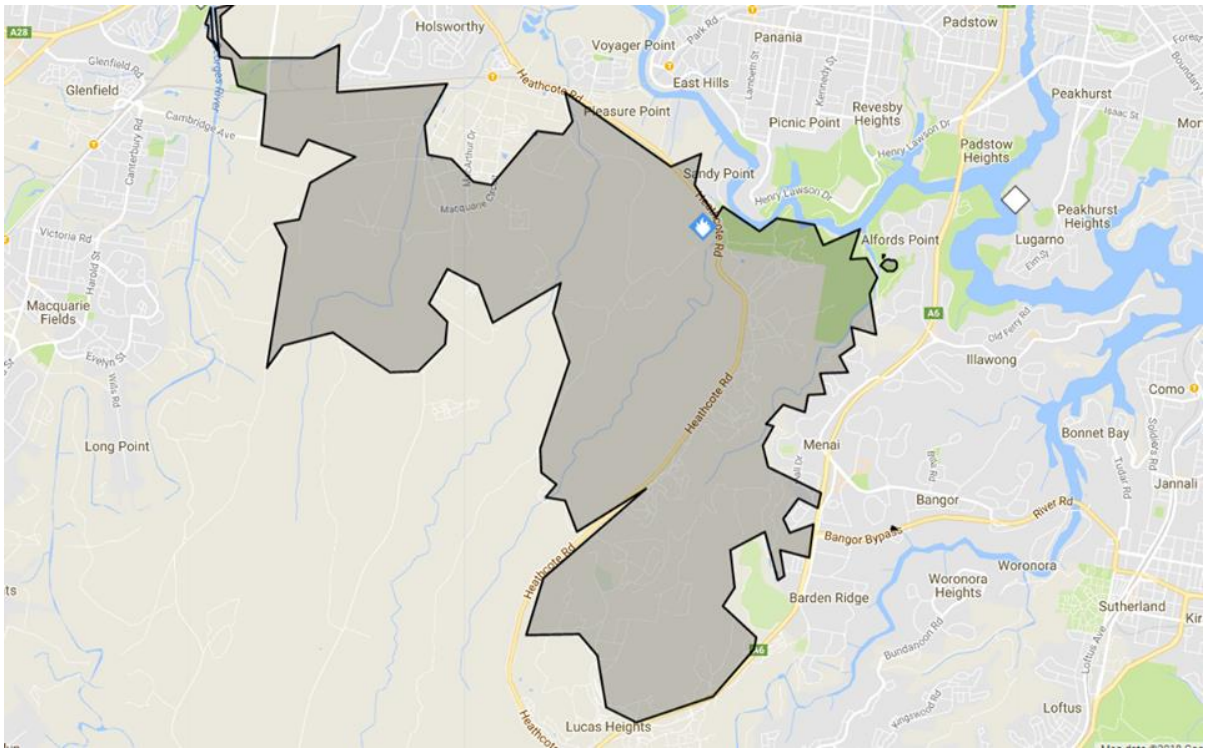

Figure 5 – Final status of fire

Throughout the whole incident, the OPAL reactor continued to operate at full power as normal and medical radioisotopes continued to be manufactured and supplied to customers. There were no implications for nuclear or radiological safety at any time.

4. Lessons Learned

Following the return to normal working conditions at the LHSTC on Wednesday the 18th April, ANSTO conducted a series of internal debriefs to identify actions and opportunities for improvement. This is standard practice following any incident in order to identify and capture lessons learned. Due to the significance of this incident, debriefs were also held for those involved in the AEOC and the CMT that identified additional actions and opportunities for improvement. Overall, a number of actions and opportunities for improvement were identified as a result of these debriefs, many of which were specific to the ANSTO situation. Some of the actions and opportunities for improvement may be relevant to other similar facilities and organisations are discussed further below.

- A number of the nuclear facilities at the LHSTC have regulatory requirements relating to emergency plans and performing appropriate emergency exercises and drills. There is also a regulatory requirement for the ANSTO itself to have an overall emergency plan for the site and to conduct exercises involving the external emergency agencies on a regular basis. However, one lesson learned was the need to review and update the ANSTO emergency plans and arrangements to improve the response to external events that do not directly endanger the ANSTO site. This would also be consistent with the IAEA guidance in SRS No.80 that says that major facilities like research reactors may be called upon to provide support to offsite emergency services and should plan accordingly even if they are not directly impacted by an extreme external event.

- Emergency Preparedness and Response needs to be practiced through drills and exercises on a regular basis. These drills and exercises need to have participation of all those who may be involved in the response, including senior management, such that all participants are familiar with their anticipated roles and responsibilities. In addition, all those who may be involved in responding to emergencies need to be appropriately trained. This includes senior management, particularly those who may be members of the crisis management team or its equivalent. Exercises that utilise the actual emergency facilities and equipment also provide an opportunity for staff to familiarise themselves with the emergency facilities and equipment, including such simple checks as verifying that they can access the facilities.
- Communication is a key aspect for optimum emergency management of an incident, both internally within the organisation and externally with the offsite emergency services and the media. Optimal communications is often reliant on ensuring numerous small items are ready and in place, such as having up-to-date emergency contact lists immediately available and pre-written scripts for staff (and possibly public) announcements. One thing that worked well during this event was the presence of an ANSTO liaison officer at the local area FCC who helped coordinate the support provided by ANSTO to the offsite emergency services as well as keeping the AEOC up to date with the fire situation. In addition, ANSTO's strong relationships with emergency services organisations developed through local emergency management committees and bushfire management committees was also of considerable benefit.
- Significant resources and facilities are needed in addition to what would normally be considered emergency equipment when responding to an emergency. An EOC or similar should not only be available and fitted out appropriately but it should also be adequately resourced with respect to both material and personnel to deal with an emergency that may last days, weeks or longer. This could include rest areas and other amenities for staff to use during breaks, meeting rooms or break-out areas separate to the main EOC for informal or informal discussions and storage areas for supplies.

Overall, whilst there were no implications for nuclear or radiological safety at any time, this incident did identify numerous actions and opportunities for improvement to ANSTO's emergency planning and preparedness that have been or are being implemented.

5. Summary and Conclusions

In April 2018, a large, fast moving bushfire in south-western Sydney resulted in the activation of the ANSTO emergency response plans. There were no implications for nuclear or radiological safety at any time and the OPAL reactor continued to operate at full power as normal and medical radioisotopes continued to be manufactured and supplied to customers.

Emergency Preparedness and Response needs to be practiced through drills and exercises on a regular basis to not only ensure that the plans and arrangements are suitable but also to train and familiarise the personnel when responding to emergencies. However, there is nothing quite like a real emergency to properly stress-test your actual preparedness. This incident did stress-test ANSTO's emergency planning and preparedness and identified numerous actions and opportunities for improvement.

ON THE ONE OF THE PRACTICAL SCIENTIFIC UTILISATIONS OF LOW POWER RESEARCH REACTOR LVR-15 IN ŘEŽ

P. MIKULA, J. STAMMERS
Nuclear Physics Institute ASCR, v.v.i., 25068 Řež, *Czech Republic*

M. ROGANTE
Rogante Engineering Office, I-62012 Civitanova Marche, Italy

A. MICHALCOVÁ
Dept. of Metals and Corosion Engineering of University of Chemistry and Technology, 16628 Prague 6, Czech Republic

ABSTRACT

At the previous conferences - IAEA International Conference on Research Reactors held in November 2015 in Vienna and RRFM/IGOR held in March 2016 in Berlin - it has been reported about the effective utilisation of the Řež research reactor LVR-15 in basic, interdisciplinary and applied research. Now, in our contribution we will focus our attention on the scientific utilisation of one of the beam tubes for plastic deformation studies of metallic polycrystalline samples by a newly developed high-resolution neutron powder diffraction method. The method consists of unconventional triple axis set up employing bent perfect crystal (BPC) monochromator and analyser with a polycrystalline sample in between (see Fig. 1). After the realisation of focusing conditions in real and momentum space at the neutron wavelength of 0.162 nm, a high angular resolution down up to $FWHM(\Delta d/d)=2\times10^{-3}$ was achieved on the standard α-Fe(110) sample (2 mm diameter) which then opened the possibility for measurements of small lattice parameter changes of samples, namely, as a result of a thermomechanical load. The feasibility of the instrument for macro- and microstrain as well as grain size studies is demonstrated on the low carbon shear deformed steel wires and the powder samples of FeAl plastically deformed by ball milling.

1. Introduction

Non-destructive X-ray and neutron diffraction techniques for studies of internal strain fields in polycrystalline materials have been successfully used for many years [1-13]. At present, the investigations of residual strains/stresses are usually carried out at the dedicated double axis diffractometers (strain scanners) with a bent perfect crystal (BPC) focusing monochromator situated on the first axis, a sample situated on the second axis and with a position sensitive detector (PSD). With respect to the experimental conditions, the BPC crystal is optimally bent which results in a highly collimated beam (often called quasi-parallel beam) reflected by the polycrystalline sample [8,11-13]. However, the $\Delta d/d$ resolution of these dedicated scanners derived from the *FWHM* of the diffraction lines is sufficiently high for small sample gauge volumes (when the width of the irradiated part of the sample is about 2 mm or less) but rarely better than 8×10^{-3} for bulk samples. Important thing is that the dedicated scanners operate with open beams without the necessity of Soller collimators. A further way, how to increase the resolution which would permit to investigate an influence of microstrains on the diffraction profile, namely, in the case of plastically deformed samples, is the use of a three axis set-up (bent perfect crystal monochromator + polycrystalline sample + bent perfect crystal analyser) when employing a third BPC crystal on the third axis as an analyser. The first attempts of the use of the three axis set-up were described two decades ago [14,15]. However, as it was

already shown in a limited case [14,15], by using the triple axis set up and by using focusing in real and momentum space, in a limited range of scattering angles a high resolution can be achieved on samples of rather large dimensions and with opened beams, i.e. also without Soller collimators (see Fig. 1). In the case of large (bulk) metallic samples, due to a low neutron attenuation factor for the most materials, neutron diffraction could be more advantageous with respect to the X-ray diffraction [16].

The drawback of such a set-up in comparison with the conventional scanners consists in using the step-by-step analysis (by rocking the BPC analyser). Therefore, the effective measurements could be carried out within a reasonable measurement time at high-flux neutron sources. From the point of view of luminosity, some improvements can be done by an employment of the BPC monochromator at a rather small Bragg angle, while the resolution can be optimized by a suitable choice of the BPC analyser and its thickness, as it was used in the present case (see Fig. 1).

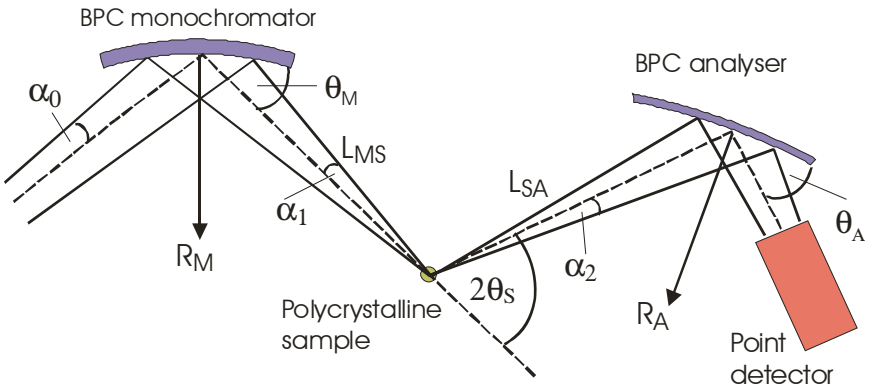

Fig. 1. Three axis diffractometer setting employing BPC monochromator and analyser as used in the experiment (R_M, R_A - radii of curvature, θ_M, θ_A - Bragg angles.

2. Experimental details

The set-up shown in Fig. 1 was experimentally realized on the three axis neutron optic diffractometer installed at the medium power research reactor LVR-15 situated in Řež. Si(111) monochromator and Si(400) or Ge(311) analysers had the dimensions of 200x40x4 mm^3 and 20x40x1.3 mm^3 (length x width x thickness), respectively. The monochromator Si(111) had a fixed curvature with a radius R_M of about 12 m. The curvature of the analyser was changeable in the range from R_M=36 m to R_M=3.6 m and finally set for the optimum radius of curvature of R_A= 9 m, where a best resolution was found. For a practical demonstration of the feasibility of using the three axis set-up for diffraction line analysis we used two types of polycrystalline samples: First, nondeformed as well as deformed α-Fe(110) wires with accumulated shear deformation, as a result of rolling with the shear of the metal ingot and conventional wire drawing. Due to the deformation the diameters of the samples are not the same, however, they were in the vicinity of 5 mm. Then, we used FeAl intermetallic alloy samples which have a known property consisting in the fact that a severe plastic deformation (e.g. ball milling) brings about a reduction of the average grain size and introduction of lattice strain defects resulting in an increase diffraction peak broadening. On the other hand, upon heating the grain size and lattice restoration can be expected [17].

3. Low-carbon shear deformed steel wires

In this case, the bent perfect Si(400) slab with the optimum radius of curvature of R_A=9 m (providing the best resolution) was used as the analyser. The description of the nondeformed as well as with accumulated shear deformation samples – (low carbon steel - Grade 08G2S GOST 1050) is shown in Tab.1. Tab. 2 describes the chemical composition of the steel.

Sample number	ϕ [mm]	Shear def. [%]	Drawing def. [%]
S.1	5.10	0	0
S.2	4.28	8	23.2
S.3	5.35	0	0
S.4	4.28	16.6	23.2
S.5	5.57	0	0
S.6	4.28	23	23.2

Tab. 1: Description of deformation of the low-alloyed steel samples. Percentage in the fourth column shows the reduction degree in drawing deformation.

Element	C	Mn	Si	S	P	Cr	Ni	Cu	N2
wt %	0,08	1,87	0,82	0,020	0,022	0,02	0,02	0,02	0,007

Tab. 2: Chemical composition of low-alloyed structural steel grade 08G2S GOST 1050 element.

3.1. Experimental results of the diffraction profiles - Radial components

The steel samples were situated on the second axis of the diffractometer in vertical position. The width of the incident beam was 8 mm and therefore, the whole volume of the sample was irradiated (within the whole diameter). The height of the incident beam was 20 mm. From the introduced individual profiles (see Fig. 2), we can detect the following features: The peak intensities and *FWHM*s related to the deformed samples differ very little. This is brought about by the fact that the diameter of the deformed samples was equal and that the shear deformation has a negligible effect. Very close values of *FWHM* point out to the fact that the lattice deformation in the radial direction was basically brought about by drawing deformation. The integrated intensity under the peak profiles related to the nondeformed samples S.1, S.3 and S.5 primarily corresponds to the irradiated volume of the sample, which is naturally maximum for the sample S.5.

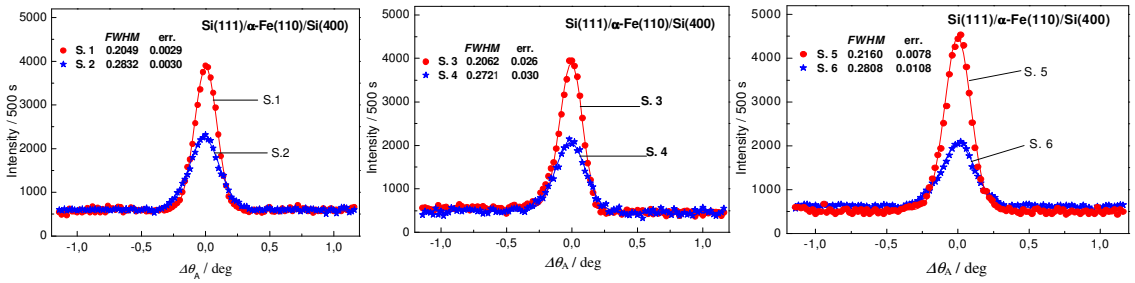

Fig. 2. Diffraction profiles related to the samples S.1 - S.6 situated in the vertical position as analysed by the bent perfect Si(400) analyser.

3.2. Experimental results of the diffraction profiles - Axial components

In the next step the steel samples were situated on the second axis of the diffractometer in the horizontal position. The obtained results are shown in Fig. 3. In comparison with the

previous case, for the samples in the horizontal position their irradiated volume is much smaller and correspondingly neutron signal was smaller. In this case, it was found that the resolution was dependent on the width of the incident beam impinging the sample and therefore, we used the slit width of 5 mm. It can be seen from Fig. 3 that the resolution represented by *FWHM* was practically the same for all nondeformed samples S.1, S.3 and S.5. Small differences in *FWHM* can be seen for plastically deformed samples. It points out to the fact that the lattice deformation was basically brought about by drawing deformation and influencing the radial strain component and much less the axial strain component.

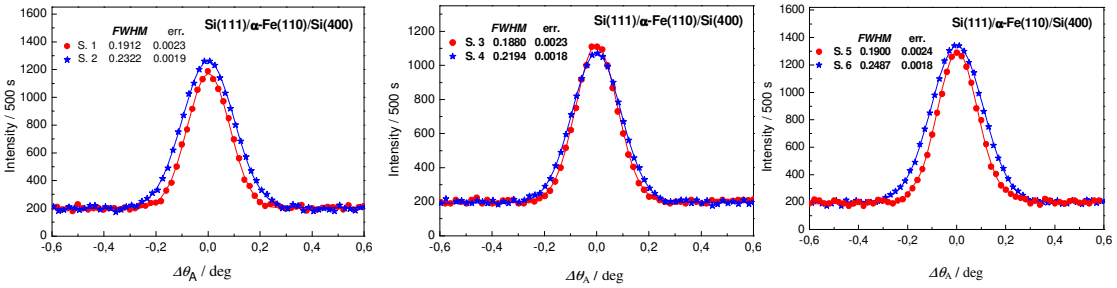

Fig. 3. Diffraction profiles related to the samples S.1 - S.6 situated in the horizontal position for measurement of the axial component as analysed by the bent perfect Si(400) analyser.

4. FeAl intermetallic alloy samples

In this case, the Si(311) bent perfect slab with the optimum radius of curvature of R_A= 9 m, was used as the analyser. The studied FeAl samples were in the form of small plates of the dimensions of about 10 x 4 x 2 mm^3 (length x width x thickness) and inserted in the neutron beam in the vertical position. As the samples were not precisely of the same dimensions, the irradiated volumes were slightly different and therefore, we could not compare the detector signal related to individual samples. First, Fig. 4 shows the effect of ball milling on *FWHM* of the analyser rocking curves for an standard powder $FeAl_E$ sample and the one after the milling ($FeAl_M$). It can be seen from Fig. 4 that the effect is remarkable. The conversion of the $\Delta\theta_A$ angles to $\Delta d/d$ provides the values of *FWHM*($\Delta d/d$) of 5.2x10^{-3} and 15.8x10^{-3} for $FeAl_S$ and $FeAl_M$ powders, respectively. After that, compacted powder samples were investigated and the related results are shown in Fig. 5. Inspection of Fig. 5 reveals that the severe plastic deformation brings about the expansion of the lattice constant of the FeAl milled powder when compared with that of compacted samples at elevated temperatures by $\Delta d/d$ of about 0.6 % for 900 °C and 0.8 % for 1000 °C and 1100 °C. The value 0.8 % is in a very good agreement with the result reported in [17].

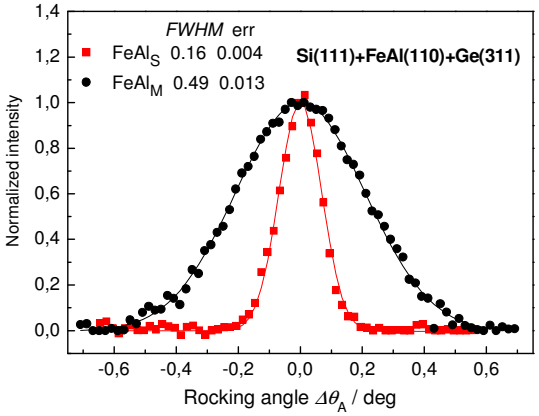

Fig. 4. Analyser rocking curves for the FeAl standard as well as the FeAl milled samples.

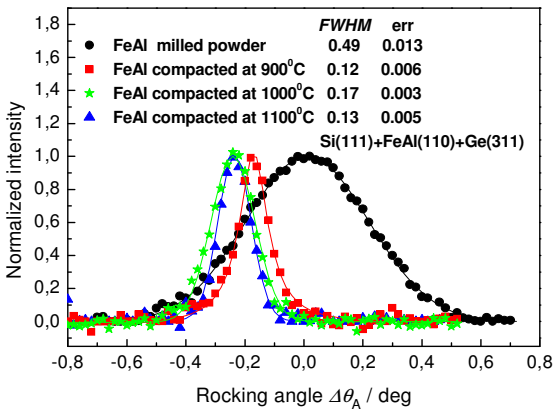

Fig. 5. Analyser rocking curves related to the individual samples.

5. Summary

Three axis neutron diffractometer setting employing BPC monochromator and analyser with the studied polycrystalline samples of FeAl between them was tested for practical application. It has been proved that the diffractometer setting provides a sufficiently high $\Delta d/d$ resolution (d is the lattice plane distance) permitting macro- and microstrain studies as well as the grain size distribution after applying shape analysis of neutron diffraction peaks [4-8]. The neutron diffraction results obtained on the samples of low-alloyed quality structural steel (Grade 08G2S GOST 1050) and FeAl document the feasibility of the unconventional three axis set-up for studies of some properties of polycrystalline samples in the plastic deformation region. It can be seen from Tab. 3 that though the *FWHM*-effects resulting from the applied deformation on the samples are very small and cannot be studied by the conventional strain scanner, thanks to the high resolution of the present experimental set-up, they are clearly measurable. In particular, such results can be used as an additional support to complement the information achieved by using the other characterization methodologies.
In the case of FeAl samples, when the ball milling and the sintering at elevated temperatures bring about much larger effect, the obtained neutron diffraction data have confirmed the expected results earlier obtained by X-ray diffraction, however, large bulk samples could be

Sample number	S.1	S.2	S.3	S.4	S.5	S.6
FWHM($\Delta d/d$) - Radial [10^{-3}]	4.09	5.66	4.12	5.44	4.32	5.61
FWHM($\Delta d/d$) - Axial [10^{-3}]	3.82	4.64	3.76	4.38	3.80	4.97

Tab. 3: Summary of the *FWHM*s as calculated in ($\Delta d/d$)-scale.

used in this case. It is clear that the shape analysis of physically broadened neutron diffraction peaks could be an attractive completion of existing procedures of integrated substructure investigation.
In this way the following favourable features of the neutron diffraction method may be mentioned: Possibility of using bulk samples under an influence of a thermomechanical load, absence of surface effects, high peak to background ratio and the possibility of investigation of real components.
Finally, it should be pointed out that contrary to the conventional double axis strain scanner, this three axis setting provides a high resolution for bulk samples e.g. of the diameter of 5-10 mm while for conventional scanner such diameter itself introduces to the resolution an uncertainty in *FWHM* of the diffraction profile at least of 1×10^{-2} rad. Thanks to the high resolution property of the three axis set-up, it can be, of course, used also for measurements of residual elastic deformation macrostresses, however, less efficiently in comparison with the conventional two axis neutron diffraction measurement [11] which has not so high resolution requirements.

Acknowledgement

Measurements were carried out at the CANAM infrastructure of the NPI CAS Řež supported through MŠMT project No. LM2015056. The presented results were also supported in the frame of LM2015074 infrastructural MŠMT project “Experimental nuclear reactors LVR-15 and LR-0”. Bragg diffraction optics investigations are, in the Czech Republic, supported by GACR project No. 16-08803J and by the ESS project LM2010011: “Contribution to Partnership in Large Research Infrastructure of Pan-European Importance”. We thank Ms. Michalcová from NPI ASCR for significant help in the measurements and basic elaboration of the data.

References

[1] NOYAN, I.C., COHEN, J.B., “Residual stress: measurement by diffraction and interpretation”, 1st edn; 1987, New York, Springer-Verlag.

[2] HUTCHINGS, M.T., KRAWITZ, A.D., (Eds.), "Measurement of residual and applied stress using neutron diffraction", NATO ASI Series, Applied Sciences, **26**, Kluwer Academic Publisher, 1992.
[3] DAYMOND, M.R., BOURKE, M.A.M., DREELE, R.B., CLAUSEN, B., LORENTZEN, T., "Use of Rietveld refinement for elastic macrostrain determination and for evaluation of plastic strain history from diffraction spectra", J. Appl. Phys. **82** (1997) 1554–1562.
[4] WEBSTER, G.A., (ed.), "Polycrystalline materials—determination of residual stress by neutron diffraction", ISO/TTA3, ISO/Technology, Trends Assessment, Geneva, Switzerland, 2001.
[5] STELMUKH, V., EDWARDS, L., SANTISTEBAN, J.R., GANGULY, S., FITZPATRICK, M.E., "Weld stress mapping using neutron and synchrotron x-ray diffraction", Materials Science Forum, **404-407** (2002) 599-604.
[6] HUTCHINGS, M.T., WITHERS, P.J., HOLDEN, T.M., LORENTZEN, T., "Introduction to the characterization of residual stress by neutron diffraction", 1st ed.; 2005, London, Taylor and Francis.
[7] MIKULA, P., VRÁNA, M., LUKÁŠ, P., "Power of Bragg diffraction optics for high resolution neutron diffractometers for strain/stress scanning", In IAEA-TECDOC-1457 "Measurement of residual stress in materials using neutrons", IAEA Vienna, 2005, pp. 19-27.
[8] PIRLING, T., BRUNO, G., WITHERS, P.J., "SALSA - Advances in residual stress measurement at ILL", Materials Science Forum, **524–525** (2006) 217–22.
[9] HOLDEN, T.M., SUZUKI, H., CARR, D.G., RIPLEY, M.I., CLAUSEN, B., "Stress measurements in welds: Problem areas", Mater. Sci. Eng. A, **437** (2006) 33–37.
[10] WITHERS, P.J., "Mapping residual and internal stress in materials by neutron diffraction", Comptes Rendus Physique, 8 (2007) 806–820.
[11] MIKULA, P., VRÁNA, M., MRÁZ, Ľ., KARLSSON, L., "High-resolution neutron diffraction employing Bragg diffraction optics - A tool for advanced nondestructive testing of materials", In Proc**.** of ASME Conference on Engineering Systems Design and Analysis, 7 to 9 July 2008, Haifa. ISBN 0-7918-3827-7**.**
[12] WIMPORY, R.C., MIKULA, P., ŠAROUN, J., POESTE, T., LI, J., HOFFMAN, M., SCHNEIDER, R., "Efficiency boost of the materials science diffractometer E3 at BENSC: One order of magnitude due to a double focusing monochromator", Neutron News, **19** (2008) 16-19.
[13] WOO, W., FENG, Z., WANG, X., DAVID, S.A., "Neutron diffraction measurements of residual stresses in friction stir welding: A review, Science and Technology of Welding and Joining", **16** (2011) N.1 23-32.
[14] KULDA, J., MIKULA, P., LUKÁŠ, P., KOCSIS, M., "Utilisation of bent Si crystals for elastic strain measurements", Physica B **180&181** (1992) 1041-1043.
[15] VRÁNA, M., LUKÁŠ, P., MIKULA, P., KULDA, J., "Bragg diffraction optics in high resolution strain measurements", Nucl. Instrum. Methods in Phys. Research A, **338** (1994) 125-131.
[16] SEONG, B.S., EM, V., MIKULA, P., ŠAROUN, J., KANG, M.H. "Unconventional performance of a highly luminous strain/stress scanner for high resolution studies", Materials Science Forum, **681** (2011) 426-430.
[17] GIALANELLA, S., "FeAl alloy disordered by ball milling", Intermetallic, **3** (1995) 73-76.

RESEARCH REACTORS SAFETY I&C MODERNIZATION LEVERAGING EXPERIENCE WITH NPPs

Arnaud DUTHOU, Aurélien MATTEI
Rolls-Royce Civil Nuclear
23, Chemin du Vieux Chêne, Meylan 38240, France
Arnaud.Duthou.cn@Rolls-Royce.com ; Aurelien.Mattei.cn@Rolls-Royce.com

ABSTRACT

Since the 1960s, Rolls-Royce Civil Nuclear has been a major stakeholder in the deployment of the French nuclear Research Reactors, supplying key safety I&C systems such as Reactor Protection, Neutron Instrumentation and Rod Control. More recently, it modernized some of their I&C systems from original analog technology to modern Digital safety systems.

Simultaneously, Rolls-Royce Civil Nuclear has been supplying its Digital or Analog safety technologies to Nuclear Power Plants (NPP) all around the world; resulting in installed and operating equipment in more than 200 NPPs worldwide. Currently, it is supplying new systems in more than 80 nuclear units, in particular in France, China and Finland.

This paper draws a parallel between NPPs and research reactors I&C modernization, to identify shared challenges and the solutions that can be applied in both cases, still assessing the specific issues of each project

In particular it will give an overview of the context: regulatory requirements, objectives and progress as well as the technologies deployed for these upgrades.

Two representative examples of successful I&C modernization for NPPs are presented, along with one for a research reactor:

- MASURCA research reactor at CEA Cadarache (France).
- 2 VVERs in Loviisa (Finland).
- 2 PWRs in Ling Ao (China).

Main similarities and differences between these projects will be highlighted and from this comparison we will extract the main challenges faced, the solutions implemented and the key success factors for such I&C modernizations. In particular, the licensing and the importance of proven and adaptable safety platforms will be assessed.

Key Words: Safety, I&C, SPINLINE, Digital, Protection System, Licensing, Hardwired, HARDLINE, Rolls-Royce

1 INTRODUCTION

Ageing of the facilities is a major trend observed worldwide for both nuclear power plants (NPP) and research reactors (RR). However, whereas the average age is about 30 years for NPPs, it is now exceeding 42 for RRs. The preservation and enhancement of their safety to the current standards must hence be achieved by the modernization of their equipment and in particular safety I&C systems. This is also a way to improve the productivity of power plants and utilization time of research reactors, and often required to apply for life operating license extension.

Modernization projects and licensing of the newly installed safety I&C systems is often seen as complex, because the new equipment must adapt to existing interfaces. Nevertheless, Rolls-Royce Civil Nuclear has led successfully several modernization projects over the past decades, basing on more than 50 years of experience in the nuclear I&C sector.

A few noteworthy examples showing the great variety of handled projects are the safety I&C modernization of 4 VVERs in Dukovany (Czech Republic), 34 units of the 900MW French PWRs, and the current retrofit of the 1300MW fleet in France (20 units, being the largest modernization project of this type in the world). Two retrofit projects for NPPs will developed in this report: the Neutron Instrumentation Systems upgrade of 2 PWR in Lingao, China and the complete safety I&C modernization of 2 VVERs in Loviisa, Finland.

In addition, Rolls-Royce was the original I&C supplier for the French research reactors since the 1960s, and carried out several modernization projects on this fleet, upgrading initial systems with both analog and digital solutions. This paper will present one of them, the modernization of the MASURCA research reactor at CEA Cadarache in France.

Each of these projects was carried out successfully based on Rolls-Royce long-term experience with modernization programs and state-of-the-art analog and digital technologies, e.g. using the Spinline digital safety platform. The paper will present the main challenges faced by each study case, and the offered solutions and best practices provided by Rolls-Royce to overcome them.

2 FIRST STUDY CASE: LOVIISA POWER PLANT

2.1 Context

The Loviisa nuclear power plant, located on the southern coast of Finland, is composed of two VVER-440 reactors (Russian design) commissioned in 1977 and 1980.

In 2014, Rolls-Royce signed an agreement with Fortum for the modernization of Loviisa nuclear power plants I&C systems, which covers mainly the nuclear safety and safety related systems. The project, named “ELSA” was implemented in three phases during 2016-2018. The aim of this modernization was to ensure the safe and reliable operation of the units until the end of the reactors’ lifetime, in 2027 & 2030. This project follows the LARA project: a partial renewal of I&C system awarded to another I&C supplier in 2005 which was not successfully completed.

While the major initial components were from Russian origins, the I&C systems were based on both Siemens technologies, Simatic and Teleperm for Normal operation and safety related systems and Russian technologies for Reactor Trip, Rod Control and Neutron Instrumentation Systems.

The modernization project awarded to Rolls-Royce concerned the reactor protection, control and power limitations systems, key safety functions and accident management systems. The new safety-classified systems delivered by Rolls-Royce (including Reactor trip) were based on the Spinline Digital safety Platform. Rolls-Royce also supplied manual backup systems for accident management using hardwired technology, and third party PLCs for monitoring and normal control systems.

To sum up, one can state that this modernization project includes a set of work and services covering hardware and software development, manufacturing, testing,

commissioning, qualification and licensing, but also the provision of spare parts and services for the estimated lifetime of the plant.

2.2 Main project-related challenges

The main challenges faced by this project were quite similar to the regular issues observed at most I&C modernization project, but other aspects were more specific. The most critical points related to this project were:

- The adaptation of the new system to the existing equipment: it is necessary to ensure the compatibility between the modernized and older systems remaining in place, which are of different technology and from several suppliers.
- The compliance with the customer's schedule: the modernized systems had to be installed during 3 regular outages between 2016 and 2018 with no increase in the length of these shutdown periods.
- The modification management: as the technology of replaced systems differs from the upgraded ones, (e.g. analog to digital for RTS) some functions could not be exactly replicated and some capabilities were added with the new architecture.
- The interface between systems that belong to different safety classes and technology necessitated a clear and strong separation policy
- The compliance with the highest standards and advanced in-house testing before shipment under tight schedule
- The assurance of economic performance offering product which are adaptable, easy to maintain and test while in operation and with a guaranteed long term support.

2.3 Schedule and offered solution

The solution offered by Rolls-Royce covered a wide variety of safety class systems: 6 SC2 and SC3 classified functions (approximately equivalent to safety and safety related) as well as 6 non-safety functions. For this modernization, one can also observe on the diagram below that several technologies were used to implement the required systems, notably digital (based on Rolls-Royce safety platform "Spinline" and industrial PLC) and analog ones. To ensure the success of this project, 10 new developments have been carried out and the total installation on-site necessitated around 100 cabinets.

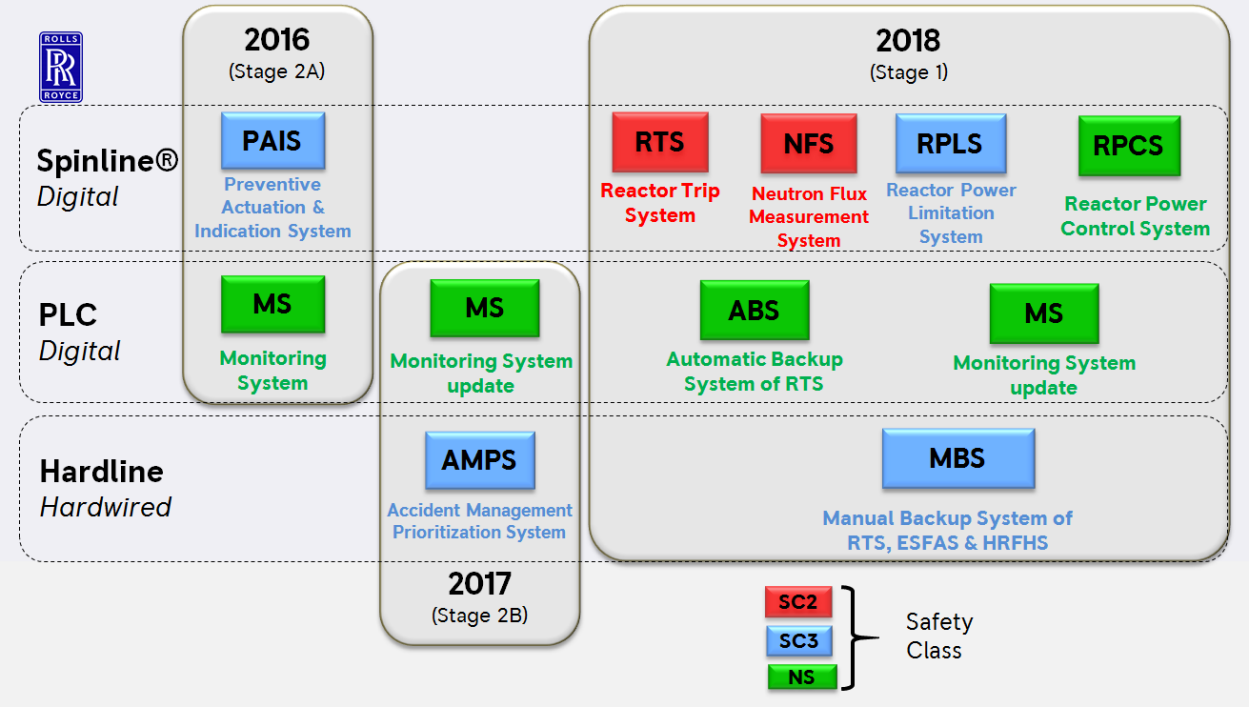

Implementation stages and related systems

This new modernization project to upgrade this nuclear power plant was awarded to Rolls-Royce in 2014, and a careful planning had to be implemented as the first onsite installation was due for 2016. A careful prioritization was hence required to target the systems to be upgraded during the first outage, while still keeping in mind the entirety of the project and the functions to be implemented in the future.

Installation was carried out successfully in three phases during outage periods from 2016 to 2018 with no increase in their length, according to the following schedule:

- Stage 2A, completed successfully in 2016: it involved the retrofit of the preventive protection functions to create clear defense in-depth lines
- Stage 2B, completed successfully 2017: it involved the retrofit of the accident management systems
- Stage 1, completed successfully in 2018: it involved the retrofit of the reactor control power limitation system as well as reactor trip system together with manual and automatic backup system

2.4 Conclusion and key success factors

The challenges of this project were numerous: a tight schedule, the cohabitation of new and old systems, the large scope covered with improvements and modifications of the architecture.

To guarantee the success of this project, Rolls-Royce leveraged the return of operating experience from large modernization projects such as the Dukovany power plant in Czech Republic (2 VVERs) or on the French EDF fleet. For the past decades, Rolls-Royce gathered a sizeable experience and know-how to manage complex projects fitting with customers' requirements and project specificities of all type (sizes, technologies, etc.)

To do so, great synergies were created with end-user (Fortum), subcontractors (e.g. INSTA for the installation) and suppliers (e.g. PROPLAN for the control panel). This close cooperation with local partners was a major lever for the success of such modernization project, thanks to the in-depth engineering dialogue with these stakeholders.

Finally, the capability of Rolls-Royce's digital safety platform Spinline to adapt to existing interfaces with limited new-development and no impact on original equipment made possible its fast deployment and on-site installation. Its renowned robustness, careful development and proven technology eased the licensing process toward one of the most stringent safety authority in the world (the Finnish STUK), and permitted Spinline to be used for safety classified systems.

As a result, four years after being awarded the contract, Rolls-Royce successfully modernized the safety I&C systems of Loviisa NPP, with the restart from outage of the last unit in October 2018. According to Mr Forsstrom, Automation Modernisation Project Owner at Fortum, "the implementation of the new safety systems was completed on time, within budget and according to high quality and required safety standards" thanks to an "extensive pre-planning phase, proactive schedule management and continuous improvement during the project".

3 SECOND STUDY CASE: LINGAO POWER PLANT

3.1 Context

The Lingao power plant comprised four nuclear reactors and operated by China General Nuclear Power Corporation (CGN). It is located on the Dapeng Peninsula, at the north of Hong Kong in Longgang District, Shenzen.

Units 1 and 2 are 950MWe PWRs commissioned in 2002 and 2003, based on the French three cooling loops design. Two additional units (3 and 4) started commercial operation later (2010 & 2011) and are based on another design: China's first domestic CPR-1000 reactors.

In 2012 CGN chose Rolls-Royce to modernize the analog Neutron Instrumentation System (NIS) initially installed on the two oldest units. The original NIS was based on SILIMOG, an analog technology installed by Rolls-Royce on the 900MW French fleet since the 1980s, hence on the Lingao 1 and 2 which are based on the same design. The main goal

of this modernization project was to replace this system by the latest digital NIS of Rolls-Royce, underpinned by the safety platform Spinline.

As Rolls-Royce initially installed SILIMOG at Lingao in the early 2000s, a first modernization of the neutron instrumentation systems after only a decade of operation may seem premature considering the robustness of the installed analog systems. In fact, this decision was mainly driven by CGN will to harmonize its I&C systems across the fleet: all of other reactors owned by this Chinese state owned enterprise embedded Rolls-Royce NIS digital technology, expect the two units aforementioned. As a matter of fact, 20 units including Lingao 3 & 4 were already using the Spinline technology for this safety function. CGN hence decided to upgrade the NIS of Lingao 1 & 2 units to standardize systems across the fleet and optimize spare parts ordering and other maintenance activities, hence increasing the efficiency of long-term services offered by Rolls-Royce.

3.2 Main project-related challenges

Although it consisted of the partial I&C modernization of two units, this project and its challenges are not directly comparable to the Loviisa retrofit, in terms of size and type of upgraded systems.

First of all, a generic yet crucial challenge when coming to modernization projects is adapting new equipment to existing interfaces. This concerns for example cabling, available place, electrical features, power supplies, etc. Moreover, as in this case the replacement only concerned one safety function, the neutron instrumentation systems, specific actions were taken to limit the changes in architecture and facilitate the integration of the new system. The Spinline technology permitted to reach this goal, thanks to the flexibility and adaptability of this safety platform. Nevertheless, new specific safety hardware were designed and manufactured in order to avoid modifying equipment remaining on-site, hence reducing the scope to be covered for the given functionality required by the final customer.

In this case, the new system had to be commissioned in a tight time schedule, according to a predefined outage period of the reactors. The new NIS hence had to be installed and tested during one outage without increasing its duration.

Finally, the installed systems had to be developed integrating the possibility for the customer to modify some parameters in accordance with local safety authorities. This could for example be required by the eventuality of a power uprate for the two reactors. Such flexibility of the offered systems can be of major interest for operators of research reactors, who may require different neutron level threshold depending on the experiment or core configuration.

3.3 Schedule and offered solution

For this retrofit project, Rolls-Royce was in charge of designing and manufacturing the equipment, as well as delivering and supporting their installation, in close collaboration with local partners. To provide a robust and performant neutron instrumentation system which could easily adapt to existing interfaces, Rolls-Royce offered a solution featuring both analog and digital technologies. This last one is underpinned by Spinline technology, embedding a 32-bit microprocessor, communication gateway and a 10mb secured network.

Regarding the global architecture, 6 electronic cabinets per unit have been replaced, including the conditioning and processing ones. The NIS architecture displayed on the following diagram shows the actual need for adaptability (colored equipment remaining unchanged) and integration of the upgraded solution with a limited scope:

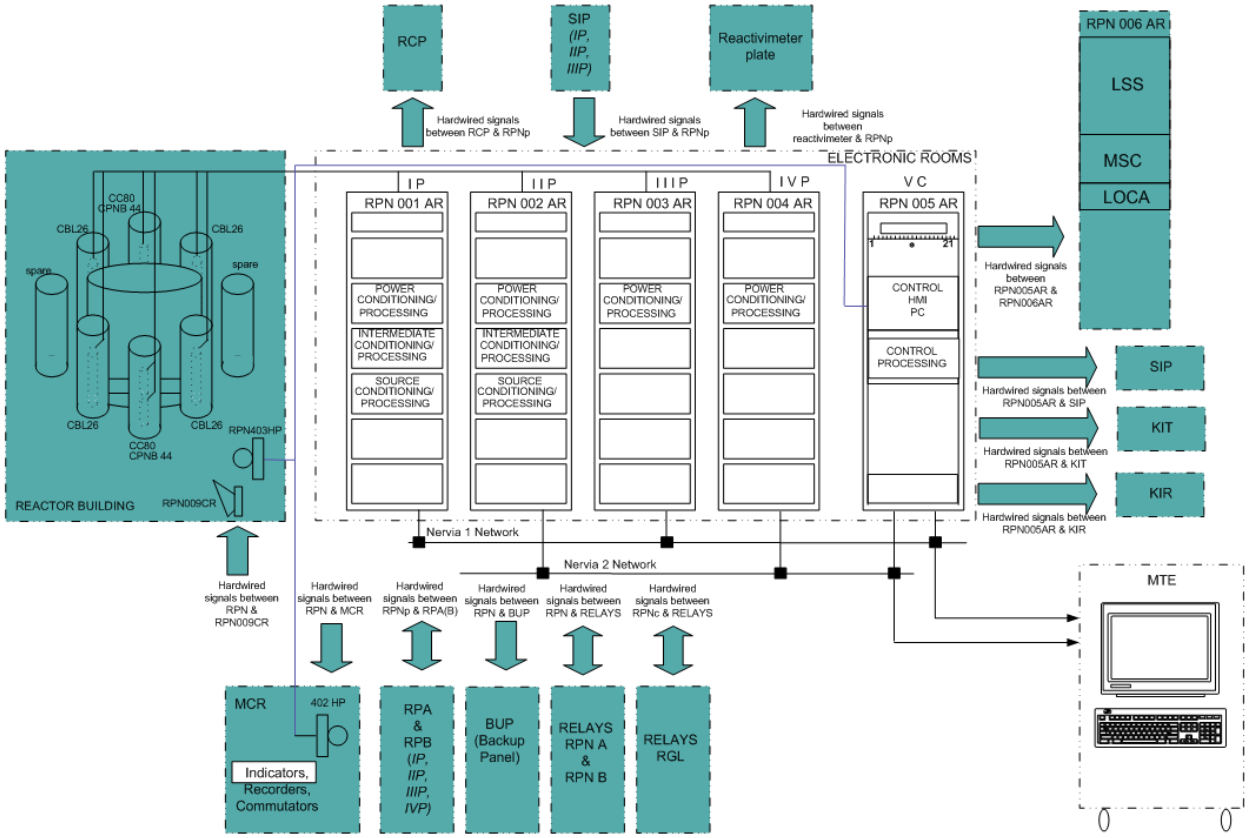

Modified systems on the NIS architecture (non-colored)

As a result, one can see that using the Spinline technology, the following new equipment have been installed for the modernization:

- 4 NIS protection cabinets IP, IIP, IIIP and IVP
- 1 NIS control cabinet VC
- 1 Maintenance Test Equipment (MTE)
- 1 Laptop computer (LDU)

Following the contract award, the design, manufacturing and validation of the systems were completed in around two years in Grenoble, France. They were then sent to China and installed by the plant operator with Rolls-Royce supervision and support. The onsite installation was completed successfully within one power outage of 45 days in November 2016.

3.4 Conclusion on key success factors

This modernization project varies greatly from ELSA presented in the previous section as the main goal was to replace a small scope of the global safety I&C, in this case the Neutron Instrumentation Systems. This experience can be relevant for research reactors as the scope is generally smaller for these facilities, and interfaces with existing systems must be ensured.

For the Lingao project, the adaptability of the installed solution was a critical point. Rolls-Royce Spinline platform is renowned for implementing new digital technologies while still ensuring the compatibility with the non-modernized equipment.

Moreover, performant integration was also the result of Rolls-Royce great knowledge of global architecture and analog technology which had to be replaced, hence reducing the scope of the modernization and fitting customer's requirements at best.

In addition, extensive collaboration between Rolls-Royce and the end-user, i.e. plant operator, permitted the smooth success of this project. This collaborative approach with the customer was taken from the design phase to the onsite installation to ensure the completion of this modernization on time. Moreover, Rolls-Royce local presence and great experience in China strengthened this relationship.

Finally, Rolls-Royce long experience with modernization projects covering a wide range of reactor type and project size, along with a particularly efficient project management were key factors for the successful installation of a new digital NIS on time and during an outage period.

Consequently, the Lingao 1 & 2 project was the first I&C modernization program in China, and Rolls-Royce completed it successfully. The new digital neutron instrumentation technology ensures the long-term safety and performance of these units, and improves maintenance management for the operator by harmonizing its neutron instrumentation across the fleet. This success was well recognized by the Chinese customer; the Lingao I&C retrofit manager expressing his "complete satisfaction of the quality of Spinline technology, as well as the project execution especially the respect of schedule and the on-site assistance."

4 THIRD STUDY CASE: MASURCA RESEARCH REACTOR

4.1 Context

Although the previous study cases just presented were related to I&C modernization of NPPs, Rolls-Royce also performed an extensive number of retrofit for the French fleet of research reactors, after having installed its original systems on a larger number of them. This is due to the fact that the company initially developed through a partnership with the CEA, the French Atomic Energy Commission. The joint creation of neutron detectors and reactivity meters was indeed at the base of the creation of Merlin Gérin nuclear division, which was later acquired by Rolls-Royce. The CEA remained strongly bounded to this entity through the years, Rolls-Royce offering I&C solutions for the neutron and protection systems of a dozen research reactors operated by the CEA, France currently having the fifth largest RRs fleet in the world.

4.2 Presentation

MASURCA is a fast reactor dedicated to studies on hard neutron spectra, using a unique design based on forced airflow cooling. This critical mock-up which operates at a maximum power of 5kW first reached criticality in 1966. The facility is located at CEA's largest research center in Cadarache, south of France. In 2004 a complete refurbishment of the facility was decided, and Rolls-Royce was chosen to replace parts of the safety I&C systems initially installed. Equipment involved in the frame of this modernization program was the neutron flux measurement and reactor trip systems.

The MASURCA refurbishment just followed another modernization for the CEA, the ISIS reactor. This RR being a 700kW pool-type design, this proves the adaptability of the installed analog and digital solutions offered by Rolls-Royce, which is suitable for a wide range of core powers and designs.

4.3 Main project-related challenges

At the time the project was awarded to Rolls-Royce, MASURCA was expected to become a reference tool for research on hard neutron spectrum and Generation IV reactors. I&C systems of the reactor had already been upgraded in 1986 using hardwired technology, but further improvements had to be made in order to ensure the compliance with upgraded safety requirements and permit the life-time extension of the facility. Such decision was also driven by the difficulty to maintain it in an operational state, due to obsolescence issues and difficulties related to spare parts provision.

In addition this retrofit project was a way to upgrade performances of control systems such as the precision, communication speed, human-machine interface etc. In the frame of the global facility retrofit, wiring and maintenance simplification were also part of the functional specification. A crucial point was also the compatibility of the new equipment with existing systems and modern supervision platform. In addition, installed system also had to adapt to detectors of different types provided by the CEA, which had to be tested and qualified before.

Another key point related to this project was the discrepancies with other modernization exercises previously performed on research reactors. As a matter of fact, the scope for the ISIS project mentioned earlier was way larger, as it involved the replacement of Rod Control, Neutron Instrumentation System and Reactor Protection systems as well as the console in the main control room. Challenges are hence different because compatibility issues were less severe, more systems being involved.

Moreover, additional challenge for this project was the use of an upgraded technology which had never been used before for a research reactor and their specific I&C architecture: this new version embedded a 32-bit microprocessor based on Spinline 3 -Rolls-Royce digital safety platform- while keeping the architecture installed on previous reactor using older version of this technology (OSIRIS in Saclay, EOLE in Cadarache etc.)

Equipment was qualified to the most stringent seismic and electromagnetic standards, and software also had to comply with the following norm:

- Software safety standard IEC 60880.
- Electrical equipment standard IEC 60980.
- Electromagnetic compatibility IEC 61000.

Although no specific software development was needed, modifications to adapt the installed system to the unique MASURCA design were performed, e.g. thresholds and other parameters.

Finally, Rolls-Royce supervised the cabinets' installation on-site and tested them for ten days. CEA employees were also trained to use this new digital equipment, Two months later, cabinets were dissembled and stored for the complete refurbishment of the MASURCA facility.

4.4 Schedule and offered solution

Basing on an already proven architecture, yet using an upgraded technology, the offered solution was delivered on time, and in accordance with the customer schedule, i.e. before the total refurbishment of the facility. As a result, the new equipment was operational in parallel to the initial systems 16 months after the contract award:

The offered solution was based on a proven architecture for research reactors, based on 2 redundant identical measurement channels featuring:

- 2-level detection to cover the total flux dynamics, using detectors provided by the CEA to which Rolls-Royce had to adapt
- Signal conditioning and processing realized by 2 rigorously identical cabinets.
- Asynchronous communication system.

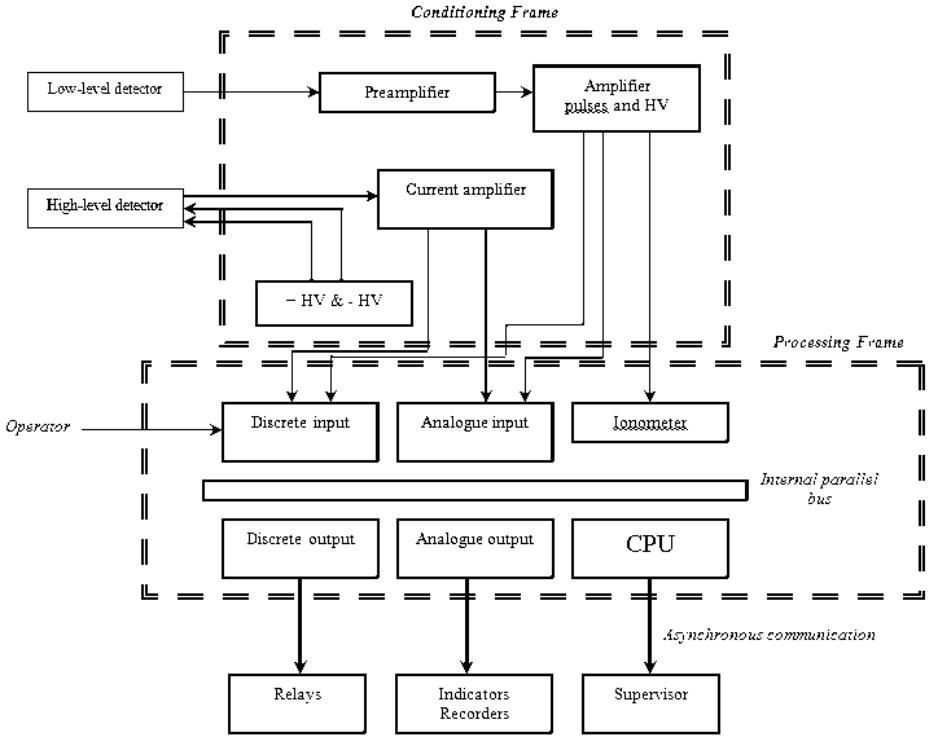

Architecture of the SIREX solution for one channel

The displayed solution uses the architecture already commissioned on different experimental reactors, namely the SIREX. This project was first developed in 1988 together with the CEA to offer a universal neutron instrumentation solution for the entire French fleet of research reactors and was installed on 7 of them during the 90s.

As a result, no new software development was required and the global functions are identical to the ones of the previous generation. The technology proposed was however improved based on Spinline 3, Rolls-Royce most advanced digital platform at this time. Such system is used to measure the neutron flux, to monitor continuously the instantaneous core power and its evolution using doubling time. Using these parameters, it permits to provide information on the reactor state and triggers alarms and emergency shut-downs following flux variations.

4.5 Conclusion on key success factors

Rolls-Royce long experience with safety I&C systems for both NPPs and RRs has been very valuable for the conduct and success of this project. As said previously, the company is present since the early times of the research reactors development, installing RPS for a large number of facilities in France. This accumulated experience is profitable for newer projects, and Rolls-Royce long-term partnership with the CEA is very valuable in the relationship with research centers, and the understanding of their special needs.

In addition, a wide variety of reactors types have been covered thanks to the diversity of the French fleet. Indeed, the great adaptability of the Spinline platform for research reactors is a key parameter for the success of such modernization projects. Moreover, the use of this state-of-the-art digital safety platform presented many advantages such as upgraded performances, and redevelopment were limited thanks to the proven SIREX architecture and software.

The previous system was based on analog associated with hard-wired logic, namely Multibloc, installed by Merlin Gérin. The global architecture was obviously changed while upgrading the neutron instrumentation to digital; however our understanding of the installed system permitted to adapt to existing equipment.

Project management was also an important point for the successful completion of this retrofit. The new system was delivered and tested in less than 16 months after the award

date, in parallel with the end of ISIS complete upgrade. This was made possible thanks to the close cooperation with client and suppliers, as well as Rolls-Royce fast understanding of research facilities' specificities.

5 GENERAL CONCLUSION

Modernization and deployment of new safety I&C systems is often seen by research reactors operators as complex and risky, mainly because of the qualification and licensing phases. However, Rolls-Royce has been a major actor in the transition to digital for research reactors in France, with for example the modernization of OSIRIS I&C at the beginning of the 90s, and more recently ISIS and MASURCA. These successes were also leaning on the gathered experience from larger modernization of nuclear power plants.

As a result, Rolls-Royce has now more than 50 years of experience in I&C for nuclear, in particular in safety classified I&C systems with equipment installed on more than 200 civil nuclear reactors worldwide and on most of the French research reactors. From this experience with retrofit, one can highlight the following best practices for I&C modernization projects on NPPs or RRs:

- The use of a proven and adaptable technology, e.g. Rolls-Royce digital platform Spinline, is necessary. It indeed permits to address easily the specificities of each reactor, whatever the size or the type, with no need to implement major changes.

- The experience in designing and implementing I&C architecture is required. To do so, knowledge of both digital and analog technologies, which are still largely present on research facilities, is crucial because the communications between all the plant systems is a key point of the defense-in-depth concept, and retrofit projects often mix different type of technologies.

- The upstream safety qualification of the used technology for NNPs and in several countries is a big advantage. It indeed permits to ease the licensing process and increase the efficiency of the overall project, which is beneficial for operators of both power plants and research facilities.

- Communication with the local safety authorities as well as extensive relationships with the end-user of the modernized systems and project management are also crucial for the success of a retrofit project

All these competences have been mastered over the years by Rolls-Royce, which is now carrying out the largest safety I&C modernization in the world with the 1300MW French fleet. The adaptability of the offered technologies, both digital and state-of-the-art analog, as well the capacity of Rolls-Royce to handle projects of all sizes in parallel makes it also able to work on I&C modernization of research reactors, as seen in the recent past.

HARDLINE™: HARDWIRED SAFETY I&C TECHNOLOGY FOR RESEARCH REACTORS

ARNAUD DUTHOU, ALAIN BOUE
Rolls-Royce Civil Nuclear
23, Chemin du Vieux Chêne, Meylan 38240, France
Arnaud.Duthou.cn@Rolls-Royce.com ; Alain.Boue.cn@Rolls-Royce.com

ABSTRACT

As the existing Research Reactors fleet is ageing, it becomes increasingly difficult to maintain old analog systems.

To meet the demands of Research Reactors to modernize their safety I&C with analog technology, Rolls-Royce has developed HARDLINE™. This modern, performant hardwired platform can be used for Cat. A / 1E safety I&C applications such as the main Reactor Protection System for Research Reactors or the Diverse Protection System for NPPs.

Hardline technology is particularly suited to research reactors as standardized safety modules are assembled to provide a wide range of I&C functions.

Leveraging the use of modern components associated with more than 50 years of experience with the design and use of non-programmed technologies for Nuclear safety I&C, Hardline platform provides the following features:

- Safety & availability: failsafe, separation of functions and channels
- Enhanced Self-diagnostics and periodic tests, optimized cabling, simple components reducing risks of failure
- Simple to license
- Standardized and adaptable: only front access needed in new cabinets, reduced footprint, racks can be integrated in existing cabinets

Hardline platform has been developed to meet IEC and RCC-E standards for Cat A functions, and US NRC 1E requirements.

This paper will present the suitability, possible uses and benefits of Hardline platform for research reactors I&C.

Key Words: Safety I&C, Reactor Protection System, Licensing, Hardwired

1. Introduction

The main I&C protection system of the first Nuclear Power Plants (NPP) and Research Reactors were implemented with analog technologies. However, they have more and more been replaced by Programmed microprocessor-based systems to handle the growing number of parameters and complex functions to handle.

Nevertheless, the software code necessary to program these systems requires long and costly verification & qualification phases to meet regulations, discouraging many Research Reactor teams planning a modernization. This has generated a renewed interest for the Hardwired systems, which are generally simpler to qualify.

As the existing Research Reactors fleet is ageing, it becomes increasingly difficult to maintain old analog systems: components are not manufactured anymore, they may drift over time, they are difficult to modify and adapt to new regulations or functionalities requirements.

To meet the demands of Research Reactors to modernize their safety I&C with analog technology, Rolls-Royce has developed HARDLINE. This modern, performant hardwired platform can be used for Cat. A / 1E (and below) safety I&C applications such as the main Reactor Protection System for Research Reactors or the Diverse Protection System for NPPs.

1.1 Research Reactors I&C

According to the IAEA Research Reactor Database (RRDB), (IAEA) 151 nuclear research facilities have reached their first criticality more than 40 years ago [1], this represents about 2/3 of operating facilities.

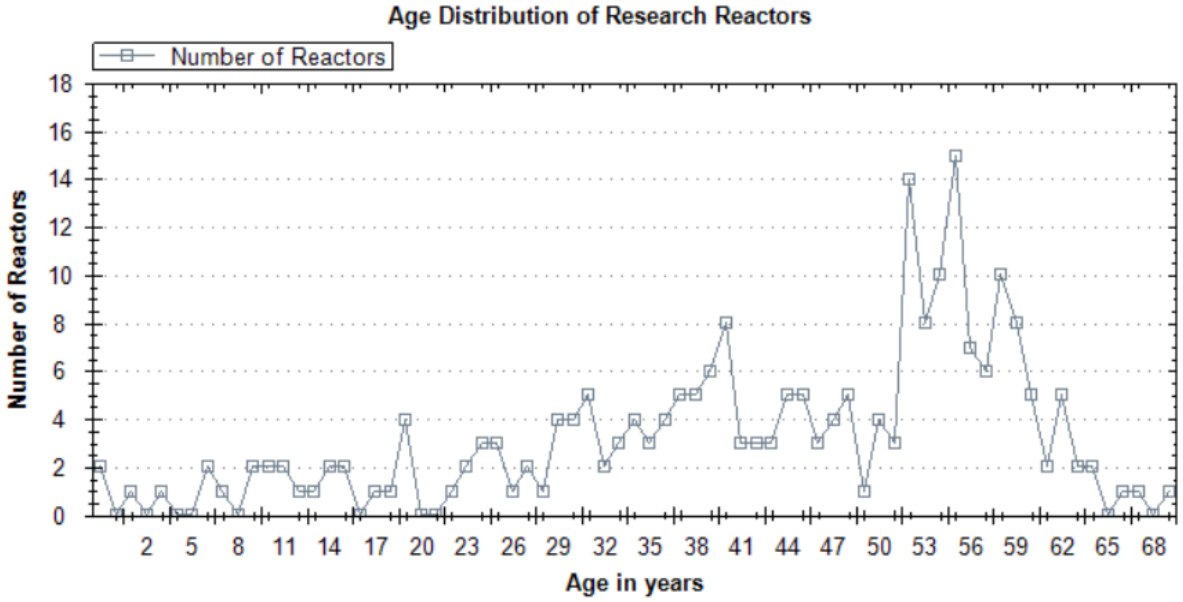

Figure 1: Age distribution of research reactors (IAEA RRDB)

Although some of them have modernized their systems, often due to obsolescence, for upgrades to reach higher fluxes, accommodate new experiments or to meet new safety requirements, most of them have not significantly modified their Safety I&C systems and still operates with their original equipment, often analog.

In that context, it is increasingly hard for them to meet all the new demands both in term of new utilization or experiments and safety requirements imposed by local regulators.

Research reactors have a broad range of uses, from isotopes production to material analysis and non-destructive testing and can be based on multiple types of design: the most commons are pool-type reactors, in particular the TRIGA design, but we can also find heavy water or graphite moderated and even a few fast reactors.

This means that the characteristics of their Instrumentation and Control equipment can greatly vary from one Research Reactor to another. Therefore it would seem natural for them to adopt Digital, microprocessor based platforms for their I&C as these are perceived to be more adaptable and could accommodate new requirements more easily. Unfortunately, the licensing of such programmed equipment has become increasingly complex and often costly in particular for the highest safety standards such as NRC 1E or IEC cat A.

Here are some of the main I&C functions of a research reactors and their safety classification according to IAEA:

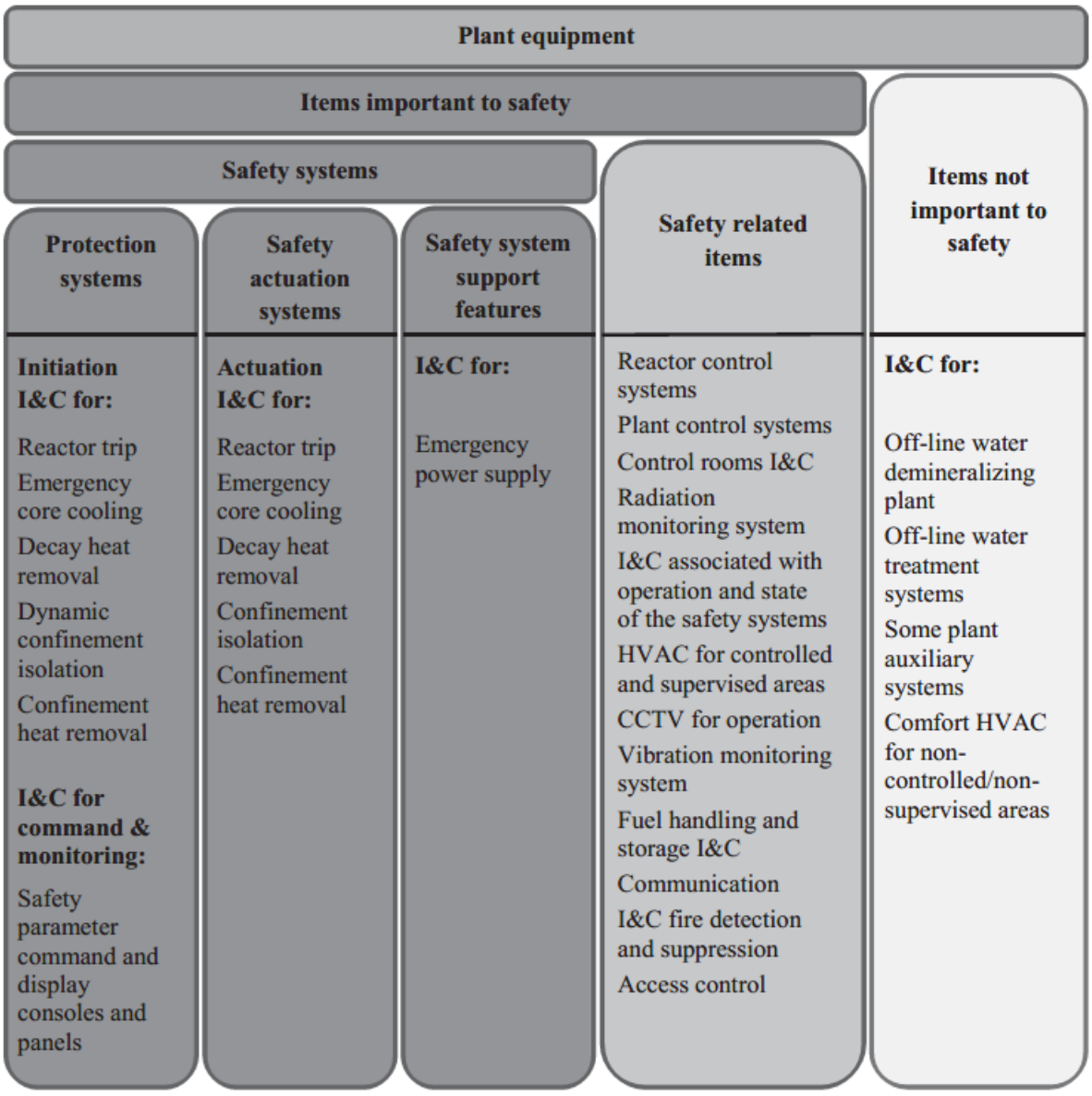

Figure 2: Example of I&C systems of a research reactor classified according to their importance to safety [2]

In that regard, Research Reactors I&C safety functions are quite similar to Nuclear Power Plants equivalent functions but the complexity and number of data to monitor and analyse are usually less demanding. This reduces the performance requirements of the systems used, and allows for a larger choice of technologies possible to implement these safety functions.

1.2 Non Programmed Analog Technologies

Microprocessor-based systems' capacity to process a large amount of complex data as well as the increasing difficulty to maintain older analog equipment led to the steady replacement of the hardwired technologies installed at the plant construction. However, their potential complexity and licensing cost, combined with new safety requirements, has generated a renewed demand for the non-programmed/Hardwired technologies that are usually simpler and cheaper to license.

As analog systems still have performance limitations, they are rarely use for the complete protection system of modern complex reactors or architectures. Nevertheless, they are well adapted for other functions such as diverse actuation systems, priority logic, post-accident systems or even main protection systems for simple architectures such as research reactors'.

Unfortunately, most existing "non-programmed" technologies did not evolve much since their creation several decades ago and as a consequence suffer from obsolescence issues and processing capability limitations. Thus the design of a truly modern, performant and purely hardwired safety I&C technology represents a progress in the catalogue of next generation technologies available for 1E/Cat A. safety I&C.

1.3 Rolls-Royce & Research Reactors

The CEA, the French Atomic Energy Commission, is a longtime partner for Rolls-Royce Nuclear I&C. Indeed, an early cooperation with the CEA on neutron detectors and reactivity meter was at the base of the Merlin Gérin nuclear division's creation in the 60s (later Merlin Gérin Nuclear division was acquired by Rolls-Royce). This strong link remained throughout the years, and Rolls-Royce was the **main I&C supplier for a dozen of research reactors** owned and operated by the CEA, the fifth largest fleet in the world.

In parallel, Rolls-Royce Civil Nuclear is currently supplying its I&C Digital safety and safety-related technologies in more than 80 nuclear facilities, in particular in France, China and Finland. Rolls-Royce nuclear I&C equipment is now installed in more than 200 Nuclear power plants in the world. With more than 50 years of experience in Nuclear I&C, Rolls-Royce has led several major I&C modernization projects in the world, on multiple types of reactors: Dukovany, Czech Republic (4 VVERs), 900 MW PWRs French fleet (34 units), 1300 MW PWRs French Fleet (20 units). More recently Rolls-Royce was awarded the modernization project of the safety I&C systems of two Fortum plants in Loviisa, Finland, based on the same methods proven during 1300MW modernization. The company was also the original I&C supplier for the French fleet of research reactors, and carried out several modernization projects in this field until 2007.

2. Research Reactors I&C

In order to demonstrate how Hardline can be used to implement the safety functions of research reactors we will first list the functions that must be realised and the corresponding standards.

2.1 Main safety I&C functions

The research reactors architecture and I&C can vary a lot depending on the specific tasks they were built to accomplish and local regulations. Nevertheless we can extract groups of similar functions that are used on all of them as they form the base of reactor protection systems.

A first group of safety functions consists in generating reactor trips. Several types of trips, whose number & relevance depend on the reactor architecture, are generally considered:

- Reactor Trip on High neutron flux
- Reactor Trip on High Power
- Reactor Trip on High neutron period / rate change

- Reactor Trip on High fuel temperature
- Reactor Trip on Low Primary Coolant Flow
- Reactor Trip on Low Reactor Pool Water Level
- Reactor Trip on failures of the conditioning units of the above signals (e.g.: neutron sensors high voltage…)
- Reactor Trip on Manuel Command in Main Control Room
- Reactor Trip from other I&C involved in essential reactor control devices (rod controls, rod position instrumentation…)

A second group of safety functions consists in managing interlocks to allow temporary and safe inhibition of reactor trips when the reactor is starting.

A third group of safety functions consists in starting Engineering Safety Actuation Features (ESFAS) after a trip to remove residual heat. Many research reactors have an intrinsic safe design, providing these features without any I&C. However, increase in safety regulation requirements might create a need for new or reinforcement of existing features that the new Safety I&C will have to implement.

2.2 **Classifications / Standards**

When it comes to Safety I&C, mainly the protection system, the classifications and standards are similar to power reactors:

The system itself is to be classified 1E / A

The relevant standards for this class of systems apply, in particular:

IAEA Safety Series No. 50-SG-D3	Protection Systems and Related Features in Nuclear Power Plants, A Safety Guide (1980).
IAEA Safety Series No. 50-SG-D8	Safety Related Instrumentation and Control Systems for Nuclear Power Plants, A Safety Guide (1984).
IEC-60671	Nuclear power plants - Instrumentation and control systems important to safety - Surveillance testing
IEC-60709	Nuclear power plants - Instrumentation, control and electrical power systems important to safety - Separation
IEC 60780-323	Nuclear facilities – Electrical equipment important to safety – Qualification
IEC 60812	Failure modes and effects analysis (FMEA and FMECA)
IEC-60880	Nuclear power plants - Instrumentation and control systems important to safety - Software aspects for computer-based systems performing category A functions
IEC 60980	Recommended practices for seismic qualification of electrical equipment of the safety system for nuclear generating stations
IEC-61226	Nuclear power plants – Instrumentation and control important to safety – Classification of instrumentation and control functions
IEC 61513	Nuclear power plants – Instrumentation and control for systems important to safety – General requirements for systems
IEC 62566	Nuclear power plants – Instrumentation and control important to safety – Development of HDL-programmed integrated circuits for systems performing category A functions
IEC 62808	Nuclear power plants – Instrumentation and control systems – Design and qualification of isolation devices
IEEE-7-4.3.2	Standard Criteria for Digital Computers in Safety Systems of Nuclear Power Generating Stations.

3. Hardline description

The Hardline platform is the result of the evolution of non-programmed nuclear-specific technologies developed by Rolls-Royce such as Multibloc, Silimog, ULS Dynamic Logic and Modumat. It takes into account all the benefits of these technologies with great operational experiences (more than 200 non-programmed systems still currently operate in nearly 100 plants).

Hardline is fully diverse from any digital I&C system: all safety functions are realized with non-programmed discrete electronics components.
Although hardwired systems have more limited data processing capabilities than programmed technologies and usually cannot be used efficiently for the complete protection system in complex NPPs, Hardline was developed to be able to address most safety I&C functions requiring Class 1E / Cat. A certification and is thus adapted to Research reactors protection systems.

As a result, a special care was given during the development phase to meet Research Reactors Safety protection functions.

First of all, the design criteria to create such platform were chosen in regards to the highest standards, in particular:

- Purely hardwired safety functions thanks to the use of non-programmed discrete electronics components
- High degree of both safety and availability
- Reduced footprint
- Optimized cabling management systems
- Quick and easy setup from design to installation
- Easiness of operation & maintenance with integrated monitoring & diagnosis features
- Flexibility to be integrated into existing cabinets or to be delivered in new cabinets
- Meet harsh Environmental qualification constraints

Then, high capabilities and performance were implemented using state of the art electronic features such as:

- Integrated physical one-way communication (diode network) for secured communication with control and monitoring systems
- Independence and separations of functions and channels
- Wide range of I&C functions

Finally, Hardline platform meets design requirements for the qualification of the to the most stringent safety standards.

3.1 Functions

The platform can implement RPS safety functions thanks to purely Hardwired modules that are completed with separate dedicated communication, diagnostic and surveillance modules

Figure 3: Hardline modules

In particular:

Binary and Analog input: • Sensor conditioners • EMC filters • Test mode switches Analog processing: • Adjustable high & low thresholds with hysteresis • Signal selectors Output: • Inhibition for tests • Output relays • Signal isolators	Binary: • Voter (1oo2, 2oo2, 2oo3, 2oo4..) • Relay-based logic circuits (OR, AND, NOT..) • Actuator control logics • Time delay controls • Signal selectors Monitoring: • Analog & binary isolated digital converters • Communication gateways Test: • Test panels for automatic tester • Communication gateways

3.1.1 Safety modules

Isolation and separation function is realized with non-programmed electronic components that ensure electrical isolation, functional separation and independence between safety functions and communication modules.
Only one-way data exchange is permitted from safety modules to communication modules. Isolation and separation function is designed and qualified according to IEC 62808 ensuring that no failure can be propagated from the communication parts to safety modules.
Isolation and separation function is integrated in safety modules, and is safety qualified.
List of main safety modules:

Table 1: list of main safety modules

Module ID	Function	Input/Output signals
A. THR 1	Adjustable high or low thresholds	Input: 0(4)..20mA / Outputs: dry contacts
A. ISO 1	Analog isolators	Input: 0(4)..20mA / Outputs: 0(4)..20mA
A. THC 1	Thermocouple type K conditioners with external compensation (0..1300°C)	Inputs: 0..60mV / Outputs: 4..20mA
A.RTD 1	PT100 conditioners (0.400°C)	Inputs: 100..247mV / Outputs: 4..20mA
B.REL 1 B. REL 2	SPDT relays with NO and/or NC contacts	Input coils: 24VDC Output contacts: dry contacts
B. REL 1	SPST relays with NO contacts	Input coils: 24VDC Output contacts: dry contacts
B. SEQ 1	TON, TOFF and TPULSE adjustable time delays and latch functions	Inputs: 24VDC / Output: dry contacts
B.PRIO ..	Priority control logic	Inputs: 24VDC / Outputs: : 24VDC
B. TST 1	Test switching features	Input and output signals: 0(4)..20mA or 24VDC Test switch command: 24VDC coil
P.DC/DC 1	24VDC isolated DC-DC converter	Input & output: 24VDC

3.1.2 Communication modules

Hardline communication modules provide one-way communication features with other I&C digital systems. As shown in Figure 4, the monitoring communication module C.11 COM 1 allows monitoring up to 11 safety modules. It is associated with Hardline Gateway allowing unidirectional communication from up to 22 units to an upper-level monitoring and diagnosis system.

3.1.3 Monitoring and Diagnostic modules

Each safety module has a one-way serial data link to provide essential signals to communication module. The communication module has a one-way serial datalink to the Hardline Gateway which communicates with an external diagnosis unit.

These external monitoring systems feature:

- Gateway capabilities to interface with higher level plant control systems
- Alarm management possibilities
- User interface for troubleshooting

3.1.4 Local HMI

Local HMI on the front panel of a Hardline cabinet is provided with a standard set of keys, push-button, LEDs to manage test mode and allow troubleshooting. Dedicated local HMI can be customized upon request.

3.2 Mechanical

Hardline modules are installed in standardized cabinets and racks. Hardline cabinets only require front access but deeper two sided cabinets can be used to densify the number of modules per cabinet.
The cabinets are IP31 and meet harshest seismic qualification requirements. The racks and cabinets can be configured to their specific functions after production (“delayed differentiation”) allowing for shorter delivery times and possible adaptations late in the design phase.

Figure 4: Hardline cabinet and rack

3.3 Standards / Technical specifications

Hardline has been developed in accordance with the following rules and standards:

Table 2: Main standards for Hardline

International	IAEA GSR part 2	Leadership and Management for safety (2016)
	IAEA SSG-30	Safety classification of structures, systems and components in nuclear power plants (2014)
	IAEA SSR-2/1	Safety of nuclear power plants: design
	IAEA SSG-2	Deterministic safety analysis for nuclear power plants
	IAEA SSG-39	Design of instrumentation and control systems for nuclear power plants
	IEC 60671	Nuclear power plants - Instrumentation and control systems important to safety - Surveillance testing
	IEC 60780	Nuclear power plants - Electrical equipment of the safety system - Qualification
	IEC 60812	Analysis technique for system reliability: procedure for failure mode and effect analysis
	IEC 60980	Recommended practices for seismic qualification of electrical equipement of the safety system for nuclear power stations
	IEC 60709	Nuclear power plants - Instrumentation and control systems important to safety - Separation
	IEC 60068-2 series	Environmental testing
	IEC 60987	Hardware design requirements for computer based systems
	IEC 61000-4 series	Electromagnetic compatibility
	IEC 61226	Nuclear power plants - I&C systems important to safety - Classification of I&C functions
	IEC 61513	Nuclear power plants - I&C systems important to safety - General requirements for systems
	IEC 62566	Development of HDL-programmed integrated circuits for systems performing category A functions
	IEC 62808	Nuclear power plants - Instrumentation and control systems important to safety - Design and qualification of isolation devices
USA	10 CFR 50	General design criteria for nuclear power plants (appendix A)
	NUREG 800, chap.7	Standard review plan for the review of safety analysis reports for nuclear power plants
	IEEE 323	Qualifying Class 1E equipment for nuclear power generating stations
	IEEE 338	Standard for criteria for the periodic surveillance testing of nuclear power generating station safety systems
	IEEE 344	Recommended practice for seismic qualification of class 1E equipment for nuclear power generating stations
	IEEE 379	Standard application of the single-failure criterion to nuclear power generating station safety systems
	IEEE 603	Standard for criteria for safety systems for nuclear power generating stations
Europe	RCC-E	Design and construction rules for electrical and I&C systems and equipment
	RFS	French ASN - Fundamental safety rules for nuclear reactors
	CRT	Technical rules file (Cahier des règles techniques EDF)
	EN 55011 (A Class)	Industrial, scientific and medical (ISM) radio frequency equipment - Radio disturbance characteristics - Limits and methods of measurement
	EN 61000-6-2	Electromagnetic compatibility - Generic immunity standard
	EN 61000-6-4	Electromagnetic compatibility - Generic emission standard
	TS 61000-6-5	Immunity for power station and substation environments

4. Possible Hardline uses for Research Reactors I&C

4.1 Architecture

Based on the developed features and achieved performances, the Hardline platform is modular and can be used for a great variety of safety functions. A typical example of Hardline systems architecture is presented on figure 1. (This architecture shows the most complex design of architecture of a research reactor or of a NPP to better illustrate the adaptability of the platform and how it can connect to various systems).
This figure highlights the redundancy principle of the system, the geographical and electrical separation of the cabinets as well as the separation of Hardline modules in charge of safety function, monitoring and communication.

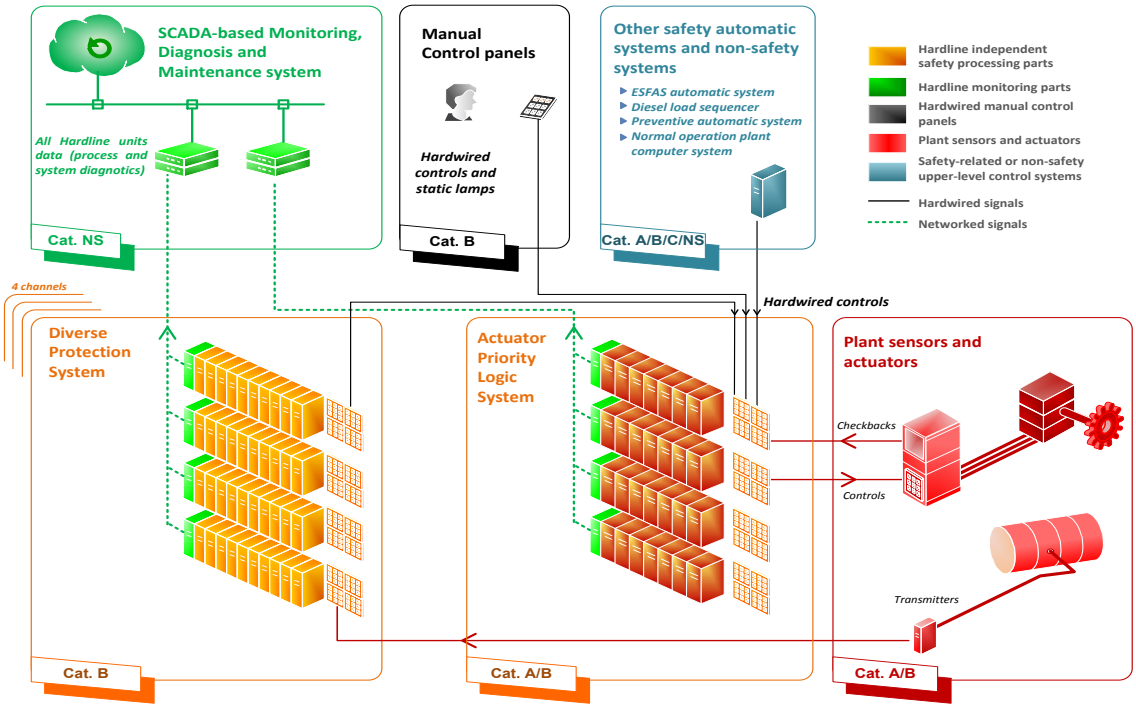

Figure 5: Possible Hardline architecture for typical application

This is how this architecture matches research reactors needs:

- The “Diverse Protection System” box of the figure becomes the main protection system of the reactor: implemented with Hardline, it provides all functions listed in §2.1. Using only analog (and up to date) technology, there is no risk of common cause failure due to common software across divisions, so there is no need for another diverse protection system.
- “Other safety automatic systems and non-safety systems”: on several reactors, there is at least a normal operation I&C, very often a digital one when a refurbishment has been done. In some cases, experiments using the reactor flux may implement a specific I&C, generally digital, which may need to limit the reactor capabilities below the safety thresholds to protect the experiment itself.
- The “Actuator Priority Logic System” is also based on Hardline. It allows each critical actuator to be safely controlled by several means: the Protection System, the Manual Control Panel, the “Other safety automatic systems and non-safety systems”. It makes sure that the order with the highest safety requirement has the highest priority.
- The “Plant sensors & actuators” box contains temperature probes, pools and/or vessel levels sensors, pressure transmitters (if any) and, most importantly, Neutron sensors and conditioning units. Rolls-Royce has a complete solution of Neutron Instrumentation System, pressure transmitters and temperature probes that can be implemented here.

As stated above, Hardline provides all functions needed to generate the trips listed at §2.1:

- Trips functions use the A.THR module to compare plant parameters (neutron flux, temperature…) to safety thresholds. If needed, thresholds detections can be voted by combining relays of the B.REL modules. The same B.REL modules are used to control actuators.
- Interlocks and permissives are implemented via B.REL modules
- Periodic Tests are implemented via the B.TST module

- ESFAS functions are based on sequential logic, implemented via B.REL modules, plus B.SEQ modules when timers and memories are needed.

The figure below is an example of a typical Hardline-based protection function, and how it is achieved with Hardline modules

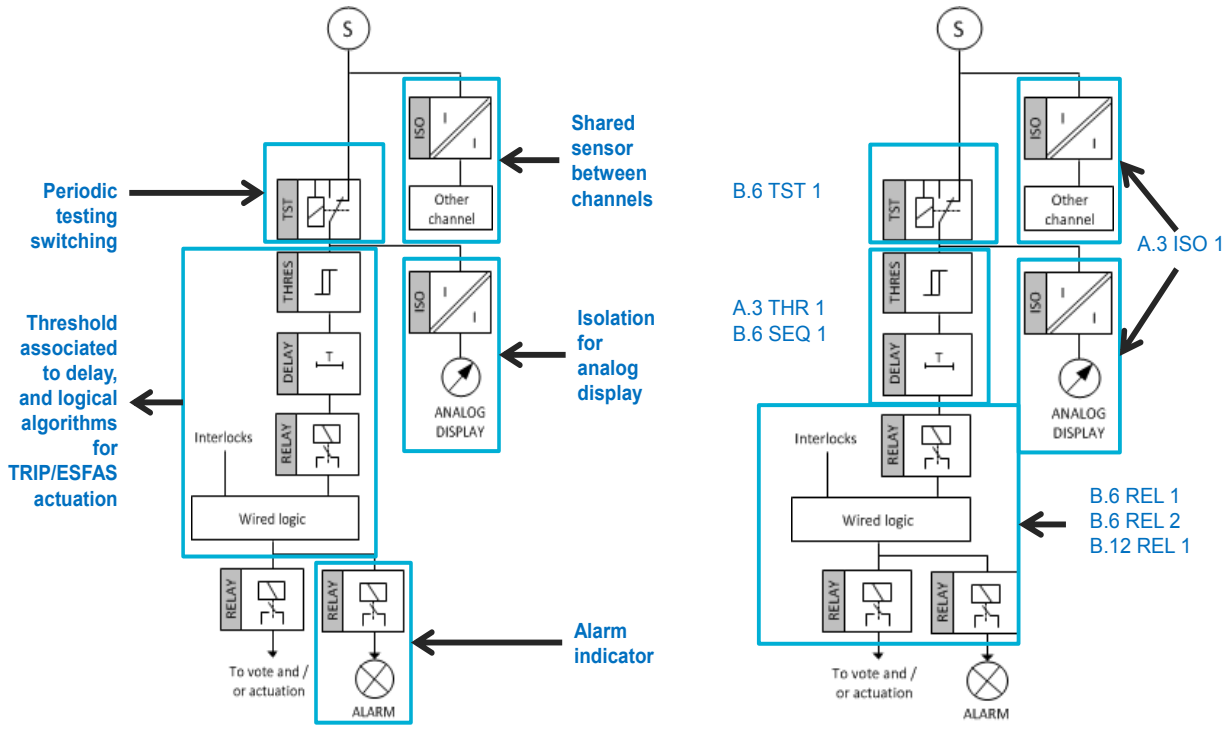

Figure 6: example of safety function implemented with Hardline modules

The simplicity of the modules and their flexibility is very well adapted to research reactors:

- It is easy for the reactor personnel to understand and master how each I&C function is implemented: there is no hidden function in some unknown software.
- Modifications and adaptations of the I&C can be needed to setup specific experiments: Hardline modular and straightforward architecture allows the reactor operator to master these changes without being heavily dependent on the original manufacturer of the technology.
- Hardline comes with a digital monitoring system. However, all Hardline I/O are analog, thus providing the maintenance engineer access to intermediate signals that are easy to measure and to check.

4.2 Signals, I/O

Signals needed to implement research reactor functions are taken in charge by Hardline modules:

- I&C formatted signals (4-20mA) can be connected directly to A.THR modules
- If a sensor is to be shared by functions that should be independent, the A.ISO module is used before A.THR
- Temperature signals are connected to A.THC or A.RTD
- Trips, ESFAS orders and all intermediate logic signals, such as interlocks, inhibitions, votes, are implemented via B.REL modules

Note that Neutron Instrumentation System signals (flux, ranges…) are delivered by a separate analog system that can be provided by Rolls-Royce, leader in this domain for more than 40 years.

4.3 Operation & maintenance

Hardline is easy to operate thanks to several features:

- Integrated monitoring and diagnosis features
- Local control and modules parametrization
- Field cables access
- Periodic tests integrated in the technology design
- Powerful engineering tool

4.3.1 Remote monitoring

Hardline integrates advanced diagnostic features with the highest separation between safety functions and monitoring devices:

- It begins with state-of-the-art hardware diagnostics capabilities implemented in each Hardline Modules.
- Then, each Hardline module sends on a dedicated line its critical parameters: health, inputs, outputs, operation modes, parameters,
- Each cabinet elaborates statuses of its own: power supplies, fans, door…
- These data are continuously acquired, consolidated and processed by an auxiliary monitoring system.
- This publication makes it easy to build both functional and maintenance views of the system. Functional views provide information to drive the system. Maintenance views give health status of the physical components of the system with the desired granularity: overall system, cabinets, racks, modules. Such a monitoring system can be installed either close to the cabinets or in a remote control room.
- The result is a software-free system that can be maintained and operated with the same efficiency as any other digital I&C system. The figure below is an example of such a monitoring system

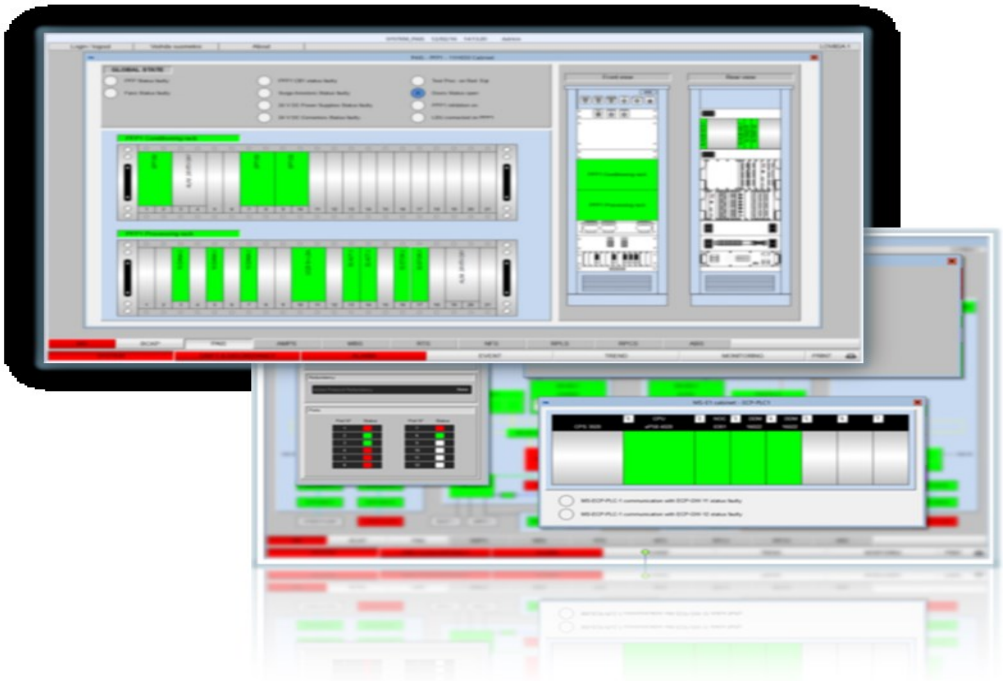

Figure 8: example of Hardline HMI for self diagnostics

When maintenance is to be performed, the faulty module / cabinet can be easily spotted thanks to LEDs on its front, giving indications of its status. The picture below shows several fronts of Hardline modules with their indication LEDs. Each module indicates its power supply status and the health (good operation) of its channels. Other indications, such as the test status, thresholds being triggered etc… are displayed according to the module functions.

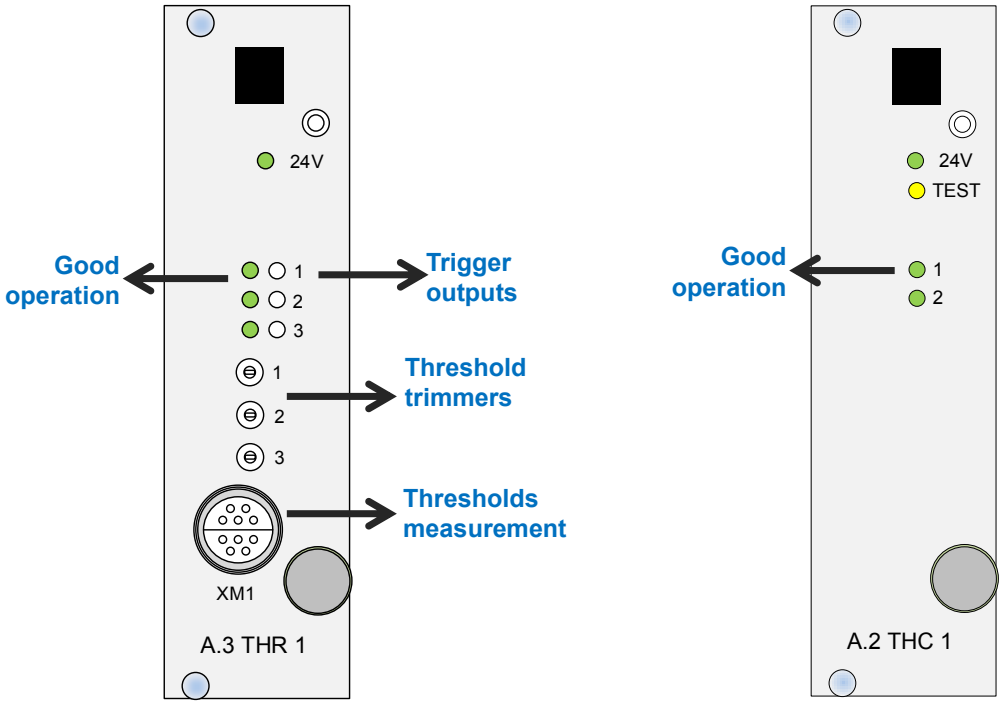

Figure 8: example of signals shown on modules front

4.3.2 Modules parametrization

Each module has several parameters that can be safely set via different means, depending on the parameter type. Threshold module is a good example of this versatility:

- The value of each threshold is set via a trimmer situated on the front of the module. A connector allows an instrument to measure the actual value set for the threshold
- The type Low or High of the threshold, is set via jumpers on the board itself,
- Some monitoring (such as sensor over current or sensor open loop) can be set of inhibited via jumpers as well,
- The safe position of the output is set very simply by choosing how to wire the output, using or not “good operation” dry contacts made available by the module. The documentation provided to Hardline users explains very clearly how wire to get the desired fail safe position.

4.3.3 Local control

On priority modules, it is possible to connect on the front of the module a special “button box”. It allows the operator to start or stop a specific actuator within the electrical room. Specific actuator tests can thus be implemented during special phases of plant maintenance.

4.3.4 Field cables access

In order to better fit in smaller Electrical rooms as in research reactors', Hardline cabinets are designed to host field cables close to the modules:

- The first main benefit is that there is no need for marshalling terminal blocks. The physical arrangement of the cabinet, the modularity of Hardline boards and the flexibility of the overall configuration allow each field signal to be directly connected to its Hardline module terminal block.
- This cabinet organization greatly simplifies the cabinet wiring, decrease the on-site installation procedures and test, facilitates the maintenance
- The changes that have inevitably to be performed during the life of an experimental installation are faster to implement.

4.3.5 Periodic tests integrated in the technology design

As illustrated in Figure 6, the B.TST Hardline module secures the periodic tests operation:

- Process and test signals are connected to this module
- The module acquires the order from the operator to start / stop the periodic test.
- This order switches all 6 inputs from process to test signal (start) or conversely (stop).
- The position of each 6 relays is read and sent to the monitoring system
- The design of the module, based on forced-guided relays, ensures that, if at least one of the signals is not correctly switched back to its process end, the malfunction is detected and the module prevents the tested division to be un-inhibited as long as the fault is not repaired.

With this module, Hardline makes it easy to design a simple protection system where periodic tests come with a very small footprint on the overall architecture and a straightforward mode of operation.

4.3.6 Engineering tool

A very powerful feature of Hardline is the engineering tool that supports systems configuration:

- It starts with a pure functional description of the system: which input / output signals, which operators are combined to provide the expected functions of the system
- This functional view can be simulated to help the system engineer to verify his implementation and to start to design his functional system tests
- Then, the functional view is broken down into an architecture view, showing which Hardline module implements which set of operators,
- In the end, the interconnection of field cables, modules and racks is automatically generated and the results can be imported in electrical and electronical CAD tools before being sent to the manufacturing of cabinets and backplanes.
- This highly integrated design tool accelerates the lead time of the system manufacturing and test. It reduces considerably the errors due to manual handling of bulky and tedious configuration data.

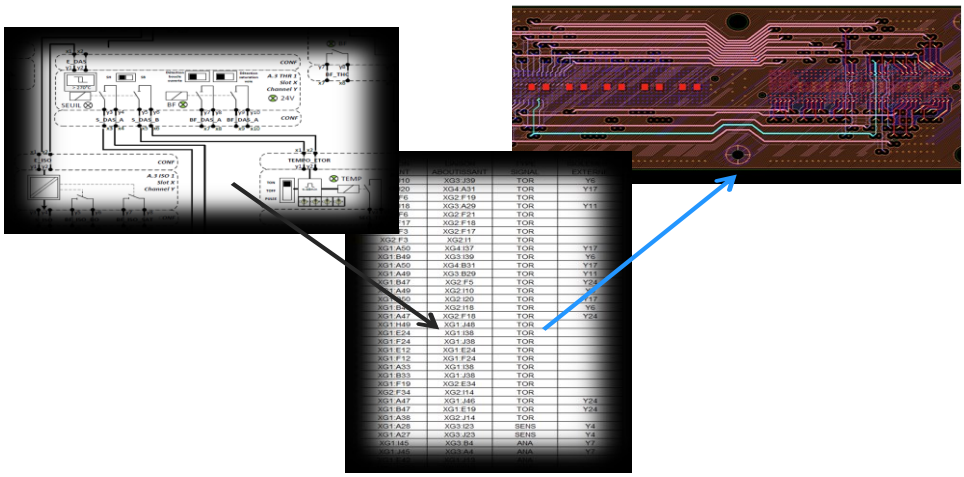

Figure 7: illustration of engineering tools flow

5. Conclusion

Designing a state-of-the-art non-programmed technology for safety I&C application led to several challenges:

- Make sure the system implemented with Hardline can be 1E / Cat. A certified
- Ensure that the safety I&C functions required for Research Reactors protection systems could be implemented
- Allow for adaptability to accommodate future demand for upgrades or new regulations/safety standards
- Provide adequate functionalities & performance expected in modern safety platforms
- Being able to guarantee long term support (components, spare parts, training) in line with Rolls-Royce standards (up to 25 years after installation)

The methodology used for this development was based on the experience acquired with previous generations of non-programmed technologies used and developed by Rolls-Royce but also all the procedures and rules applied for programmed technologies (such as Spinline, Rolls-Royce 1E / Cat. A digital safety platform). By applying the harsher design methods required for programmed technology to this non-programmed platform, the qualification and classification risks were greatly reduced.

Moreover, the return on experience from a large installed base of non-programmed equipment for various types of systems and functionalities allowed us to establish the list of functionalities and features useful to customers while meeting the most stringent safety regulations. Therefore improved features compared to previous generation of non-programmed safety I&C technologies were added such as:

- Enhance performance, in particular for Diagnostic
- Delayed differentiation (final cabling can be done later, giving more time for customization)
- Improved connectivity (no manual cabling)
- Reduced footprint

As for other Rolls-Royce technologies, a 25 year support after installation is also proposed thanks to specific components and supply chain choices.

Hardline is therefore perfectly adapted to the Research reactors I&C and provides an excellent solution for modernizations towards a simple to qualify, yet powerful and easy to operate and diagnostic platform.

6. References

[1] IAEA. (s.d.). 151 Facilities with first criticality more than 40 years ago. Accessed Jan, 21, 2019, sur IAEA: https://nucleus.iaea.org/RRDB/Content/Age/AgeHigh.aspx

[2] IAEA, Instrumentation and Control Systems and Software important to safety for Research Reactors, Specific Safety Guide No. SSG-37, 2015

IRRADIATION OF HO-PLLA MICROSPHERES IN THE MARIA REACTOR

RAFAŁ PROKOPOWICZ, KRZYSZTOF PYTEL†, JANUSZ JAROSZEWICZ, MIKOŁAJ TARCHALSKI, MICHAŁ GRYZIŃSKI, MICHAŁ DOROSZ, GAWEŁ MADEJOWSKI, ROBERT KELER, IWONA ZAGUBIEŃ, ANTONI ZAWADKA
National Centre for Nuclear Research, Otwock–Świerk, Poland

JAN SIGGER, STUART KOELEWIJN, MATTHIJS DIJK, NOORA DUIVENVOORDE
Quirem Medical BV, Deventer, The Netherlands

Introduction

Radioembolization is an innovative form of radiotherapy, e.g. of liver cancer. This is one of very promising and valuable treatment method. Radioembolization consists in delivering of radioactive substance through the blood circulation system, directly to the tumour.

In case of liver radioembolization the β-radioactive nuclide of ^{90}Y is usually used. This radionuclide has half-life of 64 h and emits β-particles of energy up to 2.28 MeV. It does not emit γ-ray, what is its huge advantage due to high liver sensitivity to radiation. However, it leads to certain difficulties in precise estimation of radioactive material distribution and dose applied. As ^{90}Y carrier glass and resin microspheres are used.

A novel radioembolization method is being currently developed. It based on ^{166}Ho radionuclide of 27 h half-life, which emits β-particles of energy up to 1.86 MeV. The microspheres containing holmium are made of biodegradable poly(L-lactic acid) – PLLA. The microspheres are developed as QuiremSpheres® by Quirem Medical BV, The Netherlands.

The microspheres are ca. 30 μm in diameter. ^{166}Ho emits ca. 80 keV γ-rays. That allows using single-photon-emission computer tomography (SPECT) to determine microspheres distribution and dose applied. Holmium is paramagnetic so it allows using also nuclear magnetic resonance (NMR) imaging to determine microspheres distribution [1].

Experiment

Recently Quirem Medical BV asked National Centre for Nuclear Research, Otwock-Świerk, Poland (NCBJ) to prepare technology of Ho-PLLA microspheres irradiation in the MARIA research reactor. The irradiation process need to assure providing precise ^{166}Ho activity (depending on microspheres mass, patient dose, transport time etc.) and sufficient microsphere physical condition (size, spherical, homogeneity, etc.).

The temperature degradation of PLLA microspheres begins above ca. 60°C. Therefore, the crucial issue is to avoid overheating of the microspheres during irradiation. The temperature of irradiation target depends on (nuclear) heat generation in the target, heat conduction and cooling water temperature. Only the last one value is known accurately. Therefore, the standard irradiation conditions led to unsatisfactory results (cf. Fig.1a).

In order to reduce nuclear heating in irradiated Ho-PLLA microspheres the peripheral irradiation channel of hydraulic rabbit system No 4 has been selected to perform the irradiations. Improved water cooling has been applied to the hydraulic rabbit system channels.

Purpose-designed irradiation vial for Ho-PLLA microspheres and filling irradiation container with helium allow more efficient heat removal from the microspheres during irradiation.

Adjacent to the irradiation channel of the hydraulic rabbit system No 4 a set of nuclear radiation detectors has been installed in order to on-line monitoring of the irradiation conditions. Two self-powered neutron detectors (equipped with silver and rhodium emitters) have been applied to determine thermal neutron flux density. They have been absolutely calibrated by means of the activation (cobalt) foils. Both the KAROLINA nuclear calorimeter and gamma-thermometer have been used to determine nuclear heat value [2]. A purpose

pressure sensor installed in the rabbit system allows determining the irradiation time with accuracy over 1 sec.

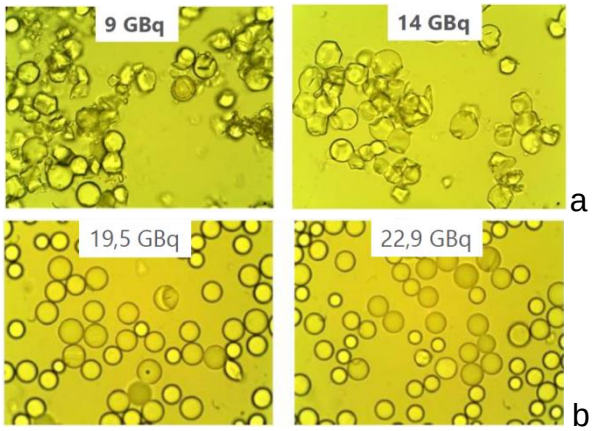

Fig. 1. Examples of irradiated Ho-PLLA microspheres:
a – standard, b – improved irradiation conditions.

Results

A series of experimental irradiation allow improving the irradiation technology (cf. Fig. 1b). That led in July 2017 to successful validation of the MARIA reactor as a supplier of irradiated QuiremSpheres®.

Since then the Ho-PLLA microspheres irradiated in the MARIA reactor are supplied by Quirem Medical BV to a number of medical centres in Europe for cancer patient treatment.

References

[1] M. Smith et al., The Lancet Oncology, vol. 13, No. 10, p. 1025–1034, Oct. 2012

[2] J. Brun et al., IEEE Trans. Nucl. Sci., vol. 63, p. 1630-1639, 2016

FULL-CORE BURN-UP CALCULATIONS USING MCNP6 CODE FOR THE JORDAN RESEARCH AND TRAINING REACTOR

I. F. FAROUKI
Jordan Research and Training Reactor, Jordan Atomic Energy Commission
Irbid - Jordan

ABSTRACT

Fuel burn-up for the initial core at the Jordan Research and Training Reactor (JRTR), due to about 18 days of intermittent full power operation during its hot commissioning, was evaluated using the MCNP6 code.

Methodology of optimizing calculation fidelity (in terms of temporal, spatial, and isotopic resolutions) is outlined. Calculation results are given in terms of radial and axial distributions of U^{235} consumption and in terms of Samarium effects on the JRTR reactivity.

Validation of the calculation methodology and results are tested by comparing predictions obtained from the updated JRTR model with critical control rod positions measured during the Initial Operation Tests (IOTs). Sources of uncertainty that need to be considered in the future to limit deviation of calculation model from actual core conditions are also identified.

1 Introduction

Determining and utilizing updated reactor fuel composition data may be considered a step towards the enhancement of the economics, safety, and performance of a reactor [1]. Tracking fuel composition changes through accurate depletion calculations is crucial to enable nuclear safety analysis, optimization of in-core fuel management schemes, and assisting with the design of core utilization and experiment facilities. At the back-end of the fuel cycle, accurate knowledge of discharged fuel composition may also help with optimizing spent fuel storage and transportation tasks, also known as implementation of burnup credit [2].

The recent availability of affordable high computing power and memory has made it possible to perform detailed, full core, 3-dimensional Monte Carlo burnup calculations [3].

Using Monte Carlo neutron transport codes, nuclear reaction rates in the reactor fuel (and in other burnable components) can be calculated at high accuracy levels, constrained only by the accuracy of the model and nuclear cross-section data, and the computational power available needed to achieve results with acceptable statistical uncertainty levels.

The study below presents the burnup calculation methodology employed for the Jordan Research and Training Reactor (JRTR), a $5MW_{th}$, open tank in pool, plate type fuelled research reactor located in the northern part of Jordan. The JRTR was operated intermittently for a total of about 18 full power days (FPDs) during its hot commissioning. The main motivation behind estimating burnup for JRTR's initial core at such an early stage was to update its calculation model so that it can be used to support planned Initial Operation Tests (IOTs) [4].

This study aims to highlight the experience of using the MCNP6 code [5], given a relatively limited computer setup, to estimate burnup in the JRTR fuel. The validity of the results is

examined through comparison of updated model predictions to criticality measurements results.

2 JRTR Core Description and Fresh Core Calculation Model

The JRTR core is fuelled with low enriched uranium silicide dispersed in aluminium. The full core consists of 18 fuel assemblies (FAs), as illustrated in Fig 1. Each FA consists of 21 plates cooled through downward forced-flow of light water. Currently the reactor is rated at 5 MW_{th} but is upgradable to 10 MW_{th}. For the initial core, four different fuel meat densities were used across the core; this is illustrated in Fig 1 by plotting FAs with different shades of grey where the darker shade represents higher fuel meat density.

Beryllium block assemblies (green colour in Fig 1) and a heavy water tank (light blue colour in Fig 1) are arranged around the reactor core acting as the neutron reflectors. Supplementary graphite thermal column is installed beyond the heavy water tank at one side of the core. Reactivity control is accomplished through withdrawal and insertion of four hafnium control absorber “Rods” (CARs), which are square hollow sections surrounding FAs 05, 07, 12 and 14 (Fig 1). CARs are vertically inserted from the top of the core and are controlled through step motors. Two boron carbide hollow cylindrical rods are also installed as secondary absorber rods and are used only for enhanced shutdown capability.

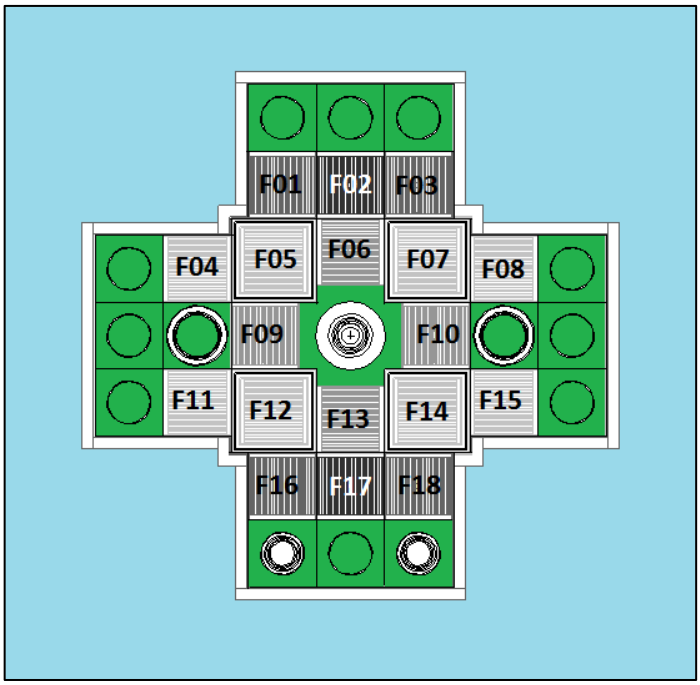

Fig 1. Core fuel assemblies (shades of grey), reflectors (green and light blue for Beryllium and heavy water, respectively), and CARs surrounding FAs 05, 07, 12 and 14.

The MCNP calculation model of JRTR’s initial fresh core used as the starting point for the depletion calculations presented below was provided by the JRTR’s project contractor - KDC (KAERI DAEWOO Consortium). The validity of that MCNP calculation model was examined during the JRTR hot commissioning phase through comparison of predicted and measured critical CAR (axial) positions for five core configurations (Tab 1). [6]

# of FAs	# of DAs	Measured Critical Position (mm) [5]	k_{eff} Calculated @ measured position*	Predicted Critical Position (mm)	Measured – Predicted (mm)
18	**-**	311.5	1.00076	310.4	1.1
17	**1**	346.1	1.00071	344.7	1.4
16	**2**	399.4	1.00055	398.2	1.2
15	**3**	454.8	1.00029	454.2	0.6
14	**4**	566.6	0.99999	565.1	1.5

*Std. of quoted values is ±0.00017.

Tab 1: Performance of the MCNP calculation model of the initial, fresh core during hot commissioning of the JRTR [6].

It is worth mentioning that the input file (calculation model) mentioned above was built based on design parameters. Small deviations between design and actual implementation of the reactor, such as the exact uranium loadings in each fuel plate which are available from the fuel fabrication reports, were not considered in the input file.

3 Calculation Model Fidelity

3.1 Temporal Decomposition of Operation History

JRTR power operation history during its hot commissioning was obtained, analysed, and segmented into time steps. For each time step, the power level, duration of operation, and CAR positions were determined, as shown in Tab 2. For each step, an *effective CAR position* was estimated for each calculation step based on the reactor operation history as follows:

$$effective\_position\ (mm) = \frac{\sum_i P(i).Pos(i)}{\sum_i P(i)}$$

Where $Pos(i)$ represents CARs position in units of mm, $P(i)$ is the power level in units of %FP (% Full Power) at index i, and i is the data point index where the summation is carried over data points covering the operation range of interest.

Step	Decay Days	Full power Days	Effective CAR Position (mm)	Step	Decay Days	Full power Days	Effective CAR Position (mm)
1	---	0.518	337	**9**	9.9	---	0
2	---	0.745	361	**10**	---	0.589	344
3	9	---	0	**11**	---	0.477	373
4	---	0.320	323	**12**	---	0.992	388
5	11.8	---	0	**13**	---	4.072	397
6	---	0.511	337	**14**	---	3.957	404
7	---	0.584	367	**15**	---	4.046	411
8	---	1.004	378	**16**	90	---	0
---	**---**	**---**	**---**	**Total**	**---**	**17.816**	**390**

Tab 2: Temporal segmentation of JRTR power operation history. These steps were followed for burnup calculations presented here-in.

3.2 Determination of Spatial Resolution

As mentioned earlier, the JRTR core consists of 18 fuel assemblies. The minimum requirement for spatial segmentation, which comes from fuel management considerations rather than accuracy-of-calculations considerations, is to average fuel burnup over no more than one single fuel assembly. However, given that reaction rates vary from plate to plate and even (transversally and axially) within a single plate, segmentation on the sub-fuel assembly level is required to achieve an acceptable level for the calculation accuracy. For this purpose, neutron flux distributions were calculated (for the fresh core) in the fuel plates of one fuel assembly, namely **F03**, and are presented in relative scale in Fig 2.

Normalized transversal flux distributions across plates of F03 and across the width of one of its plates (plate #11) are given in the Top and Bottom of Fig 2, respectively. Since CARs are inserted from the top, dramatic transversal flux tilts (with expected deviations of up to 170% from the mean) are found across each plate in the *upper part* of F03.

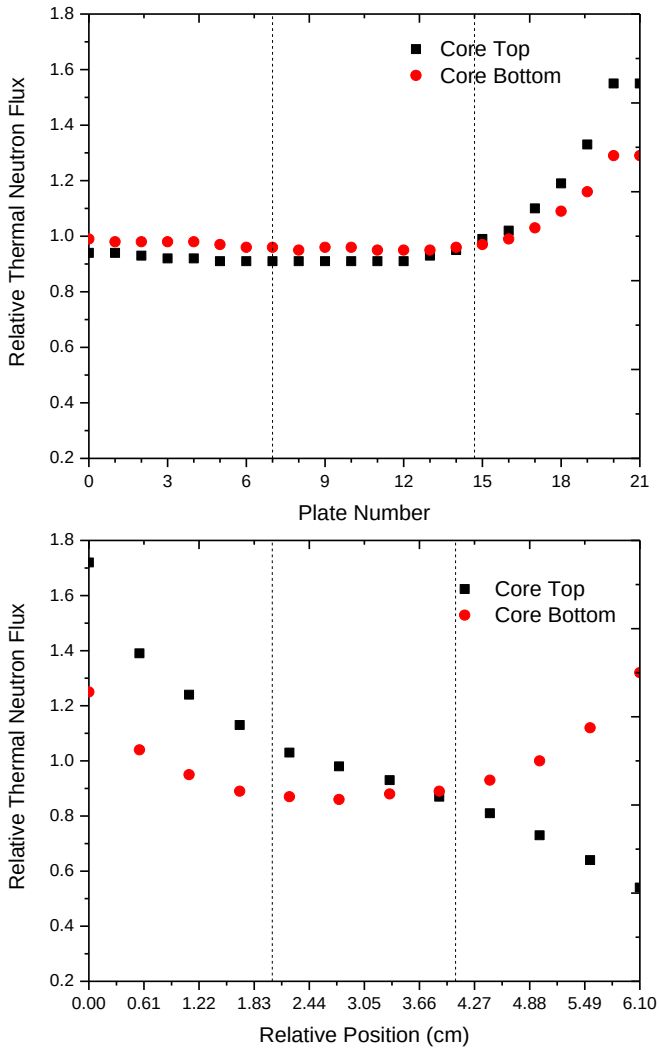

Fig 2. Flux distribution across F03 fuel plates, given for the axial and top of the F03 (Top), and the flux distribution across the width of plate #11 in F03, also given for the top and bottom of that plate (Bottom). Each set of data is normalized to its average.

The most significant source of the radial and axial flux tilting is the presence of control rods inserted from the top of the core. Beryllium and heavy water reflectors (green and light blue, respectively, in Fig 1) do contribute to the radial flux tilting. The axial flux tilt, which exists in every fuel assembly of the core, was accounted for by segmenting each fuel assembly into 10 burnup regions in the axial direction.

Radial and transversal flux tilts were taken into account by segmenting each axial region of each single fuel assembly into a 3x3 mesh, i.e., into 9 sub-regions. Therefore, the total number of fuel meat regions used for calculations was 1,620 regions (**18**FAs x **10** axial regions per FA x **9** radial meshes per axial region), each with its own composition and reaction rates that change from one-time step to the other. Fig 3 illustrates the spatial segmentation scheme used for calculations presented here.

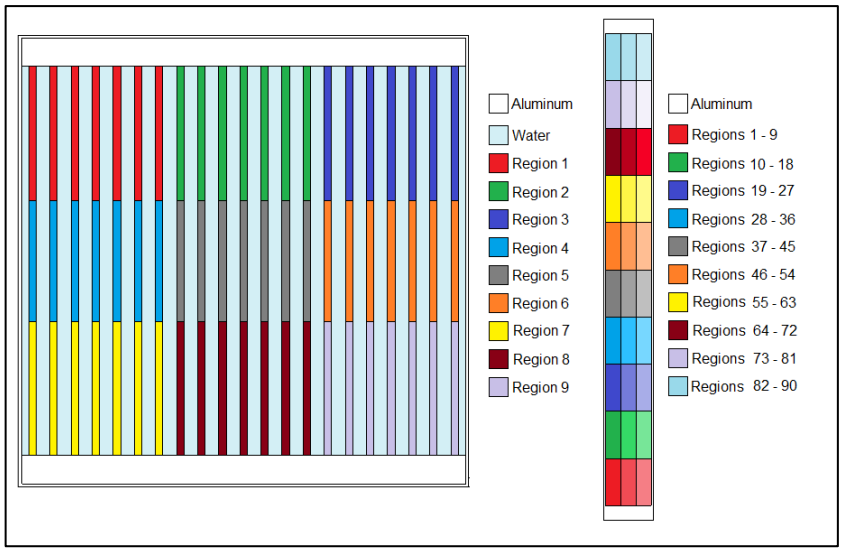

Fig 3. Spatial segmentation scheme used for burnup calculations presented here-in. Each FA was segmented into 90 sub regions, where reaction rates were calculated for each region separately.

3.3 Determination of Isotopic Resolution

For better utilization of the available computational power, the number of isotopes tracked through the depletion calculations are reduced. In order to determine which isotopes can be neglected without affecting the accuracy of calculations, the total reaction rates for 248 isotopes from a test burnup calculation with lower spatial resolution were sorted in descending order. It was found that the first 15 isotopes contribute to about 99.92% of all reactions in the fuel meat (Tab 3). At full power, U^{235}, U^{238}, Xe^{135} and Sm^{149} contribute to 98.59% of all reactions.

Isotope	Fraction	Isotope	Fraction	Isotope	Fraction
U^{235}	85.57%	**Pu^{239}**	0.35%	**B^{10}**	0.03%
U^{238}	7.27%	**U^{234}**	0.21%	**Pm^{147}**	0.02%
Xe^{135}	5.02%	**U^{236}**	0.16%	**Rh^{105}**	0.01%
Sm^{149}	0.72%	**Si^{28}**	0.08%	**Xe^{131}**	0.01%
Al^{27}	0.42%	**Sm^{151}**	0.04%	**N^{14}**	0.01%

Tab 3: Isotopes with highest neutron reaction rates, contributing to about 99.92% of all reactions in the fuel meat.

However, tracking the concentration of the two most significant neutron-poisons Xe^{135} and Sm^{149} requires tracking the concentration of their direct precursors (I^{135} and Pm^{149}, respectively). Based on that, the list of explicitly listed isotopes was limited to the 15 isotopes listed in Tab 3 in addition to I^{135} and Pm^{149}, i.e., 17 isotopes in total are tracked in the burnup calculations.

4 Code, Data Library, and Assistive Script Used for the Calculations

The MCNP6 code package along with the ENDF-VII.1 cross section data library were used to perform the calculations presented herein. It is noteworthy to mention that MCNPX 2.6.0 was

the first among the MCNP code series to employ the burnup feature. The MCNP6 code, which inherited the burnup feature from MCNPX 2.6.0, estimates depletion through internal linking of criticality problems outputs with the CINDER90 depletion code [6].

MCNP6 has made a very reliable tool to accomplish the task at hands here-in. However, difficulties were encountered using the BURN feature of MCNP. In fact, the impression gained from using the BURN feature in MCNP6 code was that this feature was designed to facilitate burnup calculations for power reactor assemblies/cores. The MCNP BURN card allows, between consecutive calculation steps, to modify materials concentrations and swap universes in a manner equivalent to changing concentration of soluble poison in coolant or shuffling fuel assemblies in a core.

Unlike power reactors, control rods positions adjustments are used at the JRTR (and similar research reactors) to compensate for reactivity changes due to build-up of poisons, temperature changes, and fuel depletion. The MCNP6 burnup feature does not enable simulating such CARs adjustment internally at the beginning of each calculation step.

In order to overcome this difficulty, the output of each burnup step, printed by the MCNP code in the form of isotope mass fractions tables, was used to produce a new input file for the next step. Once a new input file is created, the user has the freedom to adjust the CAR positions or apply any other modifications. Each burnup step, a total of 27,540 isotope mass fraction values (1,620 material-cards(regions) x 17 isotopes per material-card) had to be updated. This was achieved through an external script that enabled convenient manipulation of such a large amount of data.

A shortcoming to this (external-feedback) approach was caused by the fact that MCNP code prints output tables with isotope mass fraction values specified only up to the 4^{th} significant figure, i.e., any change in the mass fraction beyond the 4^{th} significant figure was either neglected or rounded up to four significant figures. This affected the printed mass fractions for U^{238}, since the change in U^{238} mass fraction is very small for the burnup steps under investigation (Tab 2). In order to overcome that, a subroutine was included in the assistive script to estimate the change in U^{238} mass fraction based on (n,γ) and (n,f) reaction rates printed by the MCNP code.

5 Results of Burnup Calculation

Results of the performed burnup calculations indicate that about 104 grams of U^{235} were consumed in total during the 18 full power days of operation, which took place during the

commissioning of the JRTR. Radial distribution of U^{235} consumption is illustrated in Fig 4. Results indicate that FAs 02 and 17 that neighbour the beryllium assemblies (retaining highest fuel meat density) and surrounded by three directions by other FAs, have experienced the largest amount of fission.

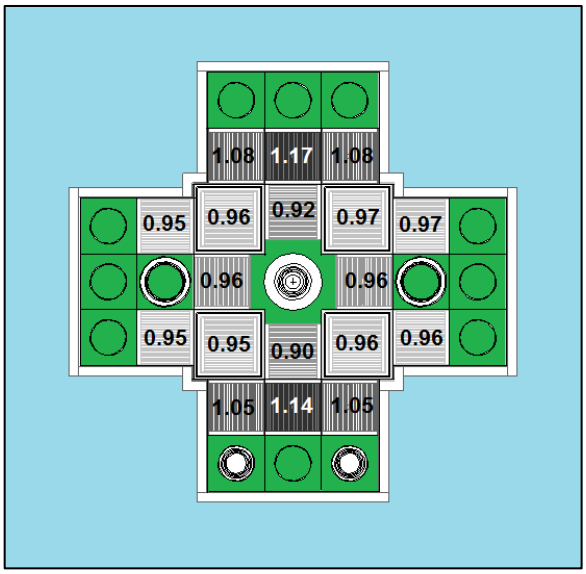

Fig 4. Radial U^{235} consumption distribution. Values normalized to the average U^{235} consumption in all FAs.

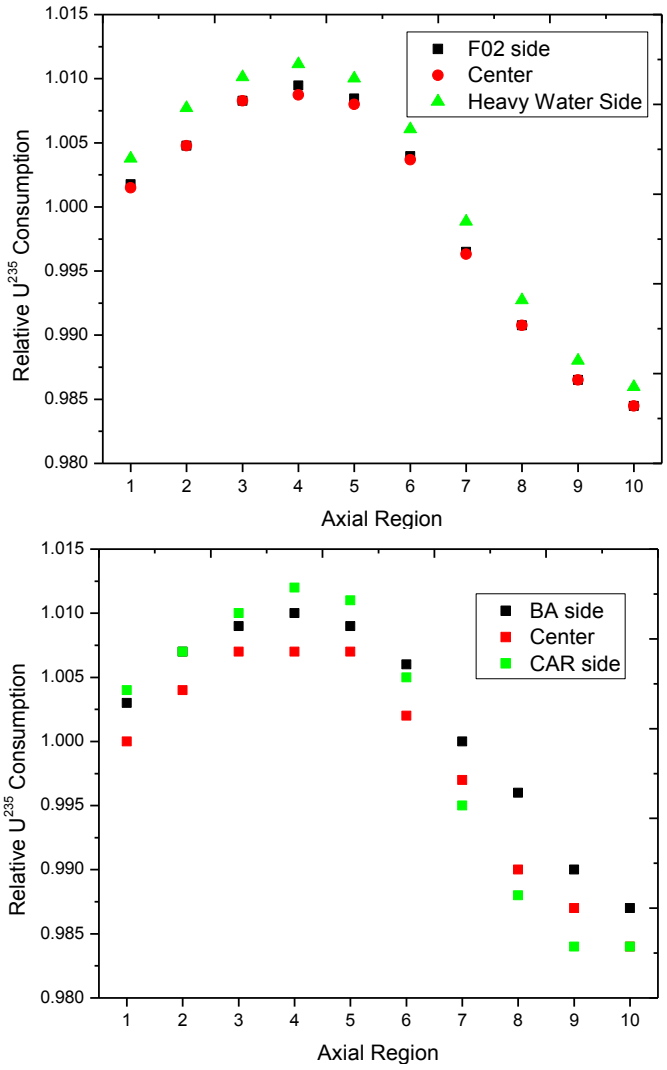

Fig 5. Normalized axial U^{235} consumption profiles, three each representing a third of F03's 21 plates (TOP), and another three each representing 7 plates of F03 (BOTTOM).

The upper portion of Fig 5 depicts three axial profiles with each profile representing seven fuel plates (in the x-direction), while the bottom portion of Fig 5 depicts three axial profiles with each profile representing a third of the 21 plates of F03 (in the y-direction).

In order to further examine the validity of the calculation results, criticality eigenvalues (k_{eff}) were calculated for the Xenon free core (Xe-135 and 131 zeroed, with all CARs withdrawn) at multiple time steps. A similar curve was also calculated for the Xenon **and** Samarium free core (Sm-149 and 151 zeroed). Results of which are shown in Fig 6.

After 18 full power days of operation, k_{eff} for the xenon-free core with all controls withdrawn was estimated to be about 1.09062, while for the xenon and samarium free core it was estimated to be about 1.10171. Compared to k_{eff} of the fresh core (with all CARs withdrawn), which was calculated to be 1.10879, it can be concluded that samarium poisoning accounts to about 61% of the total excess reactivity loss for first 18 days of full power operation. It should be noted that the x-axis of Fig 6 is in units of full power days rather than units of time, the plotted curves indicate discontinuities in k_{eff} at shutdown steps (as given in Tab 2), which is due to build-up and decay of various isotopes, most significantly Sm-149 which builds up during shutdown as evident in the Xenon free curve of the figure.

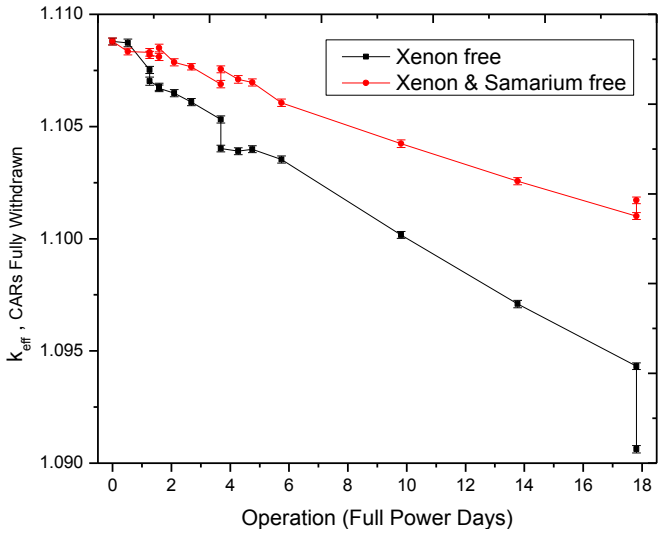

Fig 6: Calculated criticality eigenvalues change over ~18FPDs for Xenon free, and Xenon and Samarium free cores, with all CARs withdrawn.

6 Comparison of Calculation Results to Criticality Measurements

Critical CARs positions were measured for multiple core configurations at the zero-power level as part of the excess reactivity measurement tests conducted during the IOTs of the JRTR [4]. These measurements represented a great opportunity to test the validity of the developed burnup calculation scheme.

For Monte Carlo criticality and reaction rate calculations by means of power iteration method, it is conventional to confirm that sufficient number of initial iterations (cycles) are excluded (skipped) from the finalized results. [8] Typically, this is illustrated by plotting the average k_{eff} and the Shannon entropy against the number of cycles for total number (250) of cycles used. For all calculations presented in this work, including the depletion calculations, 25 cycles out of the 250 “kcode” cycles were skipped. Fig 7 presents a curve from one of the calculational runs, which indicate that after 25 cycles, variation of average k_{eff} is slow, and that the value of Shannon entropy of the fission source distribution has long reached an almost steady value.

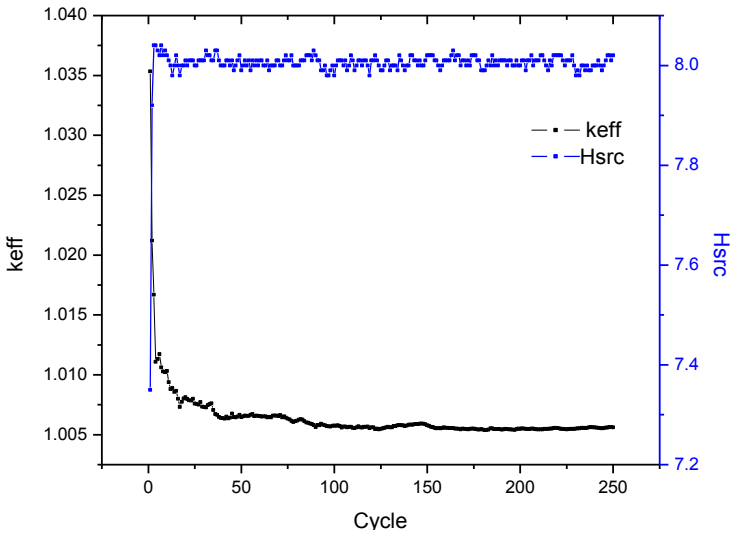

Fig 7: Average k_{eff} and the Shannon entropy against number of cycles, from one of the calculational runs.

In order to predict the critical positions, relatively quick criticality eigenvalue (k_{eff}) calculations were performed (with 4.5 million particles) for five CARs positions around an anticipated critical position, and the results (k_{eff}) is plotted against the modelled CARs position (Fig 8). Afterwards, CARs position at which k_{eff} is predicted to be equal to unity is determined using the intercept and slope from linear regression of the five points. Measured reactor pool water temperature during these measurements was25^{o}C ±1^{o}C at which criticality calculations were performed.

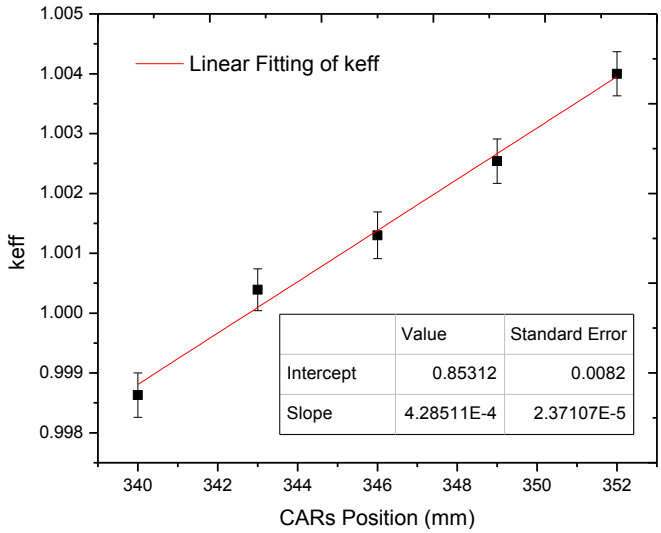

Fig 8: Results of criticality calculations at five CARs positions around a critical condition.

Summary of results for 5 of the tested core configurations are given in Tab 5. k_{eff} was recalculated at the predicted positions with higher certainty using 22.5 million particles (versus the 4.5 million used in the prediction of the critical CAR position). In addition, as a more straight-forward measure of the validity of burnup calculations, k_{eff} was calculated at measured critical positions using 22.5 million particles.

# of FAs	# of DAs	Measured Critical Position* (mm)	k_{eff} Calculated @ measured position**	Predicted Critical Position (mm)	k_{eff} Calculated @ predicted position**	Measured – Predicted (mm)
18	**-**	345.0	1.00083	342.8	0.99948	2.2
17	**1**	385.8	1.00079	384.1	0.99985	1.7
16	**2**	450.6	1.00058	450.4	1.00025	0.2
15	**3**	521.0	1.00024	519.3	0.99972	1.7

*These measurements were performed by reactor operators and senior operators.
**Std. of quoted values is between ±0.00015 and ±0.00017.

Tab 4: Results of criticality measurements and calculations.

7 Uncertainties and Sources of Inaccuracy in Depletion Calculations

Although results of the calculations performed with the updated core model has shown adequate levels of agreement with critical core configurations, this should not be interpreted

as an assurance that this methodology will be sufficient for extended burnup of the reactor core. Embedded inaccuracies in the adopted assumptions and uncertainty in the depletion calculation may propagate on the long run representing a significant source of deviation of the calculation model from actual core conditions.

The computer setup available for the JRTR allowed simulating up to 4.5 million particles (20,000 particles/cycle x 225 effective cycles) for each criticality calculation without prohibitively increasing the computational time. A summary of statistical uncertainties of reaction rates for calculations presented below are given in Tab 4. Maximum and average statistical uncertainties of **(n,γ)** and **(n,*f*)** reaction rates (over all 1,620 burnup regions) are summarized in Tab 4.

Reaction	**Max Statistical Uncertainty (std.)**			
	U^{235}	**U^{238}**	**Xe^{135}**	**Sm^{149}**
(n,γ)	5.65%	33.50%	6.73%	6.56%
(n,*f*)	6.16%	5.67%	--	--
Reaction	**Average Statistical Uncertainty (std.)**			
	U^{235}	**U^{238}**	**Xe^{135}**	**Sm^{149}**
(n,γ)	2.01%	8.06%	2.26%	2.29%
(n,*f*)	2.12%	2.17%	--	--

Tab 5: Statistical uncertainty analysis of neutron reaction rates in all 1,620 burnup regions.

Changes in the reactor core configuration and/or conditions, such as changes in pool water temperature and loading/unloading of irradiation targets may have an effect on the accuracy of the burnup calculation results if not appropriately account for in the simulation. In the calculations presented above, those variables were not taken into account and neglecting these variables from the simulations appears not to have had a significant effect on the results. Nevertheless, it is advisable that these should be considered sufficiently to avoid accumulation of error.

Other possible sources of uncertainty may stem from changes in the composition of the CARs and reflectors composition.

Finally, the accuracy of the measured reactor power history, which was obtained from data logging systems, would be another variable that should be investigated [1]. Accurate measured reactor power can be obtained only after confirming an adequate calorimetric calibration, which in many cases is a function of other factors in the reactor core, such as pool water temperature. On the other hand, accurate estimation of the Q value of the fission reaction is also required for accurate calculations, which in itself is dependent on the average energy of the neutron inducing fission.

8 Conclusion

The approach, methodology, and assumptions adopted to perform burnup calculations for the Jordan Research and Training Reactor core have been presented and discussed thoroughly.

The fidelity of the calculations, in terms of temporal, spatial, and isotopic resolution, was carefully considered in order to yield reliable results. Difficulties due to limitations in the

MCNP6 features have been discussed. Calculational results have also been presented in terms of normalized U^{235} consumption profiles, and the effects of Samarium poisoning was quantified.

Criticality calculation results were presented and compared to measurements conducted during the IOTs of the reactor, and good agreement was demonstrated. However, this shall not be interpreted as a guarantee that the given methodology and assumptions will continue to provide accurate results due to currently existing sources of inaccuracy in the depletion calculation, which were discussed in the last section.

9 Acknowledgment

The author would like to express his appreciation to all JRTR members who contributed towards generating measured data used in the validation of calculations presented above.

Special thanks to Dr. B. J. Jun for his invaluable discussions and advice and comments regarding the work presented in this paper. Thanks are also due to the JRTR senior reactor operators (SROs), to all the reactor operators, and system operators for their efforts in operating the JRTR in order to run the tests during the IOTs.

Nuclear safety team members, led by Mr. M. Omari, are commended for their support and participation in meetings and discussions related to the work presented above.

10 References

[1] Bock, H., et al. Determination of Research Reactor Fuel Burnup. IAEA, 1992.

[2] You, Guoshun, Chunming Zhang, and Xinyi Pan. "Introduction of burnup credit in nuclear criticality safety analysis." Procedia Engineering 43 (2012): 297-301.

[3] Brown, Forrest B. Recent advances and future prospects for Monte Carlo. No. LA-UR-10-05634; LA-UR-10-5634. Los Alamos National Laboratory (LANL), 2010.

[4] Farouki, I, et al. “Initial Operation Experience and Near Future Utilization Plans at the Jordan Research and Training Reactor”, RRFM Conference (2018)

[5] Fensin, Michael L., et al. The new MCNP6 depletion capability. American Nuclear Society, 555 North Kensington Avenue, La Grange Park, IL 60526 (United States), 2012.

[6] Kim, K -O, et al. “Neutronics Experiment Results in Commissioning Stage B of JRTR”, RRFM Conference (2018)

[7] Arshad, Muhammad. Study of xenon and samarium behaviour in the LEU PARR-1 cores. No. PINSTECH--142. Pakistan Inst. of Nuclear Science and Technology, 1994.

[8] Brown, Forrest. "A review of best practices for Monte Carlo criticality calculations." ANS NSCD-2009, Richland, WA 28 (2009).

CHARACTARIZATION OF VERTICAL NEUTRON IRRADIATION CHANNELS IN THE JORDAN RESEARCH AND TRAINING REACTOR

I. F. FAROUKI
Jordan Research and Training Reactor, Jordan Atomic Energy Commission
Irbid - Jordan

ABSTRACT

At the current configuration, the Jordan Research and Training Reactor core has more than 20 vertical neutron irradiation holes currently being used, or to be used in the near future, for radioisotope production, instrumental neutron activation analysis, neutron transmutation doping, as well as other applications. This work presents an attempt to characterize the JRTR core with an aim to facilitate current and near future reactor utilization activities by providing a concise description of the neutron field at available irradiation locations.

Neutron spectra are calculated, after which irradiation parameters, such as thermal to epithermal ratio (f), deviation of epithermal spectra from 1/E (α), and thermal neutron temperature (T_o) are estimated through numerical fitting applied to calculated neutron spectra. Axially averaged Values of 'f', 'α' and 'T_o' were found to range from ~6 → ~750, ~0.06 → ~0.21, and ~29 ^oC → ~60 ^oC, respectively. Axial variations of these parameters were also investigated and presented, and finally axial and radial distributions of the neutron flux were calculated and plotted.

1. Introduction

After the successful commissioning of the Jordan Research and Training Reactor (JRTR) in 2016 [1], and subsequent to the extended supplementary personnel training and qualification activities during 2017 [2], efforts are being redirected towards ramping up and enhancing utilization activities at the reactor.

Facilities for the production of Mo-99/Tc-99^m, I-131, and Ir-192 radioisotopes, and for Neutron Activation Analysis (NAA) were built and commissioned along with the reactor facility. Nonetheless, the reactor – designed and built to serve as a *multipurpose* research reactor – has a set of irradiation locations and beam tubes that are capable of serving a variety of industrial and research applications beyond Radioisotope Production (RIP) and NAA [3].

The JRTR is a tank-in-pool MTR reactor, currently rated at 5 MW_{th} but is also upgradable to 10 MW_{th}. As illustrated in Fig 1, the reactor fuel is loaded in the shape of a cross, surrounded with blocks of Beryllium as one of its reflectors, a heavy water tank as its other reflector, and a thermal column, all of which are built into a 10 meter deep pool of light water. Another beryllium block is installed in the centre of the core, representing the flux trap (IR0).

As can be noticed from the reactor core schematic of Fig 1, irradiation locations under investigation are placed within the beryllium blocks, the heavy water tank, and the Thermal Column Extension (TCE). This work aims to facilitate current reactor utilization activities by providing a concise description of the neutron field at the JRTR core, and by identifying features of the neutron field that can be exploited for effective utilization of the reactor.

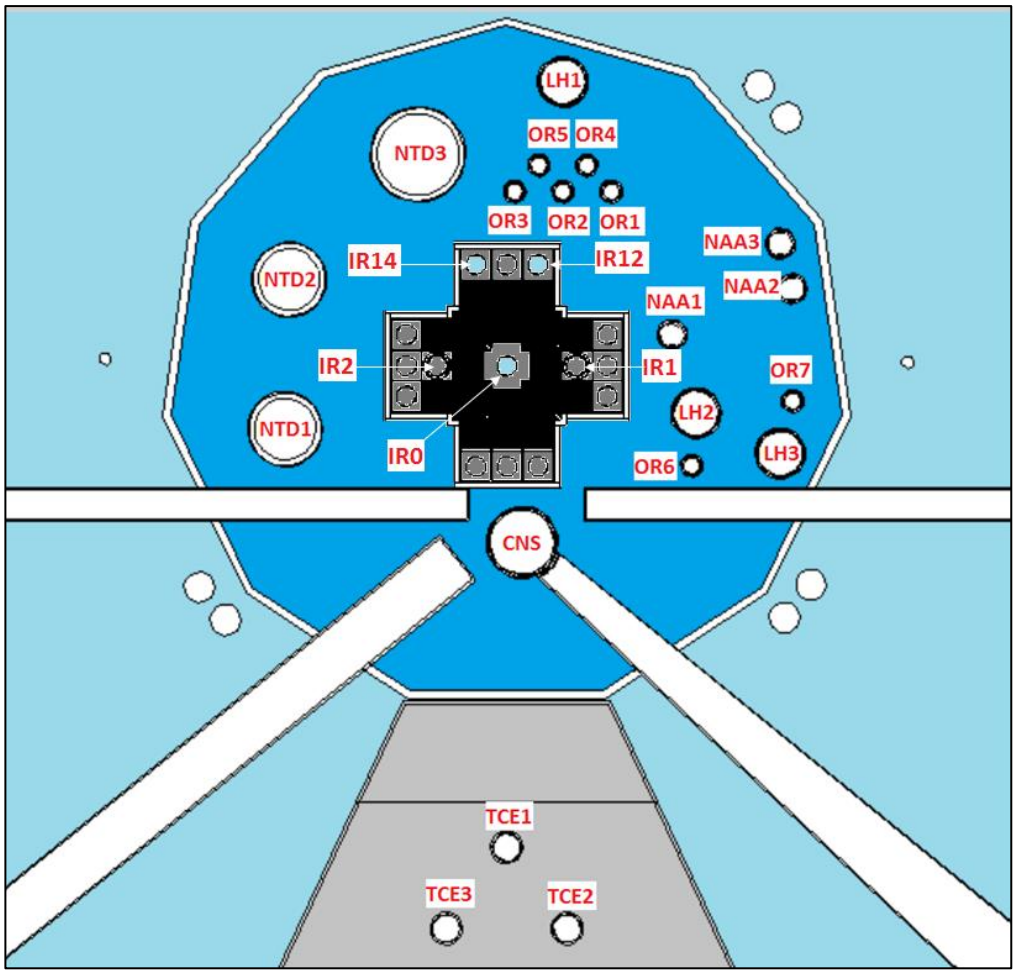

Fig 1: Top view schematic of the JRTR core, showing the MTR type fuel (black), Beryllium and Heavy water reflectors (grey and blue, respectively), TCE (light grey), irradiation holes and beam guides (white) and part of the light water pool (light blue).

2. Calculation Model and Assumptions

Neutron spectra calculations are performed using the MCNP6 code [4], along with ENDF-VII.1 data library, and covered 20 irradiation holes (Tab. 2) located in the core centre, Beryllium and heavy water reflectors, and in the Thermal Column Extension (TCE).

Full core neutron transport simulations were performed using a detailed three-dimensional MCNP model of the JRTR core. The model was provided by the contractor KAERI Daewoo Consortium (KDC) at the end of the JRTR commissioning activities [5], which was modified by the JRTR Team to allow for accurate burn-up calculations [6]. Calculations were performed using the model for the reactor core with ~20 full power days of operation, equivalent to about 100 MWD of burn-up.

For the calculations presented herein, irradiation holes were filled (in the MCNP calculation model) with materials that best match their utilization application. Neutron Transmutation Doping (NTD) holes were filled with Silicon, Cold Neutron Source (CNS), and NAA pneumatic holes were filled with He^4 gas, while all other holes were plugged with Aluminium. A list of irradiation locations and their properties are given in Tab. 1.

It is worth pointing out that calculations presented in Tab 2 modelled the temperature of reactor core components at room temperature (20 ^{o}C) and did not take into account neutrons produced through photo-neutron reactions.

	Material	Distance From Centre (cm)	Inner Diameter (cm)	Application		Material	Distance from centre (cm)	Inner Diameter (cm)	Application
IR0	Irr. Rig	0	5	Ir-192 Production	**LH1**	Al	71.4	11	Large Target
IR12	Irr. Rig	26.3	3.8	Mo99/Tc99m Production	**LH2**	Al	48.5	11	Large Target
IR14	Irr. Rig	26.3	3.8	I-131 Production	**LH3**	Al	71.5	12	Large Target
NAA1	He	41.5	3.1	NAA	**NTD1**	Si	57.3	18	Si Doping
NAA2	He	73.6	3.1	NAA	**NTD2**	Si	57.9	18	Si Doping
NAA3	He	72.8	3.1	NAA	**NTD3**	Si	56.5	23	Si Doping
OR1	Al	50.1	5	Small Target (NAA, RI)	**CNS**	He	44.2	16.8	Cold Neutron Source/Large Targets
OR2	Al	45.0	5	Small Target					
OR3	Al	42.9	5	Small Target	**TCE1**	Al	120.0	7	Small Target
OR4	Al	53.2	5	Small Target	**TCE2**	Al	140.3	7	Small Target
OR5	Al	50.0	5	Small Target	**TCE3**	Al	140.3	7	Small Target
OR6	Al	52.4	5	Small Target					
OR7	Al	71.6	5	Small Target					

Tab 1**.** Detailed summary of the JRTR core irradiation locations.

In order to cover various reactor operation conditions, calculations were performed for two cases: Xenon free core (zero power) at which the critical control rods (CARs) position is 353 mm, and for the Xenon equilibrium core (full rated power, i.e., 5 MW) at which the critical CARs position is 421 mm.

3. Calculated Neutron Spectra

Neutron flux was tallied using the F4 tally card in MCNP. The tally was segmented into 100 energy bins (groups) in order to capture the neutron energy spectrum. Except for NAA holes, tallied neutron spectra for each hole represented the average spectra over the hole's total axial length, which is about 1 meter in length. Calculations for NAA holes were averaged over the length of the in-core PTS tube. Variations across the axial direction are discussed and quantified in section 4. Neutron flux spectra are presented in terms of *neutron energy density*, i.e., Φ(E) Fig 2.

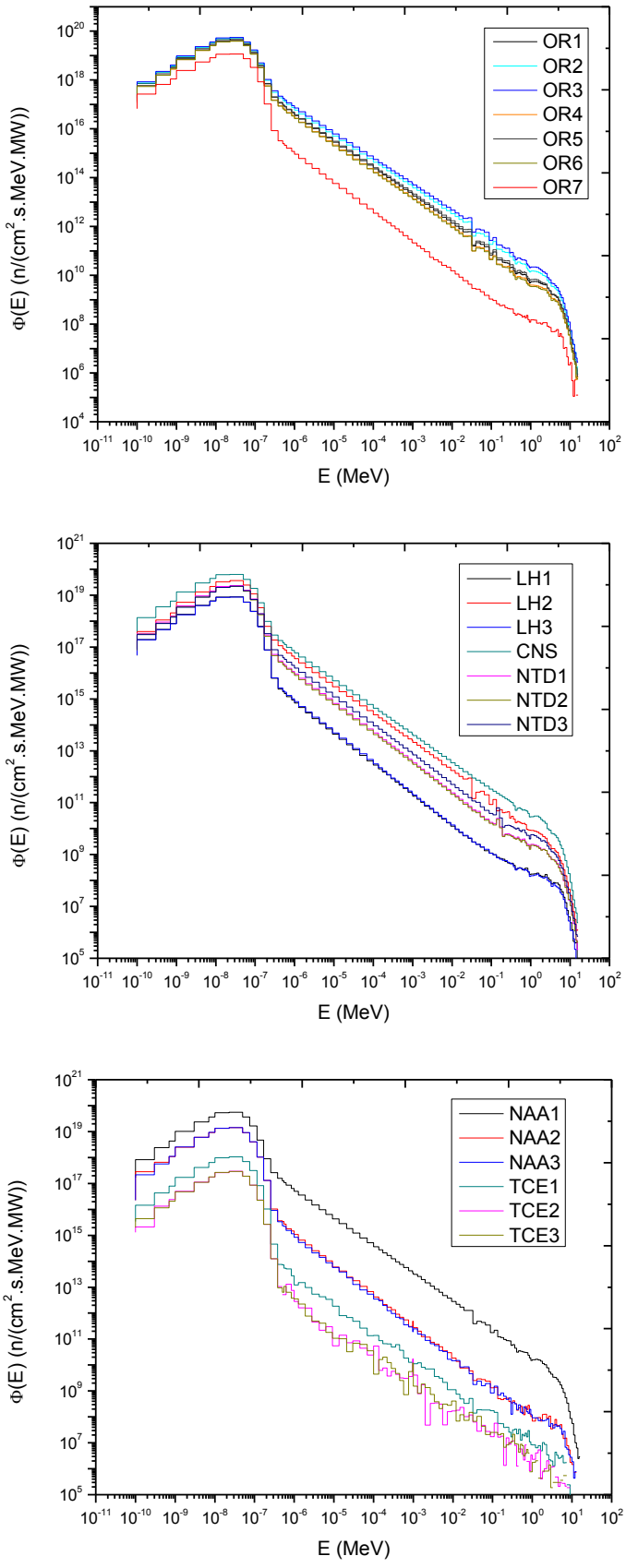

Fig 2: Axially averaged differential neutron spectra for irradiation locations OR1-OR7 (Top), for CNS, LH and NTD holes (Centre), and for NAA and TCE Holes (Bottom).

4. Thermal to Epithermal Ratio

Among the parameters of interest for utilization activities is the thermal-to-epithermal ratio (*f*) [7]. Values of (*f*) were determined by simply dividing integral flux in the two energy regions. The thermal region was defined to span energies from 0 eV → 0.55 eV, while the epithermal region was defined to span energies from 0.55 eV → 0.11 MeV, i.e., covering the entire "1/E" range, as shown in Fig 2. Results are summarized in Tab. 2 for the Xenon equilibrium configuration of the reactor core.

Irradiation Location	*f*	Irradiation Location	*f*
LH1	156.35 ±0.08	**OR1**	12.61 ±0.02
LH2	8.83 ±0.01	**OR2**	7.21 ±0.01
LH3	138.39 ±0.30	**OR3**	6.01 ±0.01
NTD1	27.89 ±0.04	**OR4**	13.78 ±0.02
NTD2	28.64 ±0.04	**OR5**	9.89 ±0.01
NTD3	14.19 ±0.01	**OR6**	14.53 ±0.02
NAA1	8.91 ±0.02	**OR7**	167.69 ±0.88
NAA2	169.17 ±2.47	**TCE1**	404.75 ±15.01
NAA3	207.03 ±3.22	**TCE2**	744.64 ±68.24
CNS	8.42 ±0.00	**TCE3**	741.96 ±69.47

Tab 2. Thermal to epithermal ratios across irradiation locations for the JRTR core at Xenon equilibrium.

Values of (*f*) were plotted against the distance of irradiation location from the centre of the core (Fig 3). Indeed, based on the reactor core configuration, the fraction of thermal neutrons increases with radial distance from the centre of the core. Fig 3 indicates that value of (*f*) increases exponentially with distance. (*f*)-values were also calculated for the Xenon-free core configuration, and results have indicated that (for irradiation holes within the heavy water reflector and beyond) axially averaged thermal-to-epithermal ratios are insensitive to the reactor core Xenon-poisoning condition**.**

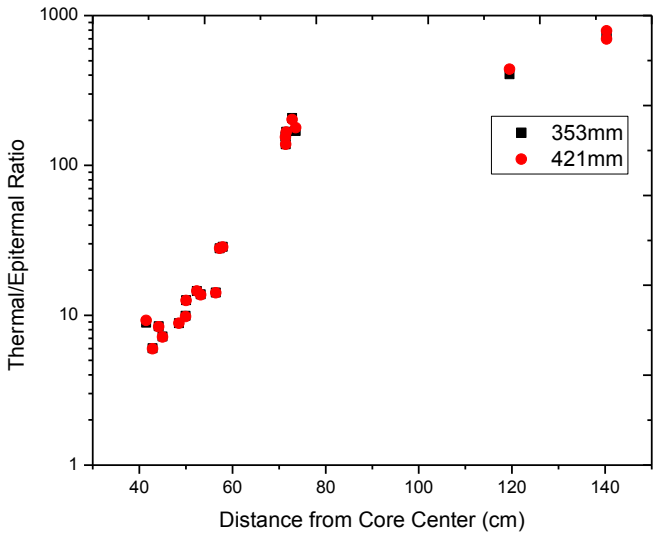

Fig 3: Thermal to epithermal ratio against distance from centre of the core.

Results reported in represent values of (*f*) averaged over the whole axial length of irradiation holes. Calculation results indicate - as expected - that values of (*f*) also vary significantly along the axial direction. In order to illustrate that, axial distributions of thermal-to-epithermal ratios are estimated by calculating thermal and epithermal flux in each of twenty regions over the whole axial length. Results are plotted for NAA hole in Fig 4.

The trend, as seen in Fig 4 for NAA and as has been confirmed for other irradiation holes, indicates that (for irradiation holes in the heavy water reflector and beyond) values of (*f*) are highest near the top of irradiation locations. It can be concluded that the top of heavy water reflector irradiation holes is suitable for localized irradiation applications that requires very well thermalized neutron flux, while irradiation applications that require fast neutrons (such as Gem-stone colouring [8]) should utilize the axial location were the flux peaks.

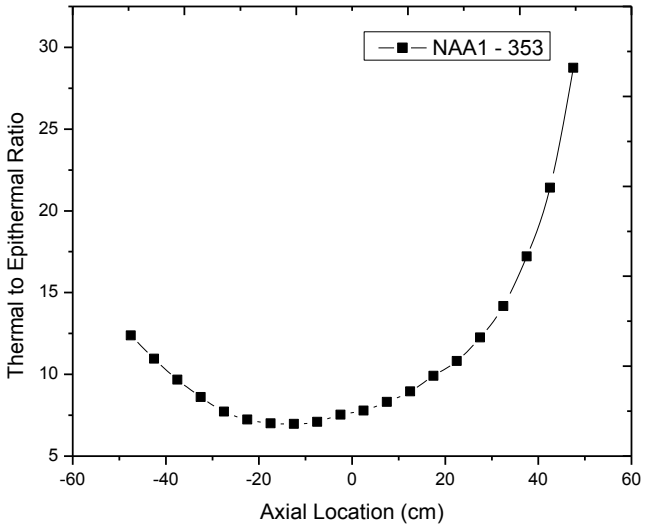

Fig 4: Thermal to epithermal ratio distribution at NAA1, at Xenon free conditions.

5. Deviation of epithermal spectrum from 1/E

The deviation of energy dependence from “1/E” in the epithermal region is accounted for through the non-1/E factor (α) according to the following equation [9]:

$$\Phi(E) = \Phi(E_o)\left(\frac{E_o}{E^{1+\alpha}}\right) \qquad \text{Equation \#1}$$

Epithermal regions of the spectra shown in Fig 2 were fitted to Equation #1. Values of the non-1/E factor (α) were found to be positive and range from ~0.05 to ~0.21. This parameter was also calculated for the Xenon-free core configuration and the results also indicated that the deviations from 1/E in the epithermal region are almost insensitive to the reactor core Xenon-poisoning condition.

Values of non-1/E factor (α) are plotted against values of thermal-to-epithermal ratios in Fig 5 as an attempt to reveal a correlation between the two. The trend shown in Fig 5 indicates that the (α) value increases (up to a certain distance) with distance from core centre.

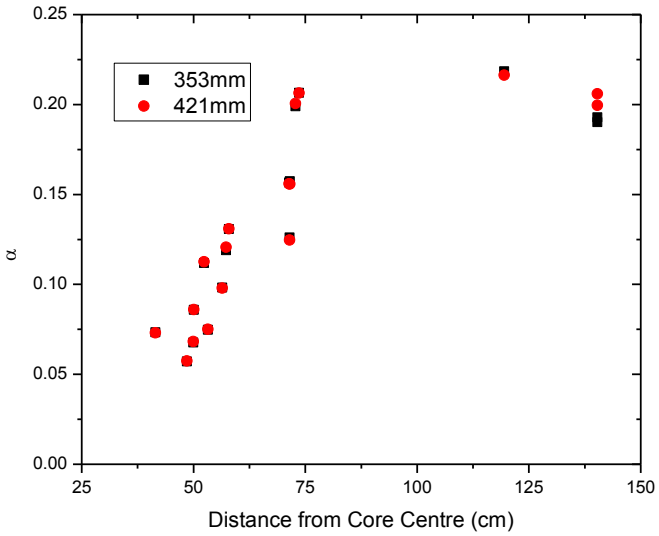

Fig 5: Non-1/E factors against distance from centre of the core.

6. Estimation of Thermal Neutron Temperature

The thermal neutron temperature (T_o) value was deduced by assuming that the thermal portion of neutron spectrum obeys a Maxwellian distribution. That portion is fitted, through nonlinear fitting, to the following equation [9]:

$$\Phi(E) = I_{th} \left(\frac{E}{E_T^2}\right) e^{\frac{-E}{E_T}} \qquad \text{Equation \#2}$$

Where I_{th} is a scaling constant and E_T is the characteristic energy, which can be converted to the thermal neutron temperature (T_o) using the following formula [9]:

$$T(\text{Kelvin}) = \frac{E_T\ (\text{eV})}{8.617\times 10^{-5}} \qquad \text{Equation \#3}$$

In addition to the distance from reactor core centre, T_o is affected by other factors, such as the size and the type of filling material in the irradiation hole. Upon grouping irradiation locations and plotting the results against distance (Fig 6), it is evident that - as expected - T_o decreases with distance from the core centre.

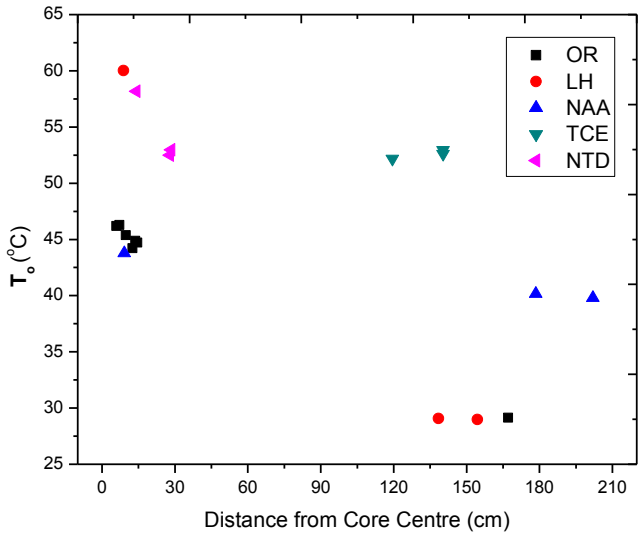

Fig 6: Thermal neutron temperature against distance from core centre.

It should be kept in mind that all spectra presented in this work were calculated using room temperature cross-section data (20 ^{o}C). Indeed, it is expected that T_o shall be sensitive to the physical temperature of irradiation locations. However, the extent to which the physical temperature affects T_o is not investigated in this work.

Similar to previous section, because the spectra used for determination of T_o (and α) are averaged over the whole axial length of the irradiation locations, these results only represent the average values of T_o and α. As explained in section 4, neutron spectra are quite sensitive to the axial location, and it would be expected that values of T_o are lowest (and that values of α are highest) near the top of the reactor core at the JRTR's current burn-up level of 100 MWD.

These fitting parameters were also determined for Xenon-free core conditions, and it has been concluded (based on calculation results) that thermal neutron temperatures (T_o) are almost insensitive to the reactor core Xenon levels.

7. Neutron Flux Distributions

In this section, attention is shifted towards presenting neutron flux distributions rather than neutron spectra. Information provided here is based on the same calculations presented above. Axial distribution of the neutron flux for IR0, IR12, and IR14 are plotted in the top of Fig 7. It has to be kept in mind that these reported distributions are perturbed by the loaded target irradiation material.

Neutron flux distributions were also calculated for irradiation locations in the heavy water reflector, and are presented in the centre and bottom parts of Fig 7.

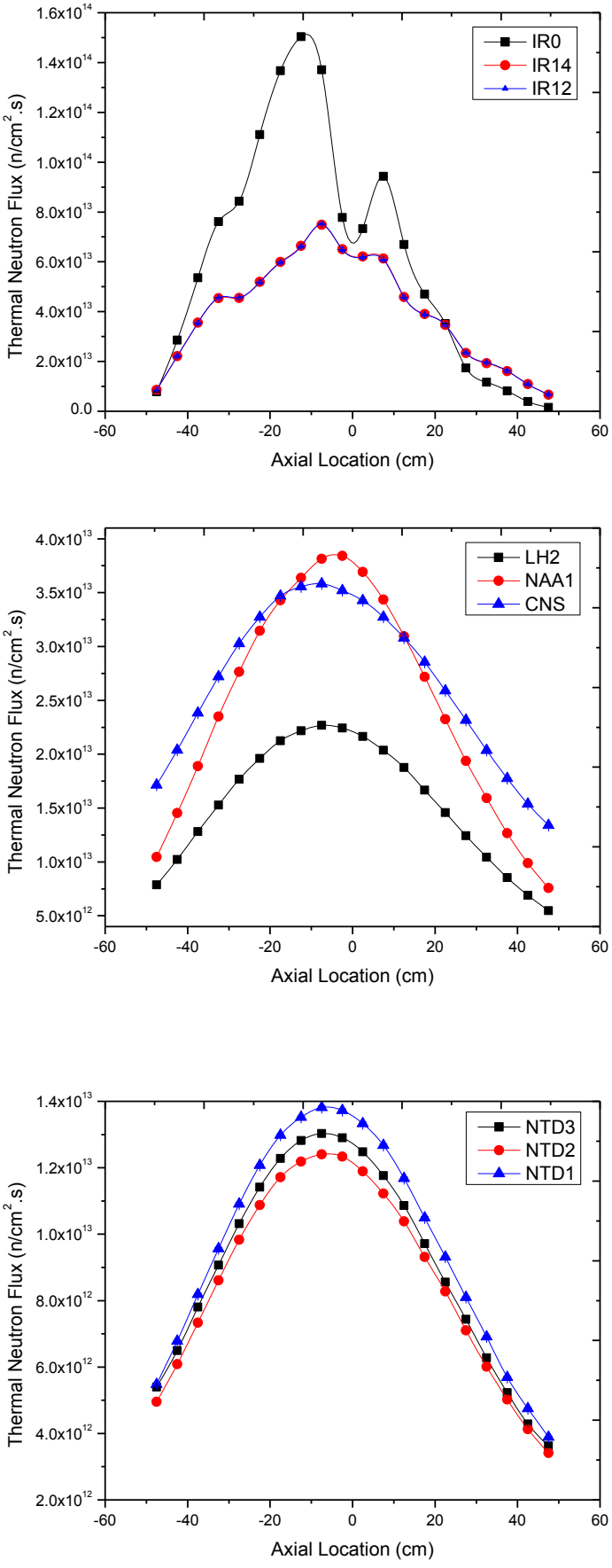

Fig 7: Axial distribution of neutron flux at IR0, IR12 and IR14 (Top), and at LH2, NAA1, CNS (Centre), and at NTD1, 2, 3 (Bottom). CAR set at 421 mm, and spectra scaled to 5 MW.

In reference to neutron flux distributions, one may quantify the neutron flux radial and axial gradients within NAA rabbits (irradiation containers) at NAA channels, which is of interest for the application of the NAA technique as pointed out by an IAEA Expert Mission held during October 2018 at the JRTR [10]. These gradients, if significant, might impact the accuracy of NAA results since flux monitors and/or reference samples will not be located at the same exact location as of the sample of interest during irradiation.

For this particular purpose, the thermal neutron flux was tallied at the NAA PTS tubes using a fine cylindrical mesh. The cylindrical mesh (10cm long and 3.1cm in diameter), was located at the bottom of the PTS tube (where a NAA rabbit is positioned during irradiation) and divided into a total of thirty regions: 10 axial regions each divided into three angular regions, where each angular region represents 120^{o} of the cylinder. A total of 4.75E+8 particles were simulated in order to obtain sufficient statistics at NAA2 and NAA3.

Fig 8 resembles normalized axial thermal neutron flux distributions within NAA1, NAA2, and NAA3 rabbits. Error bars represent standard deviation (at one sigma).

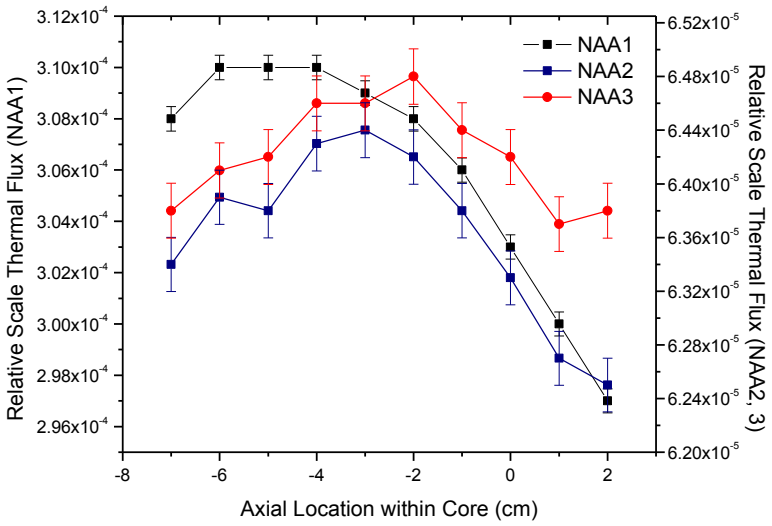

Fig 8: Axial thermal neutron flux distributions in NAA irradiation containers.

Maximum-to-minimum flux values were estimated based on these distributions and results are summarized in Tab 3 for the radial and axial directions.

	NAA1 (%)	NAA2 (%)	NAA3 (%)
Radial (max/min - 1)*	2.1 ±0.12	3.1 ±0.25	2.5 ±0.25
Axial (max/min - 1):	-	-	-
Theta 1	4.0 ±0.40	2.9 ±0.81	2.6 ±0.82
Theta 2	4.8 ±0.40	3.4 ±0.80	1.5 ±0.79
Theta 3	4.8 ±0.40	3.7 ±0.81	2.8 ±0.80
Summed Axial (max/min - 1)**	4.5 ±0.23	3.0 ±0.46	1.8 ±0.46

*Based on axially averaged flux values at three different angular positions

**Based on angularly summed axial distribution

Tab 3. Summary of thermal neutron flux gradients in NAA channels

Finally, the radial flux distribution is depicted using a contour plot in Fig 9. This plot may be more illustrative than tabular data and may be more helpful when identifying unique features of the neutron field. For example, through this figure, it can be easily identified that IR1 and IR2 holes (depicted in Fig 1) have the highest flux values after IR0 hole.

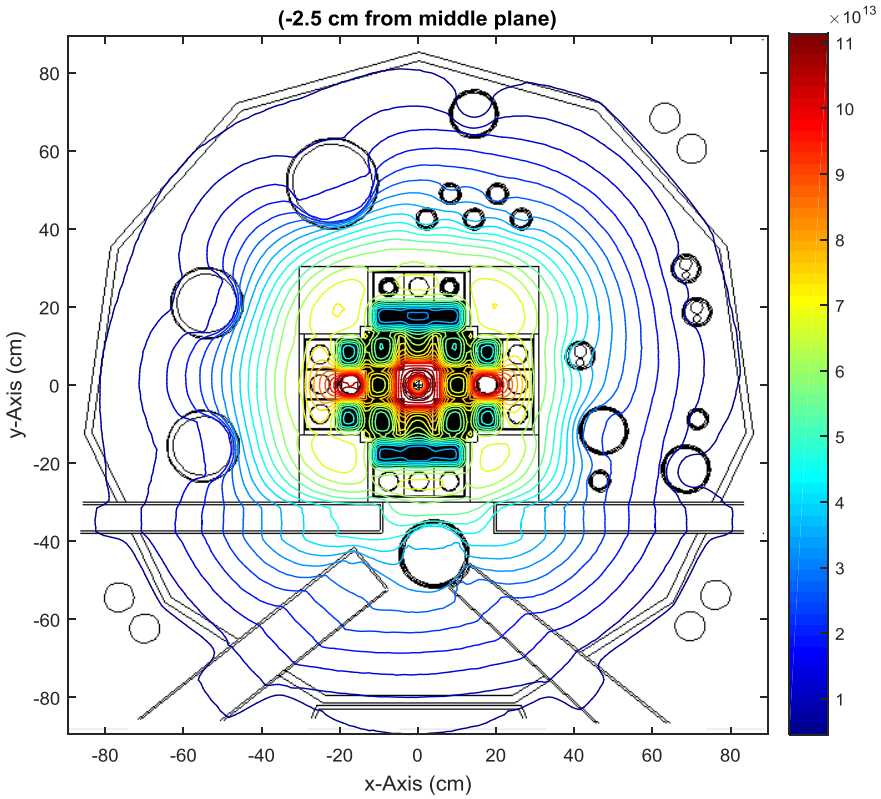

Fig 9: Thermal neutron flux contour map at the -2.5 cm plane, Xenon equilibrium at 5 MW. Units: n/cm^2.s.

8. Conclusion

Analyses have been performed to characterize the neutron fields in the JRTR reactor using the MCNP code, which is useful for the purpose of gaining an overview of the neutron field in the reactor core and for providing preliminary indications on its utilization.

Those calculations adopted a couple of assumptions, such as the core components being at isothermal room temperature and neglecting the photo-neutron source. In addition, these results are valid for the current burn-up level and reactor configuration and may change along with change of reactor core conditions and configuration.

Results presented in this work are meant to support and guide near-future utilization activities at the JRTR. Results given in this work need to be supported - for each utilization activity - by suitable measurements.

9. Acknowledgment

Nuclear safety team members are commended for their support and participation in discussions related to the work presented above and thanks to the JRTR manager for his overall kind support during the preparation of this work.

10. References

[1] AbuSaleem and K. Atrasha Y. Commissioning of the Jordan Research and Training Reactor, IGORR-2017.

[2] Farouki I.F., Hamdan K.S., Jun B.J., and Alkhafaji S.M. Initial Operation Experience and Near Future Utilization Plans at the Jordan Research and Training Reactor, RRFM-2018.

[3] Suaifan, Mahmoud, et al. "Status and perspectives on the utilization of a new nuclear research reactor in Jordan." Physica B: Condensed Matter (2017).

[4] Goorley, T., et al. "Initial MCNP6 release overview." Nuclear Technology 180.3 (2012): 298-315.

[5] Jaradat, Mustafa K., et al. "Verification of MCNP6 model of the Jordan Research and Training Reactor (JRTR) for calculations of neutronic parameters." Annals of Nuclear Energy 96 (2016): 96-103.

[6] Farouki I.F., Full-Core Burn-up Calculations Using MCNP6 Code for the Jordan Research and Training Reactor, RRFM-2019.

[7] K. S. Khoo, S. B. Sarmani, and I. O. Abugassa. "Determination of thermal to epithermal neutron flux ratio (f), epithermal neutron flux shape factor (α) and comparator factor (Fc) in the Triga Mark II reactor, Malaysia." Journal of Radioanalytical and Nuclear Chemistry 271.2 (2007): 419-424.

[8] Nassau, Kurt, "Altering the color of topaz." Gems & Gemology 21.1 (1985): 26-34.

[9] Van Hung, Tran. "Determination of neutron temperature in irradiation channels of reactor." Journal of radioanalytical and nuclear chemistry 287.1 (2011): 103-106.

[10] TC Expert Mission on Evaluation of the current status of the INAA Facility at JRTR Report, JOR1008, 21-25 October 2018

Mr. Lorenzo Stefanini

- He obtained his Master of Science in Nuclear Engineering at the School of Engineering of the University of Pisa.
- He has years working experience in the nuclear field with specialization in structural engineering and nuclear project management.
- He is currently a Project Manager at NRG, the Netherlands. His main activities are related to the project management of the High Flux Reactor Continued Safe Operations and of the European research project on Pressurized Thermal Shock. Moreover, he supports LTOs and ageing management at various NPPs.

RADIOIODINE WASTE MANAGEMENT BY USING COLD SINTERING OF CERAMIC MATRICES

Muhmood ul Hassan and Ho Jin Ryu*

*Corresponding author email: hojinryu@kaist.ac.kr

Department of Nuclear and Quantum Engineering, Korea Advanced Institute of Science and Technology (KAIST), S. Korea

ABSTRACT

Radioiodine is a volatile radionuclide present in the radioactive waste stream of the research reactor. Its long half-life and high mobility enlist it among the major causes of environmental and radiological hazards. A number of different methods have been demonstrated for the adsorption and immobilization of radioiodine. We, first time, investigated the immobilization of iodine by using ceramic matrices using cold sintering. Iodine bearing calcium hydroxyapatite (IO-HAP) and iodosodalite (I-SODA) were two ceramic matrices used as simulated waste. The IO-HAP containing 7 wt.% of iodine was sintered at 200 °C and 500 MPa whereas I-SODA with iodine contents of 14 wt.% was sintered at 300 °C and 500 MPa. Both of the ceramic matrices were cold sintered without using any binder and the achieved relative sintered densities were higher 97%. The microhardness values were 2 and 3.88 GPa for IO-HAP and I-SODA, respectively. Chemical durability of the sintered matrices was tested by using 7 days product consistency test (PCT) as per ASTM-C 1285 (1) and normalized leaching rates of the simulated waste showed very low values of 2×10^{-5} and 4×10^{-4} g/m^2·day, respectively. The measured microhardness and compressive strength values were significantly higher than the matrices being used for the immobilization of radioiodine.

1. Introduction

The wide range applications of research reactor include radioisotope production, materials irradiation behavior studies, neutron therapy and neutron activation analysis. Radioactive waste, ranging from exempt waste to high-level waste, produces during the operation of a research reactor. A number of different factors including application, operational schedule and type of reactor define the amount and type of waste produced. The nuclear industry is continuously making efforts in probing the efficient, durable, environment-friendly and technologically simple method to condition and immobilize the different types of waste being produced.

Radioiodine is a long-lived radioisotope and has high environmental mobility. Moreover, the conventional high-temperature immobilization techniques like hot pressing, thermal sintering, vitrification cannot fully retain the radioiodine due to its low volatilization temperature. Other low-temperature technologies including cementation have loading and chemical durability concerns. To overcome these challenges continuous efforts are on-going and as a part different ceramic materials are also being investigated.

Calcium hydroxyapatite and sodalite are two examples of such ceramics being considered a possible solution to the development of durable waste matrices for the immobilization of radioiodine. Both of these ceramics have the capabilities to substitute the iodine in their crystal structure both in the form of iodate and iodide. Coulon et al.[1] and Chong et al.[2] have reported the successful low-temperature synthesis of iodine substituted hydroxyapatite (IO-

HAP) and Iodosodalite (I-SODA) with very good wt.% of substituted iodine. However, the low-temperature consolidation of these synthesized ceramics waste forms was not being investigated.

Cold sintering is a very low-temperature consolidation process and a number of ceramic and ceramic composites have been sintered by using this process recently. The cold sintering is a pressure driven consolidation process achieved by making use of the transient liquid or hydrous phase. This process requires a very low temperature than the volatilization temperature of the iodine and thus can ensure the complete retention of the loaded radioiodine during the consolidation process.

We have investigated that IO-HAP and I-SODA can be cold sintered without using any organic binders and glass frit. Both of the ceramics achieved sintered relative densities >97 % and exhibited very good micro-hardness values. The sintered matrices have also shown good leach resistance and chemical durability.

2. Materials and Method

2.1 Synthesis of IO-HAP & I-SODA

The synthesis of IO-HAP and I-SODA were carried out by using reported methods. Briefly, the IO-HAP was synthesized by wet precipitation method using the anionic solution of [$(NH_4)_2HPO_4$+ NH_4IO_3] and cationic solution of [$Ca(NO_3)_2{\cdot}4H_2O$]. The synthesis was carried out at a pH of 10.5, temperature 30 °C and under continuous stirring at 200 RPM. The final product was aged for 24 hrs at room temperature, filtered and then dried at 110 °C for 12 hrs[3].

I-SODA was synthesized by hydrothermal synthesis by using the meta-kaolinite, sodium hydroxide and sodium iodide strictly following the procedure described by Chong et al. The final product was dried overnight at 110 °C in vacuum oven[2].

2.2 Characterization

Synthesized-dried ceramic powders were analysed by using advanced analytical techniques to ensure the successful synthesis of target materials. Both of the products were characterized by high-resolution XRD, XRF, XPS, NMR, FTIR, TGA-DSC, ICP, SEM and TEM techniques.
XRD, FTIR and TEM analysis confirmed the nanocrystalline nature of the synthesized ceramics with a high amorphous fraction (Fig.1). The TGA-DSC showed that both of the ceramic materials possess adsorbed water as part of their amorphous phases despite drying overnight at 110 °C. The thermogravimetric analysis also provided an upper limit for the temperature, which can be applied during the cold sintering without causing the volatilization of loaded iodine. Based on these characterizations, it was established that the synthesized products inherently have a transient phase, which can be activated under applied pressure and at low temperature. The presence of such a transient phase is a prerequisite of cold sintering and therefore the synthesized iodine bearing ceramics can possibly be cold sintered.

2.3 Cold Sintering

Cold sintering of the IO-HAP and I-SODA was carried out by using a steel mold with an internal diameter of 10 mm, a ceramic band heater and a Carver uniaxial press. The experimental set-up is shown in Fig. 4[3].

For IO-HAP the optimized cold sintering parameters were 200 °C dwell temperature for a soaking time of 10 min under constant uniaxial pressure of 500 MPa. Whereas, in the case of

I-SODA the maximum relative sintered density was achieved at 300 °C, 10 min and 500 MPa of uniaxial pressure.

2.4 Chemical Durability

Chemical durability of the cold sintered ceramic matrices was tested by 7-day product consistency test (PCT) (ASTM C1285)[4]. The test was carried out at 90 ± 2 °C using deionized water. The test specimen was sieved-washed samples of cold sintered-crushed powders. The leachate was collected at the end of the 7th day using a syringe filter and tested for the concentration of the leached elements using ICP-MS. BET-specific surface areas of the specimen were used for the calculation of normalized leaching rates (Eq. 1).

$$NLR_i = \frac{C_i}{t \times f_i \times S/V} \qquad (1)$$

3. Results and discussion

Very high sintered relative densities (≥ 97%) were achieved with ~100 % retention of loaded simulated radioiodine using very low temperature and efficient sintering process. Fig. 1 A & B shows the XRD patterns of the synthesized simulated waste forms used for the demonstration of a cold sintering process.

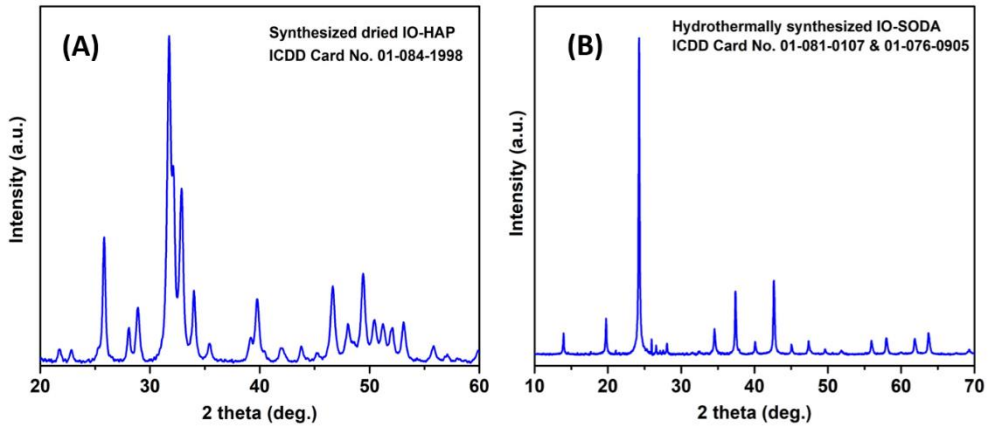

Fig. 1: XRD patterns of synthesized simulated radioiodine bearing ceramic waste forms. (A) Iodate substituted hydroxyapatite (IO-HAP). (B) Iodide substituted iodosodalite (I-SODA).

Fig. 2-A & B shows the SEM images of the fractured surfaces of the cold sintered samples. The EDAX mapping of the cold sintered samples shows the homogenized distribution of the substituted iodine inside the cold sintered matrices (Fig. 3-A & B).

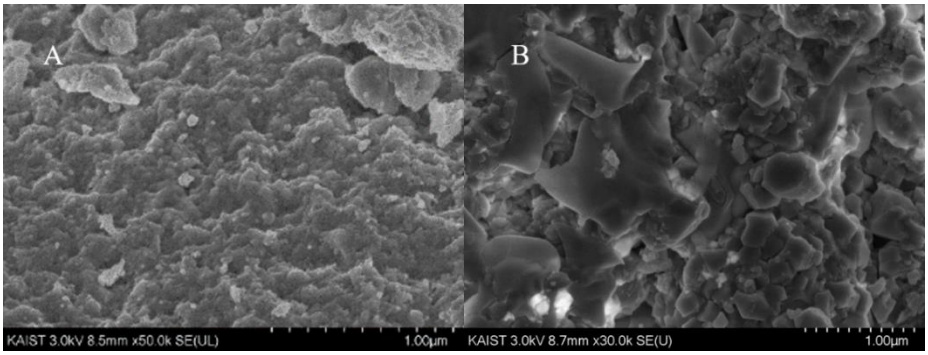

Fig. 2: SEM images of the fractured surface of cold sintered IO-HAP (A) and I-SODA (B)

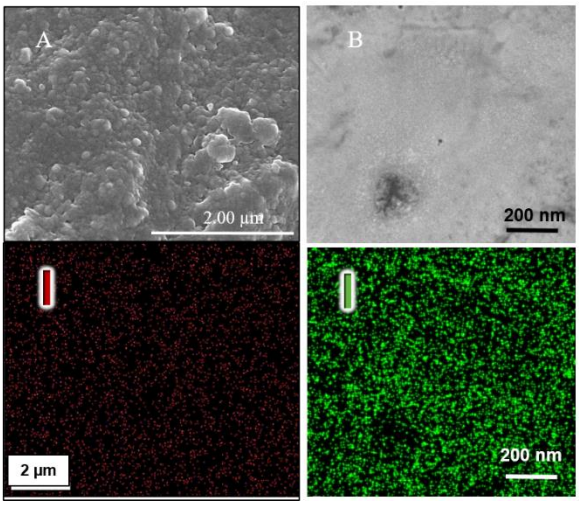

Fig. 3: EDS elemental mapping of cold sintered IO-HAP (A) and I-SODA (B)

The further verification of the sintering was carried out by testing the micro-hardness and compressive strengths of the cold sintered samples. In the case of IO-HAP, the micro-hardness and compressive strength values were 2 GPa and 174 MPa respectively. Whereas, the cold sintered iodosodalite sample exhibited the micro-hardness value of 3.88 GPa. These measured values of micro-hardness and compressive strength are much higher than the established regulatory requirements for a waste matrix[5].

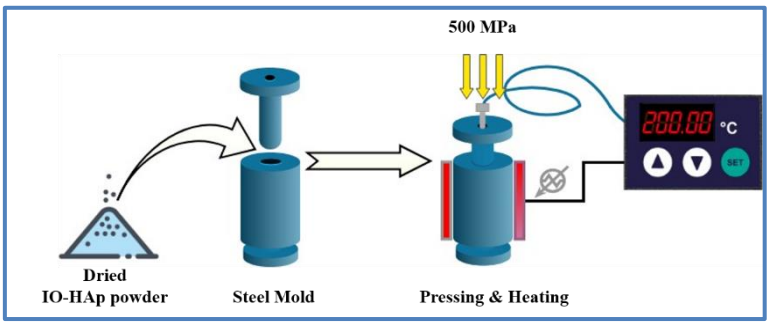

Fig. 3: Graphical representation of cold sintering set-up[3].

Cold sintering is a pressure-assisted sintering process which is facilitated by the distribution and rearrangement of a transient hydrated amorphous phase and nanocrystallites. In the cold sintering process, the highest sintered relative density is achieved by the combined mechanochemical effect triggered by the applied load and low temperature. The final stage of the densification is achieved by the dehydration of the hydrated phase and thus require low activation temperature (≤ 300 °C)[6,7]. Therefore, the cold sintering process is an effective and efficient way to consolidate ceramic waste matrices containing volatile radionuclides e.g. I-123.

ASTM C1285-PCT test was carried out without adjusting the initial pH (7.41) and the leachate samples were collected for the measurement of leached concentrations at the end of 7th day. Iodine normalized leaching rates (10^{-5} g/m^2·d) from IO-HAP cold sintered sample were of the same order of magnitude as reported by Coulon et al. [1] from spark plasma sintered IO-HAP.

In the case of I-SODA, higher leaching rates were expected due to the rapid surface dissolution, the presence of unreacted phases and the lower value of pH. Measured normalized leaching rates of iodine (10^{-4} g/m^2·d) are similar to the leaching rates reported by Maddrell et al.[8] from high temperature hot isostatically pressed sodalite and Chong et al.[9] from a glass-bonded 750 °C sintered iodosodalite sample despite the fact that Chong et al. performed the ASTM C1285 test with pH values adjusted > 10. Coulon et al.[1] and Nakazawa

et al.[10] measured reduced normalized leaching rates with high pH values in both IO-HAP and I-SODA cases, respectively.

4. Conclusions

In this study, the possibility to consolidate volatile radioactive waste over ceramic matrices was demonstrated. Low temperature, non-volatile sintering of simulated radioiodine bearing ceramic waste forms was achieved with the highest sintered relative densities. Physical and chemical durability results suggest that:

i. The cold sintering of ceramic waste forms with comparable durability is possible.
ii. The cold sintering process ensures the safety of the process by avoiding the volatilization of loaded radioisotopes.
iii. The normalized leaching rates were of the same order of magnitude as reported for the high temperature processed waste.
iv. Higher densification, ~100 % retention of the loaded volatile radionuclides, physical and chemical durability achieved by the cold sintered matrices make cold sintering process suitable for the conditioning of radioactive waste in general and for the volatile radioactive waste in particular.

Acknowledgment

These studies are supported by the grant funded by the MSIT (NRF-2018M2B2A9065746), Republic of Korea and the KUSTAR-KAIST Institute.

References

[1] A. Coulon, D. Laurencin, A. Grandjean, S. Le Gallet, L. Minier, S. Rossignol, L. Campayo, Key parameters for spark plasma sintering of wet-precipitated iodate-substituted hydroxyapatite, J. Eur. Ceram. Soc. 36 (2016) 2009–2016. doi:10.1016/j.jeurceramsoc.2016.02.041.

[2] S. Chong, J. Peterson, J. Nam, B. Riley, J. McCloy, Synthesis and characterization of iodosodalite, J. Am. Ceram. Soc. 100 (2017) 2273–2284. doi:10.1111/jace.14772.

[3] M. ul Hassan, H.J. Ryu, Cold sintering and durability of iodate-substituted calcium hydroxyapatite (IO-HAp) for the immobilization of radioiodine, J. Nucl. Mater. 514 (2019) 84-89. doi:10.1016/j.jnucmat.2018.11.024.

[4] ASTM C1285-02, Standard Test Methods for Determining Chemical Durability of Nuclear, Hazardous, and Mixed Waste Glasses and Multiphase Glass Ceramics : The Product Consistency Test (PCT) 1, ASTM, Conshohocken, USA, 2002. 15 (2002) 1–26. doi:10.1520/C1285-14.2.

[5] I.W. Donald, Waste immobilization in glass and ceramic based hosts : radioactive, toxic and hazardous wastes, Wiley, Chichester, West Sussex, 2010.

[6] M. ul Hassan, H. Ryu, Low-Temperature Processing and Consolidation of Hydroxyapatite (ICACC-S13-028-2018), in: The American Ceramic Society (Ed.), 42nd Int. Conf. Expo. Adv. Ceram. Compos., The American Ceramic Society, Daytona Beach, Florida, 2018: pp. 123–124. http://ceramics.org/wp-content/uploads/2018/01/ICACC18_Abstracts-WebFinal.pdf

[7] J. Guo, A.L. Baker, H. Guo, M. Lanagan, C.A. Randall, Cold sintering process: A new era for ceramic packaging and microwave device development, J. Am. Ceram. Soc. 100 (2017) 669–677. doi:10.1111/jace.14603.

[8] E.R. Maddrell, E.R. Vance, C. Grant, Z. Aly, A. Stopic, T. Palmer, J. Harrison, D.J. Gregg, Silver iodide sodalite – Wasteform / Hip canister interactions and aqueous durability, J. Nucl. Mater. 517 (2019) 71–79. doi:10.1016/j.jnucmat.2019.02.002.

[9] S. Chong, J.A. Peterson, B.J. Riley, D. Tabada, D. Wall, C.L. Corkhill, J.S. McCloy, Glass-bonded iodosodalite waste form for immobilization of 129 I, J. Nucl. Mater. 504 (2018) 109–121. doi:10.1016/j.jnucmat.2018.03.033.

[10] T. Nakazawa, H. Kato, K. Okada, S. Ueta, M. Mihara, Iodine Immobilization by Sodalite Waste Form, MRS Proc. 663 (2000) 51. doi:10.1557/PROC-663-51.

X-RAY 3D CT ANALYSIS FOR HIGH-DENSITY LEU DISPERSION TARGET FABRICATION

HYEONG-JIN KIM, HO JIN RYU*,
Department of Nuclear and Quantum Engineering, KAIST
Daehak-ro 291, Yuseong-gu, Daejeon, 34141, Korea
**Corresponding author: hojinryu@kaist.ac.kr*

ABSTRACT

In order to improve Mo-99 productivity, it is necessary to develop high uranium density targets with low enriched uranium (LEU). In this study, we developed a methodology to analyse the spatial distribution of uranium particles of the dispersion plate using X-ray computed tomography. Stainless steel powder was used as a surrogate for uranium particles in the aluminium matrix, and applicability of the CT technique for observing the internal microstructure of the dispersion plates was confirmed. The microstructural homogeneity of dispersion plates was evaluated by analysing the spatial distribution of the particles in the Al matrix. The effects of rolling parameters on the homogeneity of the simulated dispersion targets were investigated by the X-ray CT.

1. Introduction

Tc-99m is the most widely used radioisotope for medical diagnostic purposes. The main source of Tc-99m is Mo-99 extracted from uranium targets in the research reactors [1]. After non-proliferation policy claims minimization of highly enriched uranium (HEU) utilization in medical radioisotope production, now it is necessary to develop the low enriched uranium (LEU) targets [2]. However, due to its low U-235 content, Lethe U target has lower Mo-99 productivity than conventional HEU targets. In order to improve the radioisotope productivity of LEU targets, the development of high uranium density LEU targets is required.

In 2013, a lab-scale development of high density U-Al dispersion plates with density up to 9.0 gU/cm^3 based on the centrifugal atomization was reported [3-4]. The interaction layer (IL) consists of intermetallic compound UAl_x, was found during the fabrication process. Since IL has a low density which leads to a volumetric increase, degradation of thermal properties can occur. Larger uranium particle sizes lower the volume fraction of the IL, but the segregation of uranium particles can occur during the hot rolling process.

The optimized fabrication condition for the coarse uranium particle should be set by analysing the microstructure of the dispersion target, in order to obtain the desirable particle distribution. Currently, the internal structure of the target is mainly observed by 1) radiography, 2) optical microscopy, 3) scanning electron microscopy. In comparison with conventional techniques, the X-ray CT technique allows entire microstructure, without causing damage to the samples [5]. In this study, a methodology to figure out the particle homogeneity by using X-ray CT technique was established.

2. Methodology

2.1 Fabrication of stainless steel-aluminium dispersion plate

Stainless steel 304L (SS304L, SS) was selected as a surrogate material for uranium particle due to its similar yield strength and high X-ray attenuation coefficient [6]. SS304L powder was prepared by atomization. After sieving, the powder was mixed with Al powder with a mixing

ratio of 9.0 gU/cm^3 grade LEU target (SS:Al volume ratio = 0.471:0.529). Mixed powder was pressed into a compact with dimension of 15 mm x 15 mm x 2 mm under 400 MPa condition.

Compacts and Al6061 claddings were then assembled and welded by diffusion bonding using the spark plasma sintering technique (SPS). The joined assembly was heated to 300^{o}C with a heating rate of 30^{o}C/min, and then heated further for 10 minutes. The process was performed under 5MPa pressure, in vacuum.

Then the sample underwent a rolling process with 0.1 s^{-1} strain rate. The preheating condition was 500^{o}C for 30 minutes, and 10 minutes reheating was applied between each rolling pass. The reduction ratios are described in Table 1. After the rolling process, simulated dispersion target assemblies of 6 mm in thickness was reduced to 1.27 mm.

		Sample A	**Sample B**	**Sample C**
Hot rolling	Number of passes	9	4	3
	Reduction ratio per pass	15%	30%	40%
Cold rolling		1 pass, 10%		

Tab 1: Rolling condition

2.2 Data acquisition by X-ray CT

The fabricated sample was then observed by micro-CT. Nikon XT H 225 supporting 20 W power and X-ray voltage up to 22 5kV was used for data acquisition. The spatial resolution of the equipment was 3 μm and the minimum voxels size was 1 μm. The equipment supports high X-ray voltage which provides fine contrast resolution. Fig. 1 shows one of the cross-section images of the fabricated sample observed by XT H 225.

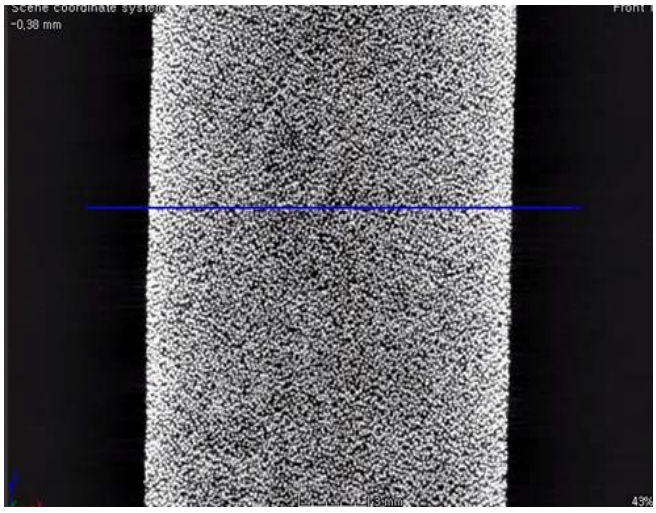

Fig 1. Cross sectional image of the fabricated sample obtained by XT H 225

3. Result and discussions

Two steps of data processing were conducted based on the MATLAB platform. First, binary segmentation of SS particles from the Al matrix on data stack was conducted by thresholding. The threshold value was set in order that stainless steel and aluminium would be separated into black and white images.

After the binary segmentation, the volume fraction of the SS particle in the sample was calculated. In the 3D stacked image, ‘cell’ which includes pixels to be calculated was set, and

calculation was conducted with n time randomly changing the position of the cell. After the calculation, the calculated volume fraction was plotted according to cell size. Convergence in the resulting graph indicates the degree of homogeneity of SS particle inside the sample. And by plotting the standard deviation plot of different samples together, comparison of their relative homogeneity is possible.

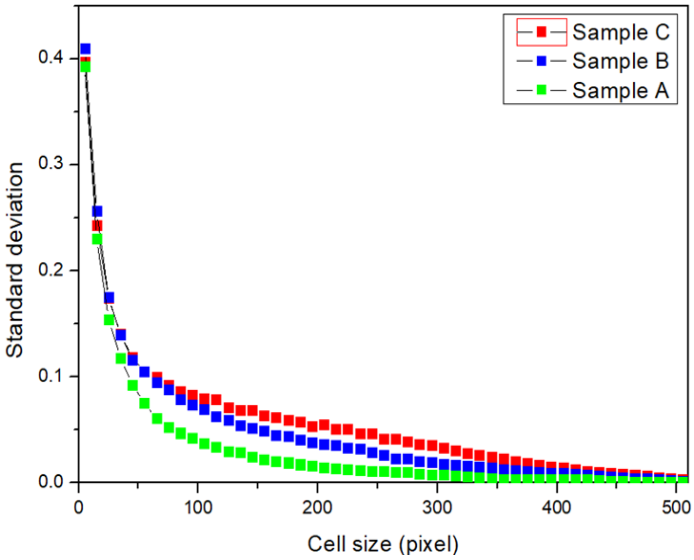

Fig 2. A standard deviation vs. cell size plot of three kinds of fabricated samples

Fig. 2 shows the standard deviation tendency depending on the reduction ratio per pass during the hot rolling process. The SS particle volume fraction converges most rapidly in the sample fabricated with the lowest reduction ratio. This phenomenon implies that the internal particle homogeneity of the high density LEU target with a larger uranium particle size, can be enhanced by reducing the rolling reduction ratio per pass.

4. Conclusions

In this study, the applicability of the X-ray CT technique on the observation of the dispersion particles in the target plate was investigated. Stainless steel and aluminium were found to be clearly distinguishable in the reconstructed CT images. From analysing the volume fraction convergence of fabricated samples, the effect of the number of rolling was identified. The homogeneity of dispersed stainless steel particle was enhanced by lowering the rolling reduction ratio per pass.

This analysis is expected to contribute to improved safety and performance of high density LEU targets by optimizing the homogeneity of dispersion particles in the target plates.

5. Acknowledgments

This study is supported by National Research Foundation, Korea (NRF-2018M2A8A1023313)

6. References

[1] Van der Marck, Steven C., Arjan J. Koning, and Kevin E. Charlton. "The options for the future production of the medical isotope 99 Mo." (2010): 1817-1820.

[2] Welsh, James, Carmen I. Bigles, and Alejandro Valderrabano. "Future US supply of Mo-99 production through fission based LEU/LEU technology." Journal of radioanalytical and nuclear chemistry 305.1 (2015): 9-12.

[3] Ryu, Ho Jin, et al. "Development of high-density U/Al dispersion plates for Mo-99 production using atomized uranium powder." Nuclear Engineering and Technology 45.7 (2013): 979-986.

[4] Ryu, Ho Jin, et al. "Metallurgical considerations for the fabrication of low-enriched uranium dispersion targets with a high density for 99Mo production." Journal of Radioanalytical and Nuclear Chemistry 305.1 (2015): 31-39.

[5] Cnudde, Veerle, and Matthieu Nicolaas Boone. "High-resolution X-ray computed tomography in geosciences: A review of the current technology and applications." Earth-Science Reviews 123 (2013): 1-17.

[6] Hubbell, J. H. "Photon mass attenuation and energy-absorption coefficients." The International Journal of Applied Radiation and Isotopes 33.11 (1982): 1269-1290.

LICENSING OF INNOVATIVE NUCLEAR RESEARCH FACILITIES

Alexander Sapozhnikov
Department for Safety Regulation of Nuclear Power Plants and Nuclear Research Facilities,
Federal Environmental, Industrial and Nuclear Supervision Service of Russia,
109147 Moscow, Taganskaya, 34, Russia

ABSTRACT

In recent years several innovative nuclear facilities have been designed and now are under construction in the Russian Federation. During the licensing process Rostechnadzor performs assessment of the applied documents justifying safety of these facilities in compliance with acting safety requirements in the field of nuclear energy use. In the process of deep and detailed analysis of the safety requirements it became clear that in case of licensing of the innovative nuclear projects, which implement modern technologies and advanced technical solutions, the existing requirements do not fully address all safety issues. The directions for further strengthening of the legislative and regulatory framework and the need for development of additional safety requirements have been identified. The paper presents the experience of licensing of nuclear research and experimental reactors, and points out directions for further improvement of the safety codes and regulations as well as licensing procedures.

1. Introduction

The analysis of current safety codes and regulations in the field of nuclear energy use in the Russian Federation (in the case of the Russian Federation – Federal Regulations and Rules - FRR) shows that they basically were harmonized with recommendations of the IAEA standards and take into account lessons learned resulting from the Fukushima Daiichi nuclear power plant accident. The volume of the FRR requirements ensures effective and sustainable safety regulation of nuclear research facilities (NRFs)[1], including those constructed many years ago as experimental facilities for needs of nuclear science and technology and demonstration of capabilities of nuclear power. At present, innovative projects of the NRF are being implemented in the Russian Federation, the objectives of which are increasing of scientific and research capabilities, significant promotion of current nuclear technologies, and testing of new equipment and fuel.

Among innovative NRFs are complex RR PIC [1], complex RR MBIR [2] and complex RR Argus-M [3], which are now in stage of commissioning. Moreover, work is underway to build a pilot demonstration power complex BREST-OD-300 [4] and pilot-industrial power unit SVBR-100 [5]. These facilities do not fully meet safety requirements for nuclear power plants, in particular the requirements for stability and reliability of operation in the power grid, the use of tested technical solutions and proven technologies. The report presents the experience of licensing of innovative research and experimental nuclear reactors, and points out directions for further strengthening FRR and improvement of the licensing procedures.

2. Licensing of nuclear research facilities innovative in the past

2.1. Licensing features

Prior to the Federal law "On the use of nuclear energy" No. 170-FZ of 21.11.1995 was put in force, the regulatory body had issued temporary permits for activities in the field of the nuclear energy use in order to bring the safety of nuclear research facilities in compliance

1 NRFs – nuclear facility including research nuclear reactors (RR), critical nuclear assembles (CA) and subcritical (SCA) nuclear assembles, and related complex of premises, structures, systems, elements, experimental facilities, and personnel that are in boundary of territory (NRF site) defined by the design for utilization of neutrons and ionizing radiation for research purposes.

with modern safety requirements. The current Russian regulatory system in the field of nuclear energy use meets, in general, the IAEA recommendations [6] and has a good practice [6]. The normative legal acts on execution by Rostechnadzor of the state function on licensing the activity in the field of nuclear energy use are given on the Internet website www.gosnadzor.ru. The full list of legislative acts and regulations in the field of nuclear energy use is presented in section II of the document P-01-01-2017 [7].

According to decree of the Government of the Russian Federation [8] the Federal service for environmental, technological and nuclear supervision (Rostechnadzor) and the State atomic energy Corporation "Rosatom" ("Rosatom") must exercise their functions related to features of conformity assessment of products, for which the safety requirements are established in the field of nuclear energy use, as well as the processes of its design (including survey work), production, construction, installation, commissioning, operation, storage, transportation, sale and disposal.

Implementation of the conformity assessment system should be based on the development (revision) of the FRRs and industry standards in accordance with national and world achievements in science and technology in the field regulated by the relevant FRR. Moreover, during the licensing of innovative nuclear facilities the necessities may be raised: 1) to assess the adequacy of the current regulatory framework for reviewing safety features of the facility; and 2) to confirm flexibility of the licensing procedures at all stages of the life cycle of the facility. These issues are considered below using examples of licensing of the research and experimental nuclear reactors (RR) that were innovative in the past. The accumulated experience of safety reviewing has been used for strengthening NRFs regulatory framework and improving licence procedures.

2.2. The First in the World NPP (RR AM-1)

The 1-st criticality was realized in 1954. The facility is water-graphite type, fuel rods are tubular with internal heat removal, moderator – graphite, coolant - water under pressure, the fuel - uranium dioxide (UO_2) enriched of 4.4% and 10 % by U235.The space inside the reactor was filled with nitrogen. A two-circuit of the heat removal to sink was used. The heat from the reactor was removed by the 1st circuit-water under pressure of 6.0 MPa, and transferred to the 2nd circuit. The reactor was designed to operate in a unit with a turbine and a generator with a nominal electric power of 5 MW. The heat of the second circuit was transferred through heating installation to the heating network of the State Scientific Center RF-IPPE. At the thermal power of the reactor 30 MW the coefficient of efficiency was 17%. The life time of the turbine- generator was expired before 1976, and since then the reactor of the First in the World NPP was used as a research reactor. The experimental work that was performed at RR AM-1 allowed starting up reactors of the Beloyarsk NPP, Bilibino NPP, and the reactors of the icebreaking ships.

A licence for operation of RR AM-1 was issued on 12.05.2000. In the licensing process, the problems were related to the life time of the structure, and systems and components (SSC) important to safety including graphite masonry of the RR AM-1, and it was a reason why since 13.03.2002 operation of RR AM-1 was carried out only in the final shutdown mode. The licence for decommissioning of the RR AM-1 was issued on 30.04.2010.

2.3. Experimental NPP VK-50 (RR VK-50)

The 1-st criticality was realized in 1964; in 1993 the facility was registered as RR VK-50. This facility is in operation since 1965. It is a nuclear facility with a pressurized water-cooled boiling reactor with natural circulation of coolant. The steam comes directly from the reactor to the turbine and the condensate of this steam in the form of feed water is returned to the reactor. Fuel-uranium dioxide (UO_2) is enriched of 3% by uranium-235. Main features of the

facility VK-50: thermal power up to 200 MW; electric power - up to 50 MW; steam consumption from the reactor-300 t / h; working pressure in the reactor vessel up to 6 MPa at a coolant temperature of 276 °C; steam pressure before the turbine - up to 2.9 MPa; specific power of the core - up to 40 kW /liter. The facility VK-50 generates electricity and transmits some heat through a heating installation into the heating network of the JSC " State Scientific Center RIAR".

The current licensing procedures provide for assessment of all safety issues of the RR VK-50, including the ageing management programme of power and heat generation equipment. The licence for the RR VK-50 operation was issued on 16.02.2000 and is updated, if necessary, by modification of licence conditions.

2.4. Experimental reactor BOR-60 (RR BOR-60)

The facility BOR-60 is experimental fast neutron reactor with two-loop three-circuit scheme for heat removal from the reactor, the maximum thermal power of the reactor is 60 MW, electrical power 12 MW. Fuel - UO_2 or a mixture of PuO_2+UO_2. The 1-st criticality was realized in 1969. The RR BOR-60 is intended for testing of advanced designs of fuel rods, fuel elements, absorbing and structural materials, testing of equipment components of NPP and non-standard equipment of sodium circuits, as well as safety justification of fast neutron reactors and production of radionuclides for the national economy. The coolant in the primary and secondary circuits is sodium; the third circuit is steam-water and includes in its composition a turbine-generator and a heating installation. The facility BOR-60 provides for generation of electricity and the transfer part of the heat through the heating installation to the heating network of the JSC "SSC RIAR".

A licence for operation of the RR BOR-60 was issued on 28.12.2001 and is updated, if necessary, by modification of licence conditions to ensure effective and sustainable operation.

2.5. Arctic modular NPP “Arbus-AST-1” (RR Arbus-AST-1)

The arctic modular nuclear facility “Arbus”, after modernization known as nuclear power plant of heat supply AST-1, was designed as an experimental facility to substantiate scientific and technical ideas for the development of nuclear power plants and low-power facilities for electricity and heating supply of industrial enterprises and settlements located in remote areas of the Far North. The 1-st criticality was realized in 1963 and then the facility was operated as a small NPP with two circuits of heat removal, thermal power 5 MW, and electricity power 750 KW. The organic coolant (gas oil) was used as a moderator and coolant of the primary circuit. Fuel - uranium dioxide (UO_2) enriched of 4,4%, 36%, 90% by uranium-235. In 1979, the facility was reconstructed into third circuits power plant of heat supply AST-1, in which high temperature organic liquid – ditolylmethane was used as a moderator and coolant in the reactor; thermal power of 12 MW. In the second and in the third circuits of the plant water was used as a coolant. The temperature of the coolant in the primary circuit at the inlet/outlet of the reactor core was 230/ 240 °C, a pressure of the coolant in the reactor was 0.5-0.6 MPa. In 1988 the facility "Arbus – AST-1" became a subject of decommissioning. In 1993 the facility was registered as RR and its safety regulation had to be conducted in compliance with FRR developed for the NRFs. The licence for decommissioning the RR "Arbus-AST-1" was issued on 24.04.2000. The decommissioning works were carried out in accordance with the FRR, extending to the NRFs. The works on the decommissioning of the facility «Arbus – AST-1" were completed and the end state in compliance with decommissioning project, namely organization of storage of high-activity RW, has been achieved.

Based on the results of the review of the completion of works on the decommissioning of the facility Arbus-AST-1, Rostechnadzor took decision from 15.08.2018 to terminate the license for decommissioning of the facility “Arbus-AST-1”. The licence for the operation of the high-activity RW storage in the building of former RR "Arbus-AST-1" was issued by Rostechnadzor on 8.12.2017.

3. Licensing of modern innovative nuclear research facilities

3.1. Complex PIC

The complex PIC is intended to conduct a wide range of research in fundamental and applied fields of nuclear physics, solid state physics, biology and other fields of science. The reactor PIK of power 100 MW is tank type water-water reactor with coolant under pressure (5 MPa), the maximum volumetric energy release in the reactor core is 6.6 MW/liter, the temperature of the coolant input/output – 50/86 °C. The reactor core (diameter 390 mm, height 500 mm, volume about 50 litres), together with the steel vessel, is placed into a heavy-water (D_2O) reflector and separated from the reflector by a double wall of the vessel. The coolant is light water (H_2O). The tank with heavy water reflector is immersed in the water pool (H_2O). Reactor facility has three loops for core cooling and three circuits for transferring the heat to the environment. Cooling towers are used as ultimate heat sink.

The material of the fuel rod composition consists of uranium dioxide (UO_2) granules dispersed in a matrix of a mixture of copper and bronze. The shell of a fuel rod is stainless steel. The fuel enrichment of U-235 is 90 %, the density of the uranium in the core is 2.2 g/cm^3, the melting point of the matrix is 1080 °C. Fuel rod is CM type that has a cruciform cross-section. The rod is twisted around its axis that ensures self-separation of fuel rods when they mounted in the fuel assembly. Similar fuel rods have more than 50 years of successful experience of operation at the SM reactor (JSC "SSC RIAR") under operating conditions that close to operating conditions at the RR PIC.

The operating organization has two licences: for construction with a validity date until 31.12.2021 and for operation at a power level less than 100 watts with a validity date until 30.12.2022. The first licence for operation of the complex PIC was issued on 21.06.2010. The first criticality of the complex PIC has been achieved in February 2011 and power level was less of permitted power 100 W. After that, the reactor core was unloaded, the fuel was moved to the fresh fuel storage, and the reactor was used in a long shutdown mode. The construction works were carried out under the licence for commissioning.

Three stages of development of reactor power were defined in the programme of the complex PIC power start-up and commissioning: 100 kW, 10 MW, and 100 MW. In 2018 the changes were made in the licence conditions for the facility operation at power level up to 100 kW.

The main difficulties during reviewing of safety are caused by the following circumstances:

- making changes to the facility project as well as to the programme of the power development;
- carrying out of refurbishment and repair works on the equipment and systems important to safety in connection with long term process of the facility commissioning since 1976;
- use of the fuel after it long-term storage;
- actualization of the safety documentation according to the results of testing and adjusting the systems and equipment;
- use of imported equipment and need to follow procedures established for assessing its conformity.

Thus, at the stage of the facility power development the safety justification of the facility could be considered as completed after achieving the design parameters of the equipment, systems and facility in the whole. In licensing process it was revealed the necessity to amend the Rostechnadzor licensing administrative procedures in term of quality check of the term of reference for reviewing of safety issues and the results of the safety examination.

In addition, the expediency of development the following safety requirements were revealed:

- ageing management of SSC important for the safety NRF;
- quality of design, manufacture, operation and storage of fuel.

3.2. Complex MBIR

The multipurpose research reactor MBIR of power 150 MW is intended to replace outdated research reactor on fast neutrons with sodium coolant BOR-60 and has the same flowsheet: two loops for core cooling and three circuits for heat transfer from the reactor to the ultimate heat sink, steam turbine, experimental loops, the complex of hot cells, and research laboratory. The sodium coolant is used in the primary and secondary circuits and in the third circuit (loop of turbine) – water/steam.

As fuel for MBIR the mixed oxide uranium-plutonium fuel is accepted. Material of the fuel rod is vibro-compacted mixture of MOX granulate (93 %) and metal uranium powder (7 %), the nominal mass fraction of the plutonium oxide in a mixture of uranium oxides and plutonium MOX granulate is 38 %.The fuel element consists of a steel shell, inside which the fuel rod and the tablets of the reproducing material of the end parts of reproduction (upper and lower) are located. The reliability of such fuel is currently not sufficiently justified. There is an idea to use alternative kinds of fuel: uranium (based on enriched uranium dioxide), dense uranium-plutonium (nitride, metal), which are of interest for future developments of nuclear energy. It is possible to use a combined vibro-compacted oxide fuel (based on plutonium and enriched uranium), which is currently used at the RR BOR-60. The most tested fuel in the nuclear energy is tablet type fuel on the basis of enriched oxide uranium (UO_2). However, it has a serious drawback for MBIR: the neutron flux with uranium fuel will be lower than with mixed uranium-plutonium MOX fuel.

At complex MBIR, it is planned to test new types of nuclear fuel for power reactors, absorbing and structural materials in steady, transient and emergency operation modes using liquid-metal, gas and liquid-salt coolants.

Rostechnadzor issued two licenses to the operating organization: in 2014 - for siting, and in 2015 - for commissioning the complex MBIR. Based on the results of the reviewing, it was concluded that there are no factors that could impede the commissioning of the complex MBIR during the stated period of up to 08.05.2025.

Nowadays, the not solved technical issues of safety justification at the construction stage of the complex MBIR include: incompleteness of projects of loop installations; incomplete confirmation of performance and reliability of the new fuel composition (MOX fuel); not full justification of the established operating life of 50 years. Moreover, resulting from Rostechnadzor inspection the shortcomings in the management system were noted.

As for the results of the analysis of the licensing procedures and completeness of the FRR requirements, there is no specific FRR for RR siting, including the requirements for the feasibility study of the site selection for RR complexes.

According to the decision of the Strategic Council of the State Corporation “Rosatom” in 2018, the initial start-up of the reactor MBIR was postponed to 2024.

3.3. Complex Apgus-M

In 1981, a stationary solution reactor “Argus” was created at the Kurchatov Institute. The reactor "Argus" is a single in the world operating RR with solution fuel. It is homogeneous nuclear reactor on thermal neutrons, operating at power 20 kW. The main purpose of the reactor is to develop innovative technologies for production of radioisotopes Mo-99, Sr-89, I-131, Xe-133. The reactor core is placed into the reactor vessel having a free volume above the fuel solution. The reactor vessel made of stainless steel is surrounded by a graphite reflector. Inside the reactor vessel there are two vertical channels for mounting control rods and a vertical central technological channel. In the reactor vessel there is a coil pipe, which is used to remove heat from the core, and an element of the reactor cooling system. The coolant is distilled water pumped by a pump through the coil pipe inside the reactor vessel (primary cooling circuit).The distillate is cooled in an external heat exchanger by technical water. During operation, the pressure inside the reactor vessel is below of atmospheric pressure and does not exceed 90.0 kPa. The gaseous products of radiolysis of the fuel solution are regenerated. Fuel is an aqueous solution of uranyl-sulphate ($U0_2S0_4$), the fuel enrichment of 90% U-235, the concentration of U-235 in solution is 73 g/liter, the solution volume in the reactor 22 liter, the neutron flux in the central channel is $5 \cdot 10^{11}$ н/см^{2}с, the time of reactor start-up and getting a reactor nominal power is 20 minutes.

The developed innovative technology for radioisotopes production from the solution fuel makes it possible getting the productivity of isotopes at the reactor power of 100-1000 times less than using the "target" technology. The efficiency of the use of U-235 is more than 90%, because the “target” is the whole fuel solution and the number of neutrons involved in the process of the generation target product multiple increases. In addition, the total amount of RW is reduced due to the exclusion of the stage of dissolution of the irradiated uranium compound from the technological cycle.

The new developed technology allows solving the urgent problem of the reducing enrichment of the used reactor fuel. Currently, the work is underway on conversion the fuel for RR Argus to low-enrichment fuel (19.8% U-235). In June 2017, the application was submitted to Rostechnadzor for changing the licence conditions for the RR Argus operation to work with low-enriched solution fuel.

The experience accumulated during the creation and operation of the RR "Argus" allowed starting the work on the implementation of the pilot nuclear-technological complex "Argus-M" (FOAK -"first of a kind"). At present Rostechnadzor is considering an application for siting and commissioning the complex Argus-M with facility of power 50 kW, fuel volume in the core 27 liter, fuel enrichment by U-235 - 19,75%, concentration of U-235 in fuel - 380,0 g/liter.

A device for loading fresh fuel provides a dosed remote fuel supply to the reactor vessel during the physical start-up of the reactor or during the planned replacement of spent fuel. The term of fuel replacement is 1 time in 10 years. The stock of the fresh fuel is stored in ampoules. A spent fuel drain device provides removal of fuel solution from the reactor vessel into ampoules for its further transportation and processing.

Licensing experience shows that the current regulatory framework for RR Argus is sufficient. However, the peculiarities of the management of solution fuel in compliance with national legislation may require the development of a special nuclear safety code for this type facility before the commissioning of the FOAK (pilot nuclear technology complex "Argus-M"). In addition, as noted above, currently there is no FRR for siting of NRF.

3.4. Licensing of demonstration modular liquid metal power nuclear facilities

3.4.1. Complex BREST-OD-300

The design of the pilot demonstration power complex BREST-OD-300 with a thermal power 700 MW and an electric power of 300 MW includes the reactor facility BREST-OD-300, a module for the processing of spent nuclear fuel, a module for the fabrication and re-fabrication of the fuel. The main objective of the design is to develop a closed-loop fuel cycle, which aims to solve the problem of radioactive waste and promote non-proliferation of nuclear materials. It is assumed to use Pu obtained from the spent fuel of WWER power reactors to manufacture mixed nitride fuel (U+Pu)N.

The mixed nitride uranium-plutonium fuel is considered as the basis fuel for future projects of commercial power fast reactors. Nitride fuel in comparison with oxide fuel has higher density and thermal conductivity; it is well compatible with liquid-metal coolant and material of the shell. Such type of fuel makes it possible to provide a closed fuel cycle without a separation of uranium and plutonium in the processing of spent mix fuel.

The integral layout is used for facility design: the core of the fast reactor, the equipment of primary circuit with lead coolant, the equipment of the fuel overloading system, as well as auxiliary systems are located in one multi-layered metal-concrete housing. The metal-concrete housing is a single monolithic reinforced concrete structure placed with a gap in the construction shaft of the reactor compartment and leaning on the foundation plate. The circulation of the lead coolant through the reactor core is realized in four peripheral cavities of the concrete housing, forming four loops, each of which includes a pump and a steam generator. The heat transfer from the reactor to the turbine is carried out by a two-circuit flowsheet. The water/steam is used in the secondary circuit.

Rostechnadzor issued a license for siting of a pilot demonstration power complex BREST-OD-300 for period from 22.01.2015 until 22.01.2025. The expert report includes the conclusion that there is no experience in operation of such type facilities, and the research and development works (R & D), as well as calculations, have not been completed for a number of technical decisions taken in the facility design. The principal safety issues, which are not now regulated by the FRR, are related to the use of liquid lead as a coolant. Among the uncompleted safety issues are the following:

- justifying operability of concrete and structural materials in interaction with lead in operation and emergency regimes;
- ensuring control of the state of the coolant and maintaining the oxygen concentration necessary to limit the corrosive effect of the coolant on the construction materials;

Moreover, the issues of radiation protection of personnel must be resolved, since in the first circuit irradiation may contribute to the formation of long-lived isotopes of lead and radioactive polonium, and in the second steam-water circuit - to the accumulation of tritium.

In the course of reviewing the justification of safety siting BREST-OD-300 the analysis of the current FRR has been performed. It shows that the requirements of acting 46 FRRs can be applied for this facility safety justification and consideration. The need was identified for the development of new FRRs and a number of industry standards containing requirements to reactor metal-concrete housing, to the reactor core elements, equipment and pipelines of the primary circuit of the facility. In accordance with licence conditions on siting of the facility ODEC BREST-OD-300 the operating organization must prepare new FRR and safety requirements agreed with Rostechnadzor before issuing the licence on it commissioning. To date, the development of the necessary safety requirements has not been completed, the calculation codes that used for safety justification have not been fully certified, R & D in support of the detailed design of the BREST-OD-300 facility has not been completed.

3.4.2. Complex SVBR-100

The project SVBR-100 is aimed at developing the technology of modular nuclear facilities for regional energy. The facility SVBR 100 is equipped with a fast reactor cooled with liquid metal lead-bismuth coolant. The heat transfer from the reactor unit to the steam turbine unit is carried out by a two-circuit flowsheet. All primary circuit equipment should be mounting in one monoblock without any pipelines or fitting valves in the primary cooling circuit. The monoblock with the reactor core is removable. In the reactor monoblock there are four steam generators installed in parallel both along the steam-water path and along the primary coolant path. Two pumps provide circulation of the coolant in the primary circuit. The secondary circuit consists of four independent circulation loops. A cooling tower is used as chiller of technical water.

The project SVBR-100 uses operation experience of Russian nuclear submarines with fast reactors and lead-bismuth coolant, as well as the results of calculations and testing of the reactor models at the prototype stands.

The potential of using different types of nuclear fuel is investigated for operation in a closed fuel cycle: uranium oxide, mixed nitrides, mixed oxides (MOX). Also work is under way to study the thorium fuel cycle, which is preferable in disposal of weapons-grade plutonium because it does not lead to its reproduction as in the case of using the U-Pu fuel cycle. For using the uranium-thorium fuel cycle, the possibilities of uranium-233 reproduction for different types of fuel are considered: oxide (U233+Th232)O2, nitride (U233+Th232)N, metal U233+Th232. The assessments and research are carried out on implementation of the uranium-plutonium fuel cycle with nitride fuel (Th+Pu)N, when plutonium is used as the initial reactor load.

The safety issues, which are not regulated by the acting FRRs are caused by the use of heavy metal (lead-bismuth eutectic) as a coolant, and are given below.

Need to ensure the corrosion resistance of structural materials and the quality of the coolant during operation by maintaining in the predetermined range the concentration of oxygen dissolved in the *coolant*.

Possibility of an intensive contamination of lead-bismuth coolant with solid impurities resulting from interaction of the coolant with construction and oxygen. The protective oxide film may be formed on the elements of the equipment only in case, that the concentration of oxygen in the coolant is maintained in a certain range. The lack of oxygen leads to increased corrosion of the equipment, and overage of oxygen in the coolant leads to formation of oxides of lead and bismuth, which, together with corrosion products, may block the flow section of the fuel assemblies.

Possibility of coolant freezing in some areas of the primary circuit due to water ingress or jamming the main circulating pump.

Possibility to loss integrity in the primary circuit due to large specific gravity of the coolant, when a hydraulic shock or seismic impact happened.

Possibility of radiation exposure to personnel by polonium-210, which can penetrate into the gaseous space from the coolant in forms of aerosol and gaseous fractions.

Possibility of generation of the hydrogen resulting from water radiolysis in the modules-evaporators, which are located in vicinity of the reactor core. In addition, hydrogen is used for cleaning of the primary circuit from depositions, that does not exclude the occurrence of explosive and fire hazardous situations.

*Possibility to loss reparability of the equipment***.** The integral (monoblock) layout of the primary circuit equipment, in which the steam generators are located near the reactor core,

can make the reactor monoblock non-repairable since operation at power levels with incomplete equipment is not foreseen in the project SVBR-100.

Possibility to loss integrity of the reactor unit housing. A dangerous consequence of a rupture of the steam generator tubes is the dynamic impact on the equipment and increasing pressure in the primary circuit, which, in the case of safety devices failure, can lead to loss of integrity of the reactor unit housing.

Possibility of melting of fuel assemblies after the reactor refueling (dismantling of the plug, removing of the reactor core unit, loading of the fresh reactor core unit). During the core overloading slag clogging of the passage flow section of the fuel assemblies may occur. It can lead to significant inequality of the coolant flow and temperature fields over the cross section of the core and creates a threat of melting of the fuel assemblies. It is known that the means of hydrogen treatment have been developed for purification of the primary circuit. However, the possibility of using modern means of hydrogen treatment of the primary circuit should be confirmed for the operating conditions of the facility SVBR-100.

On 11.02.2015 Rostechnadzor issued a licence for siting the pilot-industrial power unit SVBR-100 for period until 11.02.2020. In accordance with the licence conditions, the operating organization has to prepare safety documents for using technology of the lead-bismuth coolant before issuing the licence on commissioning the facility SVBR-100, and to develop the safety requirements reflecting features of application of heavy liquid metals as coolant.

In 2017 the Government of the Russian Federation excluded the point with plan of commissioning the power unit SVBR-100 before 2020 from the Federal target programme “Nuclear Power Technologies of New Generation for 2010-2015 and Perspectives Until 2020” of the State programme “Development of the Nuclear Power Industry”.

4. Conclusion

In the process of licensing of the innovative projects of nuclear research facilities and demonstration nuclear power complexes, the analysis of acting FRRs should be carried out and the expediency of developing the new regulatory requirements should be discussed. Safety issues of innovative projects of nuclear installations should be justified before issuing licence for their construction.

The directions of improving the compliance assessment system for products and processes were identified, including the development of new FRRs and industry standards.

One of the thematic issues for safety examination and criteria to assess is the confirmation of performance and reliability of the advanced fuel compositions.

In licensing process it was revealed the necessity to amend the Rostechnadzor licensing administrative procedures.

5. Reference

[1] Nuclear Research Facilities in Russia, M.: OJSC NIKIET, 2012.-295 pp.
[2] I.T. Tretyakov, N.V. Romanova, I.B. Lukasevich and other, “MBIR, A Reactor Facility for Validation of Innovative Designs”, Third International Scientific and Technical Conference “Innovative Designs and Technologies of Nuclear Power” (ISTC NIKIET-2014) Moscow, Russia, October 7-10, 2014, v.1, p. 83, http://www.nikiet.ru/eng/index.php
[3] Daniel Milian Pérez, Daniel E. Milian Lorenzo, Carlos A. Brayner de Oliveira Lira,Lorena P. Rodríguez Garcia «Neutronic evaluation of the steady-state operation of a 20 kWth

Aqueous Homogeneous Reactor for Mo-99 production», Annals of Nuclear Energy 128 (2019), pp. 148–159, journal homepage: www.elsevier.com/locate/anucene.
[4] Dragunov Yu.G., Lemekhov V.V., Moiseyev A.V. and other, “Detailed design of the BREST-OD-300 reactor facility: development stages and justification” Forth International Scientific and Technical Conference “Innovative Designs and Technologies of Nuclear Power” (ISTC NIKIET-2016) Moscow, Russia, 27-30 September, 2016, v.1, pp. 20-30.
[5] Ryzhov S.B., Stepanov V.S., Klimov H.H., Zrodnikov A.V. and other, «Innovative Design of Reactor Facility SVBR-100”, Problems of Atomic Science and Engineering.
Series: Physics of Nuclear Reactors, 2009, Issue 24, pp. 5–7, OKB “Gidropress” (in Russian).
[6] Integrated regulatory review service (IRRS) follow-up mission to the Russian Federation 11 to 19 November 2013, Moscow, IAEA-NS-10.
[7] The Order of Rostechnadzor from 22 November 2018 № 591 “On Approval of Item II “The State Safety Regulation in the Nuclear Energuy Use” of the List of Legislative Acts and Regulations Related to Federal Environmental, Industrial and Nuclear Supervision Service of Russia (P-01-01-2018)”.
[8] The Resolution of the Government of the Russian Federation dated June 15 2016 № 544 “On the peculiarities of compliance assessment of products, for which the safety requirements are established in the field of nuclear energy use , as well as processes of its design (including survey work), production, construction, installation, commissioning, operation, storage, transportation, sale and disposal”.

The CEA scientific and technical offer as a designated ICERR

(International Center based on Research Reactor) by the IAEA: Update as of Spring 2019 and focus on the example of support to BATAN –Indonesia for establishing an Internet Reactor Lab

Gilles Bignan[(1)], Xavier Wohleber[(1)]

French Atomic and Alternative Energies Commission
(1) Nuclear Energy Division
Cadarache and Saclay Research Centres
France
Corresponding author: gilles.bignan@cea.fr

The IAEA Director General has approved on September 2014 a new initiative, namely the IAEA designated **International Centre based on Research Reactors (ICERR)**, which will help Member States to gain access to international research reactor infrastructures. In fact, for the agency, one of the main goals of this ICERR scheme is to help Member States, mainly without research reactors, to gain timely access to research reactor infrastructure to carry out nuclear research and development and build capacity among their scientists.
CEA has decided to be candidate to its designation as an ICERR and consequently has established a candidacy report following criteria given by the IAEA in the Terms of Reference (logistical, technical and sustainability criteria). The CEA offer is covering a broad scope of activities on the 3 following topics:

- Education & Training
- Hands-On Training
- R&D Projects.

The perimeter (facilities and associated scientific and technical skills) proposed by CEA on this ICERR is centered on JHR project; its future international Material Testing Reactor under construction in Cadarache. Ancillary facilities in operation proposed in this offer include:

- ORPHÉE research reactor in Saclay, neutron beams reactor used for science, academic and industrial research, training and education to the use of neutrons scattering,
- ISIS EOLE and MINERVE zero/low power reactors located in Saclay and in Cadarache, dedicated to Core Physic and Education & Training in nuclear engineering,
- LECA-STAR and LECI hot laboratories for fuel and Material Post Irradiated Examination, located in Cadarache and in Saclay.

The designation was the result of a rigorous process, including the review of the application and support documentation, an audit mission performed at the CEA sites, as well as a comprehensive evaluation and recommendation by an international selection committee made up of representatives from the global research reactor community and IAEA staff.

CEA Cadarache and Saclay centers are the first designated ICERR by the agency; this has become official during the last General Conference on the 14th September 2015. The Director General of the agency indicated the agency motivations at a ceremony during which he awarded the designation to CEA: *"Such centers will enable researchers from IAEA Member States, especially developing states, to gain access to research reactor capabilities and develop human resources efficiently, effectively, and, probably, at a lower cost. The ICERR scheme will also contribute to enhanced utilization of existing research reactor facilities and, by fostering cooperation, to the development and deployment of innovative nuclear technologies".*

Following this designation, CEA has established a generic template as an agreement to be signed between CEA and any institutes, organization from Member State wishing to become Affiliate to CEA through this ICERR Scheme (it is question here of a bilateral agreement, the IAEA being only a facilitator).This template indicates rights and duties of both parties willing to collaborate through this ICERR scheme.

The 3 first Affiliates to CEA signed this agreement in September 2016 (JSI from Slovenia, CNSTN from Tunisia and CNESTEN from Morocco) followed by 3 others Affiliates during the first semester of 2017 (BATAN from Indonesia, COMENA from Algeria and JAEC from Jordan).Another Member State (United Arab Emirates-FANR) becomes Affiliate to CEA last September 2018.

Some first scientific and technical topics are now going-on giving some concrete examples of collaboration.

This paper presents in detail the CEA offer as an ICERR, the template agreement and shortly describes, as examples, some first scientific and technical actions recently launched with the Affiliates. Moreover, a focus on a recent example of Hands-on Training on Engineers from BATAN is given.

Introduction

The “IAEA” designated International Centre based on Research Reactor (ICERR) scheme was approved by IAEA Director General on 9th September 2014 and officially presented to the IAEA Board of Governors during the meeting held on 15th September 2014.

The ICERR scheme is intended to help IAEA Members States gain timely access to relevant nuclear infrastructure based on RRs and their ancillary facilities. ICERRs will make available their RRs and ancillary facilities and resources to organizations/institutions of IAEA Member States seeking access to such nuclear infrastructure (named Affiliates). For Affiliates, ICERRs will provide an opportunity to access RR capabilities much sooner and, probably, at a lower cost.

The implementation of the ICERR scheme will also contribute to enhance the utilization of some existing RR facilities (e.g. those that, in order to meet the criteria for designation would be stimulated to enhance their utilization and to foster their accessibility to attract potential Affiliates). On the other hand, an ICERR could benefit, for example, from additional scientific and/or technical resources made available by the Affiliate (e.g. Secondees) and by the increase of its international visibility.

By fostering wider utilization in cooperative manner of RR(s) and ancillary facilities capabilities, ICERRs could also effectively contribute to the development and deployment of innovative nuclear technologies.

Description of CEA Facilities proposed in the ICERR

CEA has decided to be candidate to its designation as an ICERR and has prepared a candidacy report indicating its motivation and answers to the Terms of Reference criteria is as being designated an ICERR-See Terms of Reference in (1). This report has been send to the Agency in January 2015 for examination.

CEA has a few decades-long experiences in operating and using research reactors for various purposes, Zero Power Reactors for Core physics, Material Testing Reactors, safety-dedicated Reactors, neutron beams reactors for science and Low Power Reactor for Education & Training.

CEA maintains a long tradition of international collaboration agreements in the field of peaceful uses of Nuclear Energy with both Member States and organizations having extensive nuclear programs, but also with new comers (potential or existing ones) or countries with no or limited nuclear power experience.

The perimeter (facilities and associated scientific and technical skills) proposed by CEA to be include in this ICERR is centered on its future international Material Testing Reactor; the Jules Horowitz Reactor under construction in Cadarache. Ancillary facilities will also be a very important part of the ICERR; they include:

- ORPHEE research reactor in Saclay, neutron beams reactor used for science, academic and industrial research, training and education to the use of neutrons scattering,
- ISIS EOLE and MINERVE zero/low power reactors located in Saclay and in Cadarache, dedicated to Core Physics and Education & Training in nuclear engineering,
- LECA-STAR and LECI hot laboratories for fuel and Material Post Irradiated Examination, located in Cadarache and in Saclay.

1) The Jules Horowitz Reactor

The Jules Horowitz Reactor (JHR) is a new Material Testing Reactor (MTR) currently under construction at CEA Cadarache research centre in the South of France. It will represent a major research infrastructure for scientific studies dealing with material and fuel behavior under irradiation (and is consequently identified for this purpose within various European road maps and forums: ESFRI, SNETP…). The reactor will also contribute to medical isotope production.

The reactor will perform R&D programs for the optimization of the present generation of Nuclear Power Plans (NPPs), will support the development of the next generation of NPPs (mainly LWRs) and also offer irradiation capabilities for future reactor materials and fuels.

JHR is fully optimized for testing material and fuel under irradiation, in normal and off-conditions:

- With modern irradiation loops producing the operational condition of the different power reactor technologies,

- With major innovative embarked in-pile instrumentation and out-pile analysis to perform high-quality R&D experiments

- With high thermal and fast flux capacity to address existing and future NPP needs.

  JHR is designed, built and will be operated as an international user-facility open to international collaboration. This results in several aspects:

- A partnership with the funding organizations gathered within an international consortium,
- Setting-up of an international scientific community around JHR through seminars, working groups to optimize the experimental capacity versus future R&D needs.
- Preparation of the first JHR International Program potentially open to non-members of the JHR consortium.

Consequently, the JHR facility will become a major scientific hub for cutting edge research and material investigations (multilateral support to complete cost effective studies avoiding fragmentation of scientific effort, access to developing countries to such state of the art research reactor facilities, supra national approach…). Many publications (2,3,4) described in

detail the JHR project. It will answer needs expressed by the scientific community (R&D institutes, TSO…) and the industrial companies (utilities, fuel vendors…).

To prepare the future JHR scientific community, CEA has started five years ago a “Secondee program” welcoming scientists, engineers in the CEA team to prepare the first experimental capacity. Up to now more than 20 Secondees from various countries have participated to this program. **This hosting possibility within JHR team will be enhanced using the recent ICERR designation.**

JHR Building site- End of 2018 (completion of civil works)

2) The ORPHEE Research Reactor

ORPHEE is a pool-type reactor specifically designed to produce thermal neutron beams primarily used by the French user community of academic and industrial researchers working on neutron scattering instruments. **ORPHEE Research Reactor has a long tradition of welcoming foreign visiting professors, scientists but also post-doctoral students and such hosting capacity is proposed here through this ICERR designation.** This reactor of 14 MW power uses light water as coolant and heavy water as reflector reaching maximum thermal flux in the reflector of 3.10^{14} $n.cm^{-2}.s^{-1}$. It has 2 CNS-Cold Neutron Sources- (20K) and 1 hot source (1400 K), 9 horizontal channels, 20 neutrons beams, 9 vertical irradiation channels and 26 experimental areas. The various devices (neutron radiography, imaging station…) around the neutron guides of the ORPHEE reactor are used for several industrial and research applications.

 ORPHEE neutron beam research reactor.

3) ISIS Research Reactor

The ISIS reactor is the neutron mock-up of the OSIRIS Material Testing Reactor (70 MW). Both reactors are located in the same facility on the CEA Saclay Research Centre. The ISIS reactor has a maximal rated power of 700 kW. Although OSIRIS has been shut down last December 2015, ISIS is scheduled to be shut down in the first quarter of 2019. The reactor was designed in the sixties to prepare and qualify the irradiation experiments before being inserted in the OSIRIS core. Its high flexibility has enabled reactivity measurements, neutron flux measurements at different spectrum indexes by dosimetry, calorimetry, and testing of new core configurations. This contributed to OSIRIS' high irradiation accuracy.

Today, ISIS is used for the tests and qualification of neutron instrumentation technologies for other reactors, whether they are electrical generators, research or even on-board. But it is mainly used for Education and Training in the frame of academic programs. An extensive panel of training courses covering the reactor operation and related activities has been developed. Since 2007, ISIS is typically operated 350 hours per year for education and training, and welcomes up to 400 trainees per year both in academic degree programs and continuing education courses for professionals. These trainees come from different fields and education levels, i.e. bachelor and master students, operation technicians, engineers and staff from various organizations including the French regulatory body. About 50% of the teaching is carried out in English for international trainees. The typical duration of a course is 3 hours, the courses being spread over 120 operating half-days.

Concerning Education and Training, it is worth quoting that ISIS reactor has been designated as an Internet Reactor Laboratory (IRL) by the IAEA for Europe and Africa since 2013. This project is partially funded by the IAEA and aims at providing countries with access to the ISIS training courses sessions by means of live video-conferences. Video signals and graphs, including all the parameters relevant to reactor operation, are transmitted while ensuring the strictest conditions of safety and security. Several campaigns have been carried out since 2014, with universities in several partner countries such as Tunisia, Belarus, Kenya and Lithuania.

Thus, further development of the education and training activity could easily be achieved within the ICERR.

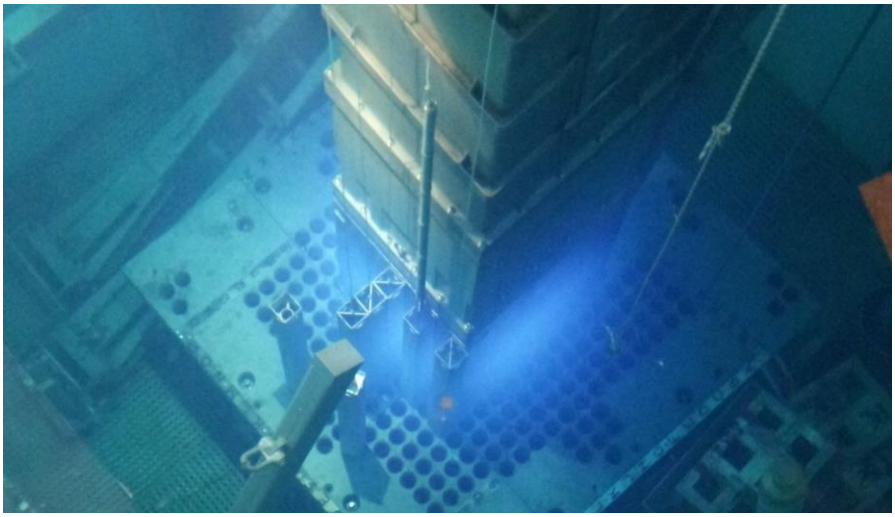

ISIS Education & Training Research Reactor

4) EOLE & MINERVE Reactor

The EOLE critical mock-up is a very low power experimental reactor (ZPR) designed to study the neutron behavior of moderated lattices, in particular those of pressurised water reactors (PWR) and boiling water reactors (BWR). The first studies specifically dedicated to the French PWRs and the qualification of core calculation tools were launched in the early eighties. EOLE provides fluxes up to 10^9 n.cm^{-2}.s^{-1}. Thanks to the high level of flexibility of the reactor, it is possible to implement complex experimental set-ups representing various core configurations to be studied. The physical measurements recorded during the experimental programmes are used to fully characterize the configurations (critical sizes, absorber weights, refined power distributions, spectral indices, material buckling, reactivity effects – boron and/or temperature, kinetic parameters, etc.) thanks to proven experimental techniques:

- Gamma spectrometry
- Measurements using miniature fission chambers
- Thermo-luminescent detectors (TLD)
- Neutron activation dosimeters.

MINERVE is also a ZPR designed for neutron studies mainly aiming to improve the nuclear database for fuel systems representative of various nuclear reactor technologies. The thermal neutron flux in the vessel is 10^9 n.cm^{-2}.s^{-1} (maximal power of 100 Watt). Physical

measurements (spectral index, conversion rates, axial and radial fission rate distributions, neutron activation) are also performed to characterize the neutron behavior of both the core and the samples under investigation. MINERVE is also used to test the performance of mini fission chamber prototypes developed by CEA and its partners. It is clearly identified as a reference facility for international collaborations on various aspects of experimental physics. MINERVE is also a key-tool for Education & Training either for Nuclear Engineering Students or for Reactor Operators. **Both these 2 Zero Power Reactors have a long tradition to host foreign scientists, PhD, Post-Doc students for E&T and R&D projects.**

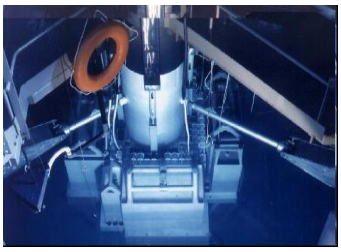

MINERVE Research Reactor for core physic studies

5) LECA-STAR Hot Laboratory

The LECA-STAR, located on the Cadarache nuclear centre, is the CEA hot laboratory in charge of the characterization of irradiated fuel for various types of nuclear industrial and/or research reactor.

The LECA-STAR was extensively refurbished between 2001 and 2011 to extend its operation. It represents a reference hot laboratory in support to the fuel experiments performed in any MTR. That means that refabricated short fuel rods to be irradiated in JHR will be manufactured there, and that fuel materials will be sent to LECA-STAR after their irradiation in JHR.

The LECA-STAR includes about 20 hot cells (up to 9 m long), with all the equipment for a wide range of irradiated fuel rod examinations, namely: non-destructive examination (visual inspection, confocal, radionuclide distribution by gamma-spectrometry, diameter measurement, eddy current testing for cladding integrity and zirconia thickness, X-rays), puncturing and fission gas release measurements, cutting, macro- and microscopy examinations. A special area is devoted to micro-analysis, with fully-shielded SEM/FIB, EPMA, SIMS and XRD, all these equipment being adapted to irradiated-fuel or material examination.

The LECA-STAR facility is mainly devoted to R&D development within French joint programs with industrial partners as EDF and AREVA. Nevertheless this laboratory is able to welcome foreign scientists and engineers in other scientific and technical areas, such as the development of new hot cell equipment, fundamental or academic research topics and safety tests required to perform PIE conducted within the framework of International collaboration.


Post Irradiation Examns of fuel at LECA Hot-Laboratory

6) LECI Hot Laboratory

The LECI, located on the Saclay nuclear centre, is the CEA reference hot laboratory in support to JHR for Material testing. This laboratory is in charge of the characterization of irradiated non fissile materials for:

- Water cooled reactors (PWR and Material Testing Reactors): Pressure Vessel life extension (embrittlement, mechanical properties), Internals (swelling, creep, stress corrosion cracking of 304 or 316 stainless steels), Zirconium alloys for fuel pin cladding and assembly (evolution of metallurgical and mechanical properties in incidental, accidental or in service reactor conditions, in storage or retrieving after interim storage conditions of spent fuel pins-corrosion-interaction between fuel pellets and cladding), and Aluminum alloys for Material Testing Reactors: vessel and cladding materials,

- Generation IV reactors: Characterization of materials for fuel pin cladding and assembly for sodium or gas-cooled reactors (steels, ODS, ceramics, refractory materials, graphite).

The LECI includes about 50 hot cells, with up-to-date scientific equipment: metallography & optical microscopy, micro-hardness, SEM, TEM, EPMA, XRD, density, Raman spectroscopy, thermoelectric power, H_2 measurements, Eddy currents, metrology, 4 autoclaves (360°C, 220 bar, 1 coupled to slow tensile testing), machining (conventional, ram and wire spark erosion machining) and welding (TIG and Laser).

The LECI was the hot laboratory in support to OSIRIS-CEA MTR- for structural materials investigation (guide tube, fuel cladding, pressure vessel steel…) when this reactor was in operation. That means that refabricated short fuel rods to be irradiated in Osiris were manufactured there or in the LECA, and that materials were and are still sent to LECI after their irradiation in Osiris. It will also be the reference non-fissile material hot laboratory for JHR.

The LECI facility is mainly devoted to R&D development within French joint programs with industrial partners as EDF and AREVA. Nevertheless, this laboratory is able to welcome foreign scientists and engineers in other scientific and technical areas, such as the development of new hot cell equipment, fundamental or academic research topics and experimental devices required to perform PIE on material.

 Post-Irradiation Exams on Materials at LECI Hot-Laboratory

Both these 2 Hot Laboratories have a long tradition to perform R&D programs within an international framework and consequently are ready to welcome scientists for Hands-On Training, R&D projects through this ICERR designation.

First Affiliates to CEA: examples of utilization of this ICERR scheme

CEA is now ready to welcome scientists, engineers within its facilities described above in the framework of this ICERR designation.

In a practical point of view, for welcoming scientists from Member States at CEA through this ICERR designation, a bilateral agreement has to be signed between the assigning party (organization from which the scientist belongs to) and CEA. Such agreement will indicate the scientific/technical topic of collaboration, and rights and duties of both parties including the financial issues. The IAEA is here a “facilitator” creating the network between its Member States and the CEA and having eventually the possibility to partially sponsor some part on a “case by case” basis (through potential TC projects).

The 3 first Affiliates to CEA signed this agreement in September 2016 (JSI from Slovenia, CNSTN from Tunisia and CNESTEN from Morocco) followed by 3 others Affiliates during the first semester of 2017 (BATAN from Indonesia, COMENA from Algeria and JAEC from Jordan).

Here are some first scientific and technical illustrations, which are on-going with these Affiliates:

Slovenia: Secondment in 2017 of a scientist from JSI to Cadarache and Saclay to perform experiments on gamma sensors (in MINERVE reactor) and to be trained on CEA Monte-Carlo core-physic code (TRIPOLI) in order to enhance future experiments in the JSI TRIGA Research Reactor.

Morocco: Expert mission of Safety Engineer from CEA to CNESTEN for analyzing safety aspects for installation of a neutron beam in the TRIGA research reactor. Review by CEA staff of the Safety report performed by CNESTEN and foreseen secondment of Safety Engineer to ORPHEE reactor team (hands-on training on safety approach when operating a neutron beam RR)

Tunisia: Secondment of 3 scientists from CNSTN (2 times in 2017) on MINERVE research reactor to perform dosimetry measurement- support from CEA to perform core-physic calculation for dimensioning a sub-critical mock-up to be established at CNSTN.

Algeria: support to COMENA on the on-going actions for refurbishment of their 2 Research Reactors (NUR and Sallaam) especially on appropriation of new Safety report and establishment of operating procedures. Secondment of a scientist to COMENA foreseen on instrumentation for research reactor (Cadarache-1st semester 2018)

Jordan: Secondment of a Safety Engineer from JAEC to Saclay for hands-on Training on thermo-hydraulic and Core-Physic CEA codes to perform complementary Safety Analysis of the JRTR core. Later on it is foreseen a secondment in ORPHEE research reactor for enhancing utilization of the JRTR neutron beams.

Indonesia: Support from ISIS reactor team to BATAN to establish their own Internet Reactor Laboratory (in collaboration with the IAEA). A secondment of scientist/engineers from BATAN to Saclay has been held last September 2018 in ISIS reactor for hands-On Training.

BATAN operates several research reactors. Two of them, TRIGAs, are useful and perfectly adapted for training. Indonesia therefore has the raw material for reactor education. There remains the choice of programmes and the way of teaching. A first meeting between the CEA and BATAN staffs took place in March 2017, leading to the signing of a cooperation agreement between the two commissions.

A delegation from the CEA went to the Serpong Centre to meet BATAN engineers and discuss the various subjects of collaboration. The INSTN (National Institute for Nuclear Science and Technology, CEA) was represented by its Director, participating in this delegation. These topics are varied and range from assistance with calculations for modifying cores, to Education & Training, with a particular focus on the IRL (Internet Reactor Laboratory [6]) topic.

It was decided to organize in September 2018 a week of exchanges and training at the CEA Centre in Saclay. Six engineers from BATAN, Yogyakarta Centre, came to France. The spirit of this meeting was to show not only the IRL system but also the upstream, i.e. the courses necessary for students before the training courses on reactor. During this week, the time was shared between lessons and lectures at INSTN, and training courses at Isis reactor. But also some visits to installations (nuclear facilities and others) were proposed. The objective was twofold:

1 - Internet Reactor Laboratory (IRL) system: how it works in the frame of the broadcast issue and the reactor work. the program planned to test the Isis - BATAN reactor connection.
2 - Pedagogical contents of the training courses: the IRL pedagogical programme but also the "classical" training courses, inserted in academic and professional curriculum. The topics covered are safety, reactor physics (with a large part of kinetics), etc.

Indonesian engineers had the opportunity to join a group of students in the *Basic Operations in Nuclear Reactor* internship, which lasted one week, thus coinciding with the mission. The picture below shows the entire team, including the trainees (in white) and the BATAN engineers (green), at the end of the last training course.

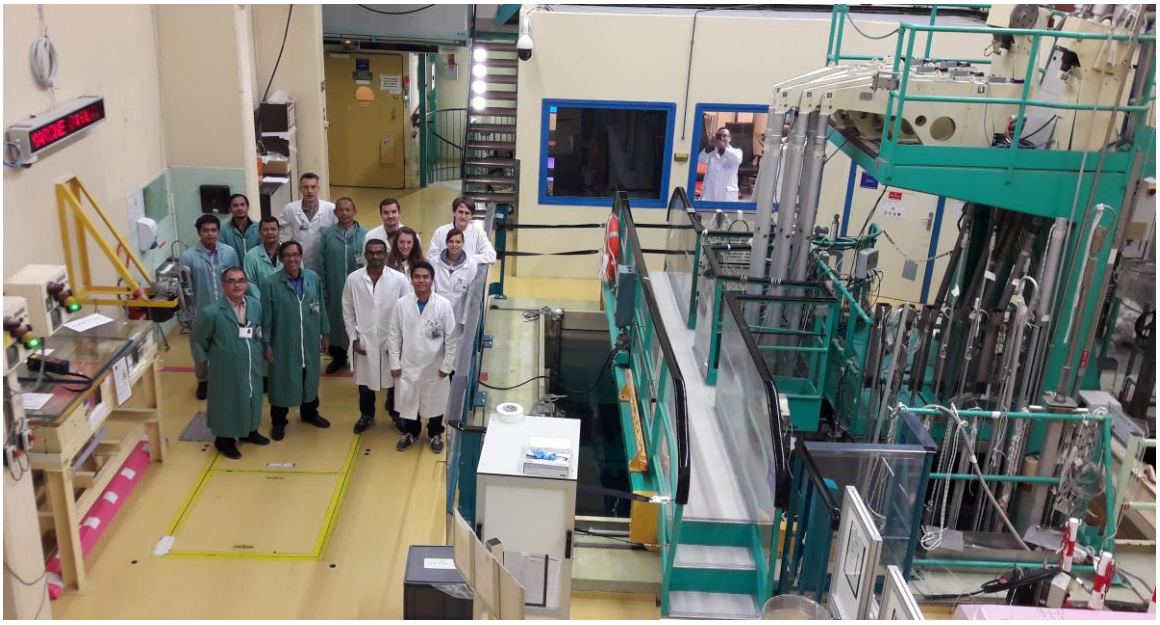

Conclusion

The IAEA's ICERR (International Center based on Research Reactors) programme facilitates access to state-of-the-art facilities for its Member States to achieve their national nuclear research and development and capacity-building objectives. The ICERR's approach is therefore to strengthen human capacities.

In this sense, the CEA, one of the first promoters of the ICERR, opens its nuclear facilities to affiliated members. This includes not only its research reactors but also a large number of experimental and education & training platforms.

A recent example is the cooperation between BATAN (Indonesia) and CEA (France) in the field of education. A delegation of Indonesian engineers was able to come in September 2018 for missions to familiarize themselves with reactor education and in particular with technical and educational access to the Internet Reactor Laboratory network.

References

(1) http:/www.iaea.org/OURWORK/ST/NE/NEFW/Technical-Areas/RRS/documents/ICERR Concept ToR Final.pdf

(2) “Sustaining Material Testing Capacity in France: From OSIRIS to JHR”, G.Bignan, D.Iracane, S.Loubière, C.Blandin, CEA (France) IGORR 2009 Conference (Beijing)

(3) “The Jules Horowitz Reactor: A new European MTR open to International collaboration” Gilles Bignan et al, IGORR 2010 (Knoxville TN-ORNL-September 2010)

(4) “The Jules Horowitz Reactor: A new European MTR (Material Testing Reactor) open to International collaboration: Description and Status” , G.Bignan, J.Estrade – IGORR 2013 – Daejeong Korea (October 2013)

(5) “The Jules Horowitz Reactor: A new high performance MTR (Material Testing Reactor) working as an International User Facility in support to Nuclear Industry, Public Bodies and Research Institutes”, X.Bravo, G.Bignan, Journal of Nuclear Energy International – December 2014.

(6) “The Internet Reactor Laboratory Project: status and experience of the Isis Research Reactor” F. Foulon et al. – RRFM March, Berlin Germany (March 2016).

RESULTS OF COMMISSIONING TESTS AND FULL POWER OPERATION OF NIRR-1 LEU CORE

S.A. JONAH[1], Y.V. IBRAHIM[1], Y.A. AHMED[1], N. ABUBAKAR[1]

Y. LI[2], D. PENG[2], X. WU[2], J. HONG[2], M. WANG[2], Q. HAO[2]

[1]Centre for Energy Research and Training, Ahmadu Bello University, Zaria, Nigeria

[1]China Institute of Atomic Energy, Beijing, China

Email: jonahsa2001@yahoo.com

ABSTRACT

The Nigeria Research Reactor-1 is the second commercial Miniature Neutron Source Reactor (MNSR) facilities outside China and the third MNSR to be converted from HEU to LEU. This follows the successful conversion of the Prototype MNSR and the Ghana Research Reactor-1 (GHARR-1) in 2016 and 2017 respectively.. NIRR-1 is loaded with 335 UO_2 fuel pins enriched to 13% as replacement for the U-AL4 HEU fuel pins enriched to 90.2%, which was discharged from the reactor vessel on October 23, 2018 after 14 years of operation. Thereafter, the first criticality with the LEU core was achieved at 11.20 am on November 02, 2018 and was followed by determination of core physics parameters at zero power. Furthermore, the reactor was safely taken to full power of 34 kW on November 27, 2018.

This paper provides an overview of the measurements of core physics data performed at zero power and a description of power rising experiments to achieve the full power. In addition, a comparison of measured data for the LEU with the HEU data is discussed as a means of returning NIRR-1 to operability after conversion.

1. Introduction

The MNSR is a compact low-power research reactor designed mainly for use in neutron activation analysis and limited radioisotope production. The prototype was built by the China Institute of Atomic Energy (CIAE), Beijing, China and was critical in 1984. Subsequently, the commercial versions of the reactor have been installed in China, Ghana, Iran, Nigeria, Pakistan and Syria. The nominal power of MNSR is approximately 30 kW and they have common operational, utilization and spent fuel management issues. The cores were designed to have HEU (>90% enrichment) as fuel with a total ^{235}U loading of approximately 1 kilogram. The Nigeria Research Reactor-1 (NIRR-1) is the eighth commercial MNSR facilities to be commissioned outside China in 2004 and it is first nuclear research reactor in Nigeria [1- 4]. NIRR-1 is the second commercial MNSR facilities outside China and the third MNSR to be converted from HEU to LEU. This follows the successful conversion of the Prototype MNSR, Beijing, China in 2016, and the Ghana Research Reactor-1 (GHARR-1), Accra, Ghana in 2017. Current NIRR-1 LEU core is loaded with 335 UO2 fuel pins enriched to 13% as replacement for the U-Al_4 HEU fuel pins enriched to 90.2%, which was discharged from the reactor vessel on October 23, 2018 after 14 years of operation. Thereafter, the first criticality with the LEU core was achieved at 11.20 am on November 02, 2018 and was followed by determination of core physics parameters at zero power. Furthermore, the reactor was safely taken to full power of 34 kW on November 27, 2018. Results of the on-site critical experiments and full power commissioning tests, which include number of fuel elements loaded to achieve criticality, measured data of some reactor components, maximum operable time at full power and other core physics data are presented

2. Materials and Method

The critical control rod method was used to make the reactor critical. In this regard, the power monitoring devices were used to determine the reactor period and thereafter the respective corresponding reactivity was taken from the Table of

reactivity versus period based on the in-hour equation for MNSR [5]. The same methodology had been deployed during the off-site zero power experiments [6]

Following the off-site zero power experiments in Beijing China, it was established that that 333 fuel elements would be required to provide the critical mass and the recommended core excess reactivity of 4 mk for NIRR-1 LEU core. However due to differences in the ambient temperatures off-site in Beijing and on-site in Zaria as well as other additional reactivity absorbing components, it was decided to load 335 fuel elements to make NIRR-1 critical and provide the required licence value of core excess reactivity of between 3.5 to 4.0 mk.

Critical Experiments

After the loading of 335 fuel elements into the 'bird cage' was completed, the reactor was made criticality by the critical control rod method using reactivity adjusting devices, while monitoring reactor's dynamic behaviour by neutron and gamma-ray counting equipment and. The core arrangement during the critical experiments is displayed in Figure 1. The equipment and devices used for critical experiments are as follows:

i. Two sets of Neutron counter devices consisting of ^{3}He detectors, two sets of power monitoring devices made up of ionization chamber and one set of γ dose monitoring devices.
ii. One Emergency shutdown Cd string absorber with the reactivity of -2.5mk inserted into an inner irradiation site (I3) See Figure 1.
iii. Four big Cd absorbers (No. 1, 2, 4 and 5), each having reactivity of -4mk were inserted into the remaining four inner irradiation sites (I1, I2, I4 and I5) respectively.
iv. Two Cd string absorbers (No. 1, 2) with reactivity of -0.5mk each were inserted into two outer irradiation sites (O3 and O5) respectively.
v. Four reactivity adjusters (No.1, 2, 3 and 4) with reactivity of -0.5mk each were inserted into the reactivity regulating tubes (R1, R2, R3 and R4) respectively.
vi. A 1 Ci Am-Be neutron source was put into the fifth outer irradiation tube (O1) to initiate the fission process

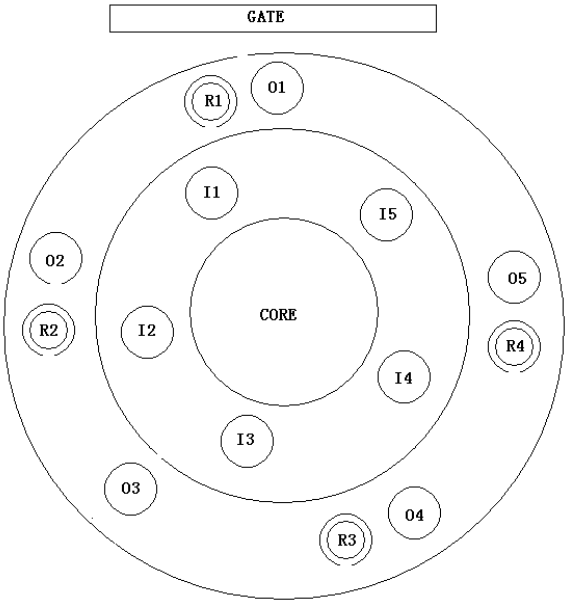

Figure1 NIRR-1 core arrangement used for the approach to critical and the on-site zero power experiments

On-site Zero Power Experiments

The zero-power experiments were conducted on-site during the Commissioning of NIRR-1 LEU core to determine the following parameters:

i. Cold core excess reactivity and its adjustment to meet the licence requirement of 3.5 – 4.0 mk;
ii. Reactivity worth of reactor components, including the worth of control rod
iii. Shutdown margin.
iv. The relationship between the excess reactivity and the critical rod position.

Power Rising Experiment

The purpose of the power rising experiment was to check reactor hot operation status, calibrate neutron flux instrument and prepare to gradually take reactor from zero power to full power. In this respect the main steps followed include:

i. The reactor was started up in the auto mode at a neutron flux of 5×10^{11} $n \cdot cm^{-2}s^{-1}$ to check the stability of operating parameters such as the variations of neutron flux and control rod position with time

ii. In the second instance, the reactor neutron flux is raised to 8 $\times 10^{11}$ $n \cdot cm^{-2}s^{-1}$ and also operated in the auto mode to check the variation of neutron flux measure and control rod position with time.

Power/Flux Calibration

Prior to the on-site experiments in Zaria, Au neutron monitor foil was irradiated in the inner irradiation site of the prototype MNSR in which the neutron flux was already calibrated. The induced radioactivity of the Au foil was determined by a portable NaI (Tl) detector. The same Au foil was irradiated for five minutes in the inner irradiation site of NIRR-1 LEU core at a neutron flux of 1×10^{10} $n/cm^2 \cdot s$, and the induced radioactivity was determined by the same portable NaI(Tl) detector setup.

Full power Experiments

The full power experiment was performed by operating the reactor at the nominal neutron flux of $1.0 \times 10^{12} n/cm^2 \cdot s$., which is equivalent of reactor power of 34 kW. During this operation the reactor is allowed to operate at the full power and maximum operable time was checked using the control rod position.

3. Results and Discussion

On the basis of the critical control rod method via the adjustments of Cd strings, the reactor became critical a rod position of 87mm for the first time on November 02, 2018 at 11:20 a.m. Results of reactivity worth of reactor devices are displayed in Table 1. Results of measured worth of representative components including reactivity regulators, irradiation tubes, Cd rabbits, and Cd strings are displayed in Table 1

Table 1 Measured reactivity worth of representative components in NIRR-1

Components	Reactivity worth, mk
Reactivity regulator	0.58
Outer irradiation tube	0.69
Inner Irradiation tube	0.70
Outer irradiation tube	0.71
Cd rabbit	1.01
Cd string	0.66

Calibration of the control rod was also performed using the setup described above. Data of critical rod position as function of core excess reactivity are displayed in Table 2 below.

Table 2 Relation between the critical rod and core excess reactivity

Critical control rod height/mm	Excess reactivity/mk
127.5	3.94
145.9	3.36
158.6	2.97
163.2	2.8
174.9	2.41
185.9	1.82
205.4	1.24
212.5	1.17

The reactivity worth of the control rod and the final core excess reactivity were determined using the period method as follows:

i. Control rod worth was found to be 7.0 mk
ii. Core excess reactivity was determined to be 3.94mk and it meet the requirement of 3.5 - 4.0 mk;
iii. Shutdown margin = Control rod worth – Core excess reactivity (7.0 - 3.94) mk = 3.06 mk, which is greater than the required value of 2.5 mk;

For the power calibration, two methods were considered, the thermal power method and foil activation method with Au foil. However, the activation method was found to be more reliable. Therefore, the same Au foil irradiated in the Prototype MNSR in Beijing was irradiated in NIRR-1. The measured radioactivity of the Au foil was found to be 30231.7Bq on-site at CERT, Zaria. When compared with similar measurement performed in the Prototype off-site, CIAE, Beijing, the neutron flux in the inner irradiation site of NIRR-1 was evaluated to be 9.51×10^{9}n/cm^2.s. This value is lower than the flux setting by 5%., thus the Computer control system and the Control Console of NIRR-1 were adjusted appropriately.

Data of power rising experiments from 1.0×10^{10}n/cm^2.s to 5.0×10^{11}n/cm^2.s and 8.0×10^{11}n/cm^2.s respectively are displayed in Table 3

Table 3 Measured data of power rising experiments at 5.0×10^{11}n/cm^2.s and 8.0×10^{11}n/cm^2.s respectively.

Test item	Power Rising Experiments					
Preset neutron flux	Data for neutron flux setting of 5×10^{11} n·cm^{-2}s^{-1}					
Time	Control rod position mm	Flux setting (nominal) n/cm2.s	Flux indication (nominal) n/cm2.s	Inlet temp. °C	Temp. diff. °C	γ dose (top) μSv/hr
10:00	166.0	5×10^{11}	4.97×10^{11}	24.2	37	6.69
10:10	167.0	5×10^{11}	5.02×10^{11}	25.1	36.1	6.58

10:20	169.8	5×10^{11}	5.01×10^{11}	25.8	37.1	6.42
10:30	171.4	5×10^{11}	5.02×10^{11}	27.8	8.1	6.38
10:40	173.3	5×10^{11}	5.03×10^{11}	27.2	38.4	6.41
10:50	174.6	5×10^{11}	5.01×10^{11}	27.9	38.6	6.81
11:00	176.4	5×10^{11}	5.02×10^{11}	28.6	39.6	7.26
11:10	177.0	5×10^{11}	5.01×10^{11}	28.5	39.6	6.41
11:20	178.1	5×10^{11}	5.01×10^{11}	28.6	39.8	6.14
11:30	179.7	5×10^{11}	4.98×10^{11}	28.7	39.8	6.02
11:31	179.4	5×10^{11}	4.99×10^{11}	28.8	39.9	6.51
11:32	179.6	5×10^{11}	5.00×10^{11}	29.1	39.8	6.25
11:33	179.4	5×10^{11}	4.99×10^{11}	28.8	39.5	6.25
11:34	179.9	5×10^{11}	4.99×10^{11}	29.2	39.8	6.30
11:35	178.4	5×10^{11}	5.01×10^{11}	29.1	40.1	6.36
11:36	179.3	5×10^{11}	4.97×10^{11}	28.7	40.1	6.34
11:37	179.7	5×10^{11}	$^{4.99}\times10^{11}$	28.9	39.3	6.65
11:38	178.6	5×10^{11}	$^{5.01}\times10^{11}$	29.5	39.6	6.60
11:39	179.9	5×10^{11}	5.02×10^{11}	29.6	39.6	6.60
11:40	179.8	5×10^{11}	4.98×10^{11}	29.1	40.4	6.39
Data for the neutron flux setting of 8×10^{11} n·cm^{-2}s^{-1}						
9:30	182.0	8×10^{11}	8×10^{11}	23.8	38.5	10.70
9:40	186.7	8×10^{11}	8×10^{11}	26.7	40.4	10.52

9:50	190.1	8×10^{11}	8×10^{11}	27.4	42.5	10.27
10:00	195.4	8×10^{11}	7.972×10^{11}	29.2	43.0	10.20
10:10	196.0	8×10^{11}	7.961×10^{11}	30.1	43.4	10.25
10:20	200.0	8×10^{11}	7.981×10^{11}	30.5	44.3	10.89
10:30	203.1	8×10^{11}	8.009×10^{11}	30.5	45.2	11.62
10:40	204.8	8×10^{11}	7.973×10^{11}	31.2	44.3	10.21
10:50	205.5	8×10^{11}	7.979×10^{11}	31.5	44.5	9.82
11:00	207.1	8×10^{11}	8.049×10^{11}	32.5	45.9	9.63
11:10	209.6	8×10^{11}	8.025×10^{11}	31.8	46.6	10.42
11:11	209.2	8×10^{11}	8.017×10^{11}	32.7	46.6	10.01
11:12	209.1	8×10^{11}	8.025×10^{11}	31.9	46.4	10.0
11:13	209.2	8×10^{11}	7.959×10^{11}	32.0	46.4	10.08
11:14	209.3	8×10^{11}	7.975×10^{11}	32.6	46.4	10.12
11:15	209.5	8×10^{11}	7.949×10^{11}	32.8	45.4	10.08
11:16	209.1	8×10^{11}	8.047×10^{11}	32.6	45.7	10.65
11:17	210.0	8×10^{11}	8.010×10^{11}	32.5	45.9	10.56
11:18	209.7	8×10^{11}	7.982×10^{11}	32.4	46.4	10.56
11:19	209.3	8×10^{11}	8.028×10^{11}	32.3	46.0	10.22
11:20	209.4	8×10^{11}	8.040×10^{11}	32.1	46.6	10.63

The reactor was operated from 10 am to 11.40 am at 5.0×10^{11}n/cm^2.s to check the neutron flux stability and other parameters on November 22, 2018. As can be seen the neutron flux is stable within 5 % pf the set value. For the setting at 8.0×10^{11}n/cm^2.s, reactor was operated from 9.30 am to 11.20 am the next day, as expected the flux data and other measured parameters were found to be stable and consistent.

NIRR-1 was then operated on at full power of 34 kW, which equivalent to a neutron flux setting of 1.0×10^{12}n/cm^2 .s on November 27, 2018 to allow for the decay Xenon so as to appropriately determine the maximum operable time at full power. Data obtained are shown in Table 4.

Table 4 Measured data of NIRR-1 at full power

Test item	Full power Experiments	Date	Nov. 29, 2018
Preset neutron flux	1×10^{12} n·cm^{-2}s^{-1}		

Time	Rod Position (mm)	ConsoleDisplay (10^{11}n/cm^2 • s)	T_{in} (℃)	T_{out} (℃)	γ dose (μSv/h)
09:50	171	10.14	25.8	43.7	40.33
09:55	172	10.01	27.2	44.4	40.92
10:00	174	9.94	28.0	44.9	40.77
10:05	177	10.00	29.1	45.8	40.85
10:10	178	9.97	29.7	46.3	40.28
10:15	184	10.10	30.2	46.9	40.78
10:20	185	10.18	31.2	47.7	41.93
10:25	187	10.01	31.9	47.1	41.90
10:30	190	9.90	31.2	48.6	40.41
10:35	192	9.96	32.4	48.9	41.17
10:40	192	10.01	32.7	49.3	40.74
10:45	193	10.05	32.8	49.4	41.70
10:50	194	10.10	33.1	49.6	42.95
10:55	195	9.95	33.2	49.8	41.56
11:00	197	10.04	33.0	50.4	42.50
11:05	200	10.13	34.1	50.2	41.77
11:10	200	10.00	34.5	50.4	41.40
11:15	201	10.04	34.5	50.7	41.40
11:20	202	9.99	35.3	51.0	41.77
11:25	202	10.05	35.4	50.2	42.16
11:30	203	10.05	35.2	51.7	43.97
11:35	204	9.95	35.4	51.3	42.77
11:40	206	9.98	35.6	51.4	42.83
11:45	208	10.10	35.8	51.7	43.76
11:50	208	10.00	36.8	51.3	41.82
11:55	209	10.03	35.9	51.7	44.05
12:00	209	10.11	35.3	51.9	46.11

12:05	209	9.98	36.4	51.9	45.27
12:10	209	10.02	35.8	52.1	44.62
12:15	210	10.02	36.3	51.2	44.91
12:20	210	10.05	36.3	51.7	45.64
12:25	211	10.08	35.8	52.0	44.14
12:30	211	10.17	37.3	52.2	45.38
12:35	212	9.92	36.6	52.6	43.35
12:40	213	10.22	36.0	52.3	43.98
12:45	214	10.01	37.3	52.6	44.45
12:50	214	9.99	37.1	52.5	44.82
12:55	216	10.10	36.4	52.5	45.49
13:00	216	10.00	36.6	52.5	46.87
13:05	217	10.16	35.9	52.2	50.38
13:10	218	10.02	36.3	53.0	49.96
13:15	218	10.04	37.3	52.6	48.25
13:20	218	9.98	36.5	52.6	46.22
13:25	218	9.99	35.4	52.2	45.80
13:30	218	10.09	36.8	52.4	45.16
13:35	219	10.15	36.9	53.3	45.85
13:40	219	10.12	37.0	53.0	44.05
13:45	219	10.10	37.8	53.4	45.69
13:50	219	9.98	36.4	52.8	45.46
13:55	220	9.94	36.9	53.0	45.27
14:00	220	9.96	37.5	53.2	44.03
14:05	222	9.96	37.3	53.3	43.78
14:10	224	9.87	37.2	53.0	43.90
14:15	224	10.09	37.9	51.6	45.01
14:20	224	9.89	37.2	53.3	45.83
14:25	225	10.06	37.7	53.3	45.95
14:30	225	10.10	38.2	53.2	43.81
14:35	225	9.98	36.9	53.3	46.18
14:40	227	10.00	37.7	53.3	45.54
14:45	228	10..06	37.2	53.3	46.49

14:50	228	10.01	37.4	53.5	45.54
14:55	228	10.03	37.6	53.7	46.07
15:00	230	10.02	37.7	53.1	45.27
15:05	230	9.98	37.3	53.6	45.29
15:10	230	9.95	37.4	53.7	43.54
15:15	230	9.89	38.5	53.28	44.72
15:20	230	9.79	38.2	53.2	44.57
15:25	230	9.70	38.2	53.1	43.44
15:26	**shutdown**				

As can be seen in the Table, the reactor was started up at 9:50 a.m. at full power and allowed to operate until 3:26 p.m. when the single control rod got to the maximum rod position of 230 mm and the power began to drop. The neutron flux stability was within 5% of the nominal value and the reactor operated for 5 hours and 36 minutes at full power. When compared with the HEU core, NIRR-1 operated for 4 hours and 30 minutes at full power in 2004.

4. Conclusion

NIRR-1 is the second Commercial MNSR facility outside China to be successfully converted from HEU to LEU under the auspices of the IAEA with the support of US-DOE, UK and Norway. The reactor's operational characteristics indicate that the neutron flux performance the LEU core is comparable with that of the HEU core and therefore has little or no impact on the operational and utilization of the facility.

5. Acknowledgements

Financial supports for the conversion came from the IAEA, US–DOE's Argonne National Laboratory (ANL) and Idaho National Laboratory (INL) as well as Governments of UK, Norway and Nigeria.

6. References

[1] FSAR, 2005. Final Safety Analysis Report of Nigeria Research Reactor-1 (NIRR-1), Technical Report-CERT/NIRR-1/FSAR-01, CRET, ABU< Zaria, Nigeria

[2] Jonah, S.A., Balogun, G.I., Umar, I.M., Mayaki, M.C., 2005. Neutron spectrum parameters in irradiation channels of the Nigeria research reactor-1 (NIRR-1) for the k0-NAA standardization. J. Radioanal. Nucl. Chem. 266, 83–88

[3] Jonah S.A., Balogun G.I., Umar I.M, Oladipo M.O.A., Adeyemo D.J., 2006. Standardization of NIRR-1 irradiation and counting facilities for instrumental neutron activation analysis. Appl. Radiat. Isotopes 64, 818 – 822

[4] Jonah, S.A., Liaw, J.R., Matos, J.E., 2007. Monte Carlo simulation of core physics parameters of the Nigeria research reactor-1(NIRR-1). Ann. Nucl. Energy 34, 953–957.

[5] Guo Chengzhen, HU Hamming, HU Zhiyi, Shi Shuankai, 1985. Prototype MNSR, Dynamic Feedback Experiments and Calculations, CIAE Technical Report. Beijing. China

[6] The Experiment Summary of Nigeria MNSR at the Zero Power Tests Facility (ZPTF), CIAE Technical Report. Beijing. China, May 2018

UTILISATION OF THE OPAL RESEARCH REACTOR

R. FRAIHAT, D. VITTORIO
Australian Nuclear Science and Technology Office (ANSTO)
New Illawarra Rd, Lucas Heights NSW 2234 Australia
Corresponding author rasmif@ansto.gov.au

ABSTRACT

The OPAL Research Reactor incorporates a number of irradiation facilities designed to accommodate various physical target sizes, flux levels and irradiation times. Since the commissioning of the OPAL Research Reactor in 2006, the utilisation of these irradiation facilities has steadily increased based on the requests from stakeholders and specific user groups. This increase in utilisation has required greater awareness of forecast demand and improved integration between the reactors digital operating systems and the enterprise wide management systems. This paper provides an overview of the OPAL irradiation facilities and how they fit in with the overall ANSTO processes together with a discussion about how forecast demand and improved integration have been implemented.

1. Introduction

The OPAL Reactor is an Open Pool 20 MW multipurpose research reactor operating with high availability and a reliable target of 98%. Operating Cycles vary between 26 to 33 days with an average of 5 days reactor shutdown between cycles. The OPAL reactor has 80 irradiation facilities split into 4 different groups to accommodate various irradiations (Fig. 1). Twenty-three of these irradiation facilities are loaded and unloaded from the pool top using dedicated lifting tools attached to a bridge hoist. The remaining 55 facilities are loaded and unloaded via a fully automated pneumatic system pressurised with nitrogen.

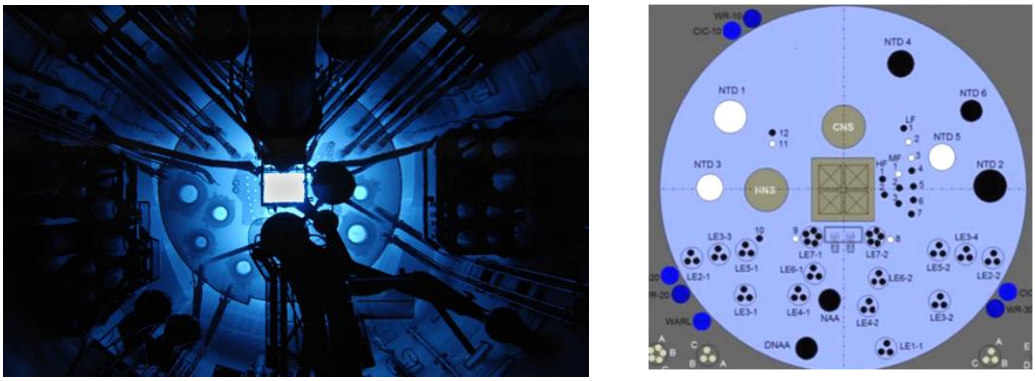

Fig 1. OPAL pool and irradiation facilities

In recent years the utilisation of the OPAL irradiation facilities has steadily increased. This increase has required greater awareness of forecast demand in utilisation and improved integration between the reactors digital operating systems and the enterprise wide management systems. A review of the OPAL utilisation facilities and the integration approach will be discussed.

2. Overview of OPAL Reactor Facilities

Forecasted demand for the utilisation of OPAL irradiation facilities is high and steadily increasing. To be able to deliver the required forecasted targets, scheduling of these irradiations becomes more challenging and time consuming (Tab 1 and Figs 2 and 3).

Irradiation Facility		Quantity	Flux Range (Thermal) n/cm2/s	Utilisation	Approximate Irradiation Duration
Bulk 	LF- Low Flux	12	Up to 1.1 E14 (peak)	Fission product Molybdenum 99 (by irradiation of LEU targets) which decays to Technetium 99m - Imaging	~3-13 Days
	MF- Medium Flux	3	Up to 1.9 x E14 (peak)	Iodine 131 by irradiation of Tellurium Dioxide – Thyroid disease diagnosis and treatment	~5-28 Days
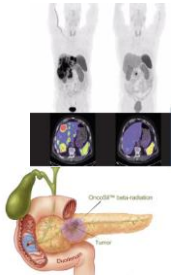	HF- High Flux IF  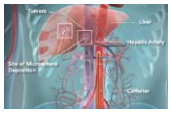	2	Up to 2.9 x E14 (peak)	Materials target compromising samples of Aluminium, Titanium, Zirconium alloys. Lutetium 177 – Cancer treatment. Yttrium -Treatment of tumours . Phosphorus -32 -Treatment for Pancreatic Cancer	~3-60 Days
Large Volume Irradiation Facilities  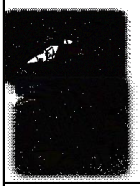	Small 136 mm dia	1	3.5 x E12	Neutron transmutation doping of single crystal silicon 4 and 5 inch diameter	~1-70 hours
	Medium 162 mm dia	3	1 x E13 to 1.9 x E13	Neutron transmutation doping of single crystal silicon 4, 5 and 6 inch diameter	~1-70 hours
	Large 213mm dia	2	3.2 x E12 to 1 x E13	Neutron transmutation doping of single crystal silicon 2, 3, 6 and 8 inch diameter	~1-70 hours
Long Residence Time General Purpose Irradiation Facilities (LRT).  	Long Residence Time - Thermal	49	2 x E12 to 1 x E14	Chromium 51 – medical uses Samarium 153 – pain management for bony metastese Lutetium 177 – Neuroendocrine cancer treatment Novel research targets Fission track samples – oil exploration industry Geological samples – mining industry	~1 hour to 30 DAYS
	Long Residence Time - Fast	6	Fast flux > 7 x E12	A508 Class 3 nuclear pressure vessel steel	~3-12 months
Short Residence Time 		2	2 x E12 to 1 x E14	Neutron Activation Analysis Delayed Neutron Activation Analysis Supports research and various industries	~3 seconds to 10 minutes

Tab.1. Utilisation of the OPAL irradiation facilities

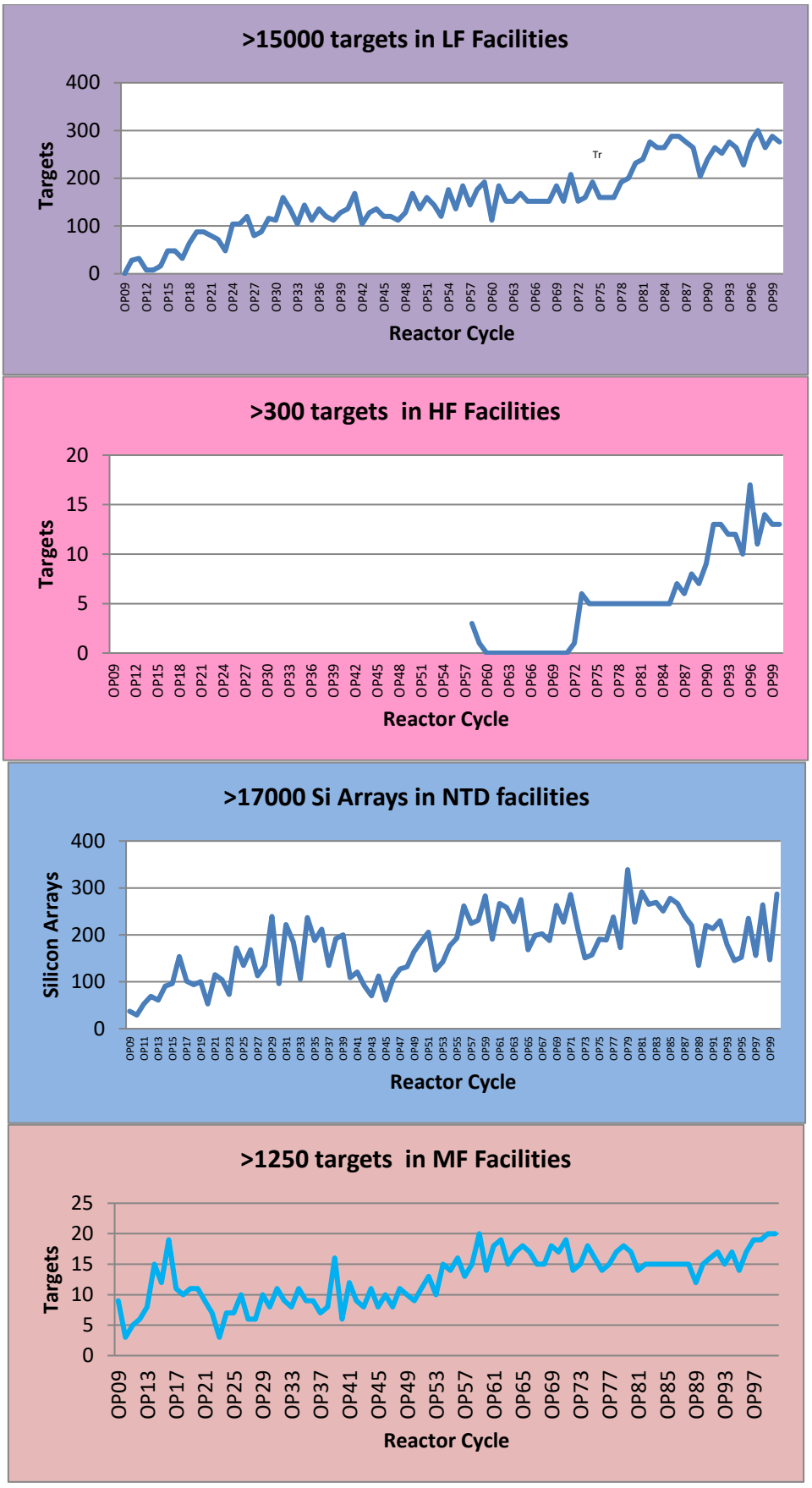

Fig 2. Irradiation graphs

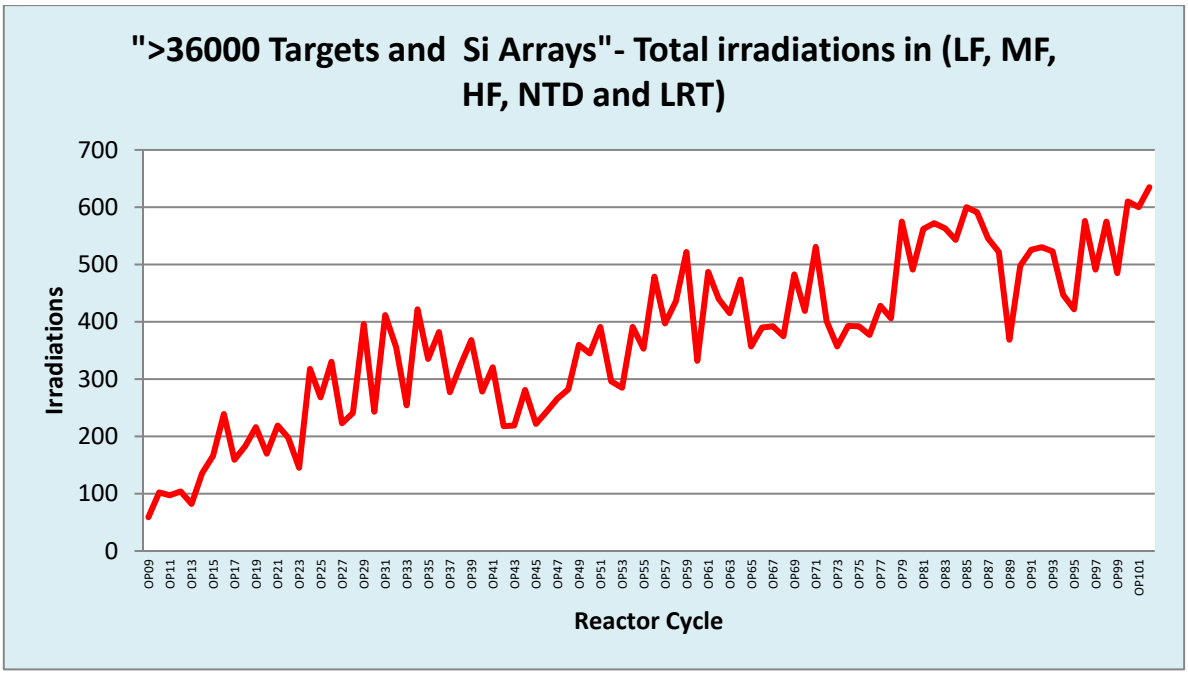

Fig 3. Total irradiations

3. Resource Planning

ANSTO Enterprise (Ae) was introduced from July 2017 to be used across all business units. The SAP component (software used to manage the Enterprise Resource Planning [ERP]) of the Ae project was introduced to ensure an integrated ERP system is available for all stakeholders with the aim to have a completed ERP system that will provide product visibility history and tools to ensure best utilisation of resources and forecasting.

The integrated system will provide an optimal plan using available critical resources such as the Operations Bridge, Utilisation Operators, Reactor Facilities, Cranes, and Hot Cells to enable on time product delivery to our stakeholders (Fig 4).

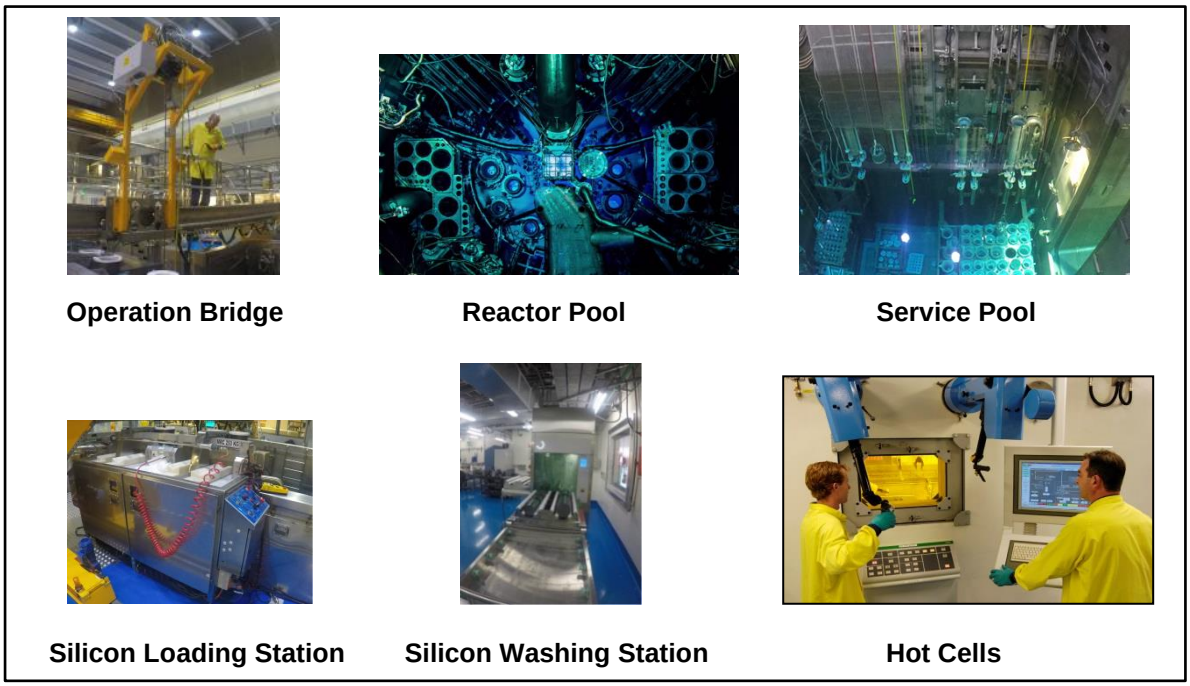

Fig 4. Critical resources

4. Manual Scheduling

Demands are received via emails or Excel spreadsheets and then manually scheduled. The Irradiation Schedule is generated and then required irradiation cards are issued. Data is transferred to the RCMS by scanning the barcode on the irradiation card and then the irradiation is visible on the RCMS. Irradiation steps are tracked via the RCMS and then data is transferred via Data Diode (Fig 5).

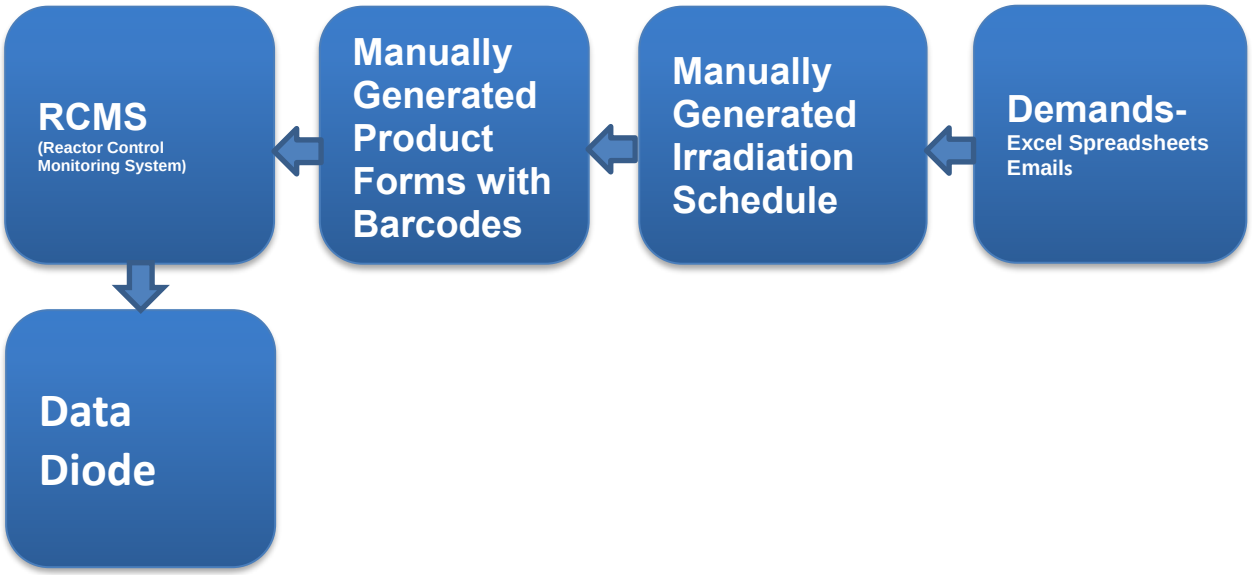

Fig 5. Manual scheduling

Issues associated with the scheduling of irradiations include the following:

- **Time consuming** - The time required to generate, review and approve the irradiation schedule.
- **Forecast visibility** - The forecast demand is tracked using Excel spreadsheets, which are not visible to everyone and not easy to change.
- **Human error** - Generating the irradiation schedule is prone to human errors, which are eliminated through experience and thorough reviews.
- **Data accuracy and reporting** - The data is manually collected and difficult to extract or update.
- **Flexibility** - Changes to the irradiation schedule have to be done manually, which involve updates to many documents.

5. Integrated Planning (SAP)

Actual and forecast demands are entered into the SAP APO (Advance Planner and Optimizer). SAP CTM (Capable to MATCH) will run to produce a 24 months rolling plan. SAP PPDS (Production Planning and Detail Scheduling) will produce a 45 days rolling irradiation schedule. Data is transferred to the RCMS by scanning the barcode on the PI-Sheet (Process Instruction Sheet), which is produced from the system and at that time the irradiation will be visible on the RCMS. Irradiation steps are tracked via the RCMS and then data is transferred via the Data Diode to the SAP system (Fig 6).

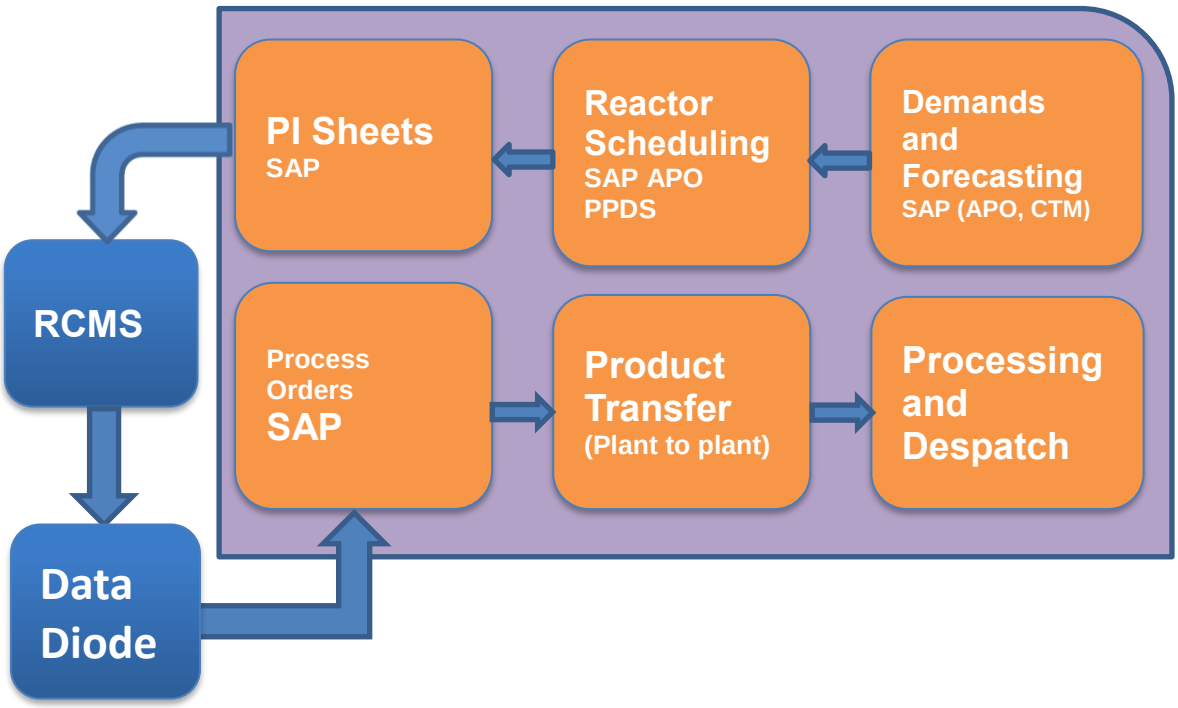

Fig 6. Integrated scheduling

The new SAP system will provide an integrated business planning tool with one source of truth with an improved data accuracy, efficiency and trend analysis. The system will enable 24 months forecasted plan visibility and a 45 days rolling schedule that will improve the supply of life-saving nuclear medicines.

6. Challenges with the New System

- **Training** - Training everyone on how to use the new system efficiently and to gain required skills on how to deal with issues arising from the new SAP system
- **Flexibility with short notice changes** - Short notice changes in the new system will require manual intervention and will require performing many SAP transactions
- **Change management** - Working with everyone to ensure change is defined understood and implemented to avoid resistance to change.
- **Master data accuracy** - Master data need to be reviewed verified to ensure the system is behaving correctly without surprises.
- **Data transfer reliability** - Data is transferred to the new system in a timely manner, the system require to be reliable with redundancy.
- **Ownership and accountability** - With the introduction of the new SAP system, process owners have changed and new roles needed to be created to ensure clear defined responsibility and accountability

7. Summary

Successful implementation of the new SAP ERP system will lead to a more robust integrated scheduling system that will enable ANSTO to have a resource planning tool to deal with short and long term challenges and provide better visibility regarding inventory, product and processes. This tool will enable ANSTO to optimise the utilisation of the OPAL reactor.

OPAL Research Reactor, Sydney Australia

OPAL Research Reactor, Main Control Room

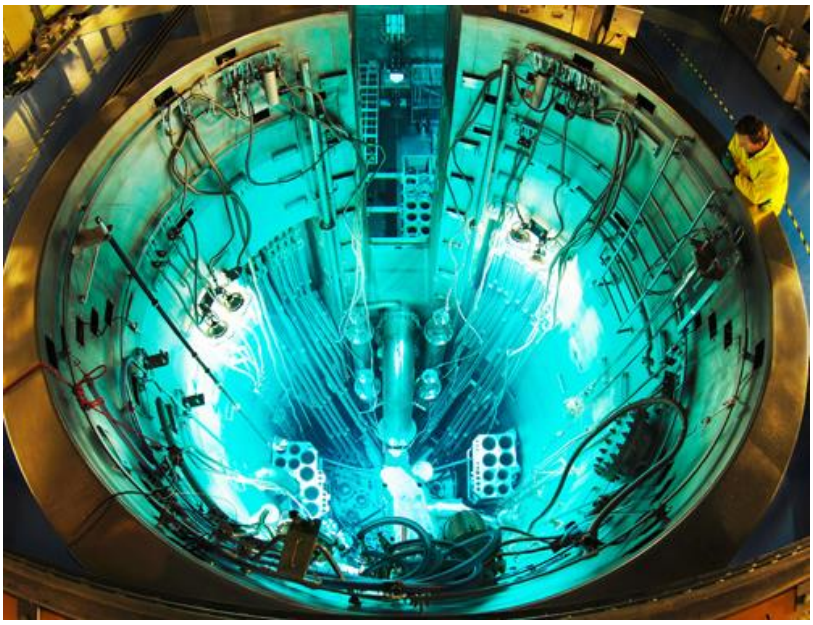

OPAL Research Reactor Pool

OPAL MULTICYCLE CORE BENCHMARK USING TRIPOLI4.10® AND COCONEUT2.0

M. DECROOCQ, C. BOURET, J. COUYBES, E. PRIVAS, N. GAVOILLE, J. KOUBBI, L. MANIFACIER(1)
TechnicAtome, CS 50497, 13593 Aix-en-Provence Cedex 3 - France

G. BRAOUDAKIS
ANSTO, Locked Bag 2001, Kirrawee DC NSW 22321 -[1] Australia

ABSTRACT

The aim of the work performed by TechnicAtome is to benchmark its codes with data provided by ANSTO on the OPAL core. Calculation schemes used are Monte-Carlo TRIPOLI4.10® (with its depletion module) and deterministic COCONEUT2.0.
After validating the models used on startup core configurations, we carry on the benchmarking process by performing the depletion calculations over cycles 7-13, as provided by ANSTO.
Use of pre and post processing tools is highlighted, making the whole process easier to cross-check. COCONEUT2.0 in its homogeneous version and TRIPOLI4.10®, even though they are very different models, both show a similar increasing trend in the k-eff within each cycle, possibly due to an overestimation of cadmium wires burnup. On the other hand, COCONEUT2.0 in its semi-heterogeneous version shows a rather flat k-eff behaviour within each cycle which could mean a better burnup calculation of both Cd and U-235. All three codes however show a trend between the cycles, consistent with that observed by other CRP participants, with an increase in the k-eff.
Burnup calculations, both with COCONEUT2.0 and TRIPOLI4.10® are satisfactory.

1. Introduction

1.1 The benchmark

OPAL (Open-pool Australian lightwater reactor) is a 20MW multipurpose RR (Research Reactor). It provides, in the frame of IAEA (International Atomic Energy Agency) CRPs (Coordinated Research Projects), a wide range of data. The aim of the work performed by TechnicAtome (TA) is to benchmark its codes with this data. Calculation schemes used are Monte-Carlo TRIPOLI4.10® (with its depletion module) and deterministic COCONEUT2.0. The latter is developed by TechnicAtome and based on CEA codes APOLLO2 and CRONOS2. All codes use JEFF3.1.1 libraries.

Data available for the fresh startup core during commissioning (CRP-1496) is first used to validate our models. The calculated results for the start-up core at low power indicate a best fit for a core power during the experiments of 41 kW rather than the suggested mean value of 36 ±6 kW, as observed by other participants. Also, local reflector environment details explain small discrepancies observed in flux profiles. All the results obtained lead TA to consider its models valid and to carry on the benchmarking process by performing the depletion calculations over cycles 7-13, as provided by ANSTO.
Use of pre and post processing tools is highlighted, making the whole process easier to cross-check. TRIPOLI4.10® geometries are generated using the powerful ROOT tool, developed by CERN.

[1] Corresponding author : Laurent Manifacier, laurent.manifacier@technicatome.com

Document [1] provides a description of the fresh OPAL core along with irradiation facilities, reflector tank, internal components as well as reloading and reshuffling strategies as described. Fig 1 illustrates briefly the startup core itself.

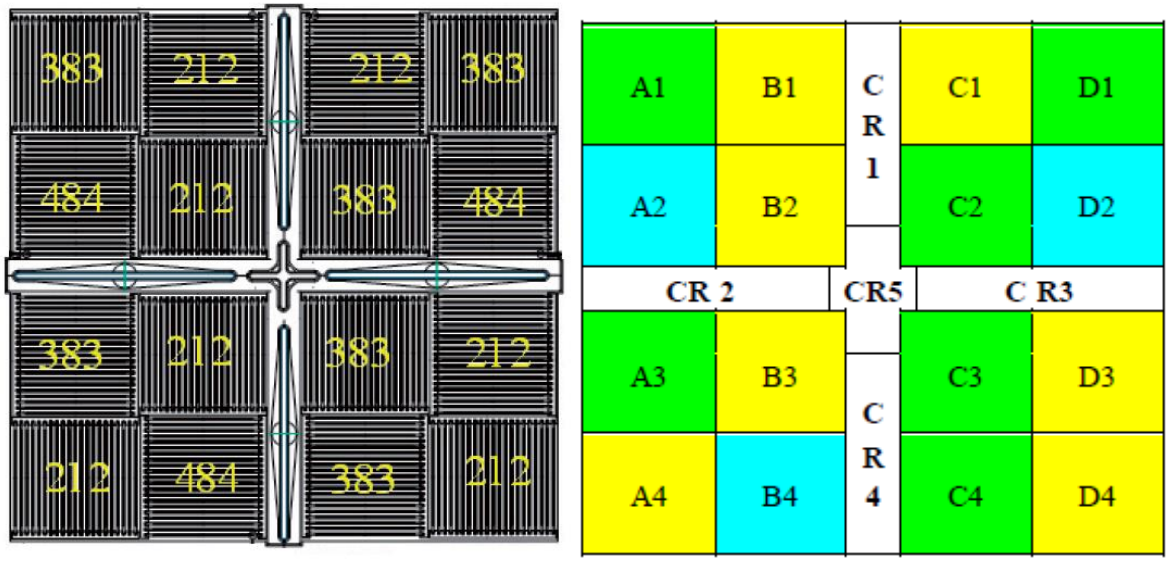

Fig 1 : OPAL core (see [1])

1.2 Summary of the codes and libraries used

This benchmark was achieved using the following codes and libraries.

TRIPOLI4® [3] (French equivalent of MCNP6) is a 3D stochastic general-purpose Monte Carlo N-Particle code used for neutron, photon and coupled neutron/photon transport and charged particles. It can use ROOT [5] (common with GEANT4) to easily generate geometry. This feature was used in this building of the model. The areas of application for these studies are neutronic, radiation protection and dosimetry, radiation shielding and experimental devices design.

COCONEUT [4] is developed by TA and based on CEA deterministic codes APOLLO2 and CRONOS2. It is a calculation scheme dedicated to RRs and includes Monte-Carlo code TRIPOLI4® in its chaining. It uses SILENE pre and post-processing and runs in 2D or 3D modes. It is designed for robust fuel rise to equilibrium and, among other features, outputs material balances as an input for TRIPOLI4® or MCNP6 continue-calculations.

2. Modelling

We present in this section the different models used by TA.

2.1 COCONEUT2.0

COCONEUT uses SILENE as a geometry interface. It is user-friendly and enables a quick generation of 2D or 3D cylindrical and Cartesian features together in variable meshes. It leads to geometries which are quite close to reality. But in this case, for simplicity reasons, no beam tubes were modelled (see Fig 2). This leads to a bias in calculations that is discussed later.

When running depletion calculations, the computed APOLLO2 model uses the following features (see Fig 3):

- 5*8 meshes in the fuel meat, per fuel plate
- 4*5 meshes per Cd wire

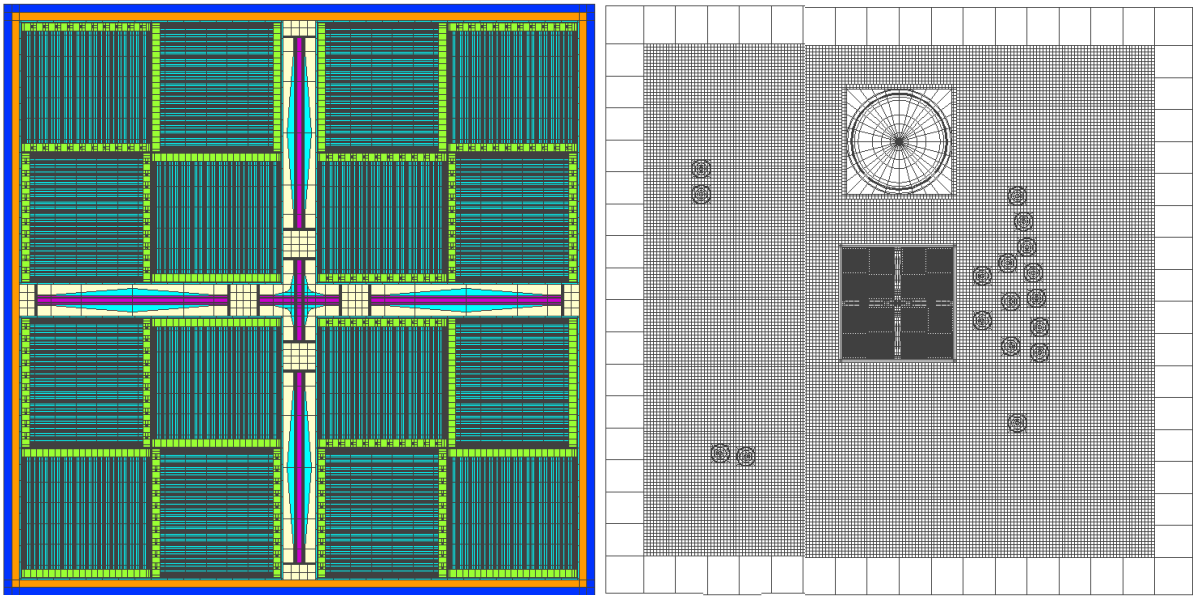

Fig 2 : 2D SILENE model of OPAL core and reactor

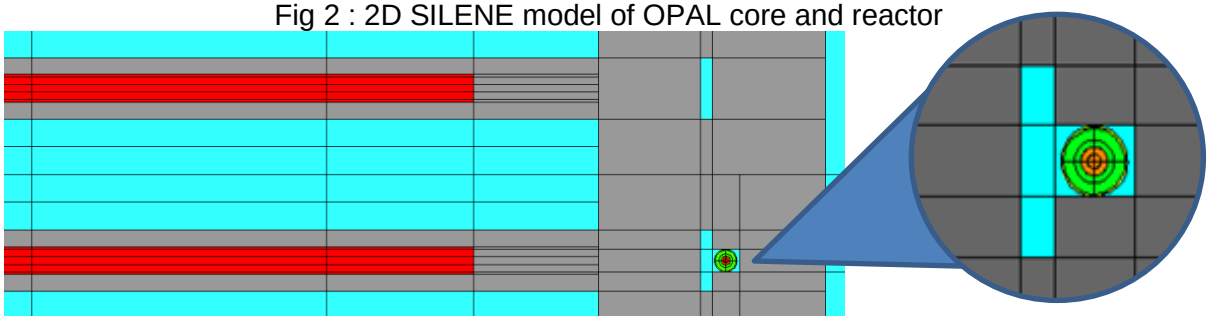

Fig 3 : 2D SILENE model of the OPAL fuel plates (with Cd wires)

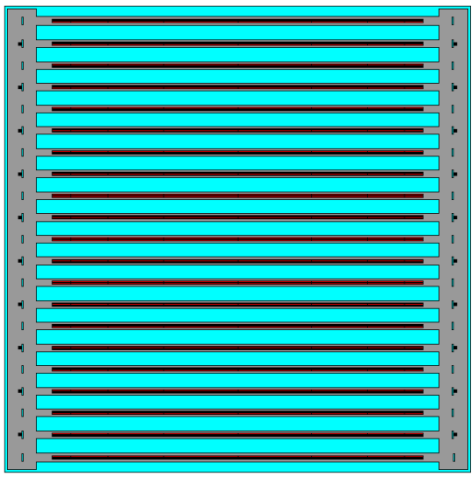

Fig 4 : 2D SILENE model of the OPAL FA (with Cd wires)

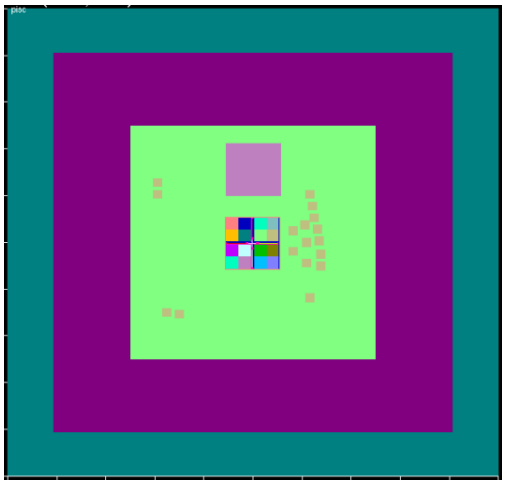

Fig 5 : 3D CRONOS2 model of the OPAL reactor

In its 3D version, the structure of CRONOS2 imposes a Cartesian mesh. Thus, several approximations were introduced:

- the control rod guide boxes are rectangular (see section 3.2)
- Outer part of the reflector is not modelled: the D2O tank is square (260 cm) with 30 cm of light water around it (Fig 5)
- The purity of D2O is constant (97.5%, as for cycle 7) (see section 3.2)

Also, when running depletion calculations, the CRONOS2 model computed uses the following features:

- 29 axial meshes in the fuel meat
- 15 axial meshes in the Cd wires thus, approximately 2 cm per mesh.

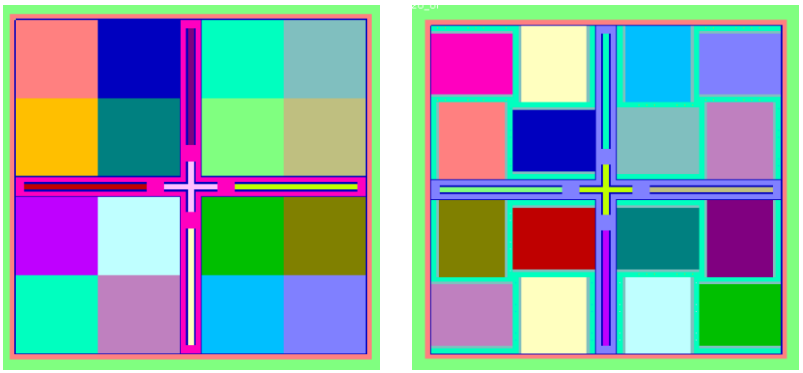

Fig 6 : zoom in views of the 3D CRONOS2 model of the OPAL core, homogeneous (left) and semi-heterogeneous (right)

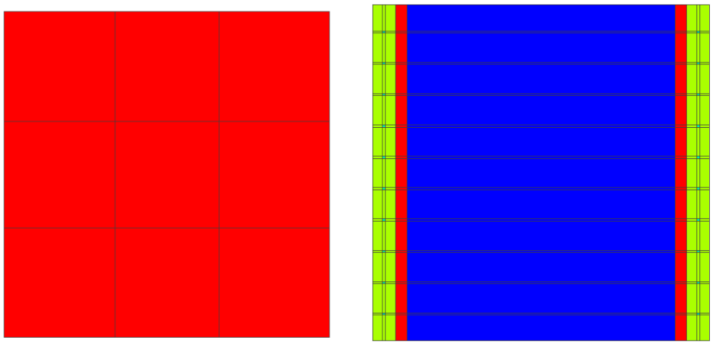

Fig 7 : 2 different modellings of the FA: homogeneous (left) and semi-heterogeneous (right) in which the side plates are fully described with Cd wires (green), water on the side is red and the fuel part (blue, centre) is homogenized with its water and cladding

For this first approach, CRONOS2 is at first used in its homogeneous version. Each FA is fully homogenised with fuel, aluminium, water, poisons etc. (Fig 6 and Fig 7, left). A full heterogeneous calculation, very time consuming, has not yet been performed, but should be in the near future. Instead, an intermediate version with a semi-heterogeneous FA is modelled (later called “heterogeneous” in this document). Mixing Cd wires in a fully homogeneous FA is expected to increase the efficiency of this poison as it is no longer self-protected inside very small cylinders (see Fig 3). We have then described a FA in which the fuel zone is still homogenized, but side plates and water in between are separated (Fig 6 and Fig 7, right). This modelling enables Cd to be fully described.

2.2 TRIPOLI4.10®

TRIPOLI4.10® models are built in this study with ROOT [5]. This powerful toolkit provides important modularity. ROOT geometry is very easy to build up and to modify, such as when it comes to the adaptation of experimental conditions (reflector purity and temperature, choice of experimental devices (ExD) in the reflector). All experimental facilities were easily created with precious time saving, and the TRIPOLI4® viewer is also compatible with ROOT geometry.

Fig 8 illustrates the ROOT generated TRIPOLI4® model used in this study.

In its depletion mode, TRIPOLI4 is run with the two following features.
A first, simple one, with:

- one depleted material per Cd wire (thus, 20 per FA)
- one depleted material per fuel plate (thus 21 per FA)

A second, more accurate one, with:

- 3 axial depleted materials per Cd wire (thus, 60 per FA)
- 6 axial depleted materials per fuel plate (thus 126 per FA)

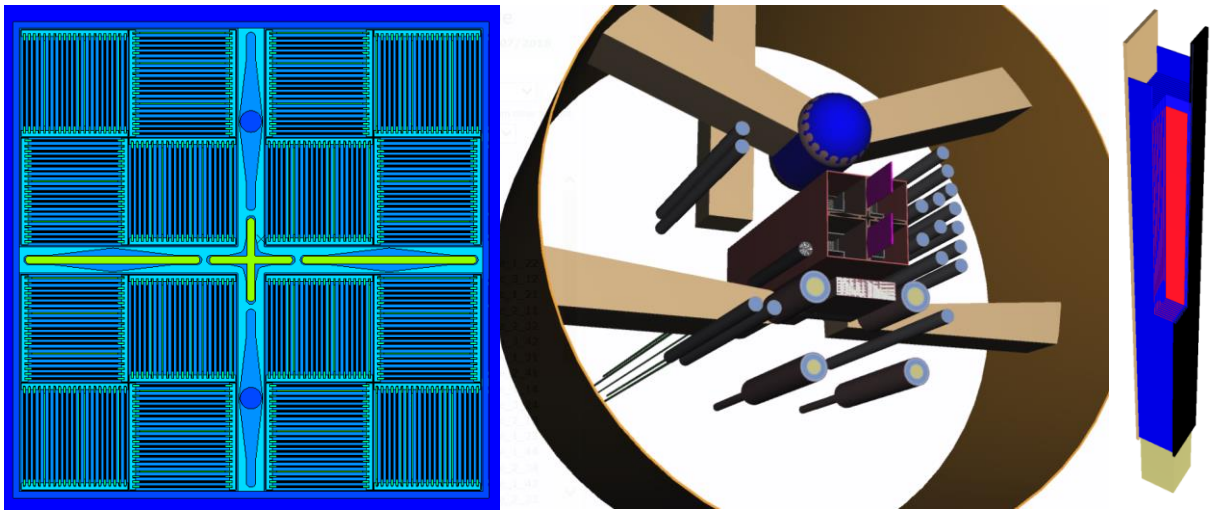

Fig 8 : ROOT geometry general views of OPAL reactor and FA

These simple features have deliberately been computed as a first step in the benchmark. However, due to very satisfactory results (see section 3.4), we don't intend to try finer meshing in the depleting materials since this would be very time consuming (even more accurate features could be modelled by adding radial meshes in Cd wires or fuel plates).

Also, in the depletion mode, for calculation time purposes, several simplifying assumptions are made:

- The CNS model is simplified
- No ExD are modelled in the reflector, just the tubes, filed in light water
- Reflector purity is computed as specified in [2] and is thus assumed constant during a given cycle

TRIPOLI4® depletion is selected with the simple Euler method computed in the "Mendel" solver. It would be possible to use Mean or Midpoint schemes [3] in order to possibly reach better results.

3. Results

We present in this section the results of calculations performed with COCONEUT2.0, then TRIPOLI4®. At first, we discuss the 2D FA calculations (APOLLO2) used to process cross sections. We then present full 3D core calculations in homogeneous and heterogeneous versions before switching to Monte-Carlo results.

3.1 2D FA calculations with APOLLO2

Full infinite lattice 2D geometry is modelled with the SILENE tool (see section 2.1), and no axial buckling. APOLLO2 2D calculations are performed in order to determine cross sections for all the materials with respect with the burnup of the fuel assembly.
In order to validate the APOLLO2 model, k-eff and neutron flux values are compared with TRIPOLI4® calculations. K-eff are very similar and it is assumed the models are correct.

Assembly type	Type 1	Type 2	Type 3
k_{eff} TRIPOLI4®	1,54795 ± 22 pcm	1,51522 ± 13 pcm	1,54784 ± 13 pcm
k_{eff} COCONEUT2.0	1,54805	1,51709	1,54960
Δρ (pcm)	**4** ±14 pcm	**81** ± 9 pcm	**73** ± 8 pcm

Tab 1 : k-eff comparisons between APOLLO2 and TRIPOLI4®, for the 3 FA types

Again, when comparing thermal flux distributions within all three FA types, COCONEUT2.0 and TRIPOLI4®, results are very close. It is assumed our models are correct.

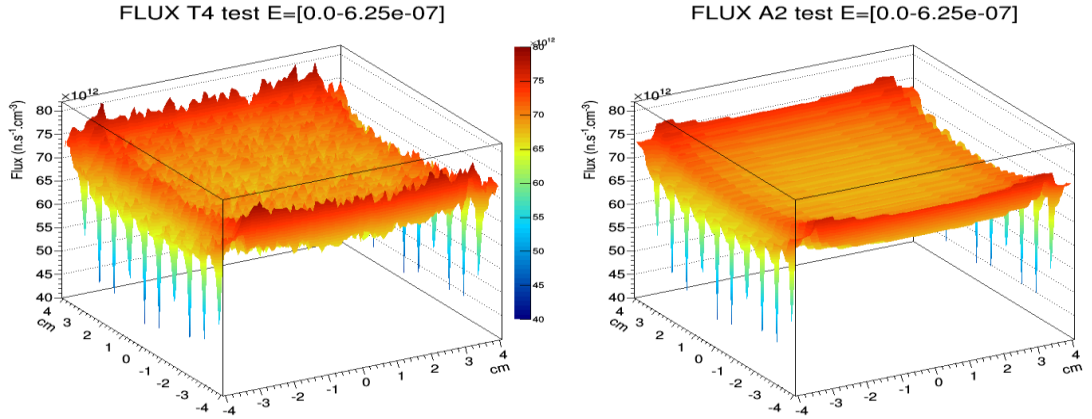

Fig 9 : Thermal flux in FA type 2. TRIPOLI4® (left) and APOLLO2 (right)

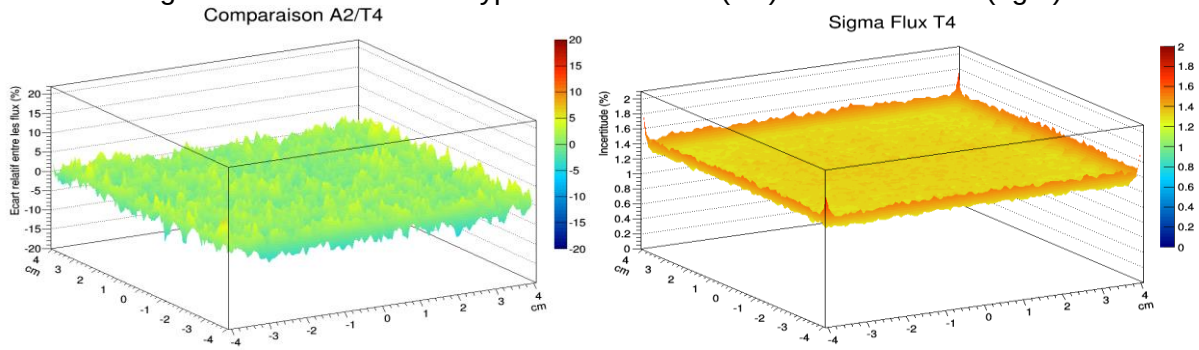

Fig 10 : Comparison of Thermal flux in FA type 2. APOLLO2 vs TRIPOLI4® (left) and standard deviation (right)

3.2 Homogeneous geometry with COCONEUT2.0

We then perform full 3D evolution of the core using the homogeneous version of COCONEUT2.0.

Reflector cross section tables in the 2.0 version of COCONEUT cannot, for the moment, be modified during the calculation. As a result, the D2O purity of the water tank is assumed to be constant and is fixed at the cycle 7 value of 97.5%. A TRIPOLI4® calculation of the first step of cycle 7 at 97.5% and 99.55% D2O purity shows a reactivity effect of +1164 pcm. We then shift the reactivity of each cycle linearly with this amplitude, depending on the exact purity of each cycle.

Cycle	%wt D2O	ρ shift
7	97.5	0
8	97.1	-227
9	96.9	-341
10	99.55	**1164**
11	99.24	988
12	98.93	812

Tab 2 : Reactivity shift (pcm) applied to COCONEUT cycles due to non-constant D_2O purity

In addition, TRIPOLI4® calculations performed on COCONEUT-like geometries reveal a -1686 pcm reactivity shift due to the fact that (mostly) neutron beams are not modelled in the reflector tank. Thus COCONEUT calculations are corrected with -1686 pcm.

In the end, Fig 14 shows the results (k-eff) of the full depletion cycle of the OPAL core during cycles 7-12, with all corrections taken into account.

The results show a bias in the k-eff values which is globally negative and increases from -1500 pcm (approx.) to zero for cycle 12. These results are satisfactory and confirm general trends observed with other CRP participants (violent power changes naturally lead to strong

Xe poisoning changes which are difficult to account for on a kinetic point of view. Thus, points occurring just at these steps have been discarded).
The mean bias in reactivity is -706 pcm, with a standard deviation of 722 pcm (see Table 4).
The effect of homogenizing all the materials within each FA is to also mix Cd, which is normally concentrated in very small wires, into the whole FA square (see Fig 7). This feature is expected to significantly amplify Cd capture and thus reduce the k-eff calculated in the homogeneous version.
One can also observe a trend within each cycle: the k-eff values increase during the cycle. This can be due to an overestimation of the Cd burnup (because of the homogenisation).

3.3 Heterogeneous geometry with COCONEUT2.0

As in the previous homogeneous case, heavy water purity is also assumed constant. K-eff values are then corrected with respect to values in Tab 2. Fig 14 also shows the results (k-eff) of the full depletion cycle of the OPAL core during cycles 7-12, in the heterogeneous version. It is reminded that in this version, the fuel area is still homogenized, but the side plates (containing Cd wires) and water surrounding them are fully described (see Fig 7).
As expected, k-eff values are much higher.
The bias is globally increasing throughout the cycles, just as in the homogeneous case, with values ranging between -300 pcm and +900 pcm. There is a noticeable exception with cycle 7 which starts with a considerable bias of approximately +1500 pcm and rapidly decreases to zero in the end. This feature still needs to be explained, but could be due to Cd wires.

Mean bias in reactivity is +567 pcm, with a standard deviation of 603 pcm (see Table 4). This is better than in the homogeneous case. These results are satisfactory and confirm general trends observed with other CRP participants.
There is a questioning in the heavy water purity correction that is applied, since a change in reactivity bias is visible after cycle 10. This should lead to further investigation.
Unlike in the homogeneous case, there is no visible trend within each cycle: the k-eff behaviour is rather flat. This could simply mean that fully modelling the Cd wires helps in better describing their depletion.

3.4 TRIPOLI4.10®

In the TRIPOLI4® case, D2O purity is computed as specified in [2] and there is no bias due to neutron beams since they are properly modelled with the ROOT toolkit.
Fig 14 shows the results (k-eff) of the full depletion cycle of the OPAL core during cycles 7-13 as calculated by TRIPOLI4® in its depletion mode. The depletion models are first simplified (as detailed in section 2.2) with a single medium per Cd wire and a single medium per fuel plate.
As for both COCONEUT 2.0 cases, there is a globally increasing trend in the k-eff. The bias is almost zero for cycle 7 (-100 pcm) and increases up to +1500 pcm at cycle 12. Mean bias in reactivity is +692 pcm, with a standard deviation of 887 pcm (see Table 4).
As in the homogeneous version of COCONEUT, a trend is clearly visible within each cycle: k-eff values increase during the cycle. This could be due to an overestimation in the Cd depletion. Indeed, there is only one material per Cd wire, which increases its burnup by not taking into account the self-protection which implies that only the outer layers of Cd in the wire deplete first.

A second calculation is performed with 3 axial meshes per Cd wire and 6 axial meshes per fuel plate (see section 2.2). The aim is to assess the sensitivity of the results to the degree of refinement of meshing depleting materials. 3 axial meshes in Cd wires and 6 in fuel plates is assumed to be quite a rough first-step refinement which is supposed to enhance the quality of the calculation.
Fig 14 reports both depletion curves for k-eff. It is clearly visible that a small refinement in the meshes has a considerable impact on the results. The trend in k-eff in each cycle (in

pcm/EFPD, see Table 4) is divided by a factor of approximately 2, and so is the global trend on the multicycle calculation. The mean bias (pcm) is also significantly reduced, dropping from +692 pcm to -124 pcm. In the last cycles (10 – 13), the bias drops from approximately 1000 pcm. Finally, standard deviation is also reduced by a factor of 2 for each individual cycle, and drops from 887 to 562 pcm on the global depletion calculation.

3.5 Isotope concentration

These data were determined with TRIPOLI4®. U-235, Pu-239 and Cd-113 masses (g) in the whole core through cycles 7-13 are plotted below. Results are obtained with the single axial mesh option (calculation number 1). Differences with the multiple axial mesh are very low if concentrations are averaged on the whole core.

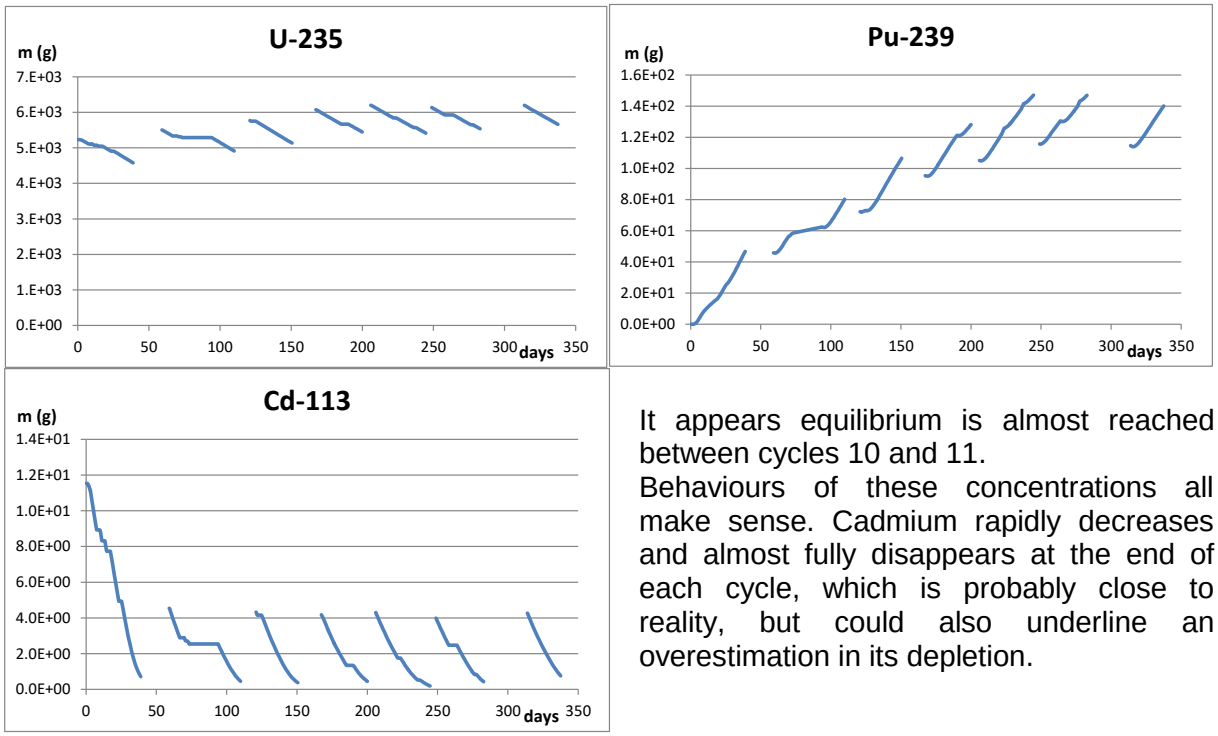

Fig 11 : U-235, Pu-239 and Cd-113 masses in the OPAL core, cycles 7-13 (TRIPOLI4®)

It appears equilibrium is almost reached between cycles 10 and 11.
Behaviours of these concentrations all make sense. Cadmium rapidly decreases and almost fully disappears at the end of each cycle, which is probably close to reality, but could also underline an overestimation in its depletion.

3.6 Burnup calculations

Fig 12 plots the burnup of the core through cycles 7-13. It is the burnup of each cycle, taken separately, thus starting at 0 each time. Processing of burnup per fuel assembly gives the burnup of the FAs at the end of each cycle, and in particular the burnup of the fuel assemblies which are unloaded (see Tab 3).
Similar burnup calculations are available at each step of COCONEUT2.0 calculations, and all are consistent with Tab 3. End of cycles 7 and 11 are shown as an example in Fig 13.

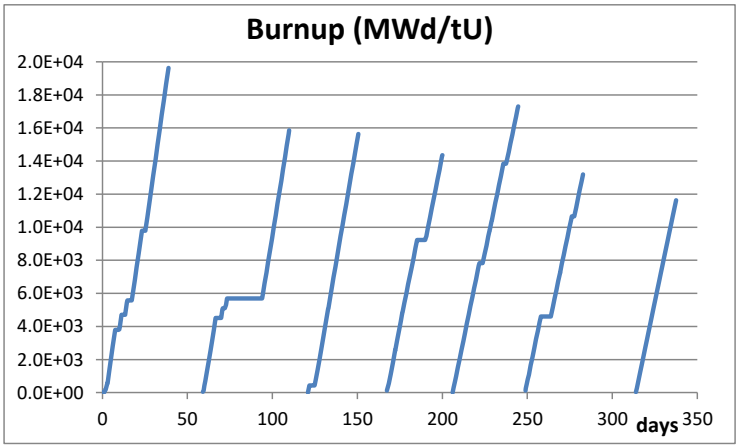

Fig 12 : Mean core burnup, calculated by TRIPOLI4® (cycles 7-13) in MWd/tU

	FA # 1	FA # 2	FA # 3
Cycle 7	26020 (T1)	25043 (T1)	24480 (T1)
Cycle 8	32459 (T1)	45050 (T1)	44167 (T1)
Cycle 9	66388 (T1)	50034 (T2)	62248 (T2)
Cycle 10	61483 (T2)	61961 (T2)	63633 (T2)
Cycle 11	76836 (Std)	73608 (T2)	72993 (Std)
Cycle 12	80428 (Std)	67812 (Std)	71985 (Std)

Tab 3 : Burnup (MWd/tU) of unloaded FAs at the end of each cycle (TRIPOLI4®)
Type of the unloaded FA is also identified (Type 1, 2, 3 or standard)

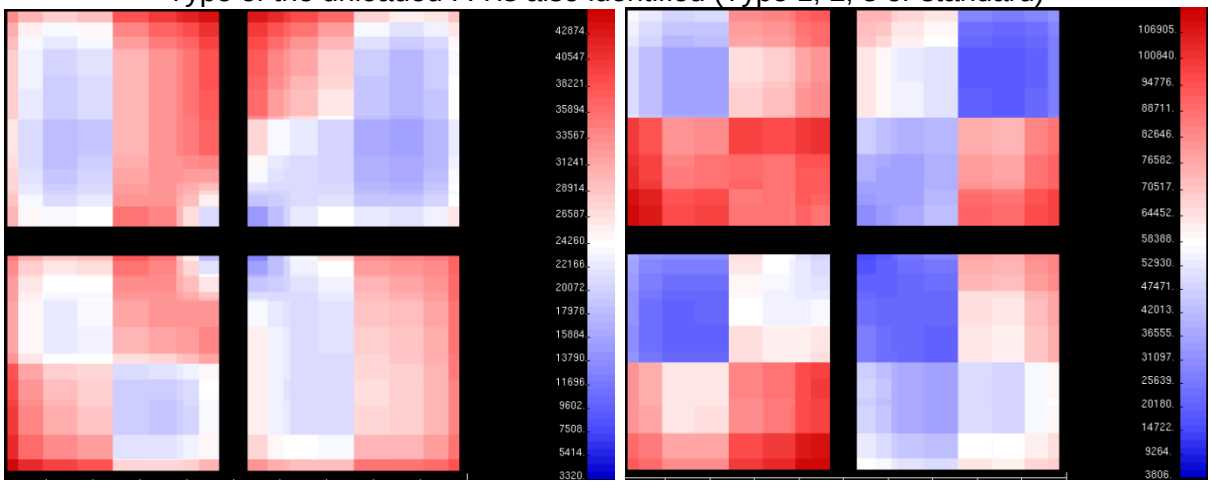

Fig 13 : Burnup (MWd/tU) of each calculation mesh (COCONEUT) in the core at the end of cycle 7 (left) and 11 (right)

4. Discussion

Fig 14 compares all calculations performed in this depletion study:

- COCONEUT2.0 in its homogeneous version
- COCONEUT2.0 in its semi-heterogeneous version
- TRIPOLI4.10® with a single axial mesh description for depleting media
- TRIPOLI4.10® with multiple axial mesh description for depleting media

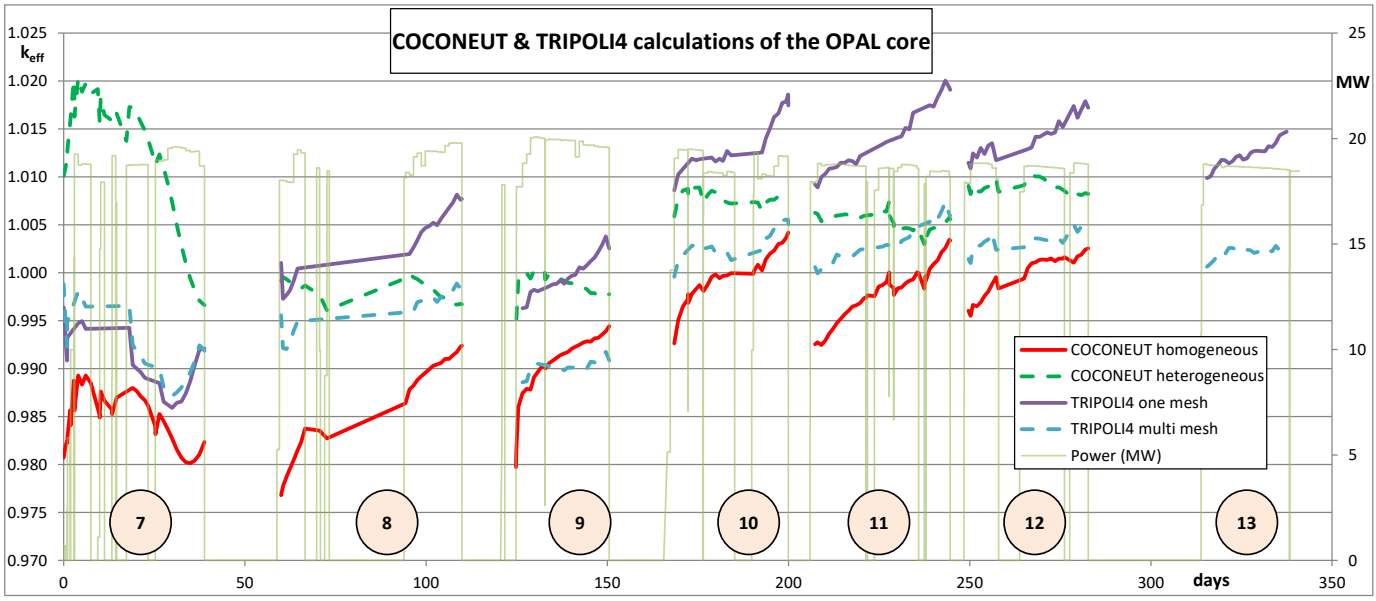

Fig 14 : Comparison of COCONEUT2.0 and TRIPOLI4® 3D core calculation of OPAL cycles 7-13, for all different models:

Also, Table 4 provides trends (pcm/EFPD), biases (pcm) and standard deviations (pcm) for all four calculations, either on each individual cycle, or globally on all cycles, or just the final cycles (10-13) once equilibrium seems to be met.

It appears that minor improvements in the modelling of the core can significantly enhance the accuracy of the results. In the deterministic case, fully describing the side plate with Cd wires (but still leaving a central homogeneous medium with fuel, water and cladding) significantly reduces trends and standard deviations (Table 4).
However, this increases the bias, suggesting compensation effects in the neutronic balance.

In the same way, and as detailed in section 3.4, a simple axial meshing in Cd depleting media also reduces discrepancies significantly. No radial meshing is introduced in Cd wires or fuel plates at this stage. This seems to be sufficient to get a better description of Cd and uranium depletion.

	Trends and Biases on calculations											
	COCONEUT2.0						**TRIPOLI4.10**					
	Trends (pcm/EFPD)		Mean bias (pcm)		Std. deviation (pcm)		Trends (pcm/EFPD)		Mean bias (pcm)		Std. deviation (pcm)	
	Homogen.	Heterogen.	Homogen.	Heterogen.	Homogen.	Heterogen.	single mesh	multi mesh	single mesh	multi mesh	single mesh	multi mesh
Global	**12.8**	**-0.9**	**-706**	**567**	**722**	**603**	**13.7**	**7.8**	**692**	**-124**	**887**	**562**
cycle 07	-17.8	-68.0	-1543	1231	288	648	-23.0	-29.8	-963	-804	325	365
cycle 08	66.9	-5.6	-1374	-193	519	143	42.5	24.9	355	-378	344	209
cycle 09	42.9	-7.0	-1014	-112	412	117	26.1	7.2	-18	-981	199	71
cycle 10	33.0	3.3	-32	758	271	146	32.1	17.2	1344	310	278	162
cycle 11	30.3	-1.1	-203	520	284	145	30.7	19.0	1350	292	337	212
cycle 12	27.4	3.5	-26	866	226	154	23.3	10.2	1397	337	192	100
cycle 13							17.9	7.6	1211	218	124	67
cycles 10-13	**3.7**	**1.5**	**-103**	**688**	**276**	**209**	**1.0**	**0.7**	**1326**	**285**	**254**	**152**

Table 4 : Trends and biases on depletion calculations.
Trends are in pcm/EFPD (pcm per Equivalent Full Power Days at 20 MW)

Cd depletion is probably overestimated in deterministic calculations with a single homogeneous cell in which Cd is homogenised with the whole FA (see section 2.1), as well in the Monte-Carlo case where a simple cylinder is coded (see section 2.2). Indeed, in the first case, Cd absorption is overestimated since self-shielding is not taken into account. As a result, reactivity of the FA increases more rapidly than it should. In the second case, Cd reaction rate is averaged over the whole cylinder, thus neglecting the bell-shape curve and amplifying Cd depletion.
Similarly, U depletion is probably underestimated in the homogenised deterministic case, which causes a positive trend in reactivity.
Again, averaging the flux in the whole fuel assembly, with the presence of mixed Cd in the medium, causes an underestimation of thermal flux due to Cd capture. Separating Cd from the fuel causes the reactivity trend to drop.

In the TRIPOLI4.10® case, effects of axial meshing in fuel plates are assessed during cycle 8. At one point, homogenising the 6 axial fuel materials in each plate of calculation n°2 leads to a reactivity effect of +754 pcm (see Fig 15). However, average U-235 in both cases differ from less than 0.1%. Thus, the effect mostly comes from axial distribution of uranium.
This confirms that modelling a single axial mesh underestimates U depletion which accounts for the majority of the difference between the two calculations. In this particular case, an additional

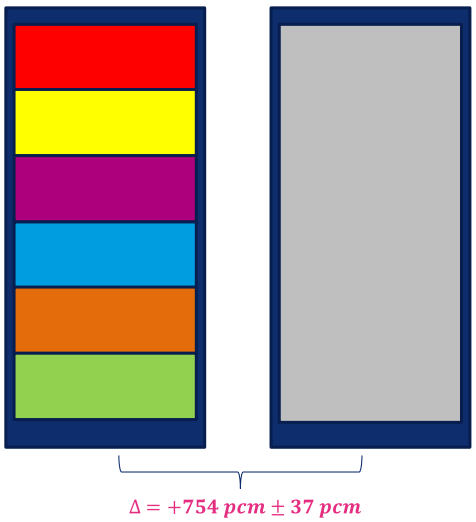

Fig 15 : Homogenising fuel cells into one, assessing the effect of axial meshing on reactivity

100 pcm, approximately, is caused by a similar meshing in Cd wires.

The effect of Cd axial meshing is illustrated by Fig 16. When we compare Cd-113 concentration in the 3 axial meshes to the average Cd concentration calculated by the similar calculation with one mesh per depleting medium, it appears that after a rather flat evolution (which is artificially amplified by a 20 day inactivity of the reactor), Cd-113 concentration in the central mesh rapidly decreases down to -20% in comparison with the "reference" homogeneous cell. In the same time, the top and bottom cells see their Cd concentration increase by 10%, which means that the Cd depletion in these cells in overestimated by 10% at the end of the cycle in the first calculation. This is simply due to the axial bell-shaped curve of the flux in the core.

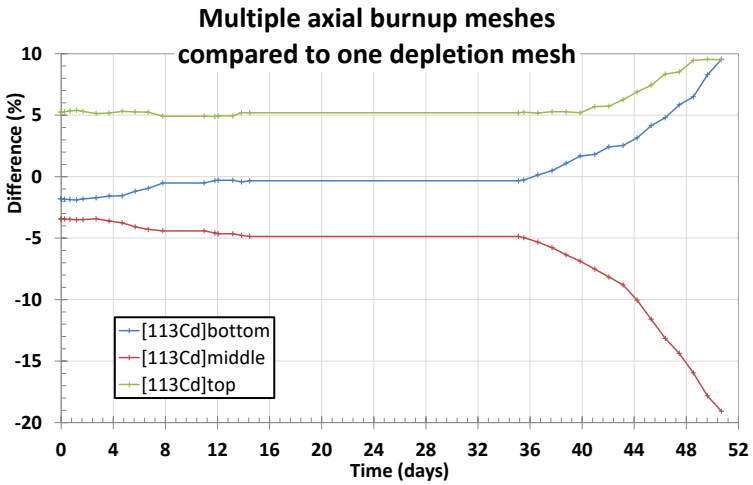

Fig 16 : Effect of axial meshing in Cd concentration in the wires: Cd concentration vs average Cd concentration in the 1 axial mesh case

Note: In Fig 16, the plotted differences start with non zero values because they refer to cycle 8, not cycle 7. Thus, due to some FAs that have already been depleted during a cycle, there are differences between the homogeneous and multi mesh cases.
In the end, a basic axial meshing in Monte-Carlo calculations or a simple semi-heterogeneous modelling of the fuel assembly in deterministic calculations is sufficient to significantly improve calculations, and reduce and almost cancel reactivity trends within the cycles.

There remains however a feature in Fig 14. Even though we can reduce trends, deviations and biases with simple modelling features, the first cycles (7 – 8 – 9) remain odd. Starting at cycle 10, there seems to be an obvious equilibrium which is met, and biases and trends are very low (see Table 4). Evolutions are significantly more chaotic before this point. Particularly, we notice important reactivity differences between two consecutive cycles that challenge interpretations.
A correlation can be found with the refuelling patterns. Indeed, cycle 10 corresponds to the point after which there are no longer type 1 transition FAs left in the core (those with the minimum U-235 load of 212g) and only 4 type 2 FAs remain in the centre. But there are no differences in matter specification for standard and transitional elements. Furthermore, measured masses in fresh FAs and dispersions are all compliant. As a result, no manufacturing tolerances issue for transition FAs can explain these relatively important features observed in k-eff variations.

5. Conclusion

The aim of the work performed by TechnicAtome is to benchmark its codes with operational data provided by OPAL. Calculation schemes used are Monte-Carlo TRIPOLI4.10® [3] (with its depletion module) and deterministic COCONEUT2.0 [4] Both are based on CEA codes APOLLO2, CRONOS2 and TRIPOLI4.10®. All codes use JEFF3.1.1 libraries.
Use of pre and post processing tools is highlighted, making the whole process easier to cross-check. Geometries in TRIPOLI4® are built very quickly with a modular technique, using ROOT [5].

After validating the models on commissioning data available for OPAL (CRP-1496), further calculations on depletion cycles are performed, both with the COCONEUT2.0 (in its homogeneous and heterogeneous versions) and TRIPOLI4® schemes.

The calculations performed for this benchmark show that both COCONEUT1.5 in its homogeneous version and TRIPOLI4.10® reveal an increasing trend in k-eff within each cycle, possibly due to an overestimation of Cd burnup (only one material per Cd wire in TRIPOLI4.10®). On the other hand, COCONEUT2.0 in its semi-heterogeneous version shows a rather flat k-eff behaviour within each cycle which could mean a better burnup calculation of both Cd and U-235.
All three models however show a trend between the cycles, consistent with that observed by IAEA CRP, with an increase in the k-eff.
Refining the modelling in deterministic case, by separating the side plates with Cd wires and fully describing them as independent depleting media, or, in the Monte-Carlo case, introducing an axial meshing of depleting fuel plates (6 cells) and Cd wires (3 cells), significantly improves calculations and almost cancels reactivity trends during cycles.
Burnup calculations, both with COCONEUT2.0 and TRIPOLI4.10® are satisfactory.
Strong remaining discrepancies in early cycles correspond to the time during which transition elements are present in the core in great numbers. But no manufacturing tolerance issue can explain these features. An equilibrium seems to be met after all type 1 elements are removed from the core (cycle 10) and full neutronic equilibrium is reached after cycle 12.

Tab 5 sums up all the main multicycle depletion features studied in this benchmark.

	TRIPOLI4®		**COCONEUT2**	
	one axial mesh	multi mesh	homogeneous	heterogeneous
Multicycle depletion	+692 pcm σ=887	-124 pcm σ =562	-706 pcm σ =722	+567 pcm σ=603
cycles 10-13 only	+1326 pcm σ=254	+285 pcm σ =152	-103 pcm σ =276	+688 pcm σ=209

Tab 5 : Summary of main results (biases and standard deviations)

References

[1] CRP-1496 - OPAL nuclear reactor: reactor specification
[2] CRP-1496 – OPAL nuclear reactor: experimental data
[3] TRIPOLI4® Project Team, “TRIPOLI-4 Version 10 User Guide”, Technical Report, CEA/DEN/DANS/DM2S/SERMA/LTSD/RT/15-5928/A
[4] COCONEUT: Enhancing neutronic design for research Reactors (J-G. Lacombe et al.), RRFM-IGORR meeting Berlin, Germany, march 2016
COCONEUT: First validation steps of the Areva TA neutronic scheme for research reactor design (C. Bouret et al.), RRFM-IGORR meeting Berlin, Germany, march 2016
[5] Root published in Linux Journal, Issue 51, July 1998. ROOT: An Object-Oriented Data Analysis Framework.

Acknowledgements

This work is performed in the frame of the CRP T12029, named “Benchmarks of Computational Tools against Experimental Data on Fuel Burnup and Material Activation for Utilization, Operation and Safety Analysis of Research Reactors” and organized by the IAEA.
Authors wish to thank Dr Laurent Chabert and Dr Claude Pascal for valuable discussions.

LESSONS LEARNED FROM MAINTAINING INSTRUMENATION AND CONTROL SYSTEMS OF JORDAN RESEARCH AND TRAINING REACTOR

YONG SUK SUH*, DANE BAANG, SEUNG KI SHIN,
SANG MUN SEO, JONG BOK LEE

Research Reactor System Design Dept., Korea Atomic Energy Research Institute, 989-111 Daedeok-daero, Yuseong Gu, Daejeon, 305-353, Republic of Korea

*Corresponding author: yssuh@kaeri.re.kr

ABSTRACT

After commissioning the Jordan Research and Training Reactor (JRTR) in December 2017, there were several issues during the operation and maintenance of instrumentation and control (I&C) systems that were designed using digital technology. The major issues were with data communication and neutronic signal processors. The data communication has dual data links and is controlled by the information processing system that connects and manages more than thirty computers. The anti-virus program is running to protect the systems from unauthorized access, which makes the systems complicated. It is difficult to detect the cause of failures when the data communication fails. This paper presents the ways of diagnosing and restoring the failure of data communication. There are eighteen neutronic detectors and digital signal processors. These components are very sensitive to electrical noises whose sources are also complex. It is also difficult to diagnose and find the cause of failure when they fail. This paper presents experiences and lessons learned from detecting, diagnosing and correcting the abnormal states of JRTR I&C systems. This paper also presents overall architecture and defence-in-depth design features of I&C systems.

1. Introduction

The JRTR construction project started in 2010 and its commissioning stage finished in 2017 [1]. After the commissioning stage, some abnormal states occurred in its I&C systems. This is a natural phenomenon because I&C systems are so complicated that they are not easily finalized. The I&C systems are usually stabilized after the upper systems, such as fluid and mechanical systems, are stabilized. The JRTR I&C systems are digital. As the reactor operation keeps going, the software of I&C systems are required to be tuned and updated. The digitalized I&C systems have the advantage of easily accepting the changes required from both the upper systems and local fields. Therefore, they are not perfectly stabilized for full power operations, although the I&C systems are successfully commissioned. Based on the operation experience of JRTR I&C systems, it takes at least one and half years to make the I&C systems stabilized after the commissioning stage because most of instrument channels should be calibrated again. During this stage, the maintenance engineers should calibrate the cannels, which were already calibrated with vendors during the commissioning stage, without the vendors for the next year. At the moment, the users should review the calibration procedures more precisely and perform it correctly. They should correct and update the procedure under their qualification control. This paper presents maintenance experiences and lessons of digital communications and neutronic signal processors as major experiences as well as lessons from maintaining the I&C systems during this stage in the next clauses.

2. Overview of instrumentation and control systems

The JRTR main control room (MCR) and supplementary control room (SCR) are facilitated with workstations. Figure 1 shows the layout of MCR where the operators start up, control and shut down the reactor via soft-control interfaces while they are sitting at the workstations. When the MCR is not available, the operators can quickly move to the SCR and safely maintain the reactor. The manual reactor trip switches are installed on the reactor protection system cabinets in the MCR and on the manual trip switch panels (MTSP) in the SCR.

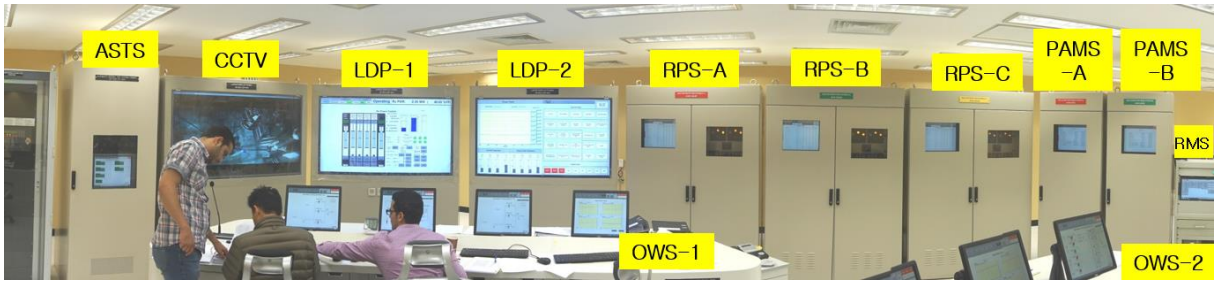

Figure 1. Panoramic view of JRTR main control room

Figure 2 shows the overall architecture of digitalized I&C systems. The "(S)" in Figure 2 marks the safety system and the "(NS)" marks the non-safety system. The reactor protection system (RPS), consisting of three Triconex™ redundant systems, automatically shuts the reactor down by cutting off electrical power to the control absorber rods (CARs) and second shutdown rods (SSRs) and actuates engineered safety features (ESFs) using a two-out-of-three voting logic when one of design bases events (DBEs) occurs. The RPS provides manual switches for reactor trips and ESF actuations. The RPS sends safety field signal values to the information processing system (IPS) via dual one-way fiber-optic data links. There are three redundant MTSPs in the SCR for the manual reactor shutdown. The post-accident monitoring system (PAMS), consisting of two Triconex™ redundant systems, displays safety field signal values not only during normal operations but also after DBEs. The PAMS also sends safety field signal values to the IPS via dual one-way fiber-optic data links. The automatic seismic trip system (ASTS), manufactured by Woori Technology™, automatically shuts the reactor down using a two-out-of-four voting logic when an operating basis earthquake occurs. The ASTS also stores field signal values and alerts the operators when an earthquake occurs. The information processing system (IPS), consisting of primary and secondary HP™ servers, acquires most of the field signal values from other I&C systems via redundant integrated monitoring and control networks (IMCNs), displays them on the operator workstations (OWSs) and large display panels (LDPs), and alerts the operators when an abnormal state occurs. The IPS stores the values and retrieves historical data. The alternate protection system (APS), consisting of two RTP™ redundant systems, automatically shuts the reactor down by cutting off electrical power to the CARs and SSRs and actuates ESFs using two-out-of-two voting logic when the RPS is not available while DBEs occur. The reactor regulating system (RRS), consisting of primary and secondary RTP™ processors, calculates the current reactor power and controls the reactivity as per the operator's demand by sending commands to the CAR stepping motors. The process instrumentation and control system (PICS), consisting of primary and secondary RTP™ processors, acquires process instrument signals and sends them to the IPS and RRS. The PICS also sends the operator's command from the OWS to the pumps and valves. The radiation monitoring system (RMS), manufactured by APANTEC™, monitors, stores and retrieves the overall radiation level inside and outside the JRTR site.

Figure 3 shows the defence-in-depth design concept of the I&C systems. In the 1st barrier, the RRS either automatically controls the reactivity in a safe state or sets the reactor power back to zero when an abnormal case occurs. The operator can manually control the reactor power through the OWS and RRS. He also can run and stop pumps and valves through the OWS and PICS. In the 2nd barrier, the RPS automatically shuts the reactor down and actuates ESFs when one of DBEs occurs. In the 3rd barrier, the APS automatically shuts the reactor down and

actuates ESFs when common mode failures occur in the RPS during the occurrence of DBE. The ASTS shuts the reactor down when the OBE occurs. In the 4th barrier, the operator can manually shut the reactor down and actuate ESFs in order to block the release of radioactive material to the public. The operator can continuously monitor the safety parameters through the PAMS until the accident is mitigated. The I&C systems support the emergency responses.

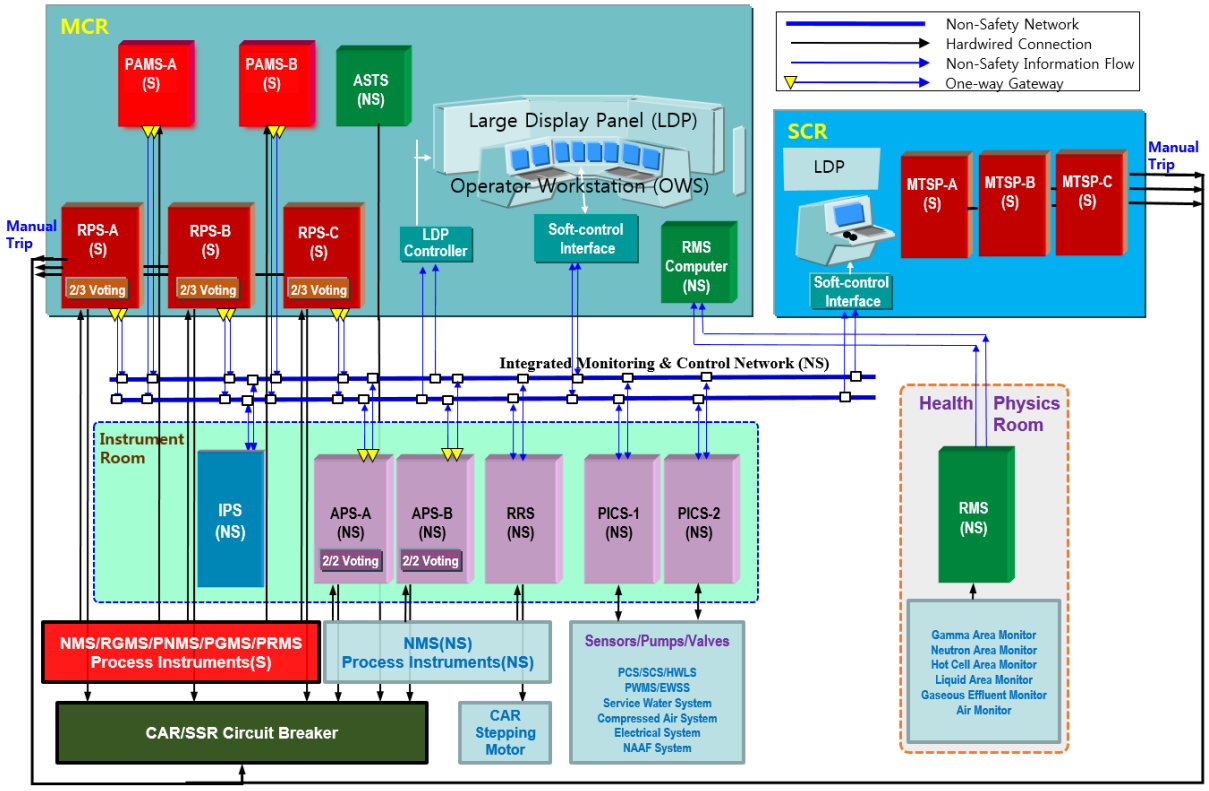

Figure 2. Overall architecture of I&C systems

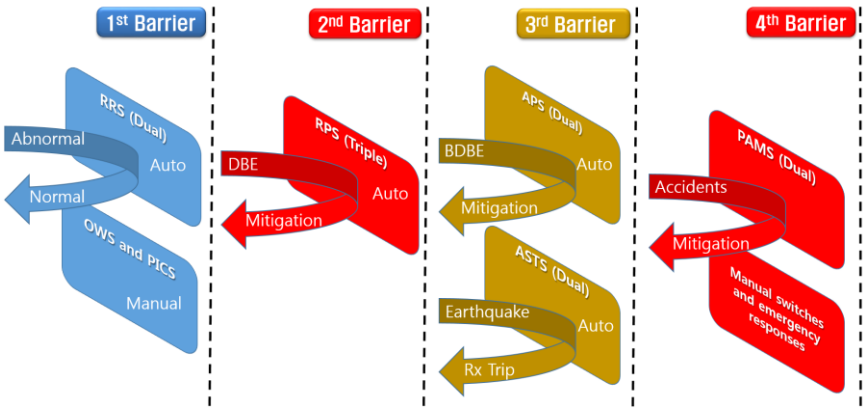

Figure 3. Defence-in-depth of I&C systems

3. Maintaining data communications

The IPS maintains the dual networks (i.e., data communications) of I&C systems, called integrated monitoring and control network (IMCN), as shown in Figure 4. The IPS uses Ethernet and TCP/IP protocol for two-way and UDP/IP for one-way data communications. During normal operation, the IPS shows network statuses in green colour in the system status overview display. When an abnormal case occurs as shown in Figure 4, the audible and visual

alarm functions alert the operators through the alarm list display. Although the operators see the status overview display that indicates abnormal components in red colour, they may not usually find the root cause of the abnormal case because many computers are connected and the operation mechanisms of hardware and software are complicated. The maintenance engineer comes to the MCR and finds the root cause by using a “ping” MS-DOS command that can directly check the network connectivity. However, it can be blocked by a firewall that is set up in the computers to block primitive access by the “ping” command to the networks. The parameters in MS-Windows for enabling the firewall are so complicated that the technician may not be able to change the parameters. For example, it should be set up with respect to private/public, inbound/outbound, and default/advanced settings in MS-Windows. There can be a conflict between the firewall of MS-Windows and an anti-virus program. The anti-virus program was not installed at the installation stage but was installed after the commission stage in JRTR because cyber security policies are adopted to the JRTR project later. A freeware anti-virus program called AVAST was first installed. Later, a commercial version called KASPERSKY replaced it. During this replacement, the configuration control was not carefully managed. For example, AVAST was not perfectly replaced with KASPERSKY over all the computers. When the anti-virus programs such as AVAST (freeware) and KASPERSKY (commercial version) are installed in a computer, it may block the incoming stream so that the “ping” command does not work. In this case, we should enable “Incoming ICMP stream” in the firewall of MS-Windows and the anti-virus program.
In conclusion, the firewall function in a computer should be carefully managed under the configuration control. We learned the following to diagnose and prevent these failures:

1) Check the cables and connectors with respect to bending, dust, light blinking, etc.
2) Check the correctness of IP addresses in the host file of each computers
3) Check the network configuration such as network speed, redundancy, and incoming and outgoing data streams
4) Check the firewall configuration such as inbound and outbound rules in the operating system, graphic tool, and the anti-virus program
5) Check the software version consistency of the operating system, graphic tool, and anti-virus program
6) Periodically reboot the IPS every six months
7) Manage configuration control of the operating system, graphic tool, and anti-virus program

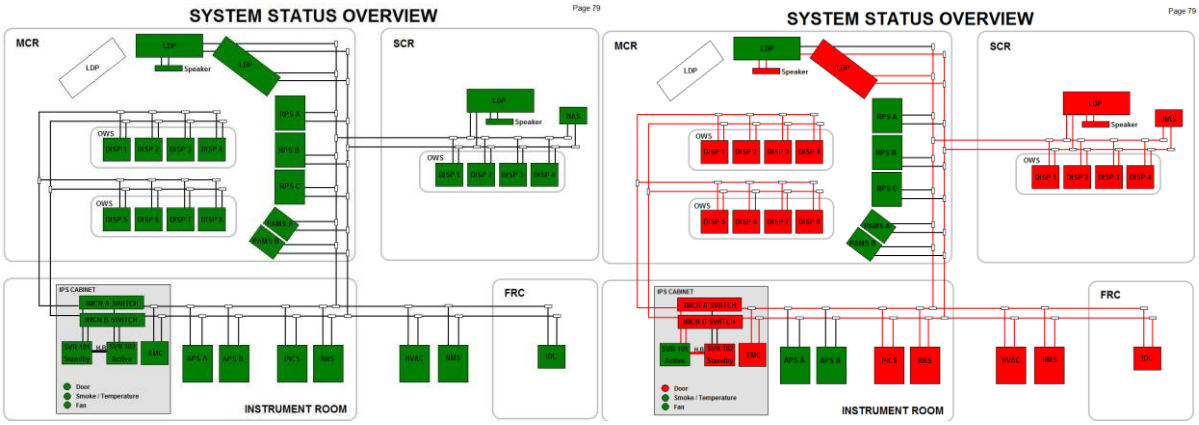

(Displaying normal status) (Displaying abnormal status)

Figure 4. System status overview displays

4. Maintaining neutronic detector signal processors

There are two manufacturers for neutronic detector signal processors: MIRRION and APANTEC. The company MIRRION manufactured and supplied six neutron measurement systems (NMSs) and three reactor gamma measurement systems (RGMSs). The company APANTEC manufactured and supplied three primary cooling system (PCS) gamma measurement systems (PGMSs), three PCS neutron measurement systems (PNMSs), and three pool-top surface radiation measurement systems (PRMSs).

The NMS consists of wide range guarded fission chambers as detectors and digital DGK250 and DWK250 as signal processors. The DGK250 sends 0 ~ 150 % full power (%FP unit) of neutron flux levels to the RPS by 4 ~ 20 mA in a linear electrical scale within 50 ms. This makes the RPS shut the reactor down promptly when it exceeds 10.5 %FP at a low power range and 115 %FP at a high power range. When the power reaches 10 %FP during start-up operation, the operator bypasses the 10.5 %FP trip setpoint in order to increase the reactor power to 100 %FP. The DWK250 sends -15 ~ 15 log rate (%FP/s unit) to the RPS by 4 ~ 20 mA in a linear electrical scale within 1 second. This makes the RPS shut the reactor down when it exceeds 8 %FP/s. The DWK250 sends 1E-8 ~ 150 %FP of log power to the RPS by 4 ~ 20 mA in a linear electrical scale within 1 second. The RPS does not use the log power for the reactor trip but for monitoring the reactor power. During the reactor start-up operation, the log rate trip by RPS channel A occurred as shown in the blue circle of Figure 5. This happened several times infrequently only in RPS channel A since early 2017. The root cause of the trip was not clearly identified because the log rates of RPS channel B and C were normal. It is suspected that unknown noises occurred near the DWK250 which were suddenly added to the normal log power signal so that the log rate increased above 8 %FP/s. The DWK250 generates the log rate using two low pass filters. The noise filtering capability can be promoted by increasing the Tau value in the filters. When MIRRION engineers came to the JRTR site for inspecting the causes of the trip, they recommended increasing the Tau value [2]. However, JRTR engineers did not have much knowledge about the Tau value increment and worried about the impact on the response time of the log rate trip. MIRRION engineers increased the Tau value by 1 second without impacting the response time and promoted the noise filtering capability because the increment impacted the processing time on the low range of neutron flux. It took too much time and cost to solve the log rate trip problem because the JRTR engineers were not fully educated to adjust the Tau value.

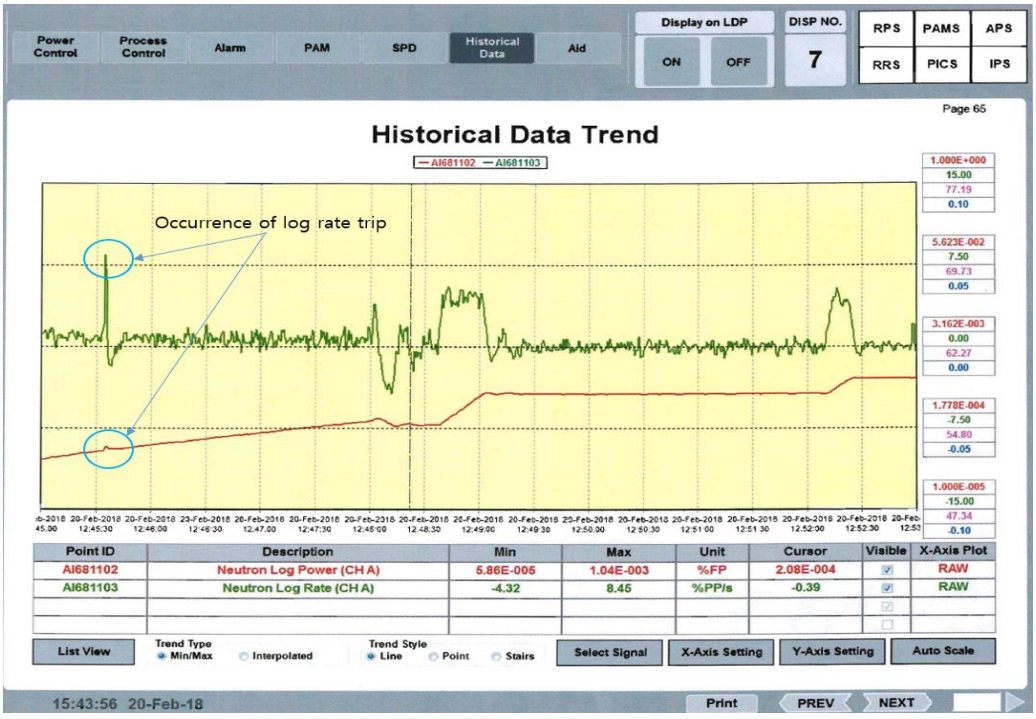

Figure 5. Log rate trip of NMS channel A

The PGMS consisting of gamma ion chambers as detectors and digital RM1Ws as signal processors that are installed near the reactor outlet PCS pipe, measures gamma level whose major source is N-16 during high power operation. It measures 1.0 ~ 1.0E6 μGy/h in a logarithmic scale. The PGMS converts the gamma level from 0 to 150 % full power and sends it to the RPS by 4 ~ 20 mA in a linear electrical scale within 30 seconds. The RPS shuts the reactor down when it exceeds 110 %FP. When the PGMS channel calibration test is performed, the input frequency, i.e., counts per second (CPS unit), is inserted as a test input value as shown in Table 1 [3]. The input frequency is divided by the scale factor (SF) which was changed according to the reactor power alignment. If the calculation method of SF is not explained well, the tester may make a mistake by inserting a wrong CPS during the test. For example, supposing the tester wants to test 37.5 %FP, i.e., 8 mA, he must know how to calculate the SF in Table 1. For this, the tester first converts the % full power to the gamma level using the %FP scale factor (%FP SF) that was determined during the reactor power alignment based on the thermal power [4]. The %FP SF is calculated by using the equation (1).

$$\%FP\ SF_{new} = \%FP\ SF_{old} \times \frac{Average\ of\ thermal\ powers}{Average\ of\ current\ neutron\ powers} \quad (1)$$

Supposing the %FP SF is 1.31E-3 %FP/μGy/h as shown in Figure 6, the gamma level 2.86E4 μGy/h is achieved by dividing the 37.5 %FP by 1.31E-3 %FP/μGy/h, which means that 2.86E4 μGy/h is equal to 37.5 %FP under the existing reactor power alignment. In order to convert the scaled gamma level to a frequency for the test, the gain, i.e., conversion factor from the frequency to gamma level is needed. However, the gain was not documented well in APANTEC documents, but explained via emails from APANTEC. There were two gains in the PGMS: 0.5 μGy/h/cps at a low gamma level and 50 μGy/h/cps at a high gamma level. Furthermore, there were two thresholds in the PGMS for switching over between a high and low gamma level: 2E4 μGy/h for low to high gamma levels and 1E4 μGy/h for high to low. The scaled gamma level 2.86E4 μGy/h is in a high level so that it can be converted to 572 CPS by dividing 2.86E4 μGy/h by 50 μGy/h/cps. There is one more important information: when switching over from low to high gamma levels, the tester should first insert the frequency representing the threshold for switching from low to high gamma levels. In other words, the tester should first insert 4E4 CPS by dividing 2E4 μGy/h by 0.5 μGy/h/cps to make the PGMS acknowledge the switch over from low to high gamma levels. Then the tester can insert the 572 CPS for testing the 37.5 %FP. This information was very important for the tester but not well documented. We learned the following to diagnose and prevent these failures:

1) Maintenance engineers should be fully trained and educated to manage the detectors and signal processors.
2) Maintenance engineers should be involved in the factory and site acceptance testing with the manufactures.
3) The maintenance work depends heavily on the manufacturer's fidelity.
4) The detectors and signal processors are sensitive to electrical noises.

Input frequency(cps)	Expected Reading (%FP)	Actual Reading (± 1%)	Expected Analog Output (mA)	Actual Analog Output (± 1%)
1/SF	0		4	
5,000/SF	37.5		8	
7,500/SF	75		12	
15,000/SF	112.5		16	
20,000/SF	150		20	

Note) Input frequency depends on given scale factor (SF) of a channel.
Table 1. PGMS channel calibration test sheet

Figure 6. PGMS %FP scale factor

It is not easy to measure the low range of neutron flux because its signal is prone to fluctuate in the range. Thus, the effective low range of the neutron flux should be evaluated with safety analysis engineers.

5. Conclusions

Even after the commissioning stage of a research reactor is completed, it takes at least one and half years to make digital-based I&C systems stabilized because of their complex connectivity among computers and software update requirements after the commissioning. There were some abnormal cases in data communications and neutronic devices in the digital I&C systems of JRTR after the commissioning. It was hard to find a root cause of the abnormal status in the data communications combined with anti-virus programs. The neutronic detectors and signal processors are sensitive to electrical noises at a low range of neutron flux. While fixing the abnormal cases, we learned that the maintenance engineer should participate in the manufacturer's testing in a factory and site and be well educated, equipment technical specification should be well documented, and configuration control should be well managed.

6. References

[1] Soo-Youl Oh, et. al, Completion of Jordan Research and Training Reactor Construction Project, 18th IGORR Conference 2017, Sydney, Australia.
[2] JR-681-MR-443-660, On-Site report Nov 17-Troubleshooting, MIRRION, Nov. 10, 2017.
[3] JR-ROP-SI-028, Channel Calibration for PGMS, Jordan Atomic Energy Commission, Dec. 13, 2016.
[4] JR-ROP-SI-008, Full Power Alignment, Jordan Atomic Energy Commission, Nov. 18, 2016.

LICENSING PROCESS OF JORDAN RESEARCH AND TRAINING REACTOR- LESSONS LEARNED: A REGULATOR'S PERSPECTIVE

B. G. ALMOMANI
Nuclear Safety Directorate, Energy and Mineral Regulatory Commission
Al-Bayader Street, Postal Code 11821 Amman – Jordan

ABSTRACT

Jordan Research and Training Reactor (JRTR) is the first nuclear reactor in Jordan imported from the Republic of Korea. Jordan's Energy and Minerals Regulatory Commission (EMRC), as a successor to Jordan Nuclear Regulatory Commission (JNRC), issued a Construction Permit (CP) on Aug. 15, 2013 and an Operating License (OL) for 10 years on Nov. 13, 2017 for JRTR that is owned and managed by the Jordan Atomic Energy Commission (JAEC). As licensing of the JRTR is a first experience for EMRC; the EMRC faced some challenges during the licensing process. Thus, this paper discusses the Jordanian regulatory framework, the experience from the JRTR licensing process, and lessons learned from the JRTR project that would be taken into account in future similar projects.

1. Introduction

The construction of Jordan Research and Training Reactor (JRTR) started on Nov. 2010 and was completed in six years. It was built at Jordan University of Science and Technology (JUST) located in the city of Irbid, 70 Km north of Jordan capital city. The Jordan Atomic Energy Commission (JAEC) signed Engineering, Procurement and Construction (EPC) turnkey contract on March 30, 2010 with Korea Atomic Energy Research Institute (KAERI) and DAEOOW Engineering and Construction Company (KAERI/Daewoo Consortium (KDC)) as a winner for designing, constructing and commissioning the first nuclear reaction in Jordan. The JRTR designed to serve as an integral part of the nuclear technology infrastructure in Jordan which encompasses a training canter to support the education and training future engineers and scientists. It also houses a radioactive waste treatment facility (RTF) for ensuring the safe conditioning and storage of radioactive waste.

Jordan's Energy and Minerals Regulatory Commission (EMRC) is the regulatory authority to regulate safe use of the energy sectors including electricity, renewable energy, nuclear energy, petroleum, and natural resources through legislation, review, inspection and licensing for protection of human and environment. For the JRTR project, the EMRC played an indispensable role in ensuring the safety regulations throughout the reactor development phase were being upheld by performing inspections, design reviews, monitoring the testing of the reactor construction materials, and systems performance that have been contributed to upholding and ensuring that the highest international safety standards are met.

As licensing of the JRTR is a first experience for EMRC; the EMRC faced some challenges during the licensing process. Thus, this paper discusses the Jordanian regulatory framework, the experience from the JRTR licensing process, and lessons learned from the JRTR project that would be taken into consideration in future similar projects.

2. Description of JRTR

The JRTR is a 5-MWt power open-in-tank-pool multi-purpose reactor cooled and moderated by light water, as well as heavy water and beryllium are used as neutron reflectors. Figure 1 illustrates the reactor assembly submerged in the reactor pool. This modern reactor aims to enhance the knowledge of nuclear and radiation technology in Jordan via the following services: education and training future engineers and scientists, radioisotope production (RIP) (e.g., Mo-99, I-131, Ir-192, etc.) for radio-pharmaceuticals and nuclear medicine applications, and neutron activation and neutron beam services for scientific and industrial use including non-destructive testing, neutron radiography, neutron diffraction, and scattering experiments [1]. In addition, several future applications are possible such as production of other radioisotopes, gemstone colouring (topaz production), cold neutron source, and neutron transmutation doping (NTD) of Silicon to enter the semiconductor research as well as to produce material for high quality semiconductor power devices with its neutron activation analysis [2]. The JRTR is equipped to aid researchers in deciphering and unlocking fine details as forefront nuclear research in Jordan and the Middle East region.

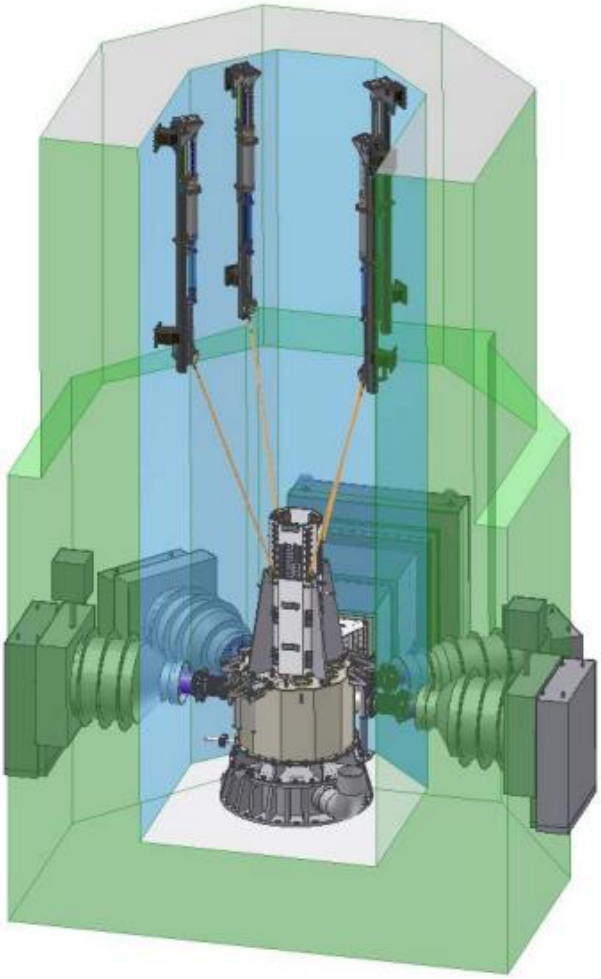

Fig. 1 Arrangement of reactor assembly, beam ports, and thermal column. [3]

The JRTR operate in two modes; training mode at low power of 50-KWt where the reactor is cooled by natural convection, and power mode at full power of 5-MWt where the reactor is cooled by forced convection using primary cooling pumps. The JRTR is operated on a very limited schedule and have a very small amount of radioactive material. Therefore, the EMRC has referred to the process of graded approach described by IAEA [4] in order to reasonably define the level of analysis, documentation and actions necessary to fulfil the safety requirements and criteria.

3. Regulatory Authority of Jordan

Jordan Nuclear Regulatory Commission (JNRC) and JAEC were established in 2007 as successors to the former Jordan Nuclear Energy Commission (JNEC), established in 2001. The Jordan's regulatory bodies including the JNRC, Electricity Regulatory Commission (ERC), and Natural Resources Authority (NRA) in relation to its regulatory tasks were merged into the EMRC in April 2014, to strengthen Jordan's radiation and nuclear regulatory infrastructure by providing more resources and influence [5]. The EMRC is adequately empowered as an administratively and financially autonomous regulatory body; the organizational chart of EMRC is illustrated in Fig. 2.

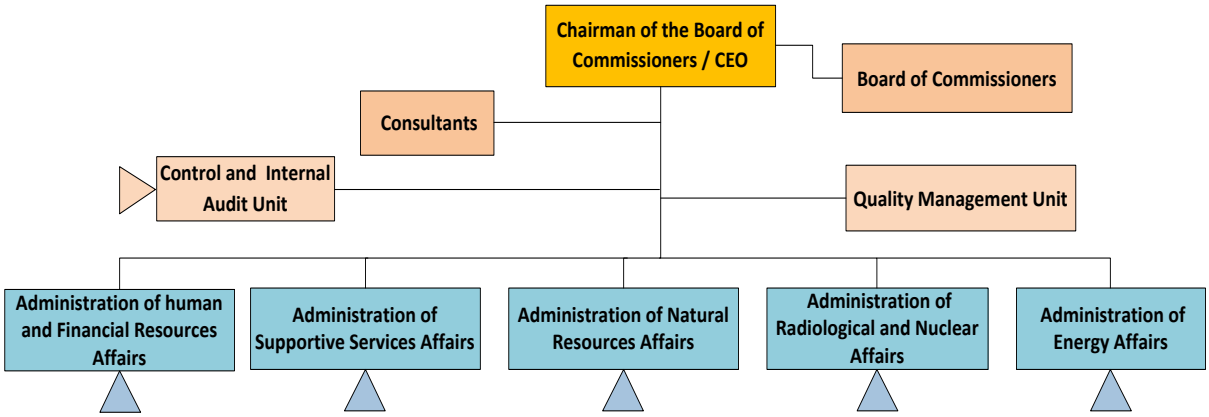

Fig. 2 EMRC organizational chart

The administration of radiological and nuclear affairs in EMRC is mainly responsible for preparing laws, regulations and instructions for nuclear installations and facilities, radioactive materials, and workers based on the principles and the requirements of safety, security, emergency and safeguards published by International Atomic Energy Agency (IAEA) and best international practices to control the safe use if nuclear energy in Jordan. In addition, EMRC reviews and evaluates the safety documents of nuclear installations and facilities, as well as carries out the tasks of field inspection through a qualified and trained inspection teams and enforcement through a systematic licensing process. The sub-organizational chart for the administration of radiological and nuclear affairs is illustrated in Fig. 3.

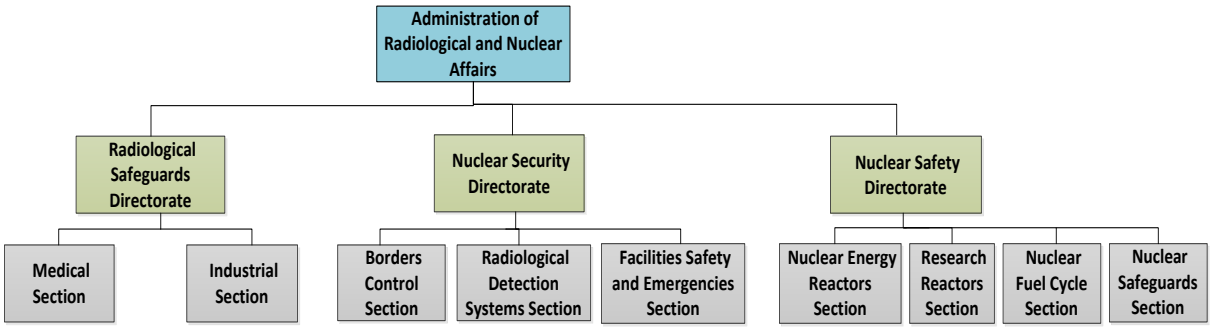

Fig. 3 Administration of radiological and nuclear affairs organizational chart

4. Experience on JRTR Licensing

4.1. Licensing Process

According to the project contract between JAEC and KDC, the JRTR design complies with the available Jordanian laws and regulations, Korean regulation and guidelines, IAEA safety standards, and internationally applicable industrial codes and standards. The licensing

procedure of the JRTR follows the licensing regime consistent with the proposed technology's country of origin, the Republic of Korea. Two-step licensing scheme, Construction Permit (CP) and Operating License (OL) are adopted for the JRTR project. While, the EMRC issued temporal permits such as a Limited Work Authorization (LWA) for excavation of the site before the CP issued. This practice helped the work progress; however, the supplier is responsible for suitability of the excavated site and the costs incurred [7].

Owing to insufficient regulatory infrastructure in Jordan, EMRC signed a cooperation agreement with Korea Institute of Nuclear Safety (KINS) in 2011, Korean's technical regulatory body, in order to have a support in performing the procedures of permitting, reviewing and approving JAEC's construction and operation of the JRTR. EMRC/JNRC-KINS bilateral cooperation covered most of the necessary aspects of the licensing stages such as site safety review, construction permit review, operation license review, pre-operational inspection (POI), quality assurance inspection (QAI), as well as EMRC's staff education and training for JRTR [6]. Therefore, the main dependence for the licensing process of the JRTR comes as a partnership between EMRC and KINS. Nevertheless, JAEC received technical support from international organizations such as IAEA, NucAdvisor, and French Alternative Energies and Atomic Energy Commission (CEA). They have reviewed the CP documents and proposed some recommendations and suggestions regarding the JRTR design. On the other hand, EMRC consulted US advisory body (AdSTM), US-NRC, and IAEA to provide technical assistance for the purpose of reviewing, evaluating and analysing the reactor safety documents as well as carrying out inspection tasks during the construction process to verify compliance with applicable legislation, requirements and special conditions for the CP and OL. The CP of JRTR was issued on Aug. 15, 2013, and the OL was issued on Nov. 13, 2017 in accordance to the IAEA's standards and requirements, the requirements of US-NRC, and the requirements of KINS. The application documents of CP and OL have been reviewed through the same process. JRTR safety is considered by lines of defence, incidental and accidental events, classification of structure, systems and components (SSCs), as well as the operability. Figure 4 illustrations the parties who involved in the joint project for JRTR licensing.

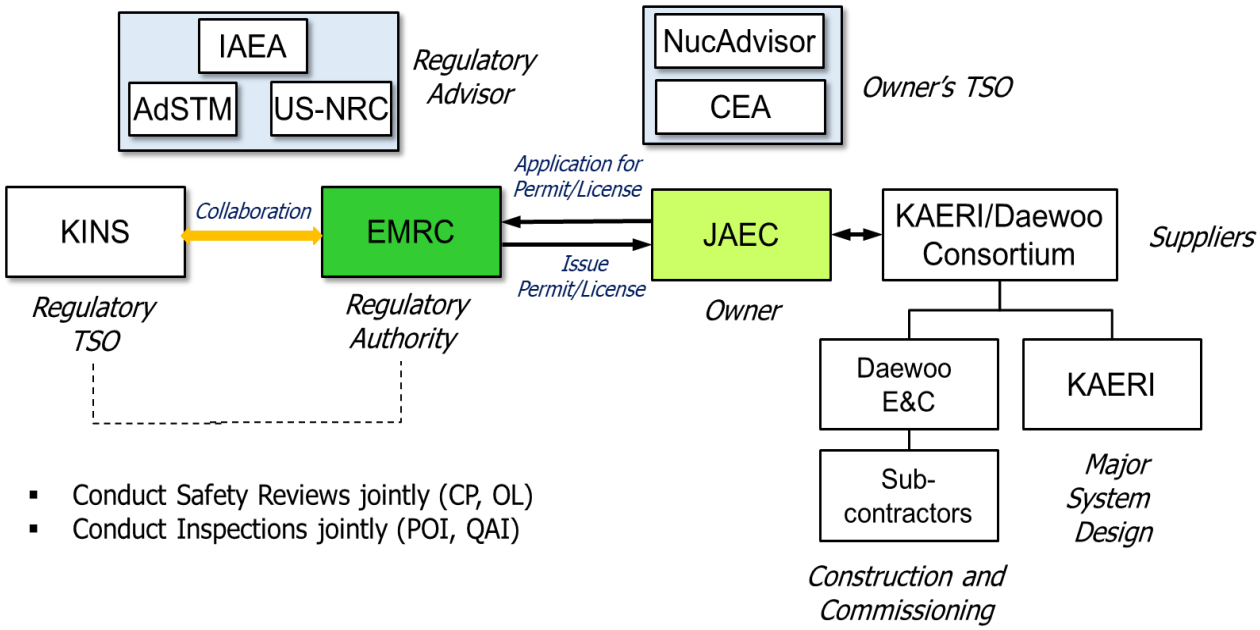

Fig. 4 Joint project for JRTR licensing

4.2. CP Licensing

The EMRC reviewed and evaluated the documents submitted from JAEC on July 2011 for the purpose of issuing the CP and to verify that the licensee follows the highest standards of safety in the design, construction, assembly, analysis, operation, etc. The EMRC reviewed mainly the following documents submitted:

a) Preliminary safety review report (PSAR).
b) Radiation environment report (RER).
c) Quality insurance manual (QIM), extended document for chapter 18 in the PSAR.
d) Description of the construction capability and purpose of the facility.

PSAR and RER reports consist of 20 and 9 chapters, receptively. Table 1 displays the topic of chapters in the PSAR and RER reports that have been reviewed by EMRC & KINS reviewers.

Tab 1: List of chapters in PSAR and RER reports

Preliminary Safety Analysis Report (PSAR)	Radiation Environmental Report (RER)
Chapter 1. Introduction and General Description of Jordan Research and Training Reactor.	Chapter 1. Overview of Construction Plan.
Chapter 2. Safety Objectives and Engineering Design Requirements.	Chapter 2. Status of Environment.
Chapter 3. Site Characteristics.	Chapter 3. Status of JRTR.
Chapter 4. Buildings and Structures.	Chapter 4. Impact Due to Construction.
Chapter 5. Reactor.	Chapter 5. Impact Due to Operation.
Chapter 6. Reactor Cooling and Connected Systems.	Chapter 6. Impact Due to Accidents.
Chapter 7. Engineered Safety Features.	Chapter 7. Environmental Radiation Monitoring Program.
Chapter 8. Instrumentation and Control.	Chapter 8. Comprehensive Assessment.
Chapter 9. Electric System.	Chapter 9. Others.
Chapter 10. Auxiliary Systems.	
Chapter 11. Reactor Utilization.	
Chapter 12. Operational Radiological Safety.	
Chapter 13. Conduct of Operations.	
Chapter 14. Environmental Assessment.	
Chapter 15. Commissioning.	
Chapter 16. Safety Analysis.	
Chapter 17. Operational Limits and Conditions.	
Chapter 18. Quality Assurance.	
Chapter 19. Decommissioning.	
Chapter 20. Emergency Planning and Preparedness.	

With close collaboration between the EMRC and KINS reviewers, they raised around 777 request of additional information (RAIs) during three rounds for the PSAR report as shown in Fig. 5, and 92 RAIs for the RER report as shown in Fig. 6. Since the reviewers are mainly focusing on evaluating of possible internal and external accidents with any environmental pollution caused by radioactive leakage as well as the design features to prevent the occurrence of such incidents or to mitigate them and treat their effects, extensive RAIs were raised especially in Ch. 3-Site Characteristic, Ch. 5-Reactor, and Ch. 16-Safety Analysis. The top tier references for safety review are US–NRC report NUREG-1537 Part 1 [8], and the following IAEA safety standards: NS-R-3 [9], NS-R-4 [10], and SSG-20 [11]. The raised RAIs are based on compliance with requirements such regulations, guides, and codes/standards, or supplementary information to provide adequate description, drawing, and references. On Aug. 2013, EMRC issued a conditional CP with 36 conditions to be fulfilled in order to obtain the full permit which it was closed on Dec. 2015.

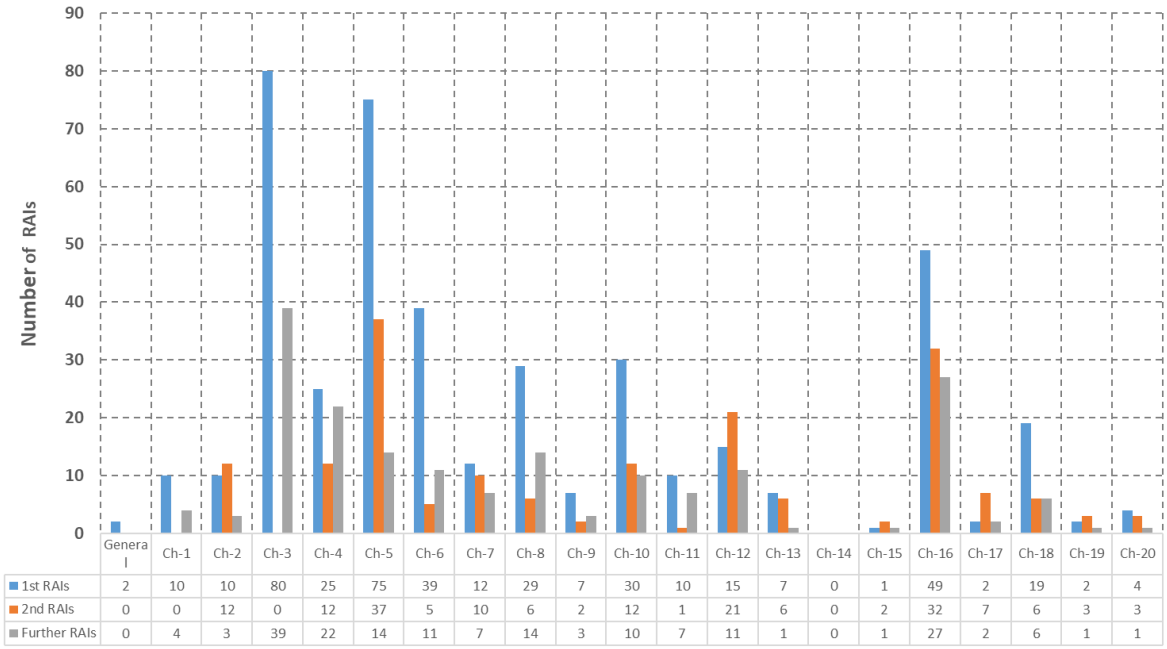

	General	Ch-1	Ch-2	Ch-3	Ch-4	Ch-5	Ch-6	Ch-7	Ch-8	Ch-9	Ch-10	Ch-11	Ch-12	Ch-13	Ch-14	Ch-15	Ch-16	Ch-17	Ch-18	Ch-19	Ch-20
1st RAIs	2	10	10	80	25	75	39	12	29	7	30	10	15	7	0	1	49	2	19	2	4
2nd RAIs	0	0	12	0	12	37	5	10	6	2	12	1	21	6	0	2	32	7	6	3	3
Further RAIs	0	4	3	39	22	14	11	7	14	3	10	7	11	1	0	1	27	2	6	1	1

Fig. 5. Request for Additional Information (RAIs) for the PSAR report during the CP stage

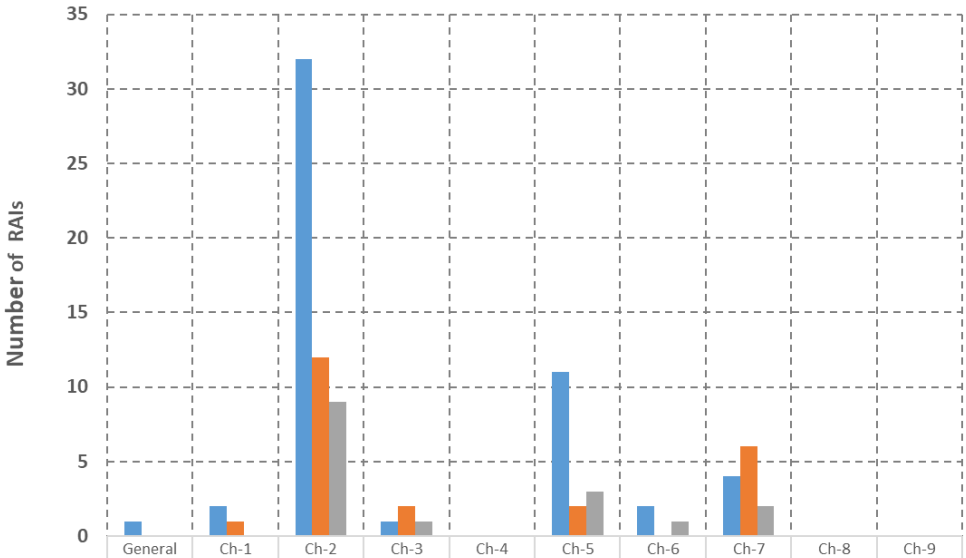

	General	Ch-1	Ch-2	Ch-3	Ch-4	Ch-5	Ch-6	Ch-7	Ch-8	Ch-9
1st RAIs	1	2	32	1	0	11	2	4	0	0
2nd RAIs	0	1	12	2	0	2	0	6	0	0
Further RAIs	0	0	9	1	0	3	1	2	0	0

Fig. 6. Request for Additional Information (RAIs) for the RER report during the CP stage

4.3. OL Licensing

After completion of the construction phase, the JRTR started the non-nuclear commissioning stage in 2015 and nuclear fuel loading in April 2016 after getting the permit from the EMRC. The reactor underwent a series of performance tests as part of hot commissioning phase demonstrating passive design features. These tests proved that the reactor is correctly installed and would be brought to a safe shutdown without the need for any active intervention. Besides, JAEC submitted the application for OL on 15 Dec. 2014 with further updatable documents and information supporting the OL application as follows:

a. Final Safety Review Report (FSAR).
b. Radiation Environment Report (RER).

c. Environmental Impact Assessment (EIA).
d. Quality Assurance Program (QAP).
e. Operational Technical Specification (OTS).
f. Operation Limits and Conditions (OLCs).
g. Others (Radiation Emergency Plan (REP), Maintenance and Periodic Testing Program (MPT), Radiation Protection Program (RP), Radioactive Waste Management Program (RWM), Security Plan, and Decommissioning Plan).

EMRC also reviewed and evaluated the reports of incidents or accidents that may occur in nuclear facilities in order to guarantee the sustainability of the safety of JRTR for continues operation. In this stage, reviewers raised around 218 RAIs in three rounds from the FSAR report as shown in Fig. 7, 24 RAIs for the RER report as shown in Fig. 8, and only 7 RAIs for the OTS report. In addition, the individuals who are the operators of the research reactor have been authorized through conducting theoretical and practical examinations and interviews to ensure the qualification and skills of the candidates. After passing the success mark for each part of the evaluation process, personal licenses are issued. Furthermore, the EMRC carried out inspection missions to ensure compliance of licensees with the applicable legislation and binding conditions, and to ensure the conformity of the information set out in the application for the license with the real situation. Therefore, POIs on structural area, functional tests, commissioning tests, and QAIs for main equipment and components were conducted by EMRC-KINS joint teams. In addition, EMRC assigned a resident site inspector at the JRTR facility that closely follows all construction activities including concrete pouring, welding activities, receipt of equipment etc. The resident inspector ensures generic compliance verification activities on-site and informs EMRC head office of the JRTR construction progress. In particular, the resident informs the reviewers/inspectors of any activities in their field of expertise to make sure that they can timely carry out inspections or reviews specific to their areas of expertise. The applied inspection criteria were based on regulation on technical standards, PSAR/FSAR reports, technical codes and standards, construction specifications, and work plan procedures.

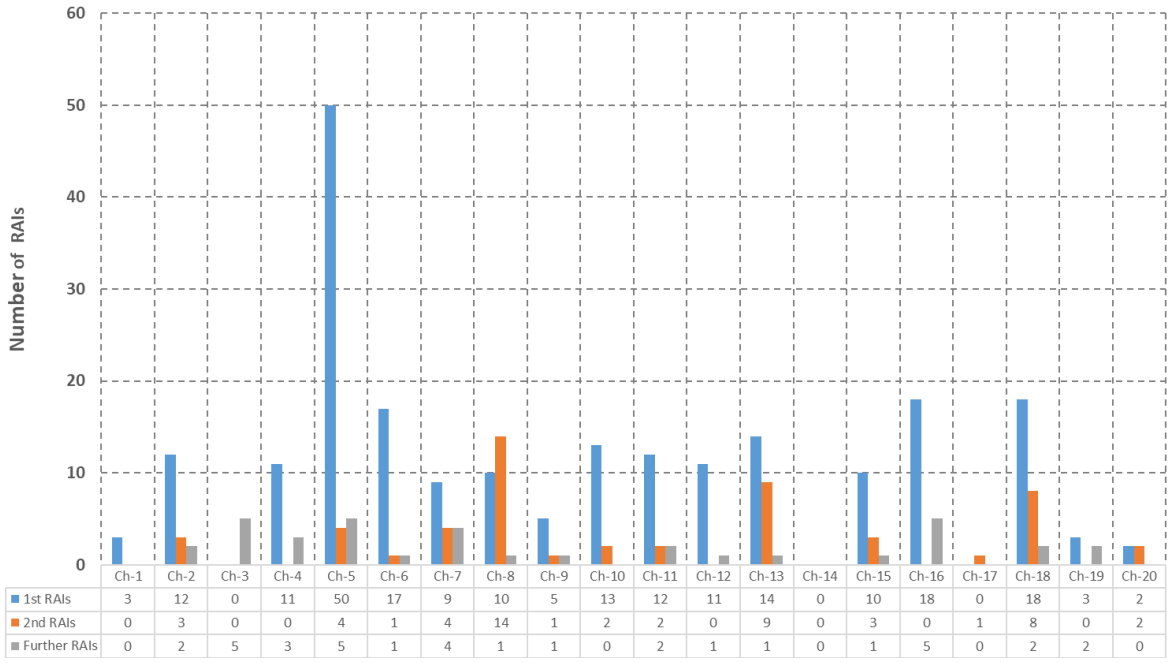

	Ch-1	Ch-2	Ch-3	Ch-4	Ch-5	Ch-6	Ch-7	Ch-8	Ch-9	Ch-10	Ch-11	Ch-12	Ch-13	Ch-14	Ch-15	Ch-16	Ch-17	Ch-18	Ch-19	Ch-20
1st RAIs	3	12	0	11	50	17	9	10	5	13	12	11	14	0	10	18	0	18	3	2
2nd RAIs	0	3	0	0	4	1	4	14	1	2	2	0	9	0	3	0	1	8	0	2
Further RAIs	0	2	5	3	5	1	4	1	1	0	2	1	1	0	1	5	0	2	2	0

Fig. 7. Request for Additional Information (RAIs) for FSAR report during the OL stage

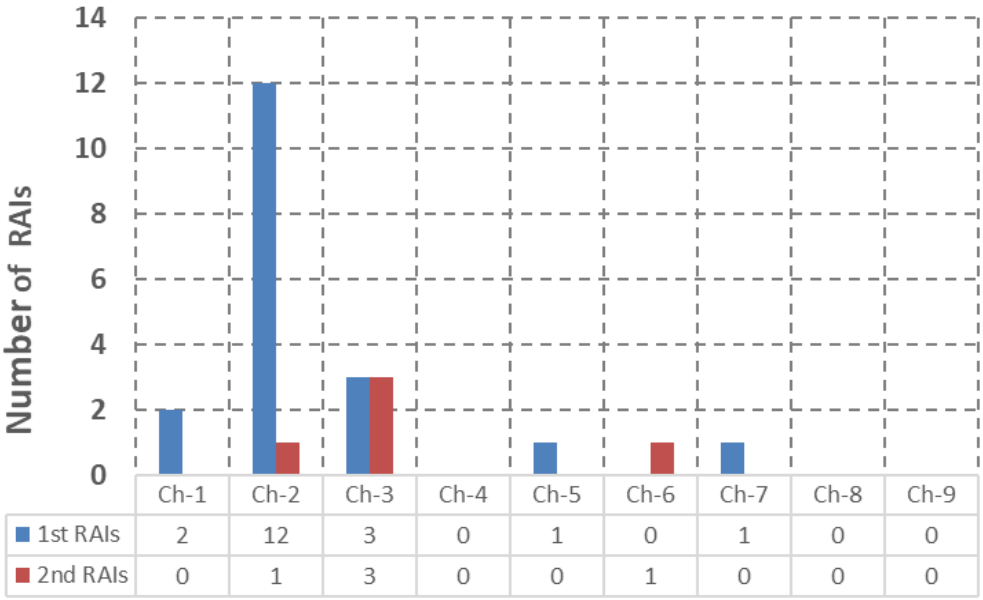

Fig. 8. Request for Additional Information (RAIs) for RER report during the OL stage

After the EMRC and KINS verified the information contained in the application for licensing through review, inspection and evaluation, and after all the requirements for personal and institutional licensing are fulfilled, the operation license for 10 years was issued on Nov. 13, 2017 in accordance with the terms and conditions.

5. Lesson Learned

One of the controversial issues that raised during the licensing process is the classification approach for SSCs. The safety classification of the JRTR follows the Korean and US classification system which based on ANSI/ANS-51.1 code [12]. The ANSI code classifies the SSCs as SC-1, 2, 3 and Non-Nuclear Safety (NNS). The SC-1 and 2 SSCs are only for pressure-retaining components, and are not applicable for the JRTR equipment. Therefore, codes and standards for design of the SSCs following the safety classification are selected in a graded approach. The JRTR's SSCs are classified only into two categories, SC-3 (important to safety) and NNS. NNS systems are divided into two subcategories, NNS with Quality Class T/Q (safety related system) and NNS with Quality Class S (not important to safety). Quality Class S is applied to general industrial equipment. Table 2 illustrates the interrelationships and the correspondences between safety classes and seismic categories, quality classes, and electrical classes.

Tab 2: Relationship between classes

Safety Class	Seismic Category	Quality Class	Electrical Class	Remarks
SC-1	I	Q	1E	Not applicable to JRTR
SC-2	I	Q	1E	
SC-3	I	Q	1E	Applicable to JRTR
NNS	I	T/Q	Non-1E	
NNS	II	T	Non-1E	
NNS	Non-seismic	T, S	Non-1E	

Since the JAEC and EMRC requested a technical support for safety evaluation by IAEA experts, some misunderstandings about the definitions of safety classifications between IAEA and KDC are raised. The IAEA's classification has three categories, safety system, safety-related system, and not important to safety. The point of the IAEA's recommendation is that some of NNS systems should be classified into safety–related system, not NNS. However, this is only a difference in classification terminology. After several hard discussions, a global agreement achieved between KDC and IAEA subject to clarifications in the presentation and wording of the classification principles and requirements associated with the different classes. It was technically clarified that the SC-3/Q is equivalent to safety system concept, while NNS/T/Q and NNS/S are equivalent to safety-related item concept and not important to safety concept, respectively; according to safety importance, design features, and nuclear environment.

For the JRTR project, a clearly-stated licensing process, legal basis, applicable standards, and guidelines on the contract conditions were stated. However, the stated legal basis and applicable standards, before signing the contract between the owner and supplier, should be discussed and agreed by the EMRC in order to select suitable foreign regulatory advisors and supporters and to avoid any misunderstanding that may cause a delay of the licensing period and project schedule. This teaches us that pre-understanding of the regulation basis by all the prospective parties is essential for a smooth project. In addition, the Korean suppliers have realized the important to propose a compromised safety classification approach of SSCs for research reactors where consensus with international standards in order to support their technology internationally [13], [14].

According to IAEA's Integrated Regulatory Review Service (IRRS) mission on 2014, the EMRC still needs to improve its regulatory infrastructure. Therefore, the EMRC determined to develop the necessary regulatory legal document relevant to research reactors and other facilities by issuing legally binding instructions pursuant to the Regulation on the Safe use of Nuclear Safety as shown in Fig 9. The issuance of legal documents follows a systematic approach outlined in the management system in accordance to its quality management manual. It is known that establishing a solid base of legal framework for prospective provision technology would eliminate the regulatory risks, i.e., changes in the safety standards and evaluations that can delay the plant construction and therefore increase the financial costs. As Jordan consider to import a small modular reactors (SMRs) instead of large reactors due to population and small grid problem, EMRC attempts to provide in advance a suitable legal documents compliance with international safety standards that fit the SMRs technology in order to avoid hurdles faced during the licensing process.

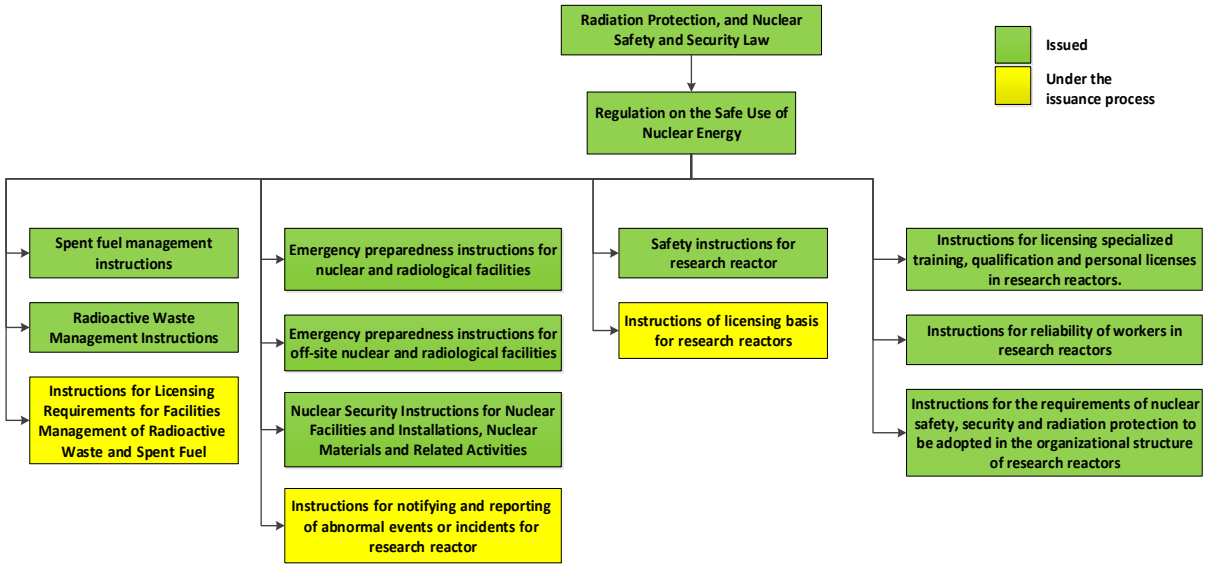

Fig. 9. EMRC relevant legal documents to research reactors

6. Conclusions

This paper briefly introduced the JRTR design and utilization, the nuclear legal framework of Jordan, and the JRTR licensing process. It is showed that the JRTR project gives a good licensing practice to EMRC. International cooperation for licensing the JRTR played a pivotal role in supporting the safe operation of JRTR. EMRC has gained a good experience from their peers in licensing the nuclear facilities through training for safety evaluation provided by international experts, review and consultation meetings, writing safety evaluation reports (SER), and conducting field inspections. The safety classification of SSCs for JRTR is discussed as an important raised issue during the evaluation process; establishing a harmonized global standard of SSCs classification for nuclear research reactors is necessary to aperient the nuclear technology trade and exchange. The major lesson during the licensing of such nuclear facility is that well-established regulatory standards and guidelines for a prospective nuclear project will help to avoid any unpredictable variables that may cause such difficulties and delay during the licensing progress. Nevertheless, a close collaboration and understanding between the regulator and applicant would help to save time and resources, reduce risk, and enhance stability and predictability.

7. Acknowledgement

The author of this paper would also like to express his sincere appreciation for Mr. Raed Al-Majali, Director of Nuclear Safety Directorate, and Mr. Mohammed Atiyat, Head of Research Reactors Section, from EMRC for providing the necessary information and documents to support this work.

8. References

[1] Mahmoud Suaifan, et. al, Status and Perspectives on the Utilization of a New Nuclear Research Reactor in Jordan, *Physica B: Condensed Matter* 551, 431-435, 2018.
[2] Official website of Jordan Research and Training Reactor (accessed 15.02.2019). http://jrtr.gov.jo/default.aspx.
[3] Ragai Altamimi, JRTR Project Overview and Licensing Processes, ANNuR/IAEA Annual Meeting on the Safety and Licensing of Research Reactors, 2016.
[4] IAEA, Safety Standards Series No. SSG-22: Use of a Graded Approach in the Application of the Safety Requirements for Research Reactors, IAEA, Vienna, Austria, 2012.
[5] Official website of Energy and Mineral Regulatory Commission (accessed 15.02.2019). http://www.emrc.gov.jo/index.php/en/.
[6] JNRC-KINS, Special Agreement for the Bilateral Cooperation on Construction and Operation Licensing on JRTR, 2011.
[7] Soo-Youl Oh, et. al, Completion of Jordan Research and Training Reactor Construction Project, 18th IGORR Conference, 2017.
[8] US-NRC. NUREG-1537-Guidelines for Preparing and Reviewing Applications for the Licensing of Non-Power Reactors, 1996.
[9] IAEA. NS-R-3-Site Evaluation for Nuclear Installations, 2016.
[10] IAEA. NS-R-4-Safety Requirements of Research Reactors, 2005.
[11] IAEA. SSG-20-Safety Assessment for Research Reactors and Preparation of the Safety Analysis Report, 2012.
[12] ANSI 51.1, Nuclear Safety Criteria for the Design of Stationary Pressurized Water Reactor Plants, 1983.
[13] Belal Al-Momani, and Jong Chull JO. Study on the Safety Classification Criteria of Mechanical Systems and Components for Open Pool-Type Research Reactors, 2013.
[14] Kim, Tae-Ryong. Safety Classification of Systems, Structures, and Components for Pool-Type Research Reactors, Nuclear Engineering and Technology 48, no. 4 1015-1021, 2016.

FEASIBILITY STUDY OF SUB-CRITICALITY MEASUREMENT USING MCNP6 IN ZERO POWER REACTOR AGN-201K

SUNGHO MOON, *SER GI HONG
Kyung Hee University, Department of Nuclear Engineering
1732 Deogyeong-daero, Giheung-gu, Yongin, Gyeonggi-do, 17104 – Korea
**Corresponding author : sergihong@khu.ac.kr*

ABSTRACT

In general, the reactor is designed to be conservatively maintain its sub-criticality under any conditions and it is very important to check the subcriticality. In particular, the accurate measurement of sub-criticality using detector signals from the reactor core is very helpful to safe operate experimental or research reactors. The noise analysis methods such as Rossi-alpha and Feynman-alpha methods have been popularly used to measure subcriticality of reactors. In this work, computational simulations of sub-criticality measurement using MCNP6 for several sub-critical conditions in AGN-201K which is unique zero power research and training reactor in our country are performed as a preliminary step to the real measurement. The comparison of the simulations with the ones obtained with MCNP6 eigenvalue calculations shows that the subcriticality measurement can be reasonably simulated with the MCNP6 and noise analysis methods.

1. Introduction

The sub-criticality of fissile assemblies for nuclear facilities is essential to safe processing, transportation, and storage operations for preventing criticality accidents. The assurance of sub-criticality requires the criticality safety assessment. As a lesson from the criticality accident, the importance of a continuous monitoring has been emerged. If the subcriticality of a nuclear reactor can be measured by using an ex-core detector's signal, excessive conservatism of the reactor can be eliminated, which enables economic and safe operation of nuclear facilities. Most of the studies measuring subcriticality has been based on the noise analysis methods such as Rossi-alpha and Feynman-alpha ones. However, it is quite difficult to accurately predict the sub-criticality condition of a reactor using a detector signal due to the fact that the detector signals are contaminated by electrical noises and the detector responses strongly depend on the detector characteristics and its position. So, the simulation of subcriticality measurement using Monte Carlo codes has been used as a preliminary step prior to the real measurement. In this study, two noise analysis methods (i.e., Rossi-alpha and Feynman-alpha methods) coupled with MCNP6 fixed source calculations are used to simulate the subcriticality measurement for AGN-201K which is a zero power research and training reactor operated by Kyung Hee university. This reactor was donated to Korea by the University of Colorado in 1976 and it is a solid-moderated reactor whose licensed maximum power is 10 Watt. In this study, we applied the weight window technique for reducing statistical errors of the detector signals generated by the MCNP6 fixed source calculations [8] and we analysed in detail the effect of the number of time shiftings for evaluating auto-correlations in Rossi-alpha method and the number of the time swaps for Feynman-alpha method. In Sec. 2, the Rossi- and Feynman-alpha methods are briefly reviewed while Sec. 3 describes the AGN-201K modelling and simulation procedures and Sec. 4 the simulation results. Finally, the summary and conclusions are given in Sec. 5.

2. Noise Analysis Method

Nosie analysis methods are based on the same basic premise that the properties of a subcritical system can be determined by measuring the fluctuations in the fission chain processes that depend on the stochastic nature of the birth and death of neutrons [7]. As shown in Fig. 1, neutron behaviour in the reactor follows a random branching process. When a neutron causes fission, the correlated neutron chain reaction occurs in a cascade. It is random that the reaction continues in this process, and each process proceeds in a branching process. The external source or fission neutrons undergo the process of scattering, fission, and absorption, and in the sub-critical system, neutrons eventually disappear because the probability of loss is greater than the probability of production. For illustration in Fig. 1, the left hand fission event during t_0 and t_0+dt_0 generates three neutrons and the event A represents a detector count during t_1 and t_1+dt_1 while the event B represents another detector count contributed from another neutron generated by the left hand fission event during t_0 and t_0+dt_0. The event A is correlated with the even B. On the other hand, the event C describes the uncorrelated event with the event A. So, if the time of the source event is measurable, the distribution of the times between the source event and the detection event would provide a direct indication of the dynamic properties of the subcritical system. In the same way, the distribution of the times between the various detection events would also provide the dynamic properties.

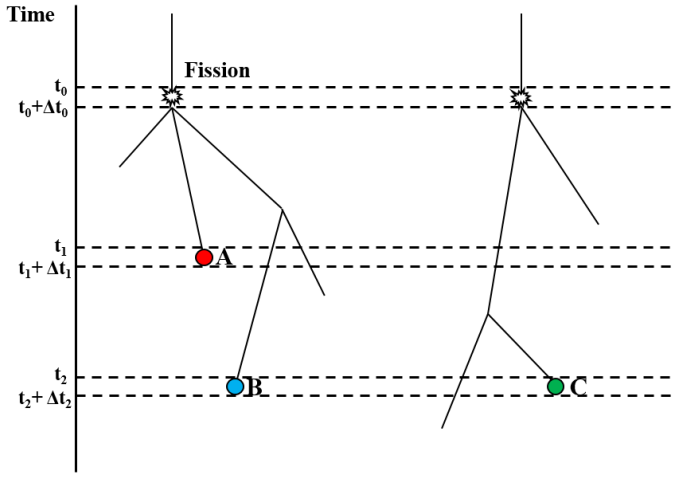

Fig. 1. Random branching process of fission neutron

2.1 Rossi-alpha method

The Rossi-alpha method can represent the fission decay process through the prompt neutron decay constant, α, using the auto-correlation of the count pairs of the detector [5]. As shown in Fig. 1. the probability of detecting two correlated neutron counts (i.e., the probabilities of detecting A, B neutrons associated with fission neutron at time $t_0 \sim t_0+\Delta t_0$) can be expressed as follows.

$$p_c(t_1,t_2)\Delta t_1\Delta t_2 = \int_{-\infty}^{t_1} p(t_1)\Delta t_1 p(t_2)\Delta t_2 F dt_0 = F\varepsilon^2 \frac{D_\nu(1-\beta)^2}{2(\beta-\rho)\Lambda} e^{-\alpha(t_2-t_1)}\Delta t_1\Delta t_2 \qquad (1)$$

where F is the average fission rate, ε is the detector efficiency, Δt_1 and Δt_2 are the small time interval around t_1 and t_2 in which the detection events (i.e., events A and B in Fig. 1) occur, β is the delayed neutron fraction, ρ is the reactivity, Λ is the neutron generation time, and D_ν is the Diven's factor. In particular, Eq. (1) considers a short detecting period to ignore the delayed neutron in measuring neutrons. The total probability of detecting two neutron counts is obtained by summing the correlated and uncorrelated probabilities, which is given by

$$P(\tau)\Delta t_1 \Delta t_2 = F\varepsilon^2 \left(F + \frac{D_v(1-\beta)^2}{2(\beta-\rho)\Lambda} e^{-\alpha\tau} \right) \Delta t_1 \Delta t_2 \quad (2)$$

where τ is the time interval between two detecting time points (=t_2-t_1). Eq. (2) can be expressed from the auto-correlation of two measurement signals.

$$R(A,B) = R(C_i^{(s)}, C_i^{(s+k)}) = \frac{1}{N-1} \sum_{i=1}^{N} \left(\frac{(C_i^{(s)} - \mu_A)^*}{\sigma_A} \right) \left(\frac{C_i^{(s+k)} - \mu_B}{\sigma_B} \right) \quad (3)$$

where R is the Pearson correlation coefficient, N is the total number of time bins, μ and σ are the mean value and standard deviation of the series of counts, respectively. The superscript s represents a reference count series and k represents the time shifting from the reference count series s (Please see Fig. 6). The form of Eq. (2) means that the prompt decay constant can be obtained using the least square fitting for the data obtained with Eq. (3) as follows [4]:

$$\text{Fitting Curve} = A * exp(-\alpha * \tau) + B \quad (4)$$

After the determination of the prompt decay constant, the effective multiplication factor can be calculated using Eq. (5) derived from point kinetics equation.

$$k_{eff} = \frac{1}{1-\beta+\alpha\Lambda}; \quad \alpha = \frac{\beta-\rho}{\Lambda} \quad (5)$$

2.2 Feynman-alpha method

The Feynman-alpha method can be derived from the correlated term of the Rossi-alpha method, ignoring the delayed neutrons and determining the prompt neutron decay constant as the ratio of the variance to mean of the detector signals during gate time, τ *(=t_2-t_1)* [3].

$$Y = \frac{\overline{C^2} - (\bar{C})^2}{\bar{C}} = 1 + Y_\infty \left[1 - \frac{1-e^{-\alpha\tau}}{\alpha\tau} \right] \quad (6)$$

In Eq. (6), Y is the variance-to-mean-ratio (VRTM) of the detector counts in the gate time τ. The saturated correlation amplitude Y_∞ includes detector efficiency, Diven's factor, reactivity, and effective delayed neutron fraction. Y_∞ and α can be obtained by fitting the measured VRTM data using least square fitting [4] as follows :

$$\text{Fitting Curve} = 1 + A \left[1 - \frac{1 - exp(-\alpha * \tau)}{\alpha * \tau} \right] \quad (7)$$

The effective multiplication factor can be evaluated using Eq. (5) as in the case of the Rossi-alpha method. In general, the Feynman-alpha method requires sufficient measurement data for improving the least square fitting. For this purpose, a method called "Time Swap" or "Moving-Bunching Technique" [3,6] is applied. Fig. 2 schematically explains this time swap technique. For example, the simple grouping of two successive bins gives only 5 bins of 2τ gate time while 9 bins of 2τ gate time can be obtained with the time swap technique. This allows a sufficient number of data to be utilized even at large gate times.

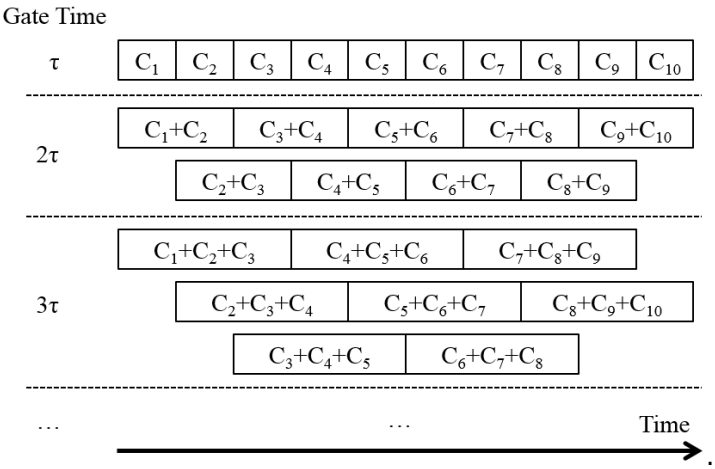

Fig. 2. Scheme of the time swap technique

3. Description of AGN-201K Model and Simulation Procedure

3.1 AGN-201K Model

AGN-201K is a zero power research and training reactor built by Aerojet General Nucleonics (AGN). It was donated to Korea by the University of Colorado in 1976. It is a solid-moderated reactor using polyethylene and licensed maximum power is 10 Watt [1]. Fig. 3 and 4 shows the axial and radial configurations of the AGN-201K modelled with MCNP6, respectively.

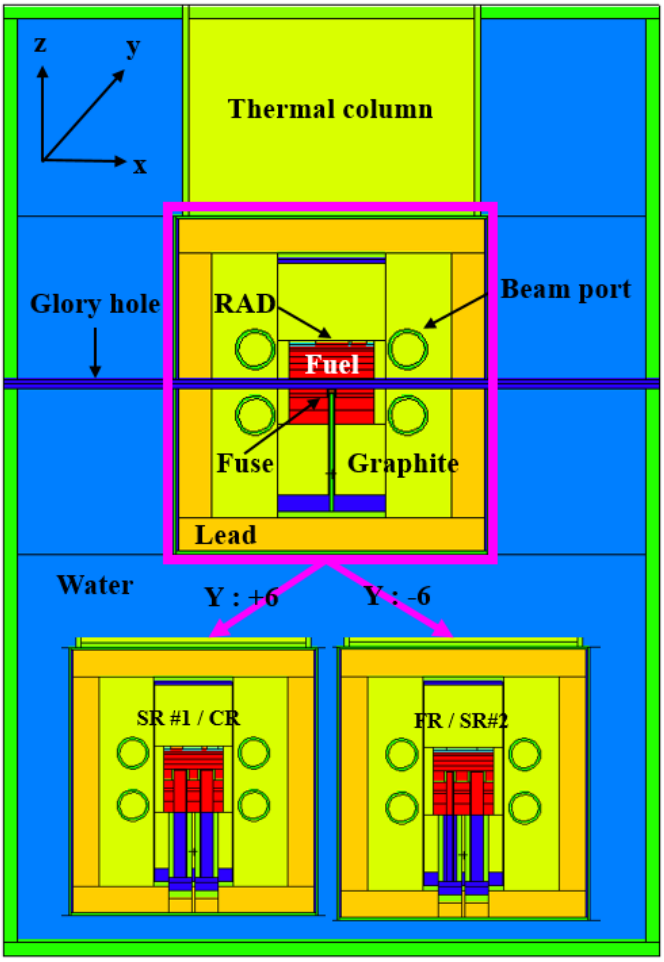

Fig. 3. Axial configuration of the AGN-201K

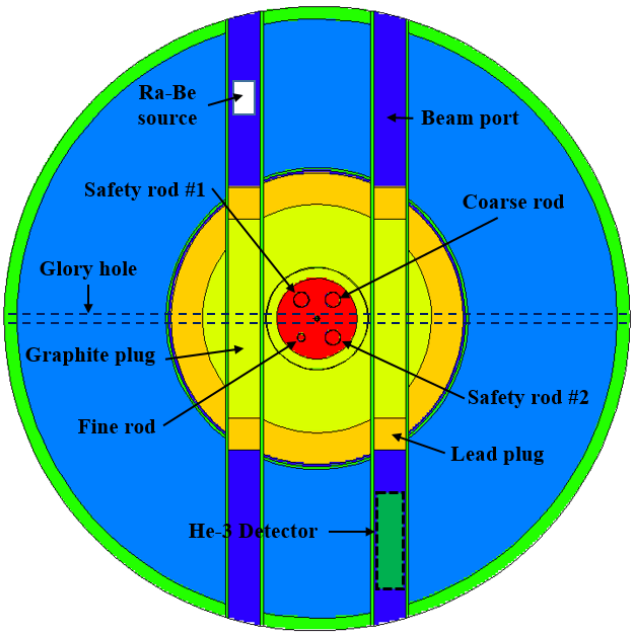

Fig. 4. Radial configuration of the AGN-201K

The fuel material is a homogeneous mixture of UO_2 and polyethylene. The fuel region is comprised of 10 disks with 12.8 cm radius [1, 2]. Uranium enrichment of the fuel is about 19.5 wt% for all rods out. The active core height is 25 cm. Four control rods are designed to pass through the fuel disks. Thermal fuses between the disks are used to separate the fuel for preventing the excessive power surge [1]. The active core is surrounded by 25 cm thick graphite reflector. The graphite reflectors are followed by a 10 cm thick lead gamma shield. For fast neutron shielding, the outside of the core tank is filled with water about 47.5 cm thick [2]. The control rod consists of 2 Safety Rods (SR), 1 Coarse Rod (CR), 1 Fine Rod (FR) that have the same composition as the fuel material [1, 2]. During operation, power is controlled by CR and FR [1]. This reactor has a one glory hole and four beam ports for experiments using neutrons. In particular, the external source neutrons are supplied at 10 mCi Ra-Be neutron source located in the left-upper beam port. For this study, we assumed a He-3 detector which is located in right-lower beam port as shown in Fig. 4. The He-3 detector is assumed to have 4 cm radius and 30 cm height.

3.2 Evaluation of Eigenvalues for Selected Subcritical States

Before the sub-criticality measurement, five sub-critical conditions are determined using the MCNP6 eigenvalue calculations (i.e., eigenvalue mode) in order to obtain the reference k_{eff} values and kinetic parameters to be used in Eq. (5). Table 1 shows the estimated multiplication factors and kinetic parameters for the five selected subcritical states and two additional cases (i.e., ARI (All Rods In) and a critical state). The MCNP6 eigenvalue calculations are performed with ENDF/B-VII.r1 cross sections, and with 50 inactive and 300 active cycles of 30000 histories each giving the standard deviations of k_{eff} less than 30 pcm. The ARI showed a maximum excess reactivity of 170 pcm Δk, which is very close to the 180 pcm Δk given in the technical specification report of AGN-201K. The critical position was shown to be a critical state in the actual experiment, but the simulation result shows a sub-critical level of 27 pcm Δk. We considered five sub-critical conditions (SCR) based on actual experimental data. The first sub-critical condition (SCR1) gives 347 pcm Δk sub-critical level with 3 cm CR and 4 cm FR withdrawals from the critical condition and the second sub-critical condition (SCR2) gives 250 pcm Δk sub-critical level with 1 cm of CR inserted from SCR1. SCR3 describes a 1 cm further insertion of CR from SCR2, which gives a 188 pcm Δk sub-critical level. SCR4 represents 1

cm further insertion of CR from SCR3, which gives a near critical state (i.e., 79 pcm Δk subcriticality). The final condition (SCR5) represents a fully withdrawn CR, which corresponds to a high sub-critical level of 1295 pcm Δk.

Table 1 : Multiplication factor and kinetic parameters according to the considered conditions

Condition	k-eff	σ (pcm)	β-eff	Λ (μsec)	Inserted rod position (cm)			
					SR#1	SR#2	CR	FR
ARI	1.00170	29	0.00834	53.25855	23.07	23.44	22.45	23.15
Critical	0.99973	27	0.00753	54.30449	23.07	23.44	20.25	16.56
SCR1	0.99653	28	0.00680	55.73110	23.07	23.44	17.25	12.56
SCR2	0.99750	26	0.00730	54.85705	23.07	23.44	18.25	12.56
SCR3	0.99812	29	0.00706	54.15084	23.07	23.44	19.25	12.56
SCR4	0.99921	28	0.00702	54.03459	23.07	23.44	20.25	12.56
SCR5	0.98705	28	0.00735	56.49639	23.07	23.44	0	12.56

3.3 Detector Signal Generation using MCNP6 Fixed Source Calculations

In order to simulate the detector signals, the He-3 detector is used to tally (n,p) reaction counts using the MCNP6 fixed source calculations. In this simulation, the external source isotropically emits 3.6 MeV neutrons in a cylindrical shape detector as shown in Fig. 4. For this simulation, 160,000,000 neutrons are assumed to be released for 0.5 seconds. Tally values are measured in units of 10 μsec. Due to this very short measurement cycle, we observed very high statistical errors for each time bin and so we used the weight window technique with the fine mesh divisions shown in Fig. 5 to reduce the statistical uncertainties of the (n, p) reaction count tally. Nevertheless, the statistical error for each time bin was as high as 10~30%.

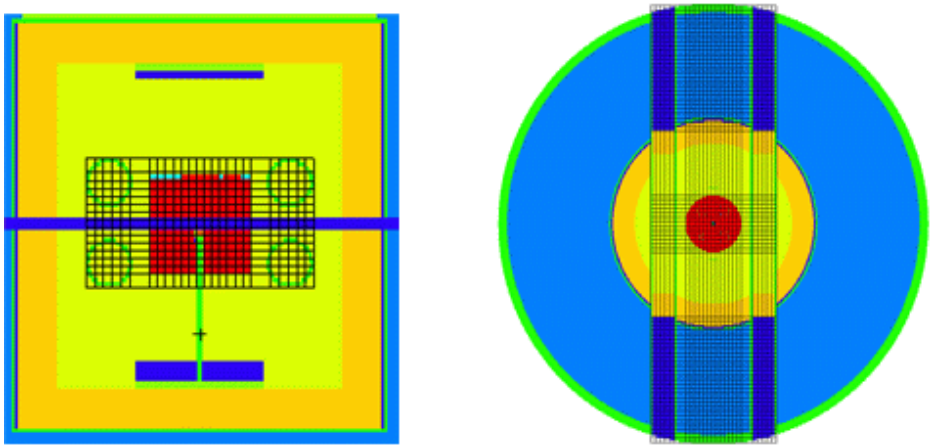

Fig. 5. Weight window mesh division on the reactor

4. Simulation Results

In this section, the simulation results for Rossi-alpha and Feynman-alpha methods are presented. In particular, we analysed the effects of the number of time shifts for Rossi-alpha method and number of time swaps for Feynman-alpha method. For example, Fig. 6 shows the change of (n, p) reaction count tally for SCR1 during 0.5 sec. As shown in Fig. 6, there are large fluctuations due to large statistical errors ranging 10~30%. We considered only the detector counts only for the first 45,000 time bins in the noise analysis. Fig. 7 shows the fitting curve of Rossi-alpha for 700 auto-correlation coefficients at SCR1 which are obtained with 700 time shifts (i.e., k=700).

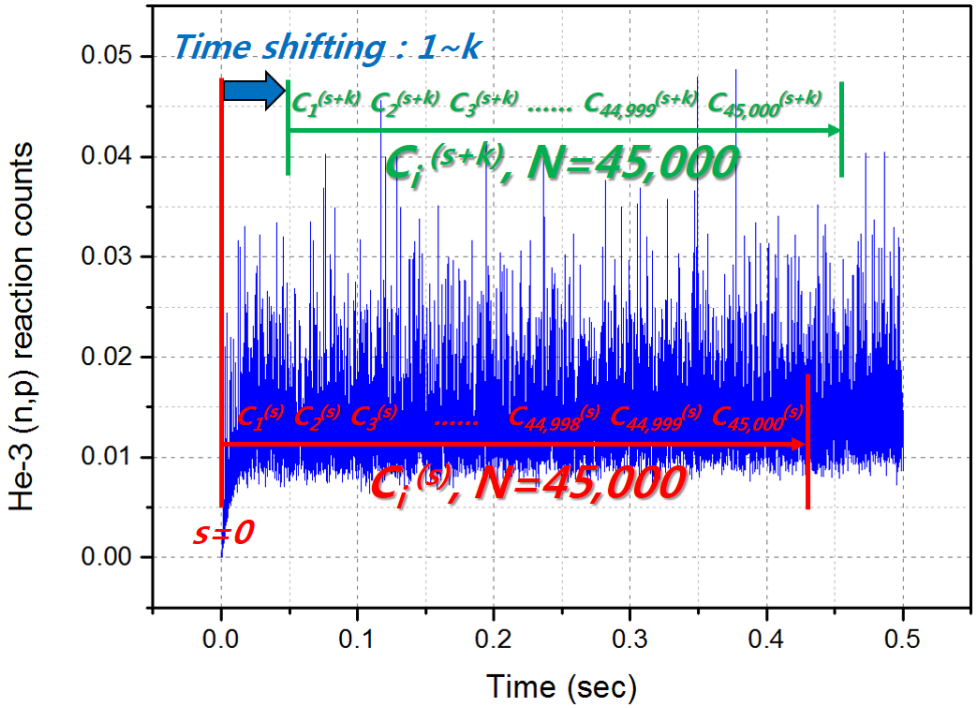

Fig. 6. Changes of the (n, p) reaction count tallies as time in case of SCR1

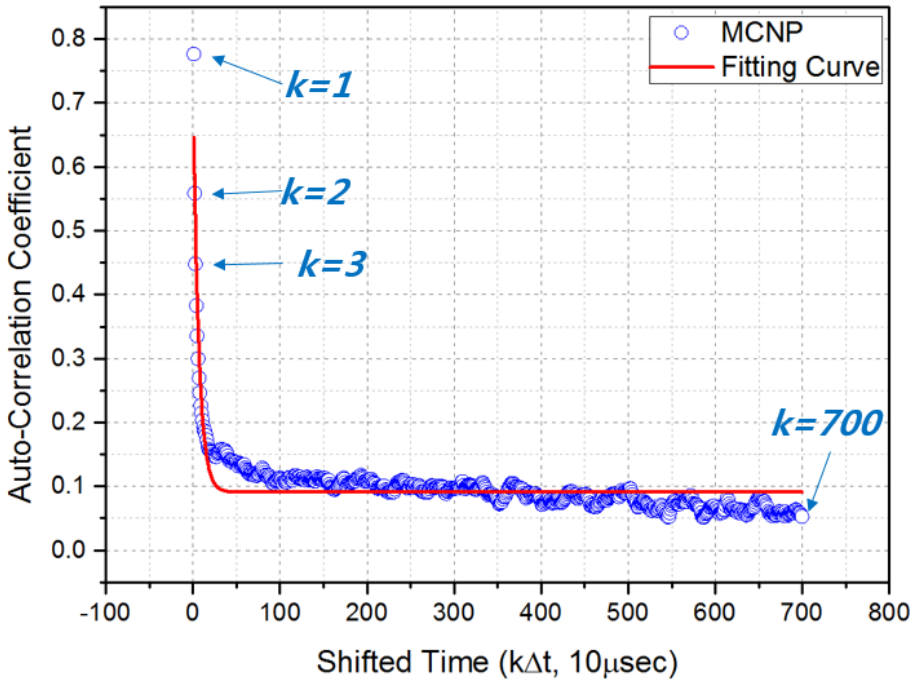

Fig. 7. Fitting curve of Rossi-alpha method in case of SCR1 (Number of time shifting, k=700)

However, since the simulated detector signals seems to be the data such as white noise, the sub-criticality measurement results can be changed depending on how the data is utilized. Therefore, we analysed the effect of the number of time shifts on the difference between the reference and estimated k_{eff} values, which are shown in Fig. 8. From Fig. 8, it can be seen that estimated k_{eff} gives good agreements as the number of time shifts increases except for the last case (i.e., SCR5) having largest subcriticality. In particular, the acceptable agreements are obtained after ~200 time shifts for SCR1~SCR4 cases.

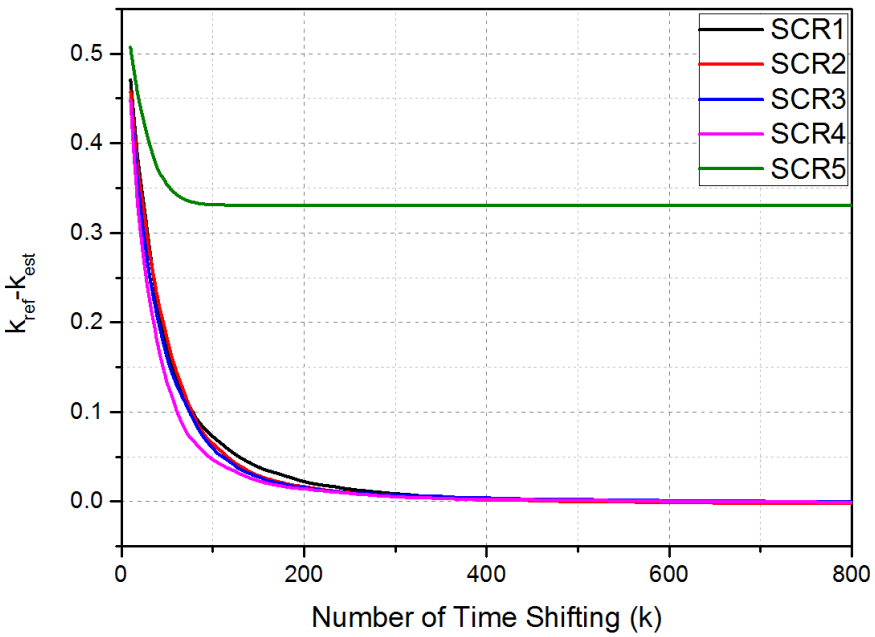

Fig. 8. Difference between reference k_{eff} (k_{ref}) and estimated k_{eff} (k_{est}) according to the number of time shifting

Fig. 9 shows the fitting curve of Feynman-alpha of SCR1 with a total of 700 time swaps. We analysed the effect of the number of time swaps on the difference between the reference and estimated k_{eff} values, which are shown in Fig. 10. As shown in Fig. 10, as the number of time swaps increases, the difference between the reference and estimated k_{eff} values gradually decreases except for the last case having largest subcriticality. However, the differences are still high up to 1000 ~ 2300 pcm even with 800 time swaps.

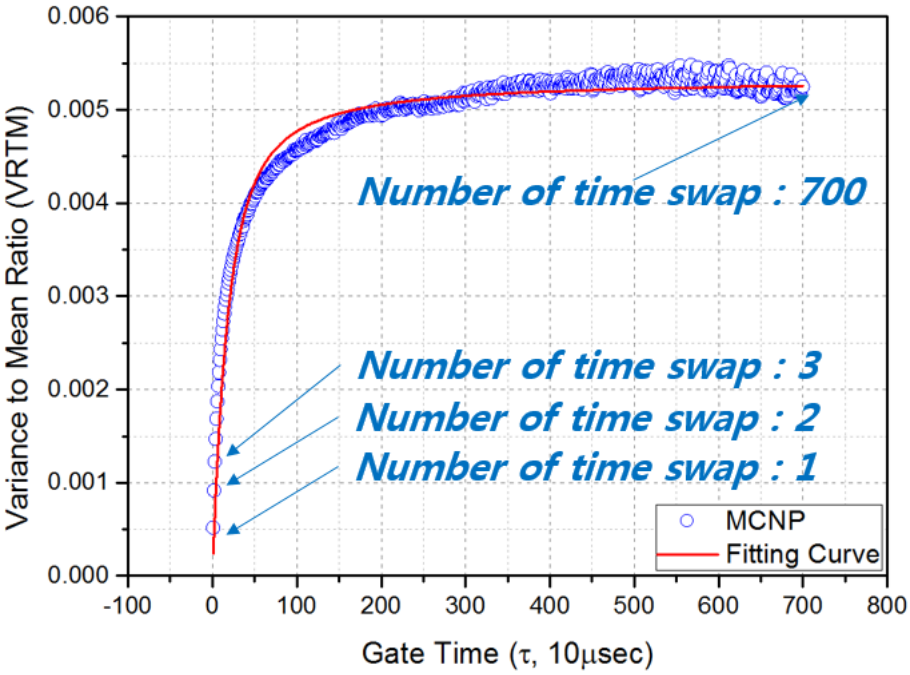

Fig. 9. Fitting curve of Feynman-alpha method in case of SCR1 (Number of time swap = 700)

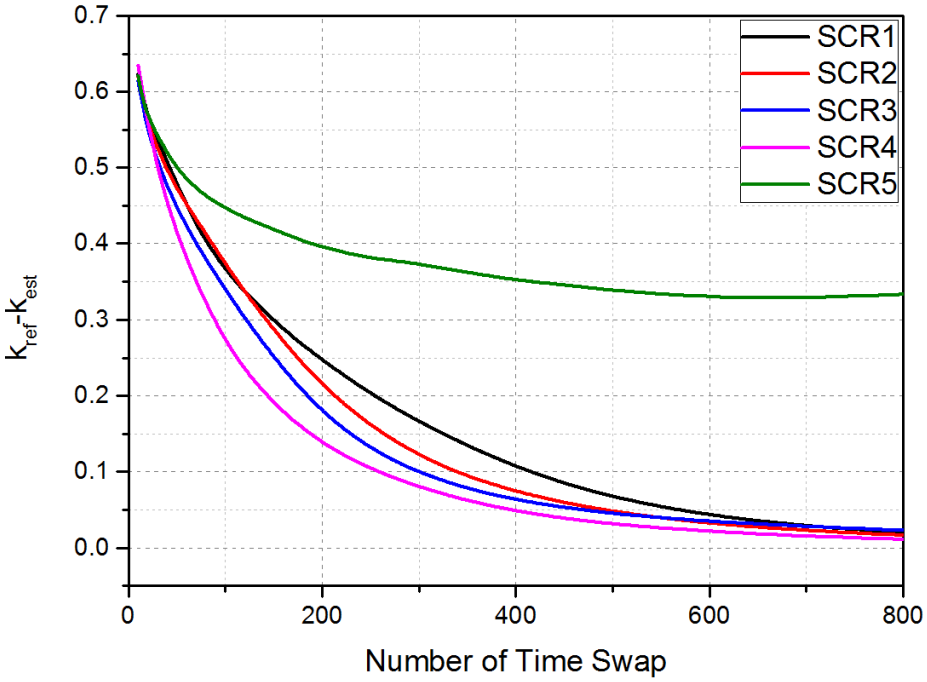

Fig. 10. Difference between reference k_{eff} (k_{ref}) and estimated k_{eff} (k_{est}) according to the number of time swap

5. Conclusions

In this study, computational simulation of noise analysis using MCNP6 was performed for zero-power reactor AGN-201K. For the five sub-critical conditions, the sub-criticality measurements were performed based on the (n, p) reaction count tally for an ex-core detector and MCNP6 fixed source mode calculations. The simulated detector signals were used to estimated k_{eff} using the Rossi- and Feynman-alpha methods and the estimated k_{eff} values were compared with those obtained with MCNP6 eigenvalue calculations. We applied the weight window technique to reduce statistical errors of (n,p) reaction counts for each time bin. In particular, we analyzed the effect of the number of time shifts and number of time swaps for Ross- and Feynman-alpha methods, respectively on the difference between the simulated and the reference k_{eff} values. The results of the simulations showed that the subcriticality can be reasonably accurately estimated with Rossi-alpha method except for the last case having the largest subcriticality if the number of time shifts is well selected while the Feynman method also gives gradual decrease of the difference between the simulated and reference k_{eff} values as the number of time swaps but the accurate estimation of subcriticality was not achieved.

6. ACKNOWLDEGEMENTS

This work was supported by the National research Foundation of Korea(NRF) grant funded by the Korean government (MSIP:Ministry of Science, ICT and Future Planning) (No. 2017M2B2B1072806).

7. REFERENCES

[1] “KHU AGN-201K Technical Specification”, Kyung Hee University, 2014.

[2] M. Gorham, “Evaluation of the AGN-201 Reactor at Idaho State University”, Idaho National Laboratory, 2006.

[3] E. Lee, et al., “A study of Ex-core detector characteristics for the estimation of effective multiplication factor in PWR”, Korea Electric Power Corporation, 2009.

[4] C. Kong, D. Lee, E. Lee, “Stability improvement of noise analysis method in the case of random noise contamination for subcriticality measurements”, Annals of Nuclear energy 71, p.245-253, 2014.
[5] G. E. Hansen., “The Rossi-alpha method”, Los Alamos National Laboratory, 1985.
[6] R. Okuda, A. Sakon, S. Hohara, et al., “An improved Feynman-alpha analysis with a moving-bunching technique”, Journal of nuclear science and technology, vol.53, p1647-1652, 2016.
[7] T. E. Valentine., “Review of subcritical source-driven noise analysis measurements”, Oak Ridge National Laboratory, 1999.
[8] J. T. Goorley, et al., “MCNP6 USER’S MANUAL Version 1.0”, Los Alamos National Security, 2013.

DECOMMISSIONING ACTIVITIES FOR IIN-3M RESEARCH REACTOR OF JSC "FOTON", UZBEKISTAN

S.A. Baytelesov, F.R. Kungurov, N.R. Maksumov, B.S. Yuldashev

Institute of Nuclear Physics of the Academy of Sciences of the Republic of Uzbekistan

The Radiational-Technological Complex (RTC) of JSC "Foton" was used in the semiconductor devices production technology.

On the ground there were: (1) IIN-3M nuclear reactor; (2) two gamma–facilities with Co-60 sources.

The total area of the RTC is 27000 m^2.

Territory of the RTC


IIN-3M reactor control panel


Gamma– facility


Gamma– facility


IIN-3M reactor vessel

IIN-3M reactor

The pulsed solution reactor IIN-3M was mounted at the Tashkent plant of electronic equipment (now JSC "Foton") in 1974-1975. Fuel loading (aqueous uranyl sulfate solution) and physical start-up of the reactor were made in December 1975.

Feasibility studies of the reactor conversion to LEU fuel were carried out and results were negative and the decision was taken to stop and decommission the reactor and gamma-facilities and clean all the territory of the RTC. The planned technological stop of the reactor was produced on 01.06.2013.

Gamma facilities

Gamma facilities have been in operation since 1976. Designated life of the installation is not determined by the project. The last charge for the units was carried out in 1990. All sources of Co-60 in installations have exhausted their service life. Dose rate in 2013 in the irradiation chambers of the facilities was about 700 Sv/h. Sources, shipped to Republican Radioactive Waste Disposal Facility (RRWDF): Cobalt-60 (**Co^{60}**) – 97 sources; Plutonium-238 (**Pu^{238}**) – 3 sources; Strontium-90(**Sr^{90}**) + Yttrium-90 (**Y^{90}**) - 2 sources.

"Foton" RTC site decommissioning stages:

– Preparation of the Decommissioning plan; – HEU fuel removal; – Removal of disused radioactive sources; – Decommissioning of RTC JSC 'Foton' site.

August 2012 – start of the decommissioning planning with the IAEA support; **2014** – permission from Uzbekistan authorities on works on decommissioning.

Works on decommissioning were performed by Consortium of the Institute of Nuclear Physics of the Academy of Sciences of the Republic of Uzbekistan and R&D Company "Sosny" (Dimitrovgrad, Russia)

Wastes from RTC site

1.Oversized solid radioactive waste - 6 containers;
2. Solid radioactive waste – 450 metalic 200 l drums – buried at RRWDF;
3. Liquid radioactive waste in quantity of 46 (20 l) canisters;
4. 2 Big-bags with wipes

Covering reactor vessel with concrete

Reactor vessel in a container with concrete

200 l drums with radioactive wastes


Liquid radioactive wastes in a 20 l canisters


Decontaminating wells in isotope storage building

Lessons learned

- Assessment on concrete activation, based on radiological survey, must be made more conservative
- Regulatory rules, norms and limits must be studied and discussed with all regulatory bodies
- Adequate technique and time frames must be considered
- Work must be divided and arranged into shorter stages to have finances available for the next stage


Decontaminating hot cell in a reactor building


Decontaminated laboratory room in a reactor building

Reactor box after decontamination

Current situation

- All works on RTC site cleaning are completed
- All radioactive wastes moved to RRWDF
- RTC site now is a so called "green field" and handed over to "Foton"

Drums with radwastes in a storage at the RRWDF

Debris from the gamma-facility building

Reactor building demolishing

Debris from the isotope storage building

EFFECTIVE UTILIZATION OF WWR-SM RESEARCH REACTOR

S.A. Baytelesov, F.R. Kungurov, B.S. Yuldashev

ABSTRACT

WWR-SM research reactor fully converted to LEU in September 2009.

After conversion reactor was upgraded and modified few times. Some of it equipment and constructional parts were replaced to strengthen safety of its operation.

Many scientific and research works are carried out using WWR-SM research reactor by laboratories of INP and institutions of Uzbekistan well as local and foreign businesses. INP jointly with foreign laboratories performed scientific works related to reactor fuel, nuclear materials.

1. WWR-SM NUCLEAR REACTOR

WWR-S research reactor with power of 2 MW, built in the Institute of Nuclear Physics of Academy of Sciences of the Republic of Uzbekistan, achieved first criticality in September 1959.

Reconstruction of the WWR-S, conducted in late 1971, with the replacement of the core vessel and reflector provided the opportunity to increase its capacity from 2 to 10 MW and the reactor was given symbolic name WWR-SM.

Conversion of WWR-SM reactor from 90% enriched fuel to the use of IRT-3M type FA 36% enriched on U-235was launched in August 1998, and completed in February 1999.

In 2009, the reactor was completely convertedfrom 36% enriched fuel to the use of LEU IRT-4M type 19,75% enriched nuclear fuel.

The most characteristic abilities to load the reactor core are shown in Fig. 1. This is loading of 24 six-tube IRT-4M type FA.

Horizontal cross-section of the reactor core

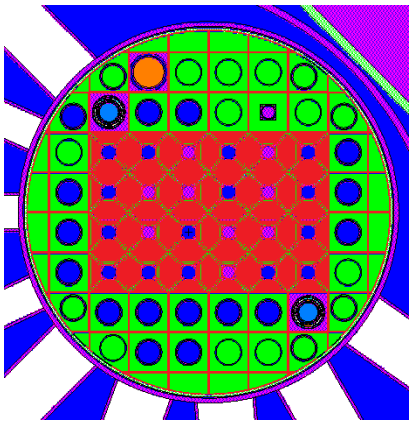

The vertical cross-section of the reactor core

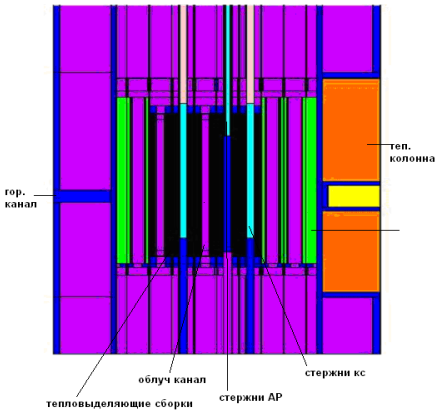

Figure 1. Horizontal and vertical cross-sections of the WWR-SM reactor core.

The maximum thermal neutron flux in the reactor core with 24 IRT-4M type fuel assemblies - 1.2×10^{14} N/cm^2*s, and the maximum fast neutron flux - 5×10^{13} N/cm^2*s.

After conversion to LEU fuel reactor had losses of about 20% in thermal neutrons flux. Maximum reachable fuel burnup decreased from 70% to 55%. Less excess reactivity is collected for the next cycle.

For these reasons, it was decided to increase the number of fuel assemblies in the active core from 20 to 24.

2. SECURING WWR-SM NUCLEAR REACTOR

IAEA, US Department of Energy, the European Commission and other international organizations, pay more attention to improving the safety of operation of the reactor, to improve its operational capabilities.

In 2004, the IAEA started a project UZB4/005 “Improving the safety of operation of the reactor WWR-SM INP”.

In 2006 - UZB9004 - Improving Operational Safety of the Research Reactor at the Institute of Nuclear Physics- Reconstruction of reactor radiation safety (put into operation a new system of stationary radiation monitoring “Pelican”) and personnel was trained in the use of the system.

In 2007 - UZB9005 - Improving Operational Safety of the Research Reactor at the Institute of Nuclear Physics (Phase II) - beginning of the project on production, supply and commissioning of complex of instrumentation and automation control systems of WWR-SM research reactor.

In 2010 - UZB1001 - Strengthening Nuclear Safety and Improving Use of the Research Reactor at the Institute of Nuclear Physics.

In 2011 - Acquisition of temperature and pressure sensors for the control and protection system of the reactor.

In 2011 - Acquisition of UPS (160 kVA) for the emergency core cooling system.

THE WORK PERFORMED UNDER THE IAEA PROJECT UZB/9/004-005.

Purchase of emergency power supply (UPS 160 kVA)

Upgrading the system for reactor control and protection

Upgraded the radiation protection system

Pic. 2. Equipment, purchased under IAEA projects.

Under IAEA TC project UZB/9/005 for the cost of 1.2 mln. USD WWR-SM research reactor’s electronic part of control and protection system was upgraded. Reason for this action was absence of spare parts for the old system on the market, which were outdated. Replacement of old electronic part of control and protection system led to gathering more accurate and advanced data on reactor operation parameters, data archiving and consequently to increased safety of reactor operation.

Pic. 3. Old control and protection system (CPS)

Pic. 4 Old and new CPS installed and operationg in parallel

Pic. 5 New CPS system.

For future works it is planned to continue the implementation of TC project UZB/9/005, in a framework of which was installed and commissioned emergency ventilation system, including the purchase and installation of radiation monitoring system for radioactive emissions from the reactor building.

IAEA PROJECT UZB/1/001 2013-2015 - Strengthening Nuclear Safety and Improving Use of the Research Reactor at the Institute of Nuclear Physics

In the framework of the project UZB/1/001it is planned to perform the following tasks:

- Reconstruction of the second cooling circuit (new pumps, piping, heat exchangers);
- Improving opportunities on WWR-SM research reactor usage, including the preparation of the production of radioisotopes for medical and industrial purposes;
- Acquisition of beryllium reflectors to create traps of neutrons;
- Performing periodic inspection of equipment to ensure safe operation of the WWR-SM reactor until 2022;
- Research works of INP staff in creation of radioisotope products.

Every year a year preventive maintenance and complex certification of instrumentation and equipment, replacement of fuel assemblies for compensation and emergency protective rods, upgraded wiring diagram pumps to supply water to the cooling system of the reactor is carried out.

Validated test instruments, perform complex tests on instruments and apparatus, safety systems with actuator, the lifting and lowering time of safety rods in the core together with the speed of loadingof compensating rods to adjust the loading of positive reactivity. Check the efficiency of the ionization chamber and measure the resistance of the cable insulation.

Quarterly conducted emergency training exercises, as well as supervision on accountingof nuclear materials.

Due to IAEA support in a forms of TC projects, trainings, seminars, the ageing management, safety, physical protection issues are always under control and that leads to reliable and safe operation of WWR-SM research reactor.

3. EFFECTIVE USE OF WWR-SM NUCLEAR REACTOR

The following laboratories of the INP usingWWR-SM research reactor nuclear reactor:

№	Name of laboratory
1	Laboratory of physics of nanostructured and superconductive materials
2	Laboratory of radiation physics of semiconductors
3	Laboratory of radiation processes in dielectric materials
4	Activation analysis laboratory
5	Laboratory of nuclear chemistry
6	Activation analysis laboratory of pure materials
7	Laboratory of physics and technology of semiconductor electronics
8	Scientific Group WWR-SM

With the use of a nuclear reactor laboratories of the institute completed and executingmore than 10 Government orders on fundamental and applied projects during last 5 years, such as:

- «Experimental studies of the properties and states of nuclear matter at high and low energies»
- «The formation of micro-inhomogeneity and their impact on the fundamental properties of nuclear-doped silicon hydrogenation»
- «Investigation using nuclear-physical methods of complexation of precious and rare earth metals with new (phosphorus) organic compounds»
- «Development of Almalyk MMC dump slag processing methods using nuclear methods»
- «Development of technology for production of radioisotopes, radiopharmaceuticals and sources of ionizing radiation for the needs of medicine and industry»
- «Development of technology preclinical treatment of tumors on the basis of a dedicated channel of a nuclear reactor INP Uzbekistan.»

and etc.

WWR-SM research reactor of INP is used by the following institutions, universities and organizations of Uzbekistan:

1. Institute of Biochemistry,
2. Institute of Bioorganic Chemistry,
3. Institute of Genetics and Experimental Biology,
4. Samarkand State University,
5. Republican Scientific Center of Oncology,
6. Design Office with PH at INP AS RU.

Research reactor WWR-SM performs contractual works on irradiation of samples with different, both local and foreign, businesses and commercial organizations.

During 10 years topaz and other stones are irradiated in WWR-SM research reactor for different customers. Technology of irradiation is fine-tuned by reactor personnel.

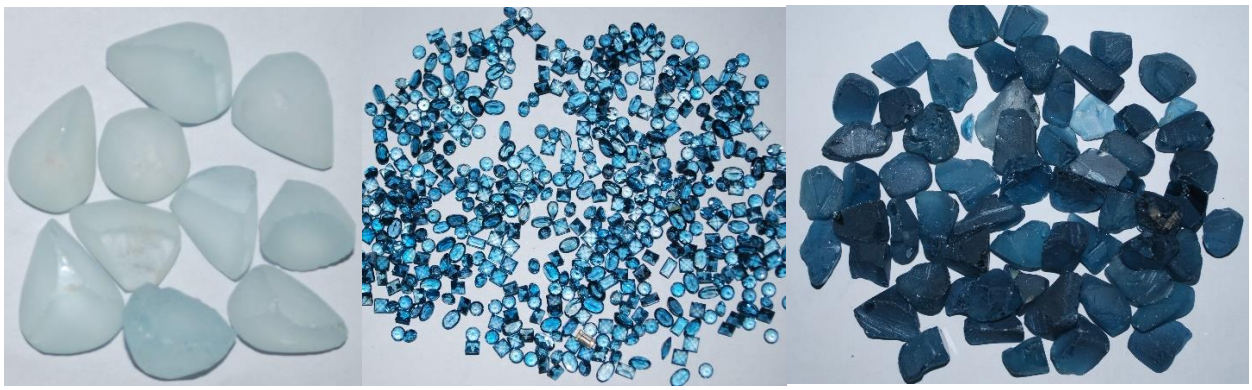

(A) (B) (C)

(D)

Pic. 6. Nonirradiated (A) and irradiated topaz stones (B), (C), (D)

State enterprise “RADIOPREPARAT” produces wide range of radioisotopes and radiopharmaceuticals for medical purposes since 1976 using WWR-SM research reactor. These preparations are used in hospitals of Uzbekistan and exported to other countries.

Obtaining Mo-99 radioisotope

Nuclear reaction:

$^{98}Mo + n \rightarrow {}^{99}Mo + \gamma$

For irradiation enrichment isotope 98Mo* is used

Isotopic content of 98Mo:

Mo isotopes	92	94	95	96	97	98	100
Content,%	0,01	0,03	0,03	0,01	0,66	98,75	9,51

* Product 98MoO3 is made in Russian

Cross-s*ection* **for 98Mo(n, γ) 99Mo reaction is about 570 mb**

(with considerations of the resonance integral)

The yield of 99Mo from the 98Mo(n, γ) 99Mo reaction 6,2 - 6,5 Ci/g

(Conditions: Tirrad.= 180 hours, Fn = 1,0•10(14) n/cm(2)•s)

Mo-99 accumulation by irradiation with Fn = 1,0•10(14) n/cm(2)•s

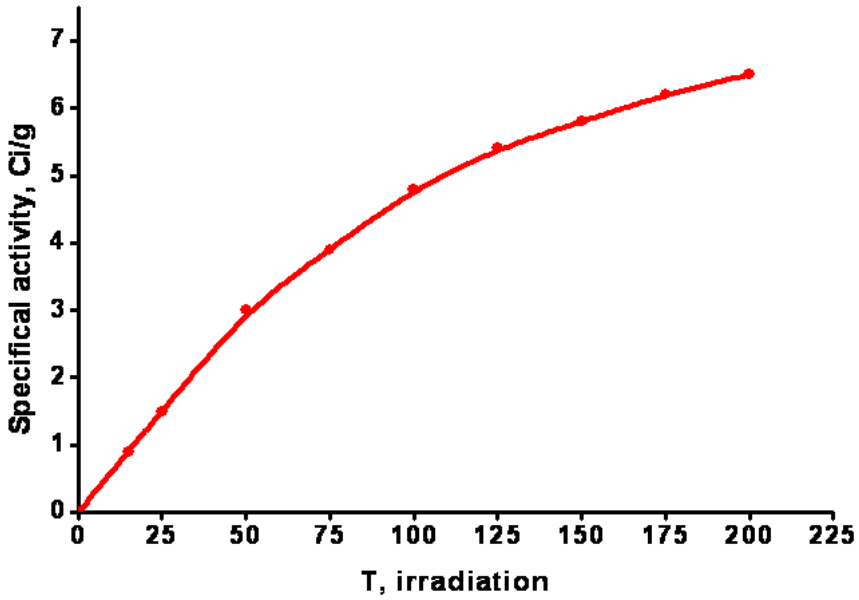

Specific activity of the Mo-99 depending on different factors.

F = 10 (14) n/sm2.s; C = 98,75 % (98Mo); A(Ci/g)

T day	γ=0	γ=0,2 L=1mm	γ=0,2 L=5mm
1	0,24	1,94	1,33
2	0,43	3,45	2,36
3	0,57	4,62	3,17
4	0,69	5,54	3,79
5	0,77	6,24	4,28
6	0,84	6,80	4,66

Pic. 7. Processing radioisotopes and samples of final products.

INP jointly with Pacific National North-West Laboratory, USA, IAEA performed research of spent nuclear fuel (SFA) using Advanced Experimental Fuel Counter (AEFC) and ^{252}Cf source. AEFC is useful device for IAEA experts to check spent fuel characteristics such as: energy release in SFA, residual mass of ^{235}U in SFA, relative ^{235}U burnup, uniformity of initial uranium enrichment in SFA and power distribution. Before using AEFC, UAEA made measurements of residual 235U mass with indirect method by detecting 662 keV peak of ^{137}Cs in SFA.

WWR-SM research reactor is one of most effectively used research reactors in the world. Reactor operation time was the most intensive in 1980-2005 – 5000 hours and above.

During the period from 1959 to 2017 the WWR-SM research reactor has been operated at a power of 237,907.7 hours.

Nowadays reactor operates almost twice less hours due to increased cost of fresh LEU fuel. For the moment, there is only one supplier of fuel for the WWR-SM research reactor, and INP looks for other suppliers, who can produce suitable LEU fuel for our reactor.

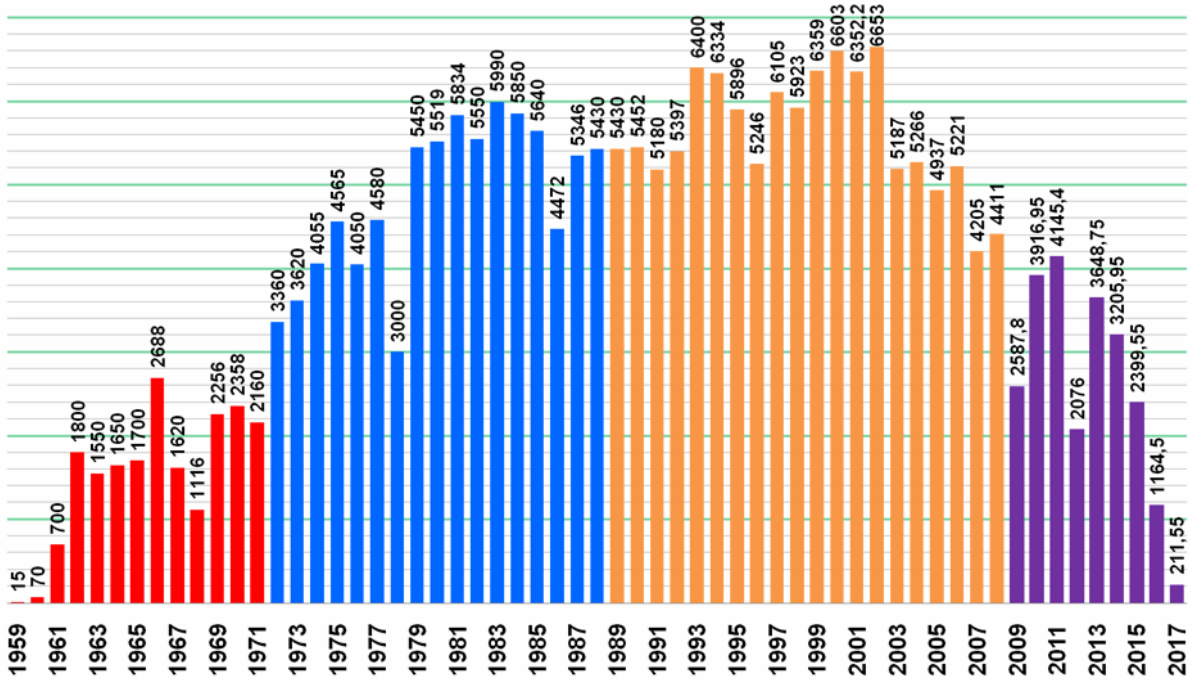

Pic. 7. WWR-SM research reactor operation hours.

INP has plans on performing neutronic and thermal hydraulic calculations for the new fuel with similar to IRT-4M geometry. Fuel will have similar to IRT-4M outer tube, but without fuel and inside this tube will be installed pin or plate type uranium-silicide fuel elements. Getting good

results will lead to manufacturing of a number of test fuel assemblies and performing their life-tests in WWR-SM research reactor.

CONCLUSION

In 2012 all HEU fuel of WWR-SM reactor was shipped to Russian Federation.

In 2015 all HEU liquid nuclear fuel off IIN-3M reactor of FOTON was shipped to Russian Federation. At the present, Uzbekistan do not have any more HEU fuel.

More than 55 years WWR-SM research reactor operates safe and reliable due to the construction of reactor and timely undertaken actions, supported by Uzbekistan government, IAEA, US DOE and Euroatom. Safe operation of reactor allows performing scientific studies of materials, production of radioisotopes and other products in stable and long terms plans. At all times, when reactor operates, almost all irradiation channels are loaded with samples for irradiation for scientific and commercial purposes for local and foreign organizations.

FUEL ASSEMBLY DESIGN FOR AN IRRADIATION IN AN EUROPEAN MEDIUM POWER RESEARCH REACTOR

M. BOYARD[1], F. HUET, C. PATURET
TechnicAtome
CS 50497, 13593 Aix en Provence, France

V. ROMANELLO, A. DAMBROSIO, M. HREHOR
Centrum výzkumu Řež
Husinec Rez 130, 25068 Husinec Rez, Czech Republic

F. GAJDOS - I. VIDOVSKY
MTA EK, Konkoly-Thege Miklos 29-33 H-1121 Budapest, Hungary

J. GAJEWSKI - M. MIGDAL
NCBJ, Ulica Andrzeja Soltana 7, 05400 Otwock, Poland

ABSTRACT

The H2020 European LEU-FOREvER Project (2017-2021)[1], associating major actors of the European research reactors community – FRAMATOME - CERCA, CEA, CV Řež, ILL, NCBJ, MTA EK, SCK·CEN, TechnicAtome and TUM, aims to foster the development of sustainable low enriched uranium (LEU) based fuel cycle for the European research reactors[2].

Some European Medium Power Research Reactors (EU_MPRR) are currently operating with a single qualified fuel based on LEU UO_2 dispersed fuel. As part of the LEU-FOREvER project goals, fuel diversification is expected for these reactors. Based on MARIA reactor conversion to LEU experience, Low Enriched Uranium silicide dispersed fuel as proven solution is expected to pave the way toward a fuel supply chain enhancement.

The following paper focuses on the first part of the project, namely core design data gathering and preliminary analysis and proposes the definition of a new fuel assembly design (standard and controlled) for LVR-15.

Thus, as a first step, data collected by TechnicAtome from LVR-15, BRR and MARIA operators are altogether analyzed. Then, relevant data for fuel assembly design and foreseen safety assessment are consolidated. Finally, realistic solutions available for LVR-15 controlled fuel assembly and promising trends for BRR fuel assembly are presented.

Currently, a first of a kind LVR-15 standard fuel assembly is manufactured by Framatome-CERCA.

The next steps will be the irradiation of the designed fuel assembly in the LVR-15 reactor and then preliminary post-irradiation examinations.

1 Introduction

The H2020 European LEU-FOREvER Project (2017-2021) [1], associating major actors of the European research reactors community, CEA, CV Řež, FRAMATOME – CERCA, ILL, NCBJ, MTA EK, SCK·CEN, TechnicAtome and TÜM, aims to foster the development of sustainable low enriched uranium (LEU) based fuel cycle for the European research reactors[2]. Key

[1] corresponding author : michel.boyard@technicatome.com

issues and related fuel development identified to secure fuel supply for European research reactors are illustrated in Fig 1.

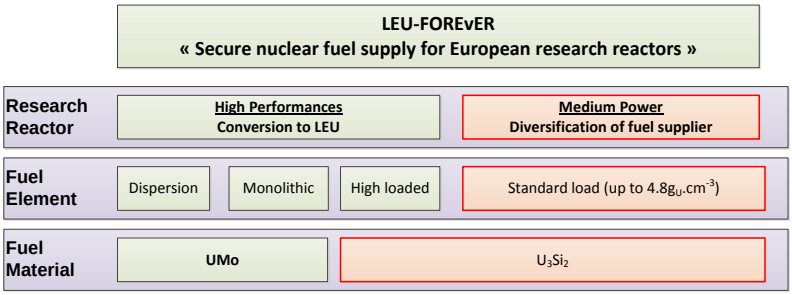

Fig 1: Key issues and related fuel development identified to secure fuel supply for European research reactors

Identified developments to reach the goal depend mainly on the research reactor power:

- High performances Research Reactor (EU_HPRR) requiring to convert to LEU: BR2, FRM2, ILL and RJH,
- Medium Power Research Reactors (EU_MPRR) already converted to LEU with a need to diversify their fuel supply chain: BRR, LVR-15 and MARIA.

Indeed, for the second type, namely BRR and LVR-15 are currently operating with a single qualified fuel based on LEU UO_2 dispersed fuel. However, based on MARIA reactor conversion experience from HEU to LEU [3], LEU silicide dispersed fuel is anticipated as a solution toward their fuel supply chain diversification.

The following paper aims to present the first steps of this diversification. For that, main characteristics of the 3 reactors are given and compared in the first part. In the second, new fuel design approach is presented. Finally design results and trends are discussed.

2 Characteristics of the 3 reactors

MARIA, LVR-15 and BRR have some similarities. However they exhibit very different cores, fuel assemblies and shutdown systems:

- MARIA core (see Fig 2) is an array of isolated cylindrical fuel assemblies (74.8mm in diameter), absorbers and experimental devices in a lattice of Beryllium blocks. The maximum thermal flux of its fuel element (FE) is up to 260 W.cm^{-2}. Each Fuel Assembly (FA) is cooled by a dedicated loop,
- LVR-15 core (see Fig 3) is a lattice of medium size square fuel assemblies (pitch 71.5mm), with an inner absorber channel in some cases, experimental devices and surrounding Beryllium blocks.
- BRR core (see
- Fig 4) is a hexagonal lattice (35mm) of fuel assemblies (hexagonal shape), absorbers and experimental devices with all around Beryllium blocks. Absorbers and experimental devices have defined locations in this pattern.

	MARIA	LVR-15	BRR
Nominal power (MWth)	30	10	10
Primary cooling system	Dedicated loops	Downward flow	Downward flow
Number of FA	≈26	28-32	≈190
Thermal neutron flux	3.0 10^{14} (in core)	1.2 10^{14} (core trap)	2.2 10^{14} (in core)
Maximum thermal power (W.cm^{-2})	260	66.3	65

Tab 1: Reactor characteristics

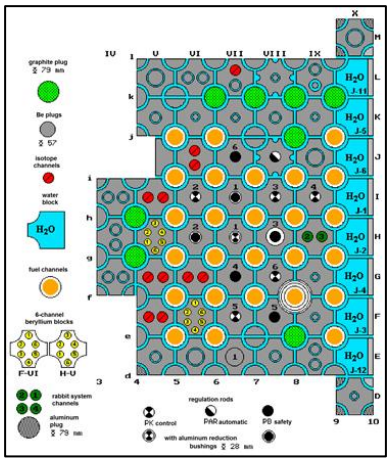

Fig 2: MARIA - Core

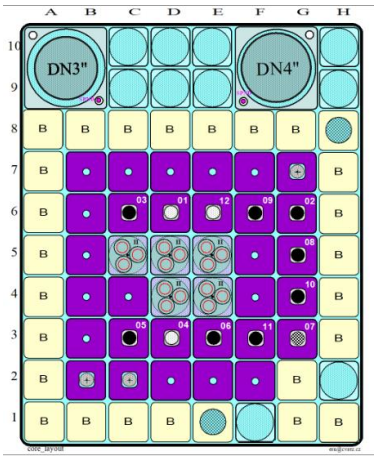

Fig 3: LVR - 15 Core

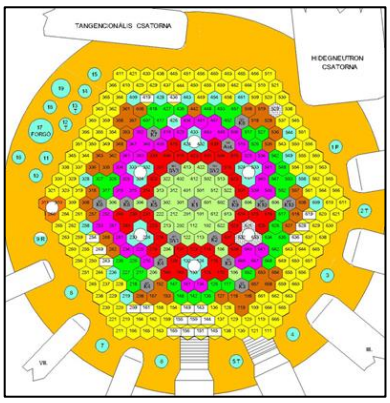

Fig 4: BRR - Core

Tab 1 summarizes the main characteristics of the 3 cores and Tab 2 characteristics of the fuel assemblies, part of the Supply Chain 1 (SC1).

	MARIA	**LVR-15**		**BRR**
	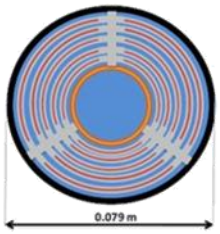	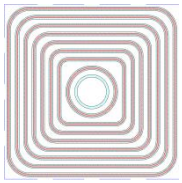		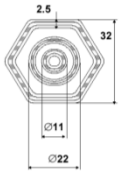
Meat	LEU Dispersed UO_2 – 19,75wt% ^{235}U			
U load	Up to 3.8 $g_U.cm^{-3}$	Up to 3 $g_U.cm^{-3}$		Up to 2.5 $g_U.cm^{-3}$
Thickness	0.8 mm	0.7		0.7
Height	1000 mm	600 mm		600 mm
^{235}U mass	~485g	~300g	~264g	~45g
Clad	SAV-1 Aluminium alloy			
Thickness	0.6 mm	≥ 0.3 mm		0.7 mm
Water velocity in FA (Max)	9 $m.s^{-1}$	4.5 $m.s^{-1}$		3.5 $m.s^{-1}$
References	[4], [5], [6], [7]	[8], [9]		[7], [10], [11], [12]

Tab 2: Fuel assemblies from the Supply Chain 1 (SC1)

3 Design approach and associated drivers

3.1 Design approach

The diversification of their fuel supply chain is a common goal of the three reactors. Nevertheless they have dedicated LEU-FOREvER project objectives:

- MARIA reactor operator has already licensed a second type of fuel assembly and offer to share his feedback of the design and licence process,
- One prototype of LVR-15's FA is to be designed, manufactured and irradiated,
- An alternative design of the current BRR's FA is to be defined.

Otherwise, Supply Chain 1 (SC1) is based on dispersed UO_2 technology for the meat and concurrent extrusion of meat and clad together, while Supply Chain 2 (SC2) uses powder technology with dispersed U_3Si_2 meat and rolling. Differences between the 3 reactors and the 2 fuel manufacturer technologies lead to different technical strategies.

As responsible for the FA design within LEU-FOREvER project, TechnicAtome has implemented a simple but effective approach thanks to the collaboration between the different partners. The following steps highlight LEU-FOREvER project overall logic:

- **Step 1**: Open exchanges between the operators and the Fuel designer to take into account fuel assemblies core environment as well as the new fuel assemblies relevant interface requirements coming from the reactor and the related facilities (see Fig. 6). Since the final objective is diversification, not a switch from one supplier to the other, the proprietary data and information of the current supply chain are preserved; it results in some limit to the exchange. New fuel requirements have been clarified at the end of this step,
- **Step 2**: Based on the requirements and proven design components (U_3Si_2 fuel element qualified manufacturing process[14]), different designs have been submitted to the operators (LVR-15 and BRR),
- **Step 3**: Mainly oriented towards LVR-15, detailed design of one prototype FA for fabrication, irradiation and characterization has been carried out,
- **Step 4:** Safety assessment of the FA prototype irradiation in LVR-15 will be done. From fuel qualification standpoint, the NUREG1313[14] and the IAEA's NF-T-5.2[13] good practices are the main guidelines.

Fig 5 focuses on LVR-15 prototype fuel assembly design process.

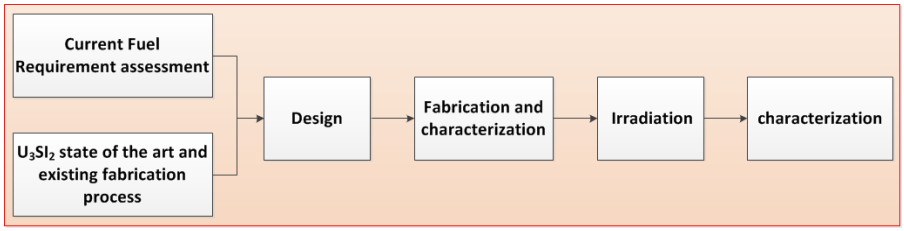

Fig 5: LVR-15 prototype fuel assembly design process

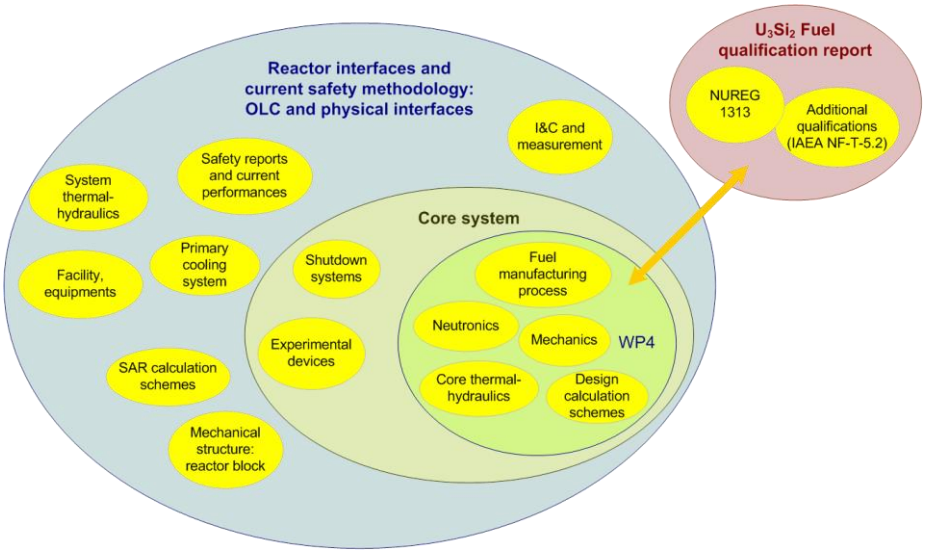

Fig 6: Fuel assembly associated interfaces

3.2 Design drivers

Main design drivers have been analysed through a methodical approach of the reactors and related facilities:

- Interfaces leading to fuel assembly manufacturing requirements: reactor block, reflector, cooling system, experimental devices and experimental loads, shutdown system, Command Control and measurement, handling, locking, storage,
- Performances impacting core performances: experimental loads, fuel consumption,

- Safety and licensing impacting operational limits and conditions: criteria, transients, safety methodology,
- Fuel conformance strategy.

Tab 3, Tab 4 and Tab 5 compare fuel assembly interfaces various standpoints (cooling system, shutdown system and selected operational topics), in order to assess Supply Chain 2 impacts on daily operations.

	Geometrical interfaces	**Functional interfaces**
Generic strategy	Identical functional interface with the primary cooling system: Similar fuel surfaces (heating and rubbing) and top and bottom nozzles head losses	Same functional interfaces with the primary cooling system: heating, rubbing and top and bottom nozzles head losses
MARIA	Slots in the Be matrix: easier management of the outer FA water gap	
LVR-15	Via the rubbing areas of the top nozzles and the other blocks (+ support grid): management of the outer FA water gap	
BRR		

Tab 3: Interfaces with the cooling system

	Geometrical interfaces	**Functional interfaces**
Generic strategy	No change of the shutdown system components Drop performances preserved (capability and time)	Design compliant with shutdown system (identical functional interface) and criticality criteria (moderating ratio, $g^{235}U/FA$)
MARIA	No interface (different slots in the Be matrix)	Absorption of the neutrons: balance at core level Heating and neutron fluence of the absorber and related mechanical structures
LVR-15	Mechanical interface inside the FA with the guide tube of the absorber ➔ implies 2 different FAs	
BRR	The same mechanical interfaces as between FA and reflector block	

Tab 4: Interfaces with the shutdown system

Locking	BRR and LVR-15: downward flow and no experimental device with significant internal mechanical energy		Passive FA locking
	MARIA: Down and upward flow		FAs inserted in field tubes
Handling	Interface with existing handling tools		Top nozzle design is compatible with current handling tools. Margin to cope with potential weight increase.
Storage	Fresh fuel	No key driver	Formal analysis for licensing by the operator
	Spent fuel	No key driver	

Tab 5: Operational topics

4 New fuel assemblies

4.1 MARIA Reactor

The design, manufacturing and licensing of SC2 have been carried out by NCBJ and FRAMATOME-CERCA. Two lead test assemblies (MC5 - Fig.7) achieved their irradiation by 17/08/2010 and 21/08/2011[3].

Feedback of both process design and licensing is part of LEU-FOREvER project.

Concerning the design, the main option has been to remain as close as possible to the geometry and the matter balance of SC1 (MR6 – Fig.6), taking into account the capabilities (higher ^{235}U volumic mass of the Uranium silicide) and the constraints (more structural components) of the fuel manufacturing technology.

The project has been a success and the operator now benefits from two different supply chains[3].

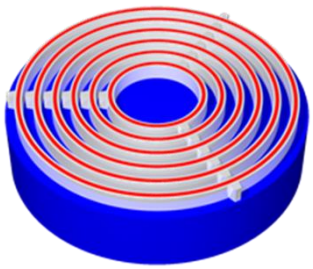

Fig 7: SC1 - MR6 type - Cylindrical tubes UO_2-Al, 3.8 gU.cm^{-3}

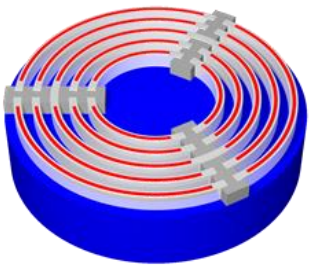

Fig 8: SC2 - MC5 type - Bended plates with stiffeners U_3Si_2-Al, 4.8 gU.cm^{-3}

4.2 LVR-15

For LVR-15, a similar process is in progress. Steps 1 and 2 are achieved, step 3 is almost completed and for Step 4, 2 tasks have been already carried out. Indeed, uncertainty management methodology for thermohydraulic safety studies[15] and benchmarks of safety assessment and design neutronics calculation schemes have been processed[16].

	Tubes	**Flat plates**		**Curved plate**		
	IRT-4M	**FA_1a**	**FA_1b**	**FA_2**	**FA_3**	**FA_4**
	8 tubes 0.7/0.45	20 plates 0.7/0.45 *0.51/0.38*	22 plates 0.7/0.45 *0.51/0.38*	8 plates, 2 stiffeners 8 mm width 0.7/0.45	8 plates, axial welding 0.7/0.45	8 plates, alone 0.7/0.45
Water gap (mm)	1.85	1.98 *2.32*	1.63 *1.98*	1.85	1.85	1.85
Heating surface ratio	1	0.92	**1.01**	0.88	**1.00**	**1.01**
Flow section ratio	1	0.91 ***1.05***	0.85 ***1.00***	0.65	0.92	0.95
^{235}U mass ratio	1	1.60 *1.16*	1.76 *1.28*	1.53	1.74	1.77

Tab 6. Standard Fuel Assembly - Main ratios between SC2 candidates and SC1 FA

A preferred design has been chosen after screening of a set of possibilities between flat plate and bended plate design (number of fuel elements, meat and clad thicknesses, ^{235}U mass). It is based on consensually balanced optimization of operator, fuel designer and fuel manufacturer considerations regarding technical and practical issues (performances towards

reactor operation, licensing of the new fuel assembly, schedule of manufacturing and irradiation of the prototype…). Tab 6 compares the main characteristic ratios of the current IRT-4M standard fuel assembly with a selection of other FAs design. In this table, for the FE description, meat thickness (mt) and clad one (ct) are noted as mt/ct (for example for IRT-4M: 0.7 mm for the meat thickness and 0.4 mm for the clad thickness).

Fig 9 and Fig 10 illustrate the standard FAs of the SC1 and SC2 and Fig 11 provides a drawing of the SC2 standard FA cross section. This design takes into account a set of adequate manufacturing tolerances thanks to the exchange with FRAMATOME-CERCA.

In parallel, a coherent process taking into account the absorber guide tube constraint has led to the controlled FA design, based on the same fuel element and same overall shape. This design is known in other research reactors, such as SILOE (see Fig 14) and HOR. This solution also offers the opportunity to add two complementary irradiation or instrumentation channels per controlled fuel assembly (available diameter up to 12 mm).

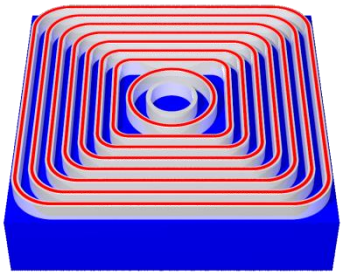

Fig 9. SC1: Standard IRT-4M

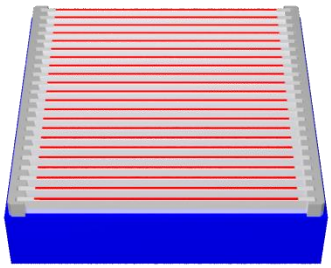

Fig 10. SC2: Standard FA (LVR-15C)

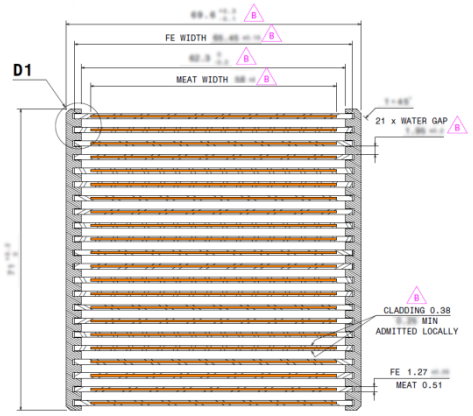

Fig 11. SC2: Drawing of the Standard FA

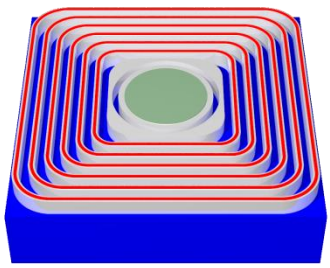

Fig 12. SC1: Controlled IRT-4M

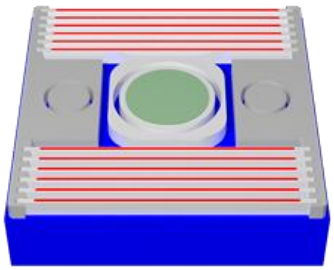

Fig 13. SC2: Controlled FA

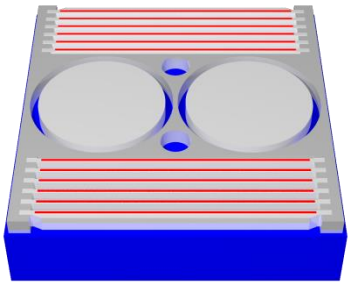

Fig 14. SILOE symmetrical irradiation FA (CEA)

4.3 BRR

For BRR, the following key points have been addressed in the fuel design:

- Core pitch is rather small: 35 mm,
- Shutdown system absorbers and experimental devices are located at fixed slots (red stars on Fig. 15) and the design choice has been to take into account the current locations without any modification,
- For an easier loading in the core support grid, the operator prefers a FA with a flexible behaviour,
- The fuel management is currently performed through 5 FA batches. For the fuel design project, one typical core has been chosen to test the compatibility of the different designs,

– Similar heating and rubbing surfaces to be compatible with the current primary and safety cooling systems have been considered.

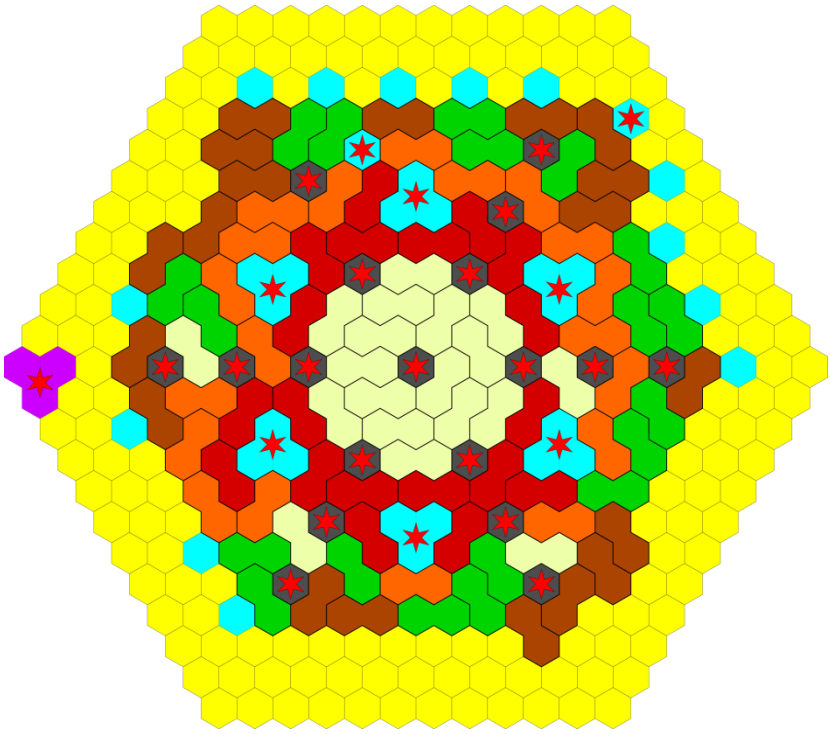

Fig 15: BRR core cross section filled with BRR_C FA taking in a account fixed slots (red stars) and 5 burnup batches.

As a consequence, a preliminary design is based on a double FA with curved plates (or chevron ones) and a flexible mechanical structure provided by the top and bottom nozzles. Fig 16, Fig 17 and Tab 7. illustrate differences between the SC1 FA (Fig 16) and the current design of the SC2 FA (Fig 17). Fig 15 gives an example of the compatibility between SC2 FA and a typical 5-batch core.

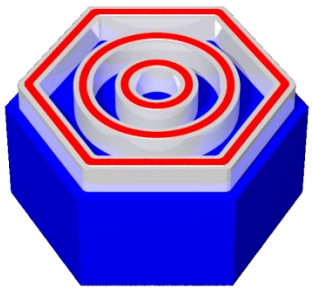

Fig 16. SC1: VVR-M2 UO_2-Al 2.5 $gU.cm^{-3}$

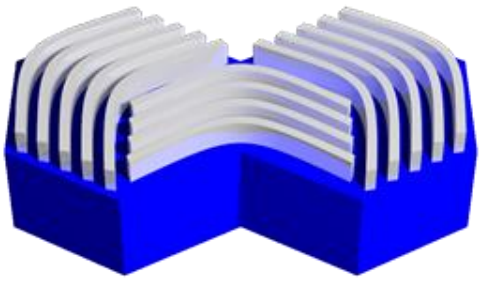

Fig 17. SC2: Preliminary BRR_C FA

	Tubes	**Curved plates**
	SC 1: VVR-M2	**SC 2: ½ BRR_C**
	3 tubes 1.0/0.75	Eq. 7 plates 0.51/0.4-0.59
Water gap (mm)	1.85	1.95 (isthmus: 1.7)
Heating surface ratio	1	1.08
Flow section ratio	1	1.22
^{235}U mass ratio	1	1.33

Tab 7. Ratios between SC1 and SC2 FA

5 Conclusion

In the frame of the LEU-FOREvER project, MARIA, LVR-15 and BRR reactors' common goal is diversification of their fuel supply chain. However, even if they present some similarities, they exhibit different reactor cores, fuel assemblies and shutdown systems. Moreover, the two alternative supply chains use different qualified fabrication processes leading to different fuel assembly designs.

Gathering together reactor operators, fuel designer and manufacturer, the project successfully achieved two fuel assembly designs (standard and controlled) in the case of LVR-15 and also promising trends in the case of BRR, thanks to MARIA's lessons learnt.

Proposed solutions are based on robust and qualified fuel element and proven fabrication process.

Testing, manufacturing and irradiation of one new standard fuel assembly is scheduled in LVR-15, by the end of LEU-FOREvER project.

6 Acknowledgments

This project has received funding from the Euratom research and training programme 2014-2018 under grant agreement No 754378.

7 References

[1] *Horizon 2020 – NFRP-2016-2017 – NFRP-11 – 754378 – LEU-FOREvER*

[2] "*The H2020 European project LEU–FOREVER*" - S. Valance et al., RRFM, 2018, Munich, Germany.

[3] *"Summary of works over MARIA Reactor Core Conversion From HEU to LEU Fuel",* W. Mieleszczenko and al., RERTR 2012, Warsaw, Poland.

[4] "*Maria research reactor conversion to LEU fuel*", G. Krzysztoszek, 2007, Institute of Atomic Energy, Poland

[5] "*Neutronics Analysis of LEU Fuel Assemblies Based on UO_2 in Maria Reactor Core*", Ł. Koszuk et al., RERTR 2012, Warsaw, Poland

[6] "*Brief history of MARIA conversion from HEU to LEU*", M. Migdal et al., RERTR 2014 Vienna, Austria

[7] *Data from IAEA Research Reactors Database* (http://nucleus.iaea.org/RRDB/RR/ReactorSearch.aspx)

[8] "*Calibration of spent fuel measurement assembly*", M. Koleska et al., Radiat. Phys. Chem., 2014, (http://dx.doi)

[9] "*Results of IRT-4M type FA's testing in the WWR-CM reactor (Tashkent)*", V.M. Chernyshov et al., RERTR 2002, San Carlos de Bariloche, Argentina

[10] "*HEU-LEU Core Conversion At Budapest Research Reactor*", G.Toth et al., International Nuclear Safety Journal, 60, vol.3 issue 3, 2014, pp. 60-67

[11] "*Advanced fuel in the Budapest Research Reactor*", T. Hargitai et al.

[12] "*A neutronic feasibility study for leu conversion of the Budapest Research Reactor*", R. B. Pond and al., RERTR 1998, Sao Paulo, Brazil

[13] "*Good Practices for Qualification of High Density Low Enriched Uranium Research Reactor Fuels*", RRFM 1997, Bruges, Belgium
IAEA NP-T-5-2, 2009

[14] "*Safety Evaluation Report related to the Evaluation of Low-Enriched Uranium Silicide-Aluminum Dispersion Fuel for Use in Non-Power Reactors*",
U.S. NRC, Office of Nuclear Reactor Regulation, NUREG1313, July 1988

[15] *"Fuel assembly thermal hydraulics design for an irradiation in an European medium power research reactor*"
R. Duperray et al., RRFM, 2019, Swemieh, Jordan.

[16] "*LEU-FOREvER project preliminary neutronic calculations status*"
J. Koubbi et al., RRFM, 2019, Swemieh, Jordan.

BENCHMARKING OF THE MTR FUEL SIMULATION CODES DART-2D AND MAIA

S. VALANCE, A. MONNIER, H. PALANCHER

CEA, DEN, DEC, Centre de Cadarache, 13108 Saint Paul lez Durance, France

B. YE, A. YACOUT

Argonne National Laboratory, 9700 S Cass Ave, Lemont, IL 60439, USA

ABSTRACT

Understanding the behavior of uranium molybdenum fuels necessitates not only the pursuit of irradiation tests but also the capacity to capitalize gained knowledge in predictive simulation codes. Both the DART-2D and the MAIA computational codes have this purpose. In this paper, a benchmark study of the two codes is carried out using the E-FUTURE test for the reference loading. Both codes are compared with a particular emphasis on the effect of the models specific to dispersed fuels.

1. Introduction

Dispersed uranium-molybdenum (UMo) LEU fuels are investigated as an alternative to the HEU fuels for Material Testing Reactors (MTR). With its utilization as standard MTR fuel, comes the question of predicting its thermo-mechanical behavior in daily operation. Modelling the fuel thermo-mechanical behavior is not only important for the fuel development phase. Robust and reliable computing codes are also crucial for preparing its standardized utilization (qualification).

Consolidating knowledge on the behavior of uranium molybdenum fuels necessitates not only the pursuit of irradiation tests but also the capacity to capitalize gained knowledge in predictive simulation codes. Both the DART-2D and the MAIA computational codes have this purpose.

The DART-2D and the MAIA codes are both dedicated to the prediction of the thermo-mechanical and irradiation behavior of MTR type fuels, and, particularly, UMo fuels. They associate classical thermal – for DART-2D and MAIA – and mechanical – MAIA – computation schemes with specific material evolution laws.

To quantify the capacity of a code to predict a behavior, a first approach usually consists in comparing the calculated data with experimental results. An alternative approach is to carry out benchmark study. Such a methodology is selected here.

In this paper, the structure of the two codes is first described. Then the conditions for the benchmark test are presented. Finally, the results from the two codes are described and commented.

2. Simulation tools description

2.1. DART-2D

The DART (Dispersion Analysis Research Tool) [1] computational code has been developed at Argonne National Laboratory for integrated simulation of the irradiation behavior of aluminum dispersion fuels used in research reactors. DART uses a mechanistic fission-gas-behavior model (the GRASS module) and a set of up-to-date empirical correlations to simulate the change of fuel morphology as a function of burnup. Since 2016, the DART code has been upgraded and modernized to enable it to simulate the irradiation behavior of full sized U-Mo fuel plates up to high burnup [2]. The updated version of the code is named as DART-2D. The current version simulates the irradiation behavior of full-size fuel plates without compromising the detailed description of microstructural changes during irradiation, such as gas bubble formation and growth and grain subdivision.

2.2. MAIA

The code MAIA (Molybdenum uranium Application for Irradiation fuel behavior Analysis) [3], developed by CEA, is a thermal and mechanical simulation code. It is based on the simulation platform PLEIADES dedicated to the behavior of nuclear fuels. With the tools of the PLEIADES architecture, MAIA offers an user-adaptive computation scheme. The meshes are either bi- or tridimensional and cover the main geometries used in MTR reactors i.e. flat and curved full size plates. The physical models include the computation of the interaction layer thickness around the fuel particles, a thermal and mechanical homogenization for the fuel core and several oxidation models for the cladding. The properties and constitutive laws of the common materials are proposed by default in MAIA. Within MAIA, the computations are done on half a transverse slice of the fuel plate as depicted on Figure 1.

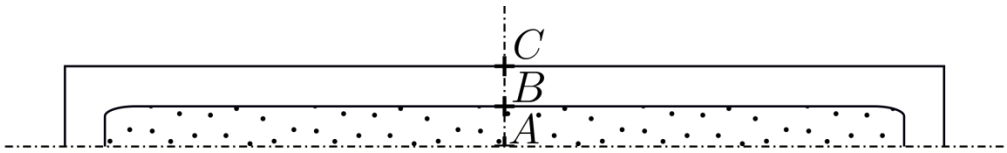

Figure 1: Schematic description of the surface where computations are done in the MAIA code: the half slice in the width-thickness plane of the plate. A stands for the middle of the meat, B for the meat/cladding interface and C is the interface between the cladding and the coolant.

3. Benchmark case description

3.1. Test case

The E-FUTURE irradiation [4] has been chosen as a reference for this benchmark. This irradiation was a selection test in which four flat, full size fuel plates with different manufacturing characteristics were irradiated in the E-FUTURE device in the BR2 reactor at representative powers and to representative burnups for high performance reactors.

The fuel plates consisted of an $8gU.cm^{-3}$ dispersion of atomized low enriched uranium (19.7% ^{235}U) based $U–7_{wght.}\%Mo$ alloy particles in an Al–Si powder mixture matrix with an as-fabricated porosity comprised between 1.2 and 2.6 %.

The E-FUTURE experiment was conducted from June to October 2010 for three BR2 reactor cycles: two times 28 EFPD (Effective Full Power Day) and one time 21 EFPD. Main irradiation features are reported in Table 1.

All plates were subjected to very similar power profiles. Due to the absence of burnable poisons, there is a gradual reduction in power with irradiation time, reaching a value of around 250 $W.cm^{-2}$ at EOL, attaining a local maximum burnup of about 70%^{235}U.

Table 1: Main characteristics of the E-FUTURE irradiation [4].

Plate id.		U7MC4111	U7MC4202	U7MC6111	U7MC6301
Fabrication data					
Cladding		AlFeNi	AG3NE	AlFeNi	AG3NE
Si in Al matrix	wght. %	4	4	6	6
Irradiation data					
Mean BU (MCNP)	$f.cm^{-3}_{U(Mo)}$	$3.36\ 10^{21}$	$3.62\ 10^{21}$	$3.53\ 10^{21}$	$3.57\ 10^{21}$
	$\%^{235}U$	48.3	48.1	47.1	47.5
Peak BU (MCNP)	$f.cm^{-3}_{U(Mo)}$	$5.53\ 10^{21}$	$5.53\ 10^{21}$	$5.31\ 10^{21}$	$5.54\ 10^{21}$
	$\%^{235}U$	71.3	71.3	68.7	71.4
Peak heat flux	$W.cm^{-2}$	457	453	465	472

For this benchmark, Plate U7MC4202 (hereinafter denoted Plate 4202) is selected for simulation. The discharge burn-up for this plate is depicted on Figure 2. At the end of irradiation, the burn-up is slightly higher on one side of the plate compared to the other, nevertheless the burn-up remains rather uniform in the width direction. In the length direction, the burn-up field evolves as expected for a plate irradiation experiment.

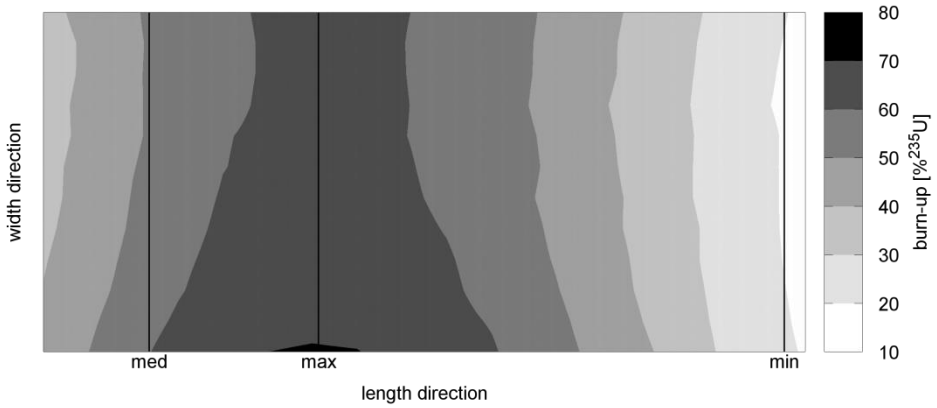

Figure 2: Burn-up field as calculated by MCNP for plate 4202 at the end of the three irradiation cycles. The lines labeled *max*, *med*, and *min* indicate the location of the calculated slices.

For DART-2D, the computations are carried out in the plane of the fuel plate and, for MAIA, in the transverse direction. To allow comparison between the two codes, three slices of the plates were selected where the discharge burn-up level was at the maximum, minimum and average value. These three locations are respectively denoted max, min and med in the following part of this paper and situated in the plate as depicted on Figure 2.

3.2. Material evolution models

In order to compare identical characteristics of the codes, a set of material models issued from the open literature has been specifically selected for benchmarking purpose. Regarding the particularities of the two codes, only the thermal computation chain is affected by these choices. They are as follow:

- Coolant temperature issued from DART-2D computation, used as a boundary condition in MAIA;
- The Colburn heat transfer correlation is used in both codes, to compute the exchange coefficient at the coolant-cladding interface;
- The model proposed by Kim *et al*. [5] is used for oxide growth onto the cladding external surface;
- Use of same thermal conductivity for the constitutive materials of the fuel element;
- The same homogenization approach is used to determine the thermal conductivity of the fuel core;
- Use of the correlation by Kim et al. [6] for the computation of the growth of the interaction layer.

3.3. Test cases

Test cases for the benchmark have been selected to point out potential difference in response to specific models used to depict the thermal behavior of MTR fuels. The test cases are described in Table 2. The test matrix is made to test independently the thermal computation chain (test case number 1) and the different material evolution models (Test cases 2 to 6). Finally, the test case number 7 permits to evaluate the codes capacity using all the MTR specific features.

Table 2: Test cases studied in this benchmark. “X” indicates that the specific model is inhibited.

Test case identification number		1	2	3	4	5	6	7
Model inhibited	Interdiffusion layer growth	X	X			X	X	
	Oxide growth	X		X		X	X	
	Thermal exchange	X	X	X	X	X		
	Thermal conductivity	X					X	

4. Results

4.1. Separate effect tests

For the test cases number 1 to 6 and the three burn-up slices selected (min, med and max), the direct comparison between the DART-2D and MAIA evolutions of central fuel core

temperature (point A on Figure 1) over irradiation time is depicted on Figure 3. It can be seen that the temperatures computed by both codes are close for all 6 test cases. Note that such a comparison has been also done for temperatures on points B and C (defined on Figure 1): a similar conclusion is obtained.

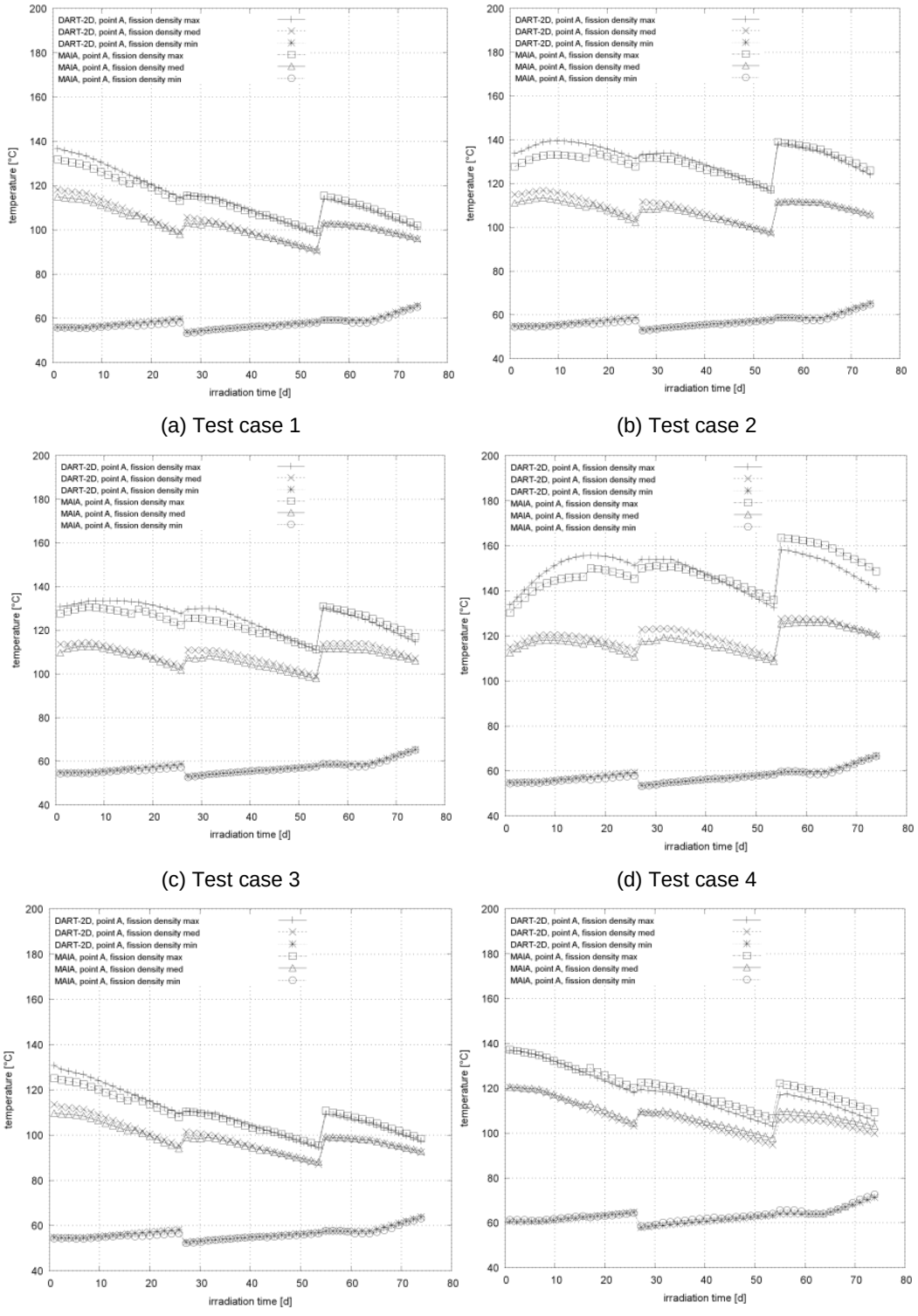

(a) Test case 1

(b) Test case 2

(c) Test case 3

(d) Test case 4

(e) Test case 5

(f) Test case 6

Figure 3: Temperature evolution during the irradiation at point A for the benchmark Test cases 1 to 6.

As shown on Figure 4, the average absolute temperature difference for all the separate effect test cases is lower than 6°C. The test case presenting the largest error is the test case 4. Then

test case number 2 and 3 present a similar error. The integration of the oxidation and interaction layer growth models brings, separately, an error of the same magnitude. When combined, their effects do not compensate and lead to the maximum observed error.

When all specific models are inhibited, as in the test case 1, the results show an average difference of less than 2°C, demonstrating that the difference in implementation does not lead to a large error in the computation. The thermal conductivity model and the thermal exchange model bring a less important error in the computed temperature.

The models for calculating the interaction layer (IL) and the oxide film (OF) thicknesses have a retroactive effect on temperature through the change of conductivity of the material: an increase of either an IL or OF induces a temperature elevation and, in turn, promotes a rise in IL and OF. It is thus not surprising that the error induced by these models is amplified with respect to the one induced by the thermal exchange and thermal conductivity models.

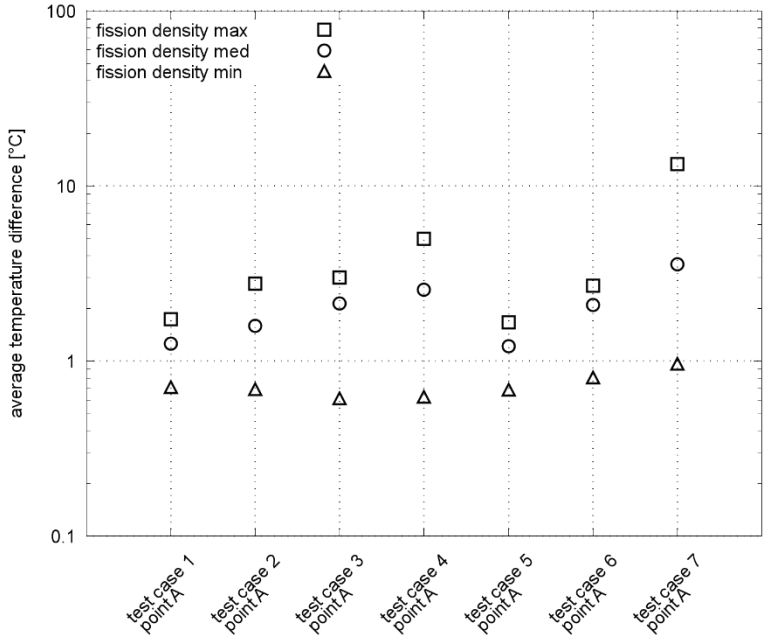

Figure 4: Average absolute temperature difference between DART-2D and the MAIA computations for the 7 different test cases described in Table 2 and at the points depicted on Figure 1.

4.2. Overall temperature difference

Test case number 7 is a full comparison between the temperatures computed with all models activated. The evolution of temperature at the three points through the plate thickness is shown on Figure 5.

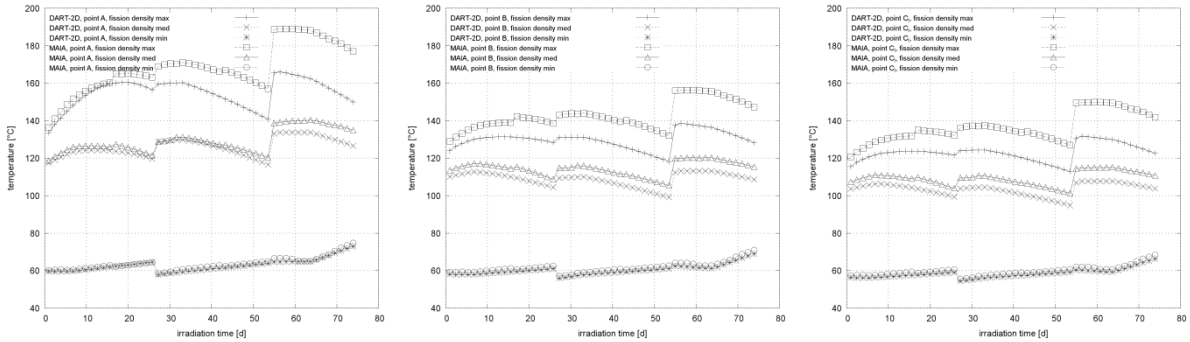

(a) point A (b) point B (b) point C

Figure 5: Temperature evolution for the test case 7 at points A, B and C depicted on Figure 1 and for the three burn-up levels.

As expected from the separate effect test cases, the error is larger when no model is inhibited. However, the results remain close, with an average temperature difference of about 10°C over the complete irradiation cycle at the fuel plate center. Also, the qualitative evolution is identical for both codes.

5. Conclusion

In this paper two computation codes (DART-2D and MAIA) for the simulation of the thermal behavior of MTR plates were benchmarked. This benchmark was focused on the definition of the influence of code structure on calculated temperatures. Therefore material evolution laws were chosen identical. The following points have been identified:

- Despite differences in the computational approach, the response of the two codes structure is close;
- The integration of models specific to MTR fuel plates material behavior increases the discrepancies in the fuel core temperature prediction;
- As expected, the difference is amplified when models included in a feedback loop with temperature are activated;
- When the codes are compared without inhibiting any specific model, the average temperature difference over the irradiation cycle remains limited i.e. about 10°C.

The next step in this study would be to quantify the effect of feedback loops on the temperature difference observed between the two codes.

Acknowledgements

BY fully acknowledges the support of the U.S. Department of Energy, National Nuclear Security Administration (NNSA), Office of Material Management and Minimization (NA-23) Reactor Conversion Program under Contract No. DE-AC02-06CH11357. Argonne, a U.S. Department of Energy Office of Science laboratory, is operated under Contract No. DE-AC02-06CH11357. The U.S. Government retains for itself, and others acting on its behalf, a paid-up nonexclusive, irrevocable worldwide license in said article to reproduce, prepare derivative

works, distribute copies to the public, and perform publicly and display publicly, by or on behalf of the Government.

References

[1] B. Ye, J. Rest, Y. Kim, G. Hofman and B. Dionne, *DART analysis of irradiation behavior of U-MO/Al dispersion fuels,* Nuclear Technology: 191(1), March 2015.

[2] B. Ye, G. Hofman, A. Leenaers, V. Bergeron, V. Kuzminov, S. van den Berghe, Y. Kim and H. Wallin, *A modelling study of the inter-diffusion layer formation in U-Mo/Al dispersion fuel plates at high power,* Journal of Nuclear Materials: 499, February 2018.

[3] V. Marelle, F. Huet and P. Lemoine, *Thermo-mechanical modelling of U-Mo fuels with MAIA,* Research Reactor Fuel Meeting, 2004.

[4] S. van den Berghe, Y. Parthoens, F. Charollais, Y. L. A. Kim, E. Koonen, V. Kuzminov, P. Lemoine, C. Jarousse, H. Guyon, D. Wachs, D. Keiser, A. Robinson, J. Stevens and G. Hofman, *Swelling of U(MO)-Al(Si) dispersion fuel under irradiation - Non-destructive analyses of the LEONIDAS E-FUTURE plates,* Journal of Nuclear Materials: 430(1-3), November 2012.

[5] T. Chae, Y. Kim and A. Yacout, *Overview of Aluminium Oxide Prediction Models or High Power Research Reactors,* ANL/RTR/TM: 18-10, September 2018.

[6] Y. Kim, G. Hofman, H. Ryu, J. Park, A. Robinson and D. Wachs, *Modeling of interaction layer growth between U-Mo particles and an Al Matrix,* Nuclear Engineering and Technology: 45(7), December 2013.

LEU-FOREVER PROJECT: PRELIMINARY NEUTRONIC CALCULATIONS STATUS

J. KOUBBI[1], M. BOYARD, F. HUET
TechnicAtome
CS 50497, 13593 Aix en Provence, France

V. ROMANELLO, A. DAMBROSIO, M. HREHOR
Centrum Výzkumu Řež
Husinec Rez 130, 25068 Husinec Rez, Czech Republic

ABSTRACT

H2020 European LEU-FOREvER Project aims to foster the development of a sustainable low enriched uranium fuel for European Research Reactors; therefore the fuel diversification option is expected as one of its goals. For this purpose, LVR-15 reactor operated by CV Řež was chosen as a case study to evaluate the impact on performances of the core due to a full conversion from LEU-UO_2 to LEU-U_3Si_2 dispersed fuel. This paper describes the status of the preliminary neutronic calculations performed to evaluate the conversion feasibility. The first step of the design process was to perform LVR-15 core calculations with its current fuel using TechnicAtome tool COCONEUT (based on APOLLO2, CRONOS2 and TRIPOLI4® codes) benchmarked with SERPENT-2 and SCALE. In the second step, the same work is done with new designed assemblies. Finally, performances comparisons and assessment between the results obtained by TechnicAtome and CV Řež on these two cores are performed.

1. Introduction

This paper presents the status of the work performed in the frame of the LEU-FOREvER Project [1], focussing on neutronic aspects.

The first part of this article details the main outlines of the project, the main characteristics of LVR-15 reactor and the overall objectives of the work presented hereafter. Then, the second part presents calculation tools used to achieve this benchmark. The synthesis of the Fuel Design process is summarized in the third one and results obtained up to now are presented and discussed in the fourth part. Finally, this paper presents the main conclusions on the work done and lists the main outlooks of this study.

1.1 FOREvER Project

H2020 European LEU-FOREvER Project (2017-2021), associating major actors of the European Research Reactors community – CEA, CV Řež, FRAMATOME - CERCA, ILL, NCBJ, SCK·CEN, TechnicAtome, TUM, aims at fostering the development of sustainable Low Enriched Uranium (LEU) fuels for European Research Reactors.

Some European Medium Power Research Reactors (EU_MPRR) are currently operated with a single qualified LEU dispersed UO_2 based fuel: as part of the LEU-FOREvER project, fuel supply chain diversification is expected for these reactors. In order to fulfil this objective, LVR-15 reactor, operated by Centrum Výzkumu Řež (CVŘ), was chosen as a case study.

[1] corresponding author: jeremy.koubbi@technicatome.com

1.2 LVR-15 Reactor

LVR-15 (Fig 1) is a light water tank-type Research Reactor placed in a stainless steel vessel under a shielding cover operating at power of 10 MWth. Its Fuel Assemblies (FA) are of the IRT-4M type (Russian design) [2] and they are cooled by forced downward flow. The reactor operates at atmospheric pressure, but the fuel is located under a ca. 4 meters water column. Reactor campaigns usually last 3 weeks, followed by an outage lasting 10-14 days for maintenance and fuel reloading; there are also other campaigns which can operate for 'short-time' experiments. Demineralised light water is used as moderator and reflector, but for the latter in some cases also beryllium blocks are included. The reactor fuel is composed of LEU UO_2 (maximum enrichment 19.75%) in an aluminium matrix, enclosed in an aluminium alloy (SAV-1) plate fuel configuration, shaped in concentric closed boxes. The maximum thermal neutron flux is 10^{14} $n.cm^{-2}.s^{-1}$ and absorbers are typically made of boron carbide (B_4C). At the bottom of the vessel are located the 7 Reactor Coolant Pumps (RCP), 5 for normal operation and 2 for emergency auxiliary conditions; pipings are equipped with both isolation and check valves. The maximum inlet and outlet coolant temperatures are, respectively, 45 and 56 °C, while the maximum flow through the primary circuit is 2000 m^3/h [3].

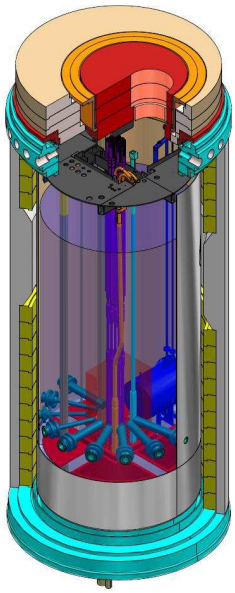

Fig 1. LVR-15 reactor sketch

LVR-15 is currently used mainly for research and industrial applications:

- Material research (irradiation of reactor pressure vessel materials, concrete samples, etc.)
- Corrosion tests of primary circuit and internal structural materials of nuclear power plants in dedicated experimental loops and rigs
- Water chemistry experiments for nuclear power plant primary circuits
- Neutron activation analysis
- Development and production of radiopharmaceuticals (^{153}Sm, ^{161}Tb, ^{165}Dy, ^{166}Ho, ^{169}Er, ^{60}Co, ^{192}Ir, ^{182}Ta, ^{198}Au)
- Production of doped silicon through neutron irradiation for the electronic industry *(the phosphorus doping of silicon utilizing neutron irradiation significantly improves specific resistance homogeneity compared to other methods)*
- Irradiation services (production of radioisotopes: ^{99}Mo-^{99m}Tc, ^{113}Sn-^{113m}In, ^{188}W-^{188}Re)
- Scientific research into horizontal channels (neutron physics and solid phase physics)

As shown in Fig 2, in a typical configuration there are 30 FAs, 15 of which are 8 tubes type and the other 15 are 6 tubes controlled type FAs. The core is always composed of a 6 x 6 "active" part (rows 2–7), in which there are FAs and some uranium irradiation targets (IRE + OK cells), surrounded by beryllium blocks and water displacers; the remaining 2 × 8 part (rows 9 and 10) are water displacers plus one or two "rotation channels" for silicon doping (DONA cells). The configuration is modified according to various the campaigns needs and goals.

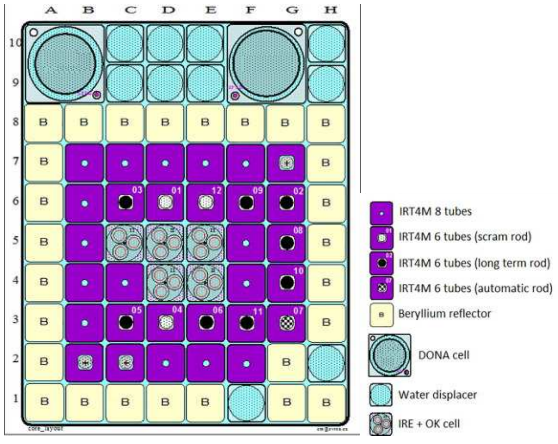

Fig 2. Core layout typical configuration

1.3 General Objectives

The main objective of the work presented hereafter is to benchmark neutronic calculation tools used both by TechnicAtome (TA, fuel and core design) and CVŘ (operation). Through this benchmark the quantification of models and calculation codes biases will be assessed and level of confidence in further calculations will be evaluated. In order to achieve this, a dedicated validation methodology is developed and presented. It aims to acquire the highest level of confidence in calculations to limit potential issues during future fuel studies, namely during support studies to obtain a new operational license from safety regulatory body in Czech Republic (Státní Úřad pro Jadernou Bezpečnost - SUJB).

In order to create a reference point, calculations with the current IRT-4M fuel are done on a dedicated core configuration. For benchmarking purposes, these calculations are performed in parallel by TechnicAtome with its neutronic calculation scheme, COCONEUT2.0 [4] and by CVŘ with SERPENT-2 [5][6] and SCALE [7] codes.
Then performances assessment of this dedicated core completely fuelled with the new fuel assemblies designed is achieved.
Finally, performances comparisons between TA and CVŘ results are provided on a set of neutronic parameters of interest.
This work gives an insight of performances reachable for LVR-15 core fuelled with LEU silicide dispersed fuel.

2. Calculation Tools

2.1 COCONEUT (COre COnception NEUtronic Tool)

Calculations performed by TA are achieved using the neutronic calculation scheme COCONEUT [4][8] (Fig 3). This calculation tool dedicated to Research Reactor design is developed and maintained by TechnicAtome. It is based on CEA (French Atomic and Alternatives Energies Commission) neutronic codes APOLLO2 [9] (deterministic cells and 2D full core transport code), CRONOS2 [10] (deterministic 3D diffusion code) and TRIPOLI4® [11] (probabilistic point wise 3D code).
Linked to COCONEUT, an additional post processing tool, recently developed and named TRAPPISM (Multicode InformationS Polygon Assisted Root Processing), is used to plot results from different calculation sources. This tool enables direct visual comparisons on 3D maps for all neutronic interest parameters, such as fluxes and reaction rates. To perform the benchmark presented here, COCONEUT 2D full core transport calculation is used for the depletion part to obtain material balances. Performances are evaluated with probabilistic code TRIPOLI4® using material balances from APOLLO2 depletion calculations.

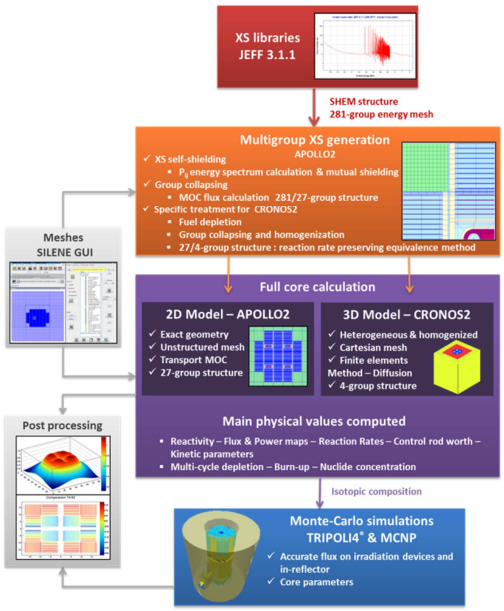

Fig 3. COCONEUT - General Overview

2.2 SERPENT-2 code

SERPENT-2 is a three-dimensional continuous energy Monte Carlo reactor physics burnup calculation code developed at the VTT Technical Research Centre of Finland since 2004. The code development started out as a simplified reactor physics tool, but the capabilities of its current version, SERPENT-2, extend well beyond reactor modelling. The applications can be roughly divided into the following main three broad categories: traditional reactor physics applications (including spatial homogenization, criticality calculations, fuel cycle studies,

research reactor modeling, validation of deterministic transport codes), multi-physics simulations (coupled calculations with thermal-hydraulics, CFD and fuel performance codes), neutron and photon transport simulations (radiation dose rate calculations, shielding, fusion research and medical physics). The neutron transport is based on a combination of conventional surface-to surface ray-tracing and the Woodcock delta-tracking method. Burnup depletion equations are solved using the matrix exponential method CRAM (Chebyshev Rational Approximation Method), providing a robust and accurate solution with a very short computation time and is entirely based on built-in calculation routines, without coupling the code to any external solver. A comparison between CRAM, ORIGEN solver and other TTA (Truncated Taylor Approximation) methods proved the advantages of the CRAM method in terms of accuracy and running time, thanks to its mathematical approach. Continuous-energy cross sections read from the library files are reconstructed on a unionized energy grid, used for all reaction modes: the use of a single energy grid results in a significant speed-up in calculation times, as the number of time consuming grid search iterations performed by CPUs is reduced to a minimum. Macroscopic cross sections for each material are pre-generated before the transport simulation: instead of calculating the cross sections by summing over the constituent nuclides during tracking, the values are read from pre-generated tables, which is another effective strategy useful in order to improve the code overall performance. SERPENT-2 was validated vs. various criticality benchmarks, experiments, research reactors tests, burnup and full core calculations, duly reported and documented in the manuals of the code.

2.3 The SCALE code

SCALE [7] is a package of neutronic computational codes developed by the Oak Ridge National Laboratory (ORNL). It can perform criticality, shielding, radiation source term, spent fuel depletion and decay, reactor physics and sensitivity analyses. The code consists of several modules, among which only 4 were used for the analyses performed for this paper: ORIGEN-S performs the fuel depletion, COUPLE executes the flux-weighted collapse of the cross sections, TRITON [12] performs XS processing and transport calculations, NEWT completes the process with a flux post-processing for the 2D depletion.
SCALE cannot be used to perform 2D Full core transport calculations.

3. Fuel Design Synthesis

This paragraph gives a summary of the Fuel Design Process applied by TA [13]. The first step of the process was to collect relevant interfaces data in order to produce a realistic design:

- Main interfaces between Fuel Assemblies (FA) and Core structures (support grid, reactivity control system…)
- Current Fuel characteristics [2] (Uranium load, ^{235}U enrichment, dimensions…)
- Operational Limits and Conditions (OLCs) (ShutDown Margin (SDM), Power Peaking Factor (PPF)…)
- Cycle length, End of life BU…

These relevant data ensure a good understanding of operational, physical and safety limits related to the reactor. Furthermore, these data are important for designing a new FA compatible with existing components taking into account main interfaces inside the core vessel. The approach adopted in the Fuel Design Process is to provide a new kind of fuel without any significant change of other reactor components (core grid, reactivity control system, cooling…). The Fuel Design Process adopted is driven by conservation of FAs external water channel.

3.1 Comparison of Fuel Assemblies

3.1.1 Standard Fuel Assembly (SFA)

Standard Fuel Assemblies (SFAs) designs are different. IRT-4M is based on concentric squared tubes while Flat Plate Fuel Assembly (FPFA) is based on parallel Fuel Elements (FE) (see Fig 4). Tab 1 gives the main characteristics of both IRT-4M and FPFA SFAs.

Parameters		**IRT-4M**	**FPFA**	$\Delta_{IRT\text{-}4M/FPFA}$
Core grid pitch		7.15cm x 7.15cm		=
Fuel Assembly (FA)	Pitch	6.96cm x 6.96cm	6.96cm x 7.15cm	To be adjusted during Fuel Design Process
	Height	88.2cm		=
Fuel Element (FE)	Meat thickness	0.070cm (UO_2-Al)	0.051cm (U_3Si_2-Al)	+37%
	Cladding thickness	0.045cm (SAV-1)	0.038cm (SAV-1)	+18%
	Meat width		6.01cm	
	Top and bottom fitting	3 cm (SAV-1)		=
	Active height	60 cm		=
	Uranium Density	2.7 $g.cm^{-3}$	4.8 $g.cm^{-3}$	-80%
Number of tubes / FE		8	22	
Inner tube / Side plate (SAV-1)		Thickness - 0.1cm	Thickness - 0.375cm	
		Cylindrical - R 0.7cm	Groove depth - 0.2cm	
Water channel	Internal	0.185cm	0.198cm	-7%
	External	0.095cm	0.095cm	=
^{235}U Mass per FA		300 g	384 g	-28%
Power/FA		328 kW		= for benchmark purposes

Tab 1: SFAs - Main Characteristics

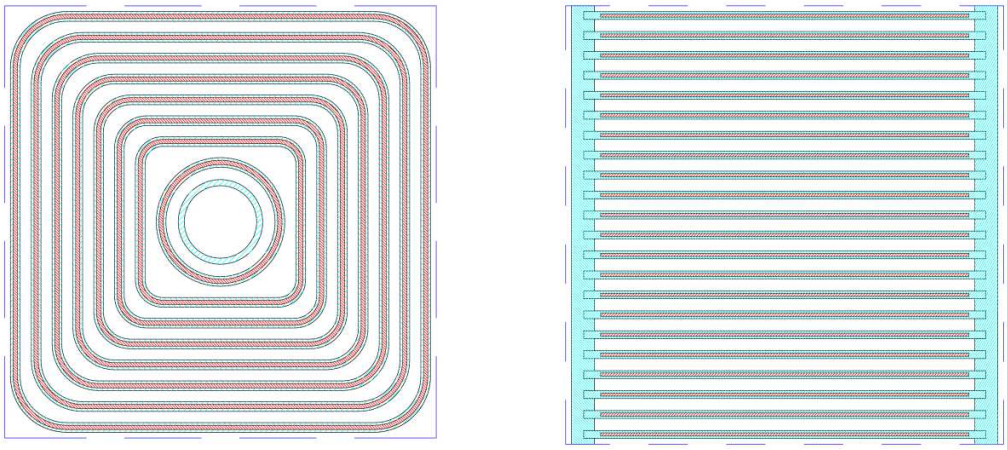

Fig 4. SFAs cross sections - Left: IRT-4M – Right: FPFA

3.1.2 Controlled Fuel Assemblies

As for SFAs, CFAs designs are different (see Fig 5). Tab 2 gives the main characteristics of IRT-4M and FPFA CFAs.

Parameters		IRT-4M	FPFA	$\Delta_{IRT-4M/FPFA}$
Core grid pitch		7.15cm x 7.15cm		=
Fuel Assembly (FA)	Pitch	6.96cm x 6.96cm	6.96cm x 7.15cm	To be adjusted during Fuel Design Process
	Height	88.2cm		=
Fuel Element (FE)	Meat thickness	0.070cm (UO_2-Al)	0.051cm (U_3Si_2-Al)	+37%
	Cladding thickness	0.045cm (SAV-1)	0.038cm (SAV-1)	+18%
	Meat width		6.01cm	
	Top and bottom fitting	3 cm (SAV-1)		=
	Active height	60 cm		=
	Uranium Density	2.7 $g.cm^{-3}$	4.8 $g.cm^{-3}$	-80%
Number of tubes / FE		6	12	
Absorber guide	Shape	Square (2.8cm x 2.8 cm) with rounded corners (R 0.45cm)		=
	Material	SAV-1		=
Absorber	Absorbing part	B_4C Rod – R_{abs} 1 cm		=
	Cladding	Stainless Steel (SS) – 0.15cm		=
Side plate	Thickness	-	0.375cm	
	Groove depth	-	0.2cm	
	Water channel plug	-	1.88cm x 2.8cm	
Irradiation channel	Water hole	-	R_{hole} 0.6cm	+
	Plug	-	R_{plug} 0.5 cm (SAV-1)	+
Water channel	Internal	0,185cm	0.220cm	-19%
	External	0,095cm	0.095cm	=
^{235}U Mass per FA		263 g	209 g	-26%
Power / FA		287 kW		= for benchmark purposes

Tab 2: CFAs - Main Characteristics

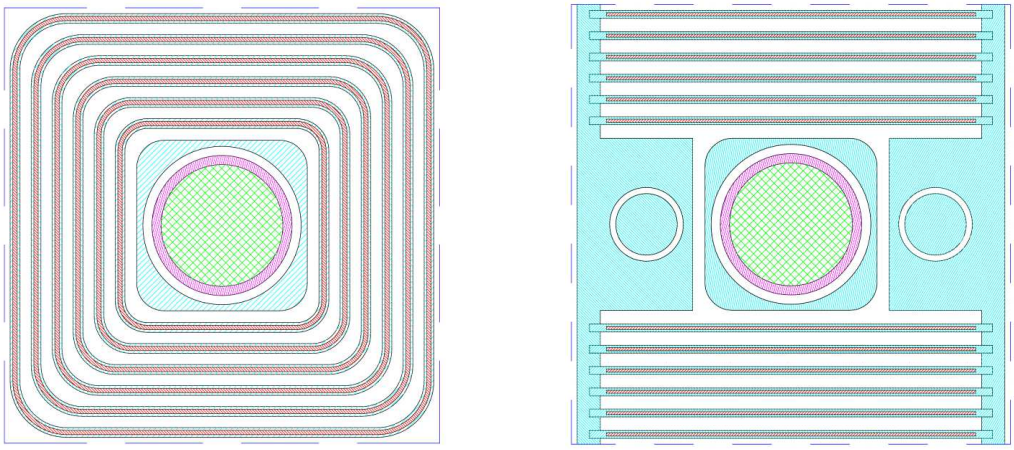

Fig 5. CFAs cross sections - Left: IRT-4M – Right: FPFA

Globally, at core level, total ^{235}U mass is 11% higher in a FPFA core compared to IRT-4M.

3.2 Reactivity

In this paragraph, results obtained for FAs are presented, analysed and discussed. It aims to demonstrate that the new FAs designed by TA and associated calculation models and results are in good agreement. This is the first step of the validation process carried out. Reactivities are compared for SFAs and CFAs without absorbers for fresh fuel in an infinite lattice.

Tab 3 to Tab 6 give Kinf and reactivity effects related to FAs calculations.

TA		**CVŘ**		**Δρ (pcm)**	
A2	1.65305	**SCALE**	1.65333	**A2/SCALE**	-10
T4 (1σ)	1.65380 (15)	**S2 (1σ)**	1.65690 (13)	**T4/S2**	-113 (20)
$\Delta\rho_{A2/T4}$ (pcm)	-27 (15)	**$\Delta\rho_{SCALE/S2}$ (pcm)**	-130 (13)		

Tab 3: SFAs IRT-4M – Reactivity Effects

TA		**CVŘ**		**Δρ (pcm)**	
A2	1.66165	**SCALE**	1.66297	**A2/SCALE**	-48
T4 (1σ)	1.66264 (15)	**S2 (1σ)**	1.66284 (13)	**T4/S2**	-7 (20)
$\Delta\rho_{A2/T4}$ (pcm)	-36 (15)	**$\Delta\rho_{SCALE/S2}$ (pcm)**	5 (13)		

Tab 4: SFAs FPFA – Reactivity Effects

TA		**CVŘ**		**Δρ (pcm)**	
A2	1.63352	**SCALE**	1.63237	**A2/SCALE**	43
T4 (1σ)	1.63417 (11)	**S2 (1σ)**	1.63359 (13)	**T4/S2**	21 (17)
$\Delta\rho_{A2/T4}$ (pcm)	-24 (11)	**$\Delta\rho_{SCALE/S2}$ (pcm)**	-46 (13)		

Tab 5: CFAs IRT-4M – Reactivity Effects

TA		**CVŘ**		**Δρ (pcm)**	
A2	1.57998	**SCALE**	1.57920	**A2/SCALE**	31
T4 (1σ)	1.57938 (13)	**S2 (1σ)**	1.57997 (13)	**T4/S2**	-24 (18)
$\Delta\rho_{A2/T4}$ (pcm)	24 (13)	**$\Delta\rho_{SCALE/S2}$ (pcm)**	-31 (12)		

Tab 6: CFAs FPFA – Reactivity Effects

Results show that both IRT-4M and FPFA reactivities are close (discrepancy max ~50pcm), Thus, models developed are in good agreement. Furthermore, it is noticeable that for these FAs, solver options, energy multi-groups libraries used and calculation procedures carried out for deterministic codes are well tuned.

These comparisons allow us to conclude that models developed and codes used:

- give consistent results
- could be enforced at core level

4. Results and Discussions

In the following paragraphs, results on the dedicated Core Configuration loaded with fresh fuel are presented.

4.1 Full core configuration

To compare and analyse the impact of FA modifications, TA and CVŘ calculate the same following core configuration (see Fig 6) for both types of FAs (including aluminium alloy):

- 20 SFAs and 12 CFAs
- No experimental devices to avoid induced disturbance.

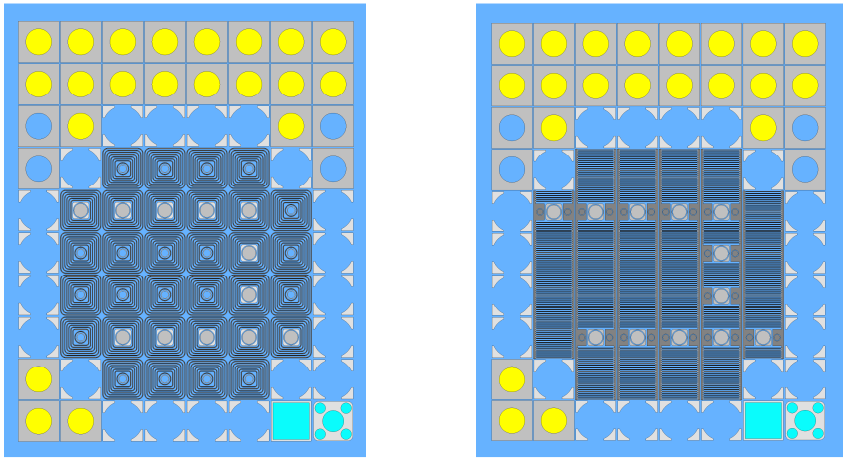

Fig 6. Theoretical core configurations studied – Left: IRT-4M fuel – Right: FPFA fuel

4.2 Neutronic parameters comparison

Tab 7 gives the following neutronic design parameters: Reactivity Excess, βeff, Total Rod Worth and Power Peaking Factor (PPF)[2].

	Fuel Type	TA		CVŘ
		A2	T4 (1σ)	S2 (1σ)
Reactivity Excess (pcm)	IRT-4M	14722	14613 (12)	14537 (7)
	FPFA	12176	12178 (12)	12187 (10)
	$\Delta_{IRT\text{-}4M/FPFA}$	***+17%***	***+17%***	***+16%***
Total Rod Worth (pcm)	IRT-4M	12335	12586 (16)	12555 (18)
	FPFA	12745	13740 (16)	12850 (18)
	$\Delta_{IRT\text{-}4M/FPFA}$	***-3%***	***-8%***	***-2%***
βeff (pcm)	IRT-4M	761.7	767.4 (4)	758.7 (1)
	FPFA	768.5	775.5 (4)	762.8 (1)
	$\Delta_{IRT\text{-}4M/FPFA}$	***-0.9%***	***-1%***	***-1%***
PPF FA	IRT-4M	1.37	1.31 (0.2%)	1.39 (0.04%)
	FPFA	1.44	1.47 (0.1%)	1.48 (0.04%)
	$\Delta_{IRT\text{-}4M/FPFA}$	***-5%***	***-11%***	***-6%***

Tab 7: Main Neutronic parameters at core level

Tab 7 shows a good agreement between deterministic and probabilistic results. Indeed, FPFA core compared to IRT-4M one exhibits:

- Reactivity Excess decrease of about 17%
- PPF rise from 5% to 10%
- similar βeff
- consistent Total Rod Worth, except for A2 (2D full core calculations are not relevant for assessing 3D effects)

Parts of these results are explained by a higher ^{235}U mass and wider water channels.
Such results at both FA and Core levels are encouraging for upcoming burnup calculations.

[2] PPF is related to a whole FA. It means a PPF axially and radially integrated into a given FA.

4.3 Fluxes maps

Fig 7 and Fig 8 present respectively IRT-4M and FPFA core Thermal Fluxes Maps obtained with the different codes used.

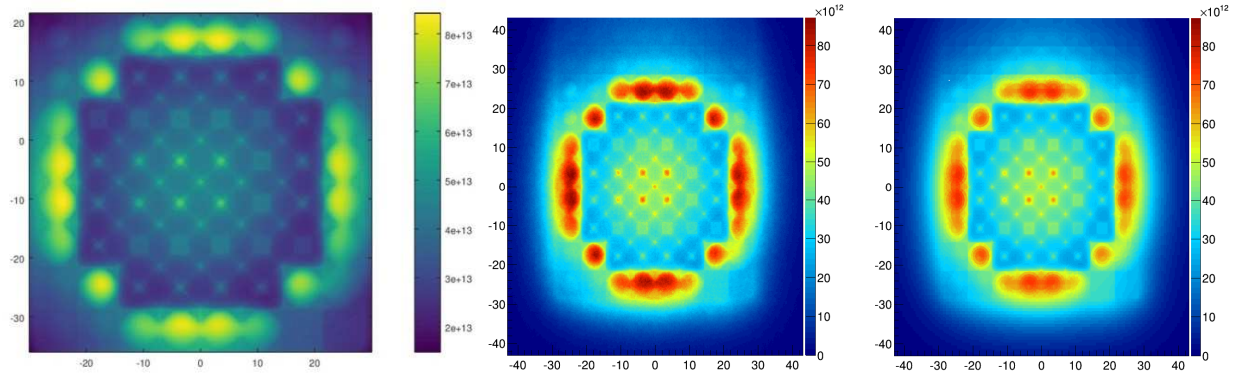

SERPENT-2 TRIPOLI4® APOLLO2

Fig 7. IRT-4M core Thermal Flux Maps

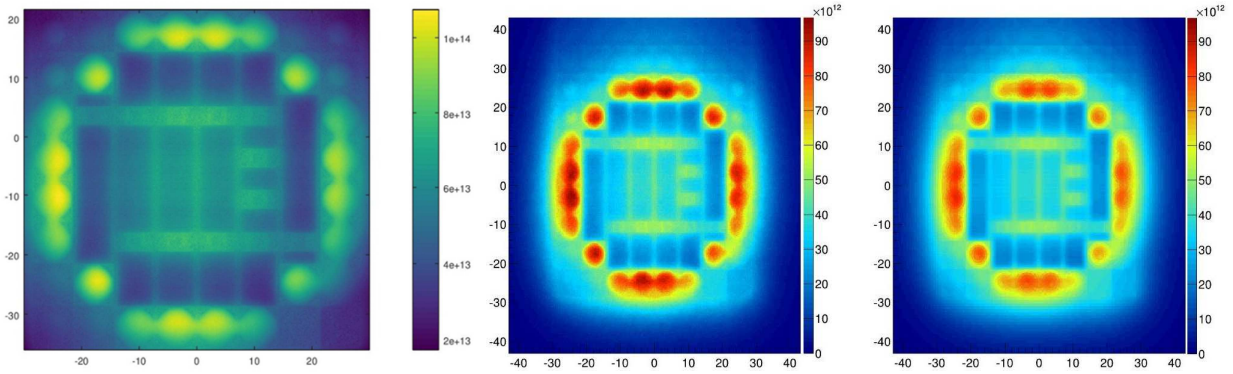

SERPENT-2 TRIPOLI4® APOLLO2

Fig 8. FPFA core Thermal Flux Maps

These maps show the same shape and close absolute values. Concerning A2 and T4 results, discrepancies are in the range $-1\% < \varepsilon < 3\%$. As thermal fluxes maps are in a good agreement, it can be assumed that all reaction rates are calculated properly at core level.

4.4 Cross Check Analyses

All along this benchmark, many Cross Check Analyses are performed at different levels. The first set of Cross Check Analyses is achieved for FAs. Models are tuned to be compliant with one another. A particular attention is paid on axial description of FAs in order to avoid perturbations linked to non-fissile materials above and below FAs.

The second step of Cross Check Analyses is performed for Core Models. Models are corrected and adjusted to be compliant. As for FAs, a particular attention is paid on axial description of component. Calculation parameters are chosen identical for both configurations in the frame of this benchmark.

All results presented here benefit from these Cross Check Analyses, performed either by TA or/and CVŘ.

5. Conclusions and Outlooks

The work performed in this study aims to benchmark TechnicAtome and CV Řez calculation tools. It is part of the LEU-FOREvER project for the fuel supply chain diversification. In this context, the first step of the fuel diversification is to check the alignment between calculations codes used. This step gives stakeholders a good level of confidence in calculation tools used for the project. The further adjustments in the Flat Plate Fuel Assembly design will not engage this confidence and results obtained here can be transposed to safety studies in support to a full FA diversification.

Fuel Assemblies and Fresh Core calculations lead to consistent results. These calculations aimed to demonstrate that results are still in good agreement and the determination of FPFA Core performances can be achieved with a high level of confidence. Moreover, Cross Check Analyses already done as well as the forthcoming ones will strengthen stakeholders in the results obtained and avoid geometry and material balance discrepancies
The next step is burnup core calculations. This phase will start soon and will be updated according to FPFA Design process evolutions.

6. Acknowledgments

The authors want to thank the European Commission for funding the LEU-FOREvER Project and for its permanent interest and support of R&D of Research Reactors in EU countries.

TechnicAtome authors acknowledge sincerely Dr. Laurent Chabert, Dr. Laurent Manifacier, Eng. Julien Couybes and Eng. Simon Nicolas for their kindliness, constant support and helpful advices along this work. Moreover, TechnicAtome authors want to thank Eng. Pierre-Adrien Calas for the first set of calculation performed during his internship. His valuable work was the starting point of this benchmark presented here.

CVŘ authors would like to thank Mr. Vlastimil Juříček for his support in the collection of the LVR-15 reactor data.

7. References

[1] Grant Agreement LEU-FOREvER
Horizon 2020 – NFRP-2016-2017 – NFRP-11 – 754378 – FOREvER

[2] Conversion of Reactor LVR-15 in Czech Republic from HEU to LEU Fuel
V. Brož et al., RRFM Conference, Rome, Italy, 2011

[3] Neutronic analysis of the LVR-15 research reactor using the PARCS code
A. Dambrosio et al., Ann. Nucl. En., vol. 117, pp. 145-154, 2018

[4] COCONEUT: Enhancing Neutronic Design for Research Reactors
J-G. Lacombe et al., RRFM-IGORR Conference, Berlin, Germany, 2016

[5] The Serpent Monte Carlo code: Status, development and applications in 2013
J. E. A. Leppänen, Ann. Nucl. Energy, vol. 82, pp. 142-150, 2015

[6] Serpent - A continuous-energy Monte Carlo Reactor Physics Burnup Calculation Code
J. E. A. Leppänen, VTT, [Online]. Available: http://montecarlo.vtt.fi/

[7] SCALE 6: A Comprehensive Modelling and Simulation Suite for Nuclear Safety Analysis and Design
S. M. Bowman et al., Oak Ridge National Laboratory, Oak Ridge (Tennessee), 2011

[8] COCONEUT: First Validation Steps of the AREVA TA Neutronic Scheme for Research Reactor Design
C. Bouret et al., RRFM-IGORR Conference, Berlin, Germany, 2016

[9] Apollo2 year 2010
R. Sanchez et al., Nuclear Engineering and Technology, 42:474-499, 2010

[10] CRONOS: a modular computational system for neutronic core calculations
J. Lautard et al., IAEA specialist meeting on advanced calculational methods for power reactors, Cadarache, France, 1990

[11] TRIPOLI-4: A 3D continuous-energy Monte Carlo transport code
C.M. Diop et al., PHYTRA1, Marrakech, Morocco, 2007

[12] TRITON: A Multipurpose Transport, Depletion and Sensitivity and Uncertainty Analysis Module
A. Jessee et al., Oak Ridge National Laboratory, Oak Ridge (Tennessee), 2011

[13] Fuel assembly design for an irradiation in an European medium power research reactor
M. Boyard et al. RRFM-IGORR Conference, Swemieh, Jordan, 2019

DEDICATED LOGISTIC PRODUCTS & SERVICES TO OPTIMIZE WASTE MANAGEMENT

CATHERINE GRANDHOMME
Orano TN,
1 rue de Hérons 78180, Montigny le Bretonneux – France

JEAN-FRANÇOIS VALERY
Orano,
Orano Tower, 1 place Jean Millier, 92400 Courbevoie – France

ABSTRACT

Research Reactors activities and dismantling operations of a Nuclear facility induce a large variety of waste to be managed by operators, such as legacy waste, operational and maintenance waste, or dismantling waste. These wastes significantly vary in form, type, volume and activity, leading to implement different transportation packaging solutions and depending of country regulations. Optimization of waste stream management is a key factor in controlling and reducing waste management costs. Orano TN provides logistic solutions for various waste streams. Thanks to its cask portfolio Orano TN can provide to waste producers shuttle transportations, certified pre-owned cask services, giving the best improved and cost and time based logistic solution when the waste form and conditioning are compatible with the cavity and performance of its cask. Besides, Orano TN is also developing new integrated services for radiolysis management or for pool cleanout and offering decision-making tools for the best waste management scenario.

1 Introduction

When operating a nuclear facility or preparing for the decommissioning of a nuclear facility, during its “end of life” management and while performing the dismantling operations, a diverse array of nuclear waste must be considered in terms of types, volumes and activities ranging from High Level Waste (HLW) to Low Level Waste (LLW) with different compositions such as: spent resins; sludge; activated fuel structures; control rods; thimble plugs; in-core instrumentation; contaminated equipment; and activated metallic core components.

The definition of a safe, technically, economically and societally acceptable waste management strategy is highly dependent on the waste policy in each country and on the already available routes. The waste generator and conditioner are responsible for establishing an appropriate waste package, considering the national policy, available conditioning techniques, transport regulations, requirements for interim storage of waste packages, and waste acceptance criteria related to disposal facilities which may not be defined yet.

As of today, when waste is segmented and ready for conditioning, operators are faced with the challenge of packaging, transport, long-term interim storage and final disposal (or preparation for final disposal if the repository is not yet available). Solutions available today are often limited to one single waste type or to a single step in the overall management route from the initial site, where the waste was generated, to its final disposal.

Research Reactors are then frequently facing the obligation of undertaking multiple and costly handling means, reconditioning or re-transferring operations from one package to another, as in the case when moving from on-site storage to transportation or from transportation to final disposal.

Optimization of waste stream management is a key factor in controlling and reducing waste management costs. Waste producers are increasingly expressing their concerns about the complexity, cost and sub-optimization of their waste management strategies.

Our mission is to go with our customers along facility waste lifecycle management whether it comes from Nuclear Installation processes or dismantling activity. Thanks to a long experience Orano TN can manage the waste logistics between producers, recycling facility interim storage zones and final disposal. Following such observations and recent feedback from customers, Orano TN has launched the development of new services to optimize the waste lifecycle management.

2 Orano TN's experience in the logistic of waste

Orano TN provides since more than 20 years, logistic solutions for all different waste streams as shown in the figure 1: for shuttle rotations or for one-way transportation needs between the waste producer and the treatment facility or to the interim storage or disposal site.

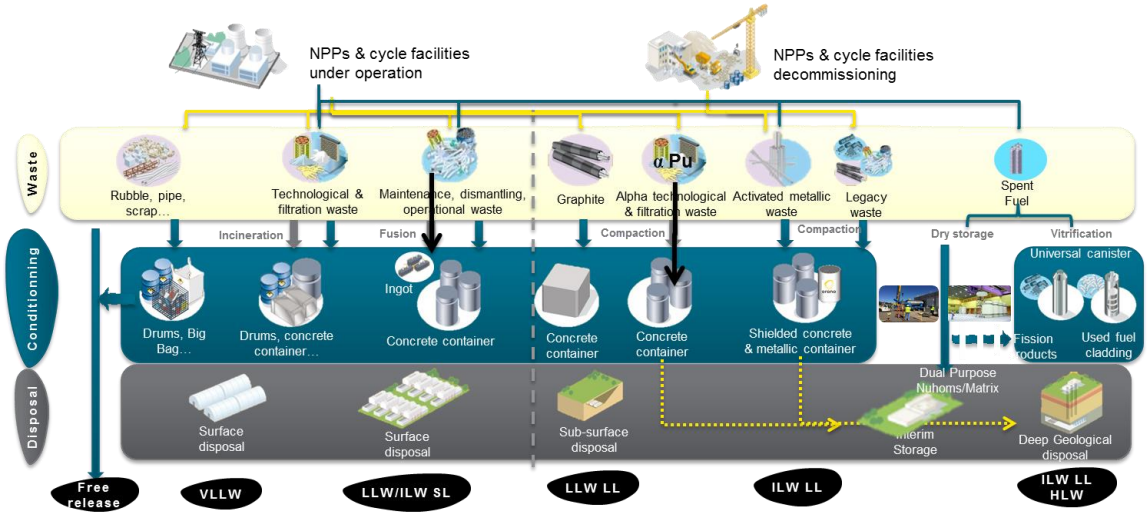

Fig.1: waste stream mapping

Orano TN owns a fleet of transportation and storage packages available for various kinds of waste and conditioning. Orano TN is also able to adapt its existing solutions to any material specificity or even develop customized transport packages with interim or final storage function when needed. By working close with its customers and surveying market and regulatory evolutions, Orano TN develops and enhances continuously its products and services.

To illustrate this capacity to implement a global strategy of waste management, Orano TN operates more than 260 transports per year of LLW / ILW Short Life waste between the Orano La Hague plant and the treatment site or disposal site. This stream is constituted by various types of waste:

- liquid waste transportation in the dedicated "Orcade" IP-2 tank,
- concrete container transportation in the dedicated shielded "CC102" IP-2 cask
- and drums transportation in specific ISO IP-2 container.

All these casks pictured in figure 2 were designed by Orano TN. Casks are proprietary of Orano TN and are leased on yearly contract for this project.

Fig.2 : IP-2 transportation casks designed by Orano TN for LLW and ILW SL waste of La Hague facility

Orano TN is then capable to oversee simultaneously different waste stream to evacuate from a Nuclear facility: benefit is an optimization of cost for the waste producer.

Thanks to its portfolio of packages, extended to the fleet of CEA's packages thanks to a partnership, Orano TN provides waste producers with certified pre-owned cask services, giving the best improved and cost and time based logistic solution. Considering the nature of the waste and its conditioning, the solution could come from its existing fleet.
If not, Orano TN propose consulting and expertise services based on an existing inventory of waste to be transported given by the waste producer.
When the waste producer owns the appropriate package, Orano TN can provide diagnostic, maintenance and repairing services to assure its full compliance with transport regulation.

The figure 3 presents the mapping of Orano TN's packaging fleet categorized by physical form of waste (solid / liquid), and spectrum of waste (alpha / gamma). Sub categories are the purpose of the packaging (transport only or transport + interim storage on site = dual purpose) and the type of transportation certificate according to AIEA (IP-2 or B).

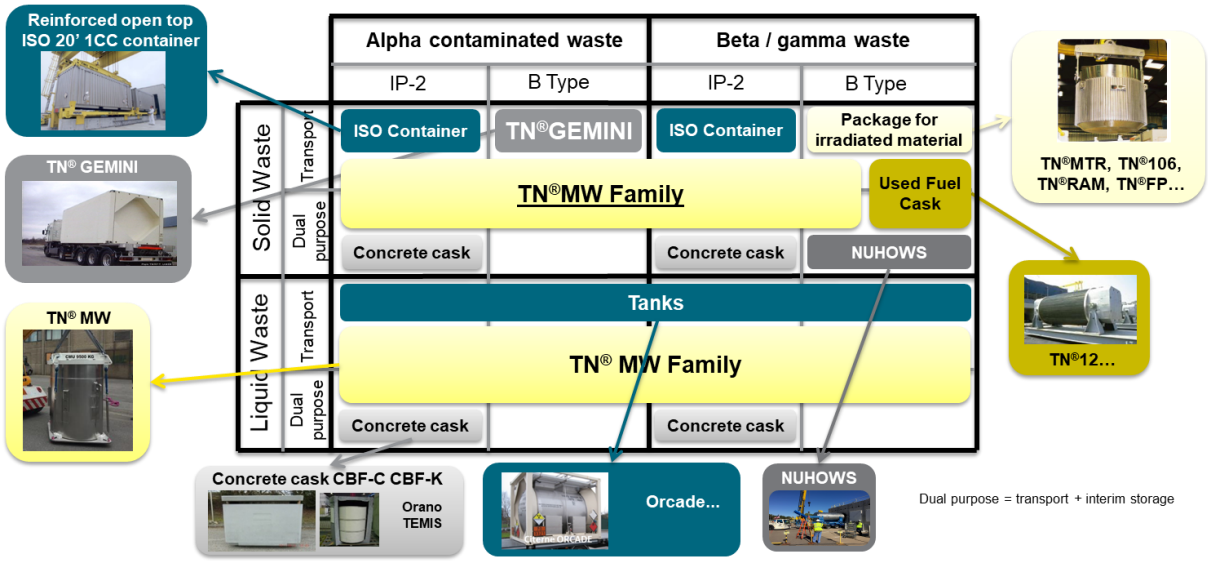

Fig.3: Orano TN's cask mapping

For waste with no existing transport and storage solutions, Orano TN is developing a new range of casks Dual Purpose compliant, and if needed Triple Purpose, to optimize the overall waste streams supply chain. This new range of casks is the TN®MW family described in the paper [1] and poster [2], gathering Orano TN proven technologies coming from its long experience and know-how from Used Fuel Dual Purposes casks and Research Reactors dedicated waste transport "compacted" casks.

2.1 Project reference of certified pre-owned cask services

Its consists in the leasing to customer of waste cask proprietary of Orano TN or its partner, which were originally designed for another project. More often the concerned casks were originally designed to transport drums of technological waste, with a type B certificate. They can now be used for on-site transfer drums or temporary storage on Nuclear facility site to gain place inside the facility.
After checking that the waste is perfectly compatible with the capacity of the cask and its certificate, Orano TN delivers the cask with its associated tools and equipment to the facility defined by the customer. It is then the responsibility of the customer to operate the cask for loading / unloading operations.
If required by the customer, Orano TN can provide technical assistance (especially for type B cask to realize leak tightness test).
The benefit of this service for customer is to minimize cost of design and licensing.

This can be demonstrated with the RD26 cask (Tab.1), which is a small cask for plutonium waste. The RD26 cask was designed as type B packaging for technological waste conditioned in drum of 100 or 118 liters and used for CEA facilities.
A Nuclear operator inside La Hague site faced to an issue of saturation of storage place in its nuclear building and need to transfer some technological plutonium waste conditioned in drums in another nuclear building inside La Hague site. After a feasibility study, Orano TN leased two units of RD26 without any modifications from its fleet for this on-site transfer. Orano TN additionally drew up specific operating instructions to be compliant to the site requirements and operational constraints. Orano TN was also in charge of technical assistance to operators to perform leak tightness tests (see figure 4). The overall duration project, from the launching of the feasibility study to find the appropriate cask candidate, until the on-site transfer operations lasted less than 2 years and finished in 2018.

Fig. 4 : On site transfer of technological waste with the RD26 cask : opening of the cask, leak tightness test after closing and loading inside the container for transport

Main Features

	Loaded	Empty
Mass	610 kg 1 344 lbs	150 kg 330,7 lbs
	Diameter	**Height**
Cavity	513 mm 20,2 in	780 mm 30,7 in
Overall	900 x 900 mm (in build pallet) 35,4 x 35,4 in	1 145 mm 45,1 in

Tab. 1: Main features of RD26 cask

This service constitutes an economic solution and is always investigated by Orano TN during the step of feasibility study to determine the best transportation scenario. This service is applicable for all types of casks even those originally designed for used fuel or irradiated

material. There were licensed as type B fissile packaging. They are now also suitable for high activated material and specially to long metallic pieces with variable geometry thanks to their large cavity. The benefit for customer is to get economic solution to transport big pieces when dismantling high activated parts of facility such as control grids, reactor vessel, by saving multiple cutting costs.

2.2 Reinstatement of customer's fleet

Thanks to experience of reinstatement of its own fleet, Orano TN is now offering this new service to his customer. When the customer owns a cask which is compatible with loading of the waste but the cask was no more used, Orano TN can offer an expertise of the state of the cask and proposes a diagnostic to reinstate the cask to be compliant with safety requirements.

As a recent example, LLW Repository Ltd, a key UK nuclear waste management company, are the custodian of 3 existing TN®Gemini NDA assets, that were manufactured and delivered by Orano TN in the early 2000 and were not operated for the past 10 years. LLW Repository provide strategic Type B transport packaging capability through this TN®Gemini fleet to transfer legacy alpha contaminated drums from different UK Nuclear Installations to an interim storage facility.

As a high-integrity waste transport solution, the TN®Gemini container (see Tab. 2) is a market-leading package, with high volumetric transport capacity, high flexibility in the variety of loaded waste and with a French and UK acclaimed safety pedigree since 2000.

LLW Repository has contracts in place with Orano TN, as TN®GEMINI Design Authority and manufacturer, to reinstate its existing UK fleet in full compliance and conformity with Safety Analysis Report (SAR) requirements. The scope of these contracts includes the modernization, the maintenance and life cycle technical services for TN®GEMINI UK fleet. Orano TN is also supplying new internal arrangements (see fig. 6), recently approved by the Nuclear Safety Authority, enhancing the TN®Gemini container capacity to transport ILW waste.

The return to service activity of the TN®Gemini fleet considers Orano TN's know-how acquired through the licensing, manufacturing, maintaining and operating this type B container for more than 20 years. To achieve full conformity and compliance of the fleet, specific and complex manufacturing operations are deployed, sometimes making use of technology transfer from other business sectors or requiring a high level of skill in the packaging manufacture. The guiding principle of all work performed to reinstate the fleet capability consists in maintaining the safety analysis report compliance thanks to an Orano TN multidisciplinary task force team.

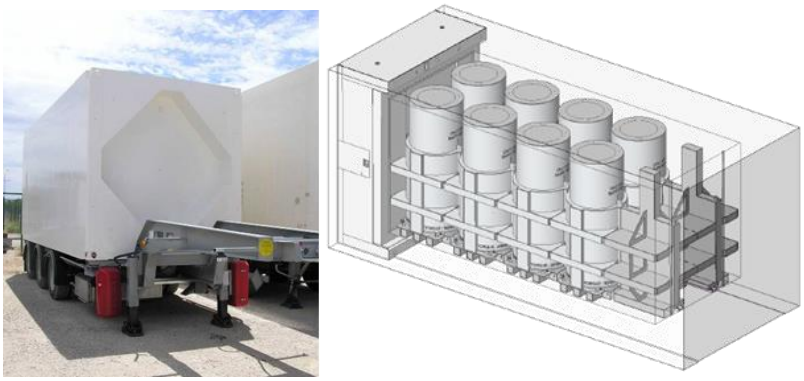

Fig. 5: TN®GEMINI type B container and a new design of internal arrangement to optimize ILW drum transportation

Main characteristics of the TN GEMINI™ packaging

Internal dimensions
Width : 1840 mm
Height : 2000 mm
Length : 4510 mm

Container with ISO corners
Dimensions: 2500 x 2650 x 6058

Mass :
Empty : 24 200 kg
Total : 30 000 kg

Tab. 2: Main features of TN®GEMINI

3 New integrated services

3.1 Management of radiolysis waste by getter oxide

The radiolysis phenomenon is of great importance in the waste conditioning issue. An evaluation/mitigation of hydrogen generation in packages is necessary to ensure that a flammable mixture will not be formed and to verify that casks do not accumulate an unsafe concentration of hydrogen (lower flammable limit (LFL) for H_2 < 4% vol. at room temperature in air).
To better adapt to changing disposal requirements, provisions have been integrated into the design of the cask to allow for different configurations or to conduct additional operations prior to disposal [1]:
- A drying system to remove moisture (free liquid for storage or disposal must be removed to avoid any chemical reaction)
- A system to fill the cask cavity with “blocking material” without having to reopen the lid
- A semi-porous gas venting system (if needed, to evacuate radiolysis gases while avoiding entry of humidity into the cask).

The evaluation of gas coming from radiolysis presents several advantages: (i) to predict and to help define the content of the waste container to avoid exceeding limits; (ii) to design the capacity of a suitable hydrogen getter.

CEA and Orano TN have carried out R&D programs [3] with the aim of qualify a getter oxide as “blocking material” (see fig. 7) until the industrial design step. Hydrogen is absorbed by these materials and chemically bound irreversibly in the crystalline structure. It presents a lot of advantages:
- Increasing safety margin during transportation to fulfill with Low Limit of explosivity criterion of H_2 in the air (4% at ambient temperature)
- Not reducing waste filling volume in the cavity
- Not having to reopen the lid
- Being predictable for long period of storage
- Reducing drying time in case of continuous evacuation

The oxide getter qualified is suitable for all contents releasing dihydrogen, for ambient atmosphere. There is no chemical interaction, no ageing, no hydrogen release even after a mechanical action. It is compact and can be put in tricky space.

It is effective up to high temperature (around 400°C) and under high gamma radiation with following performance: 1kg of getters absorbs more than 100 NL of H_2.

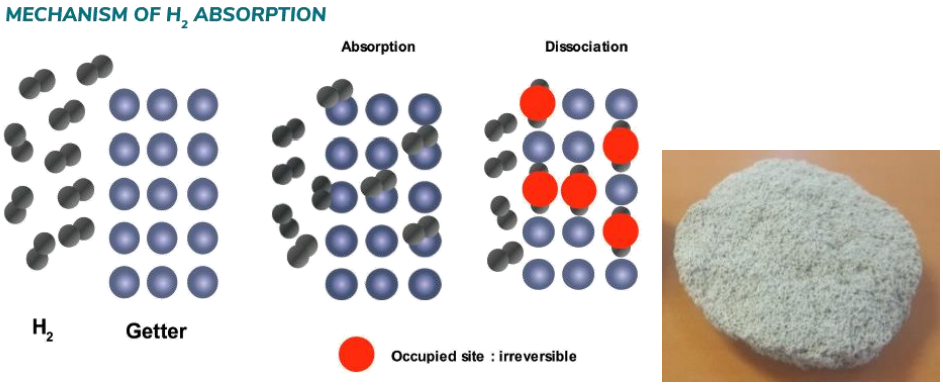

Fig. 6: Mechanism of H_2 absorption and picture of “brut” material before conditioning

The first reference of application of this getter approved by French competent authority is expected to be for the transportation of activated metallic waste in the TN®117 cask at the end of 2019.

Orano TN proposes all-inclusive services to implement this new industrial, simple and effective solution to eliminate H_2 produced by waste.

3.2 Pool clean out with reduction of waste volume

Orano TN offers also a comprehensive and optimized nuclear waste management from retrieval to disposal, through treatment and volume optimization from waste management services to decommissioning activities such as pool cleanout services.

Benefit for facility user is reduction of waste volume and optimization of transportation costs. Orano TN offers all-inclusive services including onsite support to load and unload wastes from reactors, but also transportation services to storage sites.
Orano TN has been gathering experience for LLW transport in the US since more than 30 years for irradiated waste: control rod, fuel channel. Recently in 2018 Orano TN and Babcock Services Inc. (BSI) have signed a long-term partnership to provide high quality and innovative services to nuclear power plant operators. In turn, Orano TN completed the purchase of BSI-developed, state-of-the-art and industry-proven equipment for the processing of irradiated hardware, which includes: activated services shear, activated services punch, velocity limiter shear, mobile rod cutter, and various other support and handling equipment.

As the owner of the TN®RAM cask (see Tab.3), a critical component and workhorse for irradiated reactor components transport, Orano TN can now offer turnkey services for pool cleanout projects. Orano TN will continue to utilize the full support of BSI’s engineering, innovation and project experts to ensure the highest level of quality is maintained and the most cost-effective services are provided. While these equipment and services apply more towards BWRs, PWR operators can also benefit from this technology. BSI and Orano TN recently used this equipment and expertise to successfully package irradiated hardware and remove spent fuel storage racks at a shutdown PWR nuclear power plant (see fig. 8).

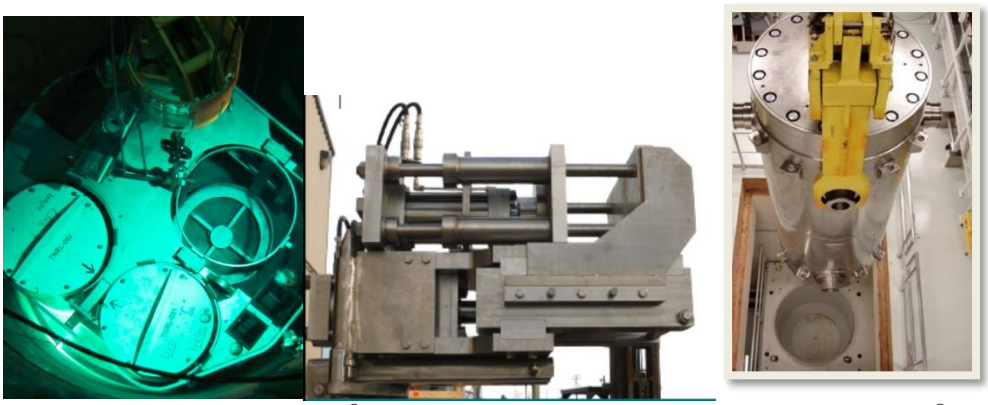

Fig.7: Example of pool to pad with TN®RAM cask: pool view, cutting machine, handling of TN®RAM cask

	Diameter	Height
External dimensions (with shock absorbers)	2336.8 mm 92 inches	4521.2 mm 178 inches
Cavity dimensions - max	889 mm 35 inches	2819.4 mm 111 inches
Maximum payload	4.3 T (9,500 pounds)	
Maximum weight (with shock absorber)	36.3 T (80,000 pounds)	

Tab.3: Main features of TN®RAM

This project shows the capacity of Orano TN to offer an integrated service to answer to dismantling operator's needs. Application for Research Reactors waste management is then possible with another cask, such as TN®MW for example.

4 Conclusions

With respect to the various waste generated during a Research Reactor's life time, such as legacy waste, operational and maintenance waste, and dismantling waste with different forms, optimization of waste lifecycle management is a key factor in controlling and reducing waste management costs.

Orano TN can oversee the global waste logistics between waste producers, recycling facility, interim storage zones and final disposal. Orano TN owns a fleet of transportation and storage packages available for various kind of waste and conditioning. Orano TN can also adapt its solutions to any material specificity or even develop customized transport packages with interim or final storage function when needed. Orano TN offers also to extend the transportation service to integrated service including the radiolysis management or the reduction of waste volume.
Working close with its customers and surveying market and regulatory evolutions, Orano TN proposes services useable as decision-making tools for customers in their waste management program:

- the definition and comparison between different logistic scenarios upgraded all along the project of the customer
- the simulation of the scenario via the virtual reality that let to integrate cask in the nuclear facility, predict the operational interface constraints and limit the risk during the realization of the project (see fig. 9).

To go further, Orano TN is developing a new way to work more closely with their customers in their facilities or in the dismantling site, based on collaborative tools which let each user to connect from any place at the same time to the same virtual site.

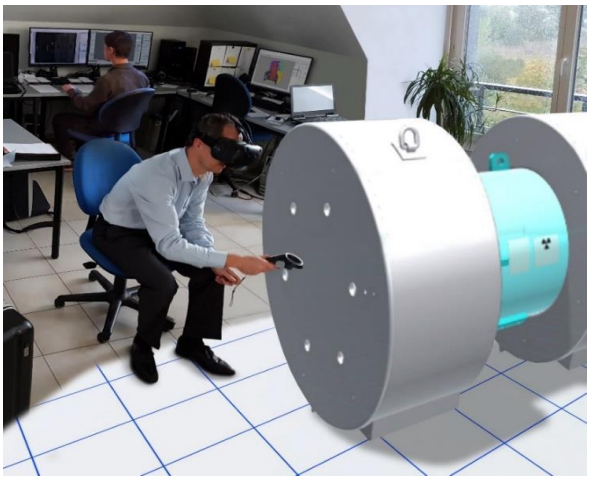

Fig.8 : Virtual reality illustration

5 References

[1] C. Lamouroux, E. Leoni, J.M. Grygiel, “Does the perfect Waste Package exist? Optimizing waste management routes”, Proceedings of Global 2017, Seoul, Korea, September, 2017.

[2] A. Talbi, M. Ghobrini, J-F. Valery, V. Vo Van, C. Lamouroux, C. Grandhomme, B. Kerr, “The TN®MW, a new optimized cask for Research Reactors’ waste management”, RRFM 2019, March 2019, Jordan.

[3] H. Issard, D. Saffré, R.Ghazal, D. Lambertin, “Technologies for integrated safety management regarding gas generation in spent fuel wet or dry transport systems IAEA CN-226, International Conference on the Management of Spent Fuel from Nuclear Power Reactors, 15-19 June 2015, Vienna, Austria

ANALYSIS OF LOW POWER, HIGH POWER AND TRANSIENT POWER COMMISSIONING TESTS IN THE CABRI REACTOR

J.P. HUDELOT, Y. GARNIER, B. DUC, P. FOUGERAS, J. LECERF, B. BIARD, L. PANTERA, O. CLAMENS
CEA, DEN, DER/SPESI, Cadarache, F-13108 Saint Paul les Durance, France

M. MAILLOT
CEA, DEN, DER/SPRC, Cadarache, F-13108 Saint Paul les Durance, France

B. BIARD
Institut de Radioprotection et de Sûreté Nucléaire
Cadarache, BP3 13115 Saint-Paul-Lez-Durance Cedex, France

ABSTRACT

This paper presents this analysis of the low power, high power and transient power commissioning tests of the CABRI reactor that were performed from 2015 to 2017. The comparison between experimental results and calculational results is given and concludes to a good consistency. Those tests allowed defining the authorized domain of operation of CABRI, better mastering the boundary conditions of the CABRI RIA tests and validating the reference neutronic calculation scheme used for safety and design studies.

1. Introduction

CABRI is an experimental pulsed reactor funded by IRSN (French Institute of Nuclear Safety and Radioprotection) and operated by CEA at the Cadarache research center. Since 1978, the experimental programs in CABRI have been aimed at studying the fuel behavior under Reactivity Initiated Accident (RIA) conditions. In order to study the PWR high burn up fuel behavior, the facility was modified to have a water loop able to provide thermal-hydraulic conditions representative of the nominal operating PWR's ones (155 bar, 300°C).

This project, which began in 2003 and ended in 2015, was driven within a broader scope including an overall facility refurbishment and a safety review. The global modification was conducted by CEA. The experiments take place in the framework of the OECD/NEA Project CIP (CABRI International Program) which is operated and managed by IRSN. IRSN finances the refurbishment and the operation of the CABRI reactor that is currently put at disposal of the IRSN for investigations into the safety of fuel.

In the framework of the reactor restart, commissioning tests were realized for all equipment, systems and circuits of the reactor. This paper particularly focuses on the analysis of low power, high power and transient power commissioning tests that were done from 2015 to 2017.

After a short description of the CABRI facility, one describes in a second part the physical parameters to be measured and the associated experimental techniques and target uncertainties. The third part describes the instrumentation that was designed and implemented in the core to enable those measurements. The fourth part gives the main experimental results that were obtained during the low power (< 100kW) neutronic commissioning tests and gives the comparison with reference calculation performed with the TRIPOLI4 French stochastic code. The final fifth part gives the main results about the core high power calibration in steady states (up to 23.7MW) and in transient states (up to ~20GW).

2. General presentation of CABRI

The CABRI facility (see Fig. 1, left figure) is made of the CABRI core and of three main systems (pressurized water loop, transient rods and primary cooling system) allowing to perform transient tests (RIA, LOCA) with a high level of representativeness, accuracy and safety [1]. Those different components of the facility are described in the following sections.

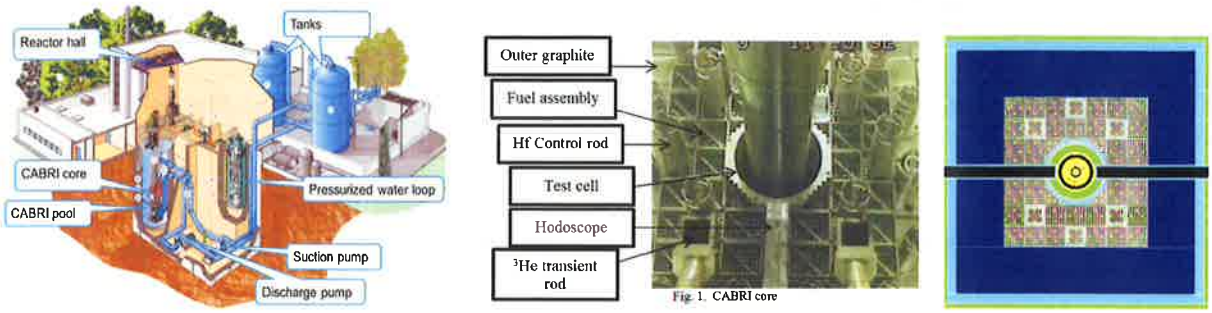

Fig. 1. Overall view of the CABRI facility (left); Top view of the CABRI core (center) – Radial cut of TRIPOLI4 model of CABRI (right)

2.1. CABRI Core

CABRI is a pool-type reactor, with a core made of 1487 stainless steel clad fuel rods with 6% enriched ^{235}U. The reactor is able to reach a 23.7MW steady state power level and ~21GW in transient state. The reactivity is controlled via 6 control and safety rods made of 23 hafnium pins each (see Fig. 1, central figure).

2.2 Pressurized Water Loop

The new test loop allows reproducing the thermal hydraulics conditions of a pressurized water reactor (300°C, 155bar, up to 6m^3/h flowrate). It is composed (see Fig. 1, left figure) of an in-pile part connected to the experimental device and of an outside tank containing the main components (pressurizer, pump, regulation valves…).

2.3 Transient Rods Circuit

The key feature of the CABRI reactor is its reactivity injection system [2]. This device allows the very fast depressurization into a discharge tank of the ^3He (strong neutron absorber) previously introduced inside 96 tubes (so called "transient rods") located among the fuel rods (see Fig.1 (right figure) and Fig. 2). The rapid absorber depressurization translates into an equivalent reactivity injection possibly reaching 4$ within a few 10ms. The power consequently bursts from 100kW up to ~20GW (see Fig. 3) in a few milliseconds and decreases just as fast due to the Doppler effect and other delayed reactivity feedbacks. The total energy deposit in the tested rod is adjusted by dropping the control and safety rods after the power transient.

2.4 Primary Cooling System

The primary cooling system [3] is illustrated in Fig. 1 (left figure). A steady water flowrate (up to 3215m^3/h) is needed to cool the fuel pins of the reactor driver core so as to respect the safety margins about the temperature of the claddings and of the oxide fuel during the power steady states and transients. The two tanks (250m^3 each) feeding the cooling system are visible in the background.

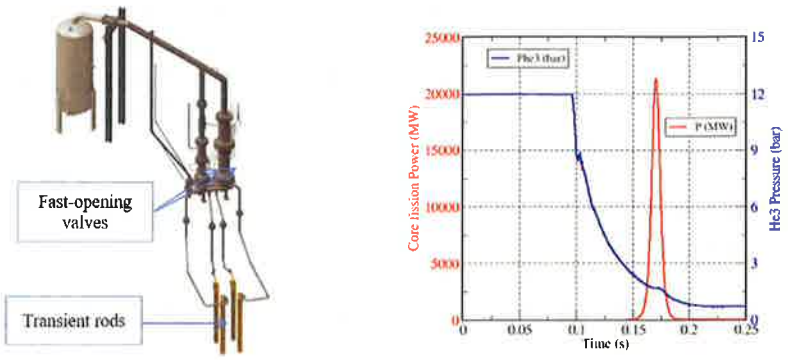

Fig. 2. Global view of the transient rods system (left) and of the typical CABRI ^{3}He Pressure and core power shapes during a RIA transient (right).

2.5. CABRI calculation scheme

Calculations were performed using a 3D and real geometry model of CABRI (see Fig. 1, right figure) with the TRIPOLI-4 French Monte Carlo code [4] and the JEFF3.1.1 nuclear data library. An important effort has been carried out to control as well as possible the metrology and the material balance of the different components of the CABRI core.

3. Measured quantities – instrumentation, experimental techniques and target uncertainties

The neutronic characterization of the core addressed three main goals:

- To prove the ability to accurately predict the safety parameters for the reactor operation and to effectively control the reactor,
- To validate the neutronic calculation scheme of the CABRI reactor,
- To provide very accurate and appropriate neutronic initial boundary conditions for the RIA tests performed in CABRI.

The neutronic parameters measured at low power are synthetized in Tab. 1 that also gives the associated instrumentation, measurement techniques and target uncertainties. A total of more than 200 measurements have been performed. Details on experimental techniques can be found in reference [5].

As for high power commissioning tests, they were conducted in 2016 and 2017. They were based on calibrating the response of experimental boron chambers vs. the power level and energy deposit in the core, measured through thermal balance measurements. This calibration was first performed during steady state operation conditions, from 8MW to 23MW. They were then followed during transient state operation conditions up to ~20GW. The measured physical quantities during thermal balance measurements are the coolant flowrate and the inlet and outlet temperatures (see Fig. 3; right figure). Associated instrumentation, experimental techniques and target uncertainties are given in Tab. 2.

3.1 Position of the core instrumentation

Fig. 3 describes the nature (see Tab. 1 and Tab. 2 for details) and the position of the different types of instrumentation that were used, both inside and outside the core.

Fig. 4 details the dosimetry program, the different types of dosimeters and their supports. Wire dosimeters were inserted inside aluminum tubes. Each tube is made of 5 gold wires and 5

cobalt wires equally alternated and positioned symmetrically as regard to the mid plane of the core. A total of 20 wire dosimeters have been irradiated in the center of the test cell in order to measure the axial flux profile. Depending on the configuration of the test cell, voided or filled, dosimeters have been irradiated at a power of respectively 2.5kW and 25kW during one hour. A total of 60 disk dosimeters (ø 4 or 10mm, thickness from 0.05 to 0.125mm) corresponding to 5 radial and 16 axial locations on a dedicated aluminum holder (see Fig. 4) were also irradiated in the core of CABRI at a power of ~2.5kW during one hour, in order to get the axial and radial flux profile inside the core.
After shipment to the MADERE platform [6] of CEA Cadarache, gamma-spectrometry measurements on measurement benches equipped with High Purity Germanium (HPGe) detectors have been performed on all dosimeters.

Measured neutronic parameters	**Instrumentation**	**Experimental technique**	**Target uncertainty (2σ)**
Critical states in several configurations of operation	Low-level Fission Chambers High-level boron chambers	Critical state	± 2mm
Integral reactivity worth of the control rods Differential reactivity worth of the control rods	Low-level Fission Chambers High-level boron chambers	Rod drop + MSM Method [7] Doubling time method	± 10% ± 10%
Isothermal temperature coefficient	Low-level Fission Chambers High-level boron chambers Thermocouples	Critical state	± 2pcm/°C
Kinetics parameters	CFUL01 fission chambers High-level boron chambers	Feynman-α and Rossi-α method [8]	± 6%
Axial and radial flux profile	Au and Co wire and disk dosimeters	Dosimetry	± 4%
Reactivity worth of helium-3 inside the transient rods	Low-level Fission Chambers High-level boron chambers Thermocouples Piezo-resistive pressure captors	Critical state + Sum of differential reactivity worth of the control rods	± 10%

Tab. 1. Neutronic parameters, associated instrumentation, measurement techniques and target uncertainties for low power neutronic commissioning tests

Measured physical quantity	**Instrumentation**	**Experimental technique**	**Target uncertainty (2σ)**
Inlet and oulet core flowrates	Annubar and ultrasonic sensor	Preliminary calibration of the detectors	
Inlet and outlet core temperatures	Thermocouples	Preliminary calibration of the detectors	
Helium-3 pressure in the transient rods	Piezo-resistive pressure captor	Preliminary calibration of the detectors	
Online Core power	Boron ionization chamber Annubar and ultrasonic sensor Thermocouples	Thermal balance [9]	Steady state : ± 5% Transient state : ± 6%

Tab. 2. Thermal balance measurements - associated instrumentation and target uncertainty

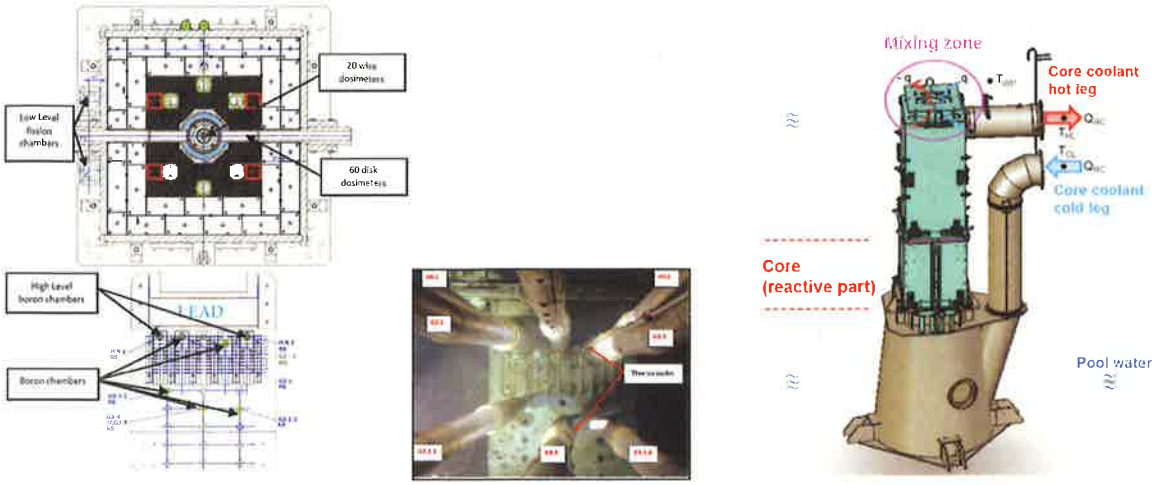

Fig. 3: nature and the position of the different types of instrumentation inside the CABRI core (left); view of experimental boron chambers (center); position of thermocouples and flowmeters outside of the CABRI core (right)

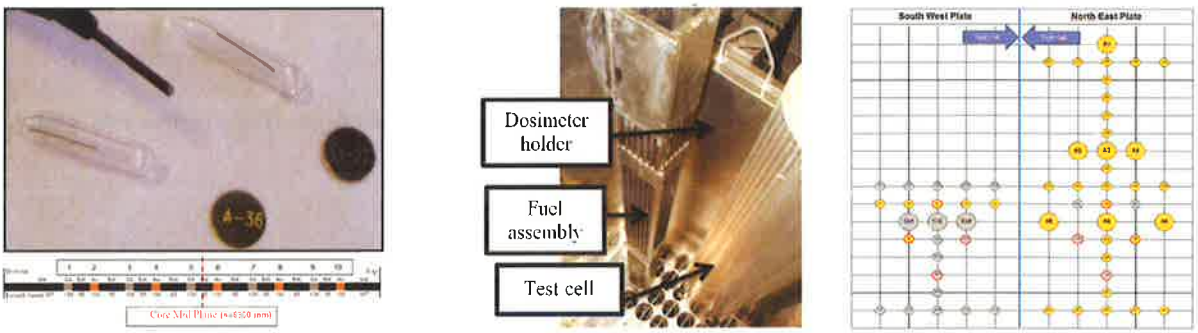

Fig. 4: top left : wire and disk dosimeters; bottom left: Co and Au wire dosimeters inserted inside aluminum tubes; center: dosimeter holder upon the hodoscope channel; right: position of Co (in grey) and Au (in yellow) disk dosimeters on the 2 plates of the dosimeter holder

4. Main results for low power neutronic characterization of the core

Hereafter are given some of the main experimental results that were obtained during the low power commissioning tests. Those results are compared to calculational ones.

4.1. Critical Position of the Control Rods

Fig. 5 shows the variation of the critical height of controls rods as a function of the Helium-3 pressure inside the transient rods. An uncertainty of 2mm (2σ) was observed on the critical height measurement, through reproducibility studies measurements.

Calculational results are consistent with experimental ones. A bias in the estimation of the multiplication factor less than 500pcm is observed, for all critical states. At the first order, this bias can be explained by the uncertainties on nuclear data and on technological data, in particular on the knowledge of the exact material balance and geometry of the hafnium control rods of CABRI.

4.2. Differential Reactivity Worth of the Control Rods

The first step of the measurement was to determine the excess of reactivity of supercritical situations using the classical asymptotic period method [5] [10] and the inhour equation of the

CABRI reactor. The differential reactivity worth of the control rods was then obtained by dividing the excess of reactivity of a supercritical situation by the difference of height of the control rods between their supercritical position and their critical position. An experimental uncertainty of about 10% (2σ) was obtained for all measurements. The calculation results are consistent with experimental ones; calculation however shows a slight overestimation of the differential reactivity worth that might be due to a lack of knowledge on the exact material balance of the control rods.

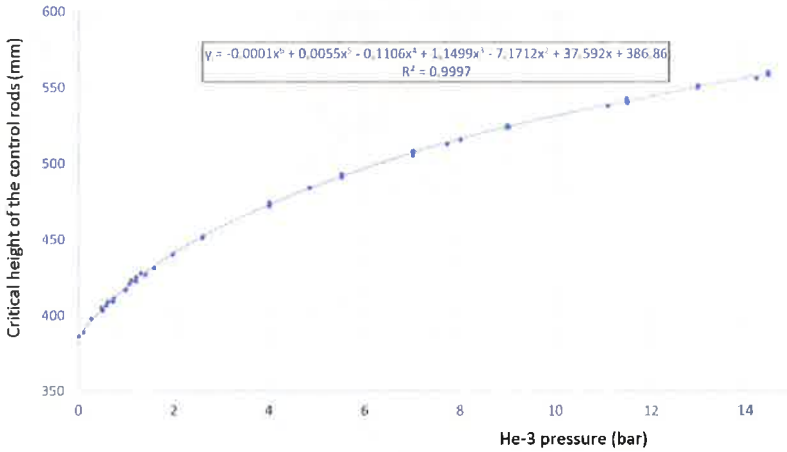

Fig. 5: critical height of the control rods as a function of Helium-3 pressure in the transient rods (moderator temperature: 20°C)

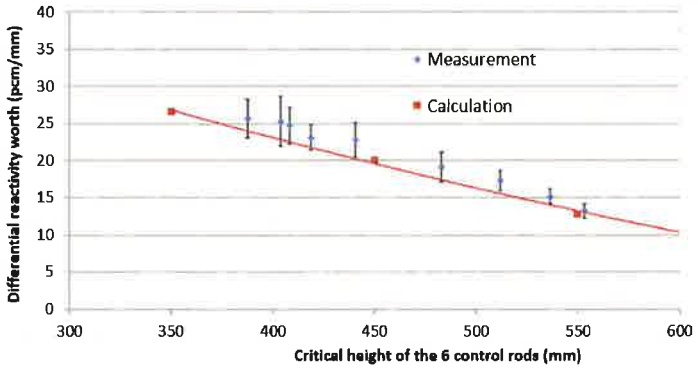

Fig. 6: differential reactivity worth of the control rods vs. the critical height

4.3. Integral Reactivity Worth of the Control Rods

The integral reactivity worth of the control rods were assessed using the rod drop technique [5] [10]. Practically, the counting of low power fission chambers (so called BN1 and BN2) has been recorded during the drop of the 6 control rods from their critical position. For measuring the integral reactivity worth of control rods, between their critical position and their fully inserted position, we used the method of inversion of the point kinetics equations [7] to convert the signal of chambers into the reactivity worth of the control rods. The reactivity worth obtained using the rod drop technique has to be corrected using the so-called *MSM correction* that takes into account the variation of the detection efficiency and of the intrinsic source of the core during the control rods shutdown [11].

The experimental uncertainty is ~7% (2σ) mostly based on the uncertainty on nuclear data used to inverse point kinetics equations. The calculation uncertainty is ~8% mostly due to the uncertainty on MSM correction factors calculation. The following results were obtained:

Critical height (mm)	Experimental reactivity worth of the control rods (pcm)	C/E (± 2σ)
386.4	BN1: -9725 BN2: -9672	BN1: 0.96 (± 11%) BN2: 0.96 (± 11%)
513.5	BN1: -11110 BN2: -12084	BN1: 1.01 (± 11%) BN2: 0.93 (± 11%)
556.0	BN1: -13138 BN2: -13631	BN1: 0.90 (± 11%) BN2: 0.87 (± 11%)

Tab. 3: integral reactivity worth of the control rods

4.4. Isothermal Temperature Coefficient

The isothermal temperature coefficient is measured between two critical states of CABRI corresponding to two different temperatures of the moderator (pool water). The isothermal temperature coefficient is then deduced throughout Equation (1): $\left(\frac{\Delta\rho}{\Delta T}\right)_{i,j} = \frac{\rho_i(T_i) - \rho_j(T_j)}{T_i - T_j}$ (1)

where T_i and T_j are the water temperatures corresponding to the two different critical states, and $\Delta\rho$ is the variation of reactivity between the two states.

Results are presented in Tab. 4. A very good consistency is observed between calculation and experiments.

Experimental isothermal temperature coefficient (pcm/°C)	Calculated isothermal temperature coefficient (pcm/°C)
-9.37 pcm/°C ± 1.92 (2σ) Temperature range [14°C – 26°C]	-9.37 pcm/°C ± 1.4 (2σ) Temperature range [20°C – 26°C]

Tab. 1: isothermal temperature coefficient of the CABRI core

4.5. Reactivity worth of Helium-3 transient rods

The reactivity worth of Helium-3 transient rods was measured by integration of the differential reactivity worth of control rods between different critical states corresponding to different pressures of Helium-3 in the transient rods. An experimental uncertainty below 1.5% (2σ) was obtained. An excellent consistency with calculational results is observed as shown in Fig. 7.

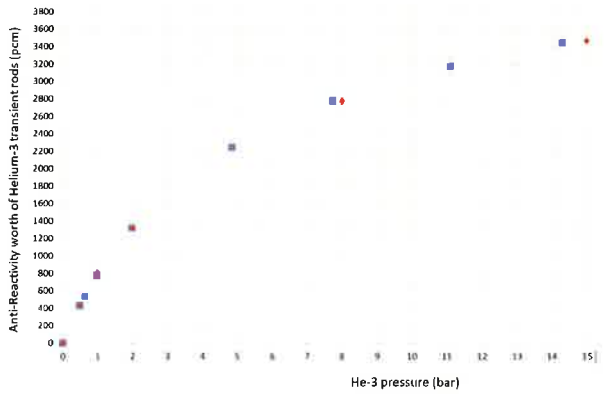

Fig. 7. Reactivity worth of Helium-3 transient rods as a function of Helium-3 pressure: experimental results in blue, calculational results in reds

4.6. Axial Distributions of Flux

The axial distribution of neutron flux will be measured using cobalt and gold dosimeters (disks and wires) at different positions [12] [13], inside the CABRI driver core and inside the central

cell in which the test fuel pin is inserted (see Fig. 8). A good consistency is observed between calculation and experiments.

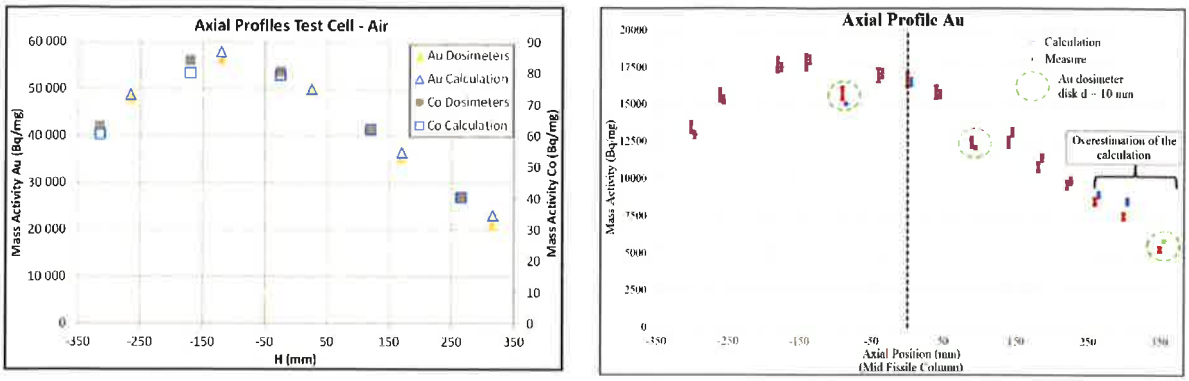

Fig. 8. Axial flux profile in the test cell measured with wire dosimeters (left); axial power profile inside the core measured with disk dosimeters of the North East plate of the dosimeter holder upon the hodoscope device – calculation to measurement comparison

6.7. Kinetic Parameters

Cross power spectral density measurements (CPSD) [5] [7] [8] have been achieved to measure the kinetic parameters (β = effective fraction of delayed neutrons and Λ = prompt neutron generation time). β and Λ were inferred using equations (2) and (3):

$$\beta^2 = \frac{2D}{F}\frac{V_{01}V_{02}}{CPSD}\frac{1}{(1+|\rho_\$|)^2} \quad (2) \quad \text{and} \quad \Lambda = \frac{\beta}{2\pi f_c} \quad (3)$$

Where CPSD is the cross power spectral density between V_{01} and V_{02} (signals of the two fission chambers positioned inside the dummy assembly outside of the core), D is the Diven factor, $\rho_\$$ is the core reactivity in dollars, f_c is the break frequency of CPSD and F is the total number of fissions in the core per unit of time.
The experimental uncertainty is at the first order due to the uncertainties on the Diven factor and on the measurement of the total number of fissions per unit of time in the core. The uncertainty on calculation is mostly due to uncertainties on nuclear data. Tab. 5 gives the comparison of experimental and calculational results. A good consistency is observed.

Parameter	Measurement ± (2σ)	Calculation ± (2σ)
β (pcm)	720.5 ± 50	760 ± 50
Λ (μs)	25.7 ± 3.6	25.6 ± 2.6
β/Λ (s^{-1})	280.3 ± 34	296.9± 30

Tab. 5: comparison of measured and calculated kinetic parameters à CABRI

6.8. Synthesis of the measurements

All measurements were performed within initial target uncertainties. An overall good consistency, within the uncertainties, is observed between experimental and calculational results for all the relevant neutronic parameters that were studied.

7. Main results for neutronic high power characterization

The accurate measurement of the absolute power and hence of the total energy deposit during transients is crucial. The power commissioning tests have been performed in 2016 and 2017. Technically speaking, the main objectives were:

- to calibrate the neutron detectors thanks to thermal balance measurements performed on water of the primary cooling system passing through the core. These measurements have been carried out up to the maximal steady state CABRI driver core power level (~23 MW),
- to verify the co-linearity of the experimental neutron detectors during the power increase as well as various steady state power levels,
- to study the consistency of the different experimental neutron detectors measurements and the linearity of each detector during power transients up to power levels of ~ 20 GW.

During steady states of power, the thermal balance method [9] consists in measuring the primary coolant heating for an accurate monitored flowrate. In the end, the current delivered by the 5 out-core experimental boron chambers (see Fig. 3) is calibrated vs. the power measured by thermal balance. Equation (4) resumes the principle of this measurement:

$$P_{ND} = P_{TB} = c.S = \rho.C_P.Q_{RC}.(T_{HL} - T_{CL}) \qquad (4)$$

With: P_{ND} = core power measured by the Neutron Detector (W)
P_{TB} = core power measured by Thermal Balance (W)
c = calibration constant counting rate of boron chambers
S = signal of boron chambers (A)
ρ.= water density (kg/m^3)
C_P = water isobar specific heat (J/kg/°C^{-1})
Q_{RC} = Reactor Coolant flow rate (m^3/s)
T_{HL} and T_{CL} = Hot Leg and Cold Leg water temperatures (°C)

Thanks to increasing distances between the driver core and the chambers, the experimental signals overlap on different ranges of operation of the chambers and electronic chains is ensured on the whole power range in the case of power transients (from few kW up to ~20 GW). G2.1 and G2.2 chambers, which are the closest to the core, are mainly used to measure power during steady state conditions (before transients). They also follow the beginning of the transients before the overlap with the G3 detectors (see Tab. 6).

Chamber	G2.1	G2.2	G3.1.1	G3.1.2	G3.4
Min Power	~10 kW		~10 MW	~100 MW	
Saturation	~450 MW		> Max transient power of CABRI		

Tab. 6: range of operation of CABRI experimental boron chambers

7.1. Steady-state high power characterization

This calibration is only possible up to the maximum deliverable power level (23.7MW) that can be obtained for a steady state operation of CABRI. During the power commissioning tests, thermal balances with increasing power levels (8, 10, 12, 15, 19 and 23MW) were used to calibrate the neutron detectors. The variation of the sensitivity of the signal of boron chambers vs. the temperature of the primary cooling system has also been taken into account.

The consistency and co-linearity of the neutron detectors power measurements was checked during the different power increases and steady states of power. Fig. 9 presents the results obtained during the different phases of the power increase. For power higher than a few kW, the signals of HN and G2 chambers are perfectly consistent. An uncertainty of about 5% (2σ) was obtained on steady-state power measurements.

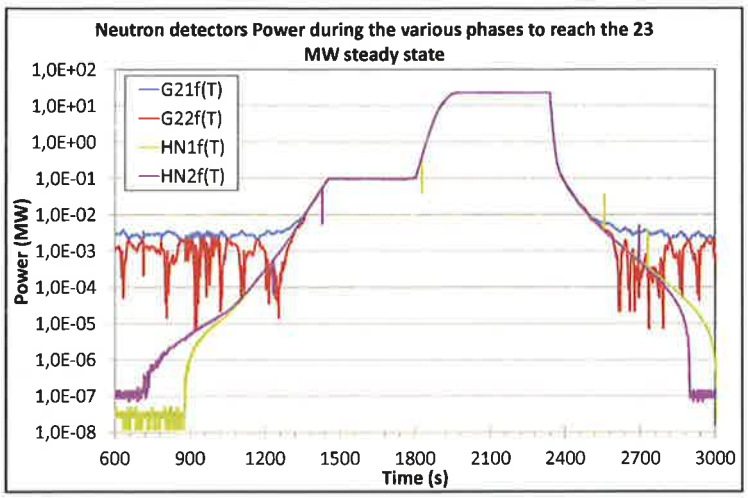

Fig. 9. Evolution of the neutron detectors signals during a 23MW steady state power level

7.2 Linearity of boron chambers during power transients

Fig. 10 presents the coherence and co-linearity of the boron chambers (G2_type and G3_type) signals based on different power transients realized with an increasing maximum power, starting from low ^{3}He pressure and low valve aperture of the transient circuit [2]. The co-linearity is excellent until 450MW that corresponds to the saturation level of G2 chambers.

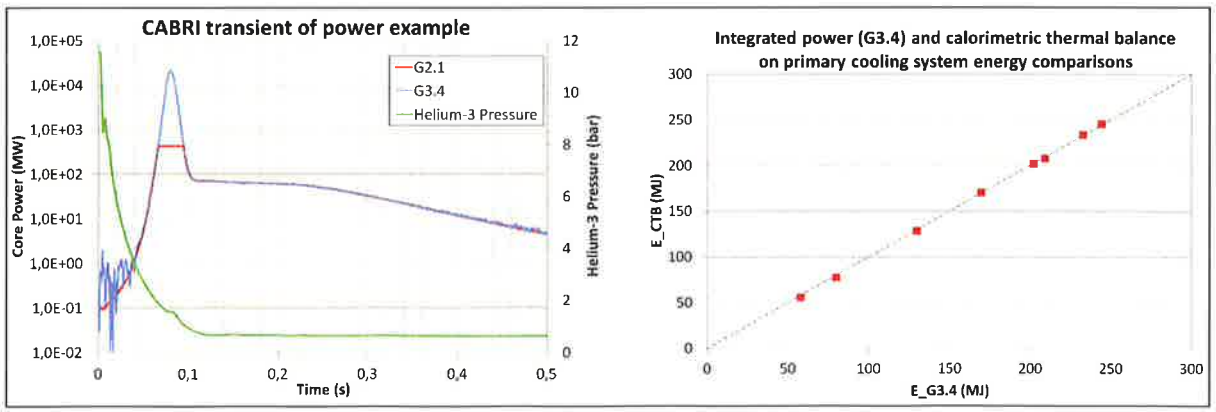

Fig. 10. coherence and co-linearity of the boron chambers (G2_type and G3_type) (left); G3.4 and calorimetric thermal balances results on the core energy comparisons (right)

The linearity of the boron chambers and their capability to measure precisely the energy deposit during power transients have been checked comparing the integral of the signal of boron chambers during transients to thermal balance measurements. Fig. 10 (right figure) shows an example of results for the G3.4 neutron detector and concludes to its very good linearity (~ 2% (2σ)) over the whole range of accessible energy deposit in the CABRI core. An uncertainty of about 6% (2σ) was obtained on transient-state power measurements.

8. Conclusion

Low power, high power and transient power commissioning tests of the CABRI reactor were successfully performed from 2015 to 2017. The experimental target uncertainties were reached in all cases. The comparison between experimental results and calculational results concludes to a good overall consistency.
Those commissioning tests allowed defining the authorized domain of operation of CABRI, better mastering the boundary conditions of the CABRI RIA tests and validating the reference neutronic calculation scheme used for safety and design studies.

9. Acknowledgement

The authors would like to acknowledge IRSN (Institut de Radioprotection et de Sûreté Nucléaire) for its financial, technical and scientific support and contribution to the CABRI experiments.

8. References

[1] JP. Hudelot, E. Fontanay, C. Molin, A. Moreau, L. Pantera, J. Lecerf, Y. Garnier, B. Duc, "CABRI facility: upgrade, refurbishment, recommissioning and experimental capacities", PHYSOR 2016 – Unifying Theory and Experiments in the 21st Century Sun Valley Resort, Sun Valley, Idaho, USA, May 1 – 5, 2016, on CD-ROM (2016)

[2] B. Duc, B. Biard, P. Debias, L. Pantera, JP. Hudelot, F. Rodiac, "Renovation, improvement and experimental validation of the Helium-3 transient rods system for the reactivity injection in the CABRI reactor," IGORR2014 conference, 17-21 November 2014, Bariloche, Argentina

[3] JP. Hudelot, Y. Garnier, J. Lecerf, M. Fournier, S. Magnetto, E. Gohier, "CABRI reactor commissioning: results and analysis of the tests on the primary cooling system and on the control and safety rods," IGORR2014 conference, 17-21 November 2014, Bariloche, Argentina

[4] E. Brun, E. Dumonteil, F. X. Hugot, N. Huot, C. Jouanne, Y. K. Lee, F. Malvagi, A. Mazzolo, O. Petit, J. C. Trama, and A. Zoia, "Overview of TRIPOLI-4 version 7 continuous-energy Monte Carlo transport code," presented at the Int. Conf. ICAPP, Nice, France, May 2011

[5] G. Bignan, P. Fougeras, P. Blaise, JP. Hudelot, F. Mellier, "Handbook of Nuclear Engineering," ISBN 978-0-387-98130-7 – Volume 3 - Reactor Physics Experiments on Zero Power Reactors – pp. 2053-2184

[6] JM. Girard, H. Philibert, S. Testanière, Ch. Domergue and D. Beretz, "The MADERE Ra-dio-activity Measurement Platform: Developments for a Better Addressing to the Experimental Needs", 978-1-4244-5208-8/09/ ©2009 IEEE

[7] G. Perret, "Amélioration et développement des méthodes de détermination de la réactivité – Maîtrise des incertitudes associées", PhD thesis, Orsay, 2003

[8] I. Pazsit, C. Demazière, "Handbook of Nuclear Engineering," ISBN 978-0-387-98130-7 – Volume 3 – Noise Techniques in Nuclear Systems – pp. 1629-1737

[9] L. Pantera, Y. Garnier and F. Jeury, « Assessment of the Online Power Measured by a Boron Chamber in a Pool-Type Ressearch Reactor Using a Nonlinear Calibration Model," Nuclear Science and Engineering, vol. 183, 247-260 June 2016

[10] JP. Hudelot, R.T. Klann, B. Micklich, M. Antony, G. Perret, N. Thiollay, JM. Girard, V. Laval, P. Leconte, "MINERVE Reactor Characterization in Support of the OSMOSE Program: Safety parameters", PHYSOR 2004 conference, Chicago (US), 2004

[11] M. Maillot, G. Truchet, J.P. Hudelot, J. Lecerf, "Analysis of the rod drop experiments performed during the CABRI commissioning tests", RRFM 2018 Conference, 11-15 March, 2018, Munich, Germany

[12] JP. Hudelot, J. Lecerf, Y. Garnier, G. Ritter, O. Guéton, AC. Colombier, F. Rodiac, C. Domergue, "A complete dosimetry experimental program in support of the core characterization and of the power calibration of the CABRI reactor", ANIMMA2015 Conference, Lisbon (Portugal), 2015

[13] J. Lecerf, Y. Garnier, JM. Girard, C. Domergue, L. Gaubert, Ch. Manenc, "Analysis of the dosimetry campaign performed during the CABRI commissioning tests," Advancements in Nuclear Instrumentation Measurement, Methods and their Applications (ANIMMA), Liege, Belgium, June 19-23, 2017

FUEL ASSEMBLY THERMAL HYDRAULICS DESIGN FOR AN IRRADIATION IN AN EUROPEAN MEDIUM POWER RESEARCH REACTOR

R. DUPERRAY, L. ROUX
Thermal hydraulics department, TechnicAtome
1100 avenue J.R. Guillibert Gautier de la Lauzière, CS 50497, 13593 Aix-en-Provence, France

ABSTRACT

H2020 European LEU-FOREvER Project (2017-2021), associating major actors of the European research reactors field – FRAMATOME - CERCA, CEA, CV Řež, ILL, NCBJ, SCK·CEN, TechnicAtome, TUM, aims to foster the development of sustainable low enriched uranium fuel for European research reactors.

Some European Medium Power Research Reactors (EU_MPRR) are currently operating with a single qualified fuel based on LEU UO_2 dispersed fuel. As part of the LEU-FOREvER project, fuel diversification is expected for these reactors. Based on collected data from LVR-15, BRR and MARIA operators, a definition of new fuel assemblies has been proposed taking into account mechanics, thermal-hydraulics and neutronics constraints.

This work focuses on the standard FA and its integration feasibility in the LVR-15 core along with its expected performances. Thermal hydraulics analyses were done with compliance with LVR-15 thermal conditions, FA constraints and safety criterions.

Several methods were engaged to evaluate the FA performances: deterministic approach, statistical approach or a combination of both. This allows investigating the different options in terms of manufacturing constraints and performance in one hand and costs in terms of methodology and safety analysis in the other hand.

Calculations were done using the thermal hydraulics code CATHARE2 RXP along with URANIE for sensitivity tests and statistical analysis.

CEA/DEN is thanked for allowing the use of CATHARE2 RXP code in this study.

1. Introduction

TechnicAtome is involved in the LEU-FOREvER project, aiming to design a new FA for the LVR-15 reactor in Czech Republic. This FA will be tested and irradiated within the LVR-15 core.

The goal of this study is to determine the effects of the manufacturing tolerances and modelling uncertainties on the new FA performances within the LVR-15 core, given the geometry of this new FA.
To achieve this, several sensitivity tests on manufacturing tolerances and models uncertainties are performed using the CATHARE2 RXP code along with the URANIE tool for sensitivity tests.

2. Methodology and hypothesis

2.1 Main hypothesis and FA data

All calculations presented in this document are performed at reference thermal conditions: 10kg/s liquid flow, 45°C inlet temperature and 1.32 bar pressure, which is representative of the LVR-15 reactor thermal conditions (reference [1]).

The chosen design for the LEU-FOREvER project is a flat plate Fuel Assembly with 22 plates (Figure 1).

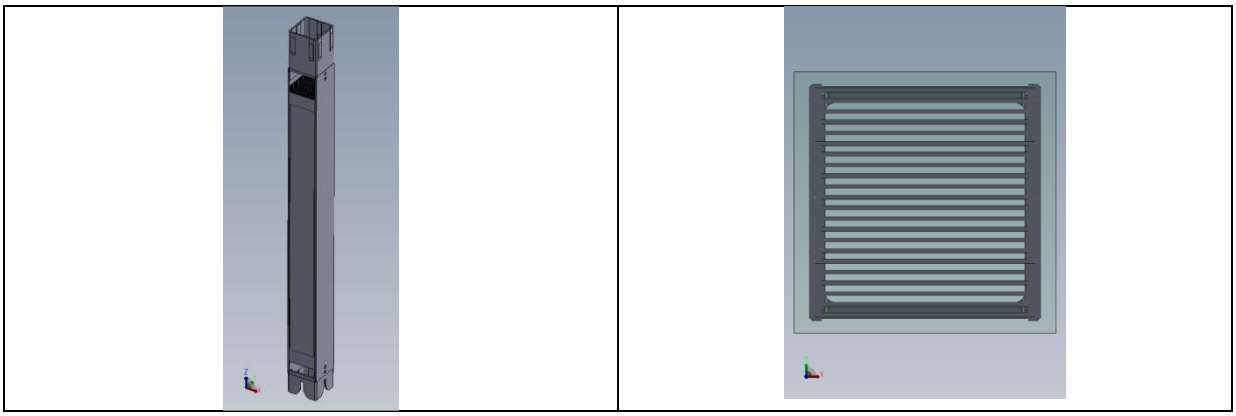

Figure 1 – LEU-FOREvER Fuel Assembly

The main geometrical characteristics of the standard Fuel Assembly to be irradiated in the LVR-15 reactor are listed in Table 1.

Number of Fuel Elements per Fuel Assembly	22
Fuel Element height (mm)	882
Meat height (mm)	600
Uranium density in fuel (g/cm^3)	4.8
Fuel Element thickness (mm)	1.27
Meat thickness (mm)	0.51
Clad thickness (mm)	0.38
Fuel Element width (mm)	65.6
Meat width (mm)	58.5
FA internal channels thickness (mm)	1.9838
FA external channels thickness (mm)	0.95

Table 1- Main FA geometrical data

2.3 Thermal-hydraulics calculation code

In this study, CATHARE2 RXP is used for thermal-hydraulics computations (reference [3]).

The CATHARE code (Code for Analysis of Thermal-hydraulic during an Accident of Reactor and Safety Evaluation) was developed to perform best-estimate calculations of pressurised or boiling water reactor accidents, but specific modules have also been implemented to allow modelling of other reactors like boiling water reactors, gas cooled reactors and pool or tank in pool experimental reactors. CATHARE is developed by CEA (French Atomic Energy Commission), EDF (Electricity of France), IRSN (Nuclear Safety and Radioprotection Institute) and FRAMATOME.

Sensitivity analyses are driven by the CEA's URANIE code based on the CERN's ROOT software toolkit.

2.4 Thermal-hydraulics safety criterions

2.4.1 Onset of Nucleate Boiling (ONB)

The ONB point is modelled with the ONB ratio (ONBR) following the Bergles and Rohsenow correlation (reference [1]) according to the CVR's thermal-hydraulics code:

$$ONBR = \frac{T_{ONB} - T_{IN}}{T_{MAX} - T_{IN}}$$

With:

- $T_{ONB} = T_{sat} + \Delta T_{sat}$; $\Delta T_{sat} = 0.556.(\frac{\Phi}{1082.p^{1.156}})^{0.463.p^{0.0234}}$
- T_{sat} : saturated temperature (K)
- Φ : surface heat flux in MW/m²
- p : pressure in bar
- T_{MAX} : maximum surface temperature along channel
- T_{IN} : Inlet fluid temperature

The surface temperature is determined with the Dittus-Boelter correlation for turbulent flows:

$$Nu = 0.023Re^{0.8}Pr^{0.4}$$

This criterion is not a technological limit but information for CVR's studies.
The technological limits for thermal-hydraulics design are (cf. reference [2]):

- The Onset of Significant Void as a precursor of the Ledinegg instability,
- The Departure from Nucleate Boiling and the critical heat flux.

2.4.2 Onset of Significant Void (OSV) and/or Departure from Nucleate Boiling (DNB)

2 criterions are calculated to detect OSV or DNB:

- Modified Saha-Zuber OSVR criterion (KIT) is calculated using correlation described below (optimized in CATHARE thanks to KIT experiment, reference [3]):
  for the thermic region ($Pe < Pe_{transition}$) : $OSVR = \frac{Nu_{OSV}}{Nu}$
  for the hydrodynamic region $(Pe > Pe_{transition})$: $OSVR = \frac{St_{OSV}}{St}$
  $Nu_{OSV} = \frac{455}{2}$, $St_{OSV} = 0.0065.\frac{1}{2}.\left(\frac{Pe}{70000}\right)^{0.4}$ and $Pe_{transition} = 37100$
  Pe being the Peclet's number, Nu the Nusselt's number and St the Stanton's number,

- Sudo DNBR criterion is calculated using the Sudo correlation:
  $DNBR = \frac{q*}{\Phi*}$, q* being the local dimensionless surface flux and Φ* the dimensionless critical heat surface flux. Both terms depend on the flow configuration and are detailed in [4].

OSV and DNB criterions are combined in one single criterion which corresponds to the first criterion among KIT and Sudo to reach 1.0.

2.5 FA performance calculation approaches

Two different safety approaches or combinations of both are implemented in this study in order to quantify the maximal FA performance: deterministic approach and statistical approach.
In both approaches, the FA performance is quantified by the maximal achievable power as regards to the OSV/DNB criterion, given the different parameters.

2.5.1 Deterministic approach

The deterministic approach consists in setting the different parameters at their most penalizing value in their variation range as regards to the maximum achievable power.
To identify which value is the most penalizing, sensitivity analysis must be made (with One-At-a-Time graphs for instance).

2.5.2 Statistical approach

The statistical approach consists in computing a batch of calculations using randomly built decks of parameters in accordance with their variation range and identified probability law.
Then, this batch is used to compute a 95% Wilks quantile with 95% confidence to determine the result of interest which is the maximum achievable power.

In study, batches of 410 calculations are done for a given thermal condition tuple. This number of calculation has been identified in reference [2] to be sufficient to guarantee that the Wilks quantile is independent of the number of calculations.

2.5.3 Studied parameters

The studied FA parameters are listed in with their variation range and associated probability laws for statistical treatment.

Parameter	Symbol	Variation range (2σ for normal probability laws)	Reference prob. law
Hot channel thickness (gap) deviation (additive)	TOL_FAB	[-0.2 mm; +0.2 mm]	Gaussian
FA Uranium density deviation (multiplicative) along a 5 mm track	FTECH	[0.95 ; 1.05]	Gaussian
Uranium density in the Hot channel spot in the core zone (multiplicative)	FTZ1	[0.895 ; 1.105]	Gaussian
Uranium density in the Hot channel spot in the dog-bone zone (multiplicative)	FTZ2	[0.762 ; 1.238]	Gaussian
Liquid convection heat flux	QCL	[0.5 ; 2.0]	Log Normal
Nucleate boiling heat flux	QEN	[0.56 ; 1.44]	Gaussian
Interface to liquid heat flux	QLLE	[0.3 ; 3.0]	Log Uniform
Wall friction coefficient	FROTTC	[0.92 ; 1.08]	Gaussian
Two phase flow phase friction	FDIPH	[0.8 ; 1.2]	Uniform
Net vapour generation	INVGP	[0.85 ; 1.15]	Gaussian
Critical heat flux	ISUDO	[0.67 ; 1.33]	Gaussian

Table 2 – Studied FA parameters

3. Results

In this paragraph, focus will be made on quantifying the expected FA performances within the LVR-15 core using the OSV/DNB criterions.
The impact of manufacturing tolerances and CATHARE physical uncertainties on the FA performances will also be treated.
Several approaches will be computed to help give clues to eventually improve the FA performances.
Power values given in this paragraph correspond to a homogeneous power FA over the FE.

3.1 Tolerances and uncertainties effect analysis

Figure 2 and Figure 3 show the power dispersion obtained via a fully statistical approach for both manufacturing tolerances and physical models uncertainties at reference thermal conditions.

In these figures:
- Spearman correlation coefficient measures the monotony correlation between two dataset, the closer to 1 or -1 the better the correlation is.
- Pearson correlation coefficient measures the linear correlation between two dataset.

As expected, the most influent manufacturing parameter on the maximum extractible power is by far the hot channel thickness deviation (see Figure 2).
Indeed, as the nominal channel is 1.98mm thick, a maximum deviation of 0.2mm on the hot channel represents 10% of its thickness, which triggers an augmentation of head loss along the channel. As a result, the liquid flow in the hot channel is 15% lower than in the nominal case

There is no significant influence of the parameters FTZ1 and FTZ2 representing the uranium local density in core and outer zones of the FE. Indeed these parameters have an influence on the critical heat flux criterion (DNB) but none on the OSV criterion. Most of the time, the OSV criterion threshold is reached before the DNB criterion, explaining why the effect of these two parameters on the DNBR is not visible on the OAT graphs.

In this FA, the calculated points are around the limit between an OSVR limited power and a DNBR limited power depending on the parameters. The effect of the Sudo correlation on the DNBR is such that the limiting criterion switches as function of this value. Depending on the limiting criterion, the effect of FTZ1 and FTZ2 is noticeable or not. This criterion switch is a good example of why the different uncertainties cannot simply be cumulated with a quadratic sum, full statistical or deterministic methods has to be performed to see all cross-effects.

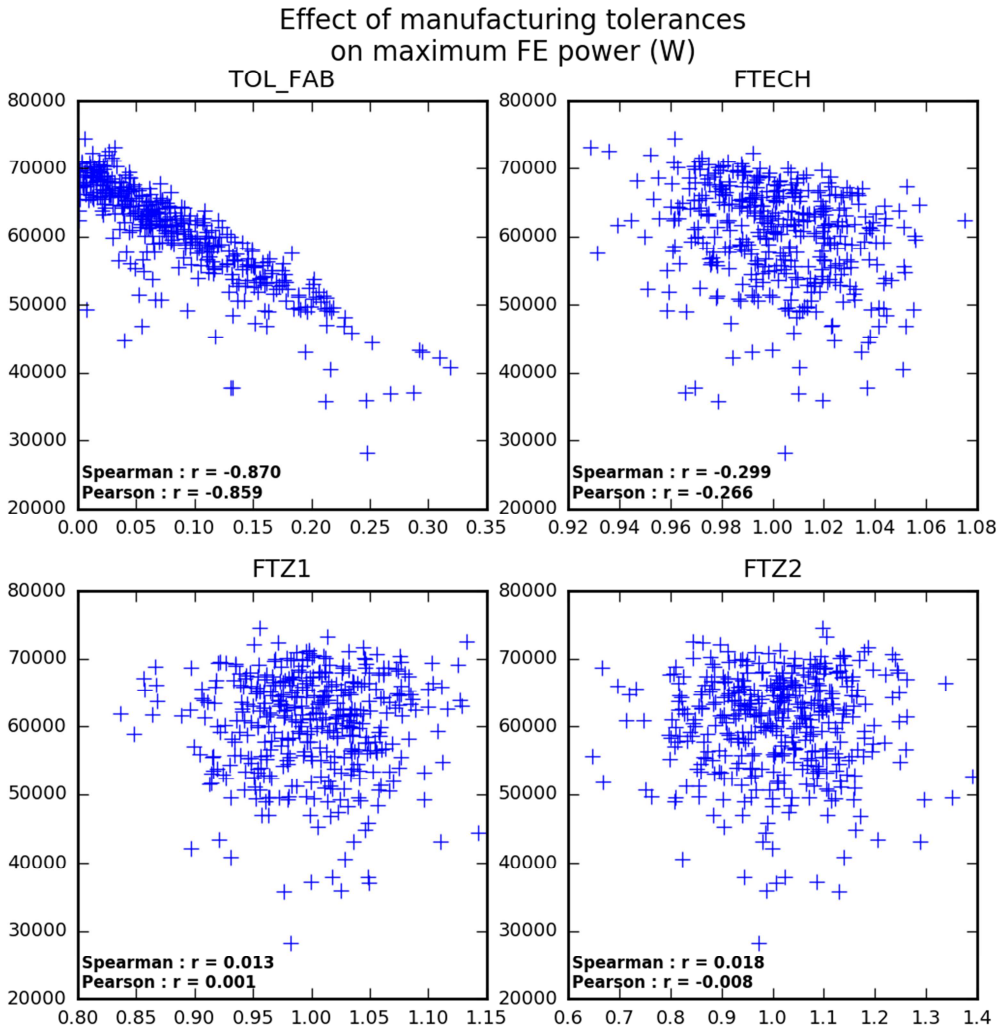

Figure 2 – Maximum OSV/DNB power dispersion at reference thermal conditions, function of manufacturing tolerances

Figure 2 shows that the hot channel thickness deviation directly determines the maximum achievable power: even with physical model uncertainties and other manufacturing uncertainties varying, the maximum power factor remains very well correlated to the channel thickness (spearman coefficient near 0.9 for fixed thermal conditions).
As a comparison, the uranium density uncertainty effect on maximum power is hidden by the effects of all the other parameters.

This shows that the effect of the hot channel thickness deviation is significant enough to overtake the effects of all the other parameters. It is the primary uncertainty to take into account in the FA studies. Two methods can be performed to take these uncertainties into account: on one hand the uncertainty can be directly modelled in the input deck just as in this paragraph, on the other hand it could be modelled with a penalizing coefficient on the ONBR criterion.

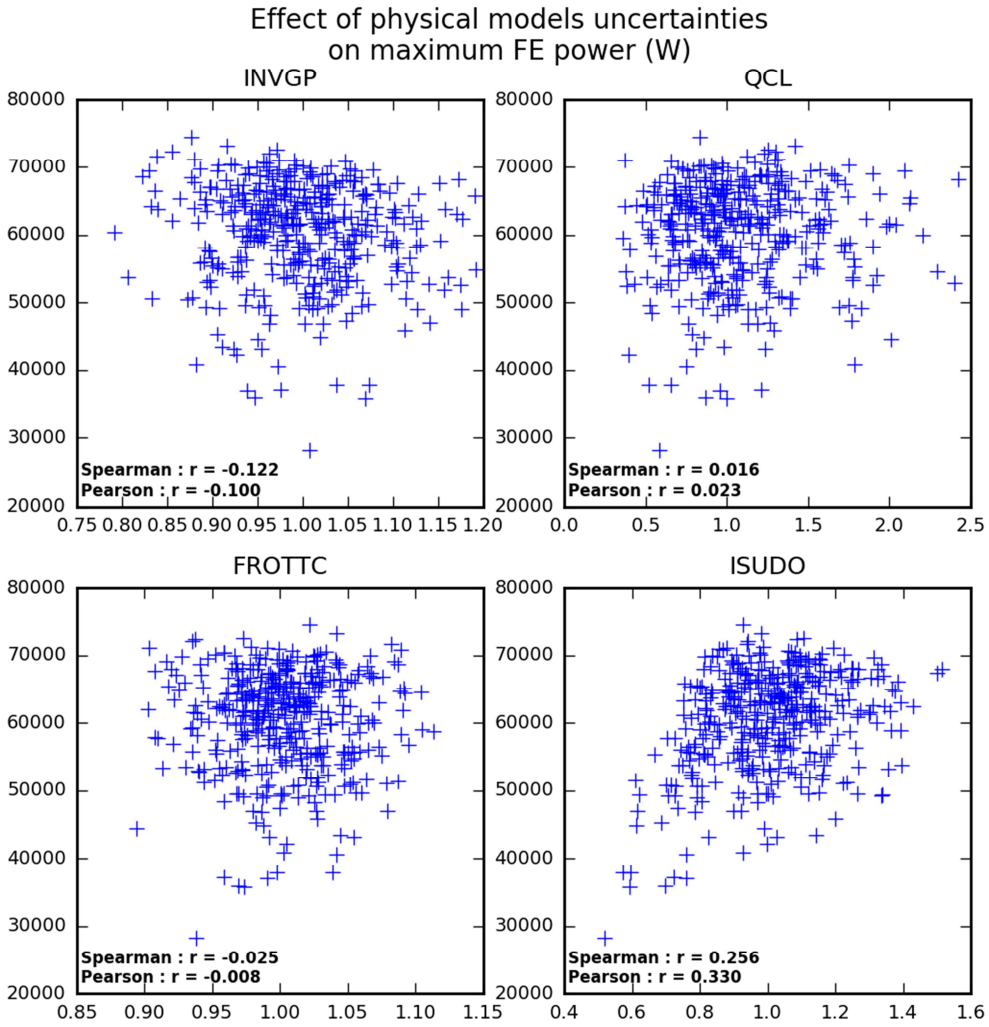

Figure 3 – Maximum OSV/DNB power dispersion at reference thermal conditions, function of physical models uncertainties

3.2 Expected FA performances as function of the safety methodology

This paragraph describes a diversity of safety methodologies applied on research reactors over the years (by Technicatome or others) and their results in terms of achievable power. Possible improvements are also shown. This could be applied to the newly designed FA within the LVR-15 core to improve performances.

Manuf. / Physics	Statistical	Deterministic
BE	1.434	1.419
Statistical	1.297	1.033
Deterministic	1.14	1.0

Table 3 – Summary of maximum achievable power relative to deterministic power with OSV/DNB criterion at reference thermal conditions

Table 3 presents the results obtained with various combinations of BE, statistical and deterministic approaches on maximum OSV/DNB power, as regards to the fully deterministic case (set at 1.0).

A statistical treatment of manufacturing tolerances could lead to a significant performance improvement (here 14% as regards to a fully deterministic approach). This result is characteristic of narrow gaps fuel assembly because of the relative cost of the absolute tolerance on the gap manufacturing (0.2mm vs 1.98mm).

It is remarkable that the effect of the methodology choice for the treatment of manufacturing tolerances is significantly lighter when calculations are done with best-estimate physical models uncertainties than with deterministic ones.
This is explained by the fact that deterministic uncertainties on physical models, and especially on the critical heat flux correlation, lead the DNBR to reach 1.0 before the OSVR. Thus, the maximum achievable power is driven by the DNBR criterion, which is more sensitive to manufacturing tolerances (because of the gap and the U5 local density) than the OSVR criterion.

3.3 Custom coefficient proposal to take tolerances into account within LVR-15 criterion

Given the influence of the several uncertainties/tolerances to take into account to determine the FA performances and the maximum achievable power of the FA, this part focuses on how to take these uncertainties into account using the Bergles and Rohsenow ONBR criterion used by the LVR-15 teams.

In this part it is proposed to tune the ONBR criterion used by LVR-15 teams in order to take into account uncertainties and tolerances in a deterministic way.
.
The approach is the following (illustrated in Figure 4):

- Two calculations are done with manufacturing tolerances set at their most penalizing value : one with best estimate physical models uncertainties and the other with physical models uncertainties set at their most penalizing value. Both calculations are performed for several thermal conditions;
- For each calculation, the maximum achievable power respecting the OSVR/DNBR gives the ONBR criterion at this point;
- Then the ONBR in a BE calculation such as the BE power equals the OSVR/DNBR power is determined;
- Ratio of the two ONBR is done to give the multiplying coefficient to apply to take into account uncertainties.

Results are summed up in Figure 5. The coefficient varies as function of the thermal conditions, in order to cover all thermal conditions we have to keep the maximal coefficient for each uncertainty treatment, see Table 4.

Uncertainties to take into account	Coefficient to apply to threshold
Only manufacturing tolerances	1.4
Manufacturing and CATHARE RXP physical models	1.76

Table 4 - ONBR threshold coefficient taking into account uncertainties

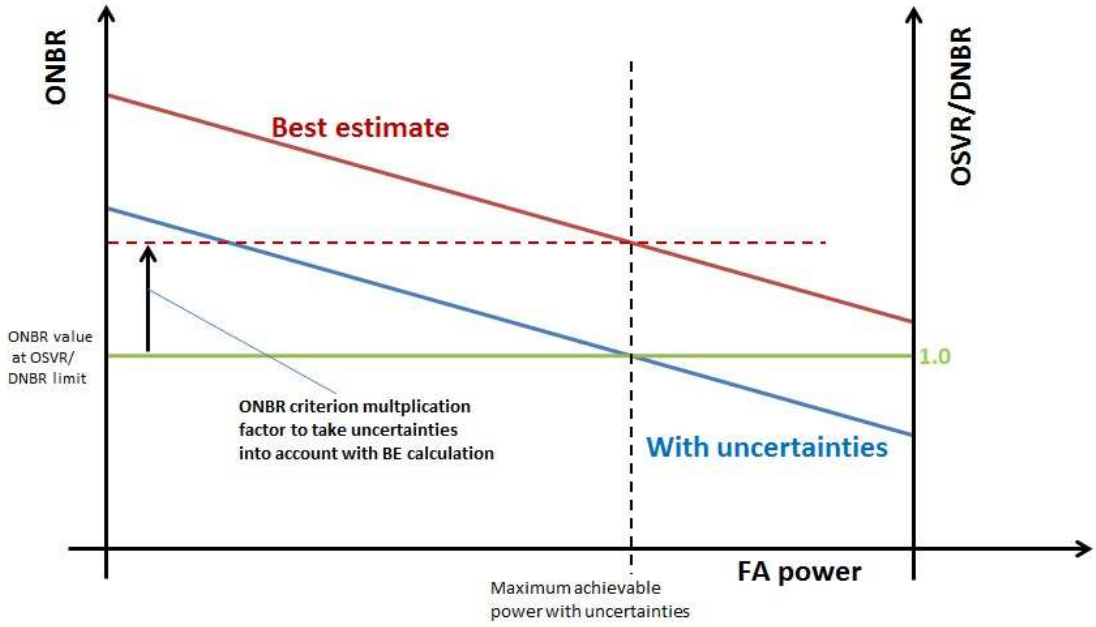

Figure 4 – ONBR criterion coefficient covering uncertainties calculation method

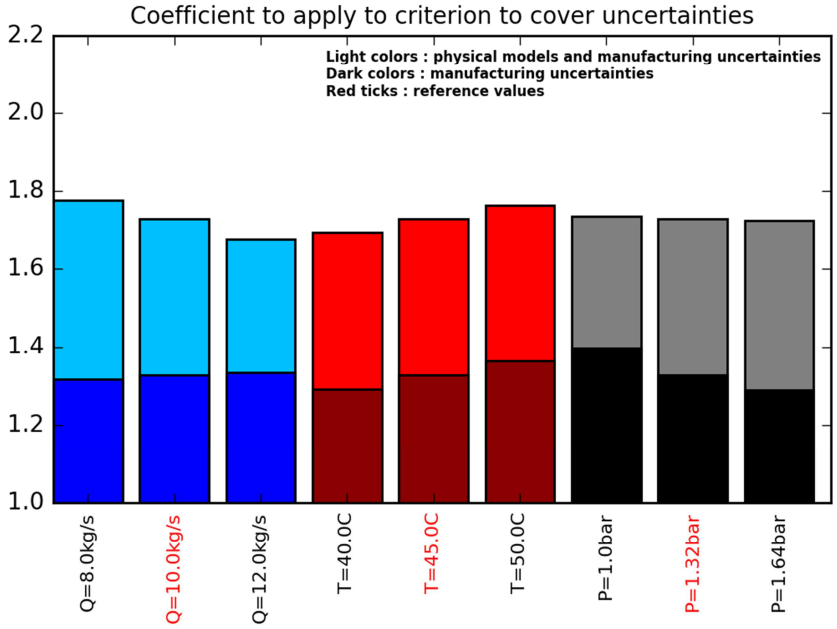

Figure 5 – Coefficient to apply to the ONBR criterion threshold to take into account various uncertainties, function of thermal conditions

4. Conclusion

In this study, the expected new FA performance within the LVR-15 core was estimated. Sensitivity analyses on various parameters (thermal conditions, manufacturing tolerances and physical models uncertainties) showed that the manufacturing tolerances have a primary effect on the final FA performance. Such tolerances cannot be simply cumulated with the other parameters with a quadratic sum; indeed this study showed that several parameters have cross-effects depending on the manufacturing tolerances.

Thus, given the effect of manufacturing tolerances, a coefficient to apply to the ONBR was proposed in order to take into account these tolerances in one go.

Taking into account tolerances and uncertainties in a more detailed way can be achieved by modelling them directly in the input deck. Depending on the method (deterministic, statistical or a combination of the two), better performances can be achieved but at the cost of more quality control on the manufacturing process and thus a more expansive FA.

5. References

[1] LEU-FOREvER – WP4 – Task 4.1 :
Data gathering for EU MPRR Fuel requirement assessment – LVR-15
TA-6289851 Ind. A *Private communication*

[2] Etude de la propagation des incertitudes des modèles physiques sur les performances thermohydrauliques des réacteurs de recherche à eau légère
TA-6107787 Ind. A - *Private communication*

[3] Réacteurs de recherche – Dossier de qualification de CATHARE2
DEN/DANS/DM2S/STMF/LATF/NT/15-036/A
EXT-6173941 Ind. A - *Private communication*

[4] Sudo Y., Miyata K., Ikawa H., Kaminaga M., Ohkawara M. : Experimental Study of Differences in DNB Heat Flux between Upflow and Downflow in Vertical Rectangular Channel, *Journal of Nuclear Science and Technology* 22(8), pp.604-618 (1985)

6. Acknowledgements

The European Commission for the funding of the LEU-FOREvER project.

CEA/DEN for allowing the use of CATHARE RXP code in this study.

EDUCATION AND RESEARCH UTILISING UTR-KINKI

G. WAKABAYASHI
Atomic Energy Research Institute, Kindai University
3-4-1 Kowakae, Higashiosaka-shi Osaka 577-8502 – Japan

ABSTRACT

UTR-KINKI is an Argonaut-type research reactor for university education and research with rated thermal power of 1 W. Since the first criticality in 1961, the reactor has been utilized in higher education, secondary education and other educational activities in nuclear science and technology in Japan. The reactor has also been utilized in various researches as a joint use facility for domestic researchers. UTR-KINKI had to be shut down for about three years from February 2014 to be relicensed under the new regulatory standards established after the Fukushima nuclear accident, but it resumed operation in April 2017 as the first research reactor approved under the new standards. In this paper, the characteristics, history and utilizations in education and research of UTR-KINKI are introduced as well as the response to Japan's new regulatory standards for research reactors.

1. Introduction

Atomic Energy Research Institute of Kindai University (Osaka, Japan) operates a research reactor, UTR-KINKI, which is one of the UTRs (University Teaching and Research Reactor) designed and developed by American Standard. The reactor is a modified Argonaut design, and the present rated thermal power is 1 W. Since its first criticality in 1961, the reactor has been utilized for education, training and research in nuclear science and technology in Japan for more than a half century. There used to be six research reactors operated by five universities in Japan, but UTR-KINKI is now one of the three university owned reactors (the other two are KUCA and KUR of Kyoto University).

After the Fukushima Daiichi nuclear power plant accident in 2011, new regulatory standards were established and applied to research reactors in 2013. All the research reactors in Japan, including UTR-KINKI, had to be shut down until they are approved under the new regulatory standards, and UTR-KINKI had been shut down for more than three years for safety reviews and inspections. In April 2017, UTR-KINKI resumed operation as the first research reactor which completed new regulatory requirements in Japan. Fifteen research reactors were in operation in Japan in 2011, but six of them have been shut down permanently after the nuclear accident. Consequently, UTR-KINKI has become increasingly important as a precious reactor for education and research in Japan.

Though the university hope to operate the reactor as long as possible to respond to expectations by the nuclear science and technology community in Japan, there are many problems for a private university such as heavy economic burdens of increasing regulatory requirements and the aging of the reactor facility.

In this paper, the characteristics, history and utilizations in education and research of UTR-KINKI are introduced as well as the response to Japan's new regulatory standard for research reactors.

2. The characteristics of UTR-KINKI

UTR-KINKI is a light water moderated, graphite reflected, heterogeneous thermal nuclear reactor. As the reactor is operated as a zero-power reactor, it does not have a cooling function, and its fuel burnup is negligible. Fig 1 shows the outer appearance of UTR-KINKI.

Fig 1. The outer appearance of UTR-KINKI

The reactor core of UTR-KINKI is shown in Fig 2. The core is divided into two parts to have dry, wide and uniform neutron irradiation field in the graphite reflector between the two fuel tanks. Each fuel tank is filled with light water moderator and contains six fuel assemblies. Each fuel assembly is composed of twelve fuel plates of Uranium-Aluminium alloy with Aluminium cladding. Four control rods, located adjacent to the fuel tanks, are Cadmium plates, and two of them (safety rod #1 and #2) are safety rods, and the rest (shim-safety rod and regulating rod) are used to vary the reactivity of the reactor. The two safety rods are completely withdrawn when the reactor is in operation. Tab 1 shows the summary of UTR-KINKI's characteristics.

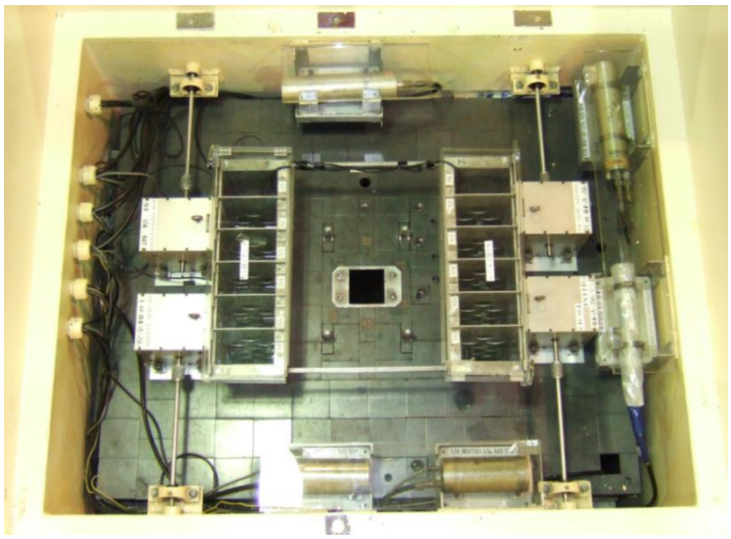

Fig 2. The reactor core of UTR-KINKI

The graphite reflector is equipped with several stringers for sample irradiations and detector installations, which are designed with educational considerations so that basic reactor physics experiments such as neutron flux mapping in the reactor with foil activations can be performed easily. The maximum thermal neutron flux of 1.2×10^{7} cm^{-2} s^{-1} is available in the central stringer hole.

Rated thermal power	1 W
Reactor core temperature and pressure	Normal temperature and pressure
The maximum integrated operating time	1 200 hours / year
Moderator	Light water
Reflector	Graphite
Fuel	Uranium-aluminium alloy
The number of fuel assemblies	12
The size of the reactor core	142 cm × 112 cm × 145 cm
Start-up neutron source	Pu-Be (1 Ci)
The maximum thermal neutron flux	1.2×10^7 cm^{-2} s^{-1}

Tab 1: The summary of UTR-KINKI's characteristics

The reactor core is surrounded by a biological shielding tank which is filled with water and sand as shielding materials. A concrete lid is installed when the reactor is in operation as an upper shielding lid. In addition to this normal shielding lid, the reactor has three types of upper shielding lids, the experimental lid A, B and C. The lid A is specially designed lid which is equipped with a large space for a small animal irradiation. The lid B is for neutron radiography, which is composed of a neutron collimator and an irradiation field. The lid C is a concrete block with an insertion hole through which an irradiation sample or a detector can be taken in and out of the reactor in operation. When the reactor is in operation, one of the lids is selected depending on the purpose of the operation.

3. The history of UTR-KINKI

UTR-KINKI is the first private and university owned nuclear reactor in Japan. In May 1959, the United States Atomic Energy Commission showed and operated a UTR at Tokyo International Trade Fair for eighteen days. The first president of Kindai University, Mr. Koichi Seko, visited this exhibition and decided to purchase this reactor to develop future nuclear engineers at his university. In the next year, the Atomic Energy Research Institute was established, and the reactor was relocated in the university campus in 1961. The first criticality was achieved at 20:53, November 11, 1961. The licensed thermal power at the time was 0.1 W, and later it was upgraded to 1 W in 1974.

Though the reactor had been operated for education and research without any trouble since the first criticality, it had to be shut down in February 2014 due to Japan's new regulatory standard for research reactors established after the Fukushima Daiichi nuclear power plant accident. As mentioned in the introduction, safety reviews and inspections based on the new regulatory standard took for more than three years, and finally the reactor resumed operation in April 2017 as the first research reactor which was allowed to be operated under the new regulatory standard in Japan. Details of the safety reviews are described in a later section.

4. Research

UTR-KINKI is open to domestic researchers belonging to universities and research organizations under a joint use program. The program began in January 1981 to promote scientific researches using UTR-KINKI and has been financially supported by the Japanese government. Researchers who want to use the reactor are invited to submit their proposals every fiscal year. The proposals are divided into three fields (physics, chemistry and biology) and reviewed by a steering committee of the program. After the review, reactor operating time is allocated to approved proposals, and travel expenses are paid to the applicants within budget. In addition to the reactor, applicants can use other facilities owned by the Atomic Energy Research Institute such as radiation detectors or X-ray apparatuses as needed. Fig 3 shows the number of approved proposals of the past decade. During the three years of the reactor shut down (2014-2016), only the proposals which can be performed without using UTR-KINKI were approved and continued.

The recent proposals in the physics field are mainly on the development of neutron detectors. There are a few proposals in the chemistry field, but neutron activation analyses are performed continuously. In the biology field, various irradiations to cells, seeds and small animals are performed using the environment where fission neutrons are available with normal pressure and temperature.

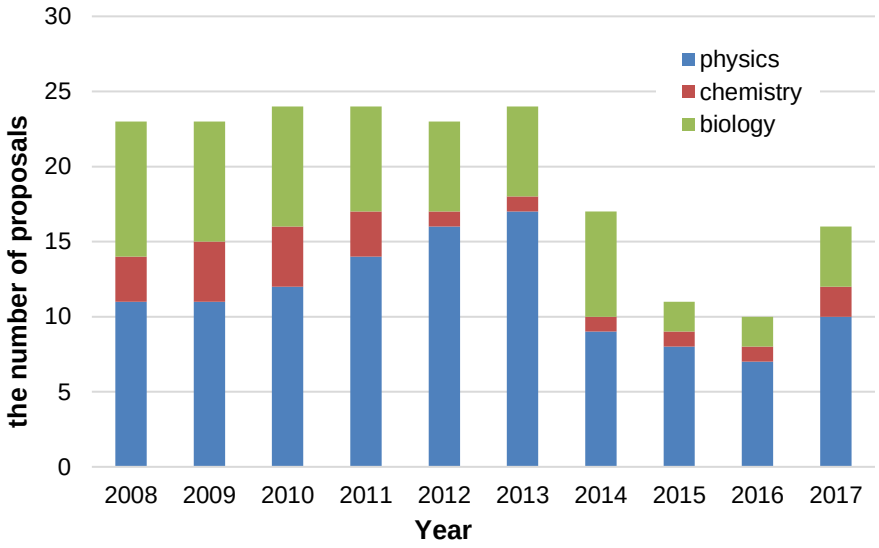

Fig 3. The number of approved proposals in the joint use program of UTR-KINKI (The reactor was not available from 2014 to 2016).

5. Education and Training

5.1 Higher education

UTR-KINKI has been mainly used in education and training for domestic nuclear engineering students. Various laboratory programs and workshops utilizing UTR-KINKI at graduate and undergraduate levels are provided. In the academic year 2017 (from April 2017 to March 2018), students from twelve universities including Kindai University attended to the laboratory programs and workshops. Tab 2 shows the list of the programs offered by the Atomic Energy Research Institute. Part of the workshops are financially supported by the Japanese government.

Basic	Reactor Operation
	Rod worth measurement
	Critical approach
	Neutron flux mapping by the activation method
	Al-foil activation and half-life measurement
	Leakage γ-ray spectrometry
	Neutron and γ-ray dose rate measurement
	Neutron radiography
Advanced	Reactor noise analysis
	Inverse kinetics analysis
	Source jerk method

Tab 2: The list of laboratory programs using UTR-KINKI

Fig 4 shows the number of students who attended the programs and workshops in the past decade. The number of students decreased after 2011 due to the impact of the Fukushima nuclear power plant accident and the decrease of grants from the government. After the three years of the reactor shut-down, the number of students is recovering to the level before the Fukushima accident.

Students also have opportunities to use UTR-KINKI by participating researches for their theses. Kindai University's students who conduct researches using UTR-KINKI are encouraged to obtain a qualification of co-operator, with which students can operate the reactor by themselves under the supervision of a qualified reactor operator.

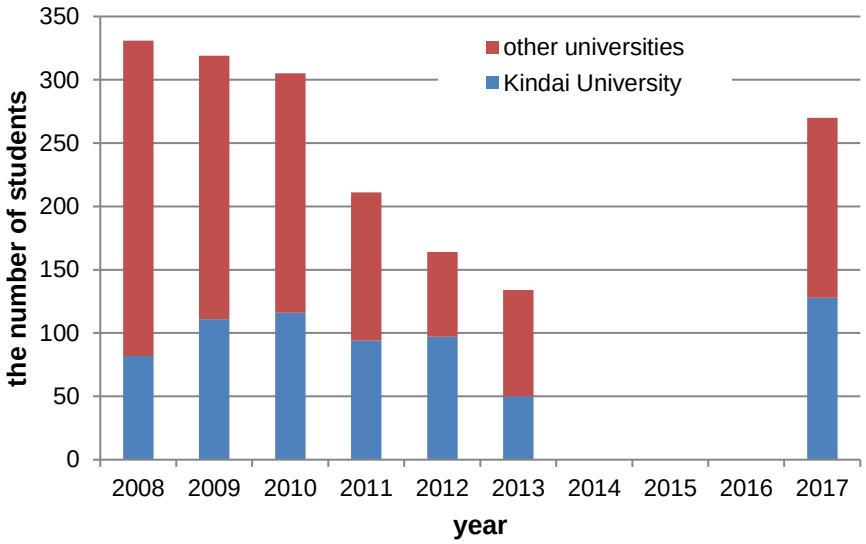

Fig 4. The number of students who attended the programs and workshops using UTR-KINKI.

5.2 Secondary education

UTR-KINKI has been utilized in educational activities for outreach to secondary education. Main activities are workshops for teachers. The aim of the workshop is to provide teachers with scientifically correct knowledge on nuclear science and technology through lectures and experiments. The workshop is usually held as a two-days program and includes several experiments using UTR-KINKI and radiation measurements. Tab 3 shows the contents of the workshop.

Experiment	Reactor operation
	Neutron radiography
	Environmental radiation measurement
	Radiation properties (radiation shielding, inverse square law)
Lecture	Safety instruction
	Basic reactor physics
	Radiation Basics
	Health effect of radiation
Tour	Tour to UTR-KINKI

Tab 3: The contents of the workshop for teachers

The workshop for teachers began in 1987 and has been continued for more than thirty years. In the academic year 2017, five workshops are held in summer, and 68 teachers attended. Fig 5 shows the number of attendees to the workshop in the past decade. Though the workshop targets secondary school science teachers, other teachers who are interested in nuclear science and technology are also accepted upon request.

Two out of the five workshops held in 2017 are co-hosted by the Japan Atomic Industrial Forum, other two are co-hosted by the Kansai Atomic Conference, and the rest is held as part of teacher's license renewal workshops offered by Kindai University.

Workshops for high school students are also offered by the Atomic Energy Research Institute to encourage young generation to pursue careers in nuclear science and technology. Two workshops were held in 2017, in which 63 students participated. The workshop included reactor operation, radiation measurements and lectures on recent topics on nuclear energy.

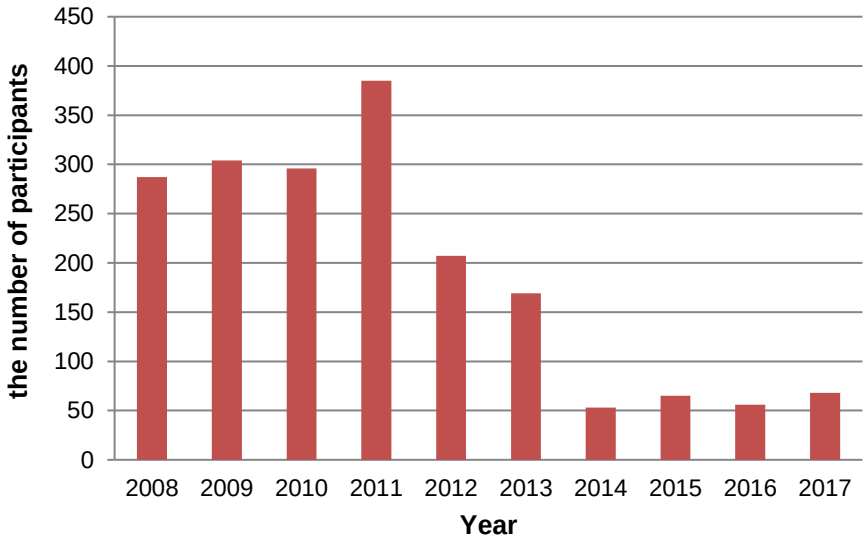

Fig 5. The number of teachers who attended workshops using UTR-KINKI

5.3 Other educational activities

UTR-KINKI is used for the training of the employees of companies in the nuclear industry. In 2017, a training workshop was held as a two-days program for the new employees of Chiyoda Technol Corporation, a company which provides services in radiation protection and applications. The workshop aimed to give all around knowledge on nuclear reactor and radiation from principles to applications through experiments and lectures.

International programs also increasingly utilize UTR-KINKI in recent years. In 2017, a two-days workshop was held for instructors from Asian countries as part of Instructor Training Program of Nuclear Human Resource Development Centre, Japan Atomic Energy Agency (JAEA). Ten trainees experienced reactor operation, rod worth measurement and neutron radiography. A regional research reactor school in 2019 using UTR-KINKI is in preparation in association with International Atomic Energy Agency (IAEA). The school is planned to be co-hosted by Kyoto University and Wakasa-wan Energy Research Centre.

6. Response to the new regulatory standards

After the Fukushima Daiichi nuclear power plant accident in 2011, Japan's nuclear regulation was revised drastically. Before the revision, research reactors were regulated by the Ministry of Education, Culture, Sports, Science and Technology (MEXT) while nuclear power plants were regulated by the Nuclear and Industrial Safety Agency (NISA) of the Ministry of Economy, Trade and Industry (METI). In 2012, the nuclear regulations were unified in the revision, and the Nuclear Regulation Authority (NRA) was established.

In December 2013, NRA enforced new regulatory standards for research reactors. Since the standards were retroactively applied to existing research reactors, UTR-KINKI had to be shut down until it is licensed again under the new regulation standards.

The new regulation standards required low power research reactors to enhance countermeasures against natural and man-induced hazards, and to prepare measures to inform users and visitors of the occurrence of an accident and evacuation instructions. The

natural hazards to be assessed for UTR-KINKI included earthquake, tsunami, flood, wind (typhoon), tornado, freezing, rainfall, fallen snow, thunderbolt, landfall, volcanic eruption, forest fire and biological events. The standards also required to assess other hazards such as internal and external fires, internal flooding, airplane crash, the loss of external power source, dam break, explosion, toxic gas, ship impact and electromagnetic interference. Furthermore, the combinations of the above-mentioned hazards are also required to be assessed.

Since each research reactor has a different risk and characteristic, and UTR-KINKI is a zero-power reactor, a graded approach was expected in the application of the regulatory requirements. However, NRA required the university to assess every regulatory requirement for UTR-KINKI according to the assessment for nuclear power plants regardless of its consequential risk. That led to the hearings and documentations for explaining more than 150 items and several modification works to make the reactor facility meet the regulatory requirements. Consequently, the safety review process for the relicense took for more than three years.

All the research and education using UTR-KINKI were cancelled for the period from February 2014 to March 2017. The limited number of researches were continued with a start-up neutron source (Pu-Be) or other facilities. Part of the laboratory programs and training workshops were continued by substituting the contents which were able to be conducted without the reactor. In the higher education programs, because no research reactor was available for education and training in Japan at the time due to the new regulatory standards, some students were selected and sent to South Korea to attend specially arranged workshops at Reactor Research and Education Centre, Kyung-Hee University, in which students experienced several reactor physics experiments with reactor operation. The workshops at Kyung-Hee University were organised by Kindai University with a financial support of MEXT.

7. Summary

UTR-KINKI is a specially designed reactor for university education and research with an Argonaut type reactor as a prototype. Since its first criticality in 1961, the reactor has been utilized in research and education in Japan, and it is now one of the three university owned reactors in Japan. The reactor is open to domestic researchers under a joint use program, which was started in 1981. Various laboratory programs and workshops using UTR-KINKI have been provided in secondary and higher education, from basic to professional levels. Due to the new regulatory standards established after the Fukushima nuclear accident, UTR-KINKI had to be shut down for about three years, but the reactor resumed operation in April 2017 as the first research reactor which was approved operation under the new regulatory standards. Though there are many problems for a private university to operate a research reactor such as heavy economic burdens on increasing regulatory requirements and the aging of the reactor facility, the Atomic Energy Research Institute hope to continue the operation of UTR-KINKI as long as possible to respond to domestic and international expectations by the nuclear science and technology community.

GRADED APPROACH FOR THE PERIODIC SAFETY REVIEW OF AGN-201K IN KOREA

J.W. PARK, K.J. LEE, S.H. HWANG, H.J. NA, T.B. YOON
FNC Technology, Inc.
13 Heungdeok 1-ro, Giheung-gu, Yongin-si, Gyeonggi-do, 16954, Korea

ABSTRACT

It is compulsory for all nuclear reactors including research reactors to be performed the periodic safety review (PSR) every 10 years in Korea. Accordingly, AGN-201K, low power educational reactor operated by KHU, has also been initiated for its first PSR. In principle, fourteen(14) safety factors identified in IAEA SSG-25 shall be used for the evaluation and review of PSR. However, IAEA SSG-22 recommends the application of graded approach in safety requirements of research reactors. The application of grading should be commensurate with the importance to safety of the activities and SSCs, and with the magnitude of the associated radiological risks. Each activities and SSCs important to safety will be identified, classified and finally graded according to the risks. The potential risks of AGN-201K from the operation and the maintenance including accidents are very low. In this paper, the graded approach on the 14 PSR safety factors of AGN-201K will be addressed with the preliminary evaluation results. Presented be also the comparison between those of HANARO and commercial power reactors.

1. Introduction

AGN-201K operated by Kyung Hee University (KHU) is a lower power reactor for education and training. Tens of AGN type reactors were widely supplied by Aerojet General Nucleonics (AGN) in 1960s. The current operating power is 10 watt at maximum, the uprated power from the original 0.1 watt. Figure 1 shows the configuration of AGN-201K [1].

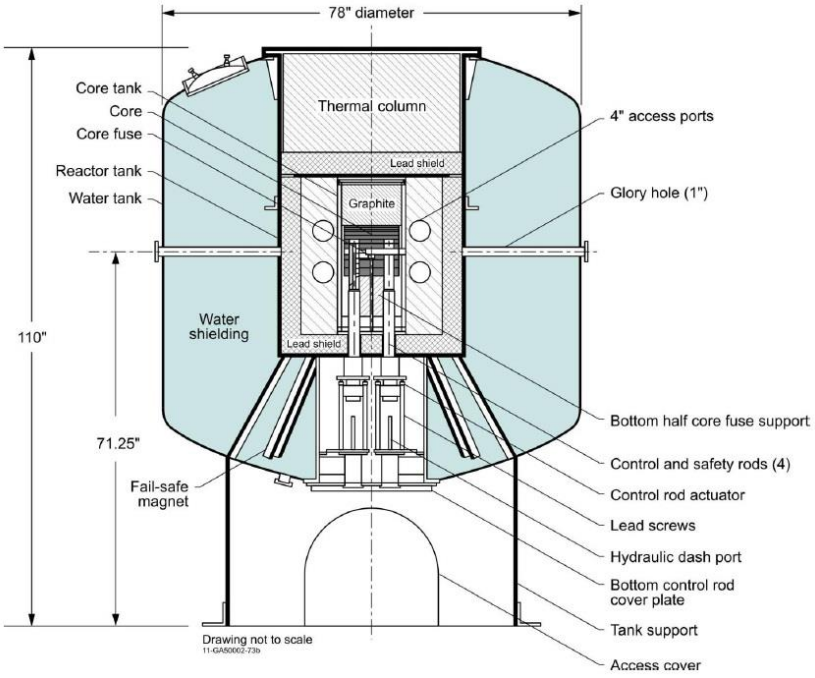

FIGURE 1. Configuration of AGN-201K

By the Korea Atomic Safety Law[2], operators of nuclear reactors shall periodically assess the safety of nuclear reactors, which shall apply to the research reactors. The Enforce Decree of the Law[3] requires that 14 safety factors identified in IAEA SSG-25[4] shall be used for the evaluation and review of PSR every 10 years. However, IAEA SSG-22[5] recommends the application of graded approach in safety requirements of research reactors.

AGN-201K was also requested to perform PSR by the Korea nuclear regulatory body (KINS). Accordingly, AGN-201K has also been initiated for its first PSR. Application of a graded approach was necessary needed for the practical and realistic purposes.

Most research reactors give rise to fewer potential hazards to the public than nuclear power plants, but they may pose greater potential hazards to operators, researchers and other users owing to the relative ease of access to radiation or radioactive materials. Qualitative categorization of the facility shall be performed on the basis of the potential hazard associated with the research reactor. For the application of a graded approach in the PSR of AGN-201K, categorization of the facility should be performed on the potential risk viewpoint. After that, each activities and SSCs important to safety should be identified, classified and finally graded according to the risks. The risks of potential radiation hazard may be impacted by many factors that affect nuclear and radiation safety of the facility. Such factors include:

- reactor power
- radiological source term
- amount and enrichment of fissile material and fissionable material
- spent fuel storage areas, high pressure systems, heating systems and the storage of flammables, which may affect the safety of the reactor
- type of fuel and its chemical composition
- type and mass of moderator, reflector and coolant
- amount of reactivity that can be introduced and its rate of introduction, reactivity control, and inherent and engineered safety features
- quality of the containment structure or other means of confinement
- utilization of the reactor (experimental devices, tests, radioisotope production, reactor physics experiments)
- location of the site, including the potential for external hazards and the characteristics of airborne and liquid releases of radioactive material

	OPR1000[6]	HANARO[7]	AGN-201K
Owner/Operator	KHNP	KAERI	KHU
Purpose	Power Generation	Research & Isotope Production	Education
Thermal Power	2,815 MW	30 MW	10 W
Fuel	UO_2 Ceramic Pellet	U_3Si+Al Metal	UO_2 PE Disk
^{235}U enrichment	< 5%	~20%	20%
Control Material	B_4C + Inconel-625	Hf	U-235
Cooling Method	PWR (H_2O)	Open Pool (H_2O)	N/A
Seismic Design	0.2 g	0.2 g	N/A
Offsite Dose Effect	Large	Small	N/A
2 Hr Accident Dose at EAB	< 250 mSv (WB) < 3,000 mSv (Thy.)	49 mSv (WB) 124 mSv (Thy.)	32 mSv (@ Reactor Area)

TABLE 1. Design Characteristics of OPR1000, HANARO and AGN-201K

Table 1 summarizes the major design characteristics of AGN-201K and compares with those of OPR1000 commercial reactors and HANARO research reactor.

The maximum thermal power of AGN-201K is 10 W with average neutron flux of $3x10^8$ #/cm^2-sec. The core was designed to be subcritical without control rods. With the insertion of control rods, the maximum excess reactivity is 1.8% Δk/k. Table 2 shows the core design of AGN-201K.

	Thickness	^{235}U Weight	Function
Fuel Disk 1,2,3,4	4 cm	102 gm x 4	Core (24 cm height)
Fuel Disk 5,6,7	2 cm	58 gm x 3	
Fuel Disk 8,9	1 cm	29 gm x 2	
Thermal Fuse		4 gm	Safe Shutdown
Safety Rod 1,2		14.5 gm x 2	Shutdown
Coarse Control Rod		14.5 gm	Control
Fine Control Rod		2.5 gm	Control
Sum of ^{235}U Weight		690 gm	
Excess Reactivity			1.8 % Δk/k

TABLE 2. Reactor Core Design of AGN-201K

Considering the contributing factor above, the potential risks of AGN-201K are very low from the operation and the maintenance including accidents. In practice, no potential radiation hazard exists exceeding the boundary of the reactor area. Consequently the graded approach will be applied to PSR in order to reflect the low risks of AGN-201K. The practical and realistic application of the IAEA safety factors is necessary for the first PSR of AGN-201K.

2. Maximum Credible Accident Analysis

IAEA SSR-3[8] and SSG-20[9] require that postulated initiating events shall be selected appropriately for the purpose of analysis present in the design of research reactors. The set of postulated initiating events shall cover all credible accidents that may affect the safety of the research reactor. They shall include all foreseeable failures of SSCs of the reactor facilities and experiments as well as operating errors and possible failures arising from internal and external hazards for all operational and shutdown states.

AGN-201K SAR updated for power uprate includes the accident analysis. It contains all postulated initiating events and describes the analysis results for each accident. They include:

- reactivity insertion
- loss of coolant
- loss of flow
- inadvertent fuel handling
- experimental error
- loss of power supply
- external events
- inadvertent equipment handling or malfunction

The maximum hypothetical accident (MHA) in AGN-201K is reactivity insertion accident. The MHA assumes that the excess reactivity of 2% Δk/k is assumed to be instantly inserted conservatively during the delayed critical state, which is impossible in the realistic condition. Except for the passive characteristics of AGN-201K and natural phenomena such as gravity, any active components or operator actions are not considered to mitigate the accident. The radiation dose from the MHA is less than 32 mSv at the vicinity of reactor site. This value is much lower than the regulatory limitation of 250 mSv at the exclusion area boundary (EAB)

for power plants. In conclusion, AGN-201K was approved to give no environmental effect in the radiological viewpoint.

3. Categorization, Classification and Grading

The application of graded approach presented in the IAEA SSG-22 begins with categorization of the facility in accordance with its potential hazard. In this step, a facility can initially be categorized into a range from facilities posing the highest risk to those posing the lowest risk. This categorization serves to provide an initial grading of the facility. The next step (Step 2) is analysis and grading of activities and/or SSCs important to safety. This second step provides more detailed grading to be applied to the particular characteristics of the facility.

Qualitative categorization of AGN-201K is performed on the basis of the potential radiological hazard, using a multi-category system:

- Facilities with off-site radiological hazard potential;
- Facilities with on-site radiological hazard potential only;
- Facilities with no radiological hazard potential beyond the research reactor hall and associated beam tubes or connected experimental facility areas.

Naturally, AGN-201K belongs to the last category according to the MHA analysis result. On the other hand, HANARO research reactor belongs to the facility with off-site radiological hazard potential[10], needless to say for commercial reactors.

The appropriateness of applying a graded approach should be determined through analysis for each of the major activities and SSCs. The application of grading should be commensurate with the importance to safety of the activities and SSCs, and with the magnitude of the associated radiological risks. All SSCs (including software for instrumentation and control) that are important to safety are required first to be identified and then to be classified according to their function and significance for safety.

In AGN-201K, no activities or SSCs is required in order to prevent or mitigate the consequences of accidents. That is, AGN-201K gives no radiological risks to personnel and environment without the help of operator actions or countermeasures. As a result, all SSCs are designated as non-safety-related, which rule out the necessity of evaluation on equipment qualification, aging, PSA and hazard analysis in the PSR evaluation of AGN-201K.

4. Implementation of Graded Approach in PSR

Evaluated are fourteen(14) safety factors identified in the IAEA SSG-25 for PSR. The evaluation on the deterministic safety analysis was conducted for the appropriateness of postulated initiating events in the accident analysis and the effectiveness of MHA analysis result. Five(5) factor are exempted in AGN-201K since no safety-related SSCs exist, including actual condition of SSCs, equipment qualification, aging, PSA and hazard analysis.

Emergency planning is exempted according to the Korean Law on the Prevention of Radioactive Disaster[11]. By the law, educational reactors with the thermal power less than 100W are excluded from the duty of development of emergency planning. Therefore, the evaluation on emergency planning is not necessary since the maximum power of AGN-201K is 10W.

Environmental radiological impact is also exempted by the Korea Atomic Law. The law requires the radiological environmental impact assessment and radiological environmental survey only on commercial nuclear power plants, research reactors with the power of 100W

higher, spent fuel storage facilities, and radwaste storage facilities. The maximum power of AGN-201K is 10W, hence the evaluation on environmental radiological impact is exempted.

As a result, the IAEA safety factors considered in the evaluation of AGN-201K PSR are as follows:

- Plant design
- Safety performance
- Use of experience
- Organization, management system, safety culture
- Procedures
- Human factors

Table 3 shows the results of graded approach on the 14 IAEA safety factors for AGN-201K PSR. Detailed evaluation has been carried out for the six(6) safety factors selected above. From the effort, two(2) tentative safety improvement items have been drawn from the evaluation, one(1) from procedures and the other one(1) from the human factors.

No	Safety Factors	Detailed Evaluation	Basis
1	Plant Design	Yes	-
2	Actual Condition of SSCs important to Safety	No	No Safety-Related SSCs
3	Equipment Qualification	No	No Safety-Related SSCs
4	Aging	No	No Safety-Related SSCs
5	Deterministic Safety Analysis	Yes	To decide the off-site radiological effect
6	Probabilistic Safety Assessment	No	No Safety-Related SSCs
7	Hazard Analysis	No	No Safety-Related SSCs
8	Safety Performance	Yes	-
9	Use of Experience	Yes	-
10	Organization, the Management System and Safety Culture	Yes	-
11	Procedures	Yes	-
12	Human Factors	Yes	-
13	Emergency Planning	No	Law the Prevention of Radioactive Disaster (100 W)
14	Radiological Impact on the Environment	No	Korea Atomic Law (< 100W)

TABLE 3. Graded Approach on 14 Safety Factors for AGN-201K PSR

5. Conclusion

The PSR on a low power educational reactor, AGN-201K has been performed. A graded approach is implemented as a tool for the practical and realistic purposes. Since the radiological risks are very low and consequently no safety-related SSCs exist in AGN-201K, several safety factors are exempted from the evaluation. Some safety factors are excluded by the laws for its low power. For other safety factors, detailed evaluation has been performed to draw countermeasures for safety enhancement.

6. References

[1] AGN-201K Safety Analysis Report, KHU, Oct. 2011

[2] Korea Nuclear Safety Law, Korea Nuclear Safety Commission, Jul. 2017

[3] Korea Nuclear Safety Law Enforcement Decree, Korea Nuclear Safety Commission, Apr. 2016

[4] IAEA Safety Standards SSG-25, “Periodic Safety Review for Nuclear Power Plants,” Vienna, IAEA, 2012

[5] IAEA Safety Standards SSG-22, “Use of a Graded Approach in the Application of the Safety Requirements for Research Reactors,” Vienna, IAEA, 2012

[6] Final Safety Analysis Report for SHINWOLSONG Units 1&2, KHNP, Rev. 1, Dec. 2011

[7] Final Safety Analysis Report for HANARO, KAERI, Oct. 2014

[8] IAEA SSR-3, “Safety of Research Reactors,” Vienna, IAEA, 2016

[9] IAEA SSG-20, “Safety Assessment for Research Reactors and Preparation of the Safety Analysis Report,” Vienna, IAEA, 2012

[10] Periodic Safety Review Report for HANARO, Dec. 2018, KAERI

[11] Enforcement Decree of Korea Law on Prevention of Radioactive Disaster, Korea Nuclear Safety Commission, Jul. 2017

SAFETY REGULATION OF DECOMMISSIONING OF NUCLEAR RESEARCH FACILITIES IN THE RUSSIAN FEDERATION

ALEXANDER SAPOZHNIKOV
Department for Safety Regulation of Nuclear Power Plants and Nuclear Research Facilities,
Federal Environmental, Industrial and Nuclear Supervision Service of Russia,
109147 Moscow, Taganskaya, 34, Russia

ABSTRACT

.
Since the beginning of the 1980s, due to raised organizational, financial and technical problems, in the Russian Federation there has been a constant increase in the number of research nuclear facilities (NRFs) that are in a state of extended or final shutdown pending their modification, refurbishment or decommissioning. The most common reasons for the termination of NRF functional use were: 1) lack of programmes for further facility use; 2) safety problems due to the need of bringing facilities in compliance with modern safety requirements. In this regard, safety regulation of the NRF in the mode of long-term and final shutdown and decommissioning of RNF is one of the most urgent tasks of Rostechnadzor mandated activity. The task is carried out in accordance with the legislation of the Russian Federation based on further development of the national regulatory framework, improvement of the licensing process and strengthening of the state supervision regime over nuclear and radiation facilities. The report provides an overview of the state of safety regulations related to decommissioning of the NRF, developed with account to recommendations of the relevant international organizations and good practices, known in this area.

1. Introduction

Most of nuclear research facilities (NRFs)[1] in the Russian Federation were designed and commissioned in 50-70th of the last century, when the legal and regulatory framework for ensuring safety of nuclear energy use was not yet developed in proper way. Since the mid of 1980s the task of decommissioning of these facilities as well as the other nuclear and radiation hazardous objects has begun to acquire a particular significance within frame of the "elimination of nuclear legacy" process. Before the collapse of the USSR, there were 119 NRFs in the Russian Federation, at present there are 63 NRFs, which are under Rostechnadzor[2] regulatory supervision (including 30 research reactors (RRs). In total about 60% of all operated nuclear research facilities are over 30 years old, and activities are being carried out to extend their service life, upgrade systems and components, make reconstruction. Some facilities are in state of preparation for decommissioning or in decommissioning mode.

The report introduces the experience, gained by Rostechnadzor in ensuring safety management of old NRFs and other small objects of the nuclear energy use (ONEU). It gives a systematic review of the regulatory issues, arisen during preparation of NRFs for decommissioning, decommissioning, and release of facilities from regulatory control, including the release with restrictions.

1 NRFs – nuclear facility including research nuclear reactors (RR), critical nuclear assembles (CA) and subcritical (SCA) nuclear assembles, and related complex of premises, structures, systems, elements, experimental facilities, and personnel that are in boundary of territory (NRF site) defined by the design for utilization of neutrons and ionizing radiation for research purposes.

2 The Federal Environmental, Industrial and Nuclear Supervision Service (Rostechnadzor) - the state regulatory authority in the field of the use of atomic energy in accordance with international conventions, www.gosnadzor.ru.

2. National decommissioning policy, strategy and funding

National policy and strategy to enable and enhance decommissioning of ONEU and environmental remediation are declared in the “Fundamentals of State Policy of Nuclear and Radiation Safety in the Russian Federation for the Period up to 2025 and Further Perspective” that was agreed by the President of the Russian Federation [1]. The document specifies the long-term goals, basic objectives, fundamental principles, priorities and crucial tools of the state policy in the field of ensuring nuclear and radiation safety in the Russian Federation. The plans, developed and implemented to perform ONEU decommissioning are closely linked to the plans on creation of storage facilities for spent fuel (SF) and disposal facilities for radioactive waste (RW), as well as creation of the appropriate infrastructure for the RW treatment and development of the legal framework [2].

According to the strategy a priority problem to be resolved is elimination of the nuclear legacy [3]. The relevant activities have been planned and realized within the Federal Target Programmes “Provision of Nuclear and Radiation Safety”. The first programme covered the time period 2008-2015, the second one was approved by the Government of the Russian Federation for the period 2016-2025. The both programmes, mentioned above, are based on adoption of the step-by-step approach for ONEU dismantling and taking deferred decisions with regard to the end state of facility.

The main part of the funds, allocated under the programmes, are intended for coping with the “nuclear legacy”, i.e decommissioning of ONEU and associated activities with the RW and SF. Funding for completion of the use of NRFs for their functional (initial) purpose and decommissioning is provided through a special fund. The mechanism for formation and use of this fund is defined by the resolutions of the Government of the Russian Federation given in Ref. [4-6].

3. Legislative basis

Implementation of the state policy in the area of decommissioning, RW management and environmental remediation are based on the following main federal laws:

- On the Use of Atomic Energy № 170-FZ dated 21.11.1995;
- On Radiation Safety of Population № 3-FZ dated 09.01.1996;
- On Protection of Environment № 7- FZ dated 10.01.2002;
- On Radioactive Waste Management № 190-FZ dated 11.07.2011.

The Federal Law “On Radioactive Waste Management” is focused onto solving of "nuclear legacy" problems and creation of the interconnected uniformed RW management system. It does not include definition of a concept of "decommissioning“, and the provisions for ONEU decommissioning there are not provided. According to the Federal Law “On the Use of Atomic Energy” the arrangements and procedures for ONEU decommissioning should be specified in the Federal Rules and Regulations (FRR) with regard to each specific type of the ONEU.

4. Regulatory basis

The work on harmonization of the national legislative and regulatory framework on decommissioning of nuclear facilities has been carried out with due account to the requirements of the IAEA Safety Standards [7] and the recommendation on setting safety criteria for release of the sites from regulatory control made by the Integrated Regulatory Review Service (IRRS) Mission to the Russian Federation [8].

To unify decommissioning procedures for various ONEU, Rostechnadzor has developed the FRR “Safety Assurance in Decommissioning of Nuclear Facilities. General Provisions”,

NP-091-14 [9]. The FRR includes a requirement that the concept of decommissioning should be planned based on graded approach at the early design stage and reconsidered throughout the lifetime of the facility. In the transition period, after the use of the facility for the functional activities had been closed, but decommissioning has not been yet started, the facility is a subject to the same safety requirements as in the operational mode. The main components of the decommissioning concept (preliminary decommissioning plan, radiological characterizations etc.) should be part of the project documentation and the Safety Analysis Report (SAR). The selected decommissioning techniques and organizational measures should provide for the following general safety principles:

- optimization of protection of workers (personnel), population and the environment from a potential negative radiation impact during the facility decommissioning;
- minimization of generated amount of RW;
- prevention of radioactive discharges into the environment in quantities exceeding the established limits;
- prevention of potential accidents and mitigating their consequences in case if they occurred.

To implement an unified technique in decommissioning Rostechnadzor developed and issued a safety guide "Recommendations for justifying the choice of option for facility decommissioning", RB-153-18, which considers the option of "Liquidation" and approaches to it implementation ("Delayed liquidation" and "Immediate liquidation"); the option with construction of a RW repository; and combination of decommissioning options.

The termination of the NRF operation and it decommissioning have some major challenges, in particular as following:

- Involvement of personal with poor experience in potentially dangerous works during NRF decommissioning. At NRFs change of personnel generations takes place and lack of new coming professionals characterizes the situation.
- Absence of the reprocessing technology for some types of fuel elements and fuel assembles. The spent fuel is kept in a temporary storage for a long time.
- The tendency to the accumulation of spent (irradiated) nuclear fuel in temporary storage facilities located on the territory of research centers. This is caused by sharply increased costs for transportation and processing of fuel at specialized enterprises.
- Unsolved problem and challenges in upgrading outdated facilities for processing and disposal of liquid and solid RW, which belong and located at research centers. The facilities, which were constructed long ago, have numerous aging problems and do not meet modern safety requirements.
- Absence of the sufficient financing for decommissioning work.

The main safety requirements to NRF preparedness for decommissioning and decommissioning implementation are systematized in the following FRR [10, 11]:

General NRF Safety Regulations, NP-033-11

FRR determines conditions for decommissioning commencement and conduct of works, including the case, when the NRF decommissioning plan does not provide technology and means for unloading nuclear materials from the reactor core or a preliminary partial dismantling of the facility constructions is required.

Safety Rules on Decommissioning of NRFs, NP-028-16

FRR sets safety requirements to organizational and technical measures of NRF decommissioning defined in NP-028-16 that is a revised version of the document NP-028-01,

issued in 2001. It was developed with account to the accumulated experience and current approaches to facility decommissioning, introduced in the IAEA Safety Standards GSR Part 6. The FRR NP-028-16 clarified the requirements to the concept of decommissioning of the NRF at all stages of the facility life cycle, substantiation of the expected end state of the site, buildings and structures, and ensuring safety during the decommissioning activity. In addition, NP-028-16 was supplemented with the requirements to the structure and content of engineering and radiation survey programs; NRF Decommissioning Plan; as well as requirements to the content and the procedure of formation of the Decommissioning Database.

The FRR NP-028-16 determines “decommissioning” as activity, which is performed after removal of nuclear materials from the site and aimed at achievement of the end state of the facility and its site, according to the Decommissioning Plan. This approach is in line with the current state of economy and social life in the Russian Federation and allows being flexible with the process of the facility decommissioning based on the financial capabilities of the operating organization, which needs to specify the end state, to establish criteria for achieving the end state, to identify stages of work implementation. All information that may be necessary or useful for preparation and conduct of NRF decommissioning should be accumulated in the database formed during facility life time. In addition, the Principal Programme, Decommissioning Plan and Safety Assessment Report of NRF decommissioning should be developed. The Decommissioning Plan should provide methods and technical means of processing, conditioning and storage of RW, technologies for decontamination, fragmentation and dismantling of equipment, technical means for transporting radioactive waste, certification of the chemical composition of materials and equipment.

The regulatory system, in addition to the general provisions of NP-091-14, includes FRRs and safety guidelines on decommissioning of specific types of ONEU and environmental remediation, storage, packaging and removal of SF and radioactive materials from the facility site.

5. Peculiarities of NRF decommissioning

Preparatory work for decommissioning (removal of nuclear and radioactive materials, decontamination) may be carried out within framework of licence for facility operation before issuing the licence for its decommissioning. The final shutdown of a NRF can be introduced only by resolution of the state nuclear authority. When a NRF is in a final shutdown mode the operating organization must perform certain organizational and technical measures to prepare the upcoming work on the NRF decommissioning, including**:**

- unloading of nuclear materials and ionizing sources from the facility core in compliance with the technology defined in the Decommissioning Plan, and removal them from the facility site or delivery to other NRF at the same site;
- removal of the radioactive working fluids from equipment and systems, decontamination of equipment, systems and constructions, processing of RW accumulated during NRF operation and (or) removal them from the NRF site;
- conduct of the comprehensive surveillance and radiation monitoring of NRF systems, equipment, constructions and buildings to monitor their engineering condition as well as to draw up the characterization of radiation dose rates and radiation contamination;
- development of the Principal Program of decommissioning activities, including general technical and organizational measures for implementation of the accepted strategy of NRF decommissioning;
- development of the Decommissioning Plan that should identify specific types of decommissioning activities including the technologies, necessary material and technical resources and the status of the NRF site after completion of the work;

- development of the D&D SAR which should justify that decommissioning technical and organizational measures are in compliance with the Principal Program and the Decommissioning Plan provides for safety conditions for the personnel and population.

For NRF operation in the final shutdown mode a decreasing of the facility staffing and maintenance might be done in compliance with the requirements established in the Decommissioning Plan and justified in the D&D SAR. Based on a graded approach it is allowed not to develop a Decommissioning Plan for CA (SCA) in case the D&D SAR has justified that a radiation risk of forthcoming works is negligible.

If the technology for unloading nuclear materials from the core requires partial dismantling of the NRF construction, these works can be carried out when NRF is in operation in the final shutdown mode, according to the Decommissioning Plan.

The set of documents on decommissioning of the NRF, in addition to the SAR, includes a Decommissioning Plan and project documentation. The Decommissioning Plan should describe the following main components of the decommissioning strategy:

- feasibility study of the chosen decommissioning option;
- main stages of the decommissioning strategy and time-scale of their implementation;
- survey of the facility site after completion of each main stage of the Decommissioning Plan.

The facility end state may be varied from “a green/brown site“ to “a buried special RW” depending on the circumstances (which force to) and conditions (which are created by) available for adoption of strategy for the execution of works. The essential circumstances for decision making are the NRF location and its technical specifications, the important conditions are the readiness of the operating organization to decommissioning activity: state of the Decommissioning Plan, personnel, availability of financial funds and others. As a rule, NRFs are located near or within cities and large settlements, and it is important that their decommissioning will not create an increased radiation risk to the population and the environment.

Taking into account the technical features of the NRFs, three specific groups of NRFs can be defined based on graded approach when choosing a decommissioning strategy:

- RRs with fixed neutron-flux density;
- pulse RRs and RRs with homogeneous core;
- stands with critical (CAs) and subcritical (SCA) nuclear assemblies.

RRs with fixed neutron-flux density are posed the most potentially hazardous facilities because of a large amount of the fission products accumulated in the spent fuel, existence of high level RW, high level of induced radioactivity in the biological shield, metal constructions and equipment. As a rule, a strategy of “the safe storage under surveillance” during a long time for reducing induced activity of construction elements to acceptable level is applied. The deferred dismantling of highly radioactive NRF equipment and the use of the reactor building for continuing operation of other NRFs located there is the most preferred strategy at present.

A comparative assessment of the cost of decommissioning of a facility with a stationary neutron flux density for the immediate dismantling option and for the delayed dismantling option shows that a significant part of the costs are treatment of RW, maintenance to support safe operation of systems and equipment, and the work on dismantling and decontamination. The time factor during deferred dismantling of the NRF reduces costs due to reducing the

activity of decommissioned structures. In addition, if the generated in the process of decommissioning RW can be brought to the acceptance criteria for disposal at the national RW management facility, then the costs associated with the temporary storage of radioactive waste at a specialized enterprise are excluded.

Critical assembles (CA), which usually have thermal power less than 1 kW and SCA have following particular features:

- irradiated fuel may be considered as "fresh fuel";
- fuel storage does not require a special cooling system, therefore a temporary storage of NRF can be used for fuel location until its removal from the facility site;
- fuel does not contain high-activity fission products and normally does not require decontamination or cleaning, in order to be used in similar facilities or to be transported to a reprocessing plant;
- induced radioactivity in biological shield, metal constructions and internal elements is low level or negligible;
- radioactive contamination of surfaces in the facility premises does not exceed the authorized level and the surfaces can be easily decontaminated;
- liquid RW (if there is any) is of low radioactive level and during normal (non-emergency) operation is accumulated in a small amount;
- practically all technological operations, such as core unloading, fuel management, dismantling of equipment, decontamination of surface and equipment are governed by acting at the facility instructions, which can be also used for NRF final shutdown and its decommissioning without essential changes.

In view of aforesaid specifics of such NRFs “immediate dismantling” strategy is usually used for their decommissioning. A scope of work and term of decommissioning works can be significant less than term of decommissioning of RRs with fixed neutron-flux density. Decommissioning period for such NRFs is commonly planned depending on the financial capabilities of the operating organizations.

Pulse RRs and RRs with homogeneous core occupy an intermediate position in the choice of decommissioning strategy. A combined decommissioning option including immediate dismantling of the low - level radioactivity part of the facility and postponed dismantling of the medium and high-level radioactivity part of the facility may be optimal.

For some types of NRFs full unloading of nuclear materials from the reactor core (for example, RRs IBR-30) or full removal of radioactive coolant from the technological system or equipment (for example, RR BR-10 with sodium coolant) can be realized only during the dismantling of the construction elements according to the NRF Decommissioning Plan.

At the final stage of the NRF decommissioning, there are two main options for achieving the final state: 1) release of the NRF building (site) or its part from the sphere of regulatory control; 2) changing of the status of the NRF, for example, use of NRF premises for storage of radioactive substances or RW (for example, RR ARBUS-AST-1).

When the final state is reached in compliance with the facility Decommissioning Plan that includes changing of the ONEU status, the operating organization should apply for closing licence for the decommissioning activities at the NRF and getting a license for a new type of activity with attached necessary set of safety documents (for example, a storage facility for radioactive substances).

6. Examples of recent decommissioning activity

Over the past 10 years, the licences for decommissioning activity have been terminated for the following NRFs due to the achievement of the facility final state:

- Join Institute for Nuclear Research (JINR) - pulsed fast neutron booster IBR-30 with injector- linear electron accelerator LUE-40 (2007)3;
- Limited liability company «Belgorodgeologiya» - SCA CO-1 (2007);
- Joint Stock Company «State Scientific Centre of the Russian Federation - Institute for Physics and Power Engineering named after A.I. Leypunsky» (SSC RF IPPE) - model of transport and small-size power reactors with intermediate neutron spectrum CGO (2008); assembly with liquid metal coolant lead-bismuth FG-5 (2007), model of nuclear rocket engine “Strela” (2010), fast neutron critical assembly «BR-1» (2011), fuel solution physical stand RF-GS (2012), critical stend AMBF-2-1600 (2017); water-water assembly with external heating MATR-2 (2018);
- Joint-Stock Company “TVEL” - critical assemble № 3 (2012);
- Sankt-Petersburg Institute of Mechanical Engineering “LMZ-VTUZ” – SCA (2012;–
- Joint-Stock Company “The Basic Institute of Chemical Technologies” (VNIIHT) – SCA CO-2M (2012);
- State Scientific Center “Scientific Institute of Atomic Reactors” (SSC RIAR) - RR RBT-10/1 (2014), RR “ARBUS-AST-1” (2018);
- Federal state unitary enterprise “Research Institute of Scientific Instruments” (NIIP) - nuclear transport engine VVRL-02 and VVRL-03 (2011), space nuclear power facility ‘’Yenisei’ (2014);
- National Research Center “Kurchatov Institute” - uranium-graphite critical stands UG (2016); Grog (2016).

Below there are the examples of NRFs (IBR-30, RBT-10/1, ARBUS-AST-1), which licences for decommissioning have been revoked due to termination of decommissioning activity, achievement of the end state and acceptable radiation conditions, defined in the Decommissioning Plan.

Pulse RR IBR-30 was a fast reactor, periodic action, air-cooling, the pulse booster on mean power less than 20 kW, fuel - U-235 90%, Pu metal. The linear electron accelerator (LUE-40) was used as the reactor injector. It was put into operation in 1969. The reactor core consisted of a stationary, two main rotating and auxiliary mobile parts. Modulation of the reactor reactivity was performed with main rotating parts. The rotating parts have been included as an alloy of uranium-235 in a steel disc. The reactor IBR-30 was finally shutdown in 2001. The strategy of immediate dismantling was adopted. The preparatory work included: commissioning of a separate building for storage of radioactive equipment resulting from the dismantling of the radioactive structures; fabrication of the special devices and tools; arrangement of the place for drilling of the uranium inserts from the disks of the main and auxiliary moving parts of the reactor core, development of models and stands for personnel training on dismantling of the reactor. The reactor was completely dismantled in 2007 and the facility internals have been decontaminated, the licence was canceled in 2007. End state - radiation -technology object, commissioning of Intense REsonance Neutron pulsed source (IREN).

A complex of research reactors RBT-10 comprises two similar in design pool-type thermal neutron reactors RBT-10/1 and RBT-10/2 that utilize spent fuel assemblies from the high flux reactor SM-3, UO2 90%. Two reactors share a building, pool, ventilation and special sewage

3 In parentheses indicate the year of termination the licence for decommissioning in connection with the achievement of the end state of the object and the completion of decommissioning activities.

systems, central vault, maintenance room, casings, water purification system, feeding and coolant filling system. The reactors were commissioned on step-by-step basis: 1982 – power startup of RBT-10/1, 1983 – RBT-10/2. In 1994, the activity at power level of the facility RBT-10/1 was stopped, and until 2008 the reactor was in final shutdown mode. In 2008, the licence for decommissioning of the RBT-10/1 reactor was issued. The strategy of immediate dismantling was adopted. As a result of decommissioning of the facility RBT-10/1, the cooling system of the facility RBT-10/2 was upgraded to increase safety and technological capabilities of the facility of RBT-10/2. The final state of the facility RBT-10/1 was reached in 2013; the licence was canceled in 2014.

RR ARBUS-AST-1 tank, organic coolant (gasoil), 12 MW, fuel - UO2, 4,4%; 36%; 90%. It was put into operation in 1963.The licence for decommissioning RR ARBUS-AST-1 was canceled in 2018, the final state of the facility - storage of RW. The licence for the operation of the high-activity RW storage in the building of former RR "Arbus-AST-1" was issued by Rostechnadzor on 8.12.2017.

Further there are the examples of NRFs (RR TVR, RR MR, RR AM, RR BR-10, RR F-1), which are currently in final shutdown or in decommissioning[4].

The facility TVR is tank, channel, heavy water, 2,5 MW, the fuel- UO_2, 90%. It was put into operation in 1949 and shutdown in 1986. The fuel was transferred to «Mayak». The decommissioning of RR TVR is carried out since 1988. During the decommissioning of RR TVR, a heavy water from the reactor and its systems after purification was drained into standard stainless steel tanks, 30 liter, of total amount about 5 tons, which are stored currently at site storage. The heavy water has a high specific activity for tritium. To prepare heavy water for shipment to the processing, its purification from mechanical impurities and its certification must be carried out. The end state was planned as electro-nuclear generator of neutrons (ELYaNG, but then as green field.

The RR MR is the pool, channel, multiloop, water-beryllium, 50 MW, fuel - UO_2, 90%. It was put into operation in 1964 and was shutdown in 1992. The fuel was transferred to «Mayak». Rostechnadzor issued a licence for decommissioning in 2016. As a basic option for the decommissioning, a strategy of immediate dismantling was adopted. The end state defined in the Decommissioning Plan is a compliance of the radiological conditions in the reactor hall, technological premises and at the facility territory with the requirements of sanitary-hygienic standards on the radiation safety of the personnel. One of the possible options for the further use of the reactor hall and the technological premises of the RR MR may be processing of SF and RW (radiation technology objects).

The nuclear facility AM was put into operation in 1954 as the First in the world NPP with electrical power 5 MW (hereinafter used as a research reactor AM). This first NPP in the world demonstrated the possibility of using nuclear energy for generation electricity and heat supply. The reactor AM is U-graphite, channel, water-cooling, thermal neutron reactor with design power 30 MW. The fuel - UO2 4,4% и 10% enrichment. The operation of the reactor AM at power was stopped in 2002, the fuel was transferred to SF storage of the operating organization. Rostechnadzor issued a licence for decommissioning in 2010. It was recognized as a national cultural and scientific heritage of the Russian Federation by certificate of 07 December, 2004. There is a decision on creation a memorial museum and educational center on the basis of the First NPP in the World in Obninsk, approved by the order of the President of the Russian Federation on 09 April, 2004. The decommissioning

4 Final shutdown – is the mode of NRF operation that includes preparation for decommissioning, unloading of nuclear materials from the reactor core and their removal from the NRF site.

strategy of the reactor AM includes four stages: preparation for decommissioning (years 2002 - 2010); preparation for long preservation under supervision and containment (years 2010 -2015); long preservation under supervision (years 2015-2080); finishing (after 2080). A problem is a disposal of the reactor graphite. In accordance with the acceptance criteria, established by FRRs and the decree of the Government of the Russian Federation for management of RW [12] graphite of RR AM is a subject to deep burial.

The RR BR-10 is tank, fast, liquid metal, 8 MW. The fuel - UN 90% + PuO_2. It was put into operation in 1959 and had a few modifications. The reactor was used for a large range of studies of fuel and structural materials, including testing of fuel rods with plutonium dioxide fuel (PuO_2) and uranium nitride fuel (UN) and various liquid metal coolant (Hg, Na-K, Na). The volume of radioactive sodium and sodium-potassium-mercury mix was about 15 m^3. Their radioactivity is caused by nuclides Na-22, Cs-137 and transuranic radio nuclides. The operation of the RR BR-10 at power was stopped in 2002; the fuel was transferred to SF storage of the operating organization (SSC RF IPPE). The liquid metal coolant is in storage at the reactor building.

Transfer of the alkaline liquid metal coolant into a solid, explosion-fire-safe, chemically neutral state that is suitable for a long-term environmentally safe storage, is tested now at a pilot installation. The installation includes three modules: 1) a module for removing mercury from the sodium-potassium alloy (NaKHg); 2) a module for conditioning the alkaline coolant (sodium and sodium-potassium alloy), using solid-phase oxidation (RF patent No. 2200991); 3) a module for neutralization of non-drained alkali metal residues by gas-phase oxidation.

In accordance with the current concept of the RR BR-10 decommissioning, the dismantling of high-activity parts of the reactor is planned after a long postponement (~ 50 years) that is necessary for reducing their radioactivity to acceptable level. The strategy of "keeping under supervision" for 50-70 years was adopted. The completion of decommissioning is planned after 2060 with the end state as radiation technology objects.

The RR F-1 is the first physical reactor in Eurasia, U- graphite, nature cooling, nominal power 24 KW. It was put in operation in 1946. The reactor is assembled with graphite units. The graphite core has cells filled with blocks of uranium metal of natural isotopic composition (2500 fuel rods), enrichment of 2% by U-235 (UO_2 2%). The reactor F-1 was used as reference neutron source for metrological certification and study of the characteristics of neutron flux measuring means for NPPs and other nuclear and physical plants. The operation of the reactor F-1 at power was stopped in 2011. It was recognized as a national cultural and scientific heritage of Russia. In 2014, the decision was made to transfer the reactor F-1 to the final shutdown mode and at present F-1 is a museum, preserving the original configuration of the basic systems.

7. Conclusion

The Russian national strategy for decommissioning nuclear facilities is based on the mandatory timely, environmentally sound and cost-effective decommissioning of the relevant ONEU and excluding the transfer of solution of this problem to future generations. At present, a legislative and regulatory framework for ONEU decommissioning has been generally established, and considerable experience has been accumulated to ensure safe ONEU decommissioning.

Seeing that the decommissioning arrangements and procedures are defined separately for each specific type of ONEU, the main direction of improving the legislative and regulatory framework in this area is: establishment of unified procedures for the safe termination of ONEU functional activities; preparation of ONEU for decommissioning; ONEU safety decommissioning; and establishing safety criteria for release of ONEU from regulatory

control in compliance with the provisions of the Joint Convention on the Safety of Spent Fuel Management and on the Safety of Radioactive Waste Management.

Based on the experience of implementing the NRF decommissioning programs, the following scientific, technical and technological tasks of NRF decommissioning have been identified as topical:

- utilization of the irradiated graphite;
- cleaning of liquid metal coolant and its conditioning into safe solid state;
- purification from mechanical impurities and certification of high-level radioactive heavy water;
- reprocessing of non-standard spent fuel, including fuel solution.

The solution of the above tasks is of a practical importance and will contribute to decommissioning of varies types of ONEU, including nuclear power plants and industrial reactors.

8. References

[1] Fundamentals of state policy of nuclear and radiation safety in the Russian Federation for the period up to 2025 and further period, approved by the order of the President of the Russian Federation from 13.10.2018 N 585.
[2] Khaperskaya A.V., Fifth National Report of the Russian Federation: On Compliance with the Obligations of the Joint Convention on the Safety of Spent Fuel Management and the Safety of Radioactive Waste Management, November 21 – 22, 2017, AtomEco, Moscow, http://www.osatom.ru/mediafiles/u/files/XII_forum_2017/Khaperskaya_A.V._National_report.pdf
[3] Abramov A., Dorofeev A., Komarov E. and other Concerning the evaluation of nuclear legacy volume in the nuclear industry and other facilities of nuclear energy peaceful use in Russia, SECNRS, Nuclear and Radiation Safety, № 3 (73), 2014, c.1-11.
[4] The order of the Government of the Russian Federation «About financing the works on decommissioning of nuclear installations, radioactive sources, disposal facility of nuclear materials, radioactive substances and radioactive waste, research and development activities to justify and enhance safety of these objects» from April 02, 1997, № 367.
[5] The order of the Government of the Russian Federation «About rules to allocate funds of organizations and enterprises, which operate specially dangerous plants and objects (Nuclear Power Plants), for resources creation to provide safety of Nuclear Power Plants at all stages of their life time and development» from January 30, 2002, № 68.
[6] The Order of the Government of Russian Federation «About rules to allocate funds of organizations, which operate specially dangerous plants and objects (excluding Nuclear Power Plants), for resources creation to provide safety at all stages of their life time and development» from September 21, 2005, № 576.
[7] INTERNATIONAL ATOMIC ENERGY AGENCY, Decommissioning of Facilities, General Safety Requirements Part 6, IAEA Safety Standards Series No. GSR Part 6, IAEA, Vienna (2014).
[8] Action plan following the results of the IAEA extended post-mission "Integrated Regulatory Review in the Russian Federation" in November 2013, approved by Rostechnadzor's order from 22 December, 2014, № 593 (In Russian)
[9] Safety Assurance of Nuclear Facilities Decommissioning. General Provisions, NP-091-14, approved by the order of Rostechnadzor from May 20, 2014, № 216 (in Russian).
[10] General Safety Regulations of Nuclear Research Facilities, NP-033-11, approved by the order of Rostechnadzor from June 30, 2011, № 348.
[11] Safety Rules on Decommissioning of Nuclear Research Facilities, NP-028-16, approved by the order of Rostechnadzor from April 04, 2017, № 108.
[12] The Order of the Government of Russian Federation "On the criteria for classifying solid, liquid and gaseous wastes as special radioactive waste, criteria for classifying

radioactive waste as special radioactive waste and removable radioactive waste and criteria for classifying removable radioactive waste" from 19.10.2012 № 1069 (In Russian).

JULES HOROWITZ REACTOR PROJECT: PREPARATION OF THE COMMISSIONING PHASE AND NORMAL OPERATION

O. MARCILLE, R. VALLÉE, G. BIGNAN, V. FEDERICI, JP. CHAUVIN, JL. FABRE, A. FARDEAU

French Alternative Energies and Atomic Energy Commission - Nuclear Energy Division
Cadarache Research Centre - France
Contact author: olivier.marcille@cea.fr

ABSTRACT

Jules Horowitz Reactor (JHR) is a new modern Material Testing Reactor (MTR), currently under construction at CEA Cadarache Research Center in south of France.

It will be a major research facility providing experimental irradiation possibilities to optimize existing power reactors as well as to support the future reactors design.

It will allow:

- to study the behavior of materials and fuels under irradiation for development and qualification needs of nuclear power plants,
- to contribute and to secure the European production of radioisotope for medical use (25% up to 50% of European needs).

The JHR is funded and steered by an international consortium gathering the following partners: EdF (France), AREVA SA (France), TechnicAtome (France), CEA (France), SCK•CEN (Belgium), NRI-CVR (Czech Republic), CIEMAT (Spain), VTT (Finland), Studsvik (Sweden), DAE (India), IAEC (Israel), NNL (United Kingdom) and European Commission and its JRC (EU) as observer.

CEA is the owner and the nuclear operator.

The construction of JHR, which started in 2009, is going on with target for a first criticality at the beginning of the next decade.

The design of the reactor provides modern experimental capacity, which will be in support to nuclear energy R&D programs for the next 50 years.

In parallel to the facility construction, the operation, in order to be safe, reliable and efficient, needs to be prepared. It is also necessary to design and implement the first experimental devices for the reactor start-up in order notably to check the performances of the reactor.

In this framework, many actions are ongoing:

- Staffing and organizational structuring for the commissioning test phases and for operation,
- Elaboration of the documentation to operate the reactor (safety analysis report, general operating rules, procedures, instructions, maintenance and periodic test programs…),
- Staff training by using dedicated facilities (simulator…),
- Performing commissioning test programs to ensure that the layout of systems and subcomponents fulfill the design requirements, the specified performances and the safety criteria,
- Designing and implementing of the first fleet of experimental devices in support to the commissioning test program and the future experimental programs.

This paper gives first an overall up-to-date status of reactor construction, and second presents one particular activity of the future operation team, the preparation of the documentation to operate the reactor.

1. Introduction

The construction of Jules Horowitz Reactor (JHR) is going-on and the facility should be operational at the beginning of the next decade. It will be operated by CEA, as an international users facility on Cadarache CEA site. The reactor design will allow providing modern experimental capacity in support to R&D programs for the next 50 years nuclear energy. It will also supply radio-isotopes for medical use (molybdenum).

JHR is a modern Material Testing Reactor (MTR). It's a pool-type reactor designed to reach a maximum power of 100 MWth. Its design allows a large experimental capacity inside and outside the reactor core (up to 20 devices). Due to the high power density, the core primary circuit is slightly pressurized.

The nuclear unit includes a reactor building and an auxiliary building. The auxiliary building hosts mainly:

- three storage pools for spent fuels, irradiated experimental devices and irradiated materials,
- four main hot cells for irradiated fuel, radioisotope targets, waste management, but also preparation, conditioning of irradiated samples,
- three small hot cells for non-destructive examinations on irradiated samples.

A transfer channel between the reactor building and the auxiliary building allows underwater transfers of all the irradiated materials (spent fuel and experimental devices).

To be ready to operate JHR reactor, CEA needs, in parallel to the facility construction, to prepare the operation of the reactor and therefore to deal with:

- Staffing: CEA has to hire around 50 people (mainly technicians) until the commissioning to reach an operation team of 85 people (shift teams and normal operation teams). This hiring has to be progressive in connection to the need of operators for the commissioning tests and with the necessity to train people before being operational,
- Staff training, requiring participation to the commissioning tests,
- Operation documentation writing: around 3600 documents such as operating rules, instructions, and forms… have to be drafted first for the commissioning tests.

After an overall up-to-date status of reactor construction, this paper will focus on this last topic.

2. Organization of the JHR project

CEA is the owner but also the future operator. CEA organization gathers several teams:

- A team responsible for project coordination, managing the design, manufacturing and commissioning tests. This team is notably in charge of supervising the prime contractor TechnicAtome,
- A team representing the future operator,
- A team in charge of managing the design, manufacturing and commissioning of the first fleet of experimental devices and associated equipments (non-destructive examination benches, laboratories…).

Of course, there are many interactions between these different teams (grouped within the program JHR).

The prime contractor, TechnicAtome, is responsible of the JHR design, manufacture and commissioning tests.

3. JHR update status

JHR construction is currently under progress. Civil work is completed.
Heavy handling equipments are on site, and acceptance tests are ongoing and should be achieved within some months.

Fig. 1 : One site pool crane commissioning tests

Hot cells work is ongoing. Liner of cells is ready and the liner tightness test of big cells has been controlled.
Biological doors are in place and filled with lead and neutron shielding. Internal cranes are manufactured in factory, assembly is underway for testing.

Fig. 2 : May 18 - lead bricks and Polyethylene on external cells door

Fig. 3 : August 18 - lead bricks on internal sliding cells door

Fig. 4 : Sept 18 - ECD Cell floor

Fig. 5 : Dec 18 - Biological doors in EPO channel

A significance milestone in 2019 is the end of the implementation of reactor pool liner, after several years' work.

Fig. 6: reactor pool liner

Fig. 7 : Crossing pipe for primary circuit

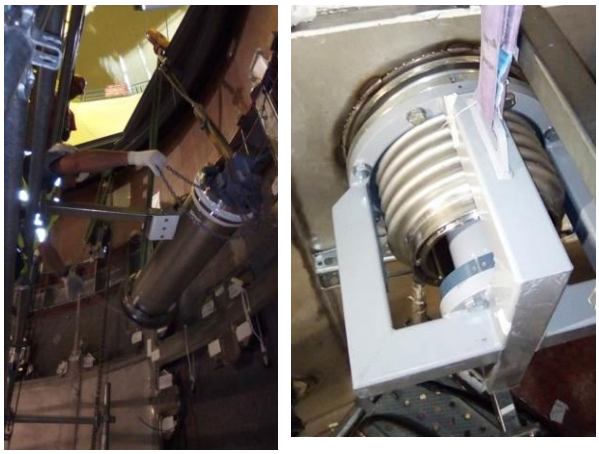

Fig. 8 : On site introduction of crossing pipe

Utilities (water, nitrogen and pressurized air) are in progress in the annex building (housing changing rooms, electrical distribution and laboratories).

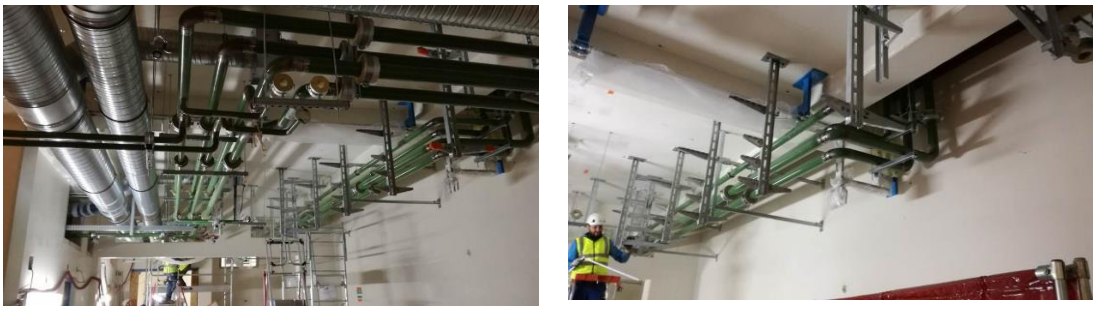

Fig. 9 : Utilities in the annex building

Fig. 10 : Air conditioning unit in the annex building

The fuel-loading machine is under acceptance tests in factory.

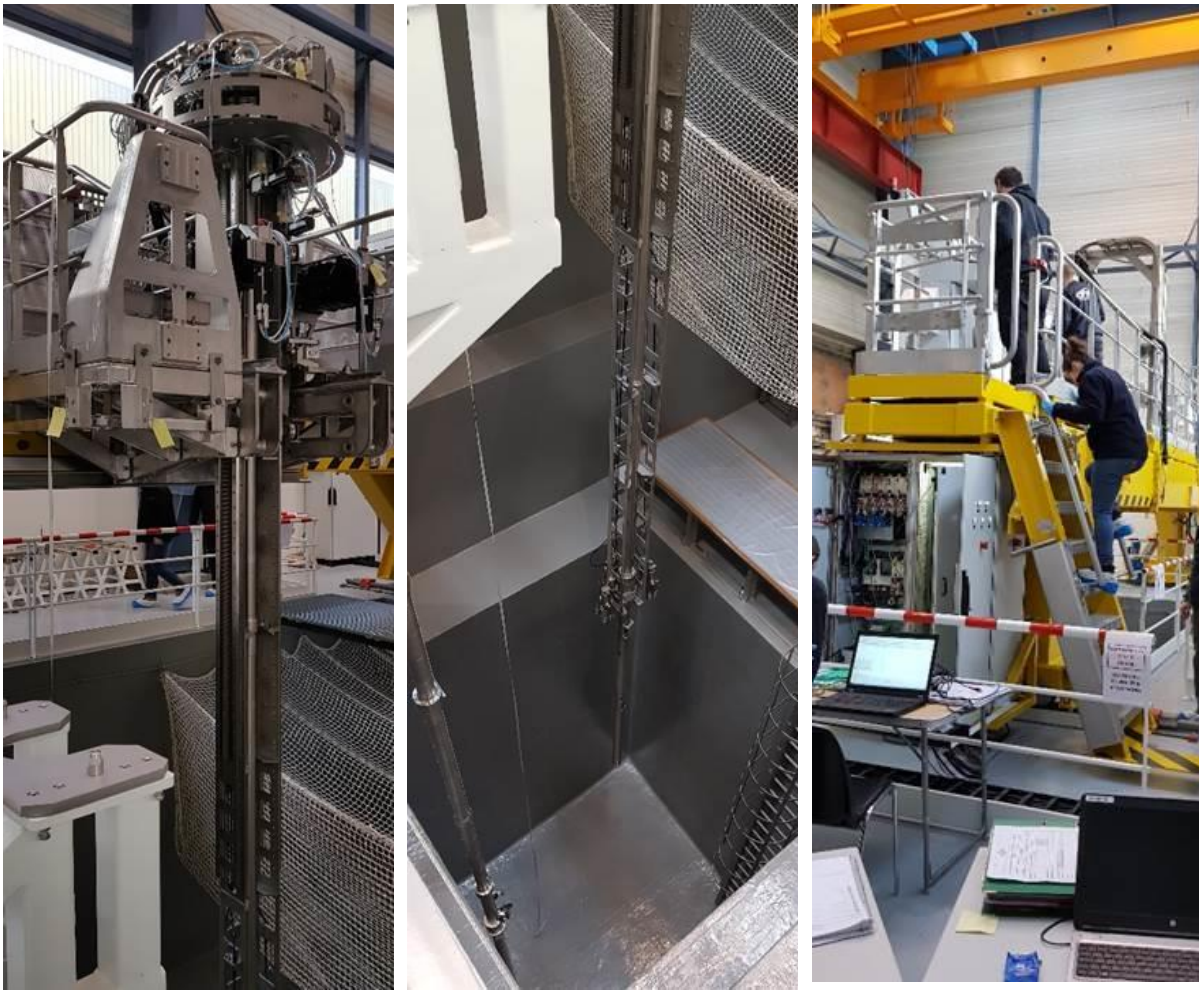

Fig. 11 : Fuel loading machine

Fig. 12 : the first primary pump under tests in factory

Fig. 13 : second primary pump (impeller)

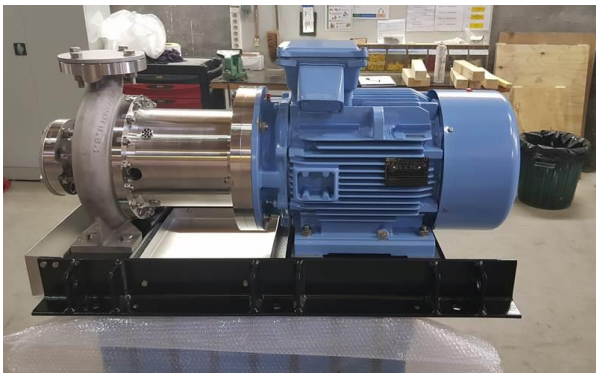

Fig. 14 : safeguard pump

After several years of development and testing, CERCA has to go on manufacturing the 100 first fuel elements, corresponding to the first JHR core and the first refuelling.

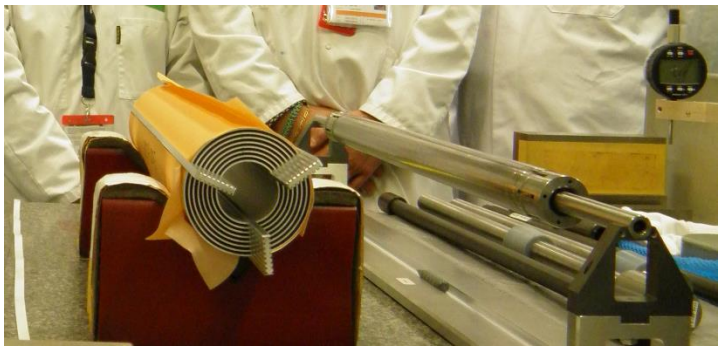

Fig. 15: first fuel RJH element

4. Operation documentation

To elaborate the operation documentation in support to the commissioning test program and the future operation (routine instructions), CEA defined the structure of the documentation based on the feedback of nuclear power plants, taking into account the specificities of experimental reactors.

In accordance with the General Operating Rules, five types of documents have to be established:

- Collection of reactor operating procedures (criticality, power increase…),
- Collection of support systems procedures (demineralized water flowing, liquid and gaseous effluents management…),
- Collection of maintenance and test procedures (cells decontamination, cells containment test…),
- Collection of experimental devices procedures,
- Collection of administrative and organizational documents (management of waste and nuclear materials, transport, nuclear materials, training…).

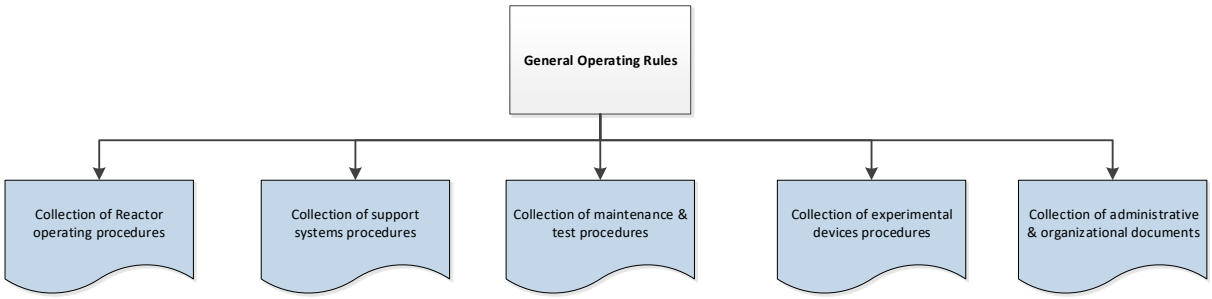

Fig. 16 : operation documentation - different collections

5. Reactor operating procedures

The reactor operating procedures concern normal situations and Incidental/accidental situations.

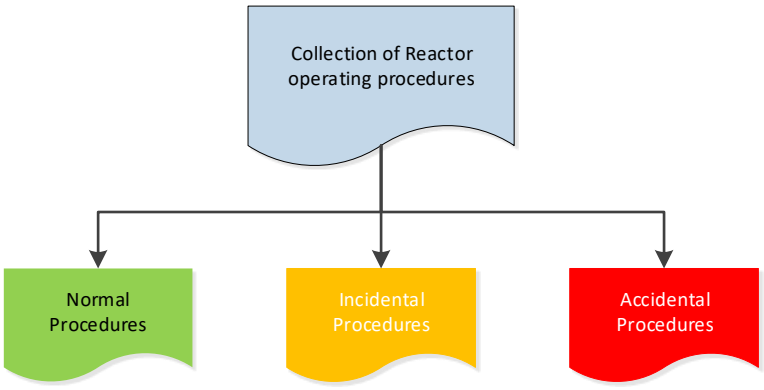

Fig. 17: structure of reactor operating procedures

These procedures are composed of rules and instructions:

- Rules identify the requirements, the strategy to operate the reactor, closed to the limits,
- Instructions, associated to the rules, provide step-by-step tasks to implement the strategy.

They are the operative declination of the General Operating Rules, and therefore are the main documentation used by the shift team to operate the reactor.
These procedures have to be in accordance with the man/machinery interface defined by the Prime Contractor TechnicAtome and have to be declined for the different team members, namely shift supervisor, reactor operator, shift electrician and mechanic.

For all alarm or deviation event, it's necessary to write message sheets which help operators to understand the event and give the tasks to be performed.

The reactor control command is designed to reduce, as far as possible, operator actions. Particularly, after an emergency shutdown, operators cannot do any action during 30 minutes from the control desk, this period is devoted to use the document «entrance to instructions».

This document named « incidental/accidental orientation document ») will allow:

- to confirm the expected automatic triggers,
- to check the safety functions parameters (controlling the reactor, cooling the fuel and containing radiation),
- to perform a diagnosis with the aim of an orientation towards the adapted instruction.

After an emergency shutdown, it is possible to go towards to incidental procedures if the safeguard systems have not been triggered.

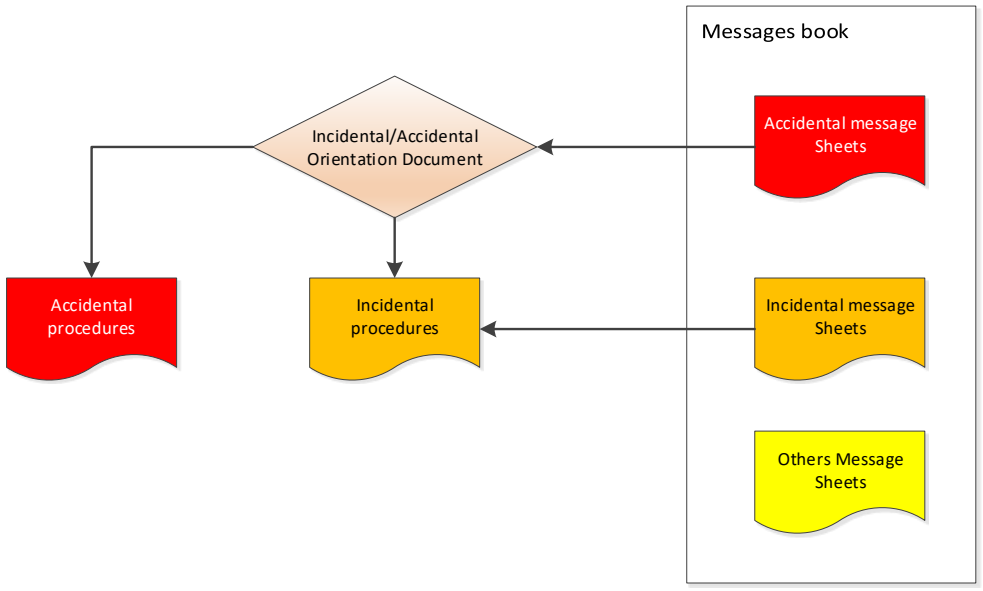

Fig. 18: entrance to instructions document

6. Documentation writing

All the documentation have to be ready for some key milestones in relation with the commissioning test program. It is also necessary to spread the workload to prevent the risk to have to write too much documents just before the fuel loading. Therefore, four milestones have be defined:

- First milestone : pools filling
- Second milestone : global tests
- Third milestone : first nuclear material acceptance
- Forth milestone : fuel loading

Collection	Type of documents	Number of documents
Reactor operating procedures	Normal procedures	≈ 180
	Message and alarm sheets	≈ 1400
	Accidental & incidental procedures	≈ 70
Support systems procedures	System instructions	≈ 120
Maintenance & test procedures	Control and test procedures	≈ 170
	Maintenance task lists	≈ 1500
Administrative & organizational documents	Organizational and general procedures	≈ 220
	Total	≈ 3660

Tab 1: number and type of documents

Therefore, more than 3600 documents have to be written before the last milestone, the fuel loading. This statement does not include the experimental devices documentation.

This task is assigned to the future operation team with the help of a service provider.
Currently, the operation team is composed of 35 people, 10 engineers and 25 technicians, future shift members (shift supervisors, reactor operators, shift electricians and mechanics).
Documentation writing is shared between the team members according to their skills and future responsibilities.

For example, shift supervisors and reactor operators are in charge of writing the normal, incidental and accidental procedures. They have to test the preliminary procedures on the simulator, to be ready to operate the reactor during the global test.

Shift electricians and mechanics have to write system instructions, in order to carry them out for the commissioning tests.

7. Conclusion

The construction of JHR is going on and the reactor should be operational at the beginning of the next decade.
In parallel to the facility construction, many actions are in progress to prepare the operation, such as staff training and documentation writing.
All the documentation has to be ready for the global commissioning test.

Writing the documentation needs a good understanding of the functioning of the reactor and all the systems. For this work, it is necessary to take into account all the contractors documentation (including prime contractor documentation) and to follow up the commissioning tests. It is considered as a part of the staff-training program.

8. References

[1] G. Bignan, D. Iracane, “The Jules Horowitz Reactor Project: A new High Performances European and International Material Testing Reactor for the 21st century”. Nuclear Energy International publication (NEI-Dec 2008)

[2] G. Bignan, P. Lemoine. X. Bravo, “The Jules Horowitz Reactor: A new European MTR (Material Testing Reactor) open to International collaboration: Description and Status”. Research Reactor Fuel Management 2011 Roma, Italy

[3] G. Bignan et al., “The Jules Horowitz Reactor: A new European MTR open to International collaboration”.13rd IGORR conference, September 2010, Knoxville,TN –USA)

[4] G. Bignan et al., ”The Jules Horowitz Reactor: A new European MTR (Material Testing Reactor) open to International collaboration: Update Description and focus on the modern safety approach”. IAEA International Conference on Research Reactors: Safe Management and Effective Utilization, November 2011, Rabat, Morocco)

[5] J. Estrade and al., “The Jules Horowitz Reactor: a new high performances European MTR (Material Testing Reactor) with modern experimental capacities – Building an international user facility”. Research Reactor Fuel Management 2013, 21-25 April, 2013, St-Petersburg, Russia.

[6] H. Beaumont and al., ”The Jules Horowitz Reactor: Engineering Procurement Construction Management missions and Construction status”. 13th IGORR conference, October 2013, Daejeon - Korea.

[7] “The Jules Horowitz Reactor: A new high performance MTR (Material Testing Reactor) working as an International User Facility in support to Nuclear Industry, Public Bodies and Research Institutes”, X. Bravo, G. Bignan Journal of Nuclear Energy International- December 2014

[8] J. Estrade and al., “The Jules Horowitz Reactor: Preparation of the commissioning phase and normal operation”. Research Reactor Fuel Management 2017, 14-18 May, Rotterdam, Netherlands

[9] O. Marcille and al., “The Jules Horowitz Reactor: Preparation of the commissioning phase and normal operation”. Research Reactor Fuel Management 2018, 11-15 March, Munich, Germany

NAC's OPTIMUS™ Packaging for Reactor Wastes

Steven Sisley, Jeff England, Juan Subiry
NAC International, 3930 East Jones Bridge Road, Suite 200, Norcross, GA 30092

ABSTRACT

NAC OPTIMUS™ packagings are a Type B(U)F-96 transportation package designed for maximum flexibility and cost-efficiency to support shipment of a wide range of challenging wastes and materials. It is a small, modular packaging meeting DOT weight limits for road transport. Contents can be accommodated in multiple configurations including standard drums of up to 110 gallons in size. The packagings also accommodate unique waste contents and fuel designs where cost-effective packaging options have been a challenge. The packagings have a simplicity of design and operational flexibility to meet both IAEA and U.S. NRC Type B requirements. Flexibility is assured by the modular design for containment, shielding and criticality control. The containment boundary design permits adaptability to content requirements by relying on interchangeable internal components or dunnage.

The OPTIMUS™ packaging utilizes the same cask containment vessel (CCV) in the OPTIMUS™-H and OPTIMUS™-L. The OPTIMUS™-L is a lightweight transportation packaging with a capability of up to ten (10) OPTIMUS™-L packages per legal-weight truck shipment. The OPTIMUS™-H has an Outer Shield Vessel (OSV) made of ductile cast iron and Impact Limiters (IL) with a higher payload capacity then the OPTIMUS™-L. The large cavity size of the CCV, can accommodate standard drums up to 110 gallons, combined with the small size and modularity of the OPTIMUS™ packaging provides unmatched flexibility for the user.

OPTIMUS™ can accommodate more radioactive waste in each drum (up to a Fissile Gram Equivalent (FGE) limit of 395g Pu-239) than larger packages can in 10 drums. Furthermore, because of its small size and weight, up to ten (10) OPTIMUS™-L packages can be accommodated per legal-weight truck shipment. Thus, one LWT shipment of 10 OPTIMUS™-L packages can accommodate more than 10 times the FGE as a large package containing 10 drums.

In this paper, NAC provides a technical overview of the OPTIMUS™ packagings and identifies the design features and technology advancements making the OPTIMUS™ product line a readily adaptable and flexible solution for packaging reactor and decommissioning wastes. The system enables the integration of these wastes into the existing waste management system process and disposition infrastructure.

1 OPTIMUS™ PACKAGING DESCRIPTIONS

The OPTImal Modular Universal Shipping (OPTIMUS™) package product line includes two different package designs; the OPTIMUS™-H and OPTIMUS™-L, shown in Fig. 1. Both packages are designated Type B(U)-F and designed to satisfy the most limiting requirements of 10 CFR 71 [1] and IAEA SSR-6 [2]. The OPTIMUS™-H packaging is used to transport radioactive materials (RAM) that require significant shielding for gamma radiation, whereas the standard OPTIMUS™-L packaging is used to transport RAM requiring minimal gamma shielding. However, the large cavity size and payload weight limit of OPTIMUS™-L allows for the addition of shield inserts inside the CCV to accommodate content with increased activities.

The general physical attributes of the OPTIMUS™ packagings are discussed in Section 1.1. Lifting and tiedown features of the OPTIMUS™-L packaging are discussed in Sections 1.2 and 1.3, respectively. Other structural, thermal, containment, and shielding features of the OPTIMUS™ packaging are

discussed in Sections 1.4 through 1.7. The contents of the OPTIMUS™ package are discussed in Section 1.8.

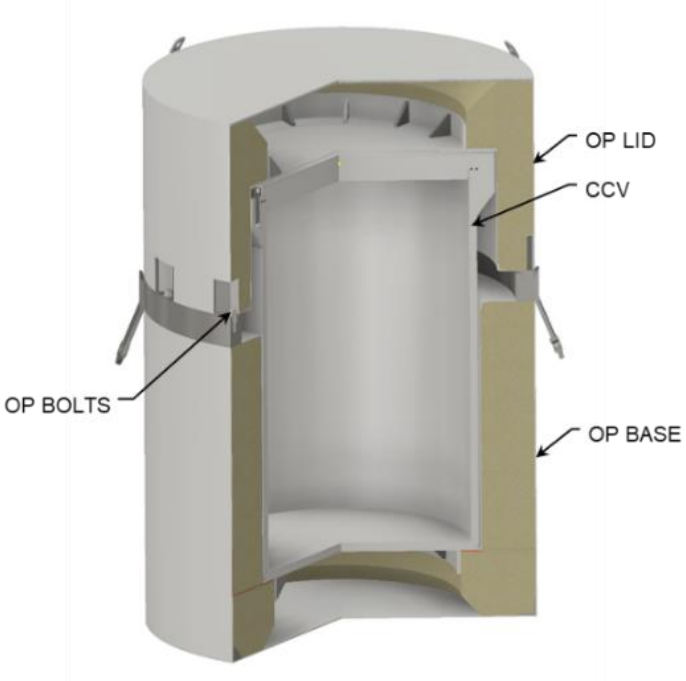

OPTIMUS™-L

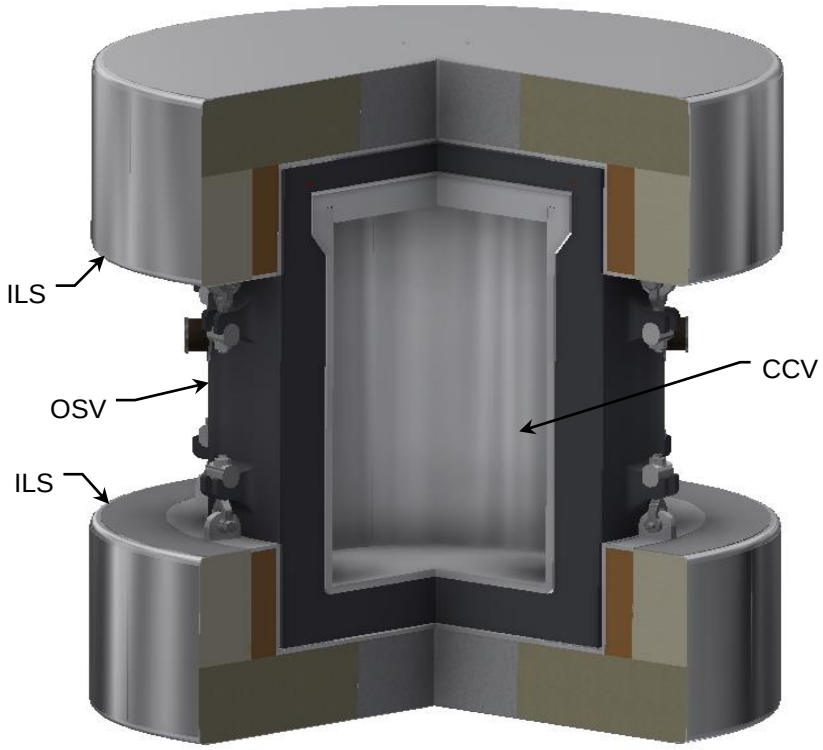

OPTIMUS™-H

Fig. 1. OPTIMUS™ Packagings

1.1 General Description

The newest addition to the OPTIMUS™ packaging product line is OPTIMUS™-L; a Type B(U)-F packaging designed to transport RAM contents requiring less radiation shielding than those shipped in the OPTIMUS™-H package. Both the OPTIMUS™-H and OPTIMUS™-L packages use the same Cask Containment Vessel (CCV). However, the outer packaging of the OPTIMUS™-H and OPTIMUS™-L differ due to shielding requirements for the intended contents. The outer packaging of the OPTIMUS™-H, designed to accommodate high-activity contents, consists of a thick-walled Outer Shield Vessel (OSV) and an Impact Limiter System (ILS), whereas the outer packaging of the OPTIMUS™-L consists of a stainless steel drum-like assembly filled with rigid polyurethane foam for impact and thermal protection. The physical attributes of the OPTIMUS™-H and OPTIMUS™-L packages are summarized in Table I.

TABLE I. OPTIMUS™ Packaging Physical Attributes

Packaging Physical Attributes	Packaging Design	
	OPTIMUS™-H	**OPTIMUS™-L**
Outer Dimensions[1]	∅188.5 cm x 211.3 high (∅74.2 in. x 83.2 in. high)	∅124.5 cm x 177.8 cm high (∅49 in. x 70 in. high)
Cavity Dimensions	∅82.6 cm x 119.4 cm high (∅32.5 in. x 47.0 in. high)	∅82.6 cm x 115.6 cm high (∅32.5 in. x 45.5 in. high)
Packaging Tare Weight	11,202 kg (24,700 lbs.)	2,721 kg (6,000 lbs.)
Max. Contents Weight	3,311 kg (7,300 lbs.)	1,429 kg (3,150 lbs.)
Gross Weight[2]	~11,338 to 14,512 kg (~25,000 to 32,000 lbs.)	~2,847 to 4,172 kg (~6,300 to 9,200 lbs.)
Gamma Shield Thickness[3]	≥ 20.3 cm (8.0 in.) iron/steel	≥ 3.3 cm (1.3 in.) steel

Notes:

1. Outer dimensions excluding lifting and tiedown protrusions.
2. Range based on variation of contents weight.
3. Shielding inserts can be added for supplemental shielding of contents, as required.

The OPTIMUS™-H and OPTIMUS™-L packagings are designed to ship similar contents with different activities, so it is likely users may require both OPTIMUS™-H and OPTIMUS™-L packagings for large shipping campaigns. By using a common CCV design in both the OPTIMUS™-H and OPTIMUS™-L packagings, operating procedures for loading contents, CCV closure, and unloading contents are largely standardized, simplifying operations for users operating both OPTIMUS™-H and OPTIMUS™-L packagings. In addition, the use of a common CCV design allows for operational flexibility and interchangeability of the CCV between packages, with clear economic benefits for users operating both OPTIMUS™-H and OPTIMUS™-L packages.

The outer packaging of the OPTIMUS™-H and OPTIMUS™-L are significantly different due to shielding requirements for the intended contents. The outer packaging of the OPTIMUS™-L consists of a stainless steel drum-like assembly that is filled with rigid polyurethane foam for impact and thermal protection, whereas the outer packaging of the OPTIMUS™-H, which is designed to accommodate high-activity contents, consists of a thick-walled Outer Shield Vessel (OSV) and an Impact Limiter System (ILS). Because of the differences in the outer packaging, the OPTIMUS™-L has a much smaller outer envelope and gross weight than the OPTIMUS™-H. As shown in Table I, OPTIMUS™-L has external dimensions of ∅124.5 cm (∅49.0-inch) by 177.8 cm (70.0-inch) high and maximum gross weight of only 4,172 kg (9,200 pounds) compared to ∅188.5 cm (∅74.2-inches) by 211.3 cm (83.2-inch) high and 14,512 kg (32,000 pounds) for the OPTIMUS™-H. The smaller size and weight of the OPTIMUS™-L package result in significant improvement in operational efficiencies for lower activity contents that larger packages. For example, OPTIMUS™-L packages can be loaded and pre-staged for shipment to minimize wait times for the driver and transport equipment, which reduces shipping costs. In addition, the per-drum content weight, decay heat, and fissile gram equivalent of RAM is much higher than that of larger transportation packages.

Loading operations for the OPTIMUS™-L package differ by content and facility type. Typical contents of the OPTIMUS™-L package with low surface dose rates may be loaded directly into the CCV. Contents with high surface dose rates may require loading via a shielded transfer cask and/or transfer adapter or via remote operations. The OPTIMUS™-L package may be loaded while mounted on the

trailer deck, or it may be removed from the trailer for loading operations performed inside a facility. The modularity of the OPTIMUS™-L packaging provides maximum flexibility for operations.

1.2 Lifting Features

Unlike most other Type B(U) packages used to transport similar RAM contents, the OPTIMUS™ packagings are relatively small and lightweight, simplifying lifting and handling operations. The primary mode of lifting and handling the OPTIMUS™ package is by forklift using a pallet, as shown in Fig. 2. The pallet allows the OPTIMUS™ packages to be quickly and easily loaded onto or unloaded from a trailer outside the secure area of a facility without the need for a mobile crane and it eliminates the need to bring the tractor and trailer into the facility's secure area.

Fig. 2. OPTIMUS™-L Packaging Secured to Pallet

The loaded OPTIMUS™-L package, with the pallet and tiedowns attached, may also be lifted from the three (3) lifting lugs attached to the OP lid using standard rigging. The OP lid lifting lugs are designed to provide minimum factors of safety of six (6) against yield strength and ten (10) against ultimate tensile strength in accordance with the requirements of ANSI N14.6 [3].

The loaded CCV assembly is lifted from the three (3) threaded holes located on the top surface of the CCV lid, into which swivel hoist rings are installed and standard rigging is attached. The CCV lifting attachments are designed to provide minimum factors of safety of six (6) against yield strength and ten (10) against ultimate tensile strength in accordance with the requirements of ANSI N14.6 [3].

1.3 Tiedown Features and Shipping Configurations

The OPTIMUS™-L package is designed to be secured to a pallet using the four (4) tiedown arms attached to the OP base bolt flange, as shown in Fig. 2. The pallets are then placed onto a trailer deck and secured in accordance with applicable transport regulations. The OPTIMUS™-L packages may also be secured directly to a trailer deck if a pallet is not used. The 127 cm (50-inch) wide pallet is sized to

permit two (2) OPTIMUS™-L packages to be placed over the width of a standard 259 cm (8'-6") trailer deck. Up to ten (10) OPTIMUS™-L packages are allowed per shipment, as shown in Fig. 3. For typical contents weighing approximately 500 pounds, ten (10) OPTIMUS™-L packages will satisfy the weight limits for a LWT shipment. For heavier contents, the number of packages may be reduced to stay within LWT limits, or shipping permits may be obtained.

Fig. 3. Typical OPTIMUS™-L Package Transport Configuration

1.4 Energy-Absorbing Features

The OPTIMUS™-L OP lid and base assemblies are designed to crush and absorb energy under NCT and HAC free drops to limit the shock loads imparted to the CCV and contents. The OP base and lid are both constructed from stainless steel shells that fully encase energy absorbing closed-cell polyurethane foam core components to create a sealed cavity to protect the foam core from the external environment. The outer shells and outer end plates of the OP lid and base are constructed from 0.5 cm (3/16 inch) thick stainless steel plate and inner shells are constructed from 14-gauge (0.2 cm (0.0751-inch) thick) stainless steel sheet. The OP shells are designed to plastically deform under NCT and HAC free drop conditions, but not fail in any manner that would expose the OP foam to the ambient environment.

The OP lid and base foam cores are comprised of 80 kg/m^3 (5 pcf) and 384 kg/m^3 (24 pcf) closed-cell polyurethane foam for optimal performance in the NCT and HAC free drop tests. The 80 kg/m^3 (5 pcf) foam cores used in the top end of the OP lid is not crushed under any NCT or HAC free drop conditions but provides thermal protection of the CCV lid O-ring seals for the HAC thermal test. All energy absorption is provided by the 384 kg/m^3 (24 pcf) foam core used in the corner and overhang regions of the OP lid and base. Shear rings attached to the top and bottom inner end plates provide backing support for the corner foam under side, corner, and oblique drop impacts.

1.5 Thermal Features

The OPTIMUS™-L packaging includes thermal insulation in the OP lid and a thermal spider in the OP base that help control the temperature of the packaging components under NCT and HAC. A 0.6 cm (¼-inch) thick layer of ceramic fiber insulation is attached to the inner surface of the OP lid outer end

plate to minimize heating of the overpack foam from insolation. This maintains the temperature of the foam under NCT below the lower-bound temperature assumed for the foam stress-strain properties used in the drop analyses. In addition, this feature minimizes the heating of the CCV closure O-ring seals during the HAC fire. The OP base includes a thermal spacer, which is designed to conduct heat from the contents through the foam core to the exterior of the outer packaging under NCT. The thermal spacer is copper plate with an annular "body" and twelve "spokes" that extend radially through the OP base foam core and are bent OP to run along the OP base outer shell. The body of the thermal spacer is sandwiched between the OP base inner bottom end plate and bottom corner foam core and compressed by the weight of the contents. The vertical legs of the thermal spider are sandwiched between the outside of the OP base foam core and the inside of the OP base outer shell.

1.6 Containment Features

The OPTIMUS™-L packaging containment system, designed to a "leaktight" containment criterion per ANSI N14.5 [4], is formed by CCV body (cylindrical shell, bottom plate, bolt flange, and all associated welds), CCV lid and its closure bolts and containment O-ring seal, and the port cover and its closure bolts and containment O-ring seal.

The CCV lid is a stepped plate secured to the CCV body by twelve (12) high strength stainless steel custom CCV lid bolts and sealed by an elastomeric O-ring. The design of the CCV lid prevents shear loading of the CCV lid bolt under NCT free drop, HAC free drop, and HAC puncture tests. The CCV lid's inner plug, which fits tightly inside the top opening of the CCV body, prevents significant lateral movement of the CCV lid relative to the CCV body bolt flange to prevent shear loading of the CCV lid bolts. The CCV lid bolts are 2.5 cm (1-inch) diameter socket head cap screws that are machined to create captured bolts. The CCV lid has twelve (12) bolt holes with scalloped pockets in which the CCV lid bolt heads are recessed and protected from impact loads.

For transport the CCV port cover is installed and sealed by an elastomeric O-ring. The CCV port cover is secured to the CCV lid by four (4) 0.6 cm (¼-inch) diameter stainless steel socket head cap screws. The CCV port cover is recessed in a pocket within the CCV lid and protected from shear loading due to free drop and puncture tests.

1.7 Shielding Features

Gamma shielding on the OPTIMUS™-L packaging is provided by stainless steel plates forming the CCV and OP inner and outer shells. The packaging radial surfaces include the CCV 2.5 cm (1-inch) thick stainless steel shell, the 0.2 cm (0.0751-inch) thick (14-gauge) OP inner shells, and a 0.5 cm (3/16 inch) thick OP outer shell, for a combined steel thickness of 3.2 cm (1.26 inches). Additional shielding thickness is provided on the top and bottom ends of the package.

Shield inserts will be added for future contents requiring additional gamma shielding or neutron shielding. With the 1,587 kg (3,500-pound) limit for the combined weight of the shield insert and the contents, the OPTIMUS™-L packaging has the capability to accommodate a wide range of contents with higher source terms.

1.8 Contents

The current contents of the OPTIMUS™ package include intermediate level waste (ILW) and irradiated fuel waste.

All waste contents shall be in secondary containers (e.g., drums or boxes). In addition, the contents shall not exceed the fissile gram equivalent (FGE) limits for plutonium contents or the Fissile Equivalent Mass (FEM) limits for low-enriched uranium (LEU) contents from Table II.

TABLE II. OPTIMUS™ Packaging Contents

Content Type	Content Limits	
	OPTIMUS™-H	**OPTIMUS™-L**
ILW and TRU Waste	≤ 390g Pu-239[(1)]	≤ 395g Pu-239[(2)]
LEU	≤ 2,268 kg (5,000 lb.), 0.96 wt% U-235[(3)]	≤ 1,134 kg (2,500 lb.), 0.89 wt% U-235

Notes:

1. FGE limit shown for hand compacted TRU waste with ≥25g Pu-240 credit. The FGE limit for hand compacted TRU waste with no Pu-240 credit is 335g Pu-235. The FGE limit for machine compacted TRU waste is 250g Pu-239.
2. FGE limit shown for hand compacted TRU waste with ≥25g Pu-240 credit. The FGE limit for hand compacted TRU waste with no Pu-240 credit is 340g Pu-239. The FGE limit for machine compacted TRU waste is 250g Pu-239.
3. Enrichment limit shown with particle size restriction of ≤ 0.1 cm and/or ≥ 8.0 cm. Enrichment limit without particle size restriction is 0.80 wt% U-235.

Shoring must be placed between loose fitting contents and the CCV cavity to prevent excessive movement during transport. The shoring may be made from any material that does not react negatively with the packaging materials or contents.

The large cavity size and high content weight limits of both the OPTIMUS™-L and OPTIMUS™-H packages allow the addition of payload shield liners (PSLs) through future amendments for higher activity contents. PSLs may be made from various materials and sizes, depending on the type and amount of shielding required. Aside from attachments for lifting, PSL do not have any other noteworthy operational features.

2 OPTIMUS™ REGULATORY APPROVALS

The OPTIMUS™-H application was submitted to CNSC in July 2018 and it is anticipated that CNSC will issue the certificate in the second quarter of 2019. The OPTIMUS™-L application to CNSC is planned for the first quarter of 2019 and it is anticipated that the certificate will be issued 9 to 12 months later. Submittals of OPTIMUS™-H and OPTIMUS™-L applications to the U.S. Department of Energy (DOE) are expected in 2019.

REFERENCES

1. U.S. Nuclear Regulatory Commission (NRC), *Code of Federal Reguations Title 10, Part 71-Packaging and Transportation of Radioactive Material*, 2017.
2. International Atomic Energy Agency (IAEA), *Regulations for the Safe Transport of Radioactive Material, Specific Safety Requirements No. SSR-6*, 2012 Edition.
3. ANSI N14.6, *Special Lifting Devices for Shipping Containers Weighing 10000 Pounds (4500 kg) or More*, American National Standards Institute, Inc., New York, 1993.
4. ANSI N14.5 2014, *American National Standard for Radioactive Materials – Leakage Tests on Packages for Shipment*, American National Standards Institute, Inc., June 19, 2014.

THE PRESENT AND FUTURE OF THERMAL-HYDRAULIC PERFORMANCE AND SAFETY ANALYSES OF RESEARCH REACTORS BY KAERI: FOCUSED ON THE JRTR

HYEONIL KIM, YOUN-GYU JUNG, CHEOL PARK, SU-KI PARK, DONGHYUN KIM, JONG-PIL PARK, DONG-WOOK JANG

Research Reactors Design Division, Korea Atomic Energy Research Institute
111, Daedeok-daero 989beon-gil, Yuseong-gu, Daejeon, 34057, Republic of Korea

IN-SUB JUN
Maritime Reactors Development Division, Korea Atomic Energy Research Institute

JEE-HAN CHUN
SMART Project Management Division, Korea Atomic Energy Research Institute

BYEONGHEE LEE
SEUNG-WOOK LEE
Thermal Hydraulics and Severe Accident Research Division, Korea Atomic Energy Research Institute

ABSTRACT

The overall activities of thermal-hydraulic performance and safety analyses of research reactors by KAERI are presented and the presentation is focused on those for the Jordan Research and Training Reactor of great success. The future program is also introduced with some examples of research and development.
Covered are the very broad efforts such as performance and safety analysis, and engineering support to system design.
The new era of the Korean nuclear society, re-structuring share of domestic energy, comes into Korea. The change requires more than safe, i.e., comfortable nuclear energy in research reactors society of Korea, too. Introduced are, the on-going research works such as addition of multi-dimensional computation for quantifying physics, improvement of the SPACE (Safety and Performance Analysis CodE) code, a licensed performance and system analysis code for nuclear power plants in Korea, into research reactors.

1. Introduction

It took about 6.5 years for a wish to come true from the preparation to operation of the Jordan Research and Training Reactor (the JRTR) project by KAERI (Korea Atomic Energy Research Institute) and Daewoo Consortium (KDC). It was a new challenging step for Korea and KAERI toward showing industrial and institutional capabilities to build a research reactor with the accumulated expertise for the engineering, procurement, and construction of the nuclear reactors for various usage to both the domestic and abroad.
It can be said that Korea nuclear society started with the operation of the first research reactor in 1962 right after the Korean War, which was imported with an international support. It was not until the HANARO, a multi-purpose high power research reactor, had been designed, constructed, and operated in a safe manner that Korea showed a well-established lifetime management of a nuclear reactor including design, construction, commissioning, and operation at least as for research reactors. Successful operation of the JRTR proved that Korea is able to provide a meaningful solution to a newly coming country.

In this paper, the overall activities of thermal-hydraulic analyses of research reactors by the KAERI are presented in focus on those for the JRTR of great success. The thermal-hydraulic analysis covers most of issues potentially related to generation and removal of heats in research reactors. As a comprehensive and systematic tool for safety assessment, it envelopes also reviews on the conformance to the performance and safety objectives and the technical specifications in the course of design, construction, commissioning, and licensing.
Covered are the very broad efforts such as performance and safety analyses, engineering support to system design including following: the established methodology for the thermal-hydraulic analysis, code verification and validation, identification and selection of the initiating events, accident and performance analyses, probabilistic safety assessment, support for the preparation of emergency operating procedures, thermal-hydraulic responses to the structures, preparation of safety analysis report and operational technical specifications.
The new era of the Korean nuclear society, re-structuring share of domestic energy, comes into Korea. The change requires more than safe, i.e., comfortable nuclear energy in research reactors society of Korea, too. Introduced are, the on-going research works, which are intended to enhance safety and comfort by the public, such as addition of validation against experiments, multi-dimensional computation for quantifying physics, improvement of the SPACE (Safety and Performance Analysis CodE) code, a licensed performance and system analysis code for nuclear power plants in Korea, into research reactors.

2. Present of Thermal-Hydraulic Analysis of Research Reactors by KAERI

2.1 Safety Achievement of the JRTR

The nuclear safety functions of the JRTR were ensured by paying particular and careful attention to the basic safety principles during the stages of design, construction, and operation. The basic safety principles adopted for the design were “defense-in-depth” and “quality assurance.”
In realizing the “defense-in-depth” principle, three basic safety functions of reactivity control, decay heat removal, and confinement of radioactive materials were assured by implementing appropriate safety systems and passive engineered safety features and also by utilizing inherent safety characteristics.
The Quality Assurance Manual (QAM) for the JRTR in accordance with ASME NQA-1:1994 was developed to achieve the quality objective that is to ensure nuclear safety.

2.2 Regulations of the JRTR: Licensing Regime

Basically, the JRTR design shall comply with the Jordan laws and regulations: Jordan’s Nuclear Energy Law, Jordan’s Radiation Protection, Nuclear Safety, and Security Law. In addition, the following documents were used as a top priority.
The JRTR design complies with IAEA safety standards and Korean regulatory requirements and guidelines. IAEA safety standards were applied as the top-tier safety requirements for the JRTR. Since IAEA standards do not cover all the engineering and/or practical requirements, Korean laws and regulations were applied for safety design of the JRTR to complement the detailed technical requirements.
KEPIC was adopted as the industrial code and standards for the JRTR, which is based on the internationally acceptable USA industrial codes and standards such as ASME, IEEE, ACI, ANSI, etc.

2.3 Safety Design Bases of the JRTR: Design Basis Events

A design basis event (DBE) is an occurrence that shall be directly considered in the design of the plant. Design basis events for the JRTR were consistent with those described in the IAEA SS NS-R-4. The JRTR design characteristics were considered in identifying DBEs. The predicted consequences of such events must fall and did within the established acceptance criteria.

DBEs can be generally classified into two categories: Normal operational transients (NOT) and abnormal operational transients (AOT). AOT can be further classified into 3 classes: Anticipated Operational Occurrences (AOOs), Accidents and Limiting Accidents. Accidents and Limiting Accidents can be a grouped and generally called as Design Basis Accident (DBA) in the IAEA SS NS-R-4. Combinations of AOTs with seismic condition were considered in the design of structures, systems, and components of the JRTR. Structures, systems, and components of the JRTR were designed to consider protection from the fire. The effect of other special internal and external conditions caused by the transients was considered in equipment design and analyses. Abnormal operational transients which need analyses or assessments were identified in IAEA SS NS-R-4. The acceptance criteria for AOT are referred to “Safety review manual for research and training reactors”, KINS/GE-N10, 2007 and “Guideline for preparing and reviewing applications for the licensing of non-power reactors”, NUREG-1537, 1996. The acceptance criteria are based on maintaining the integrity of the reactor coolant system boundary, ensuring that specified acceptable fuel design limits are not exceeded, and offsite radiological consequences are acceptable.

2.4 Establishment of Accident Analysis Methodology

Accident analysis methodology is determined in accordance with an analysis purpose. In most cases, the analysis purposes are definite and the selection of the method is clear. Accident analysis for the JRTR was performed by using the following methods [1].

The qualitative analysis is a logical thinking process that uses engineering principles and knowledge of the facility design to evaluate the consequences of event. In some cases the analysis may require quantitative calculations to support its conclusion. It is also used in identifying bounding events.

The step by step sequence of events, from event initiation to the final conditions, is clearly defined. Fault tree analysis was used in the analysis of initiating events, and for evaluating the occurrence frequencies of postulated initiating events, the reliability of a process system and unavailability of a safety system. Failure Modes and Effect Analysis (FMEA) was also considered to evaluate the effect of a single component failure in a system on the overall system effectiveness. Event tree analysis provides the possible short, middle and long-term behaviors of the reactor systems following an initiating event. In most cases, the progress path formed in the analysis ends when the reactor reaches a safe shutdown condition or a fuel damage, which is used to logically identify all of the possible event sequences.

Validated computer codes are used for the safety analysis including the reactor kinetics and thermal hydraulics simulations during operational states and accident conditions. The overall behaviors of the reactor core and systems were analyzed by the RELAP5/MOD3 with conservative initial conditions and modeling assumptions. The reactor core and primary cooling system, the reactor and service pool and the reactor protection system are modeled for the transient analysis [2][3][4].

RELAP5/MOD3.3iy (Patch04) is used for the JRTR safety analyses. It is generally thought that the RELAP5/MOD3 is typically not design-specific and is applicable to a wide variety of thermal hydraulic system transients.

In addition to the various applications for the nuclear power plants, the RELAP5/MOD3 code has also been widely used for a safety analysis of research reactors operating at low pressure and low temperature. Some examples are NBSR, ATR, HFIR, HFBR and UFTR in USA, OPAL in Australia and ETRR-2 in Egypt et al. These reactors have plate-type fuels.

However, an applicability of RELAP5/MOD3 to the research reactor with plate-type fuels may be concerned in terms of thermal hydraulic phenomena in the core and thermal hydraulic models of the code because the research reactor usually has different fuel geometries and operating conditions from those of power reactors. Thus, the applicability of RELAP5/MOD3 to the JRTR safety analyses has been investigated (Chun et al., 2013). The applicability of the RELAP5/MOD3 with the correlations to the JRTR fuel geometry and operating range was validated. Meanwhile, the set of CHF correlations obtained in vertical narrow rectangular channels (Kaminaga et al., 1998) was used to calculate the CHFR.

2.5 Accident and Performance Analysis

Accident Analysis

For instance, a Loss of Normal Electric Power (LOEP) due to either electric load troubles such as overload in the system buses or natural & environmental troubles, such as flood, storms, earthquake, etc., results in a loss of flow in the Primary Cooling System (PCS) and the Secondary Cooling System (SCS). An LOEP directly influences the Control Absorber Rod Drive Mechanism (CRDM) and the Secondary Shutdown Drive Mechanism (SSDM) which leads to an instant reactor trip.

At the beginning of the event, the reactor core is cooled by the slowing down coolant through the PCS pipe by the inertial force of pump, flywheel and coolant itself. As the PCS flow decreases, the pressure differences across the flap valves are becoming small and meet the opening condition of the valves. When the flap valves open, pool water flows into the pipe which connects to the core and a natural circulation through the flap valve is established using the pool water as a huge heat sink. In the earlier phase of the transient a natural circulation through the flap valves and the PCS pipe is established. The Siphon Break Valves (SBVs) also are opened when the flow through the PCS decreases to a preset value. The SBVs are normally closed and designed as fail-safe open. In the simulation one of the two flap valves and one of the two SBVs are assumed to open for a conservative analysis, where the effect of flow due to SBV open/close is negligible.

The reactor response to the LOEP was simulated using the RELAP5/MOD3.3 code. The minimum CHFR and maximum fuel centerline temperature were calculated using the methods. The maximum fuel temperature and the minimum CHFR in a hot channel were estimated and it was assured that no fuel failures are predicted. Even when the Class IV electric power is not recovered for long days after the event, a long-term cooling capacity of the pool water was estimated to verify the pool can successfully cool down the decay power generated in the fuels in the reactor.

The other events including excess reactivity insertion [5][6], loss of flow [4], loss of coolant, special events [7], and so on were also analyzed as above.

Performance Analysis

The power transients were analyzed for both reactivity insertion cases: reactivity insertion free of rate and reactivity insertion with limit of rate [8]. This information was used to manage the operational technical specifications [9] for reactivity insertion: this feature is not safety-limited but performance-limited for enhancing the operational safety.

The JRTR core is surrounded by a heavy water (D2O) vessel containing heavy water as a reflector. The Heavy Water System (HWS) is installed to remove the heat generated in heavy water and vessel itself and separated from the primary cooling system. The HWS is not a system critical to the safety of the JRTR, i.e., a non-nuclear safety related system but a system of great significance to operational safety and cost. The JRTR, therefore, is equipped with the Reactor Regulating System setback in order to protect the HWS from the Postulated Initiating Events (PIEs) due to failures in the HWS [10][11].

The durability of the CRDM of great importance to the nuclear safety and performance of research reactors shall be guaranteed for a certain period of time through the endurance test and a replacement period can be also proposed from the test results.

The tests are performed based on a stepping regime that means the expected stepping movements of a step motor in CRDM through the quality-guaranteed time, which is expressed in Cycles and Steps/Cycle [12]. To obtain the stepping regime, it is necessary to simulate the behaviors of the reactor and control system from the startup to the shutdown. Since reactivity change causes power perturbation, all factors to lead reactivity change must be considered to make a reasonable operational profile of the step motors. From the analysis results, the stepping regime is extracted.

The thermal-hydraulic conditions (i.e. pressure, temperature and flow rate) at various locations of the PCS including the RSA and the reactor pool during design basis events should be reflected into the basis of the corresponding Structure, Systems, and Components design. The occurrence frequency of each event is derived from the operating and design experiences of the HANARO and nuclear power plants, and engineering judgment, which are intended for design purposes only. The design frequency of occurrence reflects conservative estimates of the reactor lifetime of 40 years.

2.6 Probabilistic Safety Analysis

The PSA, according to the procedures published by the IAEA and US NRC was undertaken to identify accident sequences leading to core damage and the corresponding frequencies, to assess the level of safety for the design of the JRTR, and to evaluate whether it is probabilistically safe to operate and reliable to use. A Level 1 PSA of the JRTR PSA was performed to address the risks associated with core damage.

2.7 Development of Emergency Operating Guidelines/Procedures

A goal of the Emergency Operating Guidelines (EOGs) is to provide the best available technical information to be used for developing reactor-specific Emergency Operating Procedures (EOPs) coordinated with the existing procedures [13][14]. The EOGs/EOPs are designed to be used independently and cross referencing is minimized. Cross referencing is appropriate only when the other guideline entry conditions are achieved during the course of operation. EOGs/EOPs are divided into two classes such as event-dependent and event-independent (symptom-based) as shown in Figure 2.7-1 based on the concept of the safety functions of the JRTR.

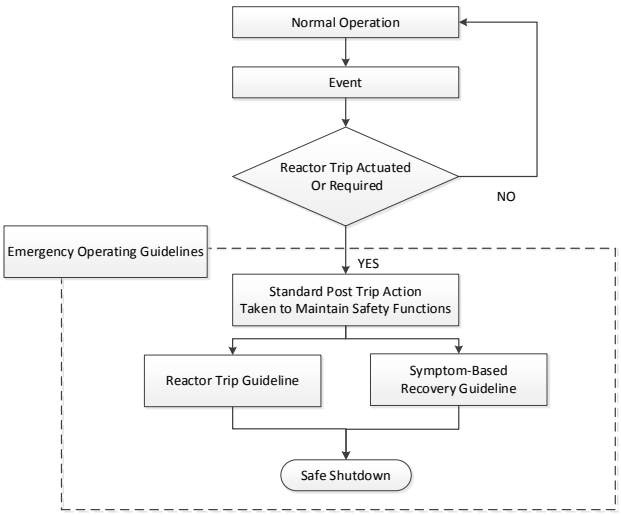

Figure 2.7-1. Structure of Emergency Operating Guidelines/Procedures.

2.8 Development of Operational Technical Specifications

The OTS of the JRTR described Safety Limits (SL), Limiting Safety System Settings (LSSS), Limiting Conditions for Operations (LCOs), required actions and completion time, surveillance requirements and frequencies, and administrative requirements, based on ANSI/ANS-15.1 and the Korean Law. The LCOs for the safe operation of the JRTR were established for each item meeting one or more of the following criteria according to 10 CFR 50.36 “Technical Specifications”, considering the characteristics of the JRTR [9].

2.9 Commissioning

To confirm the performance of safety equipment, loss of normal electric power (LOEP) [15][16] and loss of flow (LOF), possibly categorized as Anticipated Operational Occurrence (AOO), were selected as key tests to figure out how safe the research reactor is before taking over the research reactor to the owner. The intentional occurrence had shown that the nuclear safety was assured by proving that all the SSCs were performed as designed and intended and the numerical simulation, modelled by using the RELAP 5/Mod3.3 (RELAP manuals, 2010) presented the conservatism.

3. Future of Thermal-Hydraulic Performance and Safety Analysis of Research Reactors by KAERI

3.1 Multi-dimensional computation

It is clear that the resolution of 3D thermal-hydraulic phenomena can be used to improve the safety for various types of postulated accident as follows:

- Natural convection in a reactor pool for long-term cooling;
- Siphon break phenomena during loss-of-coolant accident (LOCA) including air ingress into a primary cooling system (PCS) through a siphon break line;
- Mal-distribution and starvation of coolant flow in a fuel assembly during flow blockage accident;

We, Korea Atomic Energy Research Institute (KAERI) are developing the multi-dimensional safety analysis technology by using 3D thermal-hydraulic codes in order to improve the safety performance of research reactors. Examples are presented as follows:

- When all the pumps in the Primary Cooling System (PCS) are stopped due to an accident such as a loss of electrical power, decay heat is removed by the natural circulation of the pool water through the reactor core, pool, flap valves and PCS pipes. In the pool, the coolant driven by the density difference rises from the upper part of the core and is sucked in the flap valves connecting the pool and PCS pipes during the natural circulation. Analysis of this 3D flow in the pool is very important to identify the integrity of the core and structures. Preliminary analysis was performed using the 3D module in the MARS code [17]. As shown in the Figure 3.1-1, the analysis result shows the difference between 1D model and 3D model of the pool. For detail analysis, the CUPID code, 3D thermal-hydraulic code, is being used. And the natural circulation experiments will be conducted to verify the results of the analyses.

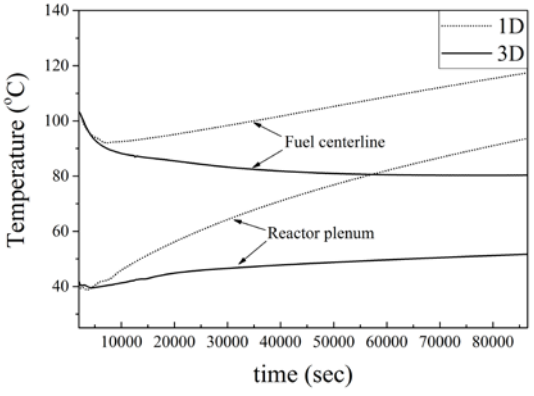

Figure 3.1-1. Comparison of coolant and fuel temperatures between the 1D and 3D models.

- The 3D numerical simulation for siphon break experiment has been performed by using CUPID code with two-fluid model [18]. The result shows that siphon phenomena during LOCA can be accurately predicted using 3D thermal-hydraulic code, CUPID. Additional simulations are being performed to assess applicability of CUPID at various siphon line sizes.
- When a number of complete blockages at cooling channels of a plate-type fuel assembly occur, the coolant flow through the blocked cooling channels will be

completely interrupted. Accordingly, the blocked cooling channels lose its own cooling capability. This event may cause mal-distribution of coolant flow in a fuel assembly and two-phase flow instability in the intact cooling channel. The preliminary studies have been performed to assure possibility of a commercial CFD code, CFX, application to onset of flow instability (OFI) in a narrow rectangular channel [19] and flow blockage in a plate-type fuel assembly [20] as shown in Figure 3.1-2 and Figure 3.1-3, respectively. Additional works are being carried out to simulate 3D thermal-hydraulic phenomena such as damage propagation due to the two-phase instability and to evaluate amount of damaged fuels during a flow blockage accident in an analytical manner.

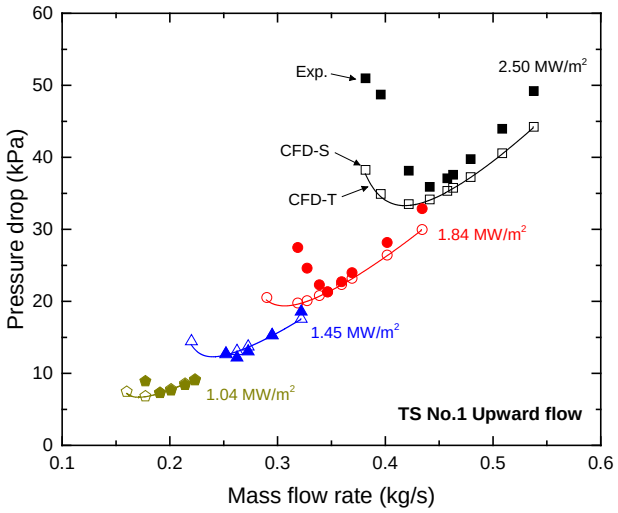

Figure 3.1-2. Two-phase pressure drop curve and OFI in a narrow rectangular channel for upward flow.

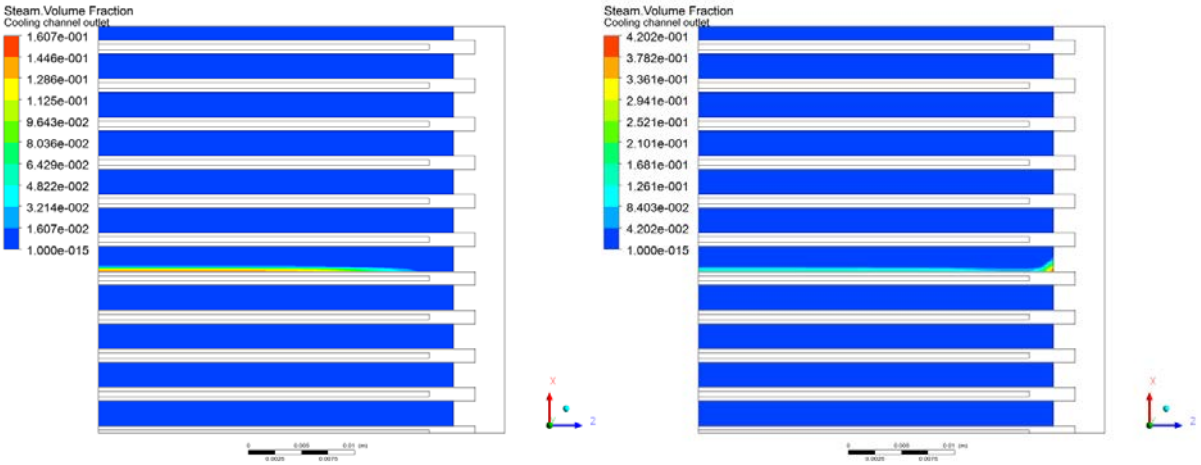

(a) 1 second (b) 2 seconds

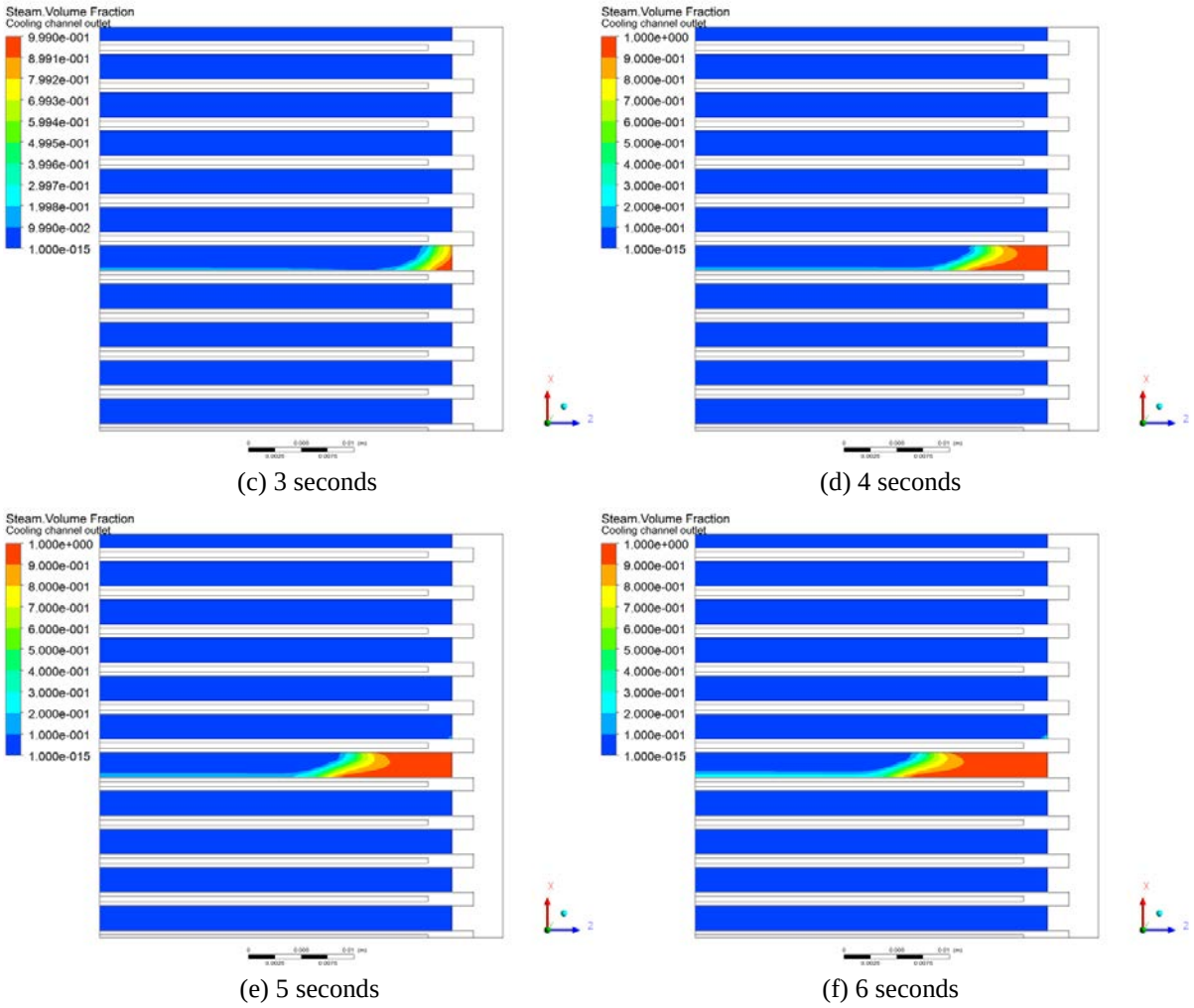

(c) 3 seconds (d) 4 seconds

(e) 5 seconds (f) 6 seconds

Figure 3.1-3. Variation of void fraction at cooling channel outlet of a plate-type fuel assembly after flow blockage accident (8 channels complete blockage)

3.2 Localization of thermal-hydraulic system code

We, KAERI have SPACE (Safety and Performance Analysis CodE) code, licensed to use for analyzing the nuclear safety of the nuclear power plants in Korea under high pressure and high temperature and want to change thermal-hydraulic numerical code by SPACE instead of using RELAP5/MOD3.

The developmental environment is as follows:

- C++ based
- Windows-XP/7 (32 bit recommended but compile and execution possible in 64 bit)
- Compiler: Visual studio 2008: SPACE 3.0 (licensed version)

The applicability of SPACE (Safety and Performance Analysis CodE) code needs to be extended to cover the operational ranges of the research reactors (RRs) such as the HANARO, the KJRR, the JRTR, and research reactors to be potentially designed in the future.

The thermal hydraulic phenomena within the research reactors are identified and the ranking tables are prepared to cover the initiating events up to beyond design basis accidents. Multi-dimensional physics is also included for the use in the future. Proposed were the RRs PIRTs, which will be the bases for the requirements for the code extension and the V&V [21].

4. Summary and Conclusions

The JRTR of great success by the Korea (war-torn nation about 70 years ago, no nuclear infra about 60 years ago) consortium is a good reference to the newly coming or upgrading nuclear society.
We, KAERI have accumulated our expertise in engineering, procurement, and construction of research reactors from small power to high power step by step since 1960s and gave a proof of competence to research reactors.
We, KAERI accomplished a comprehensive and systematic safety assessment through the design, construction, commissioning, and assurance on the conformance to the performance and safety objectives and the technical specifications. Covered are KAERI's endeavors to assure the nuclear safety of the JRTR.
We, KAERI move forward to meeting newly rising issues for the public acceptance by proactively providing more than safe and comfortable nuclear research with a set of research programs for more validation and more clear explanation about physics.

5. REFERENCES

[1] Park, S.K. (2016). Introduction to Safety Analysis Approach for Research Reactors, Transactions of the Korean Nuclear Society Autumn Meeting Gyeongju, Korea, October 27-28.
[2] Park, S.K., Jun, J.H., and Yum S.B. (2015). Cooling Performance of Natural Circulation for a Research Reactor, Transactions of the Korean Nuclear Society Autumn Meeting.
[3] Park, S.K., Lee, B.H., Kim, H.I., Park, C., and Chung, Y.J. (2013). Cooling Capability of Pool Water for a 5-MW Pool-Type Research Reactor, Transactions of the Korean Nuclear Society Spring Meeting Gwangju, Korea, May 30-31.
[4] Lee, B.H. and Park, S.K. (2015). Complete Flow Blockage of a Fuel Channel for Research Reactor, Transactions of the Korean Nuclear Society Autumn Meeting Gyeongju, Korea, October 29-30.
[5] Yum, S.B., Park, S.K., and Chung, Y.J. (2013), Sensitivity Investigation of Reactivity Induced Accidents for a 5MW Research Reactor, Transactions of the Korean Nuclear Society Autumn Meeting Gyeongju, Korea, October 24-25.
[6] Yum, S.B., and Park, S.K. (2014), Sensitivity Test of RIA in 5MW Research Reactor during Startup, Transactions of the Korean Nuclear Society Autumn Meeting Pyeongchang, Korea, October 30-31.
Park, S.K., Kim, H., Park, C., and Chung, Y.J. (2013). Cooling of Fuel Plates in an Accidental
[7] Drop of a Fuel Assembly, Transactions of the Korean Nuclear Society Autumn Meeting Gyeongju, Korea, October 24-25.
[8] Kim, H., Park, S.K., Park, C., Kim, S.J., and Noh, T.W. (2013). Simulation of power maneuvering using coupled analysis of kinetics and thermal-hydraulics in a Research Reactor. IGORR 10-1002, 70.
[9] Park, S.J., Kim, J.E., and Kim, H. (2016). A Development of Technical Specification of a Research Reactor with Plate Fuels Cooled by Upward Flow. Transactions of the Korean Nuclear Society Autumn Meeting.
[10] Kim, H., Jo, D.S., Park, S.K., and Park, C. (2015). Analysis on Thermal-Hydraulic Behavior of a Reflector System (From PRDBE to SRDBE). IAEA International Conference on Research Reactors: Safe Management and Effective Utilization in Vienna, IAEA-CN-231.
[11] Kim, H. and Park, S.K. (2014). A Preliminary Analysis on the Safety Effect of the Downgraded Heavy Water of a Research Reactor, Transactions of the Korean Nuclear Society Autumn Meeting.
[12] Kim, D.H., Kim, H. and Park, S.K. (2016). Development of Stepping Endurance Test Plan on CRDM of a Research Reactor, Transactions of the Korean Nuclear Society Autumn Meeting.
[13] Kim, H. and Park, S.K. (2015). A Proposal on EOG based on a Symptom-based approach for a Research Reactor, Transactions of the Korean Nuclear Society Autumn Meeting Gyeongju, Korea, October 29-30.
[14] Kim, H., Yum, S.B., Jung, Y. G., Lee, B.H., Jun, I.S., and Park, S.K. (2016). A Stencil to Develop an EOG for a Research Reactor, Transactions of the Korean Nuclear Society Autumn Meeting.

[15] Kim, H. and Park, S.K. (2015). A Preliminary Analysis of Reactor Performance Test (LOEP) for a Research Reactor, Transactions of the Korean Nuclear Society Autumn Meeting Gyeongju, Korea, October 29-30.
[16] Kim, H., Jung, Y.G., Jun, I.S., and Park, S.K. (2016). Development of Procedure for Stage C Commissioning: Reactor Performance Test (LOEP) for a Research Reactor, Transactions of the Korean Nuclear Society Spring Meeting Jeju, Korea, May 11-13.
[17] Kim, D.H. and Park S.K. (2017). Natural convection cooling in a 3-dimensional pool model of KJRR, Transactions of the Korean Nuclear Society Spring Meeting, Jeju, Korea, May 18-19.
[18] Park, I.K., Yoon H.Y., and Park H.B. (2018). Numerical approach to siphon break phenomena in a research reactor pool using the CUPID code, Nuclear Engineering and Design, 326, 133-142.
[19] Park, J.P. and Park, S.K. (2017). Numerical Analysis on OFI in Narrow Rectangular Channels Transactions of the Korean Nuclear Society Autumn Meeting, Gyeongju, Korea, October 26-27.
[20] Park, J.P. (2018). Numerical study for complete flow blockages of plate-type fuel assembly, Transactions of the Korean Nuclear Society Autumn Meeting, Yeosu, Korea, October 25-26.
[21] Kim, H., Lee, B.H., Park, S.K., Jung, Y.G., Park, J.P., Jang, D.W., Park, C. and Lee, S.W. (2018). Development of PIRTs for SPACE code extension to Application into Research Reactors, Transactions of the Korean Nuclear Society Autumn Meeting.

Long Term Operation and Age Management of the Advanced Test Reactor

Sean O'Kelly, David Rowsell, Hans Vogel
Idaho National Laboratory

Introduction

The Advanced Test Reactor (ATR) is currently the highest power test reactor in the world at 250 MW. The ATR's has operated for over 50 years with initial criticality occurring in 1967. The reactor mission is entirely focused on irradiation of nuclear fuels and materials for research and development and limited radioisotope production.

ATR is a light water cooled and beryllium reflected reactor with an approximate core height of 1.2 meters. The reactor primary cooling system is pressurized during operation to 2.69 MPa pressure with a typical average operating temperature of 71 C. ATR's unique design includes a four-lobe reactor core shape that creates nine large volume neutron flux traps (Figure 1). Multiple irradiation positions in the reflector around the reactor core permit many experiments to be performed simultaneously.

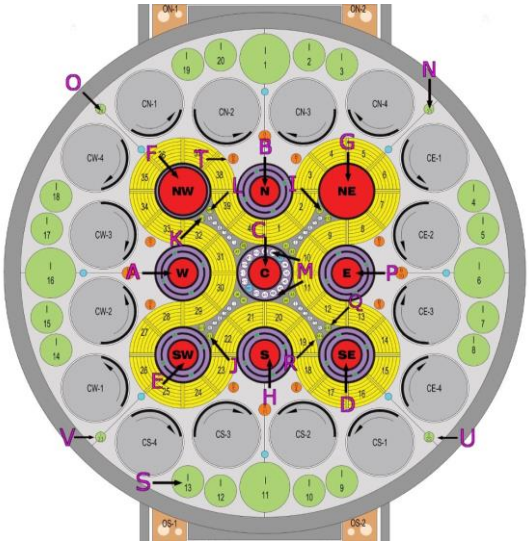

Figure 1 Advanced Test Reactor Cross-Section

Another unique feature of the ATR design is the elimination of vertical shim control rods which would change the effective reactor height as the rods were withdrawn. Movement of traditional controls rods perturbs the local power density as the rods are moved in or out of the reactor which then requires power correction on irradiated samples. To minimize power and neutron flux fluctuations during an operational cycle, ATR utilizes Outer Shim Control Cylinders (OSCC) to control reactivity. OSCC are sets of beryllium cylinders surrounding the ATR fuel with a 120 degree hafnium plate attached to one side. These cylinders are the same height as the

ATR core and absorb leakage neutrons along the full height of the ATR and thus maintain a constant power profile. The two-cylinder sets of OSCC are controlled independently and this coupled with the lobed ATR core allows significant deliberate power tilt of up to 3:1 across the reactor.

Although the ATR has already operated over five decades there is currently no replacement planned for the ATR. Current programs utilizing the ATR and its unique capabilities have required experimental irradiations scheduled for at least another two decades. To achieve such an operational goal, the ATR must continue to perform routine maintenance for operational safety and reliability now and into the future but must also begin planning for significant refurbishment or replacement of systems that have now operated beyond the original planned lifetime.

Throughout ATR's life the staff maintained the facility in accordance with industry good practice and DOE requirements but limited financial resources required decisions that often deferred some maintenance to concentrate on safety and operational requirements. In 2006, a program began that had the purpose to identify the most significant age related issues, determine a priority for ATR system refurbishment or replacement, and execute a replacement strategy. This program was called the ATR Life Extension Program (LEP) although there were different versions of these evaluation programs over previous decades. ATR does not have a planned end of life and was designed in the 1960s to operate for many years but funding for routine asset management and equipment replacement had not been sufficient to address all issues. In 1994, a decision was made by the Department of Energy, which owns the ATR, to establish an ATR shutdown date of 2014. However, by the early 2000s it was realized that ATR would continue to have an essential irradiation mission and a reactor shutdown was not desired. LEP provided resources to evaluate equipment condition and replace systems that were threatening continued operation. In 2011, ATR performance had begun to decline and the number of operational days or reactor availability each year decreased due to an increase in planned shutdowns or aging equipment issues that extended maintenance outages. That year, ATR established an equipment reliability and plant health monitoring program. This program built on previous equipment evaluations performed under LEP but also used operations and engineering staff input more effectively to monitor equipment condition in a more real-time manner with frequent system condition assessment meetings.

The ATR Equipment Reliability Program (ERP) is based upon the Institute of Nuclear Power Operations (INPO) document AP-913, Equipment Reliability Process. This process has the following components:

1. Scoping and Identification
2. Performance Monitoring
3. Corrective Maintenance
4. Preventative Maintenance Implementation
5. Continuous Equipment Reliability Improvement
6. Long Range Planning

Each of these activities had been performed at some level at ATR over the decades but had not been integrated into a formal process. It is important to note that, as with all operating facilities, unlimited funding was not available and all actions addressing equipment reliability required a structured and objective decision making process.

Scoping and Identification

This ER component requires identification of key or critical equipment that supports the overall reliability and safety of the facility and focus efforts and resources on that equipment. ATR has developed a Master Equipment List (MEL) and classified equipment on the list as Critical Component (CC), Non-Critical (NC), and Run-to-Failure (RTF). Critical Components are those pieces of equipment or systems for which a failure would cause a reactor shutdown or a reduction in power greater than 10%. ATR quickly realized that the criteria for a nuclear power plant which has a mission to provide reliable electricity would ignore some mission critical equipment at ATR. The purpose of ATR is to irradiate nuclear fuels and materials so to protect the primary irradiation mission an additional criteria was used at ATR to include experimental loops and equipment (such as data acquisition systems) that support the experimental programs. The focus of the ERP then is entirely directed towards those identified Critical Components. In practice, it was important to have a process that allowed management discretion to apply resources to non-critical equipment that supported quality of work environment such as air heating and cooling or lighting improvements.

Performance Monitoring

Tracking and trending equipment performance at ATR is a combination of real-time data from thermocouples and pressures, lagging data from periodic vibration, thermography, and human input from operator process monitoring tours and logbooks. Performance monitoring is necessary to establish a proactive, rather than a reactive, maintenance program. A core part of the equipment performance monitoring was the establishment of the Plant Health Committee (PHC) to acquire input from the various sources and make risk-based decisions as to the priority of equipment and systems to address or monitor more frequently while planning the replacement or refurbishment of the equipment. The PHC reviews system health reports for 26 systems to monitor performance and determine if any systems need to have their risk elevated for immediate attention. Overall, ATR baseline performance and trending needed an aggregate metric to inform management of program weakness or degradation in the process. This metric, called the Equipment Reliability Index (ERI). The original ERI was based on a metric created by the US nuclear power industry Equipment Reliability Working Group with EPRI (Electric Power Research Institute); however, the ATR ERI required some modification to cover all aspects of a material test reactor mission and the more frequent and shorter outage durations. Following AP-913 guidance, the ATR ERI monitors six categories which include 19 parameters. The categories are weighted to reflect their importance towards overall ATR reliability. The

weighting has been adjusted over several years to assure the right sensitivity of the ERI. The six categories are:

1. Reactor Availability
2. Challenge to Operations
3. System Health
4. Maintenance
5. Work Management
6. Long Term Planning

These categories are selected because they provide information about the current reactor reliability or failure rate but also the programs that sustain reliability such as the quality of maintenance and the replacement or upgrade strategies that are core to a good age management program. There are parameters in each category that originate from the AP-913 document but a select set is provided below.

1. Forced Loss Rate which is ratio of Lost Operational Days over planned Operational Days and reflects operational reactor reliability.
2. Unplanned Power Reductions was originally a category to agree with industry guidance but this was removed as ATR does not have a reduced power mode like a nuclear power plant and the weighted parameter was meaningless.
3. Cycle Forced Loss Events is a category that reflects equipment failures that caused a loss of operational days over a 3 month rolling period. This parameter was dropped from the ATR ERI because the operational schedule of ATR is always 2 months or less
4. Unplanned entries into Limiting Condition of Operation (LCO) reflects the control of equipment, materials, and process as inadvertent LCO entries represent a challenge to the safety envelope of the reactor.
5. Operator Work-Arounds is a measure of equipment maintenance because an operator must use some gap process to get work performed (e.g. a broken handwheel or indicator)
6. Critical Component Failure monitors the effectiveness of maintenance and age management and usually causes a reactor shutdown which supports the removal of a Cycle Forced Loss Events as a duplicative measure.
7. Safety System Unavailability is the ratio of hours that a safety system was not functioning and the hours that it was required to be in operation, either operating or shutdown.
8. Corrective Critical Work Backlog is a measure of how effectively the maintenance program is which is proportional to the performance of equipment and the planning of maintenance

Corrective Actions

The name of this function does not truly represent the activity encompassed. In this area, the action is to determine and trend failure cause analysis to understand equipment failure modes and take action to prevent future, similar failures. It is important to perform failure cause analysis in a graded approach to critical equipment and not to all failures as it would require an inordinate number of engineering resources to investigate every failure, especially when the number of failures increase due to the age of the overall reactor plant.

Preventative Maintenance (PM) Implementation

A preventative maintenance program is required for any nuclear reactor to ensure required safety systems are always available as necessary conditions to operate. However, the reliability of operation may require non-safety related systems to function and a PM program must maintain those facilities to assure reliability of operations. With limited resources, a PM program can't possibly perform PM activities on all systems at too frequent an interval or the reactor might never operate due to lengthy maintenance outages. ATR evaluated all critical components maintained in the PM system and added some equipment which had almost never been evaluated while also removing some less essential systems (i.e. making them Run to Failure systems) and increasing the frequency of the PM when it made engineering sense.

Equipment Reliability (ER) Continuous Improvement

An effective equipment reliability program must be constantly evaluating where resources should be directed to address emerging reliability issues. Because equipment failure rates are a probabilistic function there is no guaranteed way to predict when the next equipment failure will occur or which piece of equipment is most likely to fail. Therefore, information must constantly be provided to the engineers responsible for a system and adjustment to the priorities must be made as necessary. This may require cancelling one project to direct the funding to address an immediate failure that prevents reactor operation.

Life Cycle Management

Ideally, a reactor facility will establish a life cycle management program shortly after initial criticality to establish a baseline of system conditions and a schedule of equipment replacement or refurbishment linked to the overall system of age or number of hours of operation (wear-out). Such an age management program would replace a piece of equipment before the end of its design life when like for like replacements are probably still available without requiring major system redesign. In reality, with the exception of well-funded commercial or military operations, few research reactors operating in the world today had historic budgets that permitted planned periodic equipment replacements and most facilities are operating with equipment well past original design lifetimes. As facilities, such as ATR, continued to be needed for additional operating years it becomes necessary to begin equipment replacement later in operating lifetime and this creates a challenge to reactor schedules (maintenance versus operating time periods), personnel resources, and equipment reliability.

Plant Health Maintenance and Long Term Operation

Over the past thirty years, ATR has evaluated, through multiple reports, the health or condition of many critical systems required to sustain reactor operation until a time when the irradiation mission was no longer needed or if or when a replacement facility was constructed. With the exception of the core-internal changeout beryllium replacement and reactor internals overhaul, major sustained equipment refurbishment activities did not frequently occur with many replacements driven by end of life failures or obsolesce issues as spare parts were no longer available. In the period from approximately 2011 to 2015, the ATR's operational reliability became more challenged by an increasing failure rate of equipment operating beyond best-practice design lifetimes. Since 2015, there has been a strong recognition of the need for the ATR to continue to operate reliably and safely for at least the next two decades. Annual funding for equipment refurbishment or replacement has been provided under a rolling five year planning window. This requires that ATR maintain a risk-informed and reliability centered maintenance program that receives input from all staff that interact with equipment and prioritizes projects to address all age related equipment issues. The prioritization process is evaluated frequently as system health information changes (e.g. noisy bearings, higher failure rates, or indications of near-term failures). In 2017, DOE requested ATR evaluate current systems, structures, and components to develop a maintenance, operation, and funding strategy that could support ATR operations or alternate irradiation options well beyond 2040.

IDENTIFICATION OF REACTOR SPECIFIC INITIATING EVENTS USING HAZARD AND OPERABILITY ANALYSIS FOR PROBABILISTIC SAFETY ASSESSMENT OF THAI RESEARCH REACTOR-1/MODIFICATION 1

W. VECHGAMA*, K. SILVA, S. WETCHAGARUN, A. PECHRAK
Thailand Institute of Nuclear Technology (Public Organization)
9/9 Moo 7, Saimoon, Ongkharak, Nakhon Nayok, 26120 – Thailand

S. RASSAME
Department of Nuclear Engineering, Faculty of Engineering, Chulalongkorn University
254 Phayathai Rd., Pathumwan, Bangkok, 10330 – Thailand

ABSTRACT

Periodic Safety Review (PSR) of Thai Research Reactor-1/Modification 1 (TRR-1/M1) is suggested by the International Atomic Energy Agency (IAEA). It includes Probabilistic Safety Assessment (PSA). Process Hazard Analysis (PHA) is usually used to identify Initiating Events (IEs) in PSA. Hazard and Operability (HAZOP) analysis is known as one of the best PHA methods in case of limited information while Master Logic Diagram (MLD) and Failure Modes and Effects Analysis (FMEA) are recommended when complete database of components is available. The objective of this study is to identify IEs of the TRR-1/M1 using HAZOP analysis and compare IEs with MLD and FMEA from similar previous studies. As a result, IEs from HAZOP analysis is consistent with MLD and FMEA. It is found that HAZOP analysis takes a short time to assess IEs, but it cannot consider failure details of components as in MLD and FMEA.

1. Introduction

Thailand Institute of Nuclear Technology (TINT) plans for a Periodic Safety Review (PSR) of Thai Research Reactor-1/Modification 1 (TRR-1/M1) as it is required in the new Ministerial Regulation of the Office of Atoms for Peace (OAP) [1], and it is also recommended by the International Atomic Energy Agency (IAEA) [2]. Probabilistic Safety Assessment (PSA) of TRR-1/M1, which has never been done before, is one of the essential elements of the PSR. PSA is needed in order to estimate risks from a nuclear facility. PSA methodology is quite complicated since it integrates a great deal of information, e.g. plant design, operation, component reliability, human behaviour, thermal hydraulic, accident phenomena, as well as environmental and health effects [3].

PSA is a practice initially applied to a Nuclear Power Plant (NPP), especially Light Water Reactor (LWR). It is divided to three levels [4]. Level 1 PSA is an assessment of reactor pressure vessel failure in order to quantify core damage frequency. Level 2 PSA is an assessment of containment failure in order to evaluate amount of fission product release. Level 3 PSA is an assessment of consequence to people and environment from fission product release in order to assess consequence and management due to accident. Determination of initiating events (IEs) leading to accident in the LWR is an important part of PSA. IEs of NPP are identified based on both generic and plant-specific data of operation and maintenance.

Attempts have been made to perform PSA for advanced reactors [5]. However, the methodology employed for the evaluation is not identical to that of a conventional LWR due to differences of design, fuel, coolant, moderator and heat transfer system. Additionally, an

advanced reactor faces limitation in operation and maintenance records which are needed for the identification of IEs for PSA. In general, Process Hazard Analysis (PHA) techniques are used to specify hazardous events which help identify IEs in the advanced reactor. Master Logic Diagram (MLD) and Failure Modes and Effects Analysis (FMEA) are popular methods for highly detailed PHA, thus it is suitable for PSA in LWRs. On the other hand, Hazard and Operability (HAZOP) analysis is more suitable for advanced reactor because it requires less information. Design information of the advanced reactor at conceptual design stage is adequate for the identification of IEs.

For a research reactor (RR), there are also several previous studies on PSA. M. Maskin el al. [6] selected important IEs for level 1 PSA of Puspati TRIGA reactor in Malaysia. Methods to identify IEs in PSA of Puspati TRIGA Reactor include MLD and FMEA, and the assessment was done based on operating records in the IAEA's database and reactor specific data. M. Hashemi-Tilehnoee et al. [7] conducted HAZOP analysis of Iranian heavy water research reactor (IHWRR) on primary cooling system to identify IEs from Process Flow Drawing (PFD).

TRR-1/M1 is TRIGA Mark III type reactor which has no containment vessel and less effect to people and environment. Therefore, it is not necessary to conduct level 2 and 3 PSAs [6]. Since TRR-1/M1 has never prepared operation and maintenance records for PSA, HAZOP analysis is a suitable method to identify IEs because it requires less information as in the case of an advanced reactor [5]. The objective of this research is to identify IEs of the TRR-1/M1 using HAZOP analysis from internal events, and compare with previous studies where IEs of a similar type of the RR are identified by MLD and FMEA in order to see pros and cons of different methods. The paper is divided into five sections. This section introduces the background and the objective of the study. The second section explains characteristics and systems of TRR-1/M1. The third section describes HAZOP analysis. The fourth section contains the results and discussion. The last section is the conclusions.

2. Thai Research Reactor-1/Modification 1 (TRR-1/M1)

2.1 Characteristics of TRR-1/M1

Fig 1 shows the perspective view of TRR-1/M1 structures [8]. TRR-1/M1 is a TRIGA Mark III type reactor using light water as coolant, moderator, reflector and shielding. First operation started in November 1977. Maximum power based on the regulation of OAP is 1.3 MW while nominal operation power is 1.2 MW. TRR-1/M1 core is in the open reactor pool in which fuel elements include 8.5 wt.% uranium and 20 wt.% uranium. The number of fuel elements is 110, including 4 fuel follower control rods which are boron carbide.

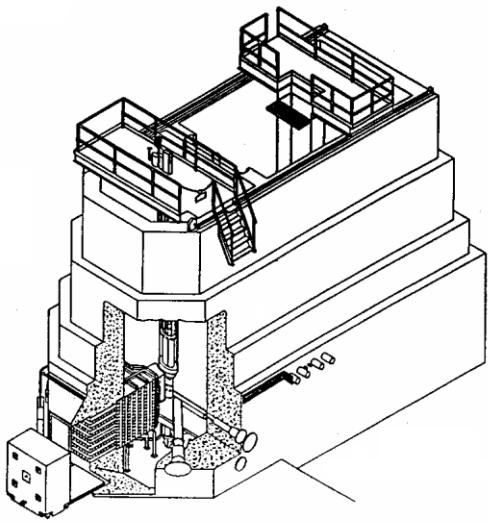

Fig 1. Perspective view of TRR-1/M1 structures [8]

2.2 Systems of TRR-1/M1

Tab 1 shows systems of TRR-1/M1 which are divided to 12 categories [9]. Each system is classified based on nuclear safety category in order to ensure it is recognized in design and operation safely. Each system of TRR-1/M1 is classified as (1) Safety Relevant-A (SR-A), (2) Safety Relevant-B (SR-B), or (1) Non-Safety Relevant (NSR). The definition of the three safety classes are as follow:

- SR-A: Items that have functions that are necessary to reactor shut down from abnormal operating conditions, prevention of loss of coolant accident (LOCA) and containment of fission products inside the fuel rods;
- SR-B: Items that do not meet the SR-A criteria but have functions to achieve proper reactor operating conditions and prevent accidents;
- NSR: Items that do not meet the SR-A or the SR-B criteria.

Tab 1: Systems of TRR-1/M1 with classifications of safety [9]

No.	Systems	Compositions	Safety class
1	Reactor core system	Core structures	SR-A
		Reactor pool structures	SR-A
		Reactor bridge and platforms	SR-B
		Fuel elements	SR-A
		Beam tubes	SR-A
		Thermal Column	SR-A
2	Reactivity control system	Control rods	SR-A
		Control rod drives	SR-A
		Control rod guide tubes	SR-A
3	Instrumentation and control (I&C) system	Reactor protection system	SR-A
		Reactor control system	SR-B
4	Reactor coolant system (RCS)	Primary coolant loop	SR-B
		Secondary coolant loop	NSR
		Pool water purification loop	SR-B
		Demineralized water makeup	NSR
5	Emergency core cooling system (ECCS)	Solenoid Valve	SR-A
		UPS for Solenoid Valve	SR-A
		ECCS Pump	SR-A
		Pressurized Tank	SR-A
		Water supply Tank	SR-A
6	Radiation monitoring system	Continuous Air Monitors	SR-B
		Remote Area Monitors	SR-B
		Ventilation Monitors	SR-B
		Personnel Monitors	SR-B
7	Electrical power supply system	Normal power supply	NSR
		Emergency power supply	SR-A
8	Experimental facilities system	In-cores	SR-B
		Out-cores	NSR
		Thermal column room	NSR
		Beam port facilities	NSR
9	Reactor building and structures system	Reactor hall	SR-B
		Reactor hall crane	SR-B
		Ventilation stack	SR-B
10	Ventilation & air conditioning (VAC) system	Normal ventilation system	SR-B
		Air conditioning system	NSR
		Reactor confinement system	SR-A
11	Fuel handling & storage system	In-pool fuel storage facility	SR-B
		Fresh fuel storage facility	NSR
		Spent fuel storage facility	NSR
		Fuel handling equipment	SR-B
12	Auxiliary systems	Auxiliary bridge and platforms	NSR
		Fire detection / protection system	SR-B
		Emergency communication	SR-B
		Evacuation alarm	SR-B
		Tap water system and sanitary drains	NSR
		Local communication system	NSR
		Lighting system	NSR
		Physical Security system	NSR
		Radioactive waste system	SR-B

3. Hazard and Operability (HAZOP) analysis

HAZOP analysis is used to assess hazards using HAZOP guide words in facilities, equipment, and processes. It is capable of assessing systems' design, operation, procedural controls, as well as physical and operational environments [10]. Methodology of HAZOP analysis is divided

to four phases including (1) definition phase, (2) preparation phase, (3) examination Phase, and (4) documentation and follow-up phase.

3.1 Definition phase

Definition phase begins with identification of scope and objective, and risk assessment team members and responsibility.

3.2 Preparation phase

Tasks in the preparation phase include identifications of supporting information, template format for assessment, and the possible HAZOP guide words. Tab 2 shows an example in the preparation phase. Findings in each abnormal element largely depend on determinations of the HAZOP guide words and parameters to identify deviations.

Tab 2: The example of basic HAZOP guide words [10]

Guide words	Meaning	Parameters (for example)	Deviation	Example
No	Negation of the design intent	Flow	No flow	No flow when production is expected
Less	Quantitative decrease	Pressure	Low pressure	Lower pressure than normal
More	Quantitative increase	Temperature	High temperature	Higher temperature than designed
Part of	Qualitative decrease	State	Degraded state	Only part of the system is shut down
As well as	Qualitative increase	One phase	Two phases	Other valves opened and not only liquid indicated (logic fault or human error)
Reverse	Logical opposite of the intention occurs	Intended objective	Mismatch	Back-flow when the system shuts down
Other than	Complete Substitution (another activity takes place)	Operation	Maintenance	Loss of electric power caused by chaotic maintenance

3.3 Examination Phase

Examination phase begins with identification of all elements or parts of the system or process to be examined. Next, important parameters which are sensitive to occurrence of hazards are applied to the prepared HAZOP guide words in order to find deviations, causes, and consequences. It may include safeguard (countermeasure), if any. Not all combinations of all HAZOP guide words and parameters are expected in the HAZOP analysis. Only credible deviations should be assessed.

3.4 Documentation and follow-up phase

The documents of the HAZOP analysis are collected and organized using a template of IEC Standard 61882 for traceability. The risk assessment team may modify the HAZOP when having more necessary requirements.

4. Results and discussion

This section shows results of HAZOP analysis of TRR-1/M1 focused on internal events. IEs are defined by grouping the results of HAZOP analysis. The results of HAZOP analysis are compared with MLD and FMEA to find pros and cons.

4.1 Results of HAZOP analysis

Since this study focuses on consequences of core damage of TRR-1/M1 based on Level 1 PSA [4] and only systems including components labelled as SR-A are included, the title of the HAZOP analysis in this study is “abnormal systems with safety class of SR-A affecting core damage of TRR-1/M1.” Schemes and information for the HAZOP analysis are referred to from the “Safety Analysis Report (SAR) for Thai Research Reactor-1 / Modification 1 (TRR-1/M1) [9].” Classification of safety is based on Tab 1. Fig 2 shows the scheme of TRR-1/M1 coolant system for the HAZOP analysis. Tab 3 shows the results of HAZOP analysis. There are several

observations. First, abnormal events which affect core damage are considered by most probable severe case of each system. Second, only components which directly affect the reactor core system are mainly considered. Third, since the determination of system for HAZOP analysis of the reactor core system covers important components with safety class of SR-B, i.e. Reactor Coolant System (RCS) and auxiliary system in Fig 2, they are also considered in HAZOP analysis.

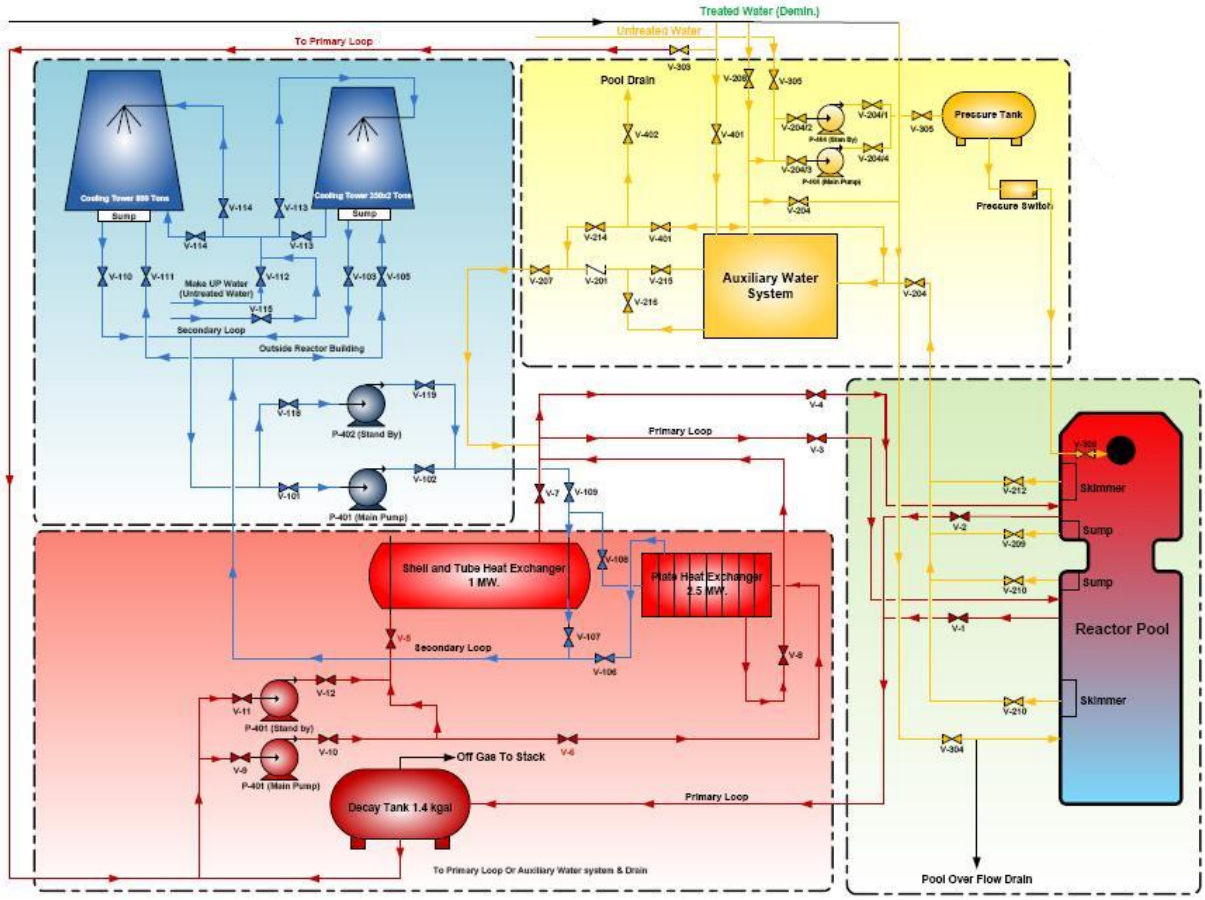

Fig 2. scheme of TRR-1/M1 coolant system [9]

Tab 3: Results of HAZOP analysis of TRR-1/M1

Title	Abnormal system affecting core damage of TRR-1/M1 base on having safety class of SR-A								
Scheme	Safety analysis report for Thai Research Reactor-1 / Modification 1 (TRR-1/M1)								
Team	Wasin Vechgama, Kampanart Silva, Saensuk Wetchagarun, Anantachai Pechrak and Somboon Rassame								
No.	Element	Parameter	Guide word	Deviation	Cause	Consequence	Safeguard	Comment	EIs group
1	Reactor core system	Flow	More	High outlet flow from small reactor pool into primary coolant loop	Control valve V-1 fail open	Core damage/LOCA	ECCS/natural convection from reactor pool	Control valve fail indication	1
					Control valve V-2 fail open	Core damage/LOCA	ECCS/natural convection from reactor pool	Control valve fail indication	1
				High outlet flow into small pool from into auxiliary coolant loop	Control valve V-209 fail open	Core damage/LOCA	ECCS/natural convection from reactor pool	Control valve fail indication	1
					Control valve V-210 fail open	Core damage/LOCA	ECCS/natural convection from reactor pool	Control valve fail indication	1
					Control valve V-212 fail open	Core damage/LOCA	ECCS/natural convection from reactor pool	Control valve fail indication	1
		Level	Less	Low water level in reactor pool	Control valve V-1 fail open	Core damage/LOCA	ECCS/natural convection from reactor pool	Control valve fail indication	1
					Control valve V-2 fail open	Core damage/LOCA	ECCS/natural convection from reactor pool	Control valve fail indication	1
					Control valve V-209 fail open	Core damage/LOCA	ECCS/natural convection from reactor pool	Control valve fail indication	1
					Control valve V-210 fail open	Core damage/LOCA	ECCS/natural convection from reactor pool	Control valve fail indication	1
					Control valve V-212 fail open	Core damage/LOCA	ECCS/natural convection from reactor pool	Control valve fail indication	1
		Reactivity	More	High reactivity in core	Failure of stuck control rod	Core damage	Safety control rod/natural convection from reactor pool	Control rod fail indication	2
		Temperature	More	High temperature in reactor core	Failure of stuck control rod control	Core damage	Safety control rod/natural convection from reactor pool	Control rod fail indication	2
		Pressure	More	High pressure of hydrogen with in cladding	Failure of stuck control rod control	Core damage	Safety control rod/natural convection from reactor pool	Control rod fail indication	2
2	Reactivity control system	Reactivity	More	High reactivity in core	Failure of stuck control rod	Core damage	Safety control rod/natural convection from reactor pool	Control rod fail indication	2
3	Instrumentation and control (I&C) system	Signal	No	No signal from channel to drop control rod	Failure of I&C trip logic of fuel temperature channel	Core damage	Reactor Regulating System (RRS)/natural convection from reactor pool	I&C trip logic fail indication	3

Title	Abnormal system affecting core damage of TRR-1/M1 base on having safety class of SR-A								
Scheme	Safety analysis report for Thai Research Reactor-1 / Modification 1 (TRR-1/M1)								
Team	Wasin Vechgama, Kampanart Silva, Saensuk Wetchagarun, Anantachai Pechrak and Somboon Rassame								
No.	Element	Parameter	Guide word	Deviation	Cause	Consequence	Safeguard	Comment	EIs group
					Failure of I&C trip logic of nuclear channel for reactor power	Core damage	RRS/natural convection from reactor pool	I&C trip logic fail indication	3
					Failure of I&C trip logic of nuclear channel for reactor period	Core damage	RRS/natural convection from reactor pool	I&C trip logic fail indication	3
					Failure of I&C trip logic of pool level float switch for water level	Core damage	RRS/natural convection from reactor pool	I&C trip logic fail indication	3
					Failure of I&C trip logic of nuclear channel for high voltage power supply	Core damage	RRS/natural convection from reactor pool	I&C trip logic fail indication	3
4	Reactor coolant system (RCS)	N/A	N/A	N/A	N/A	N/A	N/A	Safety class of SR-B and NSR/Some RCS are included in Reactor core system.	N/A
5	Emergency core cooling system	Flow	No	No inlet flow to reactor core	Failure of sensing device from pool water level	Core damage/LOCA	Natural convection from reactor pool	Sensing device fail indication	4
					Failure of water supply	Core damage/LOCA	Natural convection from reactor pool	Water supply indication	4
					Manual valve fail closed	Core damage/LOCA	Natural convection from reactor pool	Manual valve fail indication	4
					Manual shut off valve fail close	Core damage/LOCA	Natural convection from reactor pool	Manual shut off valve fail indication	4
					Latch valve fail close	Core damage/LOCA	Natural convection from reactor pool	Latch valve fail indication	4
					Failure of nozzles	Core damage/LOCA	Natural convection from reactor pool	Nozzles fail indication	4
					Failure of battery	Core damage/LOCA	Natural convection from reactor pool	Battery fail indication	4
					Failure of flow switch	Core damage/LOCA	Natural convection from reactor pool	Flow switch fail indication	4
6	Radiation monitoring system	N/A	N/A	N/A	N/A	N/A	N/A	Safety class of SR-B	N/A
7	Electrical power supply system	Electricity	No	No electricity to ECCS	Failure of emergency AC power supply to ECCS	Core damage/LOCA	Uninterruptible power supply (UPS)/Natural convection from reactor pool	Emergency AC power supply fail indication	5
					Failure of UPS to ECCS	Core damage/LOCA	Natural convection from reactor pool	UPS fail indication	5
8	Experimental Facilities	N/A	N/A	N/A	N/A	N/A	N/A	Safety class of SR-B and NSR	N/A

Title	Abnormal system affecting core damage of TRR-1/M1 base on having safety class of SR-A								
Scheme	Safety analysis report for Thai Research Reactor-1 / Modification 1 (TRR-1/M1)								
Team	Wasin Vechgama, Kampanart Silva, Saensuk Wetchagarun, Anantachai Pechrak and Somboon Rassame								
No.	Element	Parameter	Guide word	Deviation	Cause	Consequence	Safeguard	Comment	EIs group
9	Reactor building and structures	N/A	N/A	N/A	N/A	N/A	N/A	Safety class of SR-B	N/A
10	Ventilation & air conditioning (VAC) system	N/A	N/A	N/A	N/A	N/A	N/A	Safety class of SR-B and NSR/not concerned with SR-A for fission product release	N/A
11	Fuel handling & storage system	Temperature	More	High temperature of fuel and spent fuel	Failure of fuel handling	Core damage	Natural convection from reactor pool	Fuel handling fail indication	3
12	Auxiliary systems	N/A	N/A	N/A	N/A	N/A	N/A	Safety class of SR-B and NSR/Some Auxiliary systems are included in Reactor core system.	N/A

4.2 IEs selection

From Tab 3, results of HAZOP analysis of TRR-1/M1 are grouped into five IEs groups. The grouping of IEs is done by gathering core damage events due to similar causes using expert judgment. HAZOP analysis results in Tab 3 are grouped into:

- IEs group 1: Loss of coolant accident (LOCA)
- IEs group 2: Insertion of excess reactivity
- IEs group 3: Erroneous failure of equipment or components
- IEs group 4: Loss of flow accident (LOFA)
- IEs group 5: Loss of electrical power supplies

4.3 Comparison with MLD and FMEA

M. Maskin el al. [6] selected IEs for level 1 PSA of Puspati TRIGA reactor using Master Logic Diagram (MLD) and Failure Modes and Effects Analysis (FMEA). MLD method is a hierarchical depiction to show relationship between accident and initiating event. This method starts from consequences following by identification of IEs, thus the assessor team need to know thorough detail of system to identify causes of accident in hierarchy. FMEA method is appropriate to identify the potential failure modes of each component. Causes and effects of equipment failure are thoroughly showed in each component. These methods take time to identify detail of each component.

Tab 4 shows comparison of IEs groups identified by HAZOP analysis with those identified by MLD and FMEA. It is found that IEs grouping for level 1 PSA of Puspati TRIGA reactor using MLD and FMEA [6] is consistent with IEs grouping for TRR-1/M1 using HAZOP analysis.

Tab 4: Comparison of IEs identification of HAZOP analysis with MLD and FMEA

IEs group No.	HAZOP analysis	MLD and FMEA
1	Loss of coolant accident (LOCA)	• Small break loss of coolant accident (heat exchanger plate rupture) • Small break loss of coolant accident • Large break loss of coolant accident (in the reactor building) • Large break loss of coolant accident (in the basement)
2	Insertion of excess reactivity	• Insertion of excess reactivity accident
3	Erroneous failure of equipment or components	• Spurious reactor SCRAM, (7)
4	Loss of flow accident (LOFA)	• Loss of flow accident (primary) • Loss of flow accident (secondary).
5	Loss of electrical power supplies	• Loss of power supply

IEs from HAZOP analysis cover all IEs from MLD and FMEA, though the level of detail is much lower. However, identification of IEs using the HAZOP guide words can be done in a much shorter time. Therefore, in the case of the RR which is not as complicated as the LWR, HAZOP analysis is an appropriate method to identify IEs. On the other hand, although MLD and FMEA methods use a lot of details and take a long time to identify IEs, the details can help support operation and maintenance in a better manner than HAZOP analysis.

5. Conclusion

This research uses HAZOP analysis to identify IEs of TRR-1/M1. The grouping of IEs affecting core damage is shown as follows:

- IEs group 1: Loss of coolant accident (LOCA)
- IEs group 2: Insertion of excess reactivity
- IEs group 3: Erroneous failure of equipment or components
- IEs group 4: Loss of flow accident (LOFA)
- IEs group 5: Loss of electrical power supplies

It is found that IEs grouping for PSA of the TRIGA Mark type reactors using HAZOP analysis is consistent with IEs grouping using MLD and FMEA. HAZOP analysis can identify IEs in a short time but does not provide thorough detail of component failures as in MLD and FMEA.

Influence of external events and human errors on the IE identification and respective steps of PSA may need to be further studied in future research.

6. References

[1] Ministry of Science and Technology, Thailand “Ministerial Regulation on Schedule of Review and Update of Safety Analysis Report of Nuclear Facilities” 2016.
[2] IAEA “Safety of Research Reactors,” Specific Safety Requirements No. SSR-3, IAEA Safety Standards for protecting people and the environment, 2016.
[3] IAEA, “PSA and PSA Applications” Workshop Manual, 2016.
[4] Nuclear Regulatory Research, U.S. Nuclear Regulatory Commission “A Guide to the Performance of Probabilistic Risk Assessments for Nuclear Power Plants,” 1983.
[5] S. Krahn, C. Leach, B. Chisholm and et al. “Program on Technology Innovation: Early Integration of Safety Assessment into Advanced Reactor Design,” Preliminary Body of Knowledge and Methodology, Electric Power Research Institute, U.S., 2018.
[6] M. Maskin, F. Charlie, A. Hassan and et al. “Selection of Important Initiating Events for Level 1 Probabilistic Safety Assessment Study at Puspati TRIGA Reactor,” *Ann. Nucl. Energy,* vol. 92, 2016.
[7] M. Hashemi-Tilehnoee, A. Pazirandeh, S. Tashakor, “HAZOP-Study on Heavy Water Research Reactor Primary Cooling System” *Ann. Nucl. Energy,* vol. 37, 2010.
[8] K. Tiyapun, N. Klaysuban, S. Boonmark and C. Tippayakul “Current Status and Future Challenge of TRR-1/M1 Thai Research Reactor,” Thailand Institute of Nuclear Technology (Public Organization), Thailand, 2016.
[9] Thailand Institute of Nuclear Technology (Public Organization), “Thailand Safety Analysis Report for Thai Research Reactor-1 / Modification 1 (TRR-1/M1),” 2017.
[10] P. Fuchs, J. Kamenicky, T. Saska, D. Valis, J. Zajicek “Some Risk Assessment Methods and Examples of their Application” Technical University of Liberec, Czech, 2012.

LESSONS LEARNED FROM DESIGN AND CONSTRUCTION OF POOLS AND POOL OPERATION FACILITIES FOR JRTR

JEONG-SOO RYU, JINHO OH, SANGIK WU
Korea Atomic Energy Research Institute (KAERI)
111 Daedeok-daero 989 Beon-gil, Yuseong-gu, Daejeon, Republic of Korea

ABSTRACT

The Jordan Research and Training Reactor (JRTR) has potential for its applicability to most research reactor utilization areas. Research reactors are utilized for very wide and diverse areas. The pools and pool operation facilities for research reactors are designed to support radioisotope production, neutron activation analysis, neutron beam utilization, and training and education, and so on. The JRTR is arranged so that there is no interference with the pool structures, control rods, or irradiation devices, and is optimized considering ease of use. Pool operation facilities in the JRTR include an operation bridge, a pool cover, a pool door, reactor pool and service pool platforms, fresh and spent fuel storage racks and a reactor component storage rack. The function of the pools and pool operation facilities for the JRTR is introduced, and lessons learned from the design and the construction of them are summarized.

1. Introduction

Korea Atomic Energy Research Institute (KAERI) has had over 50 years of experience with research reactors, including overseeing the operation of its flagship 30 MW HANARO (Hi-Flux Advanced Neutron Application Research ReactOr) since 1995. Based on its own accumulated experience in the design, construction, and operation of HANARO, KAERI has been developing the design and technology of customized research reactor aimed at facilitating exports to other countries as well as domestic.

The Jordan Atomic Energy Commission (JAEC) commenced the Jordan Research and Training Reactor (JRTR) project by issuing a request for a proposal in January 2009. The JRTR project was officially launched in 2010, with the Korean consortium led by KAERI and Daewoo E&C (KDC). The JRTR was designed and constructed as a multipurpose reactor, which will fulfill various user requirements as an education and training tool in nuclear engineering and reactor operations, as well as neutron activation analysis, radioisotope production, neutron beam applications, and neutron transmutation doping. The JRTR started operating after obtaining its facility operation license in November 2017. The JRTR will serve as an integral part of the nuclear technology infrastructure in Jordan, and become a focal point as a center of nuclear science and technology.

The core concept of the JRTR is an open-tank-in-pool type reactor with 5 MW power, which is upgradable to 10 MW. The design life of the reactor facility is 40 years. The nuclear design of the reactor core focuses on the thermal neutron flux levels in irradiation holes and beam tubes. The target of the thermal flux level is 1.5×10^{14} n/cm2·s. The core structure is composed of the reactor structure, fuel assemblies, a D_2O reflector, control rod drive mechanisms (CRDM), second shutdown drive mechanisms (SSDM), neutron detector housings, and beam tubes. The reactor structure is composed of a stainless steel outlet plenum and grid plate, a Zircaloy reflector vessel, an aluminum chimney, and zirconium alloy flow tubes. The design

of the fuel assembly is based on well-proven box-type concepts for which multiple fuel vendors are available. A standard flat plate type has been adopted due to its high heat removal capability and positive experience in many research reactors. The fuel meat consists of U_3Si_2 particles dispersed in an aluminum matrix, and the uranium enrichment is 19.75 wt%.

The JRTR has two open pools, the reactor pool and the service pool. The two pools are partitioned by concrete walls and one pool gate. The service pool is directly connected to the reactor pool through the pool gate. Both pools can be isolated by installing a pool door to block the gate. The reactor pool contains the reactor structure assembly, four beam ports, a thermal column, the embedded plates welded to the pool liner plate for the installation of reactor control systems, instrumentation, piping supports, and pool platforms. The service pool is designed to satisfy the storage and the handling of spent fuels, reactor components, and irradiated materials. The fuel handling system to prevent the dropping of or damage to fuel assemblies during transportation was developed for safe refueling within a limited shutdown period in each operation cycle.

Pool operation facilities consist of an operation bridge, a pool cover, a pool door, reactor pool and service pool platforms, fresh and spent fuel storage racks, a reactor component storage rack, as well as other features. The function of the pools and pool operation facilities for the JRTR will be introduced in the next section, and lessons learned from the design and the construction of them are then summarized.

2. Reactor Utilization

Research reactors are used for very broad purposes. In principle, the JRTR has potential for its applicability to most research reactor utilization areas. Among the areas, neutron beam applications, radioisotope (RI) production, neutron activation analysis (NAA), and education and training are expected to be the most active ones from the early stage of the JRTR operation.

Neutron beams are an important tool in modern science and technology for investigating the microscopic structure and dynamics of materials, for looking into objects non-destructively with various neutron imaging methods, and for analyzing the elemental composition of materials. The JRTR provides four beam ports aimed basically at the neutron scattering and radiography of neutron beam applications, as well as a thermal column that provides very high quality thermal neutron flux field over a wide space.

Radioisotopes (RIs) are widely used, and the demand for them has been constantly increasing. The production of RIs is one of the major goals of the JRTR. In early reactor operation, Ir-192, I-131, and Mo-99 will be produced. Three irradiation facilities (NAA-1/2/3) with appropriate neutron flux and relatively low gamma heating are ready for the NAA. In the future, it is expected that RI production will expand not only in quantity but also in variety, and that the NAA activity will expand and additional irradiation facilities may be necessary. Neutron transmutation doping (NTD) devices will be installed for the silicon irradiation service, and several irradiation facilities will be utilized for other purposes including education and training.

One of the important utilization areas of the JRTR is education and training. All experimental facilities mentioned can be utilized for the education and training in the respective reactor utilization areas. Therefore, the reactor itself will also be utilized for the education and training of students studying nuclear engineering.

3. Reactor Pool and Service Pool

In the JRTR, two open pools, the reactor pool and the service pool, are arranged in a long rectangle of 3.6 m x 12.0 m, as shown in Figure 1. The overall pool depth is 11.2 m, filled with 10.0 m deep water. The two pools are partitioned by concrete walls and one pool gate. The service pool is directly connected to the reactor pool through the pool gate. The width of the pool gate is designed for the transport of objects between the reactor pool and the service pool. Both pools can be isolated by installing a pool door to block the gate. When lowering of the reactor pool water level is required for maintenance or inspection of the facilities in the reactor pool, the reactor pool can be isolated by the pool door. The drained water is stored in the pool water storage room and pumped back to the reactor pool. The reactor pool and the service pool are purified and cooled by the pool water management system (PWMS) during all operational modes. Leak tightness of the pool liner is monitored by the level switch with an alarm and a test port on the line of active drainage system (ADS). In addition, the pool liner plate of 9 mm stainless steel is classified as Safety Class 3 and Seismic Category I.

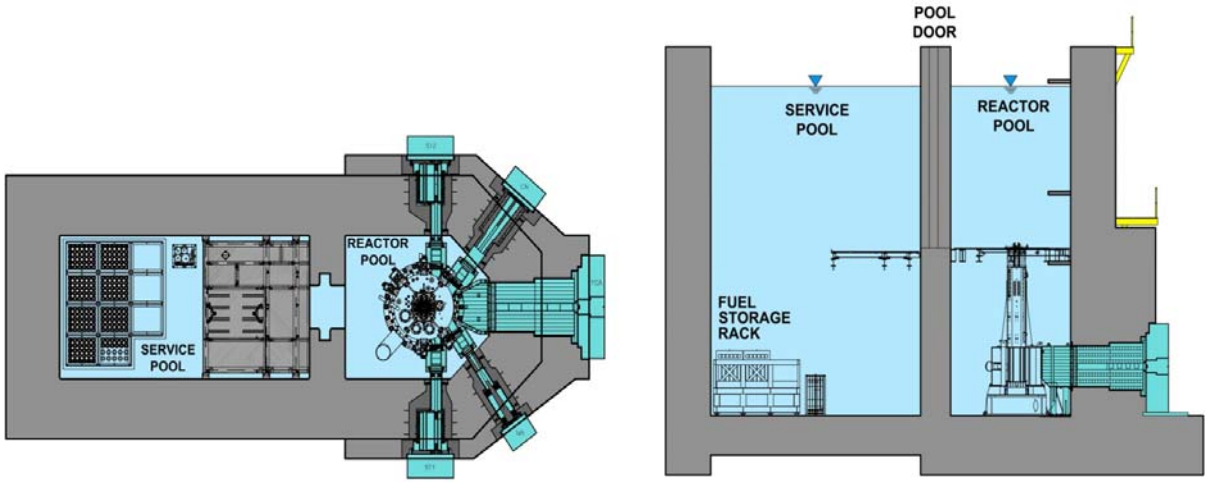

Figure 1 Pool configuration of JRTR

3.1 Reactor Pool

The reactor pool has a hexagonal horizontal section of 3.6 m x 4.0 m. A reactor structure assembly containing the reactor core and reflectors is installed at the bottom of the reactor pool, and the primary inlet and outlet pipes of the core are attached at the reactor structure. The reactor pool is constructed with heavy concrete, and the inside of the reactor pool walls is lined by stainless steel plates. The concrete structure of the pool is constructed for supporting loads acting on the reactor pool and as a biological shield. The pool liner plate is installed to be united with the concrete structure by use of a reinforcing material in order to maintain its structural integrity against seismic load.

The reactor pool contains a) the reactor structure assembly, b) embedded plates welded to the pool liner plate for the installation of reactor control systems, instrumentation, and piping supports, and c) the removable structures of pool platforms, tools, and lighting, connected with brackets fixed to the embedded plates. The gaps between the structure and the penetration are welded by using seal plates to prevent pool water leakage. Reactor pool penetrations are provided for piping, experimental facilities, SSDM, heating, ventilation, and air conditioning (HVAC), and pneumatic transfer system (PTS) tubing.

The reactor pool concrete structure is designed to satisfy the following requirements:

(a) The reactor pool performs the function of a radiation shield.
(b) The reactor pool performs the function of an ultimate heat sink to remove the decay heat generated from the reactor core.
(c) The reactor internal structures, e.g., reactor structure assembly, reactor control system, and beam tubes are installed in the reactor pool.
(d) The reactor pool is designed to endure all anticipated loads, including thermal and seismic loads.
(e) The embedded plates in the pool liner are designed with consideration of the weight and position of the structures.
(f) The underwater penetrations in the reactor pool are sealed to maintain water tightness.
(g) A leak monitoring system is attached to the welded parts of the pool liner.

3.2 Service Pool

The service pool has a rectangular horizontal section of 3.6 m x 7.0 m. The service pool provides space for underwater work and storage for experiments and radioisotope production. The two inlet and outlet primary pipes penetrate the service pool wall. Fresh fuel is temporarily stored on the service pool working platform in the service pool before transfer to the reactor core. Objects related to radioisotopes and NTD are handled on the service pool working platform. Storage space for the thermal column extensions is reserved under the service pool working platform. Junction boxes, above the normal pool water level, are provided for instruments and cables. The service pool contains a) the spent fuel storage racks, their support frames, and the reactor component storage rack, and b) removable structures such as pool platforms, tools, and lighting, are connected with brackets fixed to embedded plates.

The service pool is designed to satisfy the following requirements:

(a) It provides storage for spent fuel, damaged fuel, and reactor components.
(b) It provides space for irradiated material handling.
(c) The pool water provides radiation protection.
(d) Decay heat generated from spent fuels is removed.
(e) The service pool is designed to endure all anticipated loads, including thermal and seismic loads.
(f) The embedded plates in the pool liner are designed with consideration of the weight and position of the structures.
(g) The underwater penetrations are sealed to maintain water tightness.
(h) A leak monitoring system is attached to the welded parts of the pool liner

4. Pool Operation Facilities

4.1 Operation Bridge

The operation bridge, as shown in Figure 2, consists of a crane system with a working deck for the handling of the in-pool parts such as fuels, reactor components, and reactor utilization facilities. It allows operators to access the top of the reactor in the reactor pool and the spent fuel storage racks in the service pool.

The operation bridge comprises a lower working deck mounted on a saddle that travels on rails. Upright members are mounted on the saddle to support the upper structure and two hoist monorails. The saddle contains an anti-derail system composed of seismic lugs and guide

rollers. It travels between the reactor pool and the service pool along the rails to transport the fuel assembly, irradiated object, and reactor components in the pools by using tools. Two hoists are attached to both sides of the top girder of the operation bridge. The capacity of each hoist is 0.5 ton. The hoist is suspended from the monorail by means of a motor-driven trolley that runs along the monorail. Hoist and trolley movements are controlled from the control pendant switch. All controls are on the pendant station, and the control panel is mounted on the working deck of the operation bridge. The controls provide a means for moving the bridge, the trolley, and the hoists. The traveling speed of the bridge has four steps of 0.6 m/min, 1.2 m/min, 3 m/min, and 6 m/min. The speed of the hoist and the trolley has four steps of 0.6 m/min, 1.2 m/min, 3 m/min, and 6 m/min in both horizontal and vertical directions.

The main structural members of the operation bridge are made of carbon steel. The bridge is designed to prevent dust and oil from falling into the reactor or service pool. It was inspected and tested during fabrication and installation, and in the commissioning stage, it was tested with related procedures, and safety devices have been included to prevent abnormal operation due to human error. The accessible area of it on the pool top region is pre-defined, and the movement of it is tightly restricted by limit switches or sensors. Any simultaneous operation of hosting, traversing, and traveling is prohibited by an inter-locking system for safety. The required function and operability of the operation bridge have been tested according to relevant test procedures.

The operation bridge is classified as Non-nuclear Safety and Seismic Category II. KEPIC MCF [1] (CMAA No. 70, [2]) and KEPIC MCN [3] (ASME NOG-1, [4]) are applied as a guide in the design. It is confirmed through structural analysis and evaluation that the operation bridge maintains structural integrity against all applicable design loads and load combinations.

Figure 2 Operation bridge

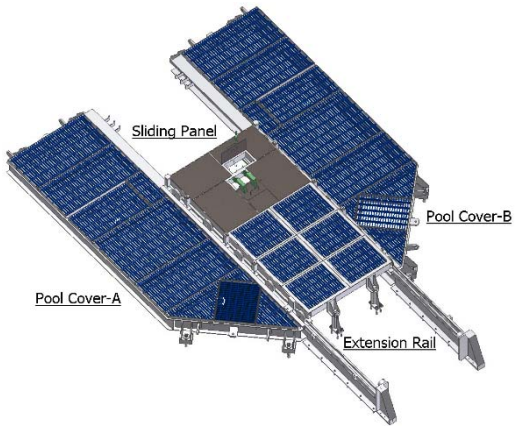

Figure 3 Pool cover

4.2 Pool Cover

The pool cover, as shown in Figure 3, has four components: Pool Cover-A, pool Cover-B, a sliding panel, and extension rails. The pool cover is located at the top of the reactor pool. It is classified as Non-nuclear Safety and Seismic Category II. It is designed to satisfy the following requirements:

(a) The pool cover prevents any foreign objects from falling into the reactor pool.
(b) It supports the on-power loading device for radioisotope (RI) rig.
(c) Neutron transmutation doping (NTD) driving devices are supported on it.

(d) A work space above the reactor pool is provided.
(e) It is designed to withstand its operational deadweight, live load, and seismic load.

Pool Cover-A and Pool Cover-B are fixed by anchor bolts to prevent movement during a seismic event. During the reactor's normal operation, the sliding panel that is traveling on Pool Cover-A and Pool Cover-B is closed and fixed by anchor bolts. When the reactor is shut down for refueling, the sliding panel is open and moves to the extension rail direction, being fixed on the extension rail by fixed bolts considering seismic events. The pool cover is made of stainless steel for resistance against corrosion.

Structural integrity is ensured by the conservative use of appropriate design standards. KEPIC MNF [5] (ASME NF, [6]) is applied for the design. It is confirmed through structural analysis and evaluation that it maintains structural integrity.

4.3 Pool Door

The principal function of the pool door, as shown in Figure 4, is to isolate the reactor pool from the service pool for maintenance. It is installed at the chase of the pool gate by using the overhead crane. For sealing, two inflatable gaskets are attached to the side frame of the pool door, and the gaskets are inflated with compressed air. The reactor pool water is drained separately after installation of the pool door.

The pool gate is opened during normal operation, and the pool door is hung on the storage bracket that is mounted on the base plate on the wall of the lift machine room in the reactor building. The design of the pool door considers deadweight, hydrostatic load, hydrodynamic load, and seismic load. It is made of stainless steel, with protection against corrosion damage effects. The main structure consists of plates and side frames. The steel parts are assembled by welded joints, and lugs are welded at the top of the pool door for clamping it to the pool gate. Non-destructive examinations were carried out at welds.

The pool door is classified as Non-nuclear Safety and Seismic Category II. It withstands all anticipated loads including seismic load induced by safe shutdown earthquake (SSE). KEPIC SND [7] (ANSI/AISC N690, [8]) is used for the design. It is confirmed through structural analysis and evaluation that it maintains structural integrity.

4.4 Pool Platforms

The reactor pool platforms consist of the reactor pool working platform (RPWP), as shown in Figure 5, top platform, middle platform, and bottom platform. The elevation of each platform is decided considering the workability and the shielding depth. The reactor pool platforms are classified as Non-nuclear Safety and Seismic Category II. The RPWP, covering the reactor pool, is designed to support the irradiation guide tubes and the refueling cover, to provide a work area near the reactor, and to suppress the rise of primary coolant flow. The top platform and the middle platform are provided to facilitate the maintenance of the CRDM, and the bottom platform is for the removal of the RPWP.

The service pool platforms consist of the service pool working platform (SPWP), the radioisotope (RI) platform, and the maintenance platform. The SPWP provides space for the RI rig and radioactive object handling, the fuel basket support, and a thermal column extension storage window. The RI platform and the maintenance platform provide RI working space and working space for instrument maintenance above the service pool water, respectively. Objects related to NTD are handled on the SPWP.

Stainless steel is used for its corrosion resistance against underwater conditions. KEPIC SND [7] (AISC N690, [8]) is applied in the design for pool platforms. It is confirmed through structural analysis and evaluation that the pool platforms maintain structural integrity.

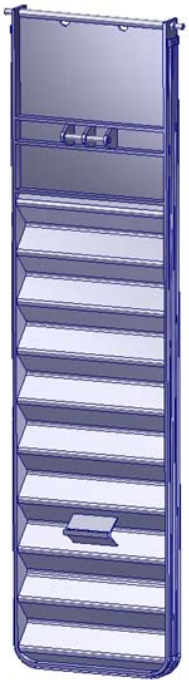

Figure 4 Pool door

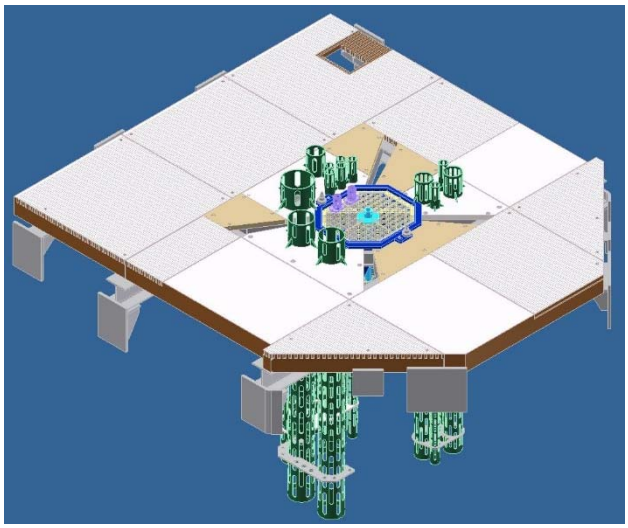

Figure 5 Reactor pool working platform (RPWP)

4.5 Fuel Storage and Handling System

The fuel storage system encompasses fresh fuel storage and spent fuel storage. The fuel handling system and handling procedure were developed for safe refueling within a limited shutdown period in each operation cycle. The operation bridge, fuel basket, fuel racks, the spring balancer, and tools are all necessary for the storage and handling of the fuel assembly in the pools.

The fresh fuel storage rack (FFSR), as shown in Figure 6, is designed to accommodate fresh fuel assemblies for two cores. Fresh fuel assemblies are stored in designated storage cell pipes in the FFSR, which is fixed by anchor bolts. Each storage cell contains one fuel assembly. The storage cell pipes maintain the positions of the fuel assemblies to prevent the fuel assemblies from moving closer to each other under normal and accident conditions. The array of the cells is designed to ensure safety with respect to sub-criticality. The effective neutron multiplication factor (k_{eff}) does not exceed 0.9 under normal and accident conditions [9]. The FFSR is classified as Seismic Category I, and is designed to maintain its function and structural integrity. Thus, the FFSR prevents damage to the fuel assemblies in the event of SSE. The FFSR is made of stainless steel for corrosion resistance, and a locking device is attached to the cover plate of the FFSR to ensure security of the fresh fuel assemblies. The FFSR is designed in accordance with KEPIC MNF [5] (ASME NF, [6]). All anticipated loadings, including dead load and seismic load, are considered in the design stage. The storage rack is designed with consideration of the safety requirements described in IAEA NS-R-4 [10] to prevent inadvertent criticality in the fresh fuel storage, and to provide storage for a sufficient number of fresh fuel assemblies. The FFSR is manufactured, installed, and inspected in accordance with the requirements of Quality Class Q. Structural analysis and evaluation confirm that the FFSR maintains its function and structural integrity.

Spent fuel assemblies are stored in the spent fuel storage rack (SFSR) within the support frame that is placed at the bottom of the service pool, as shown in Figure 7. The capacity is based on the total number of spent fuel assemblies projected to be generated during the 5-MW, 40-year operation of the reactor in addition to temporary storage of fuel assemblies and damaged fuel assemblies. The storage cells are mounted in the storage racks to protect the fuel assemblies and maintain the positions of the fuel assemblies. The support frame supports the SFSRs in the service pool and prevents the racks from being overturned. The support frame is designed to be free standing, and is placed on the floor of the pool liner. The storage racks are designed to prevent the fuel assemblies from moving closer to each other under normal and accident conditions. The effective neutron multiplication factor (k_{eff}) must not exceed 0.9 under normal and accident conditions [9]. The base plate of the rack is pierced to allow natural convection of the pool water through the fuel assemblies. The SFSRs and their support frame are made of stainless steel to prevent corrosion. The storage racks and the support frame are classified as NNS, Seismic Category I, and Quality Class Q. The design, fabrication, installation, and inspection of the storage racks and the support frame are in accordance with KEPIC MNF [5] (ASME NF, [6]) and IAEA NS-R-4 [10]. It is confirmed through a structural analysis and evaluation that the SFSRs and the support frame maintain their function and structural integrity.

The fuel handling system, which is necessary for refueling in the reactor core, is composed of the operation bridge, the fuel basket, the fuel storage racks, the fresh fuel tool, the spring balancer, and the fuel tool. The fuel tool is used for fuel replacement, fuel transport in the pools, and fuel storage. The height of the SFSR was designed and installed to be equal to the height of the fuel assembly in the core, considering the ease of handling spent fuel. The structures related to the system are the reactor pool, the service pool, and the fresh fuel storage room. The fuel handling system is designed to prevent dropping of or damage to fuel assemblies during transportation. The maximum lifting height of the irradiated fuel assembly is limited to maintain a minimum depth of pool water to keep the radiation level at the top of the pool area below the ALARA target dose. The fuel handling system is operated and managed by qualified staff. The operation of the fuel handling system complies with the operational limits and conditions specified in Operational Technical Specifications (OTS).

Fig 6. Fresh fuel storage rack (FFSR)

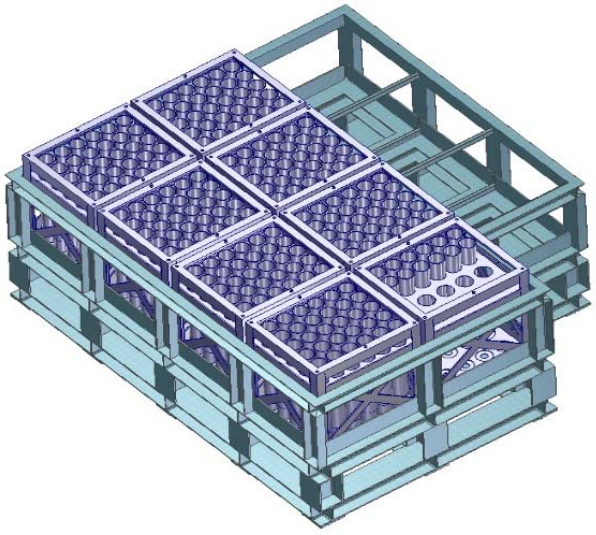

Fig. 7 Spent fuel storage rack (SFSR)

5. Lessons Learned from Design and Construction

The HANARO construction project from 1985 to 1994 included its design, construction, and commissioning. Following the operation of HANARO from 1995, many modifications and improvements were made for the enhancement of safety and operability. Based on the accumulated experience from HANARO over the years, KAERI was able to develop safe designs and technologies for the JRTR.

The design, manufacture, and installation were successfully completed by applying the improved concepts to the JRTR pools and pool operation facilities. They were designed for radioisotope production, neutron activation analysis, neutron beam utilization, and training and education. The length and width of the pools were defined considering the links between the reactor structures, cooling systems, piping, fuel handling and storage, RI production, NAA, beam facilities, and decommissioning contained within the pool. Optimal layout was implemented to avoid installation interference or operational interference.

Pool operation facilities were designed to ensure structural integrity by performing structural analysis according to codes and standards as well as to provide ease of use.

Factory fabrication inspections and tests were carried out in accordance with quality assurance procedures, and the satisfactory results could then be transferred to the JRTR sites. In the factory, problems were identified in preliminary assembly prior to the on-site installation, and this reduced the on-site installation time.

Most of the structural components manufactured in Korea were transported by sea, and after arriving at the site, they were stored at a designated warehouse or at the site. However, due to storage management problems, some of the components were contaminated with sand and dust, which had a considerable impact on the schedule and cost. Air transportation was often used in emergency situations when parts were not found. Therefore, storage management and cleaning management were very important for the construction stage.

The installation of the pool operation facility was very efficient and accurate using the Laser Tracker to manage the three-dimensional dimensions from the center of the reactor within tolerances. In order to overcome construction tolerance dimensions, some parts were re-manufactured due to design changes reflecting as-built dimensions. The accuracy of the construction is the first priority, but the designer should reflect the design tolerance of the construction errors that can occur in the field in advance.

An interlock system and limit switches were provided to prevent operator errors or mistakes resulting in fuel delivery accidents that could cause damage to the fuel assembly.

After installation, the results of commissioning tests (CAT, SPT, IST) were satisfied. They were provided for the preparation of the operating procedures.

6. Conclusion

Based on the experience gained with KAERI's HANARO, the improved design and construction of pools and pool operation facilities for the JRTR was successfully realized. To ensure the continued safe operation of the reactor after handover, lessons learned from the design and construction of the JRTR formed a valuable engineering experience, and became the basis for the preparation of operating procedures. Based on the JRTR experience, KAERI is planning to perform the design optimization and value engineering of a medium research reactor in the future.

The pool operation facilities had also been verified for reliable operability, ease of reactor utilization, and maintainability of the reactor components with remote tools. They had been constructed using the advanced Laser Tracker, and this process minimized the period of the on-site installation.

The Jordan Atomic Energy Commission (JAEC) and KDC have worked together very well by sharing the same goals, and successfully completing the JRTR project with high standards in mind. We will continue to monitor the safe operation and the full utilization of the JRTR. The safe operation of the JRTR by the JAEC personnel provides a model for nuclear research and reactor operation across the Middle East.

7. References

[1] Korea Electric Power Industry Code (KEPIC), MCF, “Fossil Power Plant Cranes,” 2005, Korea Electric Association.

[2] CMAA No. 70, “Specification for Top Running Bridge and Gantry Type Multiple Girder Electric Overhead Traveling Cranes,” 2000, Crane Manufacturers Association of America.

[3] Korea Electric Power Industry Code (KEPIC), MCN, “Nuclear Power Plant Cranes,” 2005, Korea Electric Association.

[4] ASME NOG-1, “Rules for Construction of Overhead and Gantry Cranes (Top Running Bridge, Multiple Girder),” 2002, American Society of Mechanical Engineers.

[5] Korea Electric Power Industry Code (KEPIC), MNF, 2005 Edition with 2006 Addenda, “Supports,” Korea Electric Association.

[6] ASME Boiler and Pressure Vessel Code, Section III, Rules for Construction of Nuclear Facility Components, Subsection NF, “Supports,” 2004 Edition, American Society of Mechanical Engineers.

[7] Korea Electric Power Industry Code (KEPIC), SND, “Safety-Related Steel Structures for Nuclear Facilities,” 2005, Korea Electric Association.

[8] ANSI/AISC N690, “Specification for Safety-Related Steel Structures for Nuclear Facilities,” 2002, American Institute of Steel Construction.

[9] U.S. NRC, NUREG-1537, Part 1, “Reg. Guide Guidelines for Preparing and Reviewing Applications for the Licensing of Non-Power Reactors,” 1996.

[10] IAEA Safety Requirements, No. NS-R-4, “Safety of Research Reactors,” IAEA.

THERMAL HYDRAULIC ANALYSIS OF A LOSS OF FLOW ACCIDENT IN A RESEARCH REACTOR IN RESPECT OF PROBABILISTIC SAFETY ANALYSES

V. KOPPERS, M. UTSCHICK, G. MAYER

Gesellschaft für Anlagen- und Reaktorsicherheit (GRS) gGmbH
Boltzmannstraße 14, 85748 Garching bei München, Germany

ABSTRACT

Probabilistic Safety Analysis (PSA) is an established approach to identify enveloping accident scenarios and to estimate their contribution to the core damage frequency of nuclear facilities. PSA allows to assess the relevance of initiating events with respect to the overall risk that emanates from a nuclear reactor and to identify weak points in design and operation by means of accident sequence analyses modelling the availability of safety systems to mitigate initiating events. To substantiate these accident sequences regarding sequence validation, timing and success criteria, complementary Deterministic Safety Analyses (DSA) are necessary. Therefore, an adequate thermal hydraulic reactor model is required, which represents the plant behaviour and the functionality of operational and safety systems. Currently, GRS is developing a thermal hydraulic model and a probabilistic model for a German research reactor within the frame of two research and development projects funded by the German Federal Ministry for the Environment, Nature Conservation and Nuclear Safety (BMU). This paper describes the ongoing development of the thermal hydraulic model and first application to a loss of flow event analysis. Initial and boundary conditions are defined by requirements of probabilistic analyses. The thermal hydraulic results are presented focusing on parameters regarding reactivity control, core cooling and decay heat removal.

1. Introduction

Like nuclear power plants, research reactors are subject to nuclear safety requirements. To fulfil the fundamental safety objective “to protect people and the environment from harmful effects of ionizing radiation”, the main safety functions “control of reactivity”, “removal of heat from the reactor and from the fuel storage” and “confinement of the radioactive material” have to be achieved [1]. To evaluate the safety level of research reactors, two complementary safety analysis approaches are recommended: deterministic safety analysis (DSA) and probabilistic safety analysis (PSA). DSA simulates the response of the research reactor to be analysed considering specific initial and boundary conditions to accident and transient sequences. PSA allows to assess the relevance of initiating events with respect to the overall risk that emanates from a nuclear reactor and to identify weak points in design and operation by means of accident sequence analyses modelling the availability of safety systems to mitigate initiating events. To substantiate these accident sequences regarding timing and success criteria (how many redundancies are necessary for a successful system function), additional deterministic safety analyses are necessary.

Within the PSA and DSA projects regarding research reactors at GRS, the FRM-II was chosen as a reference system for probabilistic and deterministic safety analyses studies. The concept of the FRM-II reactor is based on the use of a compact core consisting of one fuel element with a high enrichment level (93% U-235), allowing a high neutron flux at a thermal power of 20 MW [2]. It is a pool-type reactor, light-water cooled, and heavy water moderated.

Within this paper, an analysis of a loss of flow event in the reference research reactor is presented. The group of “loss of flow events” includes accidents resulting in reduction of coolant flow due to bypassing the reactor core. A failure of the piping system of the primary cooling inside the reactor pool is assumed, leading to a guillotine (2F-) break of the piping

upstream of the core position. First, a description of the selection of initiating events to be considered within PSA is introduced, followed by a presentation of the thermal hydraulic model of the reference reactor and its nodalisation with ATHLET. In section 4, the results of the thermal hydraulic analysis for the guillotine break are presented and discussed. This paper ends with a short summary and conclusion.

2. Selection of initiating event by PSA approach

Initiating events (IEs) in a PSA are those events that require either automatic or operational measures to ensure compliance with the safety objectives reactivity control, fuel element cooling, and fuel confinement. Those IEs which are relevant for a specific reactor need to be selected by a screening process. For the PSA performed for a German reference reactor in the frame of a research project, IEs were identified and grouped in accordance to the IAEA safety report No. 55 [3].

The initiating events relevant for the FRM-II can be assigned to the IE groups disturbance of reactivity control, transients, loss of coolant accidents, mechanical damages (e. g., by a heavy load drop or handling errors) or internal and external hazards. The operational states “power operation” (5770 h/a), “emergency cooling operation” (12 h/a) and “shutdown” (2978 h/a) were considered for the PSA. The IE to be investigated by means of event sequence analyses are control rod withdrawal with maximum speed, loss of offsite power (internal, external), failure of secondary or tertiary cooling systems, failure of cooling of the converter plates, primary coolant loss outside the pool, leak at the pool lining, flood and aircraft crash.

Another IE which may be postulated can be a loss of flow event due to leakage or break in the primary loop piping inside the pool. Since the leak is inside the pool no coolant is lost.

For the primary coolant piping in the primary cell and in the pool before and after the moderator tank “break preclusion” has been demonstrated during the licensing process according to a German guideline for pressurized water reactors [4]. It was stated that for the event analyses in case of a leak in the primary system a maximum leak size < 25 cm^2 is to be assumed. This leak size does not endanger the cooling by the primary and emergency cooling systems. Within the moderator tank, the central channel is made of $AlMg_3$ (due to neutron-physical considerations). This material is not included in the specifications given in [4]. However, leaks within the moderator tank are limited to a leak size of 25 cm^2 due to the double-wall design of the central channel in this area. The frequency of occurrence of this postulated IE is thus negligibly small (< 1 E-07/a). Nevertheless, the frequency of fuel damage after a postulated leak > 25 cm^2 as well as the minimum requirements for the safety systems and thus their unavailability is unknown. According to German PSA guidelines [5] IEs and respective event sequences need to be further analysed within PSA, if they contribute in sum more than about 20 % to the overall damage frequency or if one individual IE contributes more than 10 %. In other words, if an overall fuel element damage frequency of approximately 1 E-06/a is assumed, the damage frequency related to a leak in the central channel should not exceed 1 E-07/a. Since the success criteria for safety systems relevant to ensure the safety objectives in this case are not known, the IE occurrence frequency can be used as a first guess for the damage frequency.

To determine the success criteria of the safety functions required to ensure core cooling, thermal hydraulic analyses were performed for the initiating event "2F-break of the piping upstream of the core position". This event is to be considered as an enveloping case for all leaks and breaks in the primary piping inside the pool with respect to the requirements for the core cooling systems. The occurrence frequency of this IE is not known from the operational experience, thus the postulate for “break preclusion” is used (f = 1 E-07/a).

The thermal hydraulic analyses should reveal, whether the safety objectives reactivity control, core cooling and decay heat removal can be ensured. Reactivity control (reactor shutdown) can be achieved either by reactor shutdown by control rod insertion or by insertion of 4 out of 5 shutdown rods. Under certain circumstances, a 2F-break may cause the control rod to fail after scram. In a conservative approach, the shutdown function of the control rod is assumed to be unavailable. The function of the shutdown rods, however, is not affected. Core cooling can be ensured either by the primary cooling system, the emergency cooling

system or natural circulation cooling using the natural circulation flaps. The thermal hydraulic analysis should prove that the core can be cooled by the primary pumps or by natural circulation of pool water through the core. A special point of interest is the behaviour of the primary pumps and their effect on the core cooling. The pumps are expected to run into cavitation, when the suction pressure falls to a certain point. Therefore, it is assumed that they are switched off by their component protection. However, before they are switched off, it is not clear whether the running primary pumps are beneficial for core cooling or if they might hinder natural circulation of pool water through the core. The end state “fuel damage” is reached, when the maximum cladding temperature exceeds 660 °C [6]. This is analysed in the thermal hydraulic analysis presented below.
Decay heat removal function is fulfilled by the pool water, which circulates through the sieve in the piping, the fuel element and the leakage. The pool itself can be cooled by the atmosphere in the reactor hall or the pool cooling system, which transfers the decay heat to the secondary and tertiary cooling systems. Thus, decay heat removal should not be affected by the 2F break.

3. Research reactor model in ATHLET

The nodalisation for simulating the reference research reactor based on FRM-II design with ATHLET is shown in Figure 3-1. The thermal hydraulic code ATHLET uses the finite volume method and solves the ordinary differential equations matrix at discrete meshed control volumes. The control volumes are connected by junctions, which only consider momentum- and convection-related quantities.
The model of the research reactor covers a wide range of applications for analysing different initiating events within the reactor core and the primary cooling system. To achieve this, the reactor core, the primary circuit, the reactor pool, active and passive emergency systems as well as heat exchangers were modelled in detail. The secondary cooling circuit is represented by a simpler modelling approach. The moderator tank enclosing the central channel in the vicinity of the fuel element, and experimental devices are not modelled. Considering the limited technical documentation available, the reactor model is based on several assumptions.

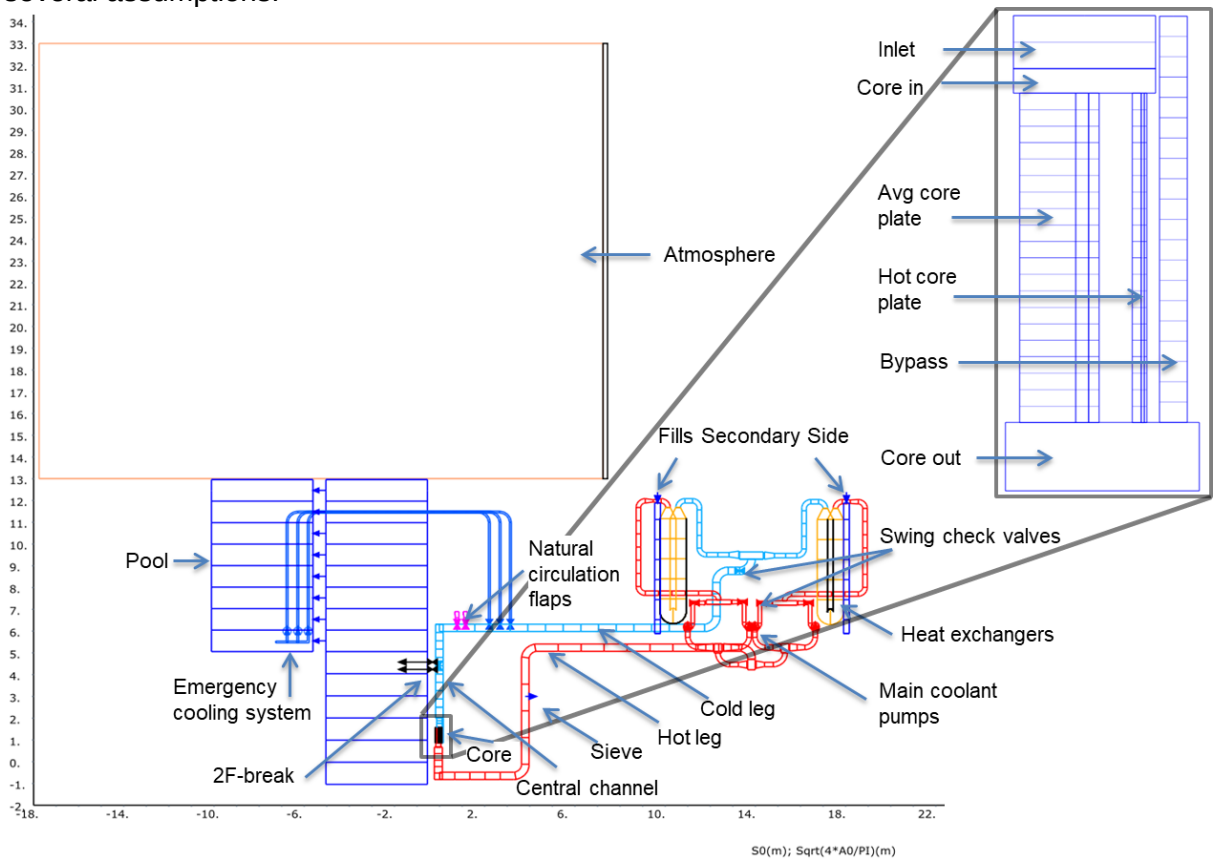

Figure 3-1: FRM-II nodalisation for ATHLET

The FRM-II compact core is in the lower part of the reactor pool in a central position within a closed primary cooling loop [2]. It consists of 113 involute curved fuel plates [2]. Each fuel plate consists of two radial zones with different uranium densities (inner zone 3.0 g/cm², outer zone 1.5 g/cm²) [2]. To consider the resulting radial power profile in the model of the reactor core, three thermo-fluid objects connected by cross connections (a series of junctions to connect two parallel pipes) are used representing one core cooling channel. This approach is used for the average core cooling channel representing 112 cooling channels using a multiplication factor as well as for one hot channel. Assuming a deviation in the manufacturing process of fuel plates, the hot cooling channel has also a reduced gap size. The point neutron kinetics model of ATHLET is used to simulate the fission process and reactivity feedbacks. The reactivity contribution of the fuel temperature, the coolant density and the coolant temperature are considered. The impact of the moderator tank on the reactor's dynamic behaviour is described to be low in [7] and therefore neglected.
For maintaining core cooling after scram, three alternative cooling systems exist: the primary cooling system, the emergency cooling system and cooling via natural circulation through the sieve and the natural circulation flaps [2]. The primary cooling system is modelled using several thermo-fluid objects, four pump components (junction related model to simulate the pump feed pressure) and two heat exchanger components. The secondary cooling system is simplified modelled, using only three thermo-fluid objects: a fill component (junction model to simulate a mass and related energy source), a pipe component (one-dimensional component for the simulation of fluid flow) as well as a time dependent volume (component to simulate a pressure-enthalpy boundary at the edge of the system). To simulate the heat transfer between the primary and secondary cooling system, the pipe components at the heat exchanger positions on the primary and secondary sides are coupled each to a common heat conduction object being assigned to the ATHLET heat exchanger model. After passing the heat exchangers, the primary coolant flows to the core via one pipe. In the cold leg and after each primary pump, a swing check valve is installed to prevent reversed mass flows in case of pump failures. Furthermore, three check valves are installed within the cold leg connecting the emergency cooling system to the primary cooling system. The emergency cooling system is modelled using a pipe and a pump component for each train. The suction points of the emergency cooling pumps are within the pool. The emergency cooling system should ensure core cooling after shutdown for at least three hours [7]. If all primary pumps and emergency pumps are shut down, the heat of the reactor core is transferred to the reactor pool by natural circulation. Therefore, the primary cooling system is equipped with two natural circulation flaps. During operation, these flaps are closed due to the pressure applied by primary or emergency cooling pumps. In case of reactor shutdown or failure of primary or emergency cooling pumps, the pressure in the cold leg drops resulting in the opening of the flaps due to gravity. This establishes a flow path of pool water from the sieve through the core to the flaps back to the reactor pool providing the coolant for core cooling. The reactor pool is modelled using two pipe components connected by cross connections. The FRM-II is an open pool reactor; therefore, an atmosphere zone above the pool components is modelled. In the hot leg, a sieve is installed allowing pressure balance between the primary cooling system and the reactor pool at this point. The connection from the primary loop to the reactor pool is modelled via a junction. To simulate the initiating event "2F-break of the piping upstream of the core position", two junctions containing valve components (junction related model to control junction mass flow) are used. Furthermore, a valve component inside the primary piping is modelled at the location of the break. This valve closes after break initiation to simulate the disconnection of the pipe.

4. Results and discussion of the thermal hydraulic analysis

In the following, the 2F-break in the primary cooling system piping upstream of the reactor core inlet is simulated using the safety analysis code ATHLET. The coolant pipe has a cross sectional area of 0.08846 m². All systems modelled are assumed to be available, except of shutdown function of the control rod. The aim of the analysis is to show, if this IE results in a fuel damage state (maximum cladding temperature > 660 °C, cf. [6]). Before the fuel damage state is reached, first fission product release can be produced by the phenomenon of blister

formation in the cladding. The blistering of cladding starts at fuel temperatures in the range from 515°C to 575°C [8]. The main thermal hydraulic results are presented focusing on parameters regarding reactivity control, core cooling and decay heat removal.

4.1 Initial plant condition

The total simulation time was 1000 s. Before initiating the loss of flow accident at 600 s, the research reactor is in power operation. The coolant flow path at 590 s is shown in Figure 4-1 and the nominal thermal hydraulic parameters during power operation are shown in Table 4-1. The model matches the nominal reference values taken from the safety report [7] as well as further publicly available data, e.g. in [9], [10], with good accuracy.

Table 4-1: Nominal thermal hydraulic research reactor parameters

Thermal hydraulic parameter	Calc. Value	FRM-II ref. Value [9], [10]	Unit
Primary Side			
Thermal power	18.20	18.18	MW
Mass flow primary circuit	300.6	300	kg/s
Mass flow core	279.7	275	kg/s
Mass flow bypass	20.9	20	kg/s
Coolant pumps Δp	10.9	-	bar
Pressure fuel plate top edge	7.1	6.1	bar
Pressure core outlet	2.16	2.3	bar
Coolant temperature core inlet	37.5	37	°C
Coolant temperature core outlet	52.09	52.5	°C
Core temperature rise	14.6	15.5	°C
Pool Temperature	29	-	°C
Average core coolant velocity	16.7	16-17	m/s
Hot core channel coolant velocity	18.8	-	m/s
Secondary Side			
Heat exchanger power	9.27	-	MW
Secondary mass flow	275	-	kg/s
Heat exchanger inlet temperature	29.5	-	°C
Heat exchanger outlet temperature	40	-	°C

4.2 Accident sequence analysis and discussion of the results

After initiating the loss of flow accident (2F-break of the piping above the reactor core) at 600 s, the pressure difference between the cold leg (position after natural circulation flap) and pool decreases below Δp_{min} = 4.6 bar at 600.37 s (see Figure 4-2, right side). The corresponding signal triggers a reactor scram with a delay of 0.2 s. The time in which the control rod drive mechanism releases the control rod (not available in this case) and shut-down rods is assumed to be 0.2 s. Reactor power decreases firstly because of negative density reactivity feedback, before the nuclear reaction is interruped by the insertion of shutdown rods (see Figure 4-3). Due to break opening, the pressure in the whole primary system decreases until the pressure of the reactor pool is reached within the central channel at the lower break opening (from core to break). The pressure at the pump suction side falls below the saturation vapor pressure. It is assumed that cavitation occurs leading to oscillations which trigger the component protection of the primary pumps at 600.56 s. This shuts down the pumps; they coast down within 100 s driven by the attached fly wheels.

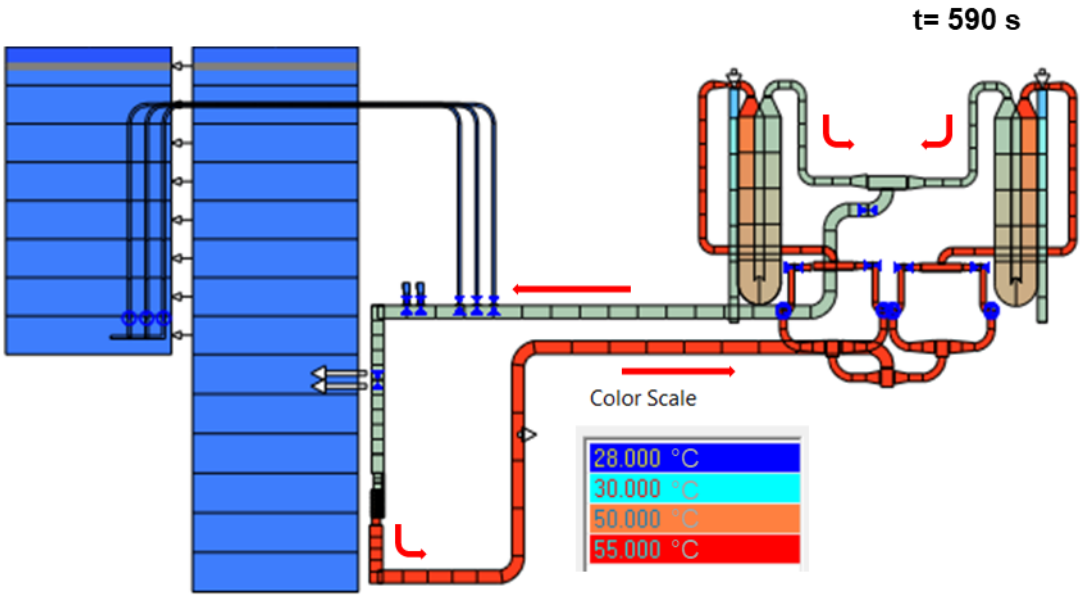

Figure 4-1: Coolant flow path during normal operation at 590 s

A given mass flow of primary pumps coast down was used as input data to the ATHLET simulation (see reference [7]) with respect to limited available pump data. In Figure 4-5 on the left side, the mass flow over primary pumps during coast down is shown. Simultaneously with the trigger for reactor scram at t = 600.57 s, the pumps of the emergency core cooling system are started. As soon as the counter-pressure from the primary pumps is low enough, pool water is pumped into the primary loop by the emergency core cooling system (see Figure 4-5 right side). In this specific accident sequence, the coolant does not reach the reactor core but flows back into the reactor pool over the break located at the piping above the core. The emergency cooling system is not effective.

Focusing on the core, the mass flow decreases suddenly with break initiation (see Figure 4-6 left side). The generated heat from the reactor core is not removed efficiently and evaporation process starts at 600.25 s (see Figure 4-10) resulting in a fuel temperature of about 160 °C and a cladding temperature of about 154 °C (see Figure 4-7 right side). Nevertheless, the coast down of the primary pumps is able to maintain the core cooling after break initiation. A coolant flow from the pool is established through the break into the core following the primary pump characteristic (see Figure 4-6). After the stop of the primary pumps, natural circulation through the core is established (see Figure 4-6). The heated coolant re-enters the pool not via natural circulation flaps, but via the break in the piping above the moderator tank position. While the core flow reverses from downward to upward direction, a second peak in the cladding and fuel temperature occurs at 720 s (see Figure 4-7 right side). Figure 4-8 shows the safety against onset of flow instabilities based on the bubble detachment parameter. Shortly after break initiation as well as before core flow reversal the safety margin is below the given minimum in [7]. The safety margin is defined as the ratio of the actual bubble detachment parameter and a statistically determined limit (only valid before core flow reversal). If the bubble detachment parameter decreases below this certain value, steam bubbles detaches from the fuel cladding. This could cause flow oscillations resulting in local burn out. Shortly after break initiation, flow instabilities are calculated for a time period of about 0.4 s. At this point of time, a departure from nucleate boiling is near the defined safety limit of 1.3, but not reached (see Figure 4-9). Void is slightly produced in the hot as well as average core channel (see Figure 4-10) at this time period.

To the end of the simulation, the research reactor reaches stable thermal hydraulic conditions having two coolant flow paths (see Figure 4-11). One is flowing through the reactor core to the reactor pool via the break and back to the reactor core via the sieve due to natural circulation. This flow path maintains the core cooling resulting in decreasing fuel temperatures. The second flow path is driven by the emergency cooling pumps. Coolant from

the reactor pool is pumped into the primary system and flows back to the reactor pool via the break.

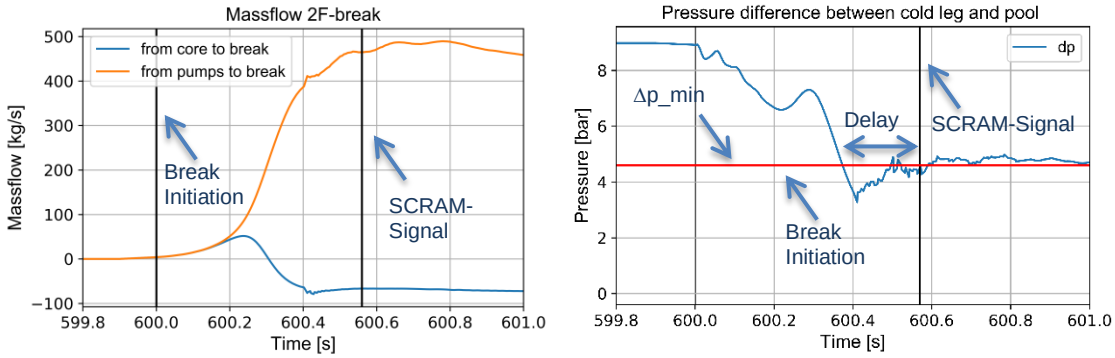

Figure 4-2: Massflow 2F-break (left side) and Pressure difference between cold leg and pool (right side)

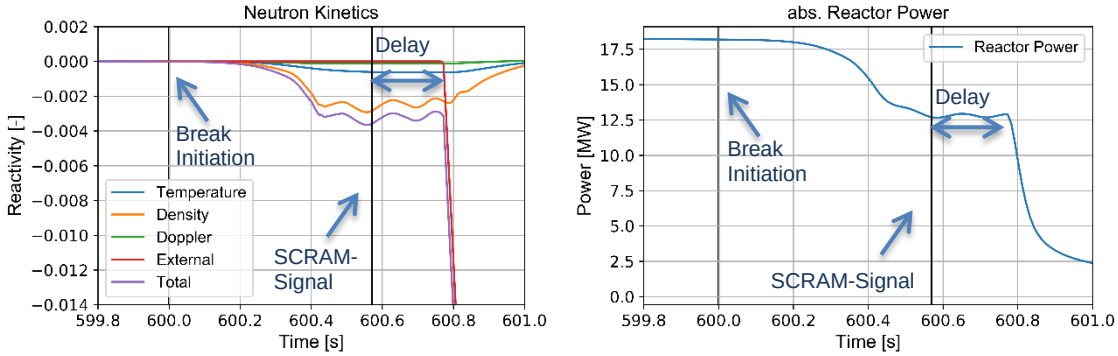

Figure 4-3: Neutron kinetics (left side) and absolute reactor power (right side)

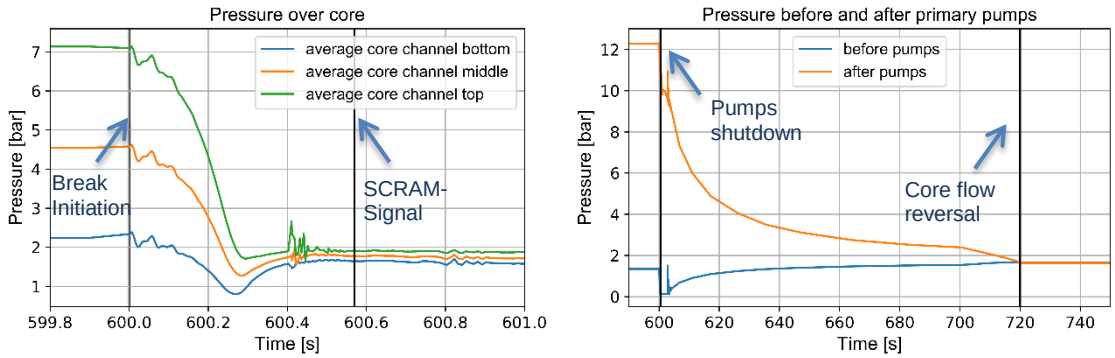

Figure 4-4: Pressure over core (left) and pumps (right)

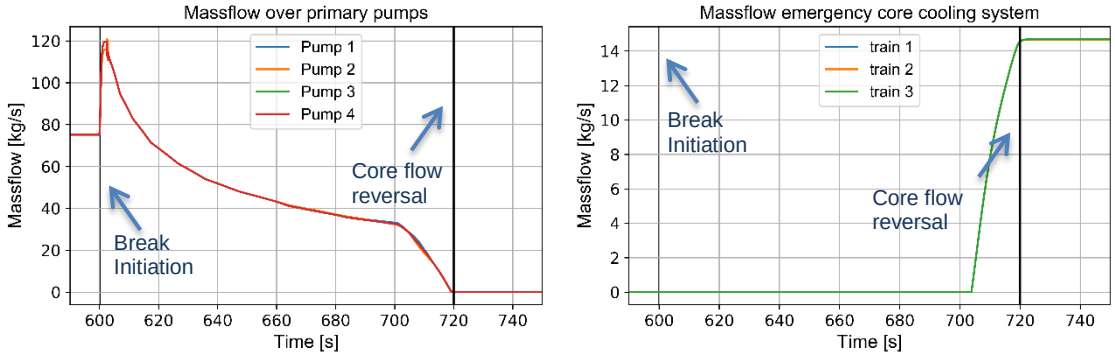

Figure 4-5: Massflows over primary pumps (left) and emergency core cooling system (right)

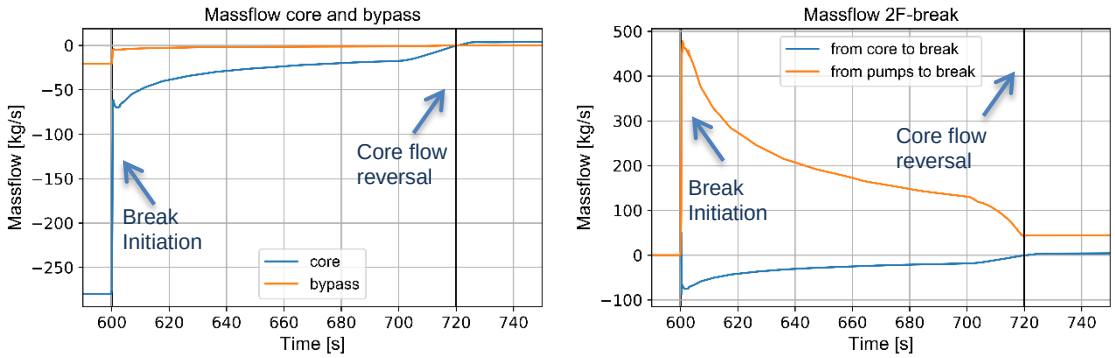

Figure 4-6: Massflow through core and bypass (left) and massflow 2F-break (right)

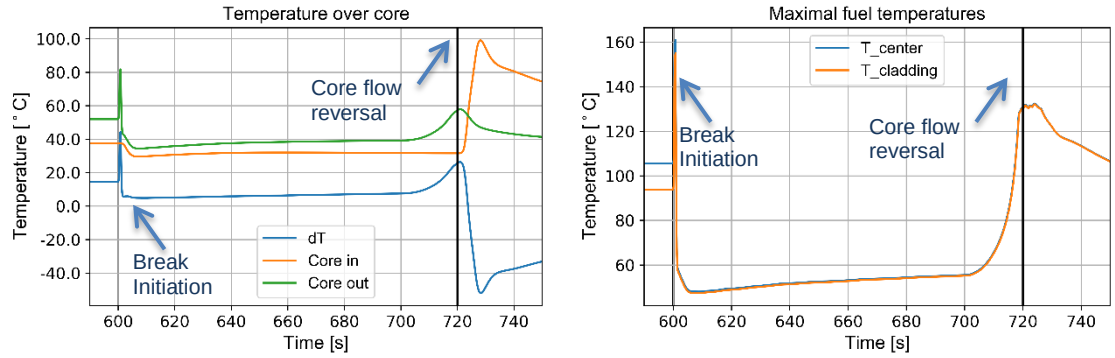

Figure 4-7: Coolant temperature over core (left) and maximal fuel and cladding temperatures (right)

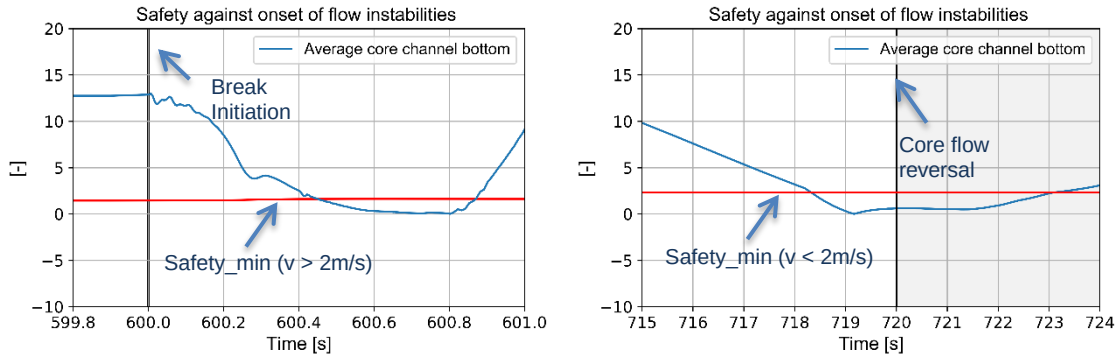

Figure 4-8: Safety against onset of nucleate boiling after break initiation (left) and before core flow reversal (right)

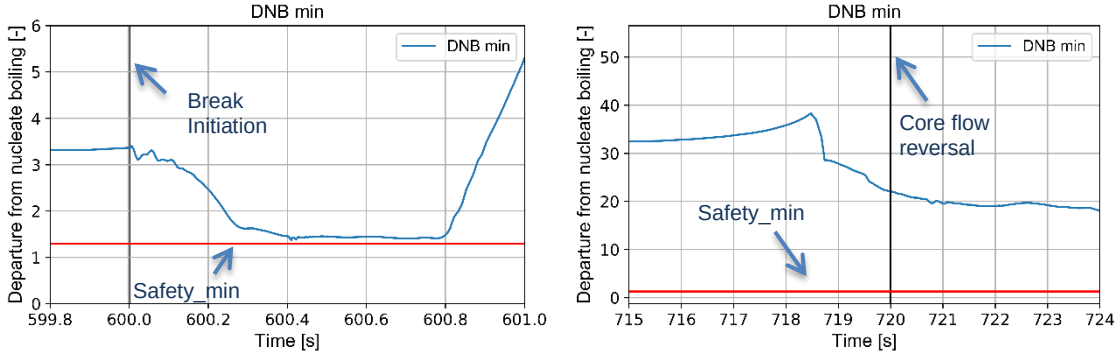

Figure 4-9: Departure from nucleate boiling after break opening (left) and before core flow reversal (right)

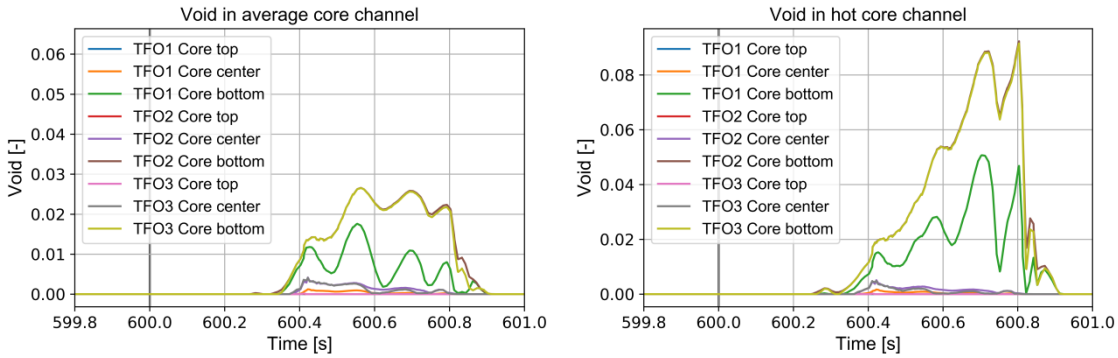

Figure 4-10: Void in the average (left) and hot (right) core channel

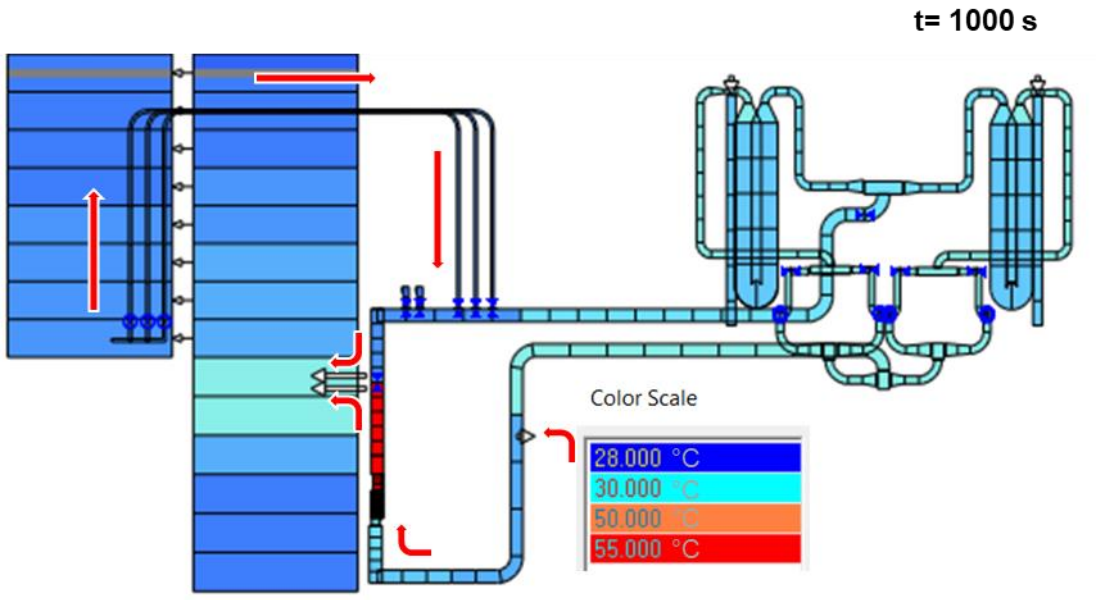

Figure 4-11: Coolant flow paths after stable condition reached during the accident phase

Focusing on the impact of the accident sequence on the safety parameters regarding reactivity control, core cooling and decay heat removal, the ATHLET simulation showed (using the mentioned assumptions), that:

- after reactor scram, the core remains subcritical;
- core cooling is maintained by pump coast down and natural circulation; the maximum fuel temperature is about 160 °C and the cladding temperature is about 154 °C << 515°C < 660°C
- decay heat removal is effective using the reactor pool and the atmosphere as ultimate heat sink.

Nevertheless, the ATHLET simulation also showed that flow instabilities shortly after break initiation occur for a short time period of about 0.4 s.

As mentioned above, a given mass flow of primary pumps coast down was used as input data to simulate the primary pumps characteristics (see reference [7]). The pump coast down influences mainly the accident sequence. Therefore, further improvements of the current pump model are planned using a dynamic pump model based on generic characteristic curves.

5 Summary and conclusions

Within this paper, the thermal hydraulic behaviour of a reference research reactor based on the FRM-II design assuming a double guillotine break in the piping upstream of the reactor core is presented. The boundary conditions are defined by PSA requirements. The

importance of this accident scenario to PSA studies is illustrated. The aim of the thermal hydraulic analysis was to check whether or with which frequency this IE results in a fuel damage state. After explaining the thermal hydraulic model, the results of the safety analysis are presented. The main safety parameter regarding reactivity control, core cooling and decay heat removal are met. Nevertheless, flow instabilities shortly after break initiation are observed for a short time period of about 0.4 s. But, fuel and cladding temperatures (fuel temperature is about 160 °C and the cladding temperature is about 154 °C) are well below the temperature of fuel damage state (maximum cladding temperature > 660 °C, cf. [6]) as well as below the starting point of cladding blistering (from 515°C to 575°C [8]).
The result of the thermal hydraulic analysis means for the event sequence analysed in the PSA that, except for the reactor scram function, no further safety functions are required to mitigate the IE. Core cooling is ensured by passive means (coast down of primary pumps, natural circulation without the need for natural circulation flap opening). The very conservative unavailability of reactor scram function by insertion of 4 out of 5 shutdown rods is 9.6 E-03/demand. Multiplied by the IE frequency (1 E-07/a), this gives a fuel damage frequency of 9.6 E-10/a << 1 E-07/a. Thus, the IE “2F-break of the piping upstream of the core position” does not contribute significantly to the overall fuel damage frequency (<< 10 % of the overall damage frequency).
The accident analysis showed that the pump coast down is important for ensuring core cooling in this accident sequence. Therefore, further improvements of the current primary pump model are planned using a more detailed pump model approach.

6 Acknowledgements

The authors want to acknowledge the support provided by the German Federal Ministry for the Environment, Nature Conservation and Nuclear Safety (“Bundesministerium für Umweltschutz und Reaktorsicherheit”, BMU) for funding of the R&D projects 4716R01325 and 4717R01368.

7 References

[1] IAEA: Safety of Research Reactors; IAEA Safety Standards No. SSR-3, 2016.

[2] Technische Universität München: (State of December 2018), https://www.frm2.tum.de/en/the-neutron-source/reactor/.

[3] IAEA: Safety Analysis for Research Reactors, IAEA Safety Reports Series No. 55, 2008.

[4] Reaktor-Sicherheitskommission, Rahmenspezifikation Basissicherheit, Stand 25. April 1979, 2. Anhang zu den RSK-Leitlinien für Druckwasserreaktoren, 1979.

[5] Facharbeitskreis (FAK) Probabilistische Sicherheitsanalyse für Kernkraftwerke, Daten zur Quantifizierung von Ereignisablaufdiagrammen und Fehlerbäumen, Stand: August 2005, BfS-SCHR-38/05, Bundesamt für Strahlenschutz (BfS), Salzgitter, Germany, 2005, https://doris.bfs.de/jspui/handle/urn:nbn:de:0221-201011243838.

[6] TÜV Süddeutschland: Gutachten über die Sicherheit des Forschungsreaktors München II (FRM-II), Standort Garching für das atomrechtliche Genehmigungsverfahren, Gutachten zur Konzeption der Anlage (Konzeptgutachten), März 1996.

[7] Neutronenquelle München FRM-II, Sicherheitsbericht Band 1, Oktober 1993.

[8] NUREG-1313: Safety Evaluation Report related to the Evaluation of Low-Enriched Uranium Silicide-Aluminium Dispersion Fuel for Use in Non-Power Reactors, U.S. Nuclear Regulatory Commission, Office of Nuclear Reactor Regulation, July 1988

[9] A. Pautz: Rechenmodellentwicklung für die Analyse von Reaktivitätstransienten mit Neutronentransporttheorie und gekoppelter Thermofluiddynamik für Hochfluss-Forschungsreaktoren, Dissertation TUM, 2001

[10] H. Breitkreutz: Coupled Neutronics and Thermal Hydraulics of High Density Cores for FRM II, Dissertation TUM, 2011

THE PERIODIC SAFETY REVIEW OF HANARO REACTOR

JIN-WON SHIN, SEUNG-GYU DOO, JAE-SAM HAN, YOUNG-SAN CHOI AND SANG-JOON PARK
HANARO Management Division
Korea Atomic Energy Research Institute
989-111 Daedeok-daero, Yuseong-gu, Daejeon, Korea

ABSTRACT

The first Periodic Safety Review (PSR) project for HANARO commenced in 2015 after operating for 20 years. According to the amendment to the National Nuclear Safety Act in 2014, research and training reactors in Korea mandatorily perform a PSR for 14 safety factors every 10 years. As the operating organization of HANARO, KAERI started the project by organizing a project management team and establishing a budget to conduct the PSR. The time schedule was set up to complete the PSR by the due date. A PSR basis document was developed, which includes the scope, major milestones, codes and standards, safety factors, a list of SSCs, and the methodology. A review of safety factors was performed by two domestic engineering companies and an internal division of KAERI. A global assessment was carried out considering all the findings derived from each safety factor review. Finally, the final PSR report was submitted to the Korean nuclear regulator by the due date. In this paper, the results of the periodic safety review of HANARO will be presented.

1. Introduction

HANARO (Hi-flux Advanced Neutron Application ReactOr) has been operating since 1995 for multiple purposes including radioisotope production, material irradiation, neutron transmutation doping, neutron activation analysis, and neutron beam utilization. Periodic inspections and in-service inspections have been regularly performed to ensure the safe operation of the facility. A special safety review after the Fukushima Daiichi Accident was also conducted to check whether the facility will remain in a safe state during and following natural or other external events such as an earthquake, flooding, loss of offsite electric power, or station blackout. As a result of the review, several recommendations were given to HANARO and their implementation for safety improvement was performed. However, a complete comprehensive safety review for the reactor facility had not been conducted before. In 2014, the National Nuclear Safety Act was amended to demand research and training reactors in Korea mandatorily perform a PSR for 14 safety factors every 10 years. As the operating organization of HANARO, KAERI composed a project management team (Task Force Team) and established a budget to conduct a PSR project. The team set up a time schedule in order to complete the PSR, which satisfies all of the requirements by the due date, and developed a PSR basis document for conducting the PSR, which includes the scope, major milestones, codes and standards, safety factors, a list of SSCs, and the methodology. A review of 12 safety factors was performed by two domestic engineering companies according to the contracts, while two safety factors, the emergency planning and the radiological impact on the environment, were reviewed by an internal division of KAERI. Considering all the positive and negative findings derived from each safety factor review, a global assessment was performed to identify the overall level of safety. The final PSR report of HANARO was submitted to the Nuclear Safety and Security Commission (NSSC) of the Korean government by the end of 2018. This paper describes the process by which the PSR of HANARO was performed and the results, which include the recommendations for safety improvement.

2. PSR Implementation

2.1 Project management team and tasks

A Task Force Team, whose members mainly consisted of staff of the HANARO Management Division, was established to perform the first PSR project of HANARO considering the available human resources in KAERI. External engineering companies and an internal division in KAERI conducted the review of the safety factors and the global assessment, whereas TFT members offered input documents, reviewed the safety review and global assessment report, and prepared the final report of PSR. The primary tasks of the project management team are summarized as follows:

- Project planning
- Budget planning
- Time scheduling
- Preparation of the basis document for PSR
- Preparation of specifications for making contracts with engineering companies for a review of safety factors and a global assessment
- Gathering input documents for the review of safety factors and offering them to engineering companies and internal experts
- Review of the safety factor review report made by engineering companies and internal experts
- Review of the global assessment report
- Preparation and submission of the final PSR documentation to the regulatory body

The quality assurance team in KAERI also participated in the project to prepare a quality assurance plan that defines the requirements for the preparation and verification of the PSR documentation. The quality assurance plan ensured the PSR documents have appropriate quality and format.

2.2 Preparation of the PSR

The project management team estimated the overall budget for the PSR project in consideration of the scope and depth of the review, the human resources available in the organization, the contracts with external companies, and the schedule. The process of estimating the project budget was supported by external consultants, who have experience in PSR for nuclear power plants. Different characteristics such as operating objectives, organizations, SSCs, safety classifications, documentation, activities, and procedures between research reactors and nuclear power reactors were taken into account while planning the budget. The project manager submitted a final proposal to the senior and executive management for the required budget and obtained approval from the government in 2015.

A time schedule including the major milestones and cut-off dates was set up to implement the project by the due date. The review of safety factors is considered to be an iterative process and time should be allowed for reviewing interfaces between the various safety factors. Thus, the project management team allocated sufficient time for the review of the safety factors and the global assessment report.

The project management team developed the PSR basis document in collaboration with an engineering company for the PSR project. The basis document identifies the scope and objectives, national regulations, codes and standards, safety factors to be reviewed, a list of SSCs, the methodology of the PSR, and the major milestones.

2.3 Review of the safety factors and global assessment

The amendment of the National Nuclear Safety Act in 2014 calls for the review of fourteen safety factors for the PSR consistent with those listed in IAEA Specific Safety Guide No. SSG-25[1] as follows:

i. Safety factors relating to the plant
   (1) Plant design;
   (2) Actual condition of the structures, systems and components (SSCs) important to safety;
   (3) Equipment qualification;
   (4) Ageing.
ii. Safety factors relating to safety analysis
   (5) Deterministic safety analysis;
   (6) Probabilistic safety assessment;
   (7) Hazard analysis.
iii. Safety factors relating to performance and feedback of experience
   (8) Safety performance
   (9) Use of experience from other plants and research findings.
iv. Safety factors relating to management
   (10) Organization, the management system and safety culture;
   (11) Procedures;
   (12) Human factors;
   (13) Emergency planning.
v. Safety factors relating to the environment
   (14) Radiological impact on the environment.

KAERI made contracts with two domestic engineering companies, KEPCO E&C and FNC Technology, to perform a review of the safety factors. They reviewed 12 out of 14 safety factors (emergency planning and radiological impact on the environment, were reviewed internally by the Nuclear Emergency and Environmental Protection Division in KAERI). Although the companies had abundant experience in conducting PSR for nuclear power plants, they needed to understand the different characteristics of structures, systems, and components of research reactors as compared to NPPs. They also considered that HANARO is an open pool-type 30MW research reactor for neutron applications and has only safety class III SSCs, for the graded approach. An objective for the review, a scope and tasks, and methodology recommended in SSG-25 were referred to in performing the review of each safety factor. An analysis of the interfaces between the various safety factors was carried out after finishing the review of separate safety factors. The global assessment was performed taking into account all the positive and negative findings from each safety factor review and what safety improvements are reasonable and practicable.

The project management team reviewed the safety factor review and global assessment report, delivered the review results back to the companies and the internal experts, and verified that feedback had been correctly reflected in the report in an iterative manner. The PSR report was also subject to an independent internal peer review through the Research Reactor Development Division in KAERI, which is in charge of developing and constructing a new research reactor in Korea. This review was incorporated into the final PSR report.

3. Results of PSR

The PSR of HANARO determined that the facility is as safe as originally intended and conforms to current national and international safety standards and practices. The review found no safety issues that can pose an immediate and significant risk to the health and safety of workers or the public or to the environment. But it identified a number of areas where improvements are necessary for achieving further safety of HANARO to ensure continued safe operation for at least the period until the next PSR. The recommendations for safety improvement listed in the final PSR report are as follows:

- Actual condition of the SSCs important to safety
  - Establishment of a maintenance management procedure for electric cables and connections, cable trays, and conduit tubes.
- Equipment qualification
  - Update of Environmental Qualification Master List (EQML).
  - Establishment of the managing procedure for Environmental Qualification.
  - Preparation of Environmental Qualification Evaluation Report (EQER).
  - Assessment of temperature and radiation conditions of the equipment rooms in the reactor hall for Environmental Qualification.
  - Corrective actions for incomplete anchoring parts of equipment for Seismic Qualification.
- Probabilistic safety assessment
  - Implementation of Probabilistic Safety Assessment (PSA).
- Hazard analysis
  - Implementation of Probabilistic Seismic Hazard Analysis (PSHA) for the area where HANARO is located.
- Safety performance
  - Improvement of the gaseous effluent sampling and monitoring system of the reactor building stack in accordance with ANSI N13.1-1999.
- Human factors
  - Improvement of the control panel interfaces of the main control room applying the principles of Human-Machine Interface.
  - Establishment of the design principles and guidelines of Human Factor Engineering (HFE) for human factor management.
- Emergency planning
  - Establishment of a managing procedure for the emergency plan distribution to the off-site organizations.

The final PSR report of HANARO was submitted to the Nuclear Safety and Security Commission (NSSC) of the Korean government by the end of 2018. Korea Institute of Nuclear Safety (KINS), as a technical support organization of NSSC, is now performing a preliminary review of the report and preparing questions and comments for requesting a supplement to the PSR report. There will be many issues to be discussed between KAERI and KINS during the review and approval process of the submitted PSR report. KAERI is planning to prepare a PSR supplement to address such issues and an integrated implementation plan for the recommendations.

4. Conclusions

The periodic safety review of HANARO has been performed consistent with Korean regulatory requirements and IAEA Specific Safety Guide No. SSG-25. It showed that the current facility design, actual conditions, operation, processes, and management system ensure the overall safety of HANARO conforming to national and international standards and good practices. The review found no safety issues that can pose an immediate and significant risk to the health and safety of workers or the public or to the environment. But it identified a number of areas where improvements are needed for achieving further safety of HANARO to ensure safe operation for the period until the next PSR. KAERI submitted the final PSR report to the regulatory body by the end of 2018 and KINS is now performing a preliminary review and preparing questions and comments. A PSR supplement and an integrated implementation plan will be prepared by KAERI.

5. References

[1] INTERNATIONAL ATOMIC ENERGY AGENCY, Periodic Safety Review for Nuclear Power Plants, Specific Safety Guide No. SSG-25

MC TYPE LEU FUEL SIPPING TEST CAMPAIGN IN MARIA RESEARCH REACTOR

M. MIGDAL

Nuclear Facilities Operations Department, National Centre for Nuclear Research
ul. Andrzeja Sołtana 7, 05-400 Otwock-Świerk, Poland

ABSTRACT

The work performed in scope of collaboration between NCNR and ANL was aimed at performing measurements of fission products release to water, so called "sipping test", for monitoring MC type LEU fuel elements irradiated during MARIA reactor operation. This work was forced by the results of sipping test measurements for LTA MC type fuel elements (MC001 and MC002), which showed significant increase of fission products release from spent fuel elements to water after 3 years of storage in reactor storage pool. Therefore it was concluded, that monitoring of state of subsequent MC type LEU fuel elements irradiated during MARIA reactor operation is necessary.
This paper will present MC type fuel construction, technology of sipping test and sipping test stand constructed in MARIA storage pool, and results of performed sipping test campaign.

1. Introduction

MARIA is a water cooled research reactor of pool type with pressurized fuel channels. It is located in National Centre for Nuclear Research (NCBJ) in Otwock, roughly 25 kilometers from Warszawa – capital of Poland. The nominal power is 30 MWth and core contains 20+ fuel elements located in individually cooled pressure tubes called fuel channels. Channels are surrounded by moderating beryllium blocks and immersed in water pool. Reactor core also consists of graphite reflector blocks. Whole core is situated in an aluminum basket.

Since 2005 in National Centre for Nuclear Research works on the fuel conversion from highly enriched uranium with 36% of 235U to low enriched one (LEU) with 235U content below 20% have been led. This is the most recent fuel conversion held in NCNR. The feasibility study for applying the silicide fuel (U_3Si_2) of 4.8 g/cm^3 density was commenced. Supplier of such fuel is the company Areva (CERCA). CERCA delivered to IAE one dummy fuel assembly (DFA) in May 2008 for hydraulic testing and two LTAs in July 2008. The proposed fuel has been tested to very high levels of burnup. Besides irradiation test, hydraulic tests was conducted. Measurements and analysis of MC fuel element design exhibited, that in comparison with MR fuel elements they have worse hydraulic and heat transfer coefficients, so main pumps system replacement was inevitable. 2009 is the beginning of LTA's irradiation, followed by inserting CERCA fuel and start of conversion in September 2012. Primary pumps replacement took place between June and September 2013. In September 2014 core conversion has ended and MARIA reactor is now operating only on LEU fuel elements.

Right now, MARIA is licensed to operate on two different LEU type fuels (similar in construction obviously, nevertheless each one has its own peculiarities): MR produced in Russian Federation, which is an uranium oxide fuel; and French MC silicide fuel. This paper focuses on the second one, as the sipping test campaign is dedicated to MC type fuel (over time, and with gradual transition to MR fuel, MR type fuel element will certainly be subjected to sipping test, but up to date of paper completion only one LEU MR fuel element was measured).

2. MC fuel type characteristics

MC type fuel element is constructed in form of five concentric fuel tubes. Each tube is made from three bend plates (in contrast to MR type fuel elements where the tubes are extruded) that are fixed together. Several of them are welded and rolled in order to form a tube (FT4). Two series of 6 of them are fixed on 3 stiffeners by swaging to form 2 tubes. All these tubes are maintained by end fitting fixed with screws on tube FT4. They are spared equally in order to ensure a correct water gap. Instead of FT1 in MC type fuel element there is an aluminium tube, serving as filling tube. Dimension of each fuel tube is given in table 1.

Tube no.	∅ outer, mm	∅ inner, mm
1*	25 ± 0.2	21
2	34 ± 0.2	30
3	43 ± 0.2	39
4	52 ± 0.2	48
5	61 ± 0.2	57
6	70 ± 0.2	66

* no fuel tube in MC assembly

Tab 1 Fuel element tubes dimensions

Axial assembly height is 1478 mm, but the core length, thus the fuel effective height is 1000 mm. Fuel used in MC type elements is U3Si2 uranium silicide dispersion (uranium/silicon alloy) in the aluminum matrix. The U235 enrichment is 19.75%. Nominal cladding thickness is 0.6 mm. Uranium meat density is 4.79 g/cm^3. In figure 1 the geometry of MC type fuel element is shown.

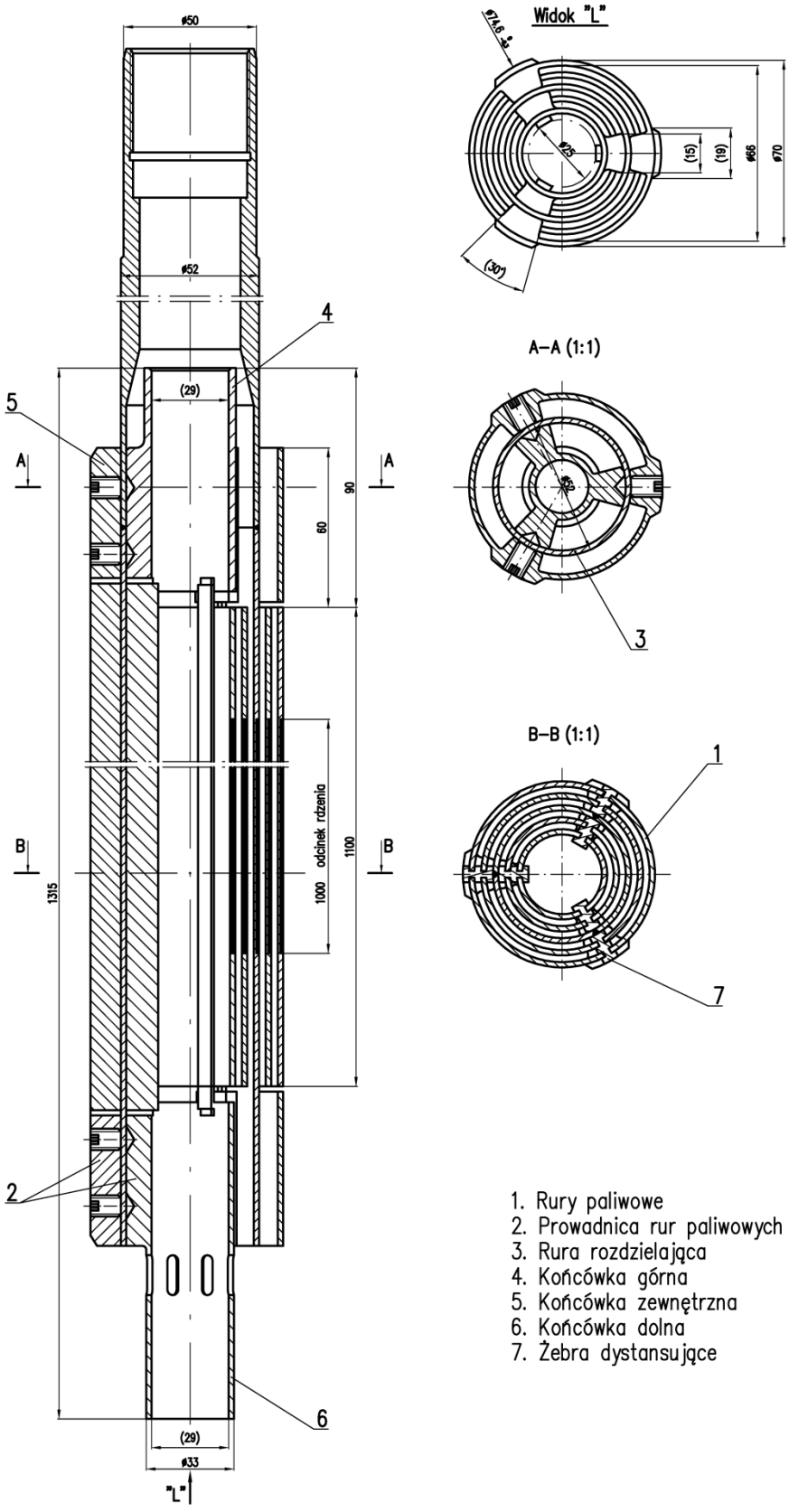

Fig. 1: MC type fuel element [1].

3. Sipping test stand construction and operation

One of the steps of MARIA core conversion to LEU fuel was irradiation test of two low-enriched LTA's. Those LTA's manufactured by Areva CERCA were tested in the MARIA reactor core from August 2009 till January 2011. First LTA reached 5899 MWh (63%) burnup and the second one 4025 MWh (43%). After unloading the elements, post-irradiation sipping tests were conducted. Those tests were repeated few times after three years of cooling down, and at that time they showed significant increase in measured activity of Cs137, which was rather alarming (it will be discussed more in "Conclusions" chapter). In cooperation with Argonne National Laboratory a measurement campaign was developed, also it was decided to build a special stand which would enable FP activity measurements without the necessity of removing the fuel element from fuel channel (LTA's MC001 and MC002 were removed from fuel channels and kept in special containers, but this isn't standard procedure. Usually spent fuel elements are kept in fuel channels and are handled in such way.)

Sipping test stand is located in the corner of MARIA's spent fuel storage pool and consists of two main parts: on-ground which allows the collection of water samples from fuel channel put into Sb-k stand or SB container, and underwater made for connecting the fuel element located in the fuel channel with on-ground part of the stand. As stated earlier there is a significant difference in technique of sipping tests of LTAs and the rest of the fuel elements. LTA's are cut off from sheaths and all measurements are done in SB measuring stand, where these two elements are stored. All the other fuel elements are kept in fuel channels, thus SB-k measuring stand is used to carry on sipping tests. The on-ground part of the stand is connected both to the SB and SB-k parts.

Stand has been constructed from 1H18N9T stainless steel. Stand itself is a supporting structure attached to spent fuel pool wall. Along this structure measuring head is moving. Spent fuel element, remaining in fuel channel, is inserted into the stand above measuring head which initially stays at the bottom of spent fuel pool. After insertion of fuel element, measuring head is pulled up to top in order to mount and connect the wires to the on-ground part of the stand. Figure 2 shows the underwater part of the stand located in the pool.

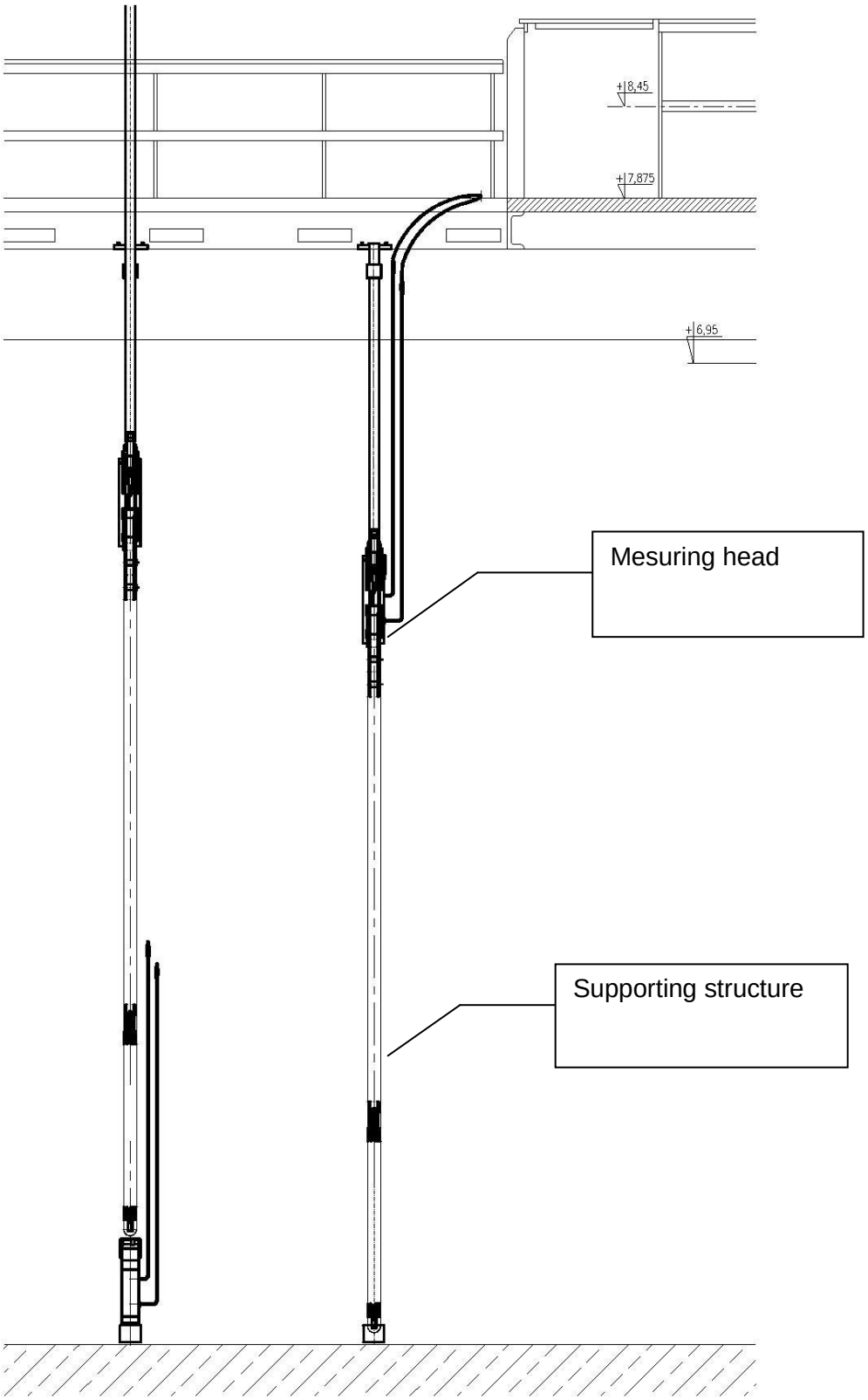

Fig. 2: Scheme of the stand for measuring the release of fission products into water from spent fuel elements remaining in channels.

In order to monitor the status of the low-enriched spent MC fuel elements remaining in the MARIA reactor storage pool, measurements of the releases of fission products into water are done by taking samples of water (the so-called "sipping test"). The principle of measurement is that a burnt fuel element and the fuel channel is inserted into the measuring head. The

measuring head is sealed, and whole channel is filled with demineralised water. Spent fuel element is flushed several times. After flushing, a sample of water for pre-measurement is taken. After final flushing water is sitting in sheath for 24 hours, then another sample is obtained and measured. The physicochemical and spectrometric parameters of water samples collected are examined and the non-leakage of the burnt fuel element is assessed according to the criteria adopted in the NCNR.

The criterion for recognizing the spent fuel element as leaking is the measurement of 24h releases of Cs137 isotope from a single fuel element above 10 kBq/day, but no more than 100 kBq/day.
If the release of the Cs137 isotope exceeds 100 kBq/day, then the fuel element should be treated as destroyed and it will be subject to a separate, case-by-case procedure that will take into account the state of the burnt fuel element.

Because over time it was observed that the stand does not guarantee the quality of the obtained results, i.e. tightness and repeatability due to the maladjustment of the structure to new needs, hence the need for its modernization.
The purpose of modernizing the test stand to measure releases from spent fuel elements to water was:

- replacement of supply hoses to the underwater SB capsule pods,
- replacement of the measuring head in the Sb-k underwater stand,
- replacement of the existing part of the on-ground measuring station with a new, completely modernized one.

The modernization of the measuring stand, after the completion of its on-ground part in accordance with the modernization project, was carried out on 30 August 2018.
The schematics of the whole measurement stand after modernization is shown in figure 3. Figure 4 shows SB stand with new hoses. Figure 5 shows modernization of the measuring head. Figure 6 shows the modernized on-ground part of the measuring stand. Beside this modernization, in the last quarter of 2018, new gamma spectrometric analyzer Genie2K was installed, which allowed to increase the measurement accuracy and reduce the measurement error (which can be seen in the results of measuring campaign).

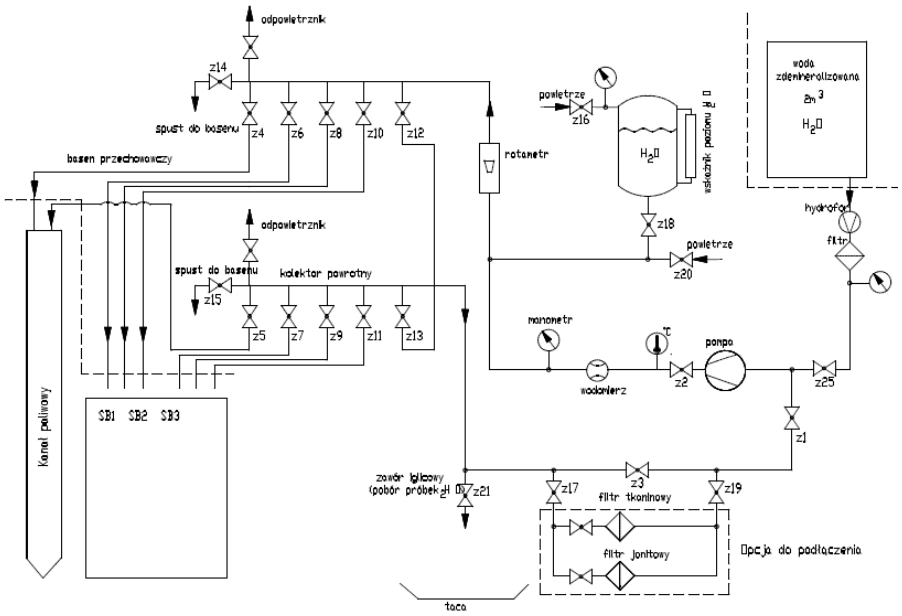

Fig. 3: Schematics of the sipping test measurement stand.

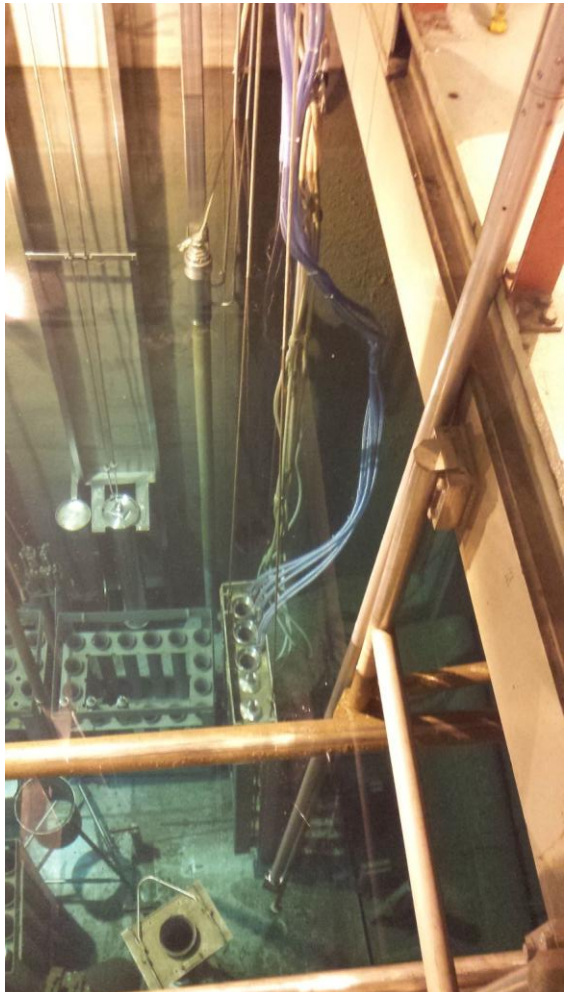

Fig. 4: SB stand with new hoses.

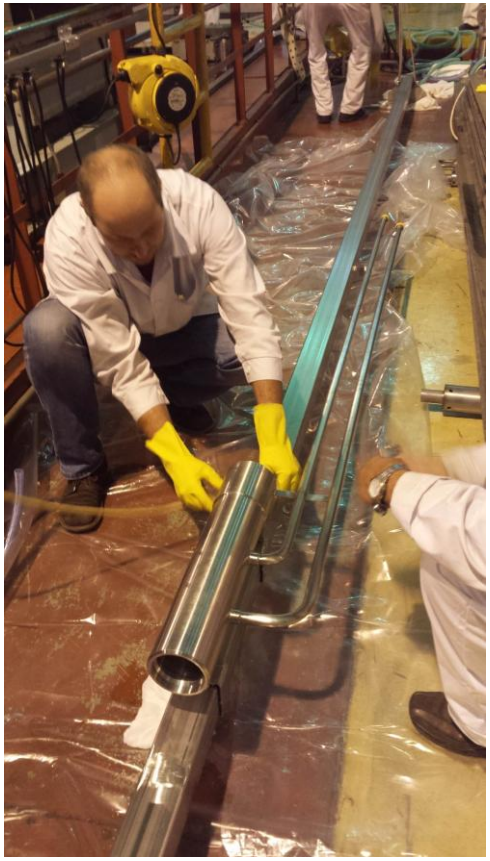

Fig. 5: Modernization of the Sb-k stand measuring head.

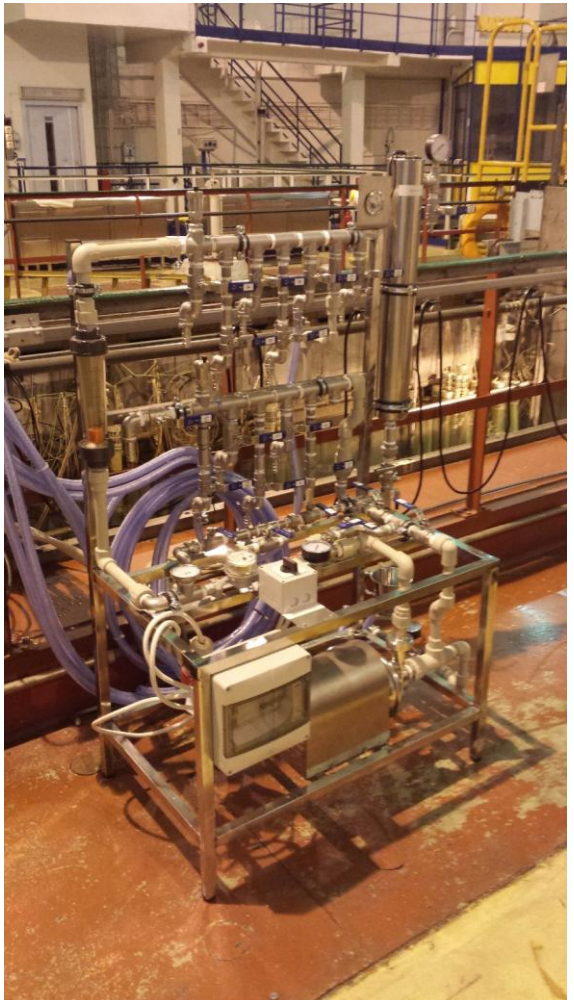

Fig. 6: On-ground, modernized part of the sipping test stand, placed above the spent fuel pool.

4. Sipping test campaign measurements results

In 2017, a total of 55 measurements, and in 2018, a total of 56 spectrometric gamma Cs137 emission measurements for the burnt MC LEU (and one MR LEU) fuel elements were made As mentioned earlier, MC001 and MC002 LTA measurements were carried out in the SB station capsules, where the volume of water is equal to 6 liters, all the other fuel elements were measured in the Sb-k stand with the water volume of 22 liters.

The results of gamma spectrometric measurements of Cs137 emission, referring to the content of Cs137 per liter of water for samples taken after 24 h from spent fuel elements, are presented in Table 2 and Table 3, below, respectively for 2017 and 2018 measurements. Last column of the table contains method measurement error, <LD is the measurement result below the spectrometer detection threshold. Results of fuel elements in bold indicate a leakage.

No.	Fuel element	Measurement Cs-137 after 24h [Bq/l]	Error [%]
1	2	3	4
1st quarter 2017			
1	MC020	10	205
2	MC021	13	70
3	MC027	1	106
4	MC030	<LD	-
5	MC033	<LD	-
6	MC036	5	220
7	MC032	12	82
8	MC026	<LD	-
9	MC010	41	44
10	MC011	<LD	-
11	MC013	<LD	-
2nd quarter 2017			
1	MC001	222	20
2	**MC002**	3291	15
3	MC004	63	43
4	MC005	32	47
5	MC006	<LD	-
6	MC007	57	38
7	MC008	18	42
8	MC012	<LD	-
9	MC014	3	325
10	MC015	<LD	-
11	MC016	<LD	-
12	MC017	11	119
13	MC019	7	200
14	MC023	50	41
15	MC024	<LD	-
16	MC025	<LD	-
3rd quarter 2017			
1	MC001	367	18
2	**MC002**	1300	16
3	MC009	24	47
4	MC027	70	10
5	MC029	<LD	-

6	MC030	11	77
7	MC032	26	53
8	MC033	2	340
9	MC034	<LD	-
10	MC037	<LD	-
11	MC039	6	213
12	MC040	<LD	-
13	MC041	<LD	-
14	MC042	4	98
15	MC043	7	192
16	MC044	<LD	-
17	MC045	5	119
18	MC046	4	216
4th quarter 2017			
1	MC038	4	300
2	MC007	54	34
3	MC005	27	50
4	MC010	32	52
5	MC006	<LD	-
6	MC020	44	40
7	MC026	<LD	-
8	MC014	105	26
9	**MC003**	10000	15
10	MC048	5	194

Tab. 2 Results of gamma spectrometric measurements of Cs137 emission for MC type fuel elements in 2017.

No.	Fuel element	Measurement Cs-137 after 24h [Bq/l]	Error [%]
1	2	3	4
1st quarter 2018			
1	**MC003**	1.8E+04	15
2	MC009	4	176
3	MC018	8	96
4	MC019	13	88
5	MC022	14	87
6	MC023	34	57
7	MC024	32	54
8	MC025	2	243
9	MC036	9	93
10	MC037	22	51
11	MC039	4	157
12	MC041	<LD	-
13	MC044	<LD	-
14	MC050	1	760
15	MC061	4	220
2nd quarter 2018			
1	MC001	241	21
2	**MC002**	1490	16
3	**MC003**	1807	16
4	MC021	<LD	-

5	MC027	<LD	-
6	MC029	3	257
7	MC030	4	235
8	MC034	8	80
9	MC042	26	66
10	MC043	<LD	-
11	MC045	<LD	-
12	MC046	<LD	-
13	MC051	8	185
3rd quarter 2018			
1	**MC001**	747	16
2	**MC002**	3363	15
3	**2212**	3786	15
4	MC005	38	48
5	MC006	13	72
6	MC010	37	47
7	MC015	10	99
8	MC017	81	15
9	MC020	206	20
10	MC031	8	97
11	MC035	36	58
12	MC038	7	130
13	MC047	36	56
4th quarter 2018*			
1	**MC001**	830.7	2.7
2	**MC002**	4074	1.7
3	**2212**	1.438E+05	1.4
4	**MC003**	1658	2.1
5	MC010	12.26	25.3
6	MC014	18.53	13.3
7	MC018	19.69	19
8	MC019	8.083	37.5
9	MC022	321.9	4.2
10	MC023	29.25	14.2
11	MC024	4.419	83.2
12	**MC025**	821.8	2.7
13	MC048	75.36	8.9
14	MC052	12.26	25.3
15	MC056	30.65	14.3

***** Results after spectrometer modernization.

Tab. 3 Results of gamma spectrometric measurements of Cs137 emission for MC type fuel elements in 2017.

5. Conclusions

The prototype fuel elements MC001 and MC002, which show increased releases of Cs-137, are located in measuring capsules of the SB test stand, isolated from the water of the storage pool, and can be monitored more frequently. Most likely cause of the releases is degradation of cladding due to storage in water or surface contamination.

Signs of leakage can be observed in fuel element MC003. We assume that there has been a degradation of the cladding of this fuel element that caused the leak. Releases from this element were monitored every quarter. After measurements in the subsequent quarters, it turned out that the release of Cs137 the fuel element into water decreases, which may mean

that there were contaminations on the surface of the spent fuel element, which are now washed out during each measurement procedure. Below, in figure 7 the graph shows the trend of 24h releases of Cs137 from MC003 fuel element to water, measured in 2018.

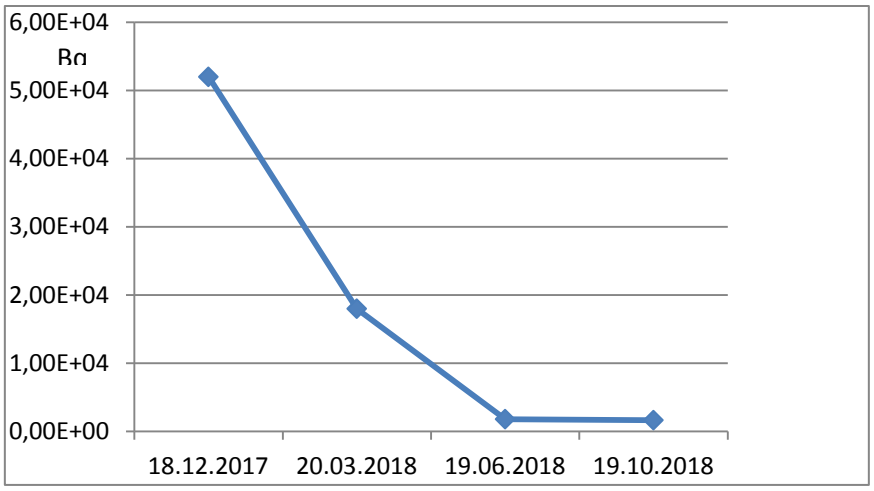

Fig. 7: Cs137 release from MC003 fuel element as a function of time.

In the fourth quarter compared to the first quarter of 2018 an increase in releases from MC022 and MC025 spent fuel elements was also observed, yet only MC025 should be classified as leaking.
The largest releases were observed from the prototype fuel element MR2212. Previous measurements carried out in 2017 didn't indicated that this element was leaking. Based on measurements in the third and fourth quarter of 2018, it was found that the releases from this spent fuel element increased significantly. It was decided that the MR2212 element will remain in the capsule pod of the SB stand, and the measurements will be repeated every quarter to monitor the state of its cladding
Remaining spent MC type fuel elements kept in the fuel channels for which measurements were made in 2017 and 2018 are tight and show no signs of leakage.

References

[1] K. Pytel et al., Maria Research Reactor Safety Report, National Centre for Nuclear Research, Otwock, Poland, 2015.
[2] K. Pytel, W. Mieleszczenko, Z. Marcinkowska, Konwersja rdzenia reaktora MARIA na paliwo MC, Annex 2012/1 to the MARIA Research Reactor Safety Report, National Centre for Nuclear Research, Otwock, Poland 2012.
[3] E. Borek-Kruszewska, A. Małkiewicz, Instrukcja prowadzenia kontroli uwolnień produktów rozszczepienia z wypalonych elementów paliwowych do wody, internal instruction no. 57-MR-2018, National Centre for Nuclear Research, Otwock, Poland, 2018.
[4] E Borek-Kruszewska, I. Wilczek, A. Zawadka, Report on control of the LEU spent fuel, internal report no. B-()/2017, National Centre for Nuclear Research, Otwock, Poland, 2017.
[5] E. Borek-Kruszewska, A. Małkiewicz, I. Wilczek, A. Zawadka, Report on control of the LEU spent fuel in 2018, internal report no. B-()/2018, National Centre for Nuclear Research, Otwock, Poland, 2018.
[6] E. Borek-Kruszewska, A. Małkiewicz, I. Wilczek, J. Wilczek, A. Zawadka, Modernization of the stand to control releasess from the LEU spent fuel to water, internal report no. B-11/2018, National Centre for Nuclear Research, Otwock, Poland, 2018.
[7] M. Migdal et al., Deliverables 12.1 and 12.2 a-e issued to Argonne National Laboratory in scope of NCNR Work Order 6J-00106-0012, Statement of Work 12 "Measurements of Fission Products Release to Water for MC type LEU Fuel Elements Irradiated During MARIA Reactor Operation", ANL-NCNR, 2015-2018.

SIMULATION OF THE RADIOLOGICAL CONSEQUENCES OF THE HYPOTHETICAL ACCIDENT IN MARIA RESEARCH REACTOR

M. LIPKA

Nuclear Facilities Operations Department, National Centre for Nuclear Research
ul. Andrzeja Sołtana 7, 05-400 Otwock-Świerk, Poland

ABSTRACT

Radionuclides propagation through the nuclear reactor safety barriers has been modelled. Mathematical model was created and coupled with the Gauss plume atmospheric dispersion model with dry and wet deposition. Finally both models have been implemented to the self-created computer code that allows to perform radiation dose calculations for reactor personnel and the public. For the purpose of calculations, hypothetical accident involving loss of the fuel element cladding integrity was considered with various scenarios of actions taken by the reactor operator.

1. Introduction

MARIA is channels-in-pool type, water cooled research reactor. She is located in National Centre for Nuclear Research (NCBJ) in Otwock, roughly 25 kilometers from Warszawa – capital of Poland. The nominal power is 30 MWth and core contains 20+ fuel elements located in individually cooled pressure tubes called fuel channels. Channels are surrounded by beryllium blocks and immersed in water pool.

When a hypothetical accident, resulting in fuel cladding integrity loss occurs, radionuclides accumulated in the fuel elements during reactor operation are released. They start to migrate through reactor safety barriers, and after weakening are finally released into the atmosphere.

This paper presents mathematical model of radionuclides transport via safety barriers and possible radiological effects on reactor staff. Additionally doses to the general public are estimated.

2. Radionuclides migration routes through safety barriers in MARIA reactor

Scheme of radionuclides migration routes through MARIA reactor safety barriers is presented in the figure 1. Rectangles represent places where radionuclides gather, arrows between them are showing radionuclides migration.

The reactor is scramed by the operator after the activity increase in the fuel element leak detection system (WNEP) or other previously obtained signal (eg. power increase or flow decrease). The ventilation system is switched in such a way that the air is released into the atmosphere through Vokes filtration system, whose task is to significantly weaken amount of radionuclides in the atmosphere.

Fission products from cracked fuel element are released to the fuel channels cooling loop and then:

- deposit in the filtration system of fuel channels cooling loop
- migrate to the pressurizer gas space
- leak through seals to the reactor pool

Radionuclides in the filtration system are not further removed but they undergo radioactive decay. Gas space in pressurizer can be discharged to the elastic balloon and later released

through intermediate filter to the ventilation system. From the reactor pool, radionuclides are released to air space below the reactor pool covers, additionally they deposit on the hall surface and some of them are desorbed back. Finally through the ventilation system protected by the Vokes filters set, radionuclides are released from the reactor stack to the atmosphere.

Reactor personnel might be exposed might be exposed to external field of β and γ radiation from filters and pressurizer, and in some cases through inhalation of the radionuclides.

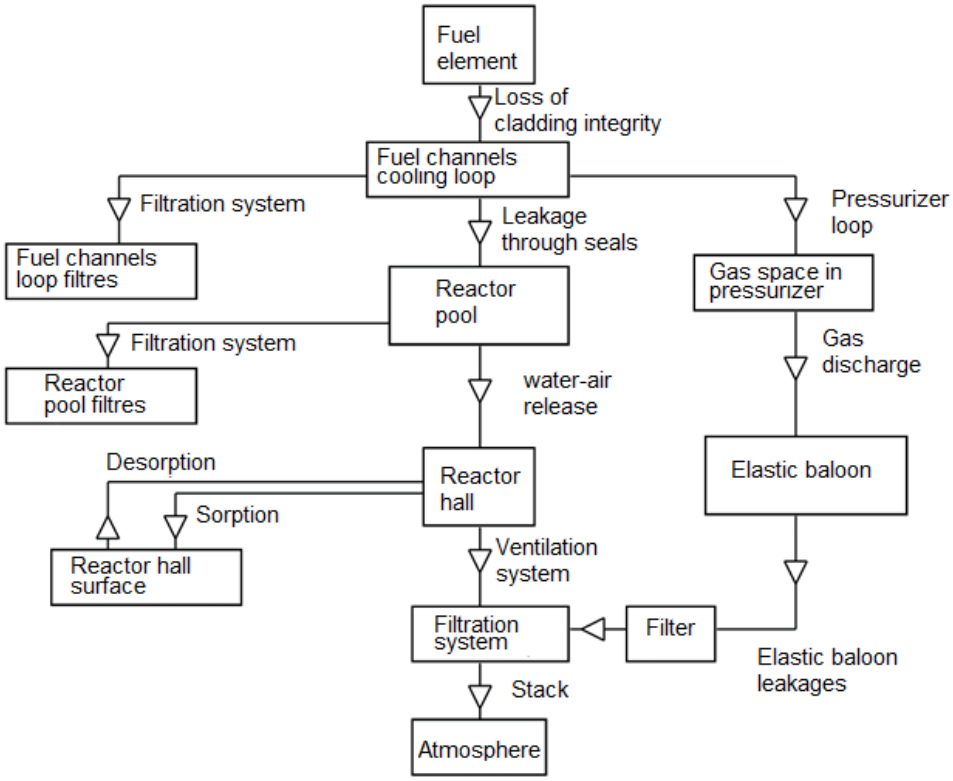

Fig. 1: Scheme of radionuclides migration routes through the safety barriers [1]

3. Mathematical model for activities

The mathematical model of activity in certain spots is based on Bateman's balance equations, individually for each of a number of radionuclides released from nuclear fuel. Parameters used in the equations are taken from the literature [2,3] or determined experimentally. Determined activity is recalculated into doses with parameters and equations taken from [4,5,6,7].

Mathematical equations for the activity balances are given below. Markings that are used in the equations, are given in the glossary at the end of the paper.

3.1 Activities inside of the reactor building

Activity balance in fuel channels cooling loop is given by

$$\frac{dX_{ok}}{dt} = Q \cdot \zeta \cdot f(t) - \left(\lambda + \lambda_{odg} + \lambda_{nb} + \lambda_{fk}\right) \cdot X_{ok}$$

Activity balance in pressurizer:

$$\frac{dX_{odg}}{dt} = \lambda_{odg} \cdot X_{ok} - \lambda \cdot X_{odg}$$

Activity balance in fuel channels cooling loop filtration system:

$$\frac{dX_{fk}}{dt}=\lambda_{fk}\cdot X_{ok}-\lambda\cdot X_{fk}$$

Activity balance in reactor pool

$$\frac{dX_{ob}}{dt}=\lambda_{nb}\cdot X_{ok}\cdot(1-\kappa_w)-(\lambda+\lambda_{fb})\cdot X_{ob}$$

Activity balance in the reactor hall

$$\frac{dX_{h}}{dt}=\lambda_{nb}\cdot X_{ok}\cdot\kappa_w-(\lambda+\lambda_{os}+\lambda_{fb}+\lambda_w)\cdot X_{h}$$

Activity balance at the reactor hall surface

$$\frac{dX_{os}}{dt}=\lambda_{os}\cdot X_{h}-\lambda\cdot X_{os}$$

Activity balance in the Vokes filtration system

$$\frac{dX_{fv}}{dt}=\lambda_w\cdot X_{h}\cdot\eta+\lambda_{nze}\cdot X_{ze}\cdot\eta\cdot(1-\eta)-\lambda\cdot X_{fv}$$

Activity released to the atmosphere

$$\frac{dX_{at}}{dt}=\lambda_w\cdot X_{h}\cdot(1-\eta)+\lambda_{nze}\cdot X_{ze}\cdot(1-\eta)^2$$

All the equations have the initial condition $X_i(0)=0$ as the zero activity before the loss of cladding integrity is assumed.

3.2 Atmospheric dispersion

For the calculations of the atmospheric dispersion, Gauss plume model have been used, as described below. Concentrations were computed in the plume axis (x=0),at the ground level (z=0). Plume is additionally depleted by radioactive decay and dry deposition (not included in the formula below)

$$C_{(x,z=0)}=\frac{X_{at}}{2\pi u\sigma_y\sigma_z}\cdot\exp\left\{-\frac{y^2}{2\sigma_y^2}\right\}\cdot\exp\left\{-\frac{H^2}{2\sigma_z^2}\right\}$$

Activities of radionuclides deposited on the ground surface have been calculated as:

$$C_{gr}=V_T\cdot C_{(x,z=0)}\ [8]$$

Activities on the ground level have been calculated together with deposited activities, and finally doses from external gamma field and some of the isotopes inhalation have been estimated as presented in chapter 4.4

4. Doses calculation in the specific spots inside of the reactor buildings

After calculations of activity in certain places of the reactor, with equations given in chapter 3, it became possible to calculate the possible radiation exposure of the reactor staff. Three potentially dangerous places have been selected in proximity of:

- Fuel channels cooling systems filter
- Pressurizer
- Vokes ventilation filtration system.

The method of calculating doses has been presented in the following chapters 4.1-4.3. Dose from external gamma field and Iodine isotopes inhalation in the reactor hall has not been calculated. It was assumed that if reactor pool covers are in place, ventilation system

prohibits radionuclides migration to the reactor hall. All of the measurements in figures 2 – 4 have been given in meters.

4.1 Gamma dose for personnel from the fission products gathered in fuel channels filtration system

Scheme of the geometry for dose from fuel channels cooling loop filtration system assessment have been presented in figure 2.

Dose have been calculated as:

$$\dot{D}_{\gamma,o}=K_{\gamma}\cdot X_{odg}\cdot\frac{e^{-\mu_{pb}\cdot d_{pb}-\mu_{b}\cdot d_{b}}}{d^{2}}$$

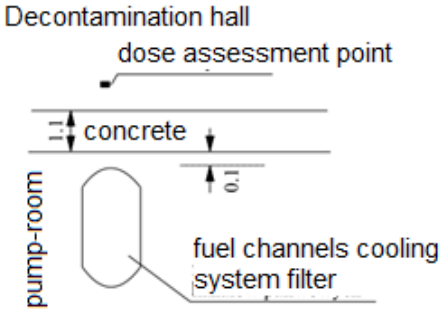

Fig. 2: Geometry for dose from fuel channels filters assesment

4.2 Gamma dose for personnel from pressurizer

Scheme of the geometry for dose from pressurizer assessment have been presented in figure 3.

Dose have been calculated as:

$$\dot{D}_{\gamma,o}=K_{\gamma}\cdot X_{odg}\cdot\frac{e^{-\mu_{pb}\cdot d_{pb}-\mu_{b}\cdot d_{b}}}{d^{2}}$$

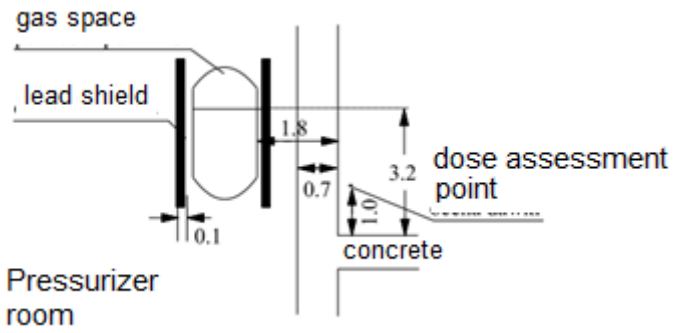

Fig. 3: Geometry for dose estimation from pressurizer

4.3 Gamma dose from the Vokes filtration system

Scheme of the geometry for dose from pressurizer assessment have been presented in figure 4.

Dose have been calculated as:

$$\dot{D}_{\gamma,v}=K_{\gamma}\cdot X_{fv}\cdot\frac{e^{-\mu_b\cdot d_b}}{d^2}$$

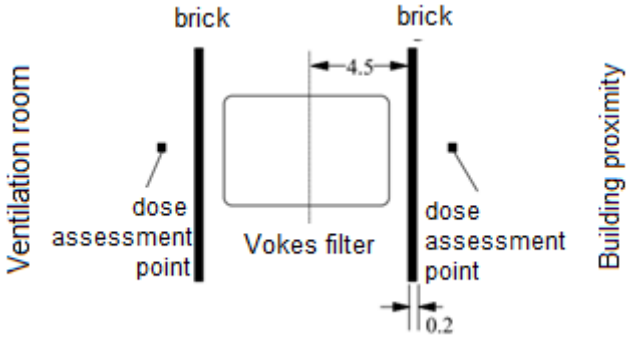

Fig. 4: Geometry for dose estimation from Vokes ventilation filtration system

4.4 Doses from the atmospheric radioactive plume

External dose from the immersion in the atmospheric discharge has been calculated as:

$$E_{im}=DF_{im}\cdot C_{(x,z=0)}$$

Internal dose due to iodine isotopes inhalation has been calculated as:

$$E_{inh}=DF_{inh}\cdot R_{inh}\cdot C_{(x,z=0)}$$

External dose from the ground deposits has been calculated as

$$E_{dep}=DF_{gr}\cdot C_{gr}\cdot\int_0^t \exp\{-\lambda t\}dt=DF_{gr}\cdot C_{gr}\cdot\left[\frac{1-\exp\{-\lambda t\}}{\lambda}\right]$$

5. Results

For the calculations the following scenario has been assumed:

1. After the loss of cladding integrity the reactor is scramed.
2. Five minutes after SCRAM, main circulation pumps are switched to auxiliary pumps to limit the pressure in fuel channels cooling loop
3. Ten minutes after SCRAM, ventilation flow is limited from 11000 to 6000 m^3/h.
4. Thirty minutes after SCRAM, all pumps are switched off.

It has been assumed that fuel element that is the source of the radionuclides has been operated at power 1 MWt and had burn-up of 245 MWd and total activity of $4.95\cdot10^5$ TBq.

5.1 Doses for the reactor staff

For the doses inside of the reactor building it has been assumed that worker is standing still in the same place for the whole time of the incident. Results have been presented in the figure 5.

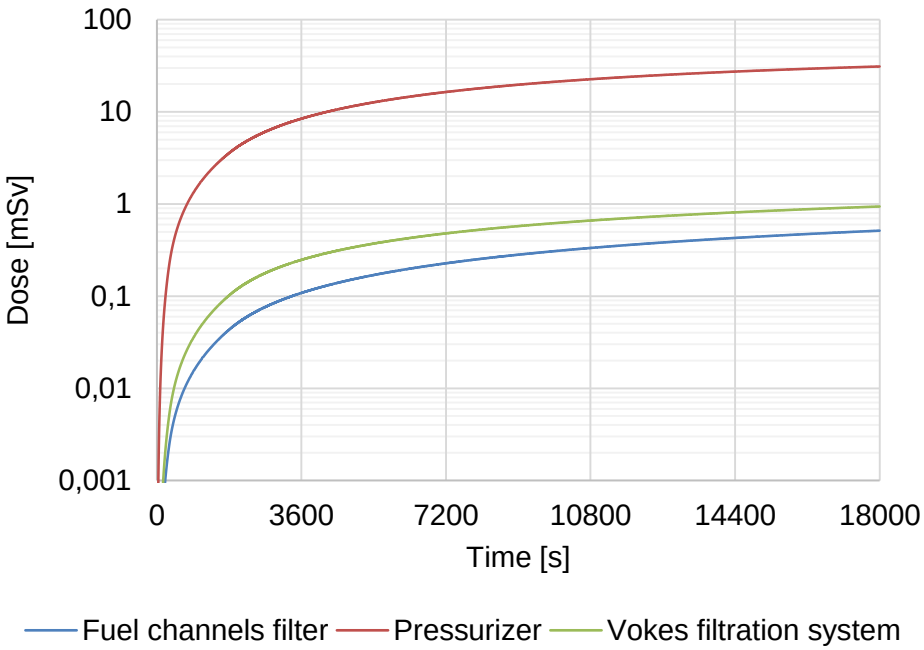

Fig. 5. Doses for the reactor worker from certain systems inside of the reactor building

5.2 Doses for the general public

For the general population dose calculation it has been assumed that representant of the critical group (child <1 y) is standing still during the time when the plume is passing by. Calculations of one-year-dose from the radioactive deposits assume that this person is outside of the building for the whole year long.

Three atmospheric situations have been assumed – most unstable, most probable and most stable (A,D, and F Pasquill stability classes respectively). For each class the lowest possible wind speed of 1m/s was taken into account

Figure 6 presents total activity released to the atmosphere. Figures 7-9 present dose from immersion, dose from inhalation and yearly dose from the ground deposits respectively.

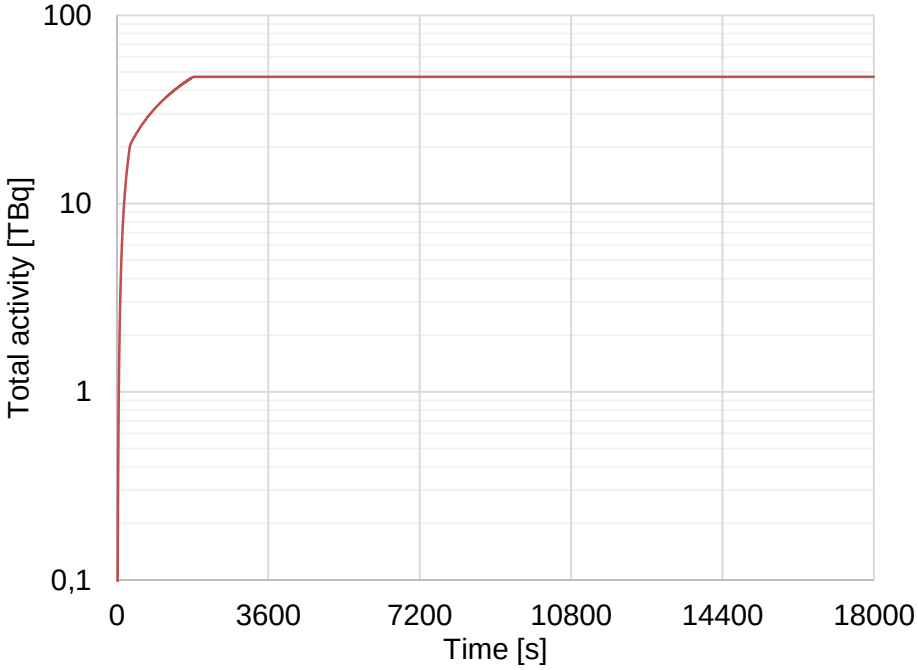

Fig. 6: Total activity released to the atmosphere

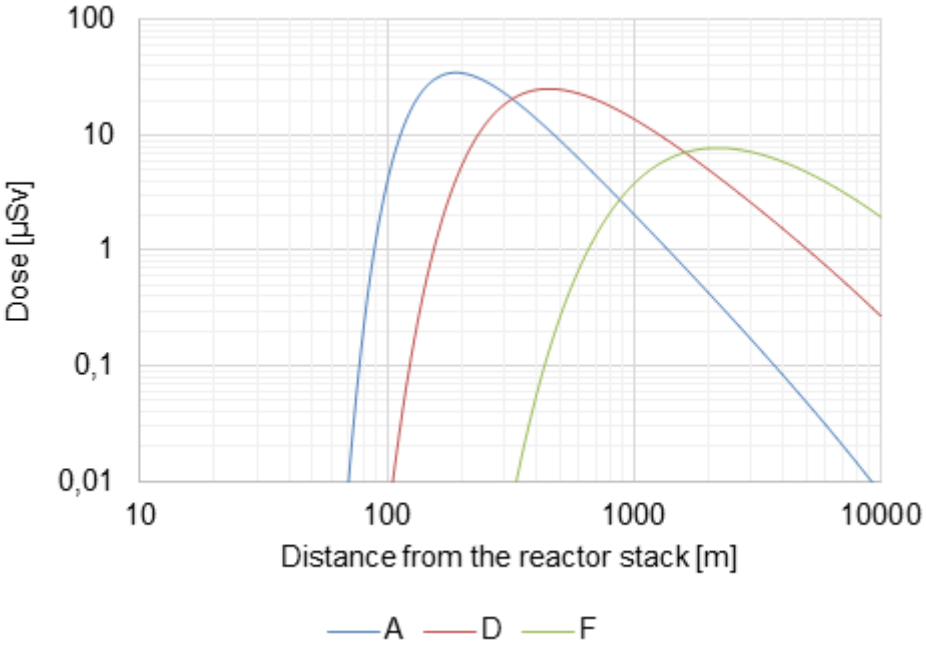

Fig. 7: External dose from the immersion in the atmospheric discharge

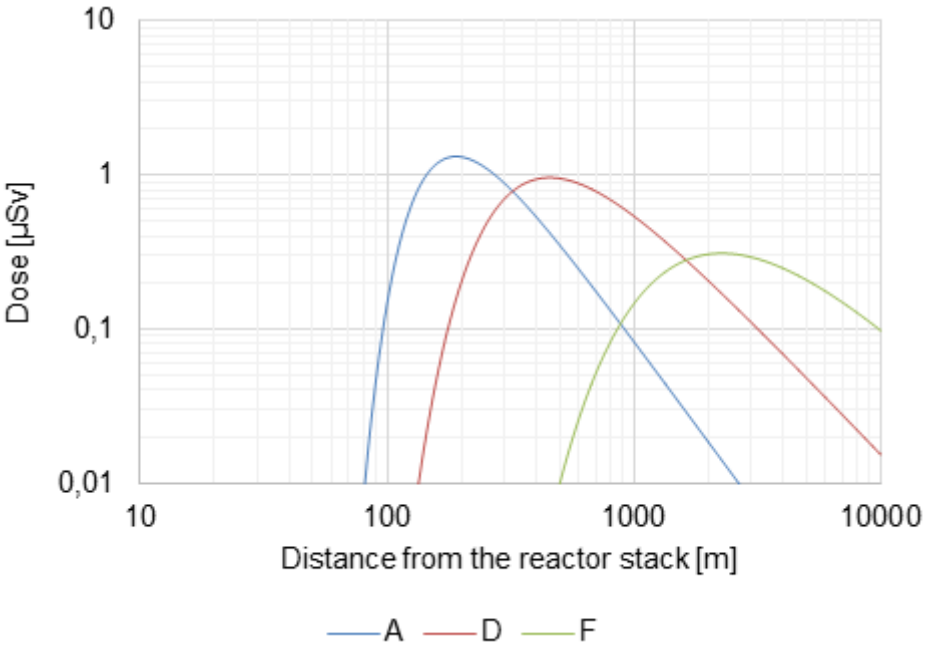

Fig. 8: Internal dose due to radionuclides inhalation

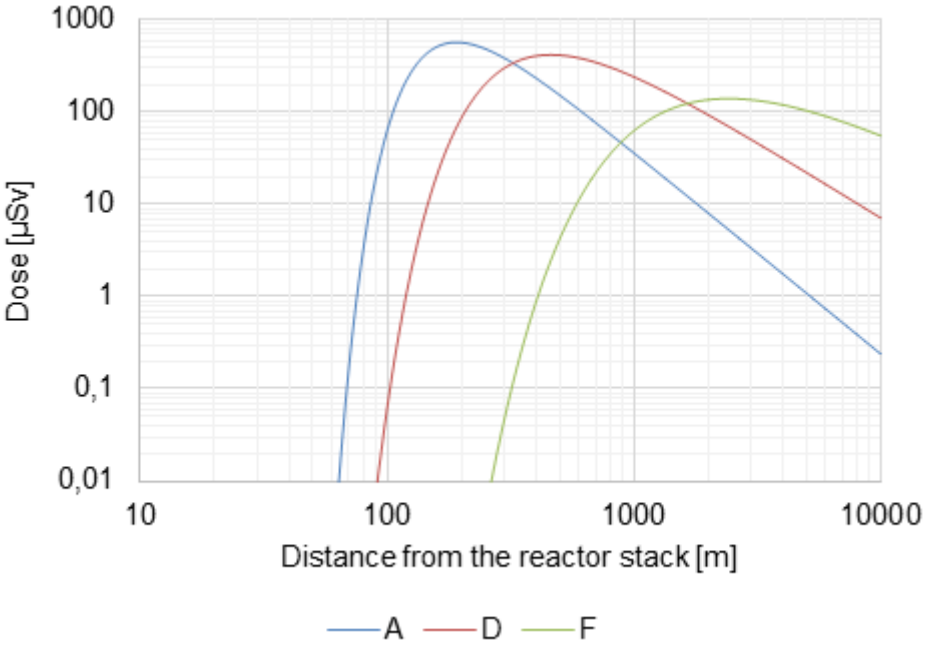

Fig. 9: External, yearly dose from the ground deposits

6. Discussion

All of the calculations presented above, have been made under pessimistic approach assuming, that representatives of the groups exposed to radiation are standing still in one place for the whole time of simulation.

Results of the calculations presented in the chapter 5 shows that reactor worker might get the biggest dose in the proximity of the pressurizer. Maximum dose in this spot equals 31 mSv which is within 100 mSv dose that worker can get during five year normal operation time [4] and 25 times lower than the permitted dose during the accident (100 mSv) [9].

From the stack to the atmosphere, 47.1 TBq of radionuclides have been discharged, containing mainly Xe-133 (40%), Kr-88 and Kr-87 (21,5% and 18.9% respectively). That activity for the representative of the critical group will get, assuming the pessimistic approach that they remain in the same spot for the whole year, is resulting in total yearly dose.

The total maximum dose for the representative of the general population, from all three routes of exposure, calculated for the whole calendar year after the accident is 0.61 mSv in the distance ~200 m from the reactor stack.

Calculated dose is not only below emergency limits described in [10] (10 mSv for staying inside the buildings) but also below 1 mSv which is yearly limit for the general population in normal operation conditions of the reactor. Dose from crops, milk and meat ingestion has not been calculated due to the lack of agricultural production around the reactor [1].

Glossary

- X_{ok} – activity in the fuel channels cooling loop [Bq]
- X_{odg} – activity in pressurizer gas space [Bq]
- X_{fk} – activity in fuel channels filtration system [Bq]
- X_{fv} –activity in the Vokes filtration system [Bq]
- X_{ob} – activity in reactor pool [Bq]
- X_{h} –activity in reactor hall [Bq]
- X_{ze} –activity in the elastic baloon [Bq]

- X_{os} - activity at the reactor hall surface [Bq]
- C – atmospheric activity concentration [$\frac{Bq \cdot s}{m^3}$]
- C_{gr} – activity deposited on the ground surface [$\frac{Bq}{m^2}$]
- DF_{im} – effective dose coefficient for immersion [Sv/s per Bq/m^3]
- DF_{inh} – inhalation dose coefficient [Sv/Bq]
- DF_{gr} – dose coefficient for exposure to ground deposits [Sv/a per Bq/m^2]
- $\dot{D}$ – dose rate [Sv/s]
- d – linear dimension [m]
- H – effective stack height [m]
- K_γ – gamma factor [$\frac{Sv \cdot m^2}{s \cdot Bq}$]
- Q – activity in the fuel element [Bq]
- R_{inh} – inhalation rate [m^3/s]
- t – time [s]
- u – wind speed [m/s]
- V_T – deposition coefficient [m/d]
- ζ – release coefficient for fuel element
- κ_w – probability of the release of the isotope from water to air
- σ – diffusion parameter [m]
- η – filter efficiency
- μ – linear gamma attenuation factor [m^{-1}]
- λ – radioactive decay time constant [s^{-1}]
- λ_{odg} – time constant of release to pressurizer gas space [s^{-1}]
- λ_{nb} - time constant of release to reactor pool [s^{-1}]
- λ_{fk} – time constant of fuel channels cooling loop filtration [s^{-1}]
- λ_{os} – time constant of the deposition at the reactor hall surface [s^{-1}]

References

[1] K. Pytel et al., Maria Research Reactor Safety Report, National Centre for Nuclear Research, Otwock, Poland, 2015

[2] K. Pytel, K. Nowicki, Model transportu produktów rozszczepienia i zagrożenia personelu w obiekcie reaktora MARIA w wyniku przepalenia paliwa, Raport Wewnętrzny IEA nr: 81/R - V/89, Instytut Energii Atomowej, Otwock-Świerk 1989

[3] В. И. Павленко, Обоснования методики оценки радиациокних последствии аварии на ЯЭУ. 1979

[4] Rozporządzenie Rady Ministrów z dnia 18 stycznia 2005 w sprawie danych granicznych promieniowania jonizującego (Regulation of the Council of Ministers regarding limiting data on ionizing radiation), Dz.U. 2005 nr 20 poz. 169

[5] D.S. Smith, M.G. Stabin, Exposure Rate Constants and lead Shielding Values for Over 1100 Radionuclides, Health Physics. 102(3):271–291, MAR 2012

[6] L.M. Unger, D.K. Trubey, Specific Gamma-Ray Dose Constants for Nuclides Important to Dosimetry and Radiological Assessment, ORNL/RSIC-45/R1, Oak Ridge National Laboratory, Oak Ridge, 1982

[7] K.F. Eckerman, J.C. Ryman, External Exposure to Radionuclides in Air, Water, and Soil, Federal Guidance Report No. 12, EPA-402-R-93-081, Oak Ridge National Laboratory, Oak Ridge, 1993

[8] IAEA Safety Reports Series No. 19. Generic Models Use in Assessing the Impact of Discharges of Radioactive Substances to the Environment, Vienna 2001

[9] Ustawa z dnia 29 listopada 2000 r. Prawo atomowe. (Atomic law), Dz.U. 2001 nr 3 poz. 1

[10] Rozporządzenie Rady Ministrów z dnia 27 kwietnia 2004 r. w sprawie wartości poziomów interwencyjnych dla poszczególnych rodzajów działań interwencyjnych oraz kryteriów odwołania tych działań (Regulation of the Council of Ministers regarding emergency limits), Dz. U. Nr 98, poz.987

PRELIMINARY UNAVAILABILITY ANALYSIS OF SHUTDOWN SYSTEM FOR AGN-201K RESEARCH REACTOR

IBRAHIM AHMED, GYUNYOUNG HEO*
Department of Nuclear Engineering, Kyung Hee University
1732 Deogyeong-daero, Giheung-gu, Yongin-si, Gyeonggi-do 17104, Republic of Korea
**Corresponding author:* gheo@khu.ac.kr

ABSTRACT

In this paper, the preliminary unavailability analysis of research and educational reactor in Kyung Hee University, AGN-201K shutdown system was performed using generic failure rate database in conservative approach or assumptions. Human reliability analysis regarding the AGN-201K shutdown system was also performed and incorporated into the overall unavailability analysis in order to evaluate the significance of human interaction on the reactor shutdown system. The critical component or combinations of components that contributed most to the overall unavailability were identified. The unavailability (fail to trip reactor on demand) of shutdown system was obtained to be 5.32E-4. The most dominant contributor cutset, which contributed about 71.99% of the unavailability, was found to be the failure of power tube and operator failure to manually initiate reactor trip. The result of these analyses might help to understand better the safety-critical characteristics of the reactor and to base any backfitting on a cost-benefit analysis which would ensure that only necessary changes are made.

1. Introduction

Research and Education Reactor, AGN-201K is a zero-power reactor which has been in operation at Suwon campus of Kyung Hee University (KHU), Republic of Korea since 1982 with a rated power of 0.1W [1]. It was originally installed at Colorado State University in 1967 and was moved to Korea in 1976. It was dedicated for educational purpose, mainly for nuclear engineering students in KHU [1]. Because of obsolescence of control system, refurbishment project was carried out with government research fund during the period of 2004 through 2007 [2]. Reactor power was up-rated and an old analog-type operational console and Instrumentation and Control (I&C) parts were replaced. Additional shielding walls and a new digital-type console for monitoring purposes were also installed during this period [2]. The average thermal flux at the central hole is 3.0×10^8 #/cm^2-sec. The maximum thermal power of AGN-201K is 10 watt. Therefore there is no cooling system for a homogeneous reactor. Core is a cylinder of 25.6 cm diameter and 24 cm height and consists of 9 disks. There is a small diameter glory hole penetrating the core central zone which is utilized for neutron activation. There are 4 beam ports (8 in total in both directions) which penetrate a 20 cm-thick graphite reflector zone outside of core. Reflector zone is surrounded by 10 cm-thick lead for gamma shield and 55 cm-thick water for neutron shield [2]. All safety shutdown functions are kept by analogue console with original safety logics. Upgraded reactor, AGN-201K is now in operation since October 2007 [2].

The I&C system in which power and research reactors rely extensively for providing several functions such as protection, control and monitoring, are installed throughout the reactor facility. The most safety-critical aspect of I&C system is reactor shutdown system or reactor protection system. In the event of accident or power excursion during operation which requires reactor trip, the first and perhaps the most important safety function requirement is reactor subcriticality which is achieved through reactor shutdown system whose purpose is to shutdown the reactor to achieve subcriticality and to avoid fuel element overheating. The AGN-201K is a low rated power reactor and has in addition to the shutdown system, inherent

safety features which include high negative feedback effects and low excess reactivity that are capable of making reactor subcritical in the event that the shutdown system fails to operate. An additional device for reactor safety against abnormal power excursion was a thermal fuse at the central part of the core. This part is designed to be melt at the 120^0C in advance of fuel melting at 200 ^{0}C in case of power excursion and make bottom-half core drop down, resulting in subcriticality due to the separation of the core [2]. However, the purpose of this paper, is to perform the unavailability analysis of the AGN-201K research reactor shutdown system in order to identify the impact of a single component failure or combination of failures on the overall unavailability of the shutdown system. In addition, human reliability analysis regarding the AGN-201K shutdown system is performed and incorporated into the overall unavailability analysis in order to evaluate the significance of human interaction on the reactor shutdown system. The result of these analyses might help to understand better the safety-critical characteristics of the reactor and to base any backfitting on a cost-benefit analysis which would ensure that only necessary changes are made.

2. System Description

Regarding the AGN-201K research reactor shutdown system, there are three single wired neutron instrument channels connected to analogue console from two BF3 ionization chambers and one proportional counter. There are three shutdown signals from these chambers and additional interlock shutdown signals: shielding water low-temperature signal, shielding water low-level signal and earthquake vibration signal. For safety and simplicity, the current study focuses on the three redundant reactor safety neutron channels. The analysis of the interlock signals, which are related with system's operation, is excluded. Therefore, all components that are not part of the safety/protection function and cannot influence the safety function are excluded.

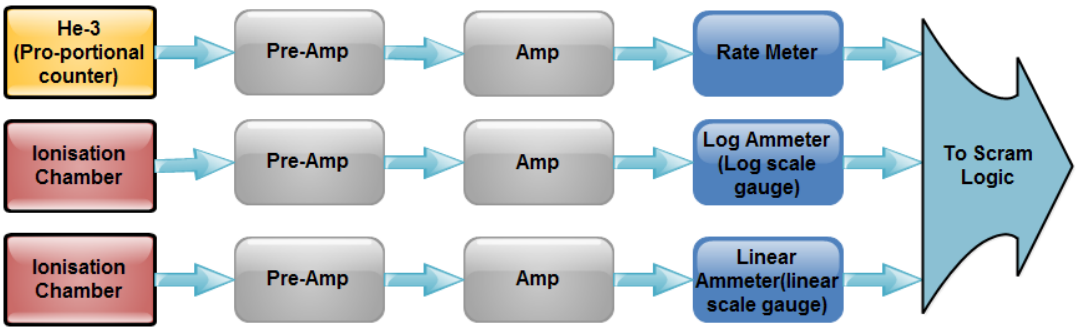

Fig 1. AGN-201K neutron instrument channels block diagram

The scram logic channels block diagram is as shown in Fig. 1. The logic consists of the three safety channels and each channel comprises of the neutron instrument channel, a meter, a sensitrol relay and a reset button. The neutron instrument channel of safety channel 1 consists of proportional counter, pre-amplifier, main amplifier and associated power supply electronics (not shown in the diagram). While that of the other two channels, safety channel 1 and 2, are ionization chamber, pre-amplifier, main amplifier and associated power supply electronics. The signals from the independent safety channels are fed to their respective independent meters whose outputs are the input to their respective sensitrol relay. The trip signals from the sensitrol relay trigger the 6L6 power tube which in turn de-energizes electromagnets that are holding the control rods (two safety rods and one coarse rod), thereby shutdown the reactor.
In addition to the three neutron safety channels, there is the period trip signal generated from the period thyratron schematic whose function is to generate reactor trip whenever the reactor power increase rate exceeds the allowable power increase rate. Also, there are two manual reactor trip buttons which, if pressed by the operator will result in reactor shutdown. The entire I&C system of AGN-201K power is supplied from the two power sources: Automatic Voltage regulator (AVR) 1 and 2. The AVR 2 supplies power to the neutron instrument channels and their respective meters while the AVR 1 supplies power to other I&C systems.

It is important to note that the neutron instrument channel whose components consist of the neutron detectors, amplifiers and the associated power supplies is considered as a single component in order to obtain the failure rate data. This is to adopt the component boundary definition of the nuclear instrument channel given in IAEA document [3] which defined the boundary of a nuclear instrument channel to include the sensor (detector), the power supply electronics and associated signal amplifiers.
It should be also noted that the results of the unavailability analysis presented in this paper regarding the AGN-201K shutdown system is preliminary because the failure data used are not specific for the AGN-201K, rather the generic failure rate data with a few conservative premises or assumptions are used. Therefore, the following assumptions are made:

Assumptions

1. The shutdown system failure is defined here as the inability of the shutdown system to trip the reactor on demand by interrupting power to the electromagnets holding the control rods.
2. The system boundaries of analysis are defined to include the components within the trip signal paths from the neutron detectors to control rod drops that must operate successfully in order to trip the reactor when required. The other trip signals paths due to interlocks and other devices such as thermal fuse and passive cooling mechanisms are outside of the system boundary of analysis.
3. The failure of offsite AC power source is not directly considered in this analysis. Rather, the failure of internal power supplies are considered and modeled explicitly in the fault tree analysis. In other words, based on the Assumption #1, modeling of the offside power loss in the fault tree is unnecessary.
4. Generic failure rate data are from different sources and used for this analysis. Hence, no specific AGN-201K failure rate data is available for use at this time.
5. Manual tripping of the reactor involves manual actuation of any of the pushbutton switches (two manual trip switches and four reset button switches). Although there are two operators in AGN-201K., this action is assumed to be strongly coupled among the pushbutton switches. Failure to manually initiate a reactor trip is therefore modeled as a single operator error.
6. The nominal human reliability analysis (HRA) procedure is not used. Instead, the screening HRA procedure is used and therefore, conservative.
7. In HRA analysis, only post-accident tasks are considered in which the screening HRA for post-accident tasks procedures is employed.
8. Failure of the 6L6 power tube is considered and assumed to be failed-short, i.e., failure to disconnect the current conduction between the anode and cathode when a trip signal is applied to the control grid terminal of the tube. Failed-open mode of the 6L6 power tube is not considered because such failure mode is fail-safe and results in reactor shutdown.

3. Unavailability Analysis

Having described the shutdown system, we performed unavailability analysis: the probability that the shutdown system failed to trip reactor when demanded.

3.1 System modelling and failure data collection

From identification of the system failure criteria, the system fault tree model is developed using AIMS-PSA developed by the Korea Atomic Energy Research Institute (KAERI) [4]. Fig. 2 shows the top-level fault tree model of the simplified shutdown system of AGN-201K.
After the development of the system fault tree model, failure data collection for all the basic events was performed. A rigorous task to develop component failure data based on plant operating experience was not performed as part of this study. Instead, generic data sources were collected and used. Table 1 shows the list of components and their respective failure mode, failure rate/probability, error factor (EF) and reference sources from where the failure

data are obtained. The failure rates/probabilities shown in the Table 1 are mean (average) values and their respective EFs are calculated as the ratio of the 95th percentile (95% upper bound, not shown in Table 1) to the average failure rate/probability. In case of a component which only its mean value is given in the reference source, the EF is conservatively assumed to be 2.4. The EFs represent a quantitative measure of uncertainty associated with component failure rate/probability, which are used in PSA for uncertainty analysis.

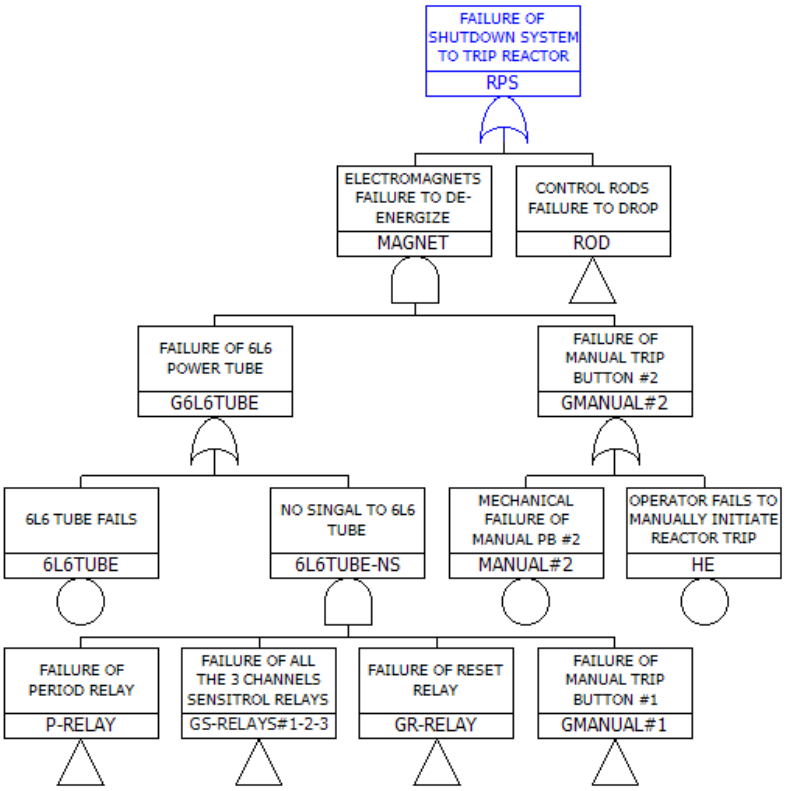

Fig 2. System modelling fault tree for AGN-201K simplified shutdown system (Top level model)

Table 1: List of components and their failure data

S/No	Component	Event Name	Failure Mode	Failure Rate(pro)	EF	Ref.
1	Neutron Instr. Ch.	CH#X-NEUTRON-INT	Fail to Function	8.89E-5/h	1.5	[5]
2	Rate Meter	R-METER	Fail to Function	3.00E-6/h	2.4*	[6][7]
3	Log Meter	LG-METER	Fail to Function	3.00E-6/h	2.4*	[6][7]
4	Linear Meter	LN-METER	Fail to Function	3.00E-6/h	2.4*	[6][7]
5	Thyratron	P-THYRATRON	Fails to Function	5.00E-5/h	2.4*	[7]
6	Sensitrol Relay	S-RELAY#X	Fails to Function	8.30E-6/h	2.4	[5]
7	Reset Relay	R-RELAY	Fails to De-energise	1.25E-4/d	2.4	[8]
8	Period Relay	P-RELAY	Fails to Energise	1.25E-4/d	2.4	[8]
9	6L6 Power Tube	6L6TUBE	Fails to Function	2.00E-5/h	2.4*	[7]
10	Manual Scram BT	MANUAL	Fails to Contact	1.25E-5/d	2.4	[8]
11	Reset Button	RESET#X	Fails to Contact	1.25E-5/d	2.4	[8]
12	Single Rod Ass.	SR#1, SR#2, CR	Fails to drop	3.00E-5/d	2.6	[8]
13	Power Sply to I&C	AVR#1, AVR#2	Fail to Function	5.00E-6/h	2.4	[5]
14	Rectifier(DC Sply)	DC-PS	Fail to Function	1.14E-5/h	2.4	[5]

*These are assumed error factor values. X = 1, 2, 3

3.2 Common cause component failure

In the system fault tree model, common cause failures (CCFs) are considered to represent multiple failures, originating from the common cause, that impact the associated system

unavailability. The CCF event tends to nullify any redundancy incorporated in the design and can make the system incapable of tripping the reactor when demanded. A screening approach was used to identify the common cause basic events and their failure modes that would be the most likely contributors to AGN-201K shutdown system unavailability. The selected components for common cause treatment are those with redundant partners. These components are: sensitrol relay, resent buttons, and neutron instrument channel. In the case of the CCF modeling of neutron instrument channel, only the neutron instrument channels of safety channels 2 and 3 are considered with assumption that neutron instrument channel of the safety channel 1 has component composition and operating mechanism, with a neutron detector, different from that of the other two safety channels. The CCF of the AVR is not considered because the power supply system basic event is explicitly modeled in the fault tree. Also, the CCF of the manual trip button is not considered because, even though the two buttons performed the same function, they are situated in different location with different operating mechanism.
Having identified the redundant components to be considered in the fault tree model, alpha factor method is used for the calculation of the CCF failure data in fault tree model. The generic CCF alpha factors are used which are obtained from ref [9] and tabulated as shown in Table 2.

Table 2: Generic CCF Alpha Factors [9]

Alpha Factor	**CCCG=2**		**CCCG=3**	
	Rate CCF	Demand CCF	Rate CCF	Demand CCF
α_1	9.70E-1	9.80E-1	9.71E-1	9.79E-1
α_2	3.05E-2	1.95E-2	1.74E-2	1.45E-2
α_3			1.19E-2	6.28E-3

3.3 Human reliability analysis

Another important analysis considered in this study is HRA where human (operator) error quantification regarding shutdown system is performed. The process used for operator error quantification here followed the procedure outlined in NUREG/CR-4772 entitled “the Accident Sequence Evaluation Program Human Reliability Analysis Procedure” (ASEP HRA) [10]. The ASEP HRA methodology is a simplified version of HRA approach model from NUREG/CR-1278 [11], and is separated into different guidelines for pre- and post-accident tasks. In this study, only post-accident tasks are considered in which the screening HRA for post-accident tasks procedures outlined in Table 7-1 of NUREG/CR-4772 [10] is employed (see Assumptions #6 and #7). Through the system modelling analysis, any post-accident operator action required for the system to successfully function when demanded was specified and added directly to the fault tree. In this case of unavailability analysis of AGN-201K shutdown system, the post-accident operator action identified which could either reduce or eliminate an abnormal event is manual reactor scram. Regarding AGN-201K, standard operating procedures direct the reactor operator to immediately scram the reactor upon any annunciation or abnormal event occurring during normal operations. Consequently, manual reactor scram can be considered a post-diagnosis task.
The result of this analysis is presented in Table 3. T_m is the maximum allowable time to have correctly diagnosed the abnormal event and to have completed the required post-diagnosis actions so as to achieve system success criteria established by systems analysts. Since no any specific accident scenario is considered in this study, a value of 60 min for T_m is assumed. The actual allowable time for a particular accident scenario might be more than this value; hence, the value of 60 min selected in this study is conservative. T_a is the estimated time needed to get to proper locations and to perform required post-diagnosis actions after a correct diagnosis. A value of 1 min for T_a is assigned in this study since the post-accident action to be performed is within the control room. This value is assigned as stated in Table 7-1 of NUREG/CR-4772 [10], which is the required travel and manipulation time combined for each control room action taken on the primary operating panels which are normally in visual access of the control room operator. T_d is then calculated as the difference between T_m and T_a ($T_d = T_m - T_a$), which is the estimated allowable time for a correct diagnosis which will still permit

sufficient time to perform required post-diagnosis actions prior to T_m. With this information, the appropriate diagnosis HEP (HEP_{dp}) and the appropriate post-diagnosis HEP (HEP_{pp}) are estimated, from where the total failure probability (HEP_{tp}) is calculated based on the procedures in NUREG/CR-4772 [10]. It is important to note that, the obtained HEP_{tp} is a median value. Therefore, for consistency with the failure data presented in Table 1, we converted the median value to mean value, HEP_{mp}, using the following equation, Eq. 1 with an EF of 10. The result was then used in the fault tree modeling analysis.

$$HEP_{mp} = HEP_{tp} * \exp\left[0.5 * \left(\frac{ln(EF)}{1.645}\right)^2\right] \quad (1)$$

Table 3: Post-Accident HRA Result

Action	T_m	T_a	T_d	HEP_{dp}	HEP_{pp}	HEP_{tp}	HEP_{mp}	EF
Manual Scram	60 min	1 min	59 min	0.001	0.01	0.01099	**0.0266**	**10**

4. Quantification Results and Discussion

In this section, the discussion of the quantification results and the sensitivity analysis performed are presented. Based on the discussion with the AGN-201K operator, the testing period interval is 1 month (720h); hence, the mission time for this analysis is set to be 720h for quantification of the unavailability of AGN-201K shutdown system (failure to trip reactor on demand). The quantification was performed using AIMS-PSA.

4.1 Unavailability distribution

An analysis was performed to calculate the uncertainty that exists for shutdown system unavailability due to the uncertainty in values used for basic event failure rates/probabilities. The results are presented as separate distribution, which is represented by the point estimate unavailability, mean value and error factor. The error factor, as earlier defined in Section 3.1, is the ratio of the 95th percentile to mean value.

The fault tree basic event uncertainties were propagated to obtain the shutdown system unavailability distribution. Monte Carlo sample size of 100,000 was used for uncertainty evaluation. Based on the uncertainty evaluation of the basic events included in the fault tree model, the unavailability distribution for the AGN-201K shutdown system failing to trip the reactor on demand is shown in Table 4 and the corresponding cumulative distribution function (CDF) and probability density function (PDF) of the distribution are presented in Fig. 3.

Table 4: Unavailability distribution result

Unavailability (point estimate)	5%	mean	95%	EF
5.32E-4	1.68E-5	5.26E-4	2.01E-3	3.82

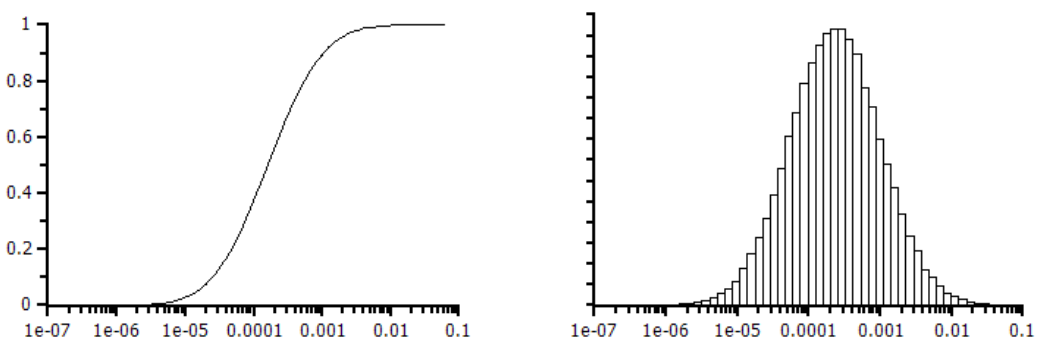

(a) CDF of the uncertainty analysis (b) PDF of the uncertainty analysis

Fig 3. Uncertainty analysis distribution result

4.2 Dominant contributors

Table 5 presented a list of the first five dominant contributors' cutsets to AGN-201K shutdown system unavailability. The cutsets represent the various combinations of basic event failures that prevent the AGN-201K reactor from tripping when demanded. Moreover, the information presented in the table for each cutset includes a description of the basic event(s) and the cutset probability.
From the result of Table 5, the relative contributions of the first five dominant cutsets are shown below:

1) 6L6 tube fails to function and operator fails to manually initiate reactor trip (**71.99%**)
2) AVR#2 fails to supply power to the designated safety channel's components and Operator fails to manually initiate reactor trip (**18.00%**)
3) DC power supply originated from AVR#1 to other components fails to function, neutron instrument channel (NIC) #2 fails to function and operator fails to manually initiate reactor trip (**2.63%**)
4) Period thyratron schematic fails to function, DC power supply originated from AVR#1 to other components fails to function and operator fails to manually initiate reactor trip (**1.48%**)
5) NIC #1 fails to function, NIC #2 fails to function, NIC #3 fails to function and operator fails to manually initiate reactor trip (**1.31%**)

Figure 4 shows the risk importance metric, Fussell-Vesely (FV) event importance, which is the fraction contribution of a risk element of a model. It can be seen that human error contributed most, follows by the 6L6 power tube and AVR 2, which are the most critical event identified in this study.

Table 5: Dominant contributors' cutsets to shutdown system unavailability

No.	Cutset Probability	Basic Event Name	Events Description
1	3.83E-4	6L6TUBE **AND** HE	6L6 tube fails to disconnect and Operator fails to manually initiate reactor trip (HE)
2	9.58E-5	AVR#2 **AND** HE	AVR#2 fails to supply power to the designated safety channel's components and HE.
3	1.40E-5	DC-PS **AND** CH#2-NEUTRON-INT **AND** HE	DC-PS originated from AVR#1 to other components fails, neutron instrument channel (NIC) #2 fails to function, and HE
4	7.86E-6	P-THYRATRON **AND** DC-PS **AND** HE	Period thyratron schematic fails to function, DC-PS originated from AVR#1 to other components fails and HE
5	6.98E-6	CH#1-NEUTRON-INT **AND** CH#2-NEUTRON-INT **AND** CH#3-NEUTRON-INT **AND** HE	NIC #1 fails to function, NIC #2 fails to function, NIC #3 fails to function and HE

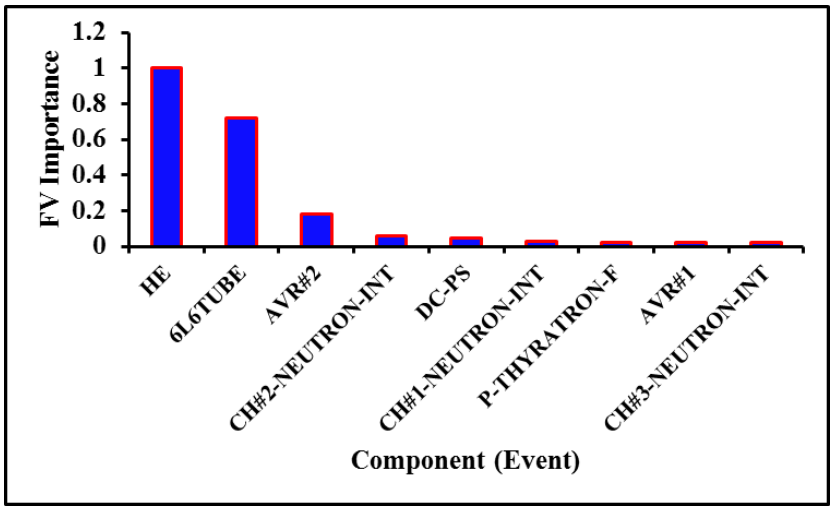

Fig 4. Fussell-Vesely (FV) event importance (HE: Human Error)

5. Conclusions

The I&C system which research reactors rely on extensively for providing several functions such as protection, control and monitoring are installed throughout the reactor facility. The most safety-critical aspect of I&C system should be reactor shutdown system or reactor protection system. Research and educational reactor in Kyung Hee University, AGN-201K is a low rated power reactor and has in addition to the shutdown system, inherent safety features which are capable of making reactor subcritical in the event that the shutdown system fails to operate. In this work, the preliminary unavailability analysis AGN-201K shutdown system is performed using generic failure data and screening HRA in order to evaluate the significance of human factor on the reactor shutdown system. Authors will be developing this model in terms of width and depth: 1) the failure rate data is replaced with the specific ones such that the specific nature of AGN-201K in KHU can be evaluated; 2) in addition to reactor shutdown system, the scope of unavailability is extended to, for instance, thermal fuse and passive cooling mechanisms; and 3) the HRA gets also more accurate by adopting the nominal analysis.

6. Acknowledgement

This work was supported by the National Research Foundation of Korea (NRF) grant funded by the Korean government (MSIP: Ministry of Science, ICT and Future Planning) (No. 2017M2B2B1072806).

7. References

[1] Myung-Hyun Kim, “Utilization of AGN-201K for Education and Research in Korea,” Research Reactor Fuel Management (RRFM-2011) Transactions, Rome, Italy, March 20-24, (2011).
[2] Myung-Hyun Kim, “Reactor Upgrade of AGN-201 in KHU, Korea,” Research Reactor Fuel Management (RRFM-2008), Hamburg, Germany, March 2-6, (2008).
[3] IAEA, TECDOC-636: *Manual on Reliability Data Collection for Research Reactor PSAs*, Vienna, Austria, 1987.
[4] Sang Hoon Han , Ho-Gon Lim , Seung-Cheol Jang, Joon-Eon Yang, “AIMS-PSA: A Software for Integrated PSA”, 13th International Conference on Probabilistic Safety Assessment and Management (PSAM 13), 2016.
[5] IAEA, TECDOC-930: *Generic Component Reliability Data for Research Reactor PSA*. 1987.

[6] B. J. Garrick, W. C. Gekler, L. Goldfisher, R. H. Karcher, B. Shimizu, J. H. Wilson, *Reliability analysis of nuclear power plant protective systems*, HN-190, US. Atomic Energy Commission report, 1967.
[7] N. A. Walter, P. M. Watson, *Component failure rates and their role in reliability prediction*, Technical report TR-71-31, 1971.
[8] IAEA, TECDOC-478: *Component Reliability Data for use in Probabilistic Safety Assessment*, Vienna, Austria, 1988.
[9] U.S. Nuclear Regulatory Commission, *CCF Parameter Estimations, 2015 Update*, http://nrcoe.inel.gov/resultsdb/ParamEstSpar/, October 2016.
[10] A. D. Swain, *Accident Sequence Evaluation Program Human Reliability Analysis Procedure,* NUREGICR-4772, SAND86-1996, Sandia National Laboratories, Albuquerque, NM, February 1987.
[11] A. D. Swain, and H. E. Guttman, *Handbook of Human Reliability Analysis with Emphasis on Nuclear Power Plant Applications*, NUREGICR1278. SAND80-0200, Sandia National Laboratories, Albuquerque, NM, August 1983.

VERIFICATION AND VALIDATION OF OSCAR-5 CORE ANALYSIS FOR THE SAFARI-1 REACTOR

L. BEDHESI, C. JACOBS, R.H. PRINSLOO, S.A. GROENEWALD, F.A. VAN HEERDEN
South African Nuclear Energy Corporation SOC Ltd, Building 1900
Pretoria, 0001 – South Africa

ABSTRACT

The latest version of the OSCAR code system (OSCAR-5) is being verified and validated for use at the SAFARI-1 reactor, operated by Necsa, South Africa. In this work we will report on the current state of this process, as it applies to reload safety and core-follow calculations. The OSCAR-5 system is a software platform which provides multi-code and multi-physics reactor calculational support for research, power and high temperature reactors. One of the main features of OSCAR-5 is the ability to create a unified code independent model of a reactor system, and deploy this model to various different codes such as MCNP, Serpent and the OSCAR nodal diffusion solver MGRAC. The platform is a fit-for-purpose tool in support of reactor operation, allowing easy data transfer between different codes. Beyond the unified model, code independent features include improved plant data processing, irradiation rig modelling, advanced homogenization methods, beryllium reflector depletion and various thermal-hydraulic coupling methods. In this paper, a subset of these new features is illustrated on SAFARI-1 core-follow with results compared to relevant plant data.

1. Introduction

There are two types of codes that are used for reactor analyses; deterministic and probabilistic codes. Historically, these two classes of solution methods have been applied to their own typical domains of application, and have been integrated rather mechanically when a specific purpose requires it. However, with the advances of computing technology, and the increased focus on code verification and validation, the lines between these distinct application areas have become blurred. A more synergistic level of integration has become necessary. Currently, the Radiation and Reactor Theory (RRT) Section at the South African Nuclear Energy Corporation Soc Ltd. (Necsa) is developing and testing the latest version of the Overall System for the CAlculation of Reactors (OSCAR), version 5. The OSCAR-5 code suite [1] is a platform that allows the user to utilize both deterministic and probabilistic calculations in a seamless fashion for a more unified approach to reactor calculational support.

In order to implement OSCAR-5 for SAFARI-1 analysis, the code has to undergo a verification and validation process. In this work, we investigate some of the calculations that were done in preparation for verification and validation analysis. We simulate core-follow calculations over a three year period as well as control rod calibration and flux wire activation experiments. We investigate the capabilities of OSCAR-5 for day-to-day full core neutronic analysis.

Core-follow and reload calculations are important for the safe operation of a nuclear reactor. Core-follow calculations are performed in order to update number densities of burnable materials in the reactor model. During the reactor operation; parameters such as control rod positions, reactor temperatures and reactor power levels are monitored and recorded. This

plant data is used at the end of each cycle, to set up a core-follow simulation of that cycle, thereby updating the number densities of the burnable materials in the OSCAR-5 reactor model. Reload calculations compose of a set of safety calculations that are performed prior to start-up of each cycle, to predict whether the reactor will remain within safety and utilization criteria during operation. At SAFARI-1, experiments are conducted at the start of each cycle to confirm control rod worth and axial flux shapes in the fuel assemblies. Simulations of these rod calibrations and flux wire activations are compared to the experimental data. This together with the reactivity trend across all core-follow calculations provides the basis for the V&V work performed in this paper.

In this paper, we simulate three years of SAFARI-1 reactor operations and investigate and quantify the impact of three specific features of the OSCAR-5 code system on this data set. These are:

- The usage of the advanced homogenization system in OSCAR-5 which constructs the nodal model in a consistent fashion. This approach uses Serpent for the generation of all non-fuel cross-sections and makes extensive use of general equivalence theory to minimize differences between the heterogeneous model and the homogeneous model results. The standard lattice solver in OSCAR-5 (called HEADE) is used for generating fuel, fuel-follower and production rig cross-sections in infinite lattice environments;

- Application of the option in OSCAR-5 to utilize Serpent directly as a lattice solver, and generate fuel and fuel-follower cross-sections directly from the unified model description. This allows the use of much more sophisticated colourseets in full geometric detail. In this case fuel elements are still modelled in an infinite lattice, but the fuel-follower is calculated in a much more realistic three-by-three mini-core configuration; and

- The option to include explicit irradiation rig schedule modelling in core-follow analysis. This is particularly important in a reactor such as SAFARI-1 where rig content has a notable impact on flux and power distributions.

2. The OSCAR-5 code system

The OSCAR-5 code suite is a system that allows for multi-code and multi-physics analysis for research reactors. OSCAR-5 contains a pre- and post-processing system. Firstly, the user builds a detailed model of each reactor component, using the Constructive Solid Geometry (CSG) module of the system. The components are then combined in a library, from which full-core configurations are constructed. At this stage, all input is code independent, meaning that the detailed reactor model is not bound to a specific target code. This is referred to as the unified heterogeneous core model.

Translators are then used to write the geometry and material descriptions of the model, as input to specific target codes. The translators are model-independent, thus ensuring that the model remains consistent when deployed to different target codes.

Monte Carlo codes such as MCNP or Serpent can model a reactor in fine detail. For nodal diffusion solvers; such as MGRAC in OSCAR-5, detailed core models cannot be used directly. OSCAR-5 therefore contains a built in tool called the OSCAR Model Preparation System (cOMPoSe) which is used to move from the heterogeneous unified description with point wise cross-section data, to a set of homogenized mixtures with energy condensed to a few group representation. Once a suitable model is prepared, it can be deployed to various analysis application codes.

Some of the neutronic codes that are available in OSCAR-5 are as follow:

- MGRAC - nodal diffusion solver in which the calculation of the steady-state neutron flux distribution is based on the solution of the three-dimensional, multi-group, time-independent diffusion equation by means of a modern transverse-integration nodal method [2];
- Serpent - Monte Carlo criticality and burnup code developed at the VTT Technical Research Centre of Finland [3], is capable of cell-level and full-core calculations for determining group constants as well as performing as a standalone simulation suite; and
- MCNP6 – Monte Carlo code that has the capability of calculating several reactor physics quantities with generalized geometries and continuous energy spectrums [4].

3. SAFARI-1

3.1 Description of SAFARI-1

SAFARI-1 is a 20 MW tank in pool material testing reactor (MTR) that is primarily used for isotope production. The reactor core is contained within a vessel which is housed inside the reactor pool. The reactor pool contains light water which is used as a coolant, moderator and shield. The core consists of 26 fuel assemblies, 6 control rod assemblies and several irradiation positions. The control rods have two regions, the absorbing region and the followers. Followers contain fuel which has to be accounted for when performing analyses. The fuel type that SAFARI-1 uses is 19.75 percent enriched uranium. Beryllium acts as a reflector surrounding the core. The beryllium is contained in an aluminium core box, surrounded by 6 beam tubes and a few ex-core irradiation facilities.

3.2 SAFARI-1 Model

The model of SAFARI-1 was developed at the Radiation and Reactor Theory section of the South African Nuclear Energy Corporation. It includes the reactor core, core box, and reactor tank and beam tubes. Inside the reactor tank is a grid plate with a rectangular arrangement of 8 × 9 positions where different assembly types can be loaded. The core is surrounded by a beryllium reflector as well as aluminium and lead assemblies. The core contains 9 different in-core target irradiation positions. A radial (X-Y) view of the OSCAR-5 model for the SAFARI-1 reactor is shown in Fig 1.

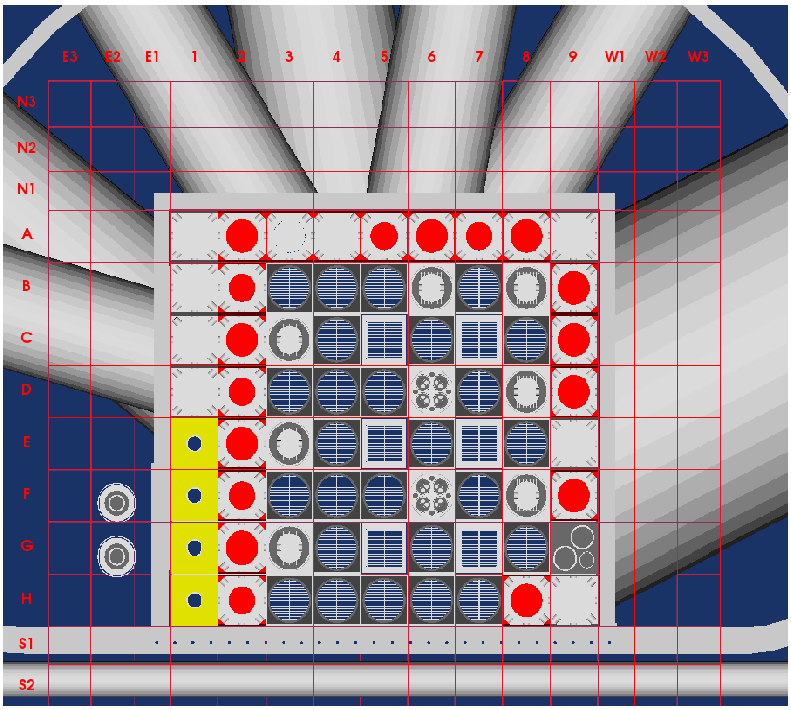

Fig 1. SAFARI-1 core configuration

Fig 2. shows a radial cut through a fuel assembly, a control rod absorber and fuel follower elements. The fuel assemblies are Material Testing Reactor (MTR) type fuel with 19 plates each. The fuel plates consist of a Uranium-Silicide-Aluminium (U3Si2-Al) powder dispersed core, enclosed in aluminium-alloy cladding.

The control rod assemblies consist of an upper absorber section and a lower fuel section connected by a rigid aluminium coupling mechanism. The absorbing section consists of an aluminium box that contains a cadmium layer as an absorber. The fuel section, also called the fuel follower, is similar to the fuel assemblies, but is encased in an aluminium box and contains only 15 fuel plates.

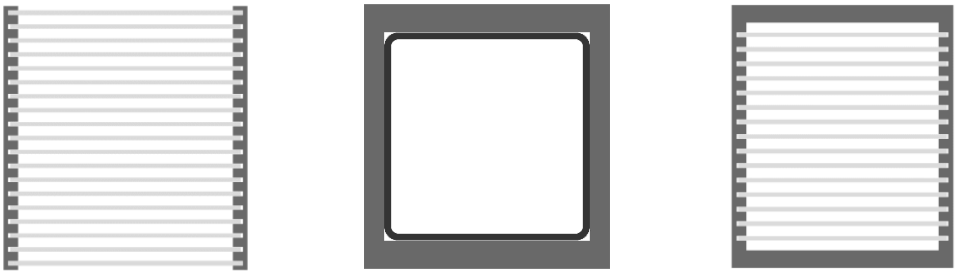

Fig 2. Radial view of a fuel assembly, a control absorber and fuel follower respectively

4. Results and Discussion

In aid of verification and validation of OSCAR-5 as applied to SAFARI-1, we construct a series of models in order to demonstrate the impact of various calculational strategies on plant experimental comparisons. Data is aggregated over a three year period (2012 to 2014) spanning about 35 operational cycles, each either 24 or 30 days long. We consider four OSCAR-5 supported modelling approaches:

- A traditional nodal approach (termed “Traditional”), in which all nodal cross-sections (fuel and non-fuel) are generated in approximate mini-core (colourset) environments with the HEADE lattice code in OSCAR-5. Most non-fuel cross-sections are generated without extensive use of equivalence theory and thus the core nodal diffusion solution would be expected to deteriorate in areas where diffusion theory does not apply. Irradiation rigs and fuelled target rigs are modelled as all loaded throughout all cycles, as this is close to the typical state of the reactor.

- The “Consistent” line, in which we use the cOMPoSe subsystem in OSCAR-5 to generate a homogenized core nodal representation directly from the unified heterogeneous core model. All non-fuel homogenized multi-group cross-sections were generated from a set of 2D full-core heterogeneous core slices from Serpent, while fuel, follower and fuelled rig models were generated from an infinite lattice in the standard HEADE lattice solver. Irradiation rigs and fuelled target rigs are modelled as all loaded throughout all cycles.

- The “Improved lattice” line, in which Serpent is used for the lattice calculations for fuel and follower components, with the latter modelled in an explicit mini-core environment. We term this line the “Serpent Lattice” line. This approach is calculationally quite expensive in generating the many burnup and state off-bases with Monte Carlo, but represents an important confirmation on the use of the HEADE lattice code for fuelled components. Irradiation rigs and fuelled target rigs are modelled as all loaded throughout all cycles.

- The “Rig schedule” line, in which case we model the in-core rig movements explicitly as applied to the “Improved lattice” model.

For both the “Consistent” and “Improved lattice” cases, five axial cuts are utilized to span the active height of the core, while two explicit cuts each are employed for the top and bottom regions. Fuel is depleted in eight axial burnup regions spanning the active height. The nodalization is shown in Fig 3, with the red grid depicting the overlay nodal mesh on which cross-sections are generated.

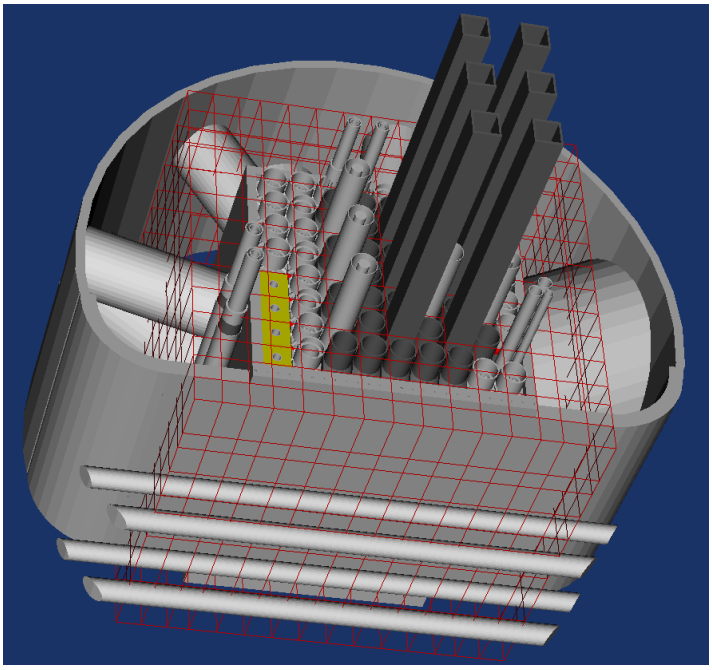

Fig 3. SAFARI-1 nodalization

We investigate the multi-year calculational error trend behaviour of reactivity, the total control rod worth (CRW) over all six rods and low power copper wire activation rates over all 26 fuel positions. We perform this analysis with all calculational lines described above, although some cases are excluded for some of the analyses and are indicated with N/A in the table below.

Line	Reactivity (pcm)	CRW (cents)	2D Activation (%)
Traditional - MGRAC	+2100 (700)	-20 (9)	7 (5)
Consistent – MGRAC	+225 (660)	17 (11)	7 (5)
Improved lattice – MGRAC	-250 (590)	16 (10)	**N/A
* Rig schedule – MGRAC	-100 (223)	N/A	N/A

Tab 1: Average error and standard deviation in error for the various models

* Only performed for year 2012, as opposed to 2012 – 2014, due to limited rig schedule. information.
** Detector constants not yet implemented for Serpent lattice option.

We note firstly an unacceptably large reactivity offset in the “Traditional” line. This is not unexpected and is largely due to the use of overly approximate mini-core (coloursets) environments for non-fuel and ex-core homogenization. The situation is further exacerbated by the use of the low-order response-matrix based lattice code HEADE, which is primarily designed for infinite lattice fuel models, but in this case also applied to non-fuel regions. In general, this offset is the primary reason why traditional nodal methods, applied to heterogeneous research reactor core designs, should always be accompanied by the proper use of equivalence theory.

We further note that the total individual control rod worth is over-estimated by about 20 cents (error averaged over the six control rods, over all cycles) in the “Traditional” model, and the flux wire experiments exhibit an average assembly integrated activation error of 7%. Standard deviation is indicated in brackets in the table.

We move on to the “Consistent” model, and note that the average reactivity offset has notably improved to just over 200 pcm. This can clearly be ascribed to the better application of full-core equivalence theory in combination with using Serpent, as opposed to HEADE, for reflector, ex-core and control rod absorber regions. Control rod worth experiments improve only marginally; the “Traditional” line under-estimates the control rod worth, whilst the “Consistent” model over-estimates. Activation rates in Cu-wires show almost no change.

The value of using Serpent as a lattice code for fuel, in combination with a better mini-core lattice environment for the follower, may be seen when comparing the “Consistent” results with the “Improved lattice” line. Differences here are marginal and we can deduce that the use of HEADE as transport solver for infinite lattice fuel models is adequate.

An area of general concern is that all models show a relatively high standard deviation in reactivity estimation. This is generally related to the way in which in-core irradiation rigs are modelled in these cases, since only a typical cycle rig loading is considered. In reality a large number of in-cycle rig loadings are performed, and these in-core changes have a significant impact on reactivity predictions. In order to mitigate this, OSCAR-5 provides the capability to include rig movements in the plant data processing step.

The “Rig movements” line attempts to capture these effects by modelling a subset of cycles with the explicit target irradiation schedule included. Here we note that the average reactivity off-set improves to about 100 pcm, and more importantly, the standard deviation in the reactivity prediction improves from 590 pcm to 223 pcm. This result shows a much improved reactivity prediction capability, with both the off-set from critical and the variation around critical at acceptable levels.

Various models show significant variation in terms of reactivity, but seem largely invariant with regard to the control calibration and Cu-wire activation experiments. In the next section, we focus on more detail related to the in-cycle reactivity behaviour for a typical cycle.

4.1 Reactivity trend discussion

From the various modelling approaches on critical estimates during core-follow analysis, we choose a typical cycle and present the detailed behaviour within this cycle.

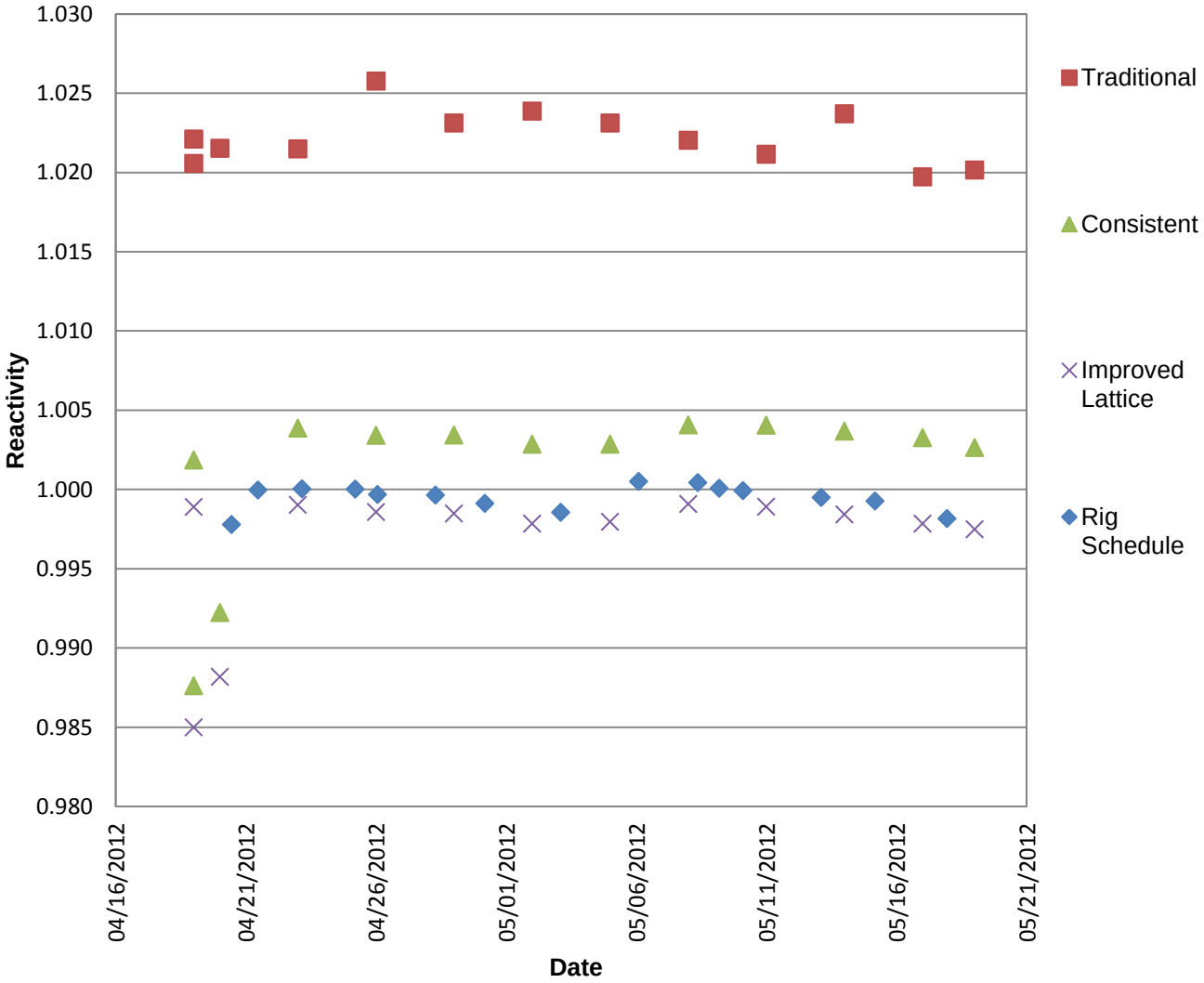

Fig 4. Comparison of the reactivity trends for cycle C1204-1 for all calculational lines considered in this study

From Fig. 4, we observe consistency with the observations made in Tab 1. When comparing the four representations above, we see that the in-cycle shape of the “Traditional” model exhibits a downward trend through the cycle (400 – 500 pcm). This can be ascribed to the rod worth underestimation in this model (as in Tab 1 by 20 cents), as reactivity estimation improves only as the rods are extracted. In contrast, the “Consistent” and “Lattice” models show much flatter in-cycle behaviour.

This improvement is largely due to the fact that the “Consistent” and “Improved lattice”, models Serpent generated cross-sections for the absorber in an exact 2D environment, as opposed to the “Traditional” model that uses nodal cross-sections with the HEADE lattice code in simplified coloursets.

From Fig. 4, we also observe that the shape of the reactivity curve for the “Improved lattice” model flattens when the production rig schedule is added to the core-follow calculations. When the rig schedules are not implemented, the models assume that the rigs are always loaded. This effect is most prominently observed at the beginning of cycle where the reactivity for the ”Consistent” and “Improved lattice” model is notably off, as opposed to when the rig schedule is implemented. We see that once the rig schedule is implemented, the reactivity curve flattens favourably.

5. Conclusion

In this paper, we explored SAFARI-1 core-follow calculations for four different OSCAR-5 supported modelling approaches. In particular, we have investigated the reactivity, control rod and activation experiments. From the “Traditional” model, it was found that the reactivity over a cycle was far from the expected value. The “Consistent” model and the “Improved lattice” models showed significant improvement in reactivity. The best results were obtained when the rig schedule was implemented in the “Improved lattice” model. In this approach the critical contributions to the “Improved lattice model” resulted from Serpent based lattice calculations for fuel and non-fuel components in accurate environments, as well as careful consideration to the in-core loading of samples and fuelled experiments.

It can be concluded that both the “Consistent” and the “Improved lattice” models can be used for reactor core analyses. To achieve a more accurate result, rig movements should also be implemented together with these models.

6. Future Work

In this paper, the impact of colourset lattice models for control rods has been studied. Similarly the lattice models for the molybdenum irradiation rigs can be improved by the use of more representative coloursets. Currently molybdenum rig cross-sections are generated from an infinite rig lattice model. Replacing this with a 3x3 colourset with some fuel and reflector assemblies included, will be investigated in future work amongst many other improvements. Initial studies indicated a significant decrease in the power error calculated in the rig assemblies when such a colourset was used.

7. References

[1] PRINSLOO, R.H., VAN HEERDEN, F.A., *et al*., “Recent Developments of the OSCAR Calculational System, as applied to Selected Examples from IAEA Research Reactor Benchmarks”, 18th IGORR conference, Sydney, Australia (2017).

[2] VOGEL, D.L., WEISS, Z.J., “A General, Multigroup Formulation of the Analytic Nodal Method”, International Topical Meeting on Advances in Reactor Physics, Charleston, South Carolina, USA (1992).
[3] LEPPÄNEN, J., “The Serpent Monte Carlo Code: Status, Development and Applications in 2013”, Ann. Nucl. Energy 82 (2015) 142–150.
[4] Werner, C.J., Bull, J.S., Solomon, C.J., *et al*.,"MCNP6.2 Release Notes", LA-UR-18-20808 (2018).

The Experiment Research of Nigeria MNSR With LEU Core

Li-Yiguo, Peng-Dan, Hong-Jingyan, Wu- Xiaobo, Lu-Jin,
Wang-Mengjiao, Hao-Qian, .

China Institute of Atomic Energy, Beijing,102413,P.O.Box 275-75,China

Abstract: Nigeria Miniature Neutron Source Reactor(MNSR) with 30kW was designed and built by China Institute of Atomic Energy (CIAE) in 2004, which is mainly used for NAA, training and teaching, testing of nuclear instrumentation. UAl_4 with ^{235}U enrichment of 90.2% is as the fuel meat，AL alloy as cladding material, metal Be as reflectors and light water as moderator and coolant.

For Nigeria MNSR conversion from HEU to LEU，the core dimensions is not changed, HEU fuel and AL cladding material are substituted by LEU fuel and Zr-4 alloy respectively.

UO2 is used as the fuel meat with density of 10.6 g/cm^3 and ^{235}U enrichment of 13%, the dimension is 4.3 mm×230 mm. The cladding material is Zr-4 alloy with wall thickness of 0.55 mm and 248 mm in length（8 mm end plug at up end, 9 mm end plug at lower end, 1 mm Helium gas between the upper end and fuel meat）

The experiment of Nigeria MNSR with LEU fuel was done on the Zero Power Facility of MNSR in CIAE, the critical mass, the control rod worth and the worth of other components are measured, the final loading of fuel elements are determined.

Key words: Nigeria MNSR; LEU; Experiment.

1 Description of equipment

The reactor with thermal power 30kW is an under-moderated reactor of pool-tank type, and UO_2 with enrichment of 13% as fuel, light water as coolant and moderator, and metallic beryllium as reflector. The fission heat produced by the reactor is removed by the natural convection. Fig. 1 shows the diagram of the experimental equipment.

There is one fuel cage with 355 lattices, the central lattice is reserved for central control rod. While the four tie rods are uniformly arranged at the eighth row, the other lattices are used for the fuel elements, the dimension of fuel cage is Ø230×258 mm, Zr-4 alloy is as material.

The UO_2 is used as the fuel meat with density 10.6g/cm^3, ^{235}U enrichment is 13%, the dimension is Ø4.3×230 mm. The cladding material is Zr-4 alloy with wall thickness of 0.55 mm

and 248 mm in length（8 mm end plug at up end, 9 mm end plug at lower end, 1 mm Helium gas between the upper end and fuel meat）

There is one Cd tube with outer dia. 4.5mm, inner dia.2.5mm and length 290mm in the central control rod, the S.S tube with dia. 6.0mm is used outside Cd tube.

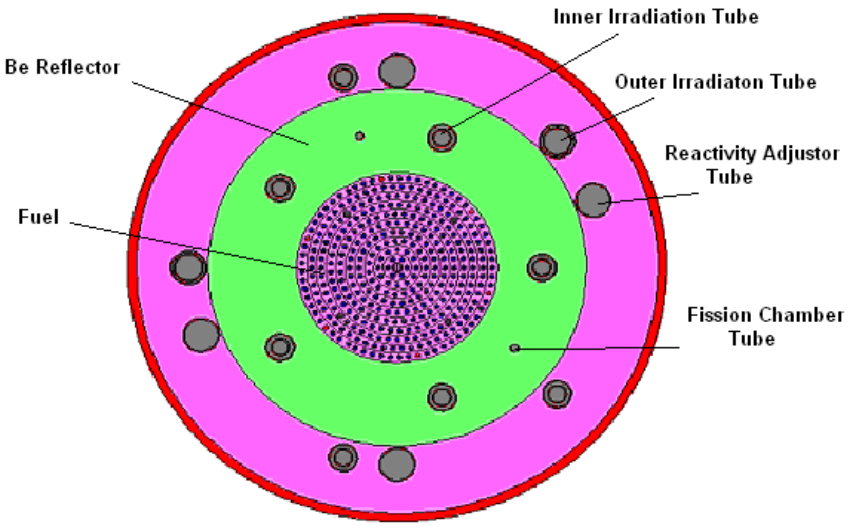

Fig.1 The diagram of the experimental equipment

Beryllium is used as the reflector around the fuel cage, there are bottom Be reflector, side Be reflector and top Be reflector. The bottom reflector with Ø290×50 mm locates the bottom of core, the side Be reflector with outer dia. 435mm, inner dia. 231mm and height 238.5mm locates in the side of fuel cage. The dimension of top Be reflectors is Ø243×109.5 mm which has different thicknessses of 1.5，3.0，6.0 and 12.0 mm, it has hole with dia. 25mm in the center of top Be reflector.

There are ten irradiation tubes in side and outer side Be reflector, 5 tubes are uniformly and vertically arranged in the side Be reflector at the radius of 165 mm, which inserts into the side Be reflector to the depth of 190.0 mm，the dimension of the irradiation tube is Ø32×1.5×190mm. other 5 tubes are uniformly and vertically arranged outside Be reflector at the radius of 232.5 mm and the insertion depth from the top surface of side Be reflector is 190.0 mm，the dimension of the irradiation tube is Ø42×1.5×190mm.

2 Zero power experimental results

The experiment was done in the MNSR zero power equipment, some parameters were measured.

2.1 Critical mass

Two ways of extrapolation and insertion were used for the measurement of critical mass when the fuel elements in the outermost ring uniformly are arranged. The results are 325.2 fuel elements when the five inner irradiation tubes and two outer irradiation tubes are in the side Be reflector and outside side Be reflector respectively and water temperature is 21.4℃.

2.2 Worth of the central control rod

The worth was measured by the period method which relates a small reactivity change with the reactor period. First, the reactivity of the core was measured with control rod fully withdrawn. Next a fraction of the rod was inserted, and reactivity re-measured. The difference in reactivity before and after the fractional insertion defines the worth of the control rod fraction. A fuel element was added to the reactor core, and the reactivity re-measured. Subsequent fractional insertions were performed until the total rod worth was measured (see Fig.2). The total worth of the central control rod of the experiment is 7.623 mk.

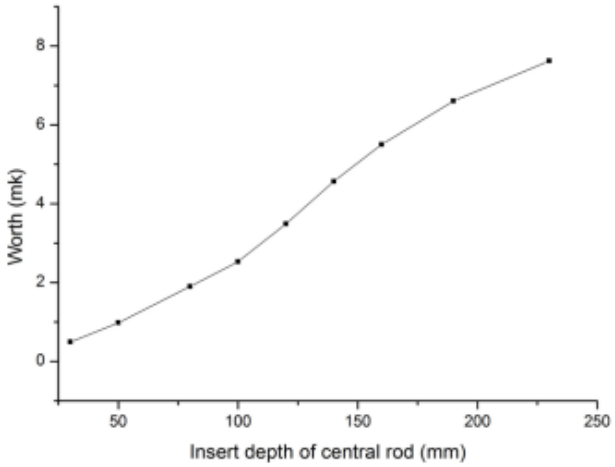

Fig.2 Central control rod worth

2.3 Worth of fission chambers and their tubes

The period method was also used to measure the worth of the two fission chambers with their tubes. The core reactivity was measured with no fission chamber and the associated tube installed. The fission chambers and their associated tubes were then installed, and the reactivity re-measured. The measured worth of both fission chambers and their associated tubes is -0.183 mk.

2.4 Worth of other components

By the period method, the core reactivity was measured with no irradiation tubes in the reflector. The one tube was then inserted, and the reactivity re-measured. Following this way, the worth of each one was measured. The total worth of five tubes is 2.738mk, the average worth of one tube was -0.548 mk. By the same way, the average measured worth of one outer tube was -0.205mk. The measured worth of the top Be tray is -0.579 mk. The measured worth of the control rod lower part is -0.618 mk

3 Final loading

At the initial state of the Nigeria MNSR with LEU core, there are five inner tubes in the side reflector; four outer tubes and one outer tube with Cd tube in outside side reflector, four reactivity regulator tubes, two fission chambers and their associated tubes, the lower part of control rod in the reactor core and an empty top Be tray installed. The total worth of all these reactor components should be considered for the selection of the final fuel loading to establish approximately 4 mk of excess reactivity.

At the experimental state of the Nigeria MNSR core with LEU, there are five inner irradiation tubes in the side reflector and two outer irradiation tubes, the reactivity was measured as 1.914 mk when 327 fuel elements were loaded, with the fuel rods uniformly arranged in the outermost ring.

Based on the measurements, the worth of one outer tube with Cd in the reactor is expected to be -0.64 mk; the worth of three outer tubes is 0.511mk; the worth of four empty reactivity regulator tubes is expected to be -0.82 mk; the worth of two fission chambers and their associated tubes is -0.183 mk; the worth of the lower part of control rod is -0.618 mk; and the worth of empty top Be tray is - 0.579 mk. Thus, a total worth of -3.351 mk is expected for the devices present in the Nigeria MNSR, but not present in the experiment.

The initial excess reactivity of the Nigeria MNSR should be approximately 4.0 mk. The average worth of one fuel element in the outermost ring is 0.96 mk. Thus, the reactivity should be increased to 5.232 mk (1.914 mk +0.205mk– 3.351 mk – 4 mk) in the experiment by using a final loading of approximately 332.45 rods (327 + 5.45). Thus, the final loading selected for the initial state of the Nigeria MNSR reactor is 333 fuel elements, with the remaining lattice positions filled by dummy elements. The measured worth of the core with 333 fuel elements in the experiment was 4.53 mk.

Fig.3 shows the arrangement of the fuel elements.

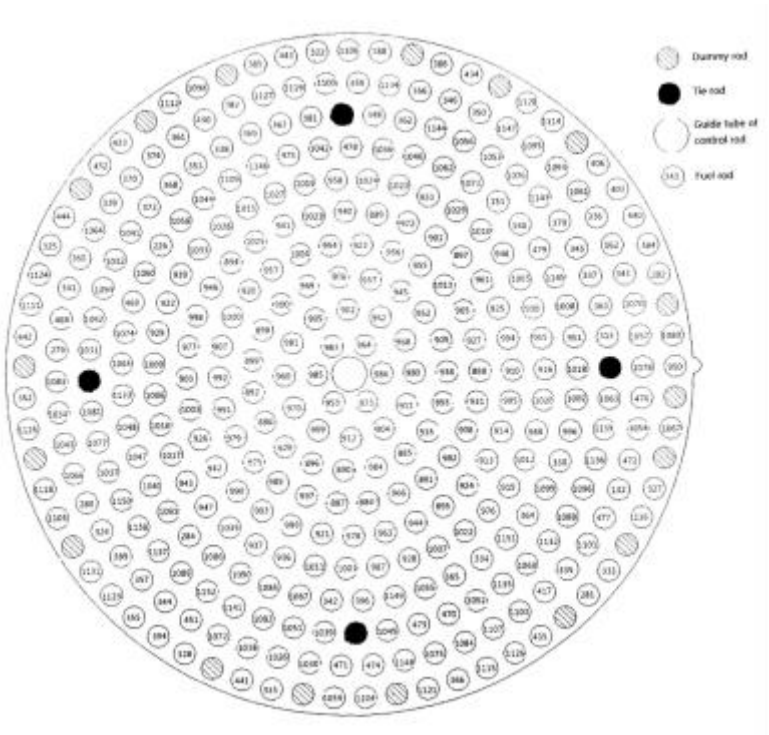

Fig. 3 The arrangement of the fuel elements.

INFLUENCE OF THE THERMOMECHANICAL PROCESS ON THE BEHAVIOR OF 6XXX ALUMINUM ALLOYS UNDER ION IRRADIATION

V. GARRIC, K. COLAS, B. KAPUSTA
DEN-Service d'Etudes des Matériaux Irradiés, CEA Université Paris-Saclay
F-91191, Gif-sur-Yvette

P. DONNADIEU
Univ. Grenoble Alpes, CNRS, Grenoble INP, SIMaP
F-38000 Grenoble

ABSTRACT

Aluminum alloys have been widely used in nuclear research reactors (NRRs) since the 1960s. This choice is mainly due to the very high neutron transparency of such alloys coupled with the low temperature of NRRs. In pressurized NRR, thicker sections are designed to achieve higher mechanical strengths, but issues arise on the irradiation damages in the thickness. Several microstructures of a typical aluminum alloy from the 6xxx series where achieved and samples with the obtained different microstructures were irradiated with different ion fluxes in order to reproduce the irradiation behavior that can be observed in reactor. The results obtained here are compared to literature results from neutron-irradiated samples and modelled in order to predict swelling behavior under irradiation.

1. Introduction

Aluminum based alloys are materials of choice for NRR due to their high thermal conductivity, low gamma heating, low activation and high neutron transparency under irradiation. Research reactors use 5xxx and 6xxx aluminum alloys for their core components to limit the activation under neutron flux. A good compromise between corrosion behavior and high mechanical strength is obtained with the 6xxx series. While increasing the safe and efficient use of NRRs, the manufacturing of such alloys can be challenging in terms of thermomechanical processing: indeed the mechanical properties of those alloys are mainly induced by very specific thermal treatments, which usually consist of annealing, quenching and artificial ageing. Due to a wide use of aluminum alloys in the automotive industry, the thermomechanical processing and its influence on the mechanical properties is already well known and documented in the literature([1], [2]). However, one of the key differences between the automotive industries applications and those of NRRs is the thickness of the manufactured components. Indeed, most of the available research data is available for thin components while the nuclear industry uses thicker ones, especially in the case of pressurized NRRs. Due to this specificity, quenching has to be carefully monitored and understood to obtain a very homogeneous material. In this study, using a typical thermal processing sequence for 6xxx aluminum alloys but varying the quenching rate, we propose to monitor the microstructure formed in aluminum components prior to irradiation in NRRs, observing the formation of dispersoïds and nanometric phases also known as hardening phases. Then, irradiating the different tempers with ion beams, targeting various DPA rates and fluences, we examined a variety of microstructures inside the material and examined in particular the formation of voids and cavities, in order to highlight the influence of the microstructure on the swelling induced by three-dimensional defects.

2. Material and methods

The base material used in this study was a 6061 alloy with the composition given in Table 1. Three 10cm side cubes specimens were extracted from a larger block and machined in order to insert thermocouples at three different positions. Then, each cube followed the same

thermal treatment excepted the quenching rates induced by different quenching fluids. The thermal treatment itself consists of an annealing at 530°C during at least 12h, then a quenching followed by an artificial ageing of 12h at 175°C with a maximum delay of 8h between quenching and ageing. One cube was quenched in water (typical T6 temper), another in oil and the last one in air. TEM specimens were extracted from various positions of the cubes, and electropolished using a 30% nitric acid in methanol solution. The quenching rates were obtained after simulation using CAST3M finite elements code. Irradiation conditions were carefully chosen to be as representative as possible of the NRR environment.

	%wt
Si	0.53
Fe	0.38
Cu	0.22
Mn	0.06
Mg	1.08
Cr	0.18
Zn	0.22
Ti	0.02
Al	*balance*

Table 1 : Composition of selected 6061 alloy (%wt)

3. Initial microstructure after thermomechanical treatment

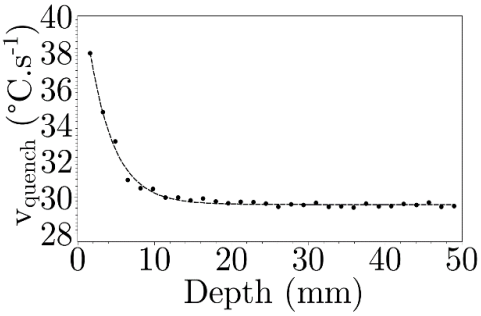

Figure 1 : Simulation of the quenching rate inside the water quenched cube

Results from the thermocouples showed a steady and slow quenching rate inside the air-quenched cube (<0.1°C/s). Water temper showed a drop of more than 10°C/s in terms of quenching rate in an area of about 12 mm as illustrated Figure 1. Due to experimental constraints on the oil quench (a sealed oven), no suitable data were acquired. Therefore, we assume the quenching rate to be between the air and water temper. The microstructure observations at submicronic scale are presented in Figure 2. Figure 2.a and b both picture dispersoïds in the water temper. Figure 2.a presents a low density of typical alpha dispersoïds inside the material near the surface of the block. Water temper at higher depth however, shows a higher density of dispersoïds as seen in Figure 2.b. These dispersoïds are the usual alpha AlMnSi phase. In the oil temper (Figure 2.c), the density of particles is higher than for the water temper sample while more elongated phases appear which were not observed in the water-temper samples. The air temper sample which has the slowest quench rate, presents a very high density of both large and regular particles as seen in Figure 2.d. Usual alpha dispersoïds are identified but new extremely large plates heterogeneously growing from alpha dispersoïds are observed. Figure 3 presents the microstructure with higher magnification (nanometric scale). All pictures here are observed along the <100> zone axis, in order to highlight the typical hardening nanophases. Contrarily to what has been observed at the submicronic scale for the water temper sample, Figure 3.a pictures a very high density of nanoprecipitates near the surface of the cube while Figure 3.b seems to present a lower density at higher depth. Oil temper (Figure 3.c) also exhibits a high density of nanometric phases but with a smaller size compared to the water temper samples. Finally, Figure 3.d pictures a dark field image in the air temper, produced with the selection usually employed to reveal hardening precipitates in 6XXX alloys. Inside the material, no signal of such particles is observed. Nevertheless, some precipitates appear located preferentially on dislocations. This observation suggests, a dislocation could be a preferential site for precipitation of nanophases in air temper samples. Additional observations such as HRTEM are needed to confirm this.

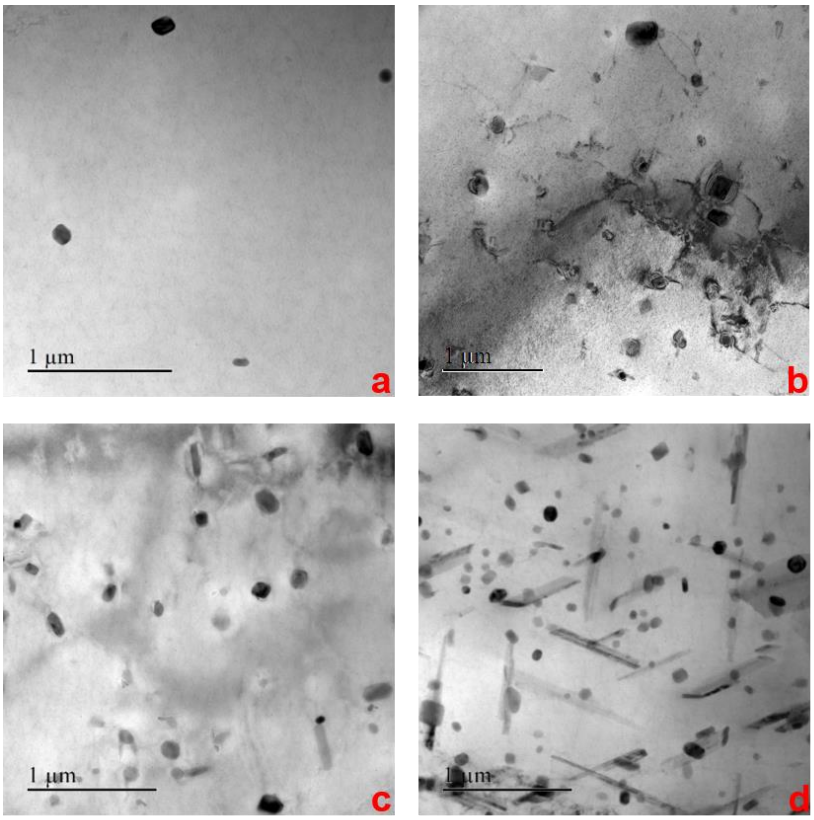

Figure 2: Typical microstructure of each temper at submicronic scale seen in TEM
(a): Water near surface, (b): Water at mid thickness, (c): Oil, (d): Air

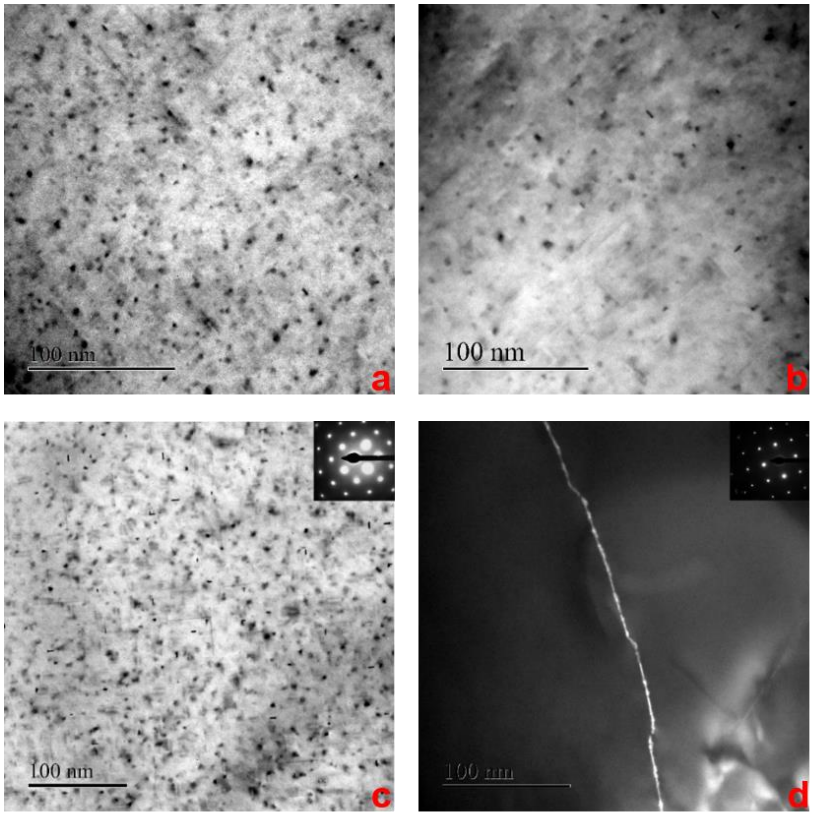

Figure 3: Typical microstructure of each temper at nanometric scale seen in TEM
(a): Water near surface, (b): Water at mid thickness, (c): Oil, (d): Air (Dark Field)

Correlated observation of both scales, Figure 2 and Figure 3, pictures an opposite behavior of precipitation correlated with the quenching rate: a higher quenching rate implies a higher density of hardening particles while lowering the density and chemical/crystallographic variety of dispersoïds while a lower quenching rate seems to imply a very heterogeneous precipitation of submicronic phases at the expense of the density of hardening phases.

4. Post irradiation observation

In the following part, specimens of each major tempers (air, oil, water near center, water near surface) were irradiated for each irradiation condition. This part focuses on qualitative observation of the voids and irradiation damages. Modelling will be presented and discussed on part 5. For brevity's sake, only two irradiation experiments and results will be detailed in this proceeding.

Paragraph	Beam	Ion	Flux (ion/cm^2.s)	Energy (MeV)	Time (h)	Fluence (ion/cm^2)	Targeted DPA (observed area)
4.1	Single	Au^{4+}	2.10^{11}	3.5	52h	$3.69.10^{16}$	100-150
4.1	Single	Au^{4+}	2.10^{11}	3.5	36h	$1.96.10^{16}$	60-90
4.2	Triple	He^{+}	$6.17.10^{11}$	0.5	5h30	$9.95.10^{15}$	35
		Si^{+}	$6.17.10^{11}$	2.5	5h30	$9.95.10^{15}$	
		W^{9+}	$3.8.10^{11}$	13	5h30	$6.15.10^{15}$	
Not detailed here	Triple	He^{+}	$6.17.10^{11}$	0.5	5h30	$9.95.10^{15}$	18
		Si^{+}	$6.17.10^{11}$	2.5	5h30	$9.95.10^{15}$	
		W^{9+}	$1.9.10^{11}$	13	5h30	$3.1.10^{15}$	
	Single	W^{9+}	$3.8.10^{11}$	13	5h30	$6.15.10^{15}$	<35
	Mixed	W^{9+}	$3.8.10^{11}$	20	5h30	$7.5.10^{15}$ (*max*)	15 *to* 50
	Mixed	W^{9+}	2.10^{11}	20	5h30	4.10^{15} (*max*)	5 *to* 25
	Mixed	W^{9+}	1.10^{11}	20	5h30	2.10^{15} (*max*)	2 *to* 10

Table 2 : Summary of ion irradiations conditions as conducted at the Jannus-Saclay facility. Temperature was set to 20°C in all experiments

4.1 Single beam irradiation with gold ions

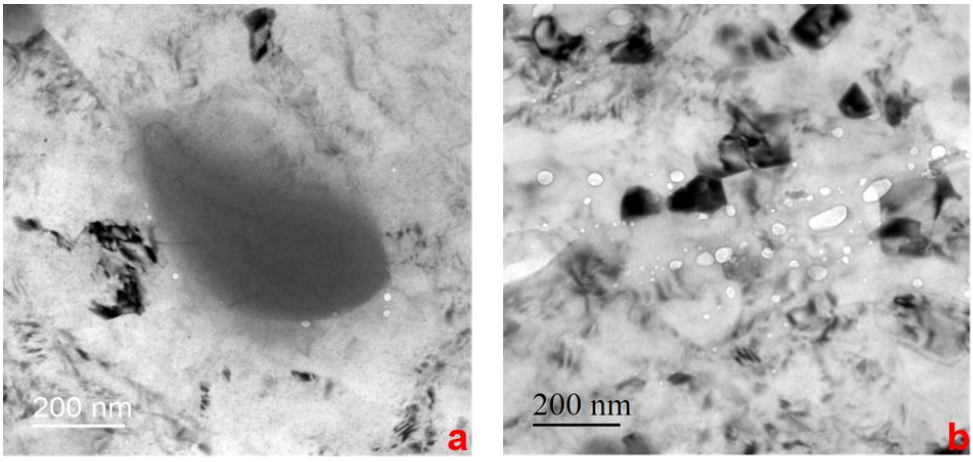

Figure 4: Observation of single beam irradiation on water temper : voids around a dissolved dispersoïd in a 60 DPA zone (a) and larger voids in a 100 DPA area (b)

Single beam irradiation with gold ions have been performed in order to obtain high damage values. Using a constant flux, two irradiation durations were used, allowing the observation of 100-150 DPA for longer duration and 60-90 DPA for the shorter duration. More details on the experimental conditions are given in Table 2.

Figure 4 pictures many different effects of the irradiation on water temper. On Figure 4.a (60 DPA), a dispersoïd is seen being dissolved and amorphized while voids begin to grow on its edges. Looking closely, background microstructure seems inhomogeneous and undefined. The microstructure observed in the 100 DPA sample exhibits many small grains all over the material. Analysis of such grains gives an average grain size of 100 nm while the material prior to irradiation presented a 100 µm average grain size. This effect was observed in the past ([3]) in different aluminum alloys and is believed to be linked with the dislocation density present in the material before irradiation. A very high density of voids is also observed in Figure 4. These voids are all aligned along what is believed to be former grain boundaries.

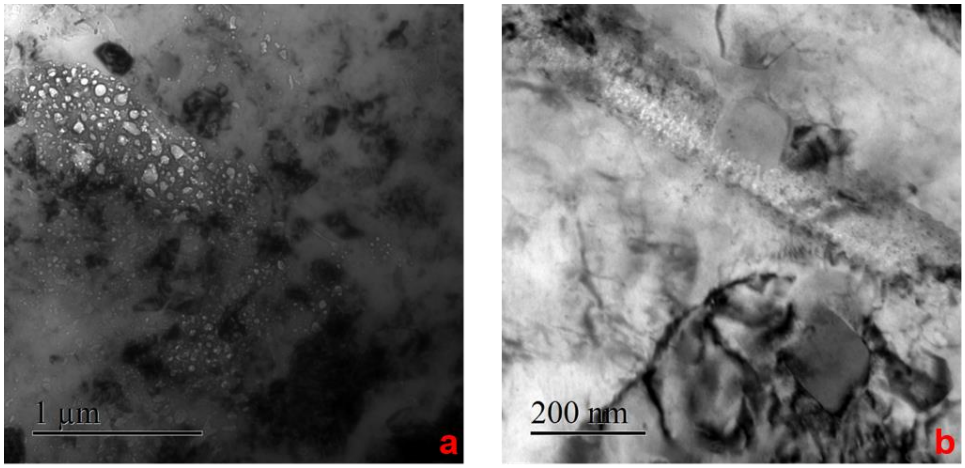

Figure 5: Observation of single beam irradiation on air temper: large void concentration in a 100 DPA area (a) and partial disolution of an elongated dispersoid at low damage value (10 DPA) (b)

Figure 5 presents air temper with two different damage levels. The 100 DPA sample presents areas with a high concentration of large voids surrounded by areas without any void. This phenomenon was observed in all the air temper specimens. In order to further understand this phenomenon, an air-tempered specimen with a low DPA value was prepared. Figure 5.b pictures the air temper at 10 DPA. Large and elongated plate is seen dissolving in the matrix while the alpha dispersoïd seems to remain crystalline and steady at such low damages.

4.2 Triple beam irradiation

Acknowledging the results of single beam irradiation, triple beam were performed in order to assess the role of helium and silicon which are produced during inside reactor irradiations with neutrons. Due to technical limitations, a lower DPA had to be targeted.

Figure 6 shows helium bubbles seen in air temper specimens. The aspect, size, distribution and location due to the implantation is different besides DPA considerations. Figure 7 presents EELS spectra obtained in two different areas in a water temper specimen. The data taken in a bubble free area, shows no peculiar edge. However, data taken from a helium concentrated area presents a peak around 25 eV that is known to be a specific edge for Helium. Finally, Figure 8 shows bubbles in a cross section oil temper specimen. Figure 8.a presents a band of bubbles of about 400 nm, which is in good accordance with our calculations. Figure 8.b, pictures helium bubble distribution, which presents the same size and distribution as seen in air and water temper with the same irradiation conditions.
Triple beam irradiations presented a different behavior toward void and bubble formation. This effect was mainly induced by the helium implantation. If this study pictured a primary role of helium in the formation of small and stable voids, more has to be carried out in order to identify clearly the role of silicon and DPA and DPA rate on the formation of voids and bubbles.

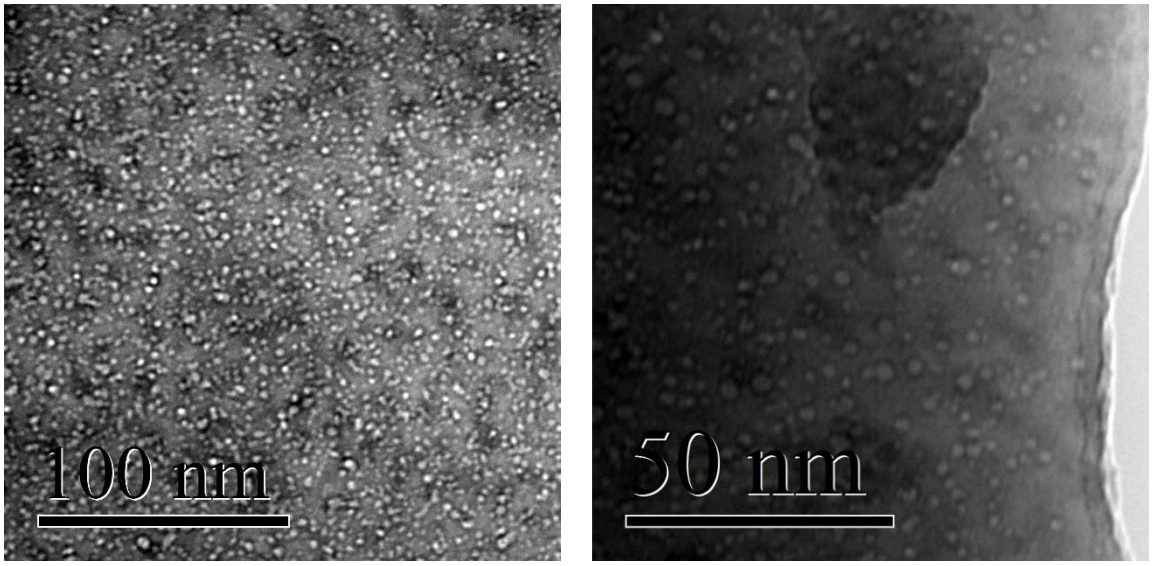

Figure 6: Helium bubbles seen in air temper with EFTEM elastic imagery

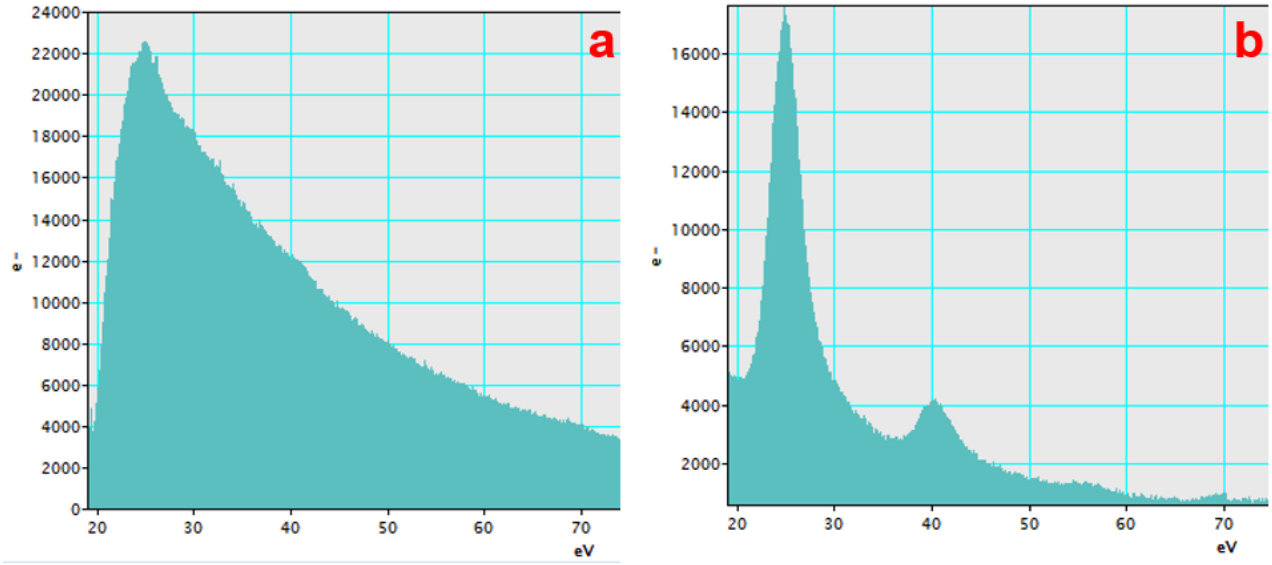

Figure 7: EELS spectrum in a bubble free area (a) and helium concentrated area (b)

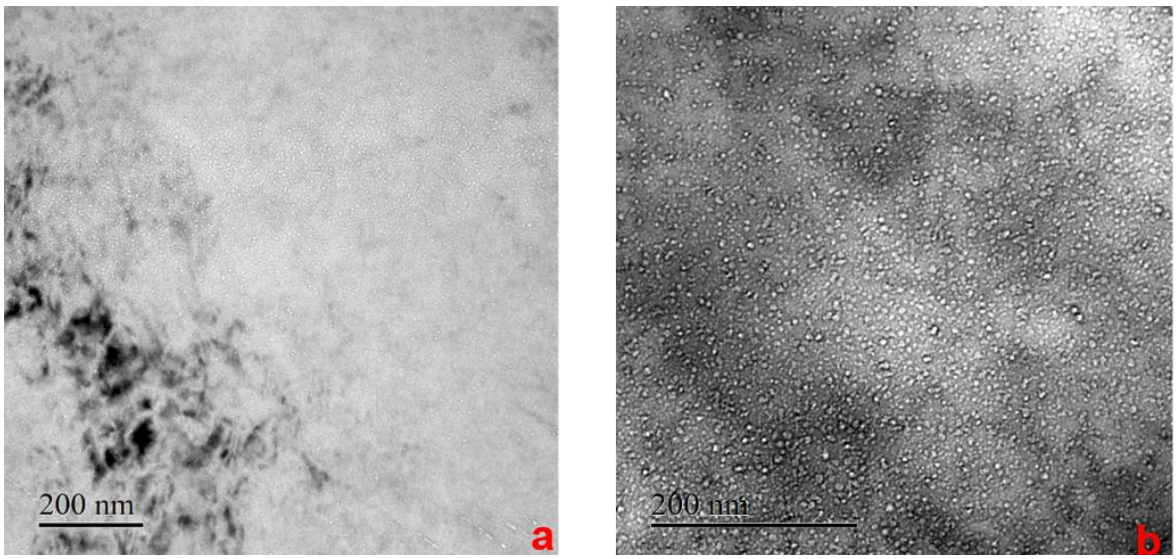

Figure 8: Helium bubbles implantation area seen in cross section sample in oil temper (35DPA)

5. Modelling

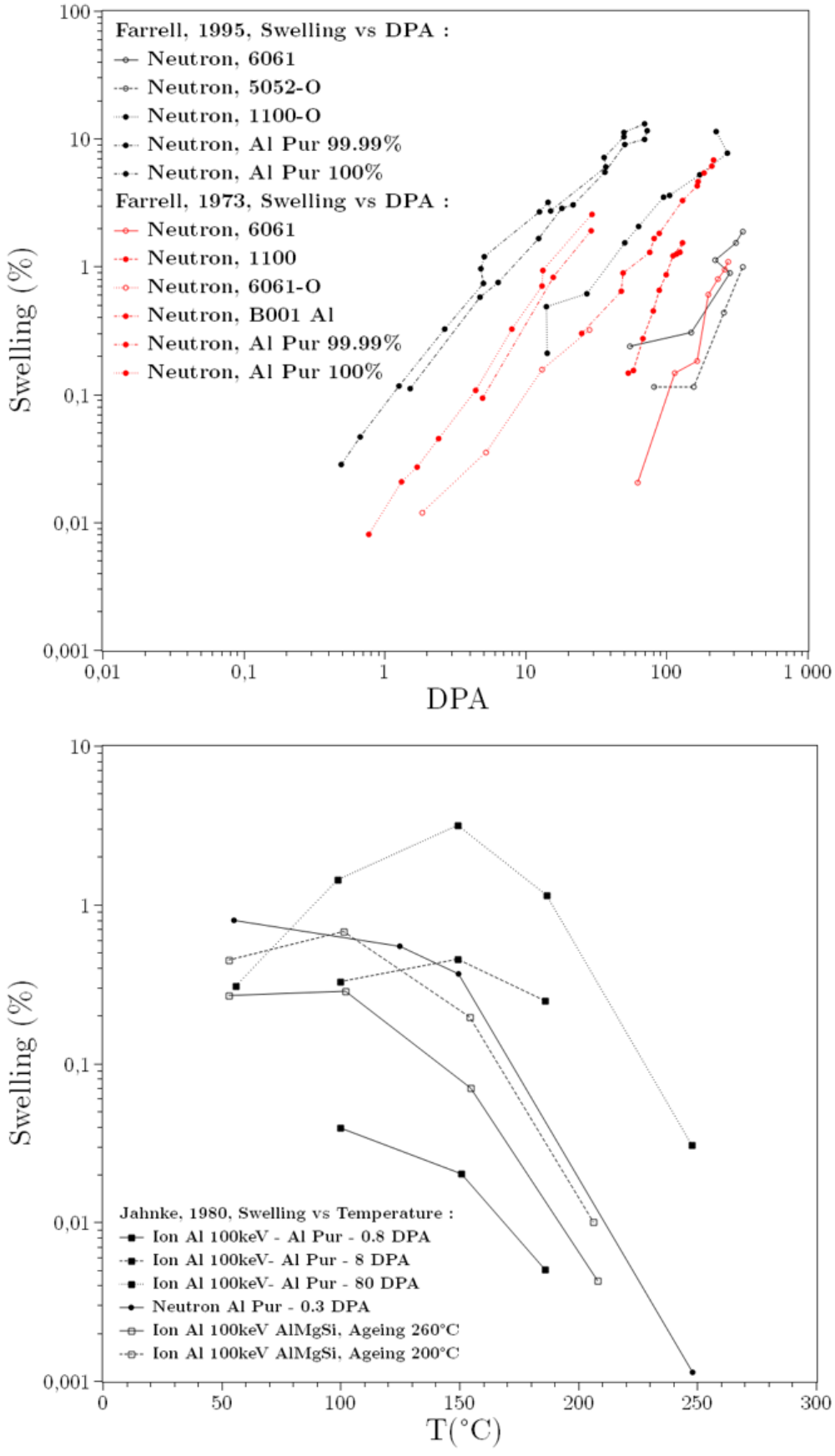

Figure 9: Synthesis of suitable data about aluminum swelling from the literature

Figure 9 represents a summary of various studies of void swelling in aluminum alloys from the literature ([3-8]) as a function of DPA, alloying elements or temperature. From this data, several observations can be made. First, for all observed irradiation conditions, alloyed aluminum swell less than pure aluminum. Secondly, a linear relation appears between swelling and DPA. In the ions irradiation experiments from Jahnke, many temperatures where tested. These observations present a peak of swelling at a given temperature which depends on the damage dose. This result is in good accordance with the general behavior of metallic materials under irradiation [10-11]. Finally, concerning the 6xxx alloys themselves, it seems that the ageing temperature, which is directly linked to the density of nanometric phases, has a great influence on the alloy swelling.
In this study, the Brailsford and Bullough (*B&B*) ([12]) model and equation as written in 1972 will be presented, explained and tracks about empirical improvements will be given. The three equations defining the B&B model are given as following:

$$(1)\ \frac{\Delta V}{V}(\%) = SF(\eta)K\Delta t$$

$$(2)\ \eta = 400\exp\left[-\frac{E_v^m}{k}\left(\frac{1}{T_s}-\frac{1}{T}\right)\right]$$

$$(3)\ F(\eta) = \frac{2}{\eta}\left[(1+\eta)^{0.5} - 1 - \frac{1}{2}\eta exp\left(-\frac{Q}{k}\left(\frac{1}{T}-\frac{1}{T_t}\right)\right)\right]$$

Symbol	Meaning	Unit	Type
S	Incubation	None	Constant to determine empirically
K	DPA rate	DPA/s	Irradiation parameter
Δt	Time	s	Irradiation parameter
E_v^m	Vacancy diffusion activation energy	J	Constant of the material
T_s	Swelling activation temperature	K	Constant of the material
Q	Vacancy self-diffusion energy	J	Constant of the material
T_t	End of swelling temperature	K	Constant of the material
T	Irradiation temperature	K	Irradiation parameter

Table 3: Synthesis of the parameters in the B&B model

Table 3 presents the meaning of major parameters in the model and the relative domain from which each parameter has to be determined. While this model seems to relatively predict the swelling behavior using only a few parameters, some results from the model do not agree with experimental observations. As seen in figure 9, T_t and T_s seem to be linked to the DPA rate in addition to material parameters, which is not taken into account in the current B&B model. Additionally the current model does not take into account any swelling plateaus which are experimentally observed. Indeed, the B&B model assess:

$$\lim_{\Delta t\to\infty}\frac{\Delta V}{V}(\%) \to \infty$$

This value is experimentally and physically not representative. Therefore, we propose some improvements of the model assessing previously detailed experiments and characterizations of the material.

Observations of the microstructure after irradiation reveal an important role of both submicronic precipitation and grain boundaries on the formation of voids and bubbles. While the role of grain boundaries in metals in swelling under irradiation has been widely studied in the literature, the effect of precipitates, which are extremely alloy dependent, has not been studied previously for the 6xxx series of aluminum alloys. The different swelling behaviors for air temper and oil temper samples raises the question of the swelling effects in thick section materials with a potential microstructure gradient. Besides being not observed nor tested in the nuclear industry, such situation may lead not to a uniform swelling but a differentiate swelling which could be expressed using the B&B model by:

$$\left(\frac{\Delta V}{V}(\%)\right)_{global} = x_i(t)\left(\frac{\Delta V}{V}(\%)\right)_{weak} + (1 - x_i(t))\left(\frac{\Delta V}{V}(\%)\right)_{strong}$$

$$\left(\frac{\Delta V}{V}(\%)\right)_{global} = \left(x_i(t)S_{weak}F(\eta)_{weak} + (1 - x_i(t))S_{strong}F(\eta)_{strong}\right)K\Delta t$$

We here introduce two swelling behaviors by separating the physics of each behavior and, furthermore, conceptualize the fact the weak zones observed in air temper will, undoubtedly, swell faster than strong zones. While being more in agreement with observations, this model is still insufficient to picture what would be observed, meaning a gradient of swelling and not a mean value of the component swelling. In other words, a spatial discretization is still missing for such model, or, mathematically speaking:

$$\frac{\partial x_i}{\partial(x, y, z)} \neq 0$$

This kind of consideration is not necessarily complicated for modelling but requires a very high knowledge of the microstructure and its gradient, which means, industrially speaking, an extremely detailed simulation of quenching rate inside the whole material.

6. Conclusion

Results presented here picture the very wide panel of microstructures which can exist in 6xxx alloys depending on the final thermomechanical treatment. This paper demonstrates a strong link between the microstructure resulting from the thermal treatment inside thick sections and the void swelling. Localization of voids, size modifications linked with the microstructure and influence of helium toward voids density have been highlighted. Particularly, it has been pictured that if a very low quenching rate is reached, formation of heterogeneous and coarse precipitation near existing alpha phase plates induces a weak area in which void formation and swelling is prevailing at low DPA.

Presenting global swelling behavior model and equations pictures the lack of representability for aluminum alloys considering thick sections. If the B&B model is globally suitable and consists in a strong outset for modeling purposes, efforts have to be made in order to take account of swelling gradient which occurs in thick sections presenting a gradient of microstructure. More, linear dependency with time has to be reconsidered facing the reality of swelling incubation and plateau.

7. Acknowledgments

The authors want to address a very special thanks to the JANNuS-Saclay facility where all the described irradiations detailed in this document took place. The expertise of all personnel and scientists of the irradiation platform and their dedication to push onward the capabilities of the

irradiators made this work possible and as much representative as possible of inside reactor conditions.

8. References

[1] D. Maisonnette, M. Suery, D. Nelias, P. Chaudet, et T. Epicier, « Effects of heat treatments on the microstructure and mechanical properties of a 6061 aluminium alloy », *Mater. Sci. Eng. A*, vol. 528, nº 6, p. 2718-2724, 2011.

[2] A. Abúndez *et al.*, « Improvement of ultimate tensile strength by artificial ageing and retrogression treatment of aluminium alloy 6061 », *Mater. Sci. Eng. A*, vol. 668, p. 201-207, 2016.

[3] A. Risbet et V. Levy, « Influence de l'ecrouissage sur la formation des cavites d'irradiation dans l'aluminium », *J. Nucl. Mater.*, vol. 46, nº 3, p. 341-352, avr. 1973.

[4] K Farrell, J. O. Stiegler et R.E. Gehlbach, « Transmuted produced silicon precipitates in Irradiated Aluminium », *Metallography*, vol. 3, p. 275-284, 1970.

[5] K. Farrell, R.T. King et A. Jostsons, « Examination of the irradiated 6061 aluminium HFIR target holder », *ORNL*.

[6] K. Farrell, A.Wolfenden and R.T. King, « The effects of irradiation temprature and preinjected gases on voids in aluminium », *Irradiat. Eff.*, vol. 8, p. 107-114, 1971.

[7] B. Jahnke et K. Ehrlich, « Void formation in an Al-Mg-Si alloy under different precipitation conditions after irradiation with 100keV Al ions », *J. Mater. Sci.*, vol. 15, p. 831-838, 1980.

[8] K. Farrell, « Assessment of aluminum structural materials for service within the ANS reflector vessel ». Rapport ORNL/TM-13049, 1995.

[9] K. Farrell, « Effects of structural imperfections on voids in aluminium – Microstructure impurity effects on void formation characteristics in neutron irradiated aluminium ». ORNL-TM-3493, 1971.

[10] « Cascade damage effects on the swelling of irradiated materials », *Proc. R. Soc. Lond. Math. Phys. Sci.*, oct. 1975.

[11] B. H. Sencer et F. A. Garner, « Compositional and temperature dependence of void swelling in model Fe–Cr base alloys irradiated in the EBR-II fast reactor », *J. Nucl. Mater.*, vol. 283-287, p. 164-168, déc. 2000.

[12] A. D. Brailsford et R. Bullough, « The rate theory of swelling due to void growth in irradiated metals », *J. Nucl. Mater.*, vol. 44, nº 2, p. 121-135, août 1972.